LATERAL INSTABILITY OF SLENDER REINFORCED CONCRETE COLUMNS IN A FIRE ENVIRONMENT

by

NICHOLAS JOHN WEEKS

A Thesis Submitted for the Degree of

DOCTOR OF PHILOSOPHY

Department of Civil Engineering and Construction
The University of Aston in Birmingham

October 1985

THE UNIVERSITY OF ASTON IN BIRMINGHAM

LATERAL INSTABILITY OF SLENDER REINFORCED CONCRETE COLUMNS IN A FIRE ENVIRONMENT

by

NICHOLAS JOHN WEEKS

A Thesis Submitted for the Degree of
Doctor of Philosophy

October 1985

SUMMARY

The research concerns the development and application of an analytical computer program, SAFE-RCC, that models material behaviour and structural behaviour of a slender reinforced concrete column that is part of an overall structure and is subjected to elevated temperatures as a result of exposure to fire.

The analysis approach used in SAFE-RCC is non-linear. Computer calculations are used that take account of restraint and continuity, and the interaction of the column with the surrounding structure during the fire. Within a given time step an iterative approach is used to find a deformed shape for the column which results in equilibrium between the forces associated with the external loads and internal stresses and degradation. Non-linear geometric effects are taken into account by updating the geometry of the structure during deformation.

The structural response program SAFE-RCC includes a total strain model which takes account of the compatablity of strain due to temperature and loading. The total strain model represents a constitutive law that governs the material behaviour for concrete and steel. The material behaviour models employed for concrete and steel take account of the dimensional changes caused by the temperature differentials and changes in the material mechanical properties with changes in temperature. Non-linear stress-strain laws are used that take account of loading to a strain greater than that corresponding to the peak stress of the concrete stress-strain relation, and model the inelastic deformation associated with unloading of the steel stress-strain relation.

The cross section temperatures caused by the fire environment are obtained by a preceeding non-linear thermal analysis, a computer program FIRES-T.

Key words: Computer, Fire, Column, Restraint, Reinforced Concrete.

ACKNOWLEDGEMENTS

I would like to express my deepest gratitude to my academic supervisor Dr. J A Purkiss who provided constant help, encouragement and valuable guidance throughout the duration of the research.

The research was financed by the Science and Engineering Research Council from whom the author was in receipt of a Research Studentship.

LIST OF CONTENTS

LIST OF CONTENTS (Cont.)

LIST OF CONTENTS (Cont.)

LIST OF CONTENTS (Cont.)

LIST OF CONTENTS (Cont.)

LIST OF CONTENTS (Cont.)

LIST OF CONTENTS (Cont.)

LIST OF FIGURES

LIST OF FIGURES (Cont.)

LIST OF FIGURES (Cont.)

LIST OF FIGURES (cont.)

LIST OF FIGURES (cont.)

LIST OF FIGURES (Cont.)

LIST OF FIGURES (cont.)

LIST OF TABLES

NOTATION

A	window area
A	convection coefficient
A_F	floor area
A_{FUEL}	area of fuel
A_c	area of concrete
A_o	floor area originally ignited
A_s	area of steel
A_{sc}	area of compression steel
A_{st}	area of tension steel
A_{s1}	area of steel corner bars
A_{s2}	area of steel side bars
A_t	area of planes enclosing compartment
a	surface absorption
a_j	elemental area
$a_{1r}, \ldots a_{jr}, \ldots a_{kr}$	areas of cross sectional elements of division point r
b	breadth of column
C	calorific value
C	compliance
C	compressive force
C_c	stiffness reduction constant allowing for cracking of section
$\underline{C}$	capacity matrix
C_m	factor for variation of axial load eccentricities
C_p	specific heat
$c_0, \ldots c_r, \ldots c_n$	division point deflections under zero load
D	depth of compartment
d	effective depth of section
d'	depth of compression steel

d_2	distance between centroid of section and centroid of steel
E_c	initial modulus of elasticity of concrete
E_m	mean initial modulus of elasticity
E_o	initial tangent modulus of elasticity
E_s	initial modulus of elasticity for steel
E_s^*	strain hardening modulus for steel
$(E_t)_{jr}$	tangent modulus of elasticity in element j division point r
E_1, E_2, E_r	initial elastic modulus of member 1, 2, r
e	eccentricity of the application of axial force
F	external heat source
f_c	concrete effective strength
f_{cu}	concrete cube strength
f_{cyl}	concrete cylinder strength
f_s	steel effective strength
f_y	steel yield strength
g_A, g_B	rigid gusset lengths at end A, B
H	sum of deflection incompatabilities
h	height of window
h	overall depth of section
I_c	second moment of area of concrete
I_s	second moment of area of steel
$I_{uncrack}$	second moment of area of uncracked section
I_1, I_2, I_r	second moment of area of member 1, 2, r
K	stiffness
$\underline{K}$	conductivity matrix
K_c	column stiffness
K_m	axial restraint parameter

<u>NOTATION</u> (Cont.)

K_1, K_2, K_r	stiffness of member 1, 2, r
k	Boltzmann constant
k	thermal conductivity
k_1	concrete creep factor
k_2	transient strain factor
L	mass of fuel
L	length of structural member
L_1, L_2, L_r	length of structural member 1, 2, r
$l_1, \ldots l_r, \ldots l_n$	segment lenghts
M	bending moment
M_A, M_B	end moments acting at A, B
M_{ac}, M_{ca}, M_{bd}, M_{db}	fixed end moments
M_u	ultimate moment at failure
M_{u1}, M_{u2}, M_{ur}	ultimate moment at position 1, 2, r
$M_0, \ldots M_r, \ldots M_n$	division point bending moments
M_1, M_2, M_r	moments at position 1, 2, r
m_1, m_2, m_3	dummy moments
N	convective power factor
N	axial restraining force
N_{fl}	number of floors above
P	axial load
P_a	axial strength of column cross section
P_c	Euler buckling load of slender column
P_o	initial axial load
P_t	total axial load supported at time t
P_u	ultimate axial load at failure
p	concrete creep factor
Q	rate of heat release

Q	external heat flow
$\underline{Q}$	external heat flow vector
q	fire load
q	rate of heat flow
R	rate of burning
R	relative stiffness of surrounding structure
R	gas constant
R	radius of curvature
T	temperature
T	tensile force
$\underline{T}$	temperature vector
$\dot{\underline{T}}$	temperature time rate of change vector
T_c	concrete temperature
T_f	fire compartment temperature
T_o	initial furnace temperature
T_s	steel temperature
t	time
t_d	fire duration
t_f	fire grading
t_r	reference time
U_a	activation energy
u_s	distance from centoid of cross section to centre of steel bar
$u_{1r}, \ldots u_{jr}, \ldots u_{kr}$	distances of element centres from column axis
V	radiation view factor
V	volume
V	shear force
W	width of compartment
x_i	distance from neutral axis to centre of element

x_{NA}	depth to neutral axis
x,y	local Cartesian coordinates
y	deflection
$y_0, \ldots y_r, \ldots y_n$	division point deflections
Z	Zener-Holloman constant
z_i	distance from extreme compressive fibre to centroid of tension steel
z_i'	distance from extreme compression fibre to centroid of compression steel
α	fire growth parameter
α	eccentricity factor
α	coefficient of thermal expansion
α	incompatability between proposed and calculated axial force
α_e	ratio of initial tangent modulus of steel to the initial tangent modulus of concrete
α_j	stress dependent constant
α_t	strength reduction constant for concrete
β	strain softening parameter
β	overconvergence factor
β	incompatability between proposed and calculated division point moment
β_o	concrete creep factor
β_t	strength reduction constant for steel
β_t'	strength reduction constant for steel corner bars
γ	compartment geometry constant
γ	thermal diffusivity
γ_m	material partial safety factor
$\gamma_0, \ldots \gamma_r, \ldots \gamma_n$	changes in slope at division points
Δ	total deformation

NOTATION (Cont.)

ΔH	activation energy of creep
ΔL	change in length
Δ_j	width of square element j
Δ_1, Δ_2	small independent change in proposed endslope
δ	column shortening
δ_o	initial column shortening
ε	strain
ε_{avtot}	average total strain
ε_{jr}	strain in element j at division point r
ε_{cr}	creep strain
$\bar{\varepsilon}_{cr}$	accumulated incremental creep strain
ε_{cro}	y axis intercept of secondary creep phase
ε_f	emissivity of radiation source
ε_{max}	value of strain at the point of maximum stress
$\bar{\varepsilon}_{max}$	value of strain at the point of maximum stress for unloaded specimens
ε_o	inelastic steel strain
ε_{shr}	shrinkage strain
ε^t	strain at ultimate concrete tensile stress
ε_{th}	thermal strain
ε_{tot}	total strain
ε_r	resultant emissivity
ε_s	surface emissivity
ε_{tr}	transient strain
ε_u	ultimate strain
ε_y	steel yield strain
ε_σ	instantaneous stress related strain
$\varepsilon_0, \ldots \varepsilon_r, \ldots \varepsilon_n$	direct strains at division points
ε_∞	total potential shrinkage strain

η	compartment geometry constant
θ	temperature compensated time
θ	absolute temperature
θ_A, θ_B	end slopes
θ_r	absolute temperature of radiation source
θ_s	absolute temperature of surface
θ_u	ultimate rotation
$\theta_0, \ldots \theta_r, \ldots \theta_n$	division point slopes
ξ_1, ξ_2	incompatability in end slope at end A, B
$(\xi_y)_0, \ldots\ldots (\xi_y)_n$	incompatability in division point deflections
ρ	density
σ	Stefan-Boltzmann constant
σ	stress
$\overline{\sigma}$	stress history
σ_{jr}	stress in element j at division point r
σ_{max}	the value of stress at the point of maximum stress or the concrete compressive strength
$\sigma_{max,o}$	the value of stress at the point of maximum stress at ambient conditions
σ_o	stress limit for linear response
σ_u^t	ultimate concrete tensile stress
τ	effective fire duration
τ_j	element retardation time
ϕ	curvature
ϕ	temperature shift function
ω	uniformly distributed load

Subscripts

i	an iteration
j	an element
$(\ )_{all}$	allowable quantity
$(\ )_c$	calculated quantity
$(\ )_i$	quantity appropriate to iteration
$(\ )_m$	modification to a quantity
$(\ )_p$	proposed quantity
$(\ )_\Delta$	change in quantity due to the effects of Δ

Superscripts

$(\ )^\Delta$	changed quantity due to the effects of Δ

CHAPTER 1

INTRODUCTION

The conventional method of assessing the performance of construction elements in a fire is through the application of the standard fire test according to BS476. The standard requires that columns should be exposed to heating from all four sides while sustaining a concentric axial load of a similar magnitude as that which would occur in the construction of which the test specimen is a part. However, this condition does not correspond to the worst loading case to which a column may be subjected to in a real fire. The worst condition is for a column heated on three sides and a moment applied in the direction of the thermal gradient. The standard also states that when it is not possible to test a full size column the maximum height of the part exposed in the furnace should be 3 metres, which will result in a column that would be slender in a structure being tested as a short column.

Since fire tests cannot be carried out on complete buildings, it is attempted to relate the fire test performance on single construction elements to the behaviour of the building. However, much evidence exists that shows the performance of a construction element in a total structure is markedly better than that for a single construction element. This is due to the beneficial effect of the presence of restraint which occurs in a real structure. It should be noted, however, that very high restraint may cause a worse effect.

In the case of a column there will be rotational restraint where beams and other columns tie into the column ends and axial restraint due to the stiffness of the structure above. In the standard furnace test a column element is free against axial restraint and subject to an indeterminate degree of rotational end restraint, the test condition is closest to being pin ended.

The standard furnace test is cumbersome, expensive, requires large specialist apparatus and fails to model satisfactorily the structural restraint and continuity likely to be experienced by a column in a real fire. More realistic conditions corresponding to columns in continuous structures can now be studied by computer simulation using calculations based on heat transfer and the structural properties of materials at high temperatures.

The first widely known computer program for analysing the structural response of reinforced concrete frames in a fire using discretization techniques was FIRES-RC by Becker and Bresler (1974). A revised version of the program was presented by Iding et al in 1977 where a tangent stiffness solution approach replaced the secant stiffness approach used by Becker and Bresler (1974) and allowance was made for the linear variation of the moment along the axis of the beam element. Anderberg established a special version of FIRES-RC in 1976 which included new material behaviour models developed by Anderberg and Thelandersson (1976) at the Lund Institute of Technology.

The various versions of FIRES-RC were based on a displacement method of analysis and neglected to take account of geometrical non-linearities or second order effects. Geometrical non-linearities as well as geometric effects were first considered by Haksever (1977) in analysing fire exposed slender L-frames where the analysis was based on a force method. Later, Forsén (1982) considered geometrical non-linearities, second order effects and material behaviour models developed at the Lund Institute of Technology in the finite element program CONFIRE. CONFIRE makes use of a displacement method of analysis, with convergence criteria based on deflections which will result in an unspecified out-of-balance loading on the structure.

The computer programs mentioned above assume that the heat flow problem is completely separable from the structural analysis and are designed to be used in conjunction with a program that predicts the thermal response of reinforced concrete frames such as FIRES-T (Becker, Bizri and Bresler (1974)) or TASEF-2 (Wickström (1979)).

All of the computer programs reported above make use of an over simplified model of restraint, either through the use of idealized linear springs or where either full restraint or pin ends are considered at the extremities of the column, neither of which are likely to occur for a member within a real structure.

This investigation is concerned with the development of a new computer program SAFE-RCC for the structural analysis of reinforced concrete columns in a fire environment. SAFE-RCC makes use of a stiffness approach where loads are tested for convergence and the resultant deflections calculated. Material behaviour models developed at the Lund Institute of Technology are included and account is taken of geometrical non-linearities and second order effects. Similarly account is taken of the problems of restraint and the interaction of the column with the surrounding structure during the fire.

Axial restraint and rotational restraint are considered independently, and not in a combined parameter, and allowance is made for the fact that the axial restraint afforded to the column increases with the height of the structure above. SAFE-RCC also models the condition of pinned and fixed rotational restraint, and free axial expansion and fixed axial restraint. Although these are conditions which are not likely to be experienced by a column in a real structure, they allow comparison with the standard furnace test.

A modified version of FIRES-T is used to determine the thermal response of the structural cross sections.

This thesis describes the thermal analysis, structural analysis, model of restraint, material behaviour models and the structure of the computer program. The computer model SAFE-RCC is shown to simulate well the structural response of a series of columns exposed to the standard test condition. A test series is further included to demonstrate the possible application of SAFE-RCC in determining the fire performance of columns that are part of a total structure. Also included in the appendices to the thesis is a users manual for SAFE-RCC.

CHAPTER 2

GENERAL DISCUSSION AND CRITICAL REVIEW OF LITERATURE

2.1 ROLE OF FIRE ENGINEERING

2.1.1 Statutory Requirements

Fire engineering is concerned with the performance of structures in a fire. At present performance is defined by the regulatory and insurance authorities. The regulations concerning fire protection in buildings have a number of aims, given in simplified form in the FIP/CEB Report (1978):

(a) Safety of occupants in (i) the fire zone
(ii) other parts of the building
(iii) the adjacent buildings

(b) Mitigation of material damage to (i) contents
(ii) the building structure
(iii) the adjacent buildings

(c) Prevention of the spread of fire

(d) Safeguarding fire fighting and rescue operations.

Fire protection strategy consists of active and passive measures. Active measures such as fire detection and alarm systems, control by sprinklers and fire fighting are designed to operate only when a fire starts. Structural fire protection is a passive measure or in-built provision. The Building Regulations of 1972 concentrate on passive rather than active means of protection. However, this raises the question whether the Building Regulations should allow interaction between active and passive measures, for example, a reduction in fire resistance period if say adequate sprinklers are installed.

Buildings are classified according to their intended use into one of eight purpose groups. A minimum period of notional fire resistance is assigned varying from 1/2 hour to 4 hours depending on the size and function of the building. The particular period of notional fire resistance is deemed to be satisfied if the structure is built in accordance with one of the specifications in Schedule 8 of the Regulations.

Present Building Regulations are based upon the findings of the 1946 Fire Grading Report, which considered fire load to be an important factor, and on the comparison of structural behaviour with the performance in fire tests (ISO 834 and BS476:Parts 20, 21 and 22). The results of standard furnace tests made on simply supported small-sized single structural elements under full design load are used to write the statutory requirements into the Building Regulations or By-laws and clauses into Codes of Practice, although recent British Standard Codes of Practice are based on rational design, for example the Steel Code BS5950, the Concrete Code BS8110 and the Timber Code BS5268.

The existing procedure for assessing the period of fire resistance is simple and not completely representative of the conditions that might obtain in a real fire, (Fire Resistance of Concrete Structures (IStructE)). While many tests have been performed on simple elements to BS476:Part 8, few studies have been carried out on real structures exposed to simulated, or even real, fires. Thus no account is taken of the effects of framing and continuity, when what evidence exists suggests that structures have a much better performance than single elements, although there is some evidence from PCA work (Carlson et al (1961) and Selvaggio and Carlson (1962, 1967)) that the presence of a very high restraint will cause problems. The FIP/CEB Recommendations (1978), however, include suggestions to take a limited allowance of the effect of continuity and restraint.

This approach has provided tabulated fire resistance data in building codes where the fire rating of each of the elements of the fire cell, eg. slabs, beams, columns or walls, is determined separately in terms of size of member and protection cover to the steel reinforcement. The Building Regulations, Schedule 8, specifies minimum concrete cover, minimum sectional dimensions and extra applied protection. Since no other documents have deemed-to-satisfy status, design engineers cannot currently use the provisions of CP110, BS5628 or CP121:Part 1 to show compliance with the regulations, but nevertheless, the codes give information for purposes of assessment or relaxation, although in practice since CP110 is deemed-to-satisfy for normal design purposes Chapter 10 is used (it is more onerous than the Building Regulations). These tables are mainly relevant to simply supported construction and are designed to provide a conservative or safe estimate of fire resistance, almost certainly for fire resistances up to 2 hours. However, fire resistances of 3 to 4 hours may be unsafe. As Sullivan and Dougill (1983) point out, for highly redundant structural frameworks the tabular method is likely to be uneconomic and unduly restrictive on design. Because of this an alternative approach having greater generality and based on analysis is required.

Structural fire engineering design philosophy can be divided into three main areas (Smith (1982)):

1. Studies and calculations to determine the heating rate and maximum temperatures likely to be encountered in fire compartments.
2. Studies and calculations of the heating rates and maximum temperatures realised in the structural members.

3. Consideration of the structural behaviour of the assembly at the elevated temperature.

Law (1983) gives a comprehensive review of the results and conclusions of the studies and calculations to determine the heating rate and maximum temperatures likely to be encountered in fire compartments, and upon which the next section is based.

2.1.2 Quantification of Fire Exposure

Structural fire engineering design philosophy needs to quantify the fire exposure and the effects of that exposure on structural behaviour to determine any reduction in loadbearing capacity. This is done through the study of compartment fires which are considered to be more representative of the degree of real fire exposure than standard fire resistance tests since direct account is taken of fire load, compartment size and ventilation.

A building fire has three main phases: ignition and growth, full development and decay. It is during the fully developed phase that most of the structural damage occurs.

2.1.3 Compartment Fires

The severity of a fire in a compartment depends upon three main factors:

(a) fuel for the fire, or fire load,

(b) ventilation (ie. air supply) to promote its growth,and

(c) the characteristics of the compartment.

2.1.4 Fire Load

The fire load represents the type, amount, porosity and distribution of the combustible materials. The fire load in a compartment is established by listing the weight of the contents and the materials used in the construction. Since combustible materials in buildings burn in a similar way to wood, equivalent fire loads of the various materials have been established and conversion factors are used to relate their calorific value to an equivalent amount of wood. A measure of the floor area is then taken to describe the fire load in terms of weight (kg of wood) or heat per unit floor area.

2.1.5 Rate of Burning

If a fire is allowed to burn out, then the duration of the fire t_d can be expressed as:

$$t_d = LC/Q \tag{2.1}$$

where: L is the mass of fuel (kg),

C is the calorific value (MJ/kg),

Q is the rate of heat release (MJ/s).

However, most experimentors have measured the rate of loss of fuel, instead of Q, and it was found that it had a constant value R (kg/s) during the fully developed period. The effective fire duration, τ, is therefore defined as:

$$\tau = L/R \tag{2.2}$$

where: R is the rate of burning.

The duration of the fully developed phase of the fire was found to be $\tau/2$, beginning when the fuel mass had dropped to 80% of its original value and ending at 30%.

2.1.6 Ventilation

The shape and size of the openings can influence the heating rate and maximum temperatures realised inside the compartment, the height of the opening being important to allow the input of cool air at the bottom of the window whilst allowing hot gases to escape at the top. Results of many experiments have shown that R was mainly controlled by the rate of flow of air which entered the compartment, being proportional to the air flow factor.

$$\text{Air flow factor} = A\sqrt{h} \tag{2.3}$$

where: A is the window area (m^2)

h is the window height (m)

For low air flows the ventilation effect can be described as below:

$$R = 0.1\ A\sqrt{h} \quad \text{(kg/s)} \tag{2.4}$$

For high air flows and when there are large window areas, the rate of burning depends upon the geometry of the fuel, A_{FUEL}, and occurs when $A\sqrt{h} / A_{FUEL}$ exceeds 0.07 to 0.08 $m^{1/2}$ giving:

$$R = 0.0062\ A_{FUEL} \tag{2.5}$$

2.1.7 Heat Transfer and Insulation

The rate of burning is also affected by the rate of heating received by the fuel and the insulation properties of the compartment materials. Consideration must be given to the characteristics of the wall lining and roof/ceiling materials. For example, with sheet steel walls heat is conducted away during the fire, with blockwood, however, heat is retained inside the compartment. The roof lining material can also disintegrate allowing dissipation of heat.

As the insulation of the compartment is increased, a rise in the rate of burning occurs since raising the temperature of the compartment increases the rate of decomposition. However, the rate of decomposition can affect the rate of heat transfer. Heat transfer within a compartment depends upon the heat balance. The total amount of heat is dependent upon the supply of fuel and the air flow which is constant for a given window opening. If there is excess fuel some will not burn and will take up heat reducing the thermal feedback to the fuel. Therefore the heat transfer rate within a compartment decreases as the fuel flow increases in relation to the air flow.

2.1.8 Heat Balance

Experiments have shown that the heat balance varies with $A\sqrt{h}$ for small values of $A\sqrt{h}$, where R is ventilation controlled, and with L for high values of $A\sqrt{h}$, where R is not ventilation controlled. From results of experiments exploring the results of different values of $A\sqrt{h}$ and L it was found that for ventilation controlled fires R was not simply proportional to $A\sqrt{h}$ but also dependent on A_t and the ratio D/W, see Figure 2.1:

$$\frac{R\sqrt{(D/W)}}{A\sqrt{h}} = f\left[\frac{(A_t - A)}{A\sqrt{h}}\right] \qquad (\mathrm{kg.m.}^{-5/2}.\mathrm{s}^{-1}) \qquad (2.6)$$

where: A_t is the area of planes enclosing the compartment, (walls, ceilings, and floors)

D is the depth of the compartment,

W is the width of the compartment.

For design purposes the following equation has been derived:

$$R = 0.18\, A \sqrt{h} \sqrt{(W/D)}(1 - \exp(-0.036\eta)) \qquad (2.7)$$

where: $\eta = (A_t)/A\sqrt{h}$

2.1.9 Fire Temperature

Early experiments showed that the compartment temperature depended on the fire load and increased with the air flow factor $A\sqrt{h}$ to a steady value. Since the outflow of hot gases is proportional to $A\sqrt{h}$ and the area of the structural surfaces to which heat is lost is expressed by $(A_t - A)$, compartments will have a different heat balance for different values of A_t, A and h for a given fire load, thus producing variations in the fire temperature. Figure 2.2 shows the variation of temperature with $\eta = (A_t - A)/A\sqrt{h}$.

Maximum temperatures were obtained for $\eta = 12$. For low values of η (high values of $A\sqrt{h}$) the rate of burning was high as were the losses through the window. For high values of η (low values of $A\sqrt{h}$) the heat loss through the window was less, as was the rate of burning. For design purposes the maximum temperature, T_f, has been defined as follows:

$$\max T_f = \frac{6000\ (1 - \exp(-0.1\eta))}{\sqrt{\eta}} \qquad (^{\circ}C) \qquad (2.8)$$

Figure 2.1 Variation of rate of burning during fully developed period measured in experimental fires in compartments. (Law (1983a)).

Figure 2.2 Average temperature during fully developed period measured in experimental fires in compartments. (Law (1983a))

However, the temperature attained depends on fire load as well as ventilation and compartment size (see Figures 2.3 and 2.4). Therefore for low fire loads this maximum T_f value may not be reached and so the temperatures are modified as follows:

$$T_f = \max T_f \, (1 - \exp(-0.05\gamma)) \qquad (^oC) \qquad (2.9)$$

where: $\gamma = \dfrac{L}{\sqrt{(A(A_t - A))}}$

2.1.10 Standard Fire

The International Organization of Standardization has defined in ISO 834 the standardized temperature-time relation in the standard fire test which is used by the national building codes of most countries, and has been adopted by British Standard BS476:Parts 20, 21 and 22:1985. The standard fire exposure is defined as:

$$T - T_o = 345 \log_{10}(8t + 1) \qquad (2.10)$$

where: t is the time (min),

T is the furnace temperature (^oC) at time t,

T_o is the initial furnace temperature.

Laboratory tests to determine fire resistance of building elements are conducted in furnaces following this relationship, where the temperature of the thermocouples adjacent to the exposed surface of the element follow the standard curve as shown in Figure 2.5. Figure 2.3 shows the standard curve imposed on some actual fire measurements.

Aston University

Illustration removed for copyright restrictions

Figure 2.3 Average temperature development with wood cribs in fire tests. Note: 30(1/4) indicates fire load of 30 kg wood per m^2 floor area, window area a quarter of the wall in which the windows are situated. (FIP/CEB (1978))

Aston University

Illustration removed for copyright restrictions

Figure 2.4 Temperature development in a compartment with different ventilation. Fire load q = 500 MJ/m^2 (wood cribs). (FIP/CEB (1978))

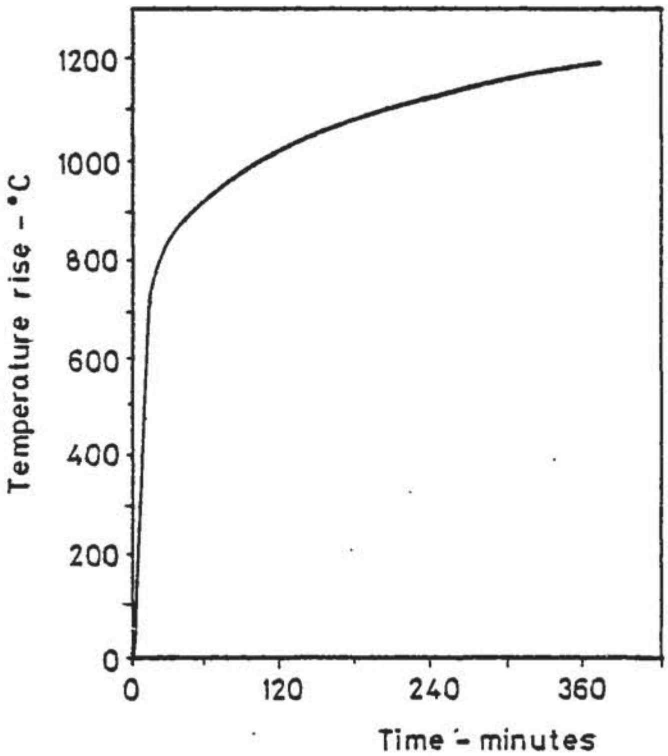

Figure 2.5 Standard time–temperature curve (BS476: Parts 20, 21 and 22)

$T = 345 \log_{10} (8t + 1)$

T = Temperature rise in °C

t = Time in minutes

It was previously mentioned that the fire resistance requirements are expressed for periods ranging from 30 minutes to 240 minutes. However, these periods do not signify the duration of an actual fire. A resistance of 60 minutes does not imply that a construction is expected to withstand a fire of 60 minutes duration, but will withstand a fire of a shorter duration whose severity corresponds to the 60 minute furnance test. The standard curve is useful for comparing actual fires. The equivalent standard fire duration, t_{eq}, is that time in the standard test which causes the same maximum effects in a structural element as the actual fire considered. The concept of equivalent severity first envisaged by Ingberg (1921) is now generally to be held untrue.

2.1.11 Real Fires

Law (1983) lists some of the uncertainties in real fires which are not taken into account in the compartment fire model, which should not be forgotten by the engineer when applying a design method:

(i) the time taken to reach full development may be much longer,

(ii) the temperature distribution is not likely to be uniform,

(iii) the fire brigade tackles the fire before all of the fuel is consumed, and

(iv) the actual fire may not behave like wood.

Information available on real building fires is mainly statistical. This information includes an assessment of fire duration and area damaged by fire.

In large buildings fires are progressive and tend to grow exponentially:

$$A_F = A_o \exp(\alpha t) \tag{2.11}$$

where: A_F is the floor area,

A_o is the floor area originally ignited,

α is fire growth parameter.

Fire doubling time has been suggested as little as 4 minutes (α = 0.0029 s^{-1}) which means that if the fire is not tackled early enough it may become uncontrollable and inextinguishable, burning until all of the fuel is exhausted.

Due to the progressive nature of real fires and the cooling effect of hoses, which prolongs burning time, a real fire may be considerably larger than a compartment fire. However, since the cooling effect is beneficial to the structure, designs based on compartment fires will tend to be on the conservative side.

Studies of industrial fires with various types of fuel have indicated that the wood cribs used in experimental fires give a realistic heat output per unit fire area and are representative of the conditions likely to occur in a real fire, except for petrochemical or similar fires for example the recent fire in Littleborough Tunnel (December 1984) where temperatures of around 4500^{o}C were reached.

2.1.12 Fire Grading

The major purpose for studying the fully developed fire is to be able to determine the appropriate fire grading for structural elements as determined by the fire resistance test. Both fire temperature and fire duration effect the structural behaviour of the building element. A relationship for fire grading, t_f, in terms of fire load per unit area is as follows:

$$t_f = k_1 L / A_f \tag{2.12}$$

where: t_f is the fire grading measured in minutes

k_1 is a constant of order unity.

A better relationship is for fire grading in terms of fire load per unit window area:

$$t_f = k_2 L / A \tag{2.13}$$

where: k_2 is a constant depending on the geometry of the compartment.

The compartment geometry can be accounted for as follows:

$$t_f = \frac{k_3 L}{\sqrt{(A(A_t - A))}} \tag{2.14}$$

where: k_3 is a constant of order unity.

2.2 COLUMN TESTING

2.2.1 Standard Furnace Tests

The performance of structural elements are determined in furnace tests where the element is subjected to a standard exposure condition following the procedure laid down in BS476:Part 8:1972 and summarized well in Fire Resistance of Concrete Structures (1975). The fire resistance of the structural element is the time during which it continues to perform its function satisfactorily during the laboratory test. Furnace tests have been used to obtain relationships between performance and a number of design factors and it is the data from these exercises that form the basis of the information contained in CP110 and in the schedules and tables attached to regulations and by-laws.

The present concept of conducting tests to determine fire resistance in the UK dates back to when the British Fire Prevention Committee (BFPC) under Edwin Sachs, carried out investigations in specially built apparatus at Regents Park during the early 1900's. The BFPC were also responsible for the first International Congress (London, 1903) when a standard time-temperature relationship was first proposed. Based largely on this work and research in the United States, Germany and Sweden, the British Standard on fire tests 1932 (BS476) defining tests for fire resistance was published. Most countries engaged in fire testing have standards for this purpose and over the last few years the major research organizations have collaborated through the International Organization of Standardization to introduce an international specification for conducting fire resistance tests, ISO 834.

The latest British Standard (BS476:Parts 20, 21 and 22:1985) is based on the ISO specifications but contains some additional features.

The heating conditions to which the constructions are exposed during the furnace tests are represented by the standard time-temperature curve shown in Figure 2.5 and represented by the formula:

$$T - T_o = 345\log_{10}(8t + 1)$$

It is important to note that the actual surface temperature of the structural element will be less than T, especially during the early stages of the heating, the difference being dependant on the geometry of the specimen and the characteristics of the furnace. The standard requires the test specimens to be realistic prototypes of the construction to be used in practice and should be full size, or for columns not less than 3m, and should be subjected to a loading that produces stresses of a similar nature and magnitude that would occur in the construction of which the test specimen is a part, i.e. the maximum design load. The standard also requires the specimen to be supported or restrained at the ends as they would be in service. The load is kept constant during the course of the test, i.e. the columns are allowed to expand due to the effects of heating.

The performance of the columns are judged on the basis of stability, integrity and insulation which are defined in BS476:Part 8:1972 as:

stability: the resistance to collapse and excessive deformation,

integrity: the resistance of passage of flames and hot gases,

insulation: the restriction of excessive transfer of heat from one side to another.

Columns are expected to resist collapse during the heating phase and the cooling down phase, identified as 24 hours after heating. The fire resistance of the structural element is expressed as the duration in minutes for which the appropriate criteria are satisfied.

Since fire tests cannot be carried out on complete buildings the fire test data on single elements are related to the behaviour of the building and in order to do this simplifications are made. An important way in which the behaviour of elements in buildings is critically different from the furnace tests concerns the boundary conditions. The intentions of the standards is to reproduce the real-life boundary conditions, but a simplified arrangement is employed where there is no restraint or nearly full restraint, however, if the load remains constant by allowing the column to expand there cannot possibly be full restraint, in any case neither condition is likely to exist and during the course of a real fire the boundary conditions can change.

Over the last few years research has been undertaken in the USA, Germany and the UK to study the effect of restraint at the end of floors and beams, the most comprehensive being conducted by the PCA in Chicago. However, no such work has been undertaken on columns. Restraint provided by continuity or end fixity can substantially improve the performance by applying a rotational restraint against the deformation due to the fire.

2.2.2 Column Testing and Simple Behaviour Prediction

The major work done on column testing has been by Thomas and Webster (1953) in England and Seekamp, Becker and Struck (1964) in Germany, both giving similar results. There was also some early work done in America by Hull (1918, 1919, 1920) and Ingberg et al (1921).

Thomas and Webster's programme of research was carried out according to the recommendations of the then current BS476, although the applied load was varied since it was required to ascertain the effect of the magnitude of the loading on the fire endurance.

The fire endurance increased appreciably for smaller test loads and the fire endurance also increased with higher concrete strength. The age of the column at test (after 7 months) had no significant effect on the results. Spalling of the arises of the columns was more marked in the larger columns.

When spalling reached a stage such that the reinforcing bars were directly exposed to the hot furnace gases, loss in strength of the bars was rapid, which could suggest that the use of high proportions of longitudinal reinforcement may be disadvantageous in fire exposed conditions. However, experimental data did not support this view since the strength of the reinforcing remained satisfactory as long as the cover remained intact. Since spalling was more pronounced at the corners of the column, due to heating from two sides, cover remained intact for longer periods of time at the sides, hence the proportion of strength left in the reinforcement depended on position of the reinforcement. Light mesh reinforcement in the concrete cover was found to substantially decrease the incidence of spalling thus increase the fire resistance considerably.

Thomas and Webster expressed the load bearing capacity of a column at any time as the sum of the strength contributions of the concrete and its reinforcement:

$$P_t = \sum f_c(T_c)\delta A_c + f_s(T_s)A_s \tag{2.15}$$

where: P_t is the total load that can be supported at time t,

δA_c is a small area of concrete cross-section,

T_c is the average temperature in element δA_c at time t,

$f_c(T_c)$ is the concrete effective strength at temperature T_c and at time t,

A_s is the cross sectional area of the steel,

T_s is the average temperature of the steel at time t,

$f_s(T_s)$ is the effective steel strength at time t.

For normal temperature conditions the ultimate strength of the reinforced concrete column was assumed by Thomas and Webster to be given approximately by:

$$P_u = 0.65f_{cu}A_c + f_yA_s \tag{2.16}$$

where: f_{cu} is the concrete cube strength,

f_y is the steel yield strength,

A_c is the cross sectional area of the concrete.

(Note, a slightly different formulation is given by the current reinforced concrete design code.)

It was considered that the effects of fire on the column could be allowed for by:

$$P_u = \alpha_t(0.65f_{cu}A_c) + \beta_t f_yA_s \tag{2.17}$$

where: α_t and β_t are constants allowing for the time of exposure.

Equating equations (2.15) and (2.17) gives expressions for α_t and β_t:

$$\alpha_t = \frac{1}{0.65f_{cu}} \cdot \sum f_c(T_c) \frac{\delta A_c}{A_c} \tag{2.18}$$

$$\beta_t = \frac{f_s(T_s)}{f_y} \tag{2.19}$$

Two approaches were pursued to obtain data on the expressions for α_t and β_t:

(i) A comprehensive series of tests on reinforced concrete columns varying the percentages of reinforcement to establish empirical values of α_t and β_t from equation (2.17) as a function of (a) time of fire exposure, (b) dimension of column and (c) the properties of concrete and steel.

(ii) Small scale tests on the concrete and steel materials to determine the functions $f_c(T_c)$ and $f_s(T_s)$, and also to determine the temperature distributions across the column cross section at various times during a standard fire test for various sizes of columns.

The test data were unsuitable for the empirical determination of both α_t and β_t, so β_t was estimated for the effect of temperature on the yield strength of steel from Lea (1920) and the measured steel temperature of the column. The relationship between β_t and the time of fire exposure can be determined from Figure 2.6.

Having obtained values for β_t, empirical values of α_t are determined from equation (2.17). Thomas and Webster sketched some curves to show the relationship between α_t and the time of exposure (Figure 2.7) and also gave an approximate indication of the relation between α_t, the column size and the time of exposure to the fire test

Aston University

Illustration removed for copyright restrictions

Figure 2.6 Yield strength of the reinforcement of columns during a fire test.
(Thomas and Webster (1953))

Aston University

Illustration removed for copyright restrictions

Figure 2.7 The effective strength of the concrete in columns during a fire test.
(Thomas and Webster (1953)).

(Figure 2.8). A comparison was made between the estimated load bearing capacity of the column at time of collapse and the actual applied test load, and between the estimated endurance period corresponding to the applied load and the actual endurance period. However, agreement was poor due to the effects of spalling on the reinforcement cover at various positions on the surface of the column. To allow for the different strengths of the side reinforcing and corner reinforcing during the fire, equation (2.17) was modified:

$$P_t = \alpha_t(0.65f_{cu}A_c) + \beta_t f_y A_{s1} + \beta_t' f_y A_{s2} \tag{2.20}$$

where: A_{s1} is the cross sectional area of the corner bars,

A_{s2} is the cross sectional area of the side bars,

β_t is the reduction constant for the corner bars,

β_t' is the reduction constant for the side bars.

Reasonable agreement was obtained using equation (2.20).

Thomas and Webster's attempt to predict test behaviour from small scale material tests were found to have little correlation with the experimental results. The main reason for this are given in Purkiss (1972):

(i) No account was taken of loading to a strain greater than that corresponding to the peak stress, ie. descending branch behaviour of the stress-strain curve of the concrete, causing a redistribution of stress, was ignored.

(ii) No account was taken of compatability of strain due to temperature and loading (ie. a total strain model such as that employed by Thelandersson was not employed).

(iii) The variation in peak stress was taken to be independent of any form of preloading.

(iv) Transient effects were also not considered.

Clarke (1960) carried out a very similar analysis to Thomas and Webster (1953) and suffered the same disadvantages. He also indicated the importance of cover and the value of column renderings such as plaster in reducing the effects of fire. This early work by Thomas and Webster (1953), Seekamp, Becker and Struck (1964), Clarke (1960), Hull (1918, 1919,1920) and Inberg et al (1921) provided the necessary information for design codes to be laid down, indeed the relevant sections on fire resistance of columns in CP110 is largely based on Thomas and Webster (1953).

Lie and Allen (1972) suggested a method of calculation for the fire resistance of concrete columns from the consideration of concrete type, cover thickness, section size, eccentricity of load, equivalent buckling length, percentage of steel, cover thickness to the steel and load intensity. The strength of the column at any time during the fire was calculated by dividing the cross section into discrete elements and using values of the temperature dependent material properties combined with the temperature distribution in the column cross section. The temperature distribution was calculated using a numerical method described in Lie and Harmathy (1972) assuming that the columns were exposed on all sides to a heat whose temperature course corresponded to the standard time-temperature curve. Typical temperature distributions of a column section are shown in Figure 2.9. Creep was neglected in the analysis as it was assumed to have only secondary effects and transient strains were not considered. Spalling also was not included since it was considered that it rarely occurred

Figure 2.8 Tentative relationships between the values of α_t and the time of exposure to fire, for various column sizes. (Thomas and Webster (1953)).

Figure 2.9 Temperature distribution along the centreline of column section for three types of concrete during exposure to standard fire, column size: 150 × 150 mm, exposure time: 1 hour (Lie and Allen (1972)).

in cover less than 40mm and in cover greater than 40mm serious spalling was prevented by the inclusion of a wire mesh in the protection.

This analysis is set out in some detail for a pin ended column subject to a constant load eccentrically applied.

Integrating over the column cross section the strength, or the total load bearing capacity, of a short column, is determined from:

Axial load: $P_t = \sum \Delta_j^2 f_{c,j} + \sum A_s f_y$ (2.21)

Bending moment: $M = \sum u_j \Delta_j^2 f_{c,j} + \sum u_s A_s f_y$ (2.22)

where: $f_{c,j}$ is the temperature dependent concrete compressive strength of concrete element j,

f_y is the temperature dependent yield strength,

Δ_j is the width of the square element,

u_j is the distance from the centroid of cross section to the centre of concrete element j,

u_s is the distance from the centroid of cross section to the centre of steel bar,

A_s is the area of steel.

The strength of slender columns is governed by the Euler buckling load, P_c:

$$P_c = \pi^2 EI/(kL)^2 \tag{2.23}$$

where: L is the column length,

kL is the equivalent length of a pin ended column, (value of k depends on end conditions)

EI is the stiffness of the cross section and is the sum of the stiffness of the steel and concrete.

i.e. $EI = E_sI_s + C_cE_cI_c$ (2.24)

where: I_s is the second moment of area for steel,

I_c is the second moment of area for concrete,

E_s is the temperature dependent modulus of elasticity for steel,

E_c is the temperature dependent modulus of elasticity for concrete,

C_c is a factor which takes into account cracking of the section.

$$C_c = 0.2 + P_u/P_a \leqslant 0.7 \quad (2.25)$$

where: P_u is the load at failure,

P_a is the axial strength of the cross section.

Integrating over the cross section gives:

$$E_cI_c = \sum E_{cj}(u_j^2\Delta_j^2 + \Delta_j^4/12) \quad (2.26)$$

$$E_sI_s = 4E_s(u_s^2A_s) \quad (2.27)$$

The initial eccentricity at mid height of a slender column under vertical eccentric loading is increased by a factor:

$$\alpha = 1/(1 - P/P_c) \quad (2.28)$$

where: P is the applied load

P_c is the Euler load from equation (2.23)

Failure of the column is assumed to occur when the load and moment corrected by factor α reach the section capacity, P_u and M_u. Since columns in buildings are subject to different eccentricities at the top and bottom, the eccentricities are modified using a factor C_m:

$$C_m = 0.6 + 0.4M_1/M_2 \geqslant 0.4 \qquad (2.29)$$

where: M_1 and M_2 are end moments, $M_1 > M_2$

Therefore the strength of slender columns is determined in the same way as short columns, only the eccentricity due to applied loads is increased by $C_m/(1 - P_u/P_c)$.

Results from this analysis were compared with the results of some German tests by Becker and Stanke (1970) carried out on columns under constant concentric load (eccentricity assumed to be 2.5mm). The analysis gave a conservative estimation of the fire resistance. The theory for eccentrically loaded columns was not checked due to the lack of suitable fire tests, however, calculations indicated a serious decrease in fire resistance with higher eccentricities.

Thomas and Webster (1953), Clarke (1960) and Lie and Allen (1972) all fail to solve the problem satisfactorily since they are based on basic equations for room temperature conditions that do not necessarily hold at elevated temperatures. The main drawbacks with Lie and Allen's method are the limited model for slenderness, failure to model additional moments as the column deflects, and failure to model structural interaction and material behaviour. The assumptions made in the analysis will hold for axially loaded members giving a conservative answer, but will not hold for any analysis made on eccentrically loaded members, the main reasons having been given by Purkiss (1972) on Thomas and Webster (1953).

Haksever and Haβ (1982) carried out fire tests on axially loaded ınd eccentrically loaded reinforced concrete columns exposed to a ıtandard fire, heated on all four sides. It was found that the fire ·esistance period of eccentrically loaded columns is significantly .ower than those for axially loaded columns. The fire resistance was 'ound to decrease by values up to as much as 50%.

The fire tests desribed so far have all been carried out .ccording to the conditions in the standard fire test. These tests ıroduce little information about what might happen in a real fire ınce it is not possible in a standard test to reproduce all the ıossible exposure conditions that might occur in a real fire. The estraint of the structure will change the thermal loading induced by hermal incompatabilities during testing. The effect and extent of palling may also change the mode of failure.

The results from the standard tests can only give a quantitative omparison of the behaviour of construction elements exposed to fire. t is generally agreed that unrestrained tests give a lower bound olution for a column under normal restraint. In order for the ehaviour of different forms of construction to be compared it is most mportant that individual elements should be tested under the onditions likely to be experienced by the element when a member in a tructure. This is recognised by the standard, however, it also tates that applied loading shall be kept constant which means the ffects of continuity are ignored and the structural component is ested as though it were unrestrained in service.

All the column tests described to date have been on axially loaded columns exposed to heat on all four sides. A recent paper by Haksever and Anderberg (1982) in Sweden deals with the qualitative verification of the structural behaviour of some reinforced concrete columns which involved the testing of columns exposed to fire on three sides, subject to eccentric loading. The support conditions were pin ends. Typical results are shown in Table 2.1. Results have indicated that moments applied in the same direction as the thermal gradient across the section decrease the fire resistance of the column, when compared to that corresponding to an axial load only, whereas moments applied against the thermal gradient increase the fire resistance.

TABLE 2.1 Tested and Calculated data (Haksever and Anderberg (1982))

Column	Load (MN)	Eccentricity (mm)	Fire Resistance (min)	
			Tested	Calculated
SL1	0.90	00.0	52	65
SL2	0.60	+60.0*	30+	55
SL3	0.30	-60.0**	120	120

* Eccentricity towards the furnace.

** Eccentricity away from the furnace.

\+ This is not a true result due to a support failure at a half hour, the likely fire resistance should be larger.

Note the fire resistance times above may be misleading since the columns were tested at loads significantly lower than the design loads. It is estimated that column SL1 was tested with a load ratio 2/3 the design load and column SL3 with a ratio of 1/5. Also high values of concrete cover to main reinforcement was employed.

2.3 STRUCTURAL RESPONSE

Very few fire tests have been performed on structural elements, either slabs, beams or columns, that model realistic structural conditions of restraint and continuity. The magnitude of restraint on a test specimen will have a considerable effect on the results of a fire test and it would appear that there exists an optimum restraint at which the specimen properties are enhanced to a maximum as suggested by Dougill (1972b) and the PCA.

In order to obtain realistic structural conditions for beams and slabs it is necessary to model continuity over the supports. This can be done by replacing the continuity by deformation induced loads and moments or by testing real continuous structures. In some tests beams have been cantilevered beyond the furnace and the cantilever is loaded together with the heated span, however, this only induces constant moments and therefore will not allow the redistribution of moments to occur which will happen in a real fire, thus reducing the fire resistance period.

The PCA (Carlson et al (1961), and Selvaggio and Carlson (1962, 1967)) model restraint and continuity by using the conditions of an allowed value of free expansion followed by complete restraint by the prohibition of both longitudinal extension and angular rotation over the supports. The PCA (Issen, Gustaferro and Carlson (1970)) take the maximum value of thermal thrust induced during the test as a measure of the restraint. However, in a structure there is a stage of elastic deformation (linear restraint) followed by non-linear deformation due to changes in material properties and the stress-strain curve, see Figure 2.10.

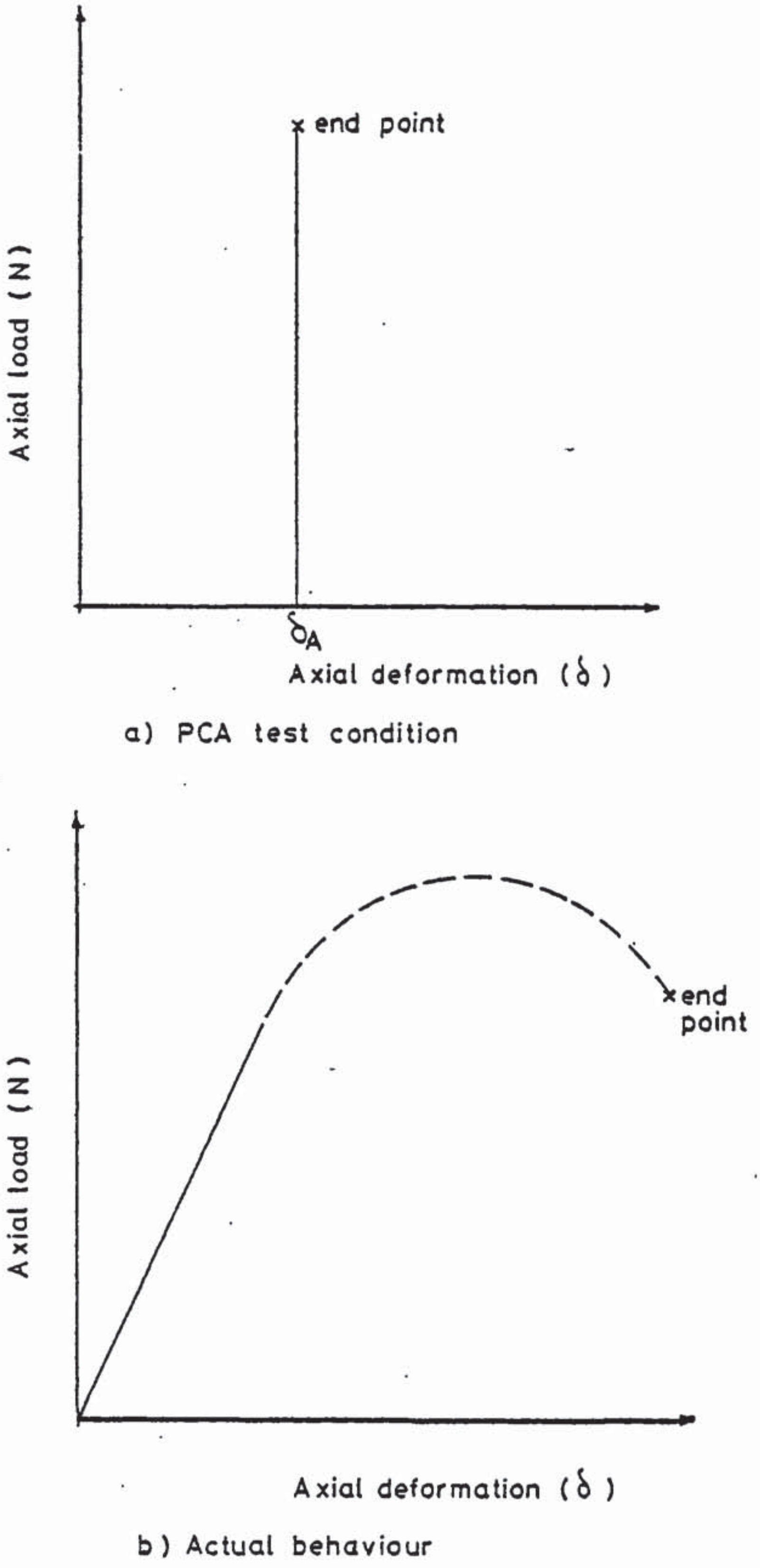

Figure 2.10 Comparison between the PCA test condition and the behaviour in a fire. (Purkiss (1972))

Both the cantilever method and the PCA approach are unsatisfactory. Bletzacker (1966) perfomed tests on protected steel beam floor assemblies and suggested an alternative measure of restraint, the sum of the absolute values of the moment due to thermal rotation and the moment due to thermal thrust acting on the specimen. None of these measures are satisfactory measures of restraint. Dougill (1972a, 1972b) suggests axial restraint and rotational restraint should be considered independently and not in a combined parameter.

Dougill (1966) described the importance of restraint on the mode of failure of columns and gave an analysis to show the effects of restraint on the type of failure incurred by a column during a fire test with restraint. The analysis deals with a single heated column in the building frame shown in Figure 2.11 subject to local heating. It is assumed that the surrounding structure is unaffected by heating. When the column is subject to a local fire the thermal expansion of the column is resisted by the axial restraint supplied by the surrounding structure inducing an additional load in the column. The restraint to the column is mainly due to the stiffness of the beams and floors and hence increases with the number of floors, N_{fl}, above. The magnitude of the induced load for a typical column can be seen from Figure 2.12.

Considering the column to be isolated from the frame, the initial shortening, δ_o, under load, P_o, is given by:

$$\delta_o = P_o/K_c \tag{2.30}$$

where: K_c is the column stiffness.

Figure 2.11 Structural arrangement of building frame and heated column. (Dougill (1966)).

Figure 2.12 Loads induced in a restrained reinforced concrete column heated according to the standard exposure condition. (Dougill (1966).

Applying results on stress-strain curves, the displacement δ is a function of load P and temperature T:

$$\delta = \delta(P,T) \tag{2.31}$$

The thermal strain in the column is given by:

$$\alpha LT \tag{2.32}$$

where: αT is the strain,

L is the column length.

Therefore the total deformation Δ at time T is given by:

$$\Delta = \alpha LT + \delta_o - \delta(P,T) \tag{2.33}$$

The structure is assumed to behave linearly with respect to the load applied, hence:

$$\Delta = \frac{P - P_o}{N_{fl}K_s} \tag{2.34}$$

where: N_{fl} is the number of floors,

K_s is the structural stiffness per floor.

In equating values of Δ from equations (2.33) and (2.34) the following is obtained:

$$\frac{\delta(P,T)}{\delta_o} + \frac{1}{R} \cdot \frac{P}{P_o} = (1 + 1/R) + \frac{\alpha LT}{\delta_o} \tag{2.35}$$

where: $R = N_{fl}K_s/K_c$ the relative stiffness of the surrounding structure i.e. a measure of the restraint afforded to the column from the surrounding structure.

The range of relative stiffness for flexible, hard and intermediate structures is shown in Figure 2.13. Dougill (1966) describes how in a flexible structure there is insufficient stiffness relative to the column stiffness to enable the column specimen to reach its ultimate strain when heated, and that it will eventually fail, when the total load on the column is approximately equal to its maximum load capacity, by the same mechanism of longitudinal instability as do unrestrained columns in the standard fire test. Conversely the load at failure on a column in a stiff structure will be small since the surrounding structure will relieve much of its load. Limiting strain is the criterion for ultimate collapse and as the relative stiffness, R, is increased the thermal strain at failure must increase. Since strain is a measure of temperature and exposure time the fire resistance of a column in a stiff structure will be greater than that for a similar column in a flexible structure.

In a later paper Dougill (1972a) has shown that instabilities can occur in panels made of concrete, a strain softening material (descending branch behaviour of stress-strain curve), during heating to high temperatures. The instabilities correspond to a mode of failure termed general or destructive spalling, the occurrence of which depends considerably upon the boundary conditions of the loading and the restraint applied to the panel.

In a following paper Dougill (1972b) demonstrated the role of loading and restraint on the occurrence of general spalling. For slender panels with full flexural restraint and no axial load, the heavy flexural restraint leads to the development of tensile stresses across the section and an early loss of stiffness due to cracking resulting in progressive failure. With the presence of an axial load the development of cracking can be delayed or inhibited. With high axial loads the section is always in compression and instability occurs as a result of the section being loaded beyond the peak stress, the time to failure being greater than that for the zero axial load condition.

Dougill (1972b) demonstrated the time to failure, or fire resistance, can be still further increased for full flexural restraint with intermediate axial loads since the occurrence of tensile stress leads to some tensile cracking, the onset of which is beneficial as it allows the section to unload and so avoid the conditions for instability, see Figure 2.14. The parameter β that appears in Figures 2.14 to 2.16 describes the form of the descending branch of the stress-strain relation and K_m is the axial restraint parameter as defined in Dougill (1972b).

The effects of various degrees of flexural restraint for a slender column are shown in Figure 2.15. Cracking occurs in the panel with zero restraint which postpones the onset of instability. For small values of applied restraint the extent of cracking is reduced which reduces the time of exposure to instability, however, with higher values of applied restraint the section remains in compression which increases the time of exposure to induce failure.

Since the occurrence of instability depends on the effect of cracking, different loadings and panel thickness effect the results. Dougill (1972b) demonstrated that applied flexural restraint would always be beneficial for thick panels since extent of cracking is less pronounced because induced tensile stresses are small as a result of a smaller proportion of the panel thickness being subjected to the effects of heating.

Figure 2.13 Limiting values of relative stiffness for different modes of structural behaviour. (Dougill (1966)).

Figure 2.14 The effect of axial load on the behaviour of panels heated under full flexural restraint with $\beta = 1$. (Dougill (1972)).

Panels subject to high axial restraint tend to fail in a flexural mode with a sudden increase in curvature. Because the curvature is prevented failure can only occur with tensile breakdown since longitudinal instability cannot occur due to the increased axial stiffness as a result of the restraining system.

Dougill (1972b) also demonstrated the effect of strain softening on the performance of flexurally restrained panels, see Figure 2.16.

2.4 COMPUTER MODELLING

Fire testing suffers a number of disadvantages. The test is cumbersome, expensive, requires large specialist apparatus and fails to model satisfactorily the structural restraint and continuity likely to be experienced in a real fire. More realistic conditions corresponding to columns in continuous structures can now be studied by computer calculation using calculations based on heat transfer and the structural properties of materials at high temperatures.

Allen and Lie (1974) studied the problems for square reinforced concrete columns using computer calculations that take into account the problems of restraint, the interaction of the column with the surrounding structure during the fire and fire curves that take into account fire load. When a column is exposed to a fire it expands. This expansion is resisted by the surrounding structure increasing the load on the column. Tendency to failure is relieved due to shortening of the column as a result of the material increased ductility at high strains and temperatures, and the fact that the column can buckle sideways, enhanced by the reduced stiffness, thus shortening the chord length, the length between column ends.

Figure 2.15 Expansion of panels heated under different degrees of flexural restraint and constant axial load of 11 N/mm^2 and with $\beta = 3$. (Dougill (1972)) .

Figure 2.16 The effect of strain softening upon the performance of flexurally restrained panels . (Dougill (1972)) .

The correct solution to the problem of interaction requires an iterative determination of the moments, curvatures and displacements along the column for each time interval considered. However, Allen and Lie (1974) carried out an approximate solution based on load deflection analysis.

The lateral deflection is calculated from the assumption that the column is fixed at both ends, and the curvature diagram varies linearly from mid-height to both supports, the curvature at mid-height and at the supports being equal and opposite as shown in Figure 2.17. The assumption is approximately correct as the column approaches failure with inelastic strains in the critical sections, but is considerably in error for elastic conditions during the early stages of the fire.

The chord shortening is calculated as a function of the curvature at the critical sections which is determined from the bending strains under eccentric load. Initial eccentricity is assumed to be 0.1t $\geqslant$ 25 mm (where t is the dimension of the column) but is reduced for increased column flexibility. The eccentricity is corrected and the bending strains and deflections recalculated if the lateral deflection at mid-height exceeds the assumed eccentricity. Axial and bending strains are determined iteratively to satisfy equilibrium. The column is said to have failed when convergence is very slow.

Allen and Lie's (1974) approximate numerical study of column-structure interaction indicated an increase in fire resistance with increased stiffness of the surrounding structure and that the assumption of no restraint is generally conservative. The temperature distribution in the column cross section was determined using the numerical method employed in Lie and Allen (1972).

Lie (1983) uses an analysis based on that given in Allen and Lie (1974), however, the boundary conditions are substantially altered. The columns which are fixed at both ends are idealized as pin ended columns of length kL, see Figure 2.18. The load on the column is intended to be concentric, however, a small eccentricity of 2.5mm is assumed due to the imperfections of the column and the loading device. The curvature of the column varies linearly as shown in Figure 2.18, at the points of zero curvature there are end moments. Deflection, y, at mid-height can be given in terms of the curvature, ϕ:

$$y = \phi(kL)^2/12 \tag{2.36}$$

The axial strain is varied until the internal moment at the mid-section is in equilibrium with the applied moment for any given curvature, and hence deflection, where the applied moment is given by:

load x (deflection + eccentricity)

A similar approach has been employed in Lie et al (1984).

The first widely known computer program for analysing the structural response of reinforced concrete frames in a fire using finite element techniques was FIRES-RC by Becker and Bresler (1974), the Fire Response of Structures - Reinforced Concrete frames. A revised version of the program was presented by Iding et al in 1977 where a tangent stiffness solution approach replaced the secant stiffness approach used by Becker and Bresler (1974) and allowance was made for the linear variation of the moment along the axis of the beam element. Anderberg established a special version of FIRES-RC computer program in 1976 which included new material behaviour models developed at the Lund Institute of Technology in Sweden by Anderberg and Thelandersson (1976) and Anderberg (1976).

Aston University

Illustration removed for copyright restrictions

Figure 2.17 Assumed column configuration near failure. (Allen and Lie (1974)).

Aston University

Illustration removed for copyright restrictions

Figure 2.18 Load deflection analysis. (Lie (1983)).

The analysis used in FIRES-RC is based on the finite element method, the approach is a non-linear, direct stiffness formulation coupled with a time step integration. An iterative approach is used to find a deformed shape that results in equilibrium between the forces due to the external loads and internal stresses within given time steps.

The material behaviour models used in FIRES-RC (1974) for concrete and steel take account of the dimensional changes caused by temperature differentials and the changes in the materials temperature dependent mechanical properties with changes in temperature. Degradation of the section by cracking and crushing, and increased rates of shrinkage and creep with increased temperatures, are also taken account of, but no account is taken of the effect of preload on the stress-strain curve. The non-linear stress-strain laws used to model the behaviour of concrete and steel take account of inelastic deformations associated with unloading. Degradation of stiffness in the structural frame as a result of exposure to fire leads to an increase in deformation which can result in the development of large secondary forces and moments, leading to instability and failure. This is more of a problem with slender columns than short columns.

Neither of the computer programs reported above took account of geometrical non-linearities. Geometrical non-linearities, as well as geometric effects, were first considered by Haksever (1977) in analysing fire exposed slender L-frames. Pin ends were taken on the L-frames so there is only a limited model of restraint. Forsén (1982) considered geometrical non- linearities and material behaviour models developed at the Lund Institute of Technology in the Finite Element program CONFIRE.

The computer program CONFIRE is developed from the computer program CONFRAME by Åldstedt (1975) and employs a beam element with three degrees of freedom at each node and one internal axial degree of freedom, where the total strain is taken as linear over the cross section. Time dependent stresses, strains and structural displacements are obtained step by step by use of the Newton-Raphson iteration method by solving the linearized incremental system equilibrium equation. Gaussian integration with fixed integration points is employed to obtain the linear element stiffness matrices and the element stress resultant vectors. The geometric element stiffness matrix is obtained using analytical integration.

Forsén (1982), in his computer program CONFIRE, uses an over simplified model of restraint where either full restraint is considered at the ends of the column or pin ends are considered, neither of which are likely to occur for a member within a real structure. However, Forsén does consider secondary effects, the additional moment that arises from the eccentricity of the axial force as the column deflects under load. Figure 2.19 shows the marked effect between including, or not including, second order effects in the calculation of the restraint forces in a reinforced concrete plate exposed to an ISO fire, using the computer program CONFIRE.

The computer programs FIRES-RC and CONFIRE are designed to be used in conjunction with a program that predicts the thermal response of the reinforced concrete frames such as FIRES-T or TASEF-2.

Figure 2.19 Predicted axial restraint forces in a reinforced concrete plate strip with different permissible expansions followed by complete restraint. (Forsén (1982))

FIRES-T, a computer program for the Fire Response of Structures-Thermal developed by Becker, Bizri and Bresler (1974), evaluates the temperature distribution history of structural cross sections in fire environments by solving the heat balance equation in matrix form using a finite element method coupled with a time step integration. The approach is based on the work of Wilson and Zienkiewicz and extended to the fire situation by Bizri (1973).

The problem is formulated in two dimensions through the assumption that no heat is flowing along the longitudinal axis of the stuctural member. Due to the temperature dependence of the thermal properties of structural materials and the heat transfer mechanisms associated with fire environments, the heat flow problem is non-linear. These non-linearities are handled by a local linearization about a current temperature distribution which requires the use of an iterative approach within the given time steps. The finite element mesh employed in FIRES-T can be made up of quadrilateral or triangular elements. Convective and radiative mechanisms are used to model the fire environment to which the structural member is exposed.

A revised version of FIRES-T, FIRES-T3, has also been developed by Iding, Bresler and Nizamuddin (1977) and allows a three dimensional solution to the heat flow problem.

TASEF-2, a computer program for the Temperature Analysis of Structures Exposed to Fire was developed by Wickström (1979). The concept is similar to FIRES-T, based on the finite element method where the Fourier heat balance equation is solved in matrix form for two dimensional field by the use of an explicit forward integration method.

Similarly the finite element mesh may employ quadrilateral or triangular elements and, an arbitrary external temperature time curve, which is defined by the user, simulates the fire exposure. However, TASEF-2 is sensitive to the choice of time increments which gives problems of over convergence as a result of Wickström employing a smaller computer memory core than that required by FIRES-T.

Bandyopadhyay (1975) developed a computer method for the elastic and inelastic analysis of two dimensional and three dimensional skeletal structures taking into account the effect of temperature stresses, creep and deterioration of material properties as a result of fire exposure. The program obtains an approximate temperature distribution in the member by assuming a mathematical curve and minimizing the error. It can predict the formation of a plastic hinge or hinges in an overstressed member as a result of an excessive bending moment and is capable of continuing the analysis after the hinges have formed, until the structure, or part of the structure, becomes a mechanism.

Although the program may not accurately predict the time and temperature at failure, it gives a clear indication of the mode of failure and the order of formation of plastic hinges. Bandyophyay's computer program recognises the fact that the formation of plastic hinges in a multistorey structure will effect the stiffness of the structure as a whole and thus will effect the restraint afforded to any structural member subject to the fire exposure. It is also noted that the section of the structure exposed to the fire may not necessarily contain the critical sections where plastic hinges form. Since no fire tests have actually been performed on a multistorey structure there is no way of confirming this result.

As far as it is known, of the available computer programs, only CONFIRE takes into consideration the additional moment that arises from the eccentricity of the axial force as the column deflects under load, which have been well demonstrated by researchers, such as Forsén, to considerably reduce the fire resistance period. Since Becker, Bresler et al, neglect to consider this additional induced stress as a result of the axial force eccentricity, failure of slender columns due to buckling mode are likely to occur earlier than that predicted by programs such as FIRES-RC. However, this will not effect short columns since they tend to fail by maximum stress criteria.

It is also questionable whether a satisfactory model of restraint has been employed in any of the available computer programs. Only a limited model of restraint is considered, either through the use of idealized linear springs, where the value of restraint is proportional to a spring of stiffness K, or through the use of the idealized condition of pinned and fixed restraint.

Cranston presented a paper in 1967 for the analysis of restrained columns and deals with all stages, from zero load up to and beyond maximum load, which takes account of the additional moment due to axial load eccentricity and the slenderness of the column. The column is divided into segments and the analysis is based on the cross sections at the division points between the segment lengths.

The analysis consists of determining successive solutions as the load on, or the deflection of, the column is increased in steps. A stage in the analysis comprises the finding of each seperate solution using an iterative procedure. Initial proposals are made for the deflected shape of the column and bending moments are computed for each division point. This satisfies equilibrium conditions.

Curvatures at each division point are computed using an iterative procedure where the cross sections are idealized into elements which are small enough for the stress in them to be assumed uniform. Strain profiles across the section are proposed which enable the calculation of values of axial load and bending moment. If these calculated values agree closely with the loading applied to the section the curvatures corresponding to the proposed strain profile are taken as correct. If not the strain profile is modified and the procedure repeated. This procedure automatically takes account of the influence of axial load on the moment-curvature relation.

When curvatures have been calculated for all division points the deflected shape is calculated and compared with that initially proposed. If agreement is close a valid solution has been obtained and compatability has been satisfied. If not the deflection proposals are modified and the whole procedure repeated.

With the introduction into the analysis by Cranston (1967) of material behaviour models of the type developed at the Lund Institute of Technology in Sweden, and used in conjunction with a program such as FIRES-T to evaluate the thermal response of a column, the analysis could be applied to the analysis of restrained reinforced concrete columns in a fire environment.

2.5 MATERIAL PROPERTIES

In order to understand the behaviour of load bearing structures under fire conditions and predict their performance by numerical methods it is necessary to have a knowledge of the relevant materials material properties. A knowledge of thermal properties is also important since they influence the rate of heat transfer into the construction.

Some of the physical and mechanical properties are influenced by the mode of testing. The classical method for the determination of strength is to gradually heat a material to a known temperature and apply an increasing load to failure. This procedure is then repeated for different temperatures to obtain the relationship between the material parameter and temperature.

However, this procedure bears little relation to the conditions likely to be encountered in actual fire conditions. The determination of material properties under transient conditions are a truer representation where the material is subject to a degree of preload and a transient type of heating regime. Malhotra (1982) has listed six different ways in which mechanical properties can be established, shown diagramatically in Figure 2.20.

2.5.1 Concrete

2.5.1.1 Density

Density of concrete depends primarily on the aggregate type. Concretes made with dense aggregates have a density range of 2 to 2.4 t/m^3 whereas concretes made with lightweight aggregates have a density range of 1 to 1.5 t/m^3.

Figure 2.20 Different testing regimes for determining mechanical properties. (Malhotra (1982))

Heating of the concrete drives away free moisture when the temperature exceeds 100°C but the effect on density is insignificant and it can be assumed constant for heating regimes up to 800°C when some aggregates begin to decompose.

2.5.1.2 Thermal Conductivity

The thermal conductivity of concrete depends upon the nature of the aggregate, porosity of the concrete and the moisture content for temperatures below 100°C. Harmathy (1970) investigated various concretes and obtained performance bands as shown in Figure 2.21. Thermal conductivity decreases with increasing temperature but during subsequent cooling the change is reversible. The thermal conductivity decreases slightly for dense aggregate concretes from about 1.25 W/m°C to 1.0 W/m°C at 800°C, but for lightweight aggregate concrete it remains constant around 0.3 W/m°C. Similar results have been found by other workers, however, actual values differ between investigators due to the variations in materials and experimental technique.

2.5.1.3 Specific Heat

Specific heat is the amount of heat required to raise the temperature of a unit mass of material by one degree. Harmathy's (1970) data on specific heat are compared with data from Collette (1976) and Odeen (1972) in Figure 2.22. For dense aggregate concretes specific heat increases from 0.8 KJ/kg°C to 1.2 and for lightweight aggregate and limestone concretes from 0.8 to 1.0 KJ/kg°C.

Aston University

Illustration removed for copyright restrictions

Figure 2.21 Effect of temperature on thermal conductivity of concrete. (Malhotra (1982))

Aston University

Illustration removed for copyright restrictions

Figure 2.22 Effect of temperature on specific heat of concrete. (Malhotra (1982))

2.5.1.4 Thermal Diffusivity

The thermal diffusivity can be expressed as:

$$\gamma = K/\rho C_p \qquad (m^2/h) \qquad (2.37)$$

where: γ is the thermal diffusivity,

K is the thermal conductivity (W/m^oC),

ρ is the density (kg/m^3),

C_p is the specific heat (J/kg^oC).

Figure 2.23 shows the relation between temperature and thermal diffusivity for dense and lightweight aggregate concretes. As temperature increases, thermal diffusivity decreases, i.e. the rate of heat transfer decreases, for dense concrete it decreases to virtually half its value at 700°C.

2.5.1.5 Thermal Deformation

A number of workers have attempted limited descriptions for concrete in compression subject to high temperature exposure, such as Becker and Bresler (1974) and Anderberg, Pettersson and Thelandersson (1978). The approach generally used is by an extension of procedures used at normal or only slightly elevated temperatures when cracking is insignificant and behaviour may be assumed to be linear.

In this way, a computer orientated constitutive model for concrete in compression applied at transient high temperatures was presented in Anderberg and Thelandersson (1976) based on the concept that the total strain, ε, can be separated into four components. This is also supported by the work of Schneider (1976).

The total strain is considered to be the sum of an instantaneous strain due to stress, the free thermal movement, creep and a correction term included to take account of the additional strain that occurs during temperature change.

$$\varepsilon = \varepsilon_{th}(T) + \varepsilon_{\sigma}(\bar{\sigma},\sigma,T) + \varepsilon_{cr}(\sigma,T,t) + \varepsilon_{tr}(\sigma,T) \qquad (2.38)$$

where: ε_{th} is the thermal strain, including shrinkage, measured in specimens under variable temperature,

ε_{σ} is the instantaneous, stress related strain, based on stress-strain relations obtained under constant stabilized temperature,

ε_{cr} is the creep strain or time dependent strain measured under constant stress and stabilized temperature,

ε_{tr} is the transient strain accounting for the effect of temperature increase under stress, derived from tests under constant stress and variable temperature,

σ is the stress,

$\bar{\sigma}$ is the stress history,

T is the temperature,

t is the time.

The importance of the strain components can be obtained from Figure 2.24, predominance of transient strain is obvious. As Dougill (1983) points out, although agreement with experimental results is good for the rates of heating used with small laboratory samples, there must be some uncertainty with models of this sort when used with the fast rates of heating that occur in concrete sections exposed to fire.

Figure 2.23 Effect of temperature on thermal diffusivity of concrete. (Malhotra (1982))

Figure 2.24 Different components of thermal strain. (Anderberg & Thelandersson (1976))

Another fundamental flaw is that this form of model appears to ignore degradation or micro-cracking as a major influence on the stress-strain law and has only been validated for stress levels where the concrete behaves in an almost linear elastic manner.

The deformation of concrete is dependent on a number of factors, including aggregate type, heating rate and the magnitude of the externally applied forces. Researchers such as Schneider (1976) have demonstrated the fact that an increase in applied load significantly decreases the total deformation of concrete. The effect of load on the nett deformation of siliceous (dense) concrete when heated at 5°C/min with varying loads from 0 to 67.5% is shown in Figure 2.25. Normal thermal expansion is represented by the zero curve. It can be seen that the effect of load reduces the expansion significantly. As the deformation curves become vertical, the deformation rates approach infinity and failure occurs.

2.5.1.6 Thermal Strain

Much work has been done on this subject by researchers including Harada (1949-53), Philleo (1958) and Zoldners (1960). The thermal strain during heating is a simple function of temperature, directly given by the thermal expansion curve. Since drying shrinkage is included, the thermal expansion depends on the initial moisture content and the rate of heating is not critical. It can be assumed that the thermal expansion is fully reversible, although it is not quite in reality since the shrinkage that occurs is irrecoverable. Figure 2.26 shows the thermal expansion of dense concrete.

Aston University

Illustration removed for copyright restrictions

Figure 2.25 Thermal strain under different loading conditions. (Malhotra (1982))

Aston University

Illustration removed for copyright restrictions

Figure 2.26 Thermal expansion of quartz aggregate concrete. (Anderberg (1976)).

Some early experiments by Cruz (1966) measuring the thermal expansion of concrete as the temperature is raised show that concretes can be divided into three groups depending on the aggregate used, see Figure 2.27. Cruz and Gillen (1980) investigated the thermal expansion of portland cement paste, mortar and concrete at high temperatures. Although the cement paste contracted when subjected to elevated temperatures, the thermal expansion of mortar and concrete was dominated by the thermal expansion of the mineral aggregate. Cruz and Gillen (1980) also present average values of the coefficient of expansion for the materials tested. A comparison of thermal strains for the materials tested is given in Figure 2.28.

2.5.1.7 Transient Strains

Transient strains are those strains that cannot otherwise be accounted for due to the physical breakdown of the cement paste. They occur under compressive stresses as the temperature increases, essentially permanent, irrecoverable and only occur under first heating. Transient strain is temperature dependent and independent of time. Figure 2.29 shows the effect of temperature on transient strain.

Anderberg and Thelandersson (1976) demonstrate that:

$$\varepsilon_{tr} = \sigma g(T)/\sigma_{max,o} \tag{2.39}$$

where: $g(T)$ is a function of temperature,

σ is the applied stress,

$\sigma_{max,o}$ is the compressive strength at ambient conditions.

Inspection shows that $g(T)$ is approximately proportional to ε_{th} i.e. the temperature dependence of transient strain is very similar to that of thermal strain.

Aston University

Illustration removed for copyright restrictions

Figure 2.27 Thermal expansion of concretes made with different aggregates. (Malhotra (1982))

Aston University

Illustration removed for copyright restrictions

Figure 2.28 Comparison of thermal strains. (Cruz & Gillen (1981))

Figure 2.29 The ratio $\varepsilon_{tr}/(\sigma/\sigma_{max,o})$ as a function of temperature. (Anderberg & Thelandersson(1976))

However, the model only holds for temperatures below 550°C due to the alpha-beta quartz phase change.

The Anderberg and Thelandersson model for transient strain appears to be the only computer orientated model available, the model also demonstrates reasonable agreement with data from Weigler and Fischer, and Schneider in Anderberg and Thelandersson (1976).

2.5.1.8 <u>Creep</u>

Cruz (1968) at the PCA was one of the first researchers to investigate the time dependent behaviour or creep behaviour of concrete at high temperatures. Typical results are shown in Figure 2.30. Cruz found that the creep strains at elevated temperatures are substantially higher than those at ambient conditions.

A large amount of data are available on the time dependent or creep behaviour of concrete under transient conditions in the temperature range 20°C to 150°C for example Bazant and Panula (1978). At this temperature regime it was originally thought that creep was a linear function of the applied stress and the notion of specific creep, creep/unit stress, was considered to be a valid model.

It is now considered that for applied stresses greater than 0.3 times the concrete strength, creep no longer appears to be a linear function of the applied stress, as demonstrated by Freudenthal and Roll (1958). This view is supported by Purkiss (1972) and Bali (1984). Although Freudenthal and Roll carried out their investigations at ambient conditions, their conclusions may reasonably be expected to hold at elevated temperatures. Freudenthal and Roll (1958) demonstrated for linear creep:

Aston University

Illustration removed for copyright restrictions

Figure 2.30 Time dependent strains in concrete maintained under load at high temperatures. (Cruz (1968)).

$$\varepsilon_{cr} = \frac{\sigma}{\sigma_{max}} \frac{(C_M T_M (1 - e^{-t/T_M}))}{\sigma_o/\sigma_{max}}$$

$$+ \sum_{j=1,2,m} \frac{\sigma}{\sigma_{max}} (\alpha_j \sigma_{max} (1 - e^{-t/\tau_j})) \tag{2.40}$$

and for non-linear creep:

$$\varepsilon_{cr} = C_M T_M e^{2.62(\sigma/\sigma_{max} - \sigma_o/\sigma_{max})} (1 - e^{-t/T_M})$$

$$+ \sum_{j=1,2,m} \frac{\sigma}{\sigma_{max}} (\alpha_j \sigma_{max} (1 - e^{-t/\tau_j})) \tag{2.41}$$

where: α_j is a stress dependent constant,

T_M is a constant,

$C_M = Ce^{-b}$,

C is a constant of magnitude 1,

b is a dimensionless constant,

σ_o is the stress limit for linear response,

t is the time,

τ_j is the element retardation time,

σ_{max} is the maximum compressive strength,

m is the number of elements.

For the model of high temperature creep in FIRES-RC (Becker and Bresler (1974)), the Freudenthal and Roll (1958) creep concept, for an effective stress that accounts for non-linear effects at high stress levels, was combined with a temperature compensated compliance function suggested by Mukaddam (1974), for the linear behaviour at lower stress levels. Mukaddam's compliance model is demonstrated to compare very favourably with experimental results obtained by Cruz (1968) in Becker and Bresler (1974).

The compliance function suggested by Mukaddam (1974) is:

$$C(t) = \sum_{j=1}^{m} J_j (1 - e^{-\lambda_j \phi(T) t}) \tag{2.42}$$

where: $C(t)$ is the compliance,

J_j is a linear constant,

λ_j is an exponential constant,

$\phi(T)$ is the temperature shift function based on data from Cruz (1968),

t is the time,

m is the number of elements.

Bazant and Panula (1978) carried out a numerical analysis involving activation energy to access the effect of temperature on creep and Maréchal (1969, 1970) has demonstrated that the activation energy approach holds at very high temperatures. Both Bazant and Panula (1978) and Maréchal (1970) accept that activation energy remains constant for any particular concrete type. Maréchal demonstrated that the variation of creep with temperature above 500°C, follows the equation:

$$\varepsilon_{cr} = C\sigma^{\alpha/k\theta}\, e^{-U_a/k\theta} \tag{2.43}$$

where: U_a is the activation energy,

θ is the absolute temperature,

k is the Boltzman constant,

α and C are constants varying with θ.

This model does not seem to hold for temperatures below 150°C due to the presence of moisture. For concrete with no free moisture, however, the model appears to be satisfactory.

Anderberg and Thelandersson (1976) developed a creep model for constant temperature and constant stress, where the creep is proportional to the actual stress divided by the concrete strength for the test temperature. The model is developed assuming linearity of behaviour although this is not exactly true. The model is extended for use for changes of temperature and stress by using the concept of the strain hardening rule.

It is a generally held view that a power law will best describe the variation of creep with respect to time and an activation energy approach with respect to temperature. Anderberg and Thelandersson (1976) employ a power law for time variation. However, an activation energy approach is not employed. The variation of creep with temperature is given by:

$$\varepsilon_{cr} = \beta_o \sigma (t/t_r)^p e^{k_1(T - 20)} / \sigma_{max}(T) \qquad (2.44)$$

where: $\beta_o = -0.53 \times 10^{-3}$,

$\sigma_{max}(T)$ is the maximum compressive stress for temperature T,

t is the time,

t_r = 3 hours,

$k_1 = 3.04 \times 10^{-3} {}^oC^{-1}$,

p = 0.5.

Gillen (1981) investigated the effects of temperature on creep and has shown the rate of creep strain is not constant but continually decreasing with time, the magnitude of creep strains increased with temperature and that there is no consistent relation between age of concrete and creep. Gillen compared his experimental data with three mathematical expressions frequently used to model creep strain as a function of time, namely:

$$\varepsilon_{cr}(t) = f[\log(t+1)] \quad \text{logorithmic function,}$$

$$\varepsilon_{cr}(t) = f[t^k] \quad \text{power function,}$$

$$\varepsilon_{cr}(t) = f[t/k+t] \quad \text{hyperbolic function.}$$

The power function gave best agreement in the form:

$$\varepsilon_{cr}(t) = At^b \tag{2.45}$$

where: A is a constant dependent on increasing load or temperature,

$b = 0.5 \pm 0.05$

For creep as a function of temperature satisfactory agreement was achieved with a model expression of the form:

$$\varepsilon_{cr}(T) = f[\exp(cT)] \tag{2.46}$$

where: c is a constant dependent on concrete type.

Combining expressions (2.45) and (2.46) gave a creep model of the form:

$$\varepsilon_{cr}(t,T) = Kt^b\exp(cT) \tag{2.47}$$

where: K is a function of load and material variables.

Reasonable agreement is obtained between this model and the Anderberg and Thelandersson (1976) model.

Schneider (1976) investigated creep and deformation characteristics of concretes up to 450°C and compared transient creep data, i.e. data derived from transient temperature conditions, with creep data which were measured at constant elevated temperatures. The importance of transitional thermal creep in the temperature range 80°C to 300°C due to physical disintegration and chemical decomposition is pointed out.

Schneider's (1976) results appear to be in good agreement with the results of other workers, such as Maréchal (1970), as can be seen in Figure 2.31. The Figure clearly indicates the significant influence of the load level on the creep values. Schneider points out the need for further experimental creep data at high temperatures.

Gross (1973) recorded isothermal creep strains developed in concrete specimens subject to moderate and high stresses and temperatures and modelled the problems of thermal creep using a digital computer. The models that Gross formulated were based on the notion of specific creep, hence the stress and temperature dependent non-linearities in strains developed under sustained loads were reduced to the problem of linear thermoviscoelasticity.

2.5.1.9 Stress-strain Relationships

Furamura (1966) was the first researcher to obtain the complete stress-strain curve for concrete. Harada (1957) and Harmathy and Berndt (1966) had earlier only managed to obtain the initial portion of the stress-strain curve due to their use of soft testing machines. Furamura (1966) used a testing machine which was sufficiently stiff to obtain the descending portion of the stress-strain relation. Some researchers appear to have failed to reach the peak stress. However, the complete stress-strain characteristic has since been obtained by Purkiss (1972) and Bali (1984).

Several investigators have only considered certain aspects of the stress-strain curve for example Malhotra (1956) has measured the effect of temperature upon the compressive strength of concrete, (Figure 2.32) whilst Philleo (1958) and Cruz (1966) have investigated the effect of temperature on the modulus of elasticity (Figure 2.33).

Figure 2.31: Unit creep strains of concrete at high temperatures. (Schneider (1976))

(Malhotra (1982))

Figure 2.32 Compressive strength of dense concrete at high temperature - no preload.

However, results of these studies are difficult to compare since Malhotra, Philleo and Cruz have all shown that the numerical values of the physical properties are strongly influenced by factors such as the age and the aggregate type, although all the researchers show similar trends in peak stress that shows a slight rise up to 300°C then at greater temperatures a very large drop occurs.

Zoldners (1960) in his investigation found that the flexural strength of concrete decreases to a much greater degree than does the compressive strength. Figure 2.34 shows the loss of flexural strength with temperature from Zoldners' results.

Anderberg and Thelandersson (1976) investigated the stress-strain curve characteristics for concrete but obtained only the initial portion of the curve yet postulated a constant descending branch behaviour, see Figure 2.35, however, there is sufficient evidence from Furamura (1966), Purkiss (1972) and Bali (1984) that indicate the magnitude of the slope of the descending branch does not remain constant but decreases with increasing temperature. At high temperatures pseudo ductile behaviour is approached which means the stress-strain relation flattens and therefore a linear slope is not possible. Some typical stress-strain curves of Furamura are shown in Figure 2.36.

Baldwin and North (1973) reviewed Furamura's data on the effects of temperature upon the relationship between stress and strain for concrete under compression and have shown that the effects of temperature can be represented by the equation of the form:

$$\frac{\sigma}{\sigma_{max}} = \frac{\varepsilon}{\varepsilon_{max}} \exp(1 - \varepsilon/\varepsilon_{max}) \qquad (2.48)$$

Figure 2.33 Effect of temperature on Young's modulus of concrete.
(Philleo (1958))

Figure 2.34 Effect of temperature on flexural strength of concrete.
(Zoldners (1960))

Figure 2.35 Stress-strain relationships for dense concrete (no preload). (Anderberg & Thelandersson (1976))

Figure 2.36 Stress-strain relationships for dense concrete (no preload). (Malhotra (1982)) where: functional form is independent of temperature,

σ_{max} is the value of stress at the point of maximum stress for the temperature,

ε_{max} is the value of strain at the point of maximum stress.

The relationship is shown in Figure 2.37. The result is significant since it implies that the stress-strain curves for high temperature can be derived entirely from the stress-strain curves measured at room temperature together with the variation of the compressive strength of the material with temperature, corresponding to the peak of the curve, and the strain at this point.

In most cases of fire the temperature acts on 'preloaded' concrete members and so it is desirable to determine the stress-strain relationship of preloaded concrete specimens at elevated temperatures. The influence of applied load on peak stress have been investigated by such researchers as Malhotra (1956) and Abrams (1970). However, the most exhaustive in this field has been carried out by Fischer (1970). Fischer et al show that with preloaded specimens there is a smaller strength loss at elevated temperatures. Schneider (1976) has investigated the effects of preload on the stress-strain relationship of concrete specimens at elevated temperatures and indicates three significant differences between the stress-strain relations for preloaded specimens when compared with those for no preload, see Figure 2.38:

(a) the high temperature strength of heated preloaded specimens increases with total load during heating,

(b) the high temperature elasticity of preloaded specimens increases with the total load during heating,

Figure 2.37 Normalized stress-strain curves (data from Furamura).
(Baldwin & North (1973))

Figure 2.38 Comparison of the effects of temperature on the stress - strain curves for preloaded and unloaded concrete specimens . (Schneider (1976))

(c) the high temperature strains at peak stress of preloaded specimens decrease significantly with the total load during heating.

This trend has been confirmed by Bali (1984).

2.5.1.10 Bond Strength

Bond strength of steel and concrete at high temperatures is of major importance in the determination of the behaviour of concrete structures in a fire. However, there is limited detailed information available on the subject despite investigations of such researchers as Reichel (1978), Morley and Royles (1979), Diedrichs and Schneider (1981) and Hertz (1982).

Unfortunately there has been little uniformity in test procedures which has often led to differences in results. The researchers generally agree that the surface of the reinforcing bars and type of concrete are important factors. Deformed bars or plain bars with heavily rusted rough surfaces show higher bond strengths at elevated temperatures than smooth bars. Figure 2.39 shows typical results obtained by Diedrichs and Schneider (1981) for the relative bond strengths of various reinforcing bars as a function of temperature. Concretes with lower thermal strain characteristics show higher bond strengths at elevated temperatures than concretes with high thermal strain characteristics. The decrease in bond strength with temperature follows a similar trend to the loss in compressive strength or tensile strength of the concrete. However, it is likely the bond strength will be more influenced by the tensile strength.

2.5.2 Steel

Behaviour of steel at high temperatures depends on the type of steel and the method of manufacture. Considerable information on this is now available including Anderberg et al (1978), Harmathy and Stanzack (1970) and Malhotra (1982).

2.5.2.1 Density

The density of steel is unaffected by high temperatures and is taken to be 7850 kg/m^3.

2.5.2.2 Thermal Conductivity

The thermal conductivity of steel at room temperature is about 50 W/m^oC and much higher than that for concrete. It is often assumed that steel sections have a high enough conductivity to aquire a uniform temperature throughout the section. Figure 2.40 shows the decrease of thermal conductivity with increased temperature, which depends upon the chemical composition of the steel, at 700^oC it is reduced by about 50%.

2.5.2.3 Specific Heat

Specific heat appears to be independent of the nature of the steel. The effect of temperature on specific heat is shown in Figure 2.41, it increases progressively nearly doubling in value up to 700^oC before reaching a peak and then descending. Specific heat can be expressed by the following equation for temperatures up to 700^oC (from Stirland (1980)):

$$C_p = (6.01x10^{-7}T_s^2) + (9.46x10^{-5}T_s) + 0.475 \text{ (KJ/kg}^oC) \quad (2.49)$$

where: C_p is the specific heat,

T_s is the temperature of the steel.

2.5.2.4 Thermal Diffusivity

The effect of temperature on the thermal diffusivity of steel is shown in Figure 2.42. The thermal diffusivity is 0.84 m^2/h at 20^oC decreasing linearly to 0.28 at 700^oC and can be represented by the following equation:

$$\gamma_s = 0.87 - (T_s x 0.84x10^3) \quad (m^2/h) \quad (2.50)$$

2.5.2.5 Thermal Deformation

It is generally agreed that the deformation process of steel at high transient temperatures can be described by three strain components, defined by the constitutive equation:

$$\varepsilon = \varepsilon_{th}(T) + \varepsilon_\sigma(\sigma,T) + \varepsilon_{cr}(\sigma,T,t) \quad (2.51)$$

where: ε_{th} is the thermal strain,

ε_σ is the instantaneous, stress related strain based on stress-strain relations obtained under constant, stabilized temperature,

ε_{cr} is the creep strain or time dependent strain.

Unlike concrete, steel does not undergo transient strain.

Page removed for copyright restrictions.

2.5.2.6 Thermal Strain

The thermal strain of steel is generally expressed by the coefficient of thermal expansion. The temperature dependence of the coefficient appears to be very similar for different steels and a linear relationship is often used. The thermal expansion of steel is commonly determined by heating steel specimens to various temperatures and measuring the increase in length. Figure 2.43 shows experimental data which apply to most steels. The coefficient of expansion can be expressed by the following equation:

$$\alpha = \frac{\Delta L}{L} = (0.4x10^{-8}T_s^{\,2}) + (1.2x10^{-5}T_s) - (3x10^{-4})\ (m/m) \quad (2.52)$$

where: α is the coefficient of thermal expansion,

ΔL is the increase in length,

L is the original length,

T_s is the temperature rise of the steel.

However, a constant value for the steel coefficient of thermal expansion equal to 1.5×10^{-5} is often used in calculation.

2.5.2.7 Creep

Creep of steel occurs in three phases (see Figure 2.44), primary creep as soon as the load is applied, the secondary creep continues at a steady rate during the heating period until the failure stage approaches when high strains in the tertiary phase lead to rupture. Data related to the primary and secondary phase are of most interest in fire conditions since heating periods rarely exceed a few hours. The rate of creep for two steels is shown in Figure 2.45 as obtained by Harmathy (1970).

Figure 2.43 Thermal expansion of steel.
(Malhotra (1982))

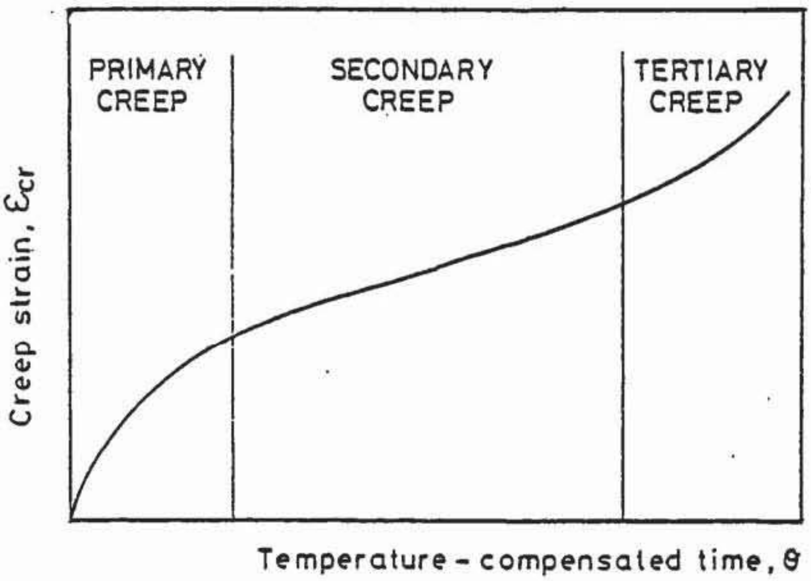

Figure 2.44 Phases of steel creep.

Models of creep are in most cases based on the concept put forward by Dorn (1954), in which the effect of variable temperature is considered. The model can be extended so that it is applicable to variable stress by the use of the strain hardening rule. The creep strain is assumed to be dependent on the magnitude of the stress and on the temperature compensated time given by the following expression:

$$\theta = \int_0^t \exp(-\Delta H/RT)dt \qquad \text{(hours)} \tag{2.53}$$

where: ΔH is the activation energy of creep (J/mol),

R is the gas constant,

t is the time.

Figure 2.46 shows the relation between creep strain and temperature compensated time. Using Harmathy's comprehensive creep model with Dorn's theta method, the following equation can be obtained:

$$\frac{\partial \varepsilon_{cr}}{\partial \theta} = Z\coth^2(\varepsilon_{cr}/\varepsilon_{cro}) \tag{2.54}$$

where: ε_{cr} is the creep strain,

Z is the Zener-Holloman constant,

θ is the temperature compensated time,

ε_{cro} is the y axis intercept of secondary creep phase.

2.5.2.8 Stress-Strain Relationship

Different steels have different stress-strain diagrams. Figure 2.47 shows the classical stress-strain relationship for mild steel which enable first yielding of the material to be observed (where strain occurs without an increase in stress), the 0.2% proof stress and the ultimate strength.

Pages removed for copyright restrictions.

The modulus of elasticity can be obtained from the early part of the curve where there is a linear relationship between stress and strain.

These strength properties of reinforcing steels have been studied in great detail by various workers but whether the steel has been tested at the required temperature or allowed to cool to room temperature before testing influences the results considerably.

Crook (1980) and Holmes et al (1982) reviewed the physical properties of reinforcing steels. The general view is that yield strength of reinforcing steel reduces above temperatures of 300°C and a 50% reduction occurs between 500°C and 600°C. Some typical results of the variation of yield strength with temperature are shown in Figure 2.48. As temperature increases the yield point becomes more difficult to pin point.

The ultimate strength of reinforcing steel increases for temperatures up to 300°C, after which the strength is progressively reduced. Typical results for the ultimate strengths are shown in Figure 2.49. The modulus of elasticity shows a steady reduction with temperature, most steels show a reduction of about 25% between room temperature and 600°C as can be seen in Figure 2.50.

An analytical description of the stress-strain curve as a function of temperature can be made in different ways as illustrated in Figure 2.51 and Figure 2.52. In Figure 2.51 the curve is approximated by two straight lines (as used in FIRES-RC and CONFIRE) or can be refined as in Figure 2.52 where an elliptic branch is placed between the straight lines. It is further supposed that the stress-strain relation in compression is identical to that in tension.

For the stress-strain models of the type in Figure 2.51 the stress-strain envelope for reinforcing steels can be completely described by three material parameters: the yield stress, the initial modulus of elasticity and the strain hardening modulus.

The subject of this research is concerned with the development of an analytical process that models the effect of a fire environment on a reinforced concrete column that is part of an overall structure. The following Chapter takes the form of a statement of the problem and its solution.

CHAPTER 3

STATEMENT OF PROBLEM AND ITS SOLUTION

Thermal gradients and thermal expansion of structural elements in fire environment, are sources of internal stress from local estraint within the member and global restraint from the overall tructural system. As a consequence of internal stress, cracking, rushing or spalling occurs, resulting in reductions in strength and tiffness of the structural member. This combination of phenomena ontrols the fire response of the structural system. An analytical ethod is used to predict the stress and deformation histories of a einforced concrete column that is part of an overall structure xposed to a fire environment.

In order to model the fire response of a reinforced concrete olumn, it has been assumed that the heat flow problem is separable rom the structural analysis. This separation simplifies the evelopment of appropriate analytical models and related computer rograms. The computer analysis is therefore carried out in two tages. The thermal response of the member is evaluated using an xisting computer program FIRES-T developed by Becker, Bizri and resler (1974). FIRES-T, the Fire Response of Structures - Thermal, akes use of a non-linear finite element approach coupled with a time tep integration. A new computer program, SAFE-RCC, which is the main ubject of this research, predicts the structural response of the einforced concrete column using the thermal histories predicted by IRES-T. Figure 3.1 shows the main composition of the computer nalysis.

The computer program SAFE-RCC, Structural Analysis of Fire xposed Reinforced Concrete Columns, used to evaluate the structural esponse of reinforced concrete columns in a fire environment, as resented in this thesis, includes several significant developments.

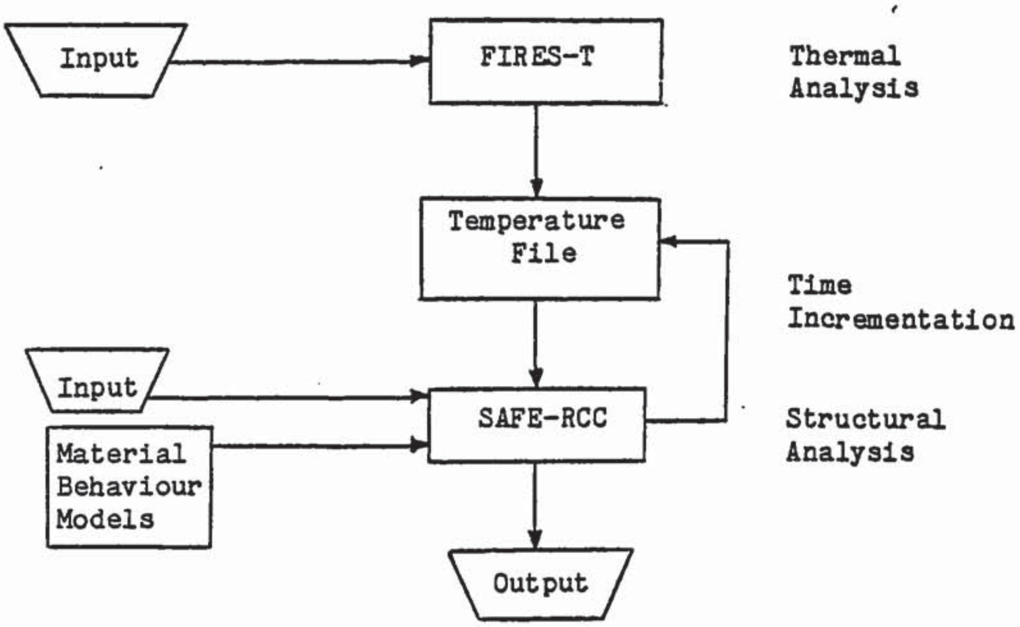

Figure 3.1 Main composition of the computer analysis.

Computer calculations are used that take into account the problems of restraint and the interaction of the column with the surrounding structure during the fire. In order to obtain realistic structural conditions it is necessary to model continuity over the supports, and to allow for the redistribution of moments to occur that will happen in a real fire. The solution to the problem requires an iterative determination of the moments, curvatures and displacements along the column for each time interval considered, until equilibrium is satisfied between the forces due to the external loads and internal stresses. This is achieved using a computer method for the analysis of restrained columns similar to that presented by Cranston in 1967.

The Cranston analysis (1967) provides automatic consideration of slenderness and second order effects. Second order effects occur with the degradation of the stiffness of the column as a result of the fire exposure which results in the development of large secondary forces and moments due to the axial force and increased lateral displacement leading to instability and failure.

The structural response program SAFE-RCC includes a realistic model of restraint and continuity likely to be experienced by a column in a real structure. In a structure there is a stage of elastic deformation (linear restraint) followed by non-linear deformation, due to changes in material properties and the stress-strain curve. In addition to modelling this behaviour, SAFE-RCC includes the option of the restraint system being exposed to, or not being exposed to, the fire environment.

Axial restraint and rotational restraint are considered independantly as suggested by Dougill (1972a, 1972b) and not in a combined parameter. Allowance is made for the fact that the axial restraint afforded to the column increases with the number of floors above. SAFE-RCC also models the conditions of pinned and fixed rotational restraint, and free axial expansion and fixed axial restraint. Although these are conditions which are not likely to be experienced by a column in a real structure, they allow comparison with the standard furnace tests.

The structural response program includes a total strain model (Anderberg and Thelandersson (1976)) which takes account of the compatability of strain due to temperature and loading. The material behaviour models for concrete and steel take account of the dimensional changes caused by temperature differentials and changes in the material mechanical properties with changes in temperature. Account is taken of loading to a strain greater than that corresponding to the peak stress of the concrete stress-strain curve, i.e. descending branch behaviour of the stress-strain curve which causes a redistribution of stress. Inelastic deformation associated with unloading of the steel stress-strain relation is also modelled.

Degradation of the section by cracking and crushing, and increased rates of shrinkage and creep with increased temperatures, are also taken account of, but no account is taken of the effect of preload on the stress-strain curve. SAFE-RCC does not attempt to model spalling as the calculated temperature distribution history is based on the assumption that the cross section remains intact.

In order to present the computer analysis in this thesis, the analysis is broken down into several stages. The thermal analysis, structural analysis, model of restraint and material behaviour models are described in separate Chapters. The following Chapter, Chapter 4, deals with the thermal analysis.

CHAPTER 4

THERMAL ANALYSIS

4.1 Introduction

The thermal response for the structural cross sections of the column system is calculated using a modified version of FIRES-T, a computer program for the Fire Response of Structures Thermal, developed by Becker, Bizri and Bresler (1974). FIRES-T evaluates the temperature distribution history of structural cross sections in fire environments by solving the heat balance equation in matrix form using a finite element method coupled with a time step integration. The problem is formulated in two dimensions as it may be assumed that no heat is flowing along the longitudinal axis of the structural member. It is also assumed that there is no contact resistance to heat transmission at the interface between the reinforcing steel and the concrete.

Owing to the temperature dependence of the thermal properties of structural materials and of the heat transfer mechanisms associated with fire environments, the heat flow problem is non-linear. These non-linearities are handled by a local linearisation about a current temperature distribution which requires the use of an iterative approach within the given time steps. The finite element mesh employed in FIRES-T can be made of quadrilateral or triangular elements. Simulation of the fire environment is through the use of a standard ISO fire, expressed as a time dependent curve, while convective and radiative mechanisms are used to model the fire boundary conditions. FIRES-T can also model the effects of protective coatings, for example plaster.

Since FIRES-T, at present, appears to be a perfectly satisfactory program for the prediction of temperature distributions in structural cross sections, it is to be used in this research as the preliminary program to evaluate the temperature distribution history, on the basis of which the structural analysis program, SAFE-RCC, evaluates the structural response.

The following section on the thermal model and solution procedure is based largely on the documentation of FIRES-T from Becker, Bizri and Bresler (1974).

4.2 Thermal Model and Solution Procedure

A finite element, time step integration technique is used to solve the two dimensional heat flow equation:

$$\rho C_p \frac{\partial T}{\partial t} = \frac{\partial}{\partial x}\left(k \frac{T}{\partial x}\right) + \frac{\partial}{\partial y}\left(k \frac{T}{\partial y}\right) \tag{4.1}$$

where: x,y are Cartesian coordinates,

ρ is the temperature and space dependent density,

C_p is the temperature and space dependent specific heat,

k is the temperature and space dependent isotropic conductivity,

T is the temperature,

t is time.

The finite element formulation is simplified by the following statement of the heat balance equation:

$$\begin{bmatrix}\text{Rate at which heat is}\\ \text{stored in elements}\\ \text{adjacent to a node}\end{bmatrix} + \begin{bmatrix}\text{rate at which heat}\\ \text{flows from elements}\\ \text{adjacent to a node}\end{bmatrix} = \begin{bmatrix}\text{rate at which}\\ \text{external heat}\\ \text{enters a node}\end{bmatrix} \tag{4.2}$$

This heat balance equation is given in matrix form by the following equation:

$$\underline{C}(\rho(T),C_p(T))\dot{\underline{T}} + \underline{K}(k(T))\underline{T} = \underline{Q}(\underline{T},F(t)) \qquad (4.3)$$

where: $\dot{\underline{T}}$ is the temperature time rate of change vector,

$\underline{C}$ is the capacity matrix,

$\underline{K}$ is the conductivity matrix,

$\underline{Q}$ is the external heat flow vector,

$\underline{T}$ is the temperature vector,

$\rho(T)$ is the density as a function of temperature,

$C_p(T)$ is the specific heat as a function of temperature,

$k(T)$ is the conductivity as a function of temperature,

$F(t)$ is the external heat source (e.g. standard fire).

Boundary conditions are an integral part of the heat flow equation and represent the effect of an external environment on the cooling or heating of a structures surface. The boundary conditions are introduced as either a prescribed boundary temperature or a prescribed boundary heat flow per unit area of exposed surface, or heat flux, see Section 4.5.

4.3 Conductivity Matrix $\underline{K}$

The terms of the conductivity matrix are associated with the rate of heat flow from the elements adjacent to each node. These terms are dependent on the conductivity k(T). The conductivity matrix for the system being analysed is assembled from element conductivity matrices, initially condensed from a system of triangular elements with linear temperature distributions. A process of static condensation is used to reduce the system of linear triangles to an element conductivity matrix.

The conductivity matrix of a triangular element with a linear temperature distribution is:

$$K^m = \frac{k(T)}{2\lambda}\begin{bmatrix} e^2 + d^2 & y_k e - x_k d & -y_j e + x_j d \\ & y_k^2 + x_k^2 & -y_j y_k - x_j x_k \\ & & y_j^2 + x_j^2 \end{bmatrix} \tag{4.4}$$

where: x_k, x_j, y_k, y_j, e, d and λ are defined in Figure 4.1(a).

A quadrilateral element is constructed from four linear triangles through the addition of a fifth node (see Figure 4.1(b)). The coordinates of this node are specified as the average of the original four nodes. It is assumed that there is no external heat flow at node 5. A typical term of the quadrilateral conductivity matrix is given by:

$$K_{i,j} = K_{i,j} - \frac{K_{i,5}\, K_{5,j}}{K_{5,5}} \tag{4.5}$$

These element conductivity matrices are then assembled into the conductivity matrix for the system, where:

$$\underline{K} = \sum_i K^i \tag{4.6}$$

4.4 Capacity Matrix C

The heat capacity associated with a node is the rate at which heat is absorbed for a unit rate of change of the temperature of that node. The capacity matrix contains terms that are dependent on the heat capacity $C_p(T)$ and density $\rho(T)$ of the elements immediately adjacent to each node.

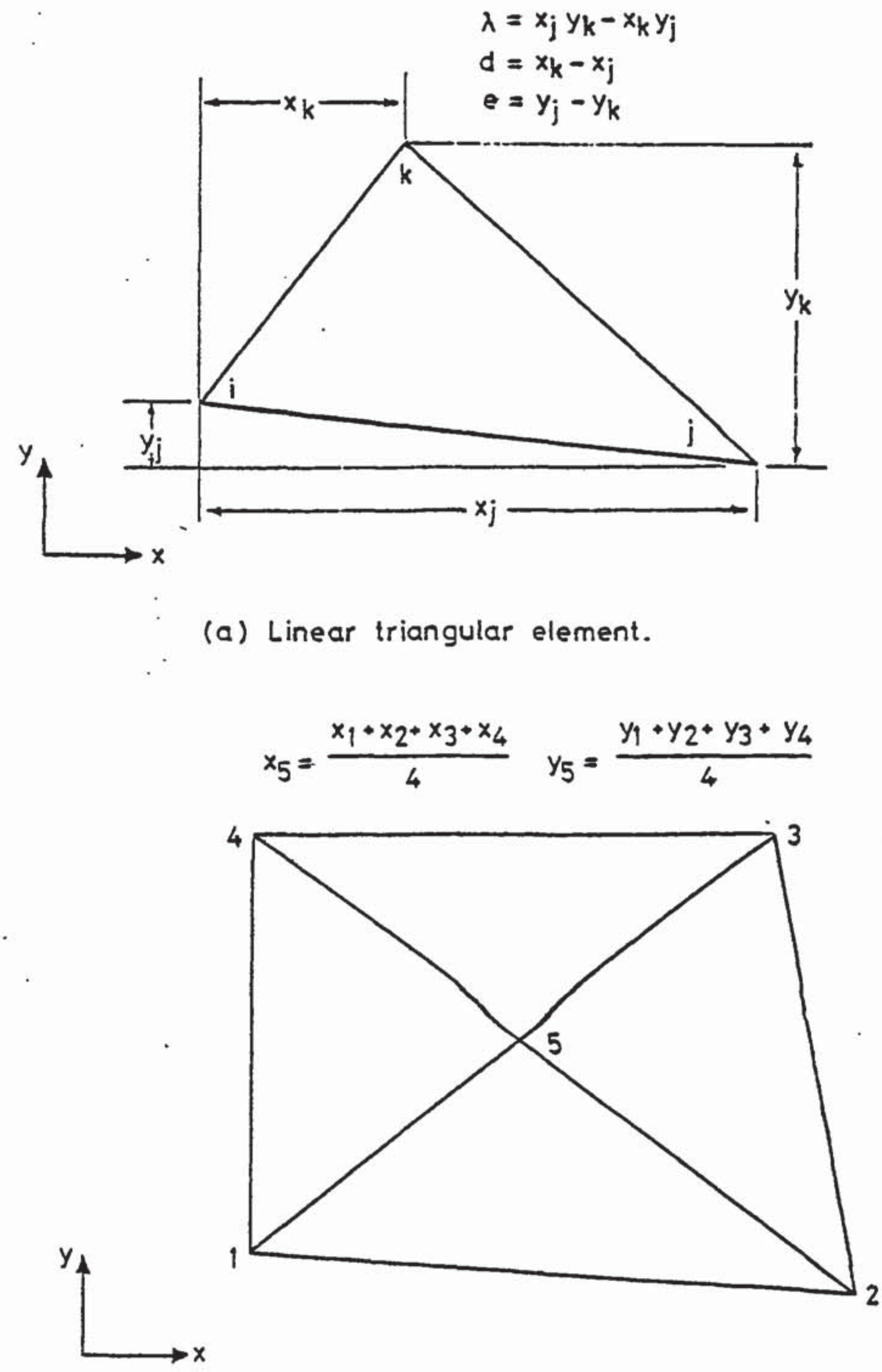

(a) Linear triangular element.

(b) Quadrilateral assembly of four linear triangles.

Figure 4.1 Quadrilateral finite element.

The capacity matrix can be diagonalized by lumping at each node the heat storing capacity of the material adjacent to that node. The problem is thus simplified by making the capacity term for each node independent of the temperature time rate of change of neighbouring nodes. The capacity matrix is idealized by delineating the volume adjacent to a node by a perimeter drawn through the midpoints of element boundaries and the internal nodes previously associated with the conductivity matrix (see Figure 4.2).

The heat capacity for an element is given by:

$$C_m = V_m \rho(T) C_p(T) \tag{4.7}$$

where: V_m is the volume of element which is equal to unit thickness times area of element.

Since areas are a function of the linear triangles associated with an element, the contribution of an element, m, to a particular node, i, is given by:

$$C_{m,i} = \rho(T) C_p(T) \frac{(a_j + a_k)}{2} \tag{4.8}$$

where: a_j, a_k are areas of triangles in elements adjacent to node i, hence the heat capacity of a node, i, is:

$$C_i = \sum^{m'} C_{m,i} \tag{4.9}$$

where: m' is the number of elements adjacent to node i, and the capacity matrix is:

$$\underline{C} = \sum_{i=1}^{n} C_i \tag{4.10}$$

where: n is the number of nodes.

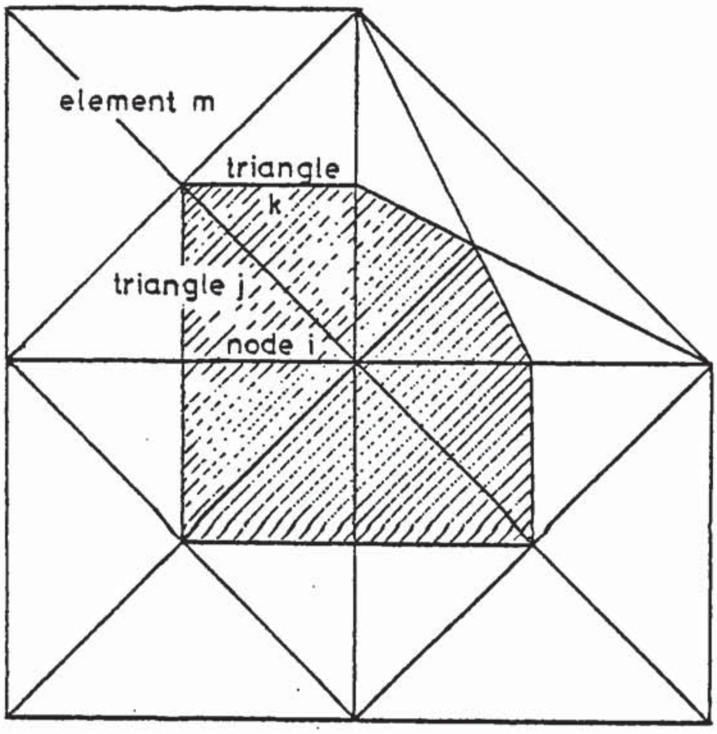

Figure 4.2 Heat capacity idealization.

4.5 External Heat Flow Vector Q

In solving a heat flow problem one of two conditions must be known, the temperature of the node or the external heat flow into the node. The external heat flow is expressed in the following summation:

$$Q = Q_K + Q_E + Q_F \tag{4.11}$$

where: Q_K is a prescribed heat flow,

Q_E is the resultant of an exothermic reaction within the system,

Q_F is the heat flow caused by the exposure of the system to an external source.

In a fire environment Q_F is the primary heat source, therefore it is assumed $Q_E = 0$ and Q_K is directly entered as data. Q_F is considered to be a function of convective and radiative mechanisms and the time-temperature relationship is represented by the function F(t). The external heat flow over a surface can be represented by:

$$Q_F = l * q(T_s, T_f) \tag{4.12}$$

where: l is the length between adjacent nodes i and j,

q is the rate of heat flow per unit area,

T_s is the average surface temperature = $(T_i + T_j)/2$,

T_f is the temperature of standard fire F(t).

The heat flow per unit area of the exposed surface can be modelled using linear heat transfer or non-linear heat transfer.

4.5.1 Linear Heat Transfer

$$q = h(T')(T_f - T_s) \tag{4.13}$$

where: $h(T')$ is the heat transfer coefficient,

$T' = (T_f + T_s)/2$

4.5.2 Non-Linear Heat Transfer

$$q = A(T')(T_f - T_s)^{N(T')}$$

$$+ \sum_{i=1}^{rs} V\sigma(a(T_s)\varepsilon_r(T_r)\theta_r^4 - \varepsilon_s(T_s)\theta_s^4 \tag{4.14}$$

where: $A(T')$ is the convection coefficient,

$N(T')$ is the convection power factor,

V is the radiation view factor,

σ is the Stefan-Boltzmann constant,

$a(T_s)$ is the absorption of the surface,

$\varepsilon_f(T_r)$ is the emissivity of radiation source,

$\varepsilon_s(T_s)$ is the surface emissivity,

θ_r is the absolute temperature of radiation source,

θ_s is the absolute temperature of surface,

rs is the number of sources of radiation.

Through the assumption that the standard fire is the only radiation source and the elimination of the temperature dependence of the controlling parameters, equation (4.14) is reduced to:

$$q = \underbrace{A(T_f - T_s)^N}_{\text{convection term}} + \underbrace{V\sigma(a\varepsilon_f\theta_f^4 - \varepsilon_s\theta_s^4)}_{\text{radiation term}} \tag{4.15}$$

where: ε_f is the emissivity of the flame associated with the standard fire,

θ_f is the absolute temperature of the standard fire.

4.6 Numerical Scheme

The heat flow equation and associated boundary conditions are solved using a finite element method. The technique reduces the differential equation to a system of algebraic equations. Simplifying equation (4.3) the matrix equations solved are:

$$\underline{C}\,\dot{\underline{T}}_i + \underline{K}\,\underline{T} = \underline{Q} \tag{4.16}$$

where: i is the i^{th} time step.

Substituting a linear approximation for the temperature rate of change vector,

$$\dot{\underline{T}}_i = (\underline{T}_i - \underline{T}_{i-1})/\Delta t \tag{4.17}$$

where: Δt is the time step interval,

into equation (4.16) gives:

$$\underline{C}(\underline{T}_i - \underline{T}_{i-1})/\Delta t + \underline{K}\,\underline{T}_i = \underline{Q} \tag{4.18}$$

Defining the modified conductivity matrix as:

$$\underline{K}^* = \underline{K} + \underline{C}/\Delta t \tag{4.19}$$

and the modified external heat flow vector as:

$$\underline{Q}^* = \underline{Q} + \underline{C}\,\underline{T}_{i-1}/\Delta t \tag{4.20}$$

the solution to equation (4.16) is from the solution of the following set of linear equations:

$$\underline{K}^*\,\underline{T}_i = \underline{Q}^* \tag{4.21}$$

$\underline{K}^*$, $\underline{Q}^*$, $\underline{K}$, $\underline{C}$ and $\underline{Q}$ are all functions of the current temperature $\underline{T}_i$. This problem can be resolved by either using the temperature distribution from the previous time step, $\underline{T}_{i-1}$, or by the use of an iterative solution. FIRES-T contains the option of either solving the entire problem iteratively or iterating only on the boundary condition aspect of the iteration.

An overconvergence factor, β, is used in the iterative process to estimate the temperature distribution for the next iteration, j+1, in order to accelerate convergence.

$$\underline{T}_i^{\,j+1} = \underline{T}_i^{\,j} + \beta(\underline{T}_i^{\,j} - \underline{T}_i^{\,j-1}) \tag{4.22}$$

Becker, Bizri and Bresler found from experience that a value of β in the interval of -0.10 to -0.40 gave satisfactory convergence for the non-linear fire condition, although values of β up to -0.60 have been necessary in order to achieve convergence in the application of FIRES-T reported in this thesis. Convergence is achieved when:

$$\frac{2\ (\ T_i^{\,j} - T_i^{\,j-1}\ )}{(\ T_i^{\,j} + T_i^{\,j-1}\ )} < \text{permissible error} \tag{4.23}$$

Flow charts of FIRES-T and its main control subroutine, HEATFLO, are presented in Figures 4.3 and 4.4, a listing of the computer program is presented in Appendix L.

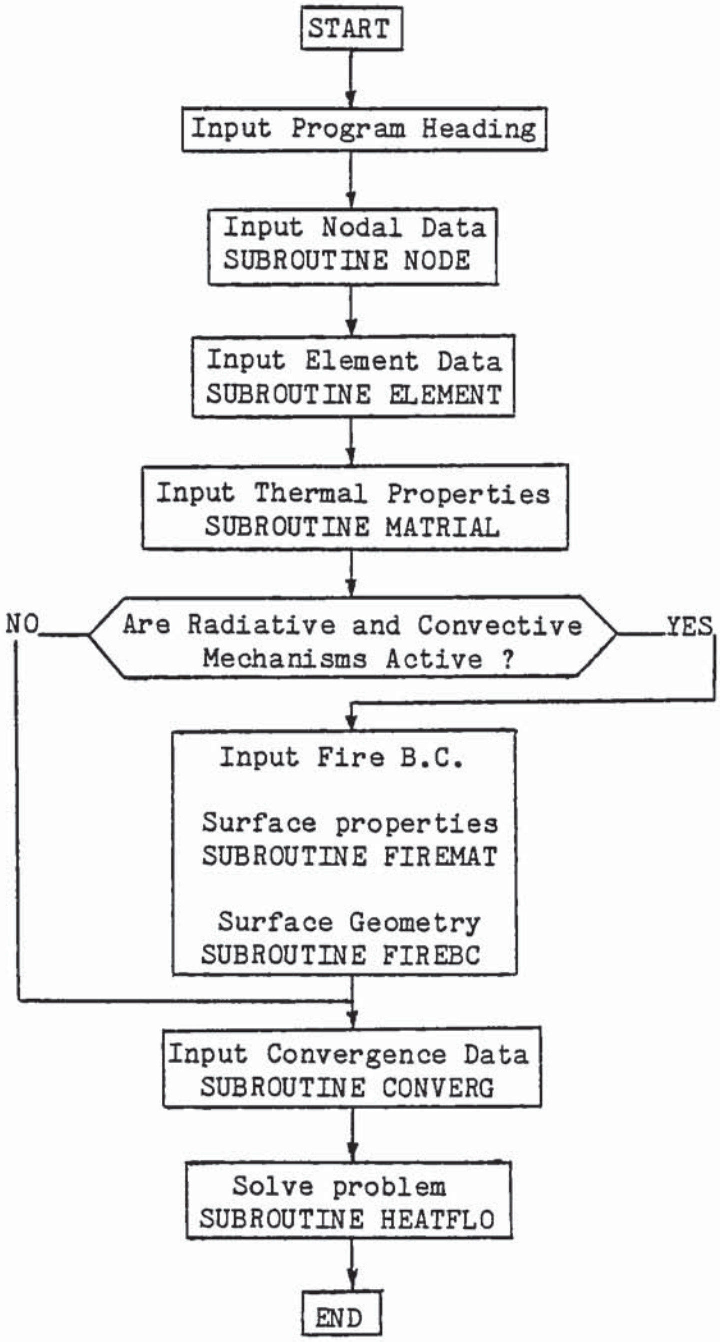

Figure 4.3 Flow chart for program FIRES-T (Becker, Bizri and Bresler (1974))

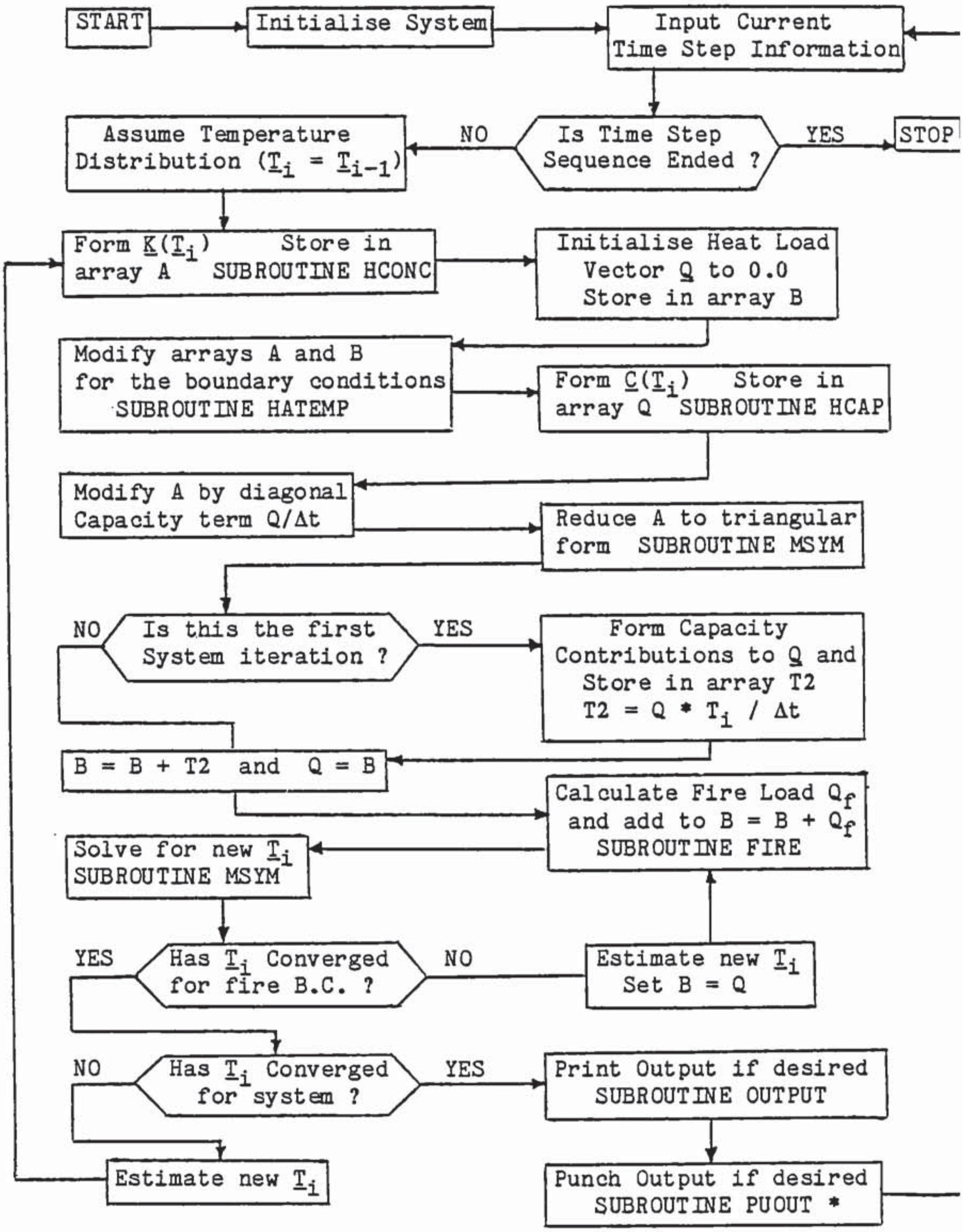

* Subroutine PUOUT in the modified version of FIRES-T used in this research writes output to a file.

Figure 4.4 Flow chart for Subroutine HEATFLO assuming a fire b.c. (FIRES-T, Becker, Bizri and Bresler (1974))

4.7 Use of FIRES-T

In order to use the computer program FIRES-T, the column cross section must be divided into a finite element mesh that may be constructed from quadrilateral or triangular elements. The mesh chosen is at the discretion of the user. However, concrete is not a highly conductive material and therefore the thermal gradients near the surface are high. The influence of this effect becomes even more extreme when contrasted with the well dampened gradients observed at the interior of a structural member due to the insulative nature of the depth of surrounding concrete. In order to overcome this effect it is advisable to use a finer element mesh near the surface of the column section and a coarser mesh at the interior of the section. Once the mesh has been chosen, the number of nodal points are entered as data and then the nodal points are plotted and entered as data in coordinate form.

For FIRES-T the origin of the coordinate axis is arbitrary, but in order for it to be used in conjunction with the structural response program SAFE-RCC, the origin must correspond with the longitudinal axis of the column, since the finite element mesh used in FIRES-T is passed directly over to SAFE-RCC in the form of element areas and centroidal distances of the elemental centroids to the xx axis. This stipulation is necessary in order to produce the correct balance of positive and negative centroidal distances about the principal axis of bending for the calculation of stresses and strains in the structural response program SAFE-RCC (see Figure 4.5).

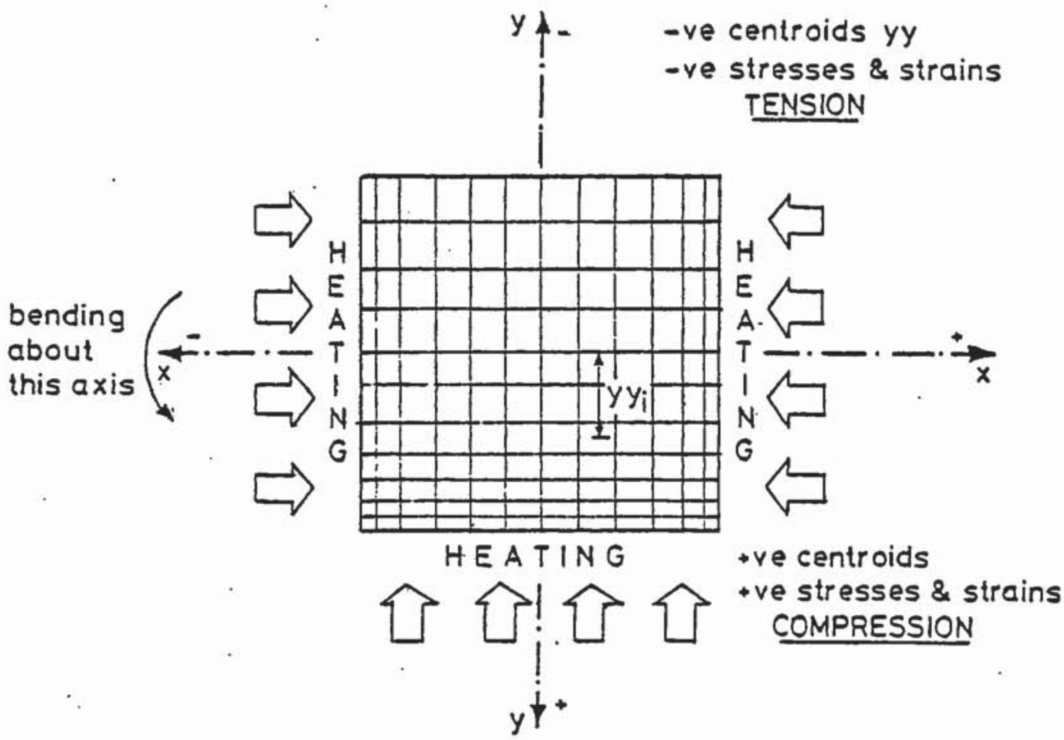

Figure 4.5 Origin of coordinate axis with respect to finite element mesh for tension and compression sign convention incorporated in SAFE - RCC for column cross sections.

When running FIRES-T for the restraint system, the origin of the coordinate axis must coincide with the top of the restraint beam, see Figure 4.6. This stipulation is necessary in order for calculated centroidal distances to be compatable with the theory in subroutine ULTIMOM of SAFE-RCC. Subroutine ULTIMOM calculates the ultimate moments of the restraint beam.

The number of elements and details of their corresponding nodal points, in addition to a material type designation for each element, are then entered. The thermal properties are then entered for each material allowing for their temperature variation. Specification of the boundary conditions with the parameters of the heat flow equation for each material exposed to fire are the data next required. This is followed by details of the fire exposure in the form of a series of fire temperatures against time, and which elements of the column cross section are exposed to the fire. The time increments required are then entered and the elemental temperatures of the column cross section are then calculated for each time increment in accordance with the theory covered in the previous sections. For full user instructions the user manual in FIRES-T (Becker, Bizri and Bresler (1974)) should be consulted.

Heat flow through the specimen surface will be dependent on the values chosen for the parameters of the heat flow equation of the fire boundary condition, however, there seems to be little conformity in the values chosen by other researchers.

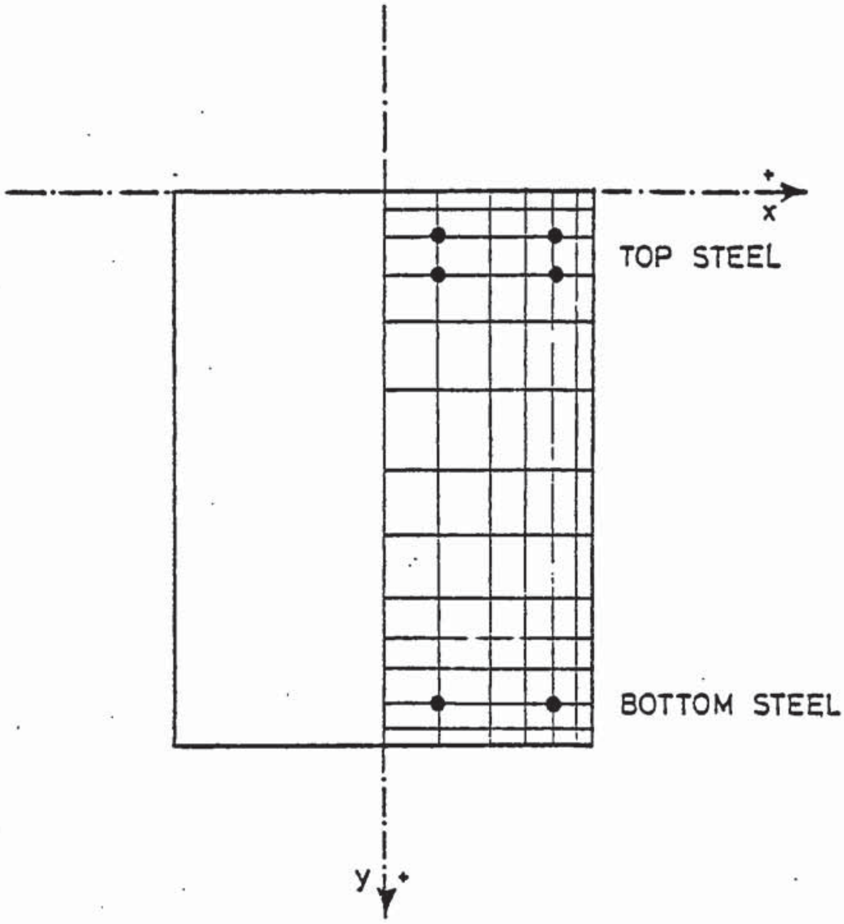

Figure 4.6 Origin of coordinate axis with respect to finite element mesh for calculation of ultimate moment capacities in SAFE-RCC for the restraint beam sections.

The heat flow per unit area of the exposed surface due to radiation from equation (4.15) is given by:

$$q_r = V\sigma(a\varepsilon_f\theta_f^4 - \varepsilon_s\theta_s^4)$$

or

$$q_r = V\sigma\varepsilon_r(a\theta_f^4 - \theta_s^4) \tag{4.24}$$

where: ε_r is the resultant emissivity = $1/(1/\varepsilon_f + 1/\varepsilon_s - 1)$.

Bresler and Iding (1983) state that emissivities should range in value from 0.5 to 0.9 and considered values for the concrete surface (ε_s) of 0.9 and values for the flame (ε_f) of 0.5 and 0.7 in calculations. Pettersson, Magnusson and Thor (1976) took a value for the emissivity of a steel surface of 0.8 and state the emissivity of flames should be in the interval of 0.6 to 0.9, 0.85 was used in calculation.

Other researchers state values of resultant emissivity (ε_r). Odeen (1968) found that ε_r of 0.6 for horizontal bottom surfaces and ε_r of 0.2 for vertical sides gave best agreement between test and theoretical results. Anderberg (1976) suggests that the resultant emissivity should be in the range of 0.6 to 0.8. Correspondingly Anderberg (1976) and Wickström (1979) employ ε_r of 0.8. However, Malhotra (1982) suggests a value of ε_r of 0.5 and CEB (1982) take a resultant emissivity of 0.4 in fire resistance design calculations.

It should be noted that the emissivity values are probably found from direct adaptation to measured temperature distributions and will most likely vary with the thermal properties of the materials and furnace from one laboratory to another.

Bresler and Iding (1983) suggest that view factors (V) may be taken in the interval of 0.0 to 1.0, and employ a value of 1.0 for horizontal surfaces and 0.5 for vertical surfaces in calculations. The surface absorption (a) is usually set to around 0.9.

The heat flow rate per unit area due to convection from equation (4.15) is expressed as:

$$q_c = A(T_f - T_s)^N \tag{4.25}$$

Many researchers suggest a simple estimate of the heat transfer coefficient (A) in the range of 10 to 30 $W/m^{2o}K$, while setting the convection power (N) equal to 1.0, is adequate in most standard fire resistance calculations. Odeen (1972) indicates the coefficient should be in the interval of 23 to 29 $W/m^{2o}K$. Correspondingly CEB (1982) and Malhotra (1982) take a value of 25 $W/m^{2o}K$ and Pettersson et al (1976) state a value of 23 $W/m^{2o}K$. In theoretical calculations verified by tests Anderberg (1976) employs a value equal to 12 $W/m^{2o}K$.

Wickström (1979) has evaluated the paramters A and N based on a complex theoretical approach in relation to a specific test program and found that for a cool side $A = 2.2\ W/m^2K^{1.25}$, $N = 1.25$ and for an exposed side $A = 1.0\ W/m^2K^{1.33}$, $N = 1.33$.

However, at elevated temperatures the heat flow rate from convection is of secondary importance when compared to the heat flow from radiation and therefore a simple estimation of A taking N as 1.0 can be adequate.

4.8 Modifications to FIRES-T

The program is used in a form essentially as that developed by Becker, Bizri and Bresler (1974) except that it has been compiled with no comment lines and a substantially different PUOUT subroutine to suit the requirements of the structural analysis program.

4.8.1 Subroutine PUOUT

The original subroutine PUOUT has been replaced and a new subroutine has been written that writes all the finite element details and results of the thermal analysis into a specified file which can then be used as data for the structural analysis program. There is a choice of output that can be obtained from PUOUT, either data for the temperature distribution of the column cross section in the form of elemental temperatures, or data for the temperature distribution of the restraint system in the form of average layer temperatures.

When the output option for the restraint system is selected subroutine PUOUT will lump together elements of the same material type and centroid to form a layer, taking the layer temperature as the average elemental temperature. This is done due to the limitation of available storage space within the structural response progam SAFE-RCC.

In the program FIRES-T as developed by Becker, Bizri and Bresler, different punched output options, from subroutine PUOUT, could be requested for each time step by entering either 0, 1, 2 or 3 as part of the fire history data (refer to user instructions FIRES-T, Becker, Bizri and Bresler (1974)). The modified version of FIRES-T, used in this research, makes use of these output options to request different filed output options.

Output for the column cross section and output for the restraint system is requested by entering 1 and 2 respectively for the punched (filed) output option for FIRES-T as described in the users manual FIRES-T (1974).

Subroutine PUOUT will write into a file:

(output option 1 - data for column section)

number of elements,

centroidal distance of each element from axis of bending,

area of each element,

time of fire exposure, } each element, each time step

average element temperature, } each element, each time step

or Subroutine PUOUT will write into a file:

(output option 2 - data for restraint system)

number of layers,

centroidal distance of each layer from top of beam,

area of each layer,

average layer temperature - for each layer, each time step.

The file produced by subroutine PUOUT is then edited with the inclusion of additional data necessary to calculate the structural response, and then used as the data file for the structural response program SAFE-RCC. Full details of the data file for SAFE-RCC are given in Appendix A.

The next Chapter, Chapter 5, describes the structural analysis.

CHAPTER 5

STRUCTURAL ANALYSIS

5.1 Introduction

The structural analysis used in the computer program SAFE-RCC, is based on 'A Computer Method for the Analysis of Restrained Columns' developed by Cranston (1967), which was used by Cranston to develop a model for the effective lengths of short and slender columns presently in use in CP110. The analysis was designed so that solutions for a given column bent about one of the principal axes of the cross section, in a non fire environment, are obtained in stages as loading is applied from zero up to a maximum load in specified load increments. Solutions are found, corresponding either to a specified load or to a specified deflection, using an iterative method. Cranston's analysis is based on the following assumptions:

(i) plane sections remain plane during bending,

(ii) lateral deflections of the column are small in comparison with its length,

(iii) the longitudinal stress at any point in the column is dependent only upon the longitudinal strain at that point,

(iv) the stress-strain relations for the column materials are known,

(v) material strained into the inelastic range and subsequently unloaded follows a linear unloading line,

(vi) the moment-rotation relations for the end restraint systems are known,

(vii) the effects of deformations due to shear forces are negligible,

(viii) under zero loading, the segment lengths are straight,

(ix) under loading, the curvature varies linearly along the segment.

However, for the fire situation some of these assumptions do not hold, namely, lateral deflections of the column may not necessarily be small in comparison with its length due to the increased elasticity of the column materials at elevated temperatures, and the effects of axial deformation are also no longer negligible due to the thermal expansion of the column at elevated temperatures, and thus these effects must be included.

In order to apply the analysis developed by Cranston to a fire situation the notion of a total strain model, of the type developed by Anderberg and Thelandersson (1976), must be employed. The Anderberg and Thelandersson model (1976) is based on the concept that the total strain is the sum of four components: the thermal strain, the stress related strain, the creep strain, and the transient strain (see Chapter 8). Hence two types of strain must be used in the structural analysis for the computer program SAFE-RCC, the stress related strain for the determination of stress from the known stress-strain relations, and the total strain for the calculation of axial deformation.

Another fundamental change in the analysis is that the load is no longer applied in stages from zero load up to a maximum load, but a specified load is applied to the column. As the fire progresses, strains as a result of the fire load increase, so according to the total strain model, the instantaneous stress related strain complement of the total strain, as a fraction of the total strain, must decrease.

The analysis has also been developed so that axial restraint of the column and rotational restraint at the column supports are considered as two separate parameters. The analysis is capable of dealing with any of the following combination of restraint conditions:

(a) free axial restraint or free axial expansion,

(b) normal axial restraint - the axial restraint likely to be experienced in service, either temperature dependent or temperature independent,

(c) fixed axial restraint,

(d) pinned rotational restraint end A,

(e) normal rotational restraint end A - the rotational restraint likely to be experienced in service, either temperature dependent or temperature independent,

(f) fixed rotational restraint end A,

(g), (h), (i) rotational restraints for end B.

Examples of end fixities are shown in Figure 5.1.

Cranston (1967) covers two methods of analysis: a method of analysis for finding a solution corresponding to a specified deflection and a method for finding a solution corresponding to a specified load. The general load-deflection response to be expected from reinforced concrete columns can be seen in Figure 5.2. For curves of the type illustrated as case III, there are two equilibrium positions corresponding to the same loading in regions close to the peak of the curve. In order to avoid difficulties in such cases, Cranston found it convenient to find solutions corresponding to a specified deflection. In this way, the behaviour of the column can be traced up to and beyond maximum load if desired.

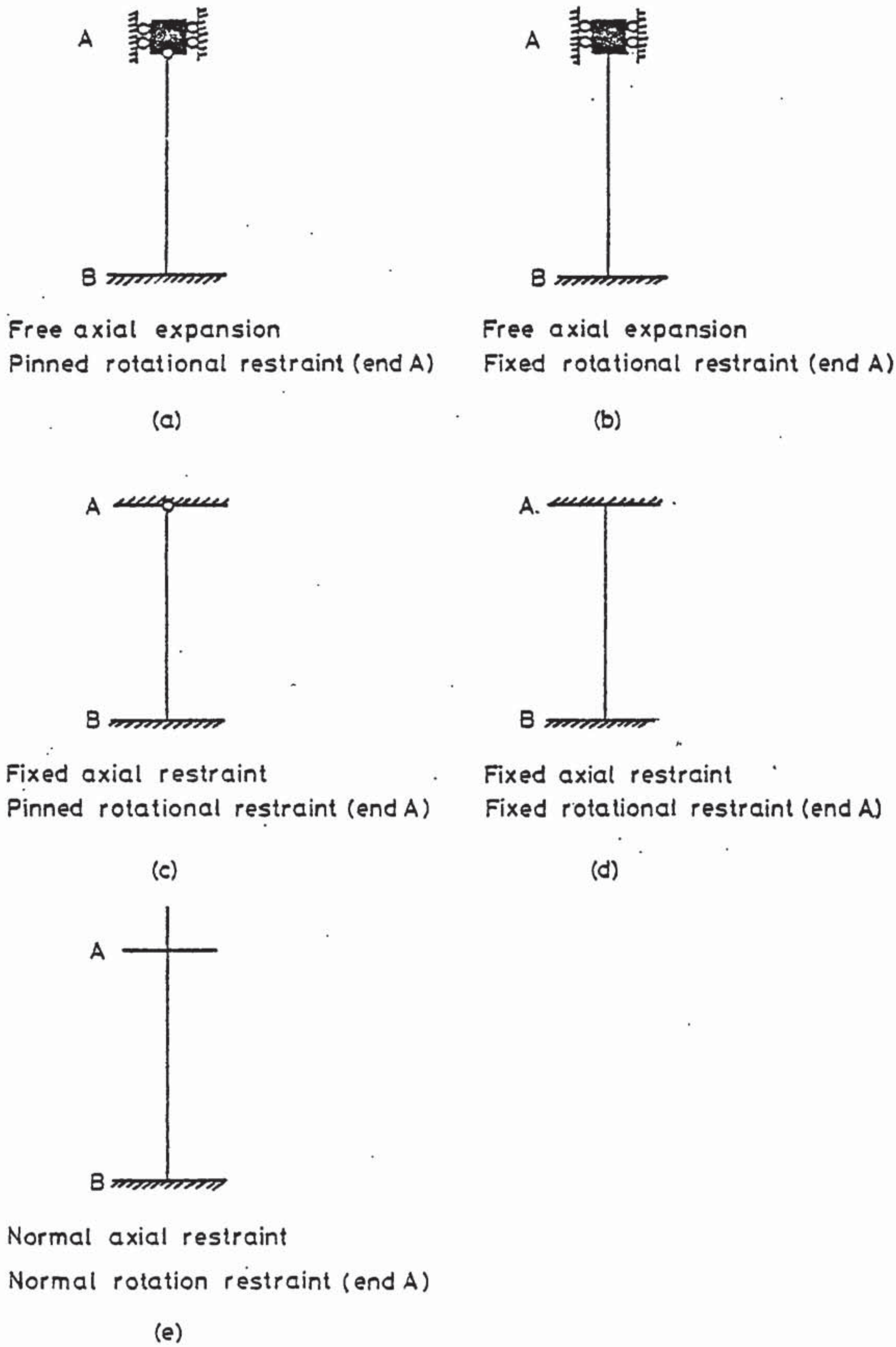

Figure 5.1 Examples of end fixities for column.

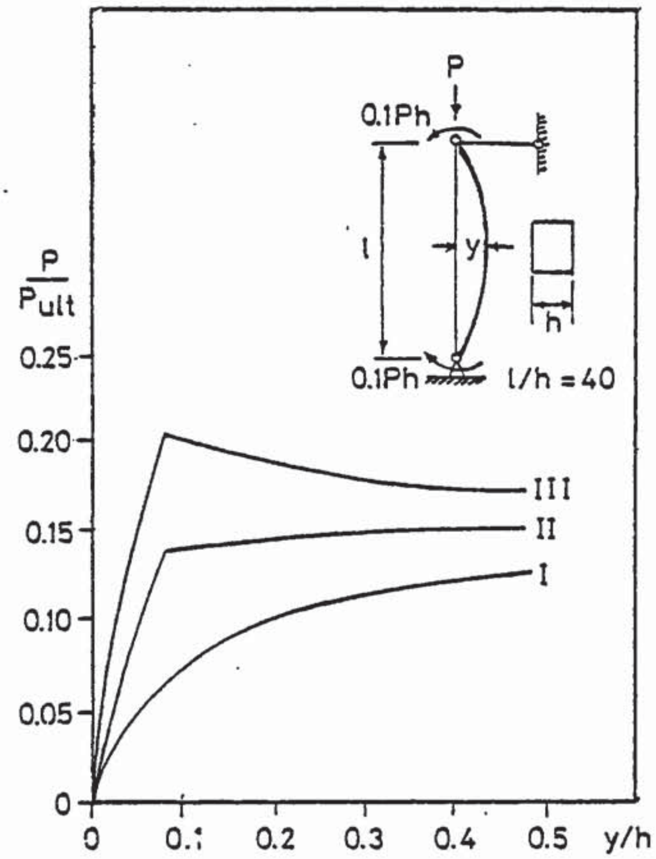

Figure 5.2 General load deflection relations.
(Cranston (1972))

Cranston thus designed the analysis to find successive solutions as the load on (or deflection of) the column is increased in steps (for the non fire situation). The finding of each of these separate solutions is said to comprise a stage in the analysis.

However, the column system analysed in this research will have constant specified external structural loads, and increase in load will be due to the increased strains in the column subslice elements due to the elevated thermal environment of the fire condition or due to the induced restraining moment from the moment-rotation relations as a result of increased end rotation. Thus the method of analysis corresponding to specified load only can be used since calculating incompatabilities when equilibrium is not satisfied with the specified deflection method of analysis (that is when calculated deflection and specified deflection of a point are incompatible) involves making changes in the applied load to satisfy equilibrium.

The following sections are based largely upon Cranston (1967) and the method of analysis for finding solutions corresponding to a specified load is covered in detail.

5.2 Description of Analysis

5.2.1 System Analysed

The system analysed is shown in Figure 5.3. The column AB is held by restraining systems at A and B, which provide rigid restraint against sway movement but which are, however, capable of rotation. The loading is shown in Figure 5.3(b) and consists of an axial load, P, acting along the line AB and end moments M_A and M_B.

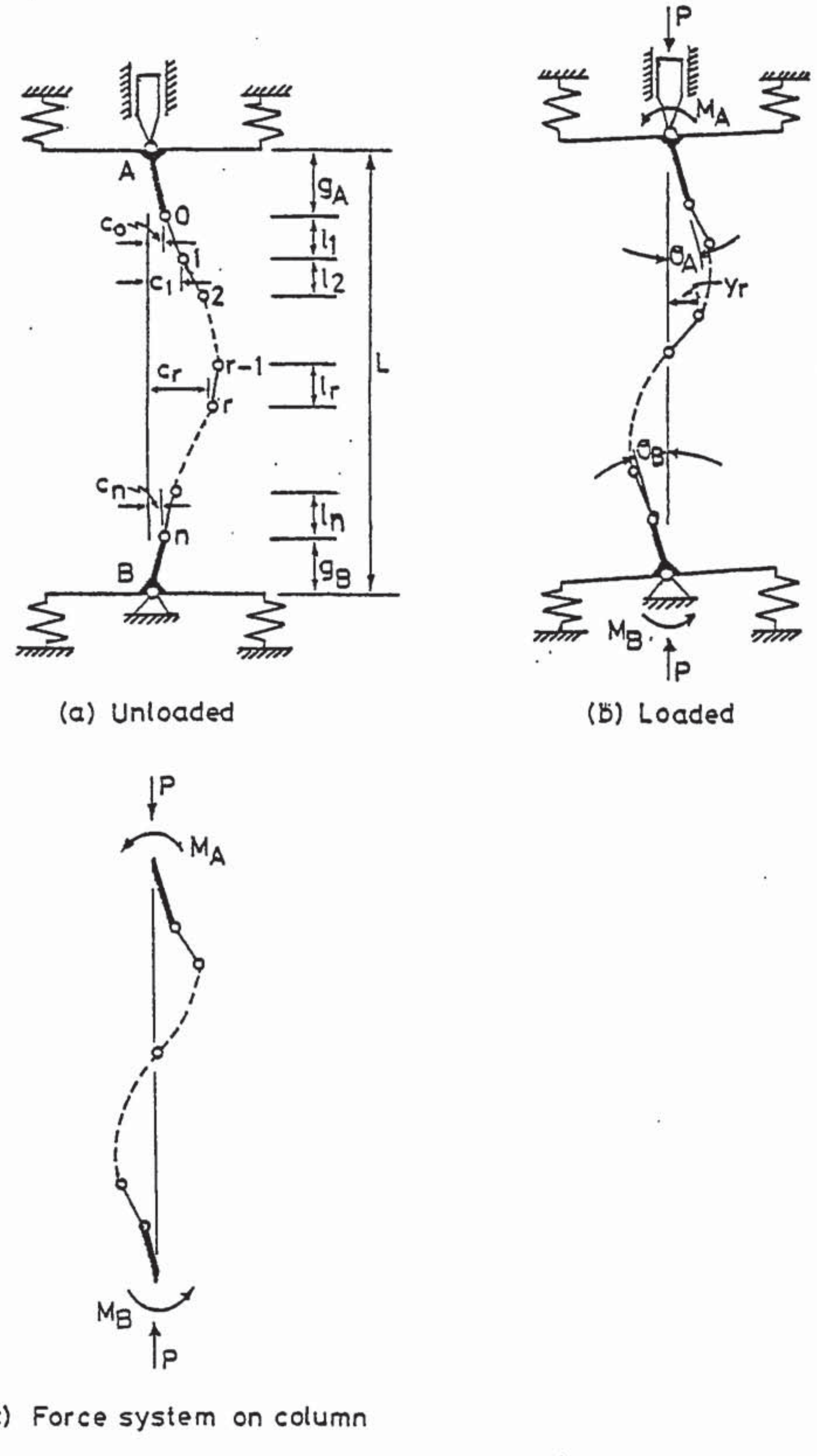

(a) Unloaded

(b) Loaded

(c) Force system on column

Figure 5.3 Systems analysed.

The column length, L, is considered to be made up of two rigid gusset or end lengths, g_A and g_B, the remainder being divided into segments having lengths l_1, l_2,..... l_r,..... l_n. The analysis is based on the cross section behaviour at the division points between these segments. The division points are numbered 0, 1,..... r,.... n. The column may possess initial deformations under zero load, these are defined by division point deflections c_0, c_1,..... c_r,..... c_n, measured from a line passing through A and B to the column axis.

The deflections of the column under load are denoted by y_0, y_1,..... y_n, and are again measured with respect to a line passing through A and B. The end slopes, θ_A and θ_B, along with the division point slopes, θ_0, θ_1,..... θ_n are also measured with respect to this line. Division point slope is defined as the slope just below the division point.

5.2.2 Sign Convention

The sign convention is as follows. P, M_A and M_B are positive, as drawn on Figure 5.3(b). c_0, c_1,..... c_n and y_0, y_1,..... y_n are positive when the column deflects to the right of the line AB. θ_A, θ_0, θ_1,..... θ_n, θ_B are positive if the deflection is increasing in the direction A to B. Division point curvatures, denoted by ϕ_0, ϕ_1,..... ϕ_n are positive when the slope is increasing in the direction A to B, and moments within the column length are positive when they produce negative curvature. See Figure 5.4. Compressive stress and strain are taken as positive.

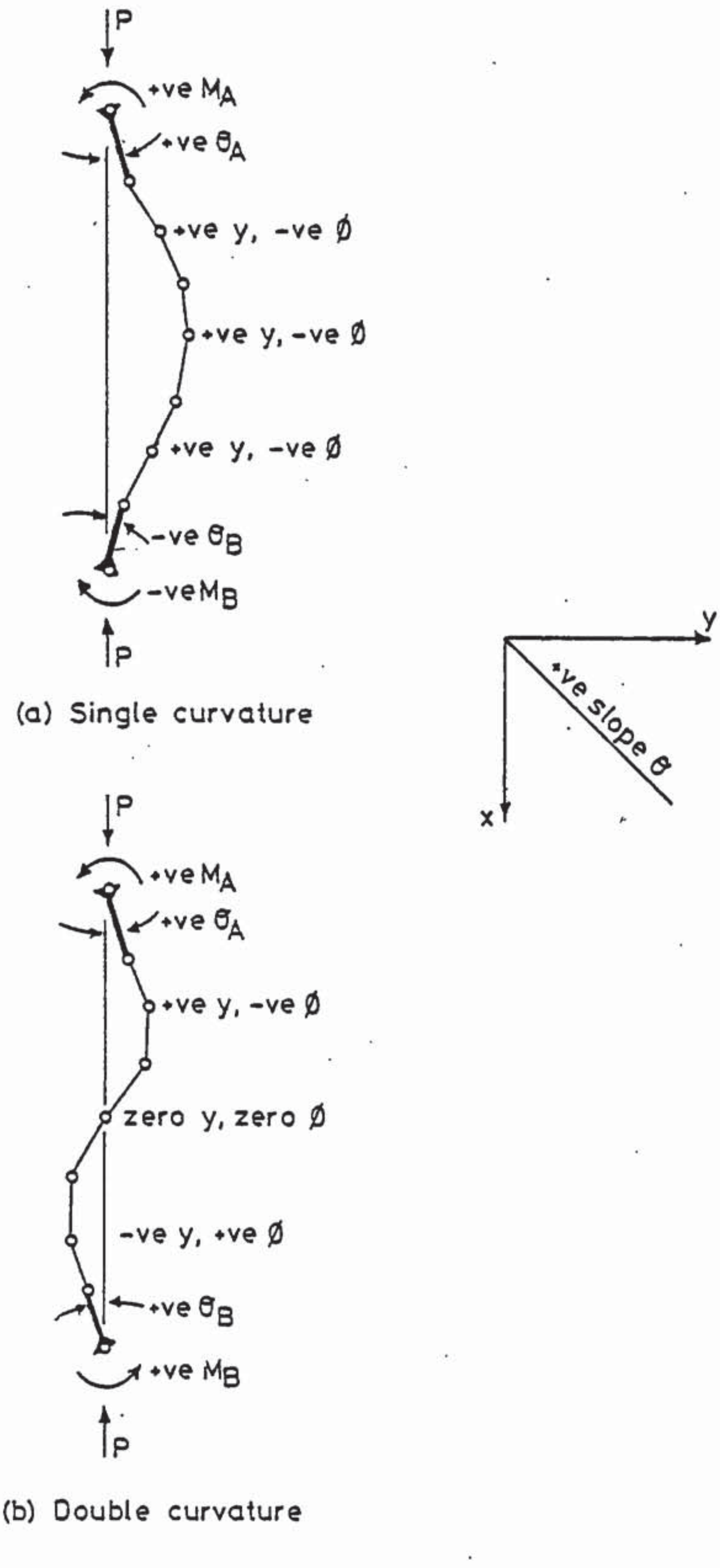

Figure 5.4 Column examples showing sign convention.

5.2.3 Method for Finding a Solution Corresponding to a Specified Load

5.2.3.1 General Description

The end loads on the column P, M_A and M_B are specified. The first step is to make proposals for the division point deflections denoted by $(y_0)_p$, $(y_1)_p$,...... $(y_r)_p$,...... $(y_n)_p$, and for the end slopes denoted by $(\theta_A)_p$ and $(\theta_B)_p$. Based on these proposals, division point moments, denoted by M_0, M_1,...... M_r,...... M_n, are calculated. This part of the procedure ensures that equilibrium conditions are satisfied.

The division point curvatures, denoted by ϕ_0, ϕ_1,...... ϕ_r,...... ϕ_n, are now calculated using a subsidary iterative procedure. From these curvatures calculated values are obtained for the division point deflections, denoted by $(y_0)_c$, $(y_1)_c$,...... $(y_r)_c$,...... $(y_n)_c$, and for end slopes, denoted by $(\theta_A)_c$ and $(\theta_B)_c$.

If the calculated values are the same as those initially proposed, compatability conditions are satisfied and a valid solution has been obtained. Normally this is not the case on the first iteration, and modifications to the proposals must be made and the procedure repeated until the compatability conditions are satisfied. The various steps in the procedure are now described in detail.

5.2.3.2 Calculation of Bending Moments

The proposed end slopes, $(\theta_A)_p$ and $(\theta_B)_p$, produce an induced restraining moment at the column ends, denoted by M_A and M_B, and an axial force P. The end moments are found from the appropriate M_R-θ relations, which are dependent upon the type of rotational restraint afforded to the column. The rotational restraint characteristics are covered in Chapter 6. The loads P, M_A and M_B are therefore specified, however, they vary with endslope.

The force system acting on the column length must now be considered, this is shown in Figure 5.3(c). The division point bending moments (calculated about the axis of the column) are given by:

$$M_r = -M_A + \frac{(M_A + M_B)(g_A + \sum_{r=0}^{r} \sqrt{(l_r^2 - ((y_r)_p - (y_{r-1})_p)^2)})}{L} - P(y_r)_p \qquad (5.1)$$

setting r = 0, 1,...... n. In equation (5.1) (and subsequently), l_0, which does not formally exist is taken as zero.

5.2.3.3 Calculation of Curvatures

The curvature must now be calculated at each division point corresponding to the appropriate loading worked out above. The procedure for division point r is desribed below.

The cross section is divided into k elements, small enough for the stresses in them to be assumed uniform. These elements, having areas a_1, a_2,...... a_k, have ordinates u_1, u_2,...... u_k, measured to the column axis as shown in Figure 5.5. 'u' values are taken as positive when the elements lie to the right of the column axis.

The loading on the cross section comprises an axial load, $(P_r)_s$, acting along the column axis, and a moment, $(M_r)_s$, where:

$$(P_r)_s = P \quad \text{and} \quad (M_r)_s = M_r \qquad (5.2)$$

The subscript, s, denotes specified values to distinguish them from the values calculated below.

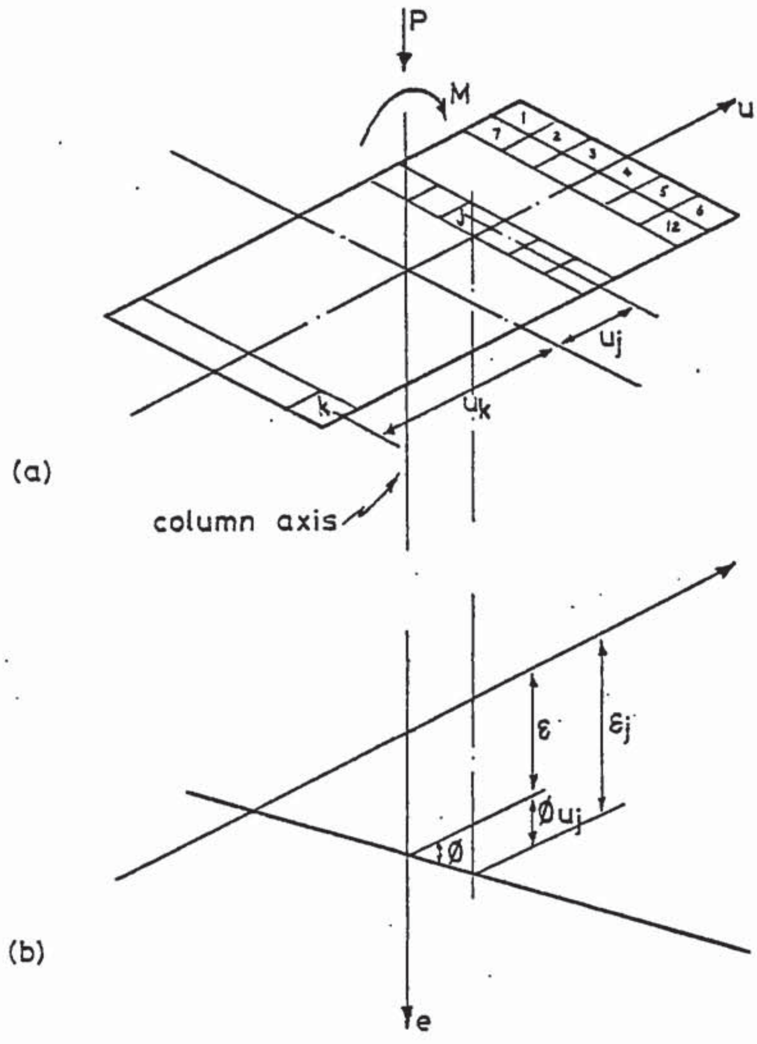

Figure 5.5 Idealization of cross-section.

The procedure is iterative, initial proposals being made for ε_r, the direct strain at the column axis and ϕ_r, the curvature. These proposals define the strain profile across the section, from which the calculated values of axial load and bending moment, denoted by $(P_r)_c$ and $(M_r)_c$ are obtained. If they are reasonably close to the specified values, the proposed values of ε_r and ϕ_r are taken as correct. If they are not within close limits, the proposals for ε_r and ϕ_r are modified and the procedure repeated. Full details are given below, the subscript r being omitted for convenience.

Referring to Figure 5.5, the total strain, ε_j, at the centre of the element j is given by:

$$\varepsilon_j = \varepsilon + \phi u_j \tag{5.3}$$

According to the Anderberg and Thelandersson total strain model, see Chapter 8, the total strain is given by:

$$\varepsilon_{tot} = \varepsilon_{th} + \varepsilon_\sigma + \varepsilon_{cr} + \varepsilon_{tr} \tag{5.4}$$

where: ε_σ is the instantaneous stress related strain,

ε_{th}, ε_{cr}, ε_{tr} are strain components due to the effects of exposure to fire.

Hence the instantaneous stress related strain is given by:

$$\varepsilon_{\sigma,j} = \varepsilon_j - (\varepsilon_{th} + \varepsilon_{cr} + \varepsilon_{tr})_j \tag{5.5}$$

where ε_{th}, ε_{cr} and ε_{tr} are calculated using the material behaviour models described in Chapter 8 and are dependent upon the individual elemental temperatures.

The corresponding stress, σ_j, is found by interpolation from the appropriate stress-strain relation described in Chapter 8, along with the corresponding value of tangent modulus, denoted by $(E_t)_j$, which is required later in the procedure. The stress-strain relation is also dependent upon the elemental temperature. When the stresses in all the elements have been found, P_c and M_c are given by:

$$P_c = \sum_{j=1}^{k} \sigma_j a_j$$
$$M_c = \sum_{j=1}^{k} \sigma_j a_j u_j \tag{5.6}$$

If P_c and M_c are close to P_s and M_s respectively, the proposed values for ε and ϕ are taken as correct. The magnitudes appropriate for the permissible differences are discussed in Section 5.2.3.9.

Normally, on the first iteration, P_c and M_c will not be close to P_s and M_s, and modifications to ε and ϕ must be made. The first step is to calculate α and β, defined as follows:

$$\alpha = P_c - P_s$$
$$\beta = M_c - M_s \tag{5.7}$$

However, P_s is not taken to be equal to P, the axial load applied, for all division points. The axial force acting on each segment length is determined from resolving verically at each division point, see Figure 5.6. P_s is given by:

$$P_s = P\cos\theta \tag{5.8}$$

where: θ is the slope of the segment length just below the division point.

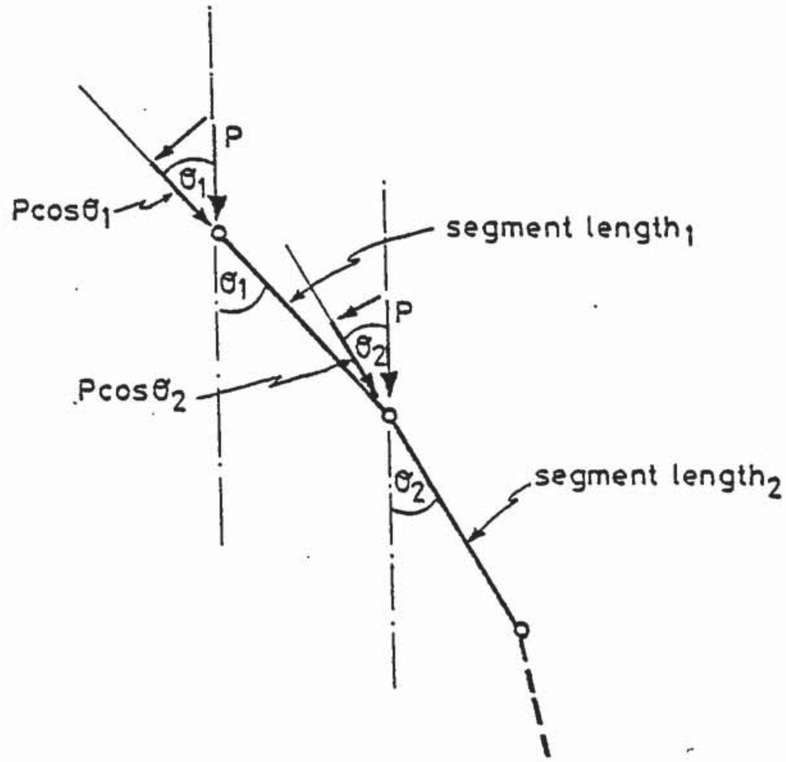

Figure 5.6 Variation of axial force due to axial load, throughout segment lengths.

The modifications to ε and ϕ must reduce α and β to zero on the next iteration. Denoting these modifications by ε_m and ϕ_m, the following pair of partial differential equations hold:

$$\frac{\partial\alpha}{\partial\varepsilon}\varepsilon_m + \frac{\partial\alpha}{\partial\phi}\phi_m = -\alpha$$

$$\frac{\partial\beta}{\partial\varepsilon}\varepsilon_m + \frac{\partial\beta}{\partial\phi}\phi_m = -\beta \tag{5.9}$$

Differentiating equation (5.7) gives:

$$\frac{\partial\alpha}{\partial\varepsilon} = \frac{\partial P_c}{\partial\varepsilon} \quad : \quad \frac{\partial\alpha}{\partial\phi} = \frac{\partial P_c}{\partial\phi}$$

$$\frac{\partial\beta}{\partial\varepsilon} = \frac{\partial M_c}{\partial\varepsilon} \quad : \quad \frac{\partial\beta}{\partial\phi} = \frac{\partial M_c}{\partial\phi} \tag{5.10}$$

The partial differentials on the right hand sides of equation (5.10) are determined by considering the effects of small changes in ε and ϕ on P_c and M_c. These small changes are denoted by $\delta\varepsilon$ and $\delta\phi$.

$\delta\varepsilon$ produces an increment of strain, $\delta\varepsilon$, at each element in the cross section. The corresponding stress changes at element j is thus $\delta\varepsilon(E_t)_j$. The resulting change, δP_c, in P_c is given by:

$$\delta P_c = \sum_{j=1}^{k}(E_t)_j a_j \delta\varepsilon$$

$$\text{i.e. } \frac{\partial P_c}{\partial\varepsilon} = \sum_{j=1}^{k}(E_t)_j a_j$$

$$\text{similarly, } \frac{\partial M_c}{\partial\varepsilon} = \sum_{j=1}^{k}(E_t)_j a_j u_j \tag{5.11}$$

$\delta\phi$ produces an increment of strain equal to $\delta\phi u_j$ at element j. The resulting change δP_c in P_c, in this case is given by:

$$\delta P_c = \sum_{j=1}^{k} (E_t)_j a_j u_j \delta\phi$$

$$\text{i.e. } \frac{\partial P_c}{\partial \phi} = \sum_{j=1}^{k} (E_t)_j a_j u_j \tag{5.12}$$

$$\text{similarly, } \frac{\partial M_c}{\partial \phi} = \sum_{j=1}^{k} (E_t)_j a_j u_j^2$$

Substituting in equations (5.9) and (5.10), and rewriting equation (5.8) in matrix form gives:

$$\begin{bmatrix} \sum_{j=1}^{k} (E_t)_j a_j & \sum_{j=1}^{k} (E_t)_j a_j u_j \\ \sum_{j=1}^{k} (E_t)_j a_j u_j & \sum_{j=1}^{k} (E_t)_j a_j u_j^2 \end{bmatrix} \begin{bmatrix} \varepsilon_m \\ \phi_m \end{bmatrix} = - \begin{bmatrix} \alpha \\ \beta \end{bmatrix} \tag{5.13}$$

Defining A as:

$$\begin{bmatrix} \sum_{j=1}^{k} (E_t)_j a_j & \sum_{j=1}^{k} (E_t)_j a_j u_j \\ \sum_{j=1}^{k} (E_t)_j a_j u_j & \sum_{j=1}^{k} (E_t)_j a_j u_j^2 \end{bmatrix} \tag{5.14}$$

equation (5.13) can be rewritten as:

$$\begin{bmatrix} \varepsilon_m \\ \phi_m \end{bmatrix} = - A^{-1} \begin{bmatrix} \alpha \\ \beta \end{bmatrix} \tag{5.15}$$

Using equation (5.15), ε_m and ϕ_m are obtained. Denoting the proposed values of direct strain and curvature for the current iteration by ε_i and ϕ_i, those appropriate to the next iteration, i+1, are given by:

$$\begin{aligned} \varepsilon_{i+1} &= \varepsilon_i + \varepsilon_m \\ \phi_{i+1} &= \phi_i + \phi_m \end{aligned} \tag{5.16}$$

Using these modified values the procedure is repeated.

Figure 5.7 gives a flow diagram for the sequence of calculations described above.

While the cross section remains linearly elastic, the values of tangent modulus E_t appearing in equations (5.11) and (5.12) will remain constant, with the result that equation (5.15) will be exact. In such cases only one modification will be required to give the correct values for ε and ϕ. When the non-linear range is entered, however, the values of E_t for the relevant elements will vary as ε and ϕ vary, with the result that equation (5.15) will become approximate. Several iterations through the procedure may then be necessary. It should be noted that there is no guarantee that the procedure will converge to a solution, some discussion on this point is given in Section 5.2.3.9.

5.2.3.4 Calculation of Deflections

The deflections are obtained by double integration of the curvatures, making allowance for the initial deflections c_0, c_1,..... c_n. It is assumed that under zero load the segments are straight, this means that there may be changes in slope at each division point, denoted by γ_1, γ_2,..... γ_r,..... γ_n. These changes are given by:

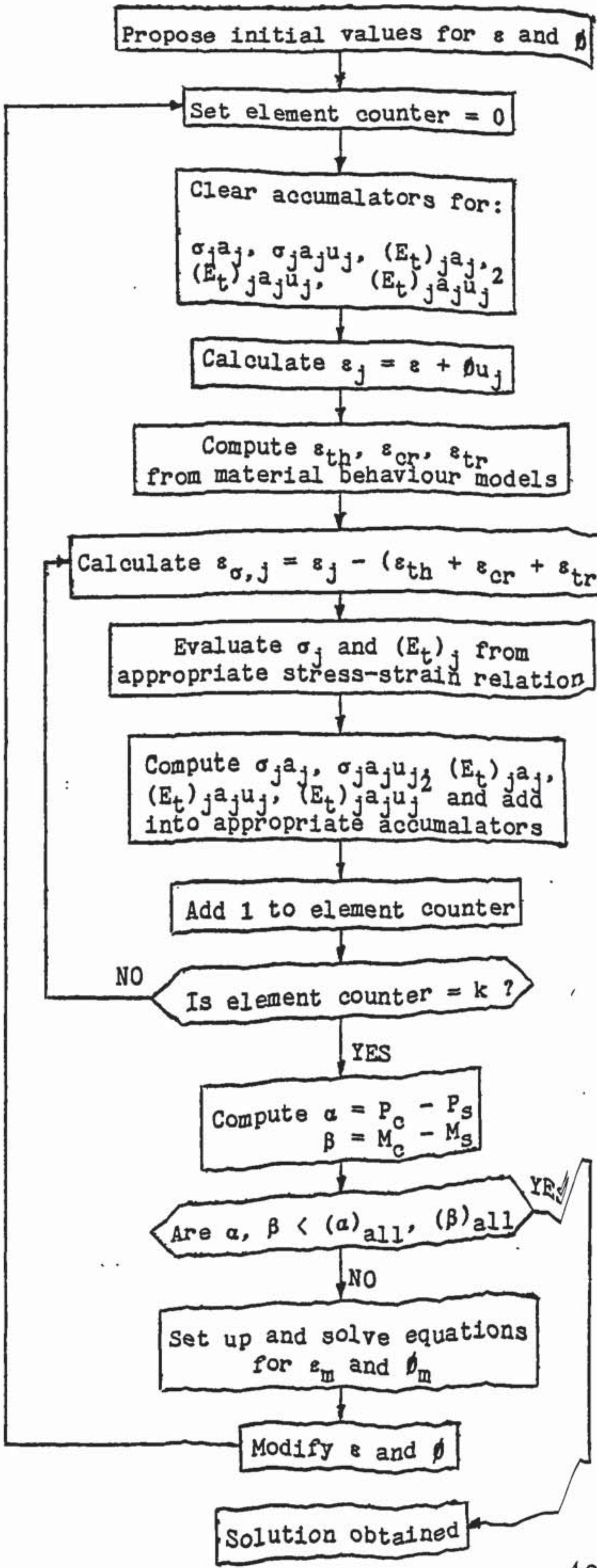

Figure 5.7 Flow diagram for curvature calculation

Changes γ_1 to γ_{n-1} are given by:

$$\gamma_0 = \frac{c_1 - c_0}{l_1} - \frac{c_0}{g_A} \tag{5.17}$$

$$\gamma_r = \frac{c_{r+1} - c_r}{l_{r+1}} - \frac{c_r - c_{r-1}}{l_r} \tag{5.18}$$

setting r = 1, 2,..... n-1.

γ_n is given by:

$$\gamma_n = \frac{-c_n}{g_B} - \frac{c_n - c_{n-1}}{l_n} \tag{5.19}$$

In the special case where a segment length or gusset length is equal to zero, the slopes of such lengths are taken as zero.

The deflections are calculated starting at end A and working along the column. Provisional slopes, denoted by θ'_0, θ'_1,..... θ'_r,..... θ'_n, θ'_B, and deflections, denoted by y'_0, y'_1,..... y'_r, ... y'_n, y'_B are calculated taking the slope at end A equal to $(\theta_A)_p$. y'_B should be equal to zero, and if this is not the case corrections are applied to give final calculated deflections and end slopes.

Referring to Figure 5.8 it will be seen that:

$$\begin{aligned} \theta'_0 &= (\theta_A)_p + \gamma_0 \\ y'_0 &= (\theta_A)_p g_A \end{aligned} \tag{5.20}$$

θ'_1..... θ'_n and y'_1..... y'_n are obtained from the following recurrence formulae, setting r = 1, 2,..... n:

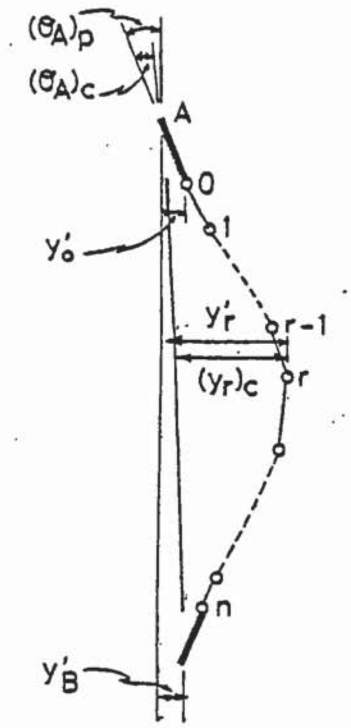

Figure 5.8 Deformation of column.

$$\theta'_r = \theta'_{r-1} + \frac{(\phi_{r-1} + \phi_r)l_r}{2} + \gamma_r$$

(5.21)

$$y'_r = y'_{r-1} + \theta'_{r-1}l_r + \frac{l_r^2(2\phi_{r-1} + \phi_r)}{6}$$

These formulae are based on the assumption that the curvature varies linearly between division points. θ'_B and y'_B are given by:

$$\theta'_B = \theta'_n$$

(5.22)

$$y'_B = y'_n + \theta'_n g_B$$

The corrected, i.e. calculated deflections are given by:

$$(y_r)_c = y'_r - \frac{y'_B(g_A + \sum_{r=0} l_r)}{L} \tag{5.23}$$

setting r = 0, 1,..... n. The calculated end slopes are given by:

$$(\theta_A)_c = (\theta_A)_p - \frac{y'_B}{L}$$

(5.24)

$$(\theta_B)_c = \theta'_B - \frac{y'_B}{L}$$

5.2.3.5 Checking Compatability Conditions

When the deflected shape has been calculated as outlined in the preceding section the compatability conditions must be checked. This is done in two stages, the first of which involves the calculation of the incompatabilities in end slopes, as follows:

$$\xi_1 = (\theta_A)_c - (\theta_A)_p$$

(5.25)

$$\xi_2 = (\theta_B)_c - (\theta_B)_p$$

For a valid solution, ξ_1 and ξ_2 should be less than their allowable values, and if this is not the case the procedure described in Section 5.2.3.6 is followed to produce modified values for $(\theta_A)_p$ and $(\theta_B)_p$. When modified values for $(\theta_A)_p$ and $(\theta_B)_p$ have been produced, a new iteration is begun by returning to calculate division point bending moments as described in Section 5.2.3.2.

Where ξ_1 and ξ_2 are acceptable, the second stage of checking is carried out, involving the comparison between the proposed and calculated division point deflections. The incompatabilities in deflection are calculated using the following equation:

$$\xi_{yr} = (y_r)_c - (y_r)_p \tag{5.26}$$

setting $r = 0, 1, \ldots\ldots n$.

If these values are below a given allowable value a valid solution has been obtained, if not, the procedure described in Section 5.2.3.7 is entered to produce modified values for $(y_0)_p$, $(y_1)_p, \ldots\ldots$ $(y_n)_p$.

The selection of appropriate values for the various incompatabilities is discussed in Section 5.2.3.9.

5.2.3.6 Modifications to Proposed End Slopes

The procedure in this Section is applied where ξ_1 and ξ_2 are not below their allowable values. The modifications to $(\theta_A)_p$ and $(\theta_B)_p$ must therefore be such that, on repeating the procedure, ξ_1 and ξ_2 are reduced to zero. Denoting the modifications by $(\theta_A)_{pm}$ and $(\theta_B)_{pm}$, the following set of equations hold:

$$\frac{\partial \xi_1}{\partial(\theta_A)_p}(\theta_A)_{pm} + \frac{\partial \xi_1}{\partial(\theta_B)_p}(\theta_B)_{pm} = -\xi_1$$

$$\frac{\partial \xi_2}{\partial(\theta_A)_p}(\theta_A)_{pm} + \frac{\partial \xi_2}{\partial(\theta_B)_p}(\theta_B)_{pm} = -\xi_2 \tag{5.27}$$

The partial differentials in equation (5.27) are found by considering the effects of small independent changes in $(\theta_A')_p$ and $(\theta_B')_p$, denoted by Δ_1 and Δ_2 respectively.

The effects of Δ_1, a small independent change in $(\theta_A')_p$, will now be discussed. The column end moments will be affected by Δ_1. From consideration of moment rotation relations it follows that:

$$(M_A)_{\Delta_1} = \Delta_1 \frac{dM_A}{d\theta_A'}$$

$$(M_B)_{\Delta_1} = 0 \tag{5.28}$$

where: $dM_A/d\theta_A'$ is the slope of the M_A-θ_A diagram when $\theta_A' = (\theta_A')_p$.

Δ_1 is used as a subscript to denote changes in quantities due to Δ_1.

The changes in axial load at each division point are given by:

$$(P_r)_{\Delta_1} = P_{\Delta_1} \tag{5.29}$$

$$P_{\Delta_1} = -6\Delta_1 K_2/L_2 \tag{5.30}$$

See Chapter 6 and Appendix B for derivation of equation (5.30).

Note: K_2, the stiffness of the top restraint beam, is adjusted with the formation of plastic hinges.

The changes in division point bending moments are given by:

$$(M_r)_{\Delta_1} = -(M_A)_{\Delta_1} + \frac{((M_A)_{\Delta_1} + (M_B)_{\Delta_1})(g_A + \sum_{r=0}^{r} \sqrt{(l_r^2 - ((y_r)_p - (y_{r-1})_p)^2)}}{L} - P_{\Delta_1}(y_r)_p \tag{5.31}$$

setting r = 0, 1,..... n.

The task now is to determine the changes in division point curvature that result from the changes in division point loading. These can be conveniently assessed by reference to equation (5.15) used in the calculation of curvature. Substituting from equations (5.7) and restoring the subscript r, equation (5.14) becomes:

$$\begin{bmatrix} (\varepsilon_r)_m \\ (\phi_r)_m \end{bmatrix} = A_r^{-1} \begin{bmatrix} (P_r)_s - (P_r)_c \\ (M_r)_s - (M_r)_c \end{bmatrix} \tag{5.32}$$

This equation, as it stands, gives the modifications to ε_r and ϕ_r required to bring the calculated values of P_r and M_r equal to the specified values. It can also be interpreted as giving the changes in ε_r and ϕ_r which will result from applying changes in P_r and M_r equal to $(P_r)_s - (P_r)_c$ and $(M_r)_s - (M_r)_c$ respectively. Thus the following equation holds:

$$\begin{bmatrix} (\varepsilon_r)_{\Delta_1} \\ (\phi_r)_{\Delta_1} \end{bmatrix} = A_r^{-1} \begin{bmatrix} (P_r)_{\Delta_1} \\ (M_r)_{\Delta_1} \end{bmatrix} \tag{5.33}$$

Applying equations (5.30) to (5.33) to division points 0, 1,..... n gives the required change in curvature $(\phi_0)_{\Delta_1}$, $(\phi_1)_{\Delta_1}$,..... $(\phi_n)_{\Delta_1}$.

The changes induced in ξ_1 and ξ_2 by these changes in curvature are now assessed. The changes in curvature are then added to the curvatures originally calculated, giving changed curvatures as follows:

$$\phi_r^{\Delta_1} = \phi_r + (\phi_r)_{\Delta_1} \tag{5.34}$$

where: Δ_1 is used as a superscript to denote changed quantities.
The procedure described previously to calculate deflections, Section 5.2.3.4, is then used to give calculated deflections and end slopes based on the curvatures given by equation (5.34). These deflections and endslopes are denoted by $(y_0)_c^{\Delta_1}$, $(y_1)_c^{\Delta_1}$,...... $(y_n)_c^{\Delta_1}$, and $(\theta_A)_c^{\Delta_1}$, $(\theta_B)_c^{\Delta_1}$ respectively. The incompatabilities, taking account of Δ_1 are thus as follows:

$$\begin{aligned} \xi_1^{\Delta_1} &= (\theta_A)_c^{\Delta_1} - ((\theta_A)_p + \Delta_1) \\ \xi_2^{\Delta_1} &= (\theta_B)_c^{\Delta_1} - (\theta_B)_p \end{aligned} \tag{5.35}$$

and plainly:

$$\begin{aligned} \frac{\partial \xi_1}{\partial (\theta_A)_p} &= \frac{\xi_1^{\Delta_1} - \xi_1}{\Delta_1} \\ \frac{\partial \xi_2}{\partial (\theta_A)_p} &= \frac{\xi_2^{\Delta_1} - \xi_2}{\Delta_1} \end{aligned} \tag{5.36}$$

The effects of Δ_2 are studied in a manner similar to that used for Δ_1, and enable the two remaining partial differentials in equation (5.27) to be found.

Equations (5.27) are now solved for $(\theta_A)_{pm}$ and $(\theta_B)_{pm}$. Denoting the proposals for the previous iteration by $(\theta_A)_{p,i}$ and $(\theta_B)_{p,i}$, those appropriate to the next iteration are given by:

$$
\begin{aligned}
(\theta_A)_{p,i+1} &= (\theta_A)_{p,i} + (\theta_A)_{pm} \\
(\theta_B)_{p,i+1} &= (\theta_B)_{p,i} + (\theta_B)_{pm}
\end{aligned}
\tag{5.37}
$$

A new iteration is begun by returning to calculate division point bending moments.

A slightly different procedure must be followed for the modifications to end slopes for a pin ended column. Consider first the effects of Δ_1. Any change in endslope will not effect the applied loading i.e. $(M_A)_{\Delta 1} = 0$, $(M_B)_{\Delta 1} = 0$ and $(P_r)_{\Delta 1} = 0$, and therefore the change in curvature $(\phi_r)_{\Delta 1}$ will be zero. To overcome this it is necessary to consider the induced change in division point deflections that result from a change in end slope, in order to be able to evaluate the change in moment at each division point due to the second order effect of axial load eccentricity. Subsequently on application of equations (5.30) to (5.33) the change in curvature $(\phi_r)_{\Delta_1}$ corresponding to a change in end slope Δ_1 will not be zero.

The change in division point deflections $(y_r)_{\Delta_1}$ corresponding to the change in end slope Δ_1 are given by the following equation derived in full in Appendix G:

$$
(y_r)_{\Delta_1} = \frac{3\Delta_1}{L}\left[\frac{x_r^3}{6L} - \frac{x_r^2}{2} + \frac{Lx_r}{3}\right] \tag{5.38}
$$

where: $x_r = g_A + \sum_{r=0}^{r} l_r$

The effects of Δ_2 are studied in a similar manner to that for Δ_1.

A further problem arises for a pin ended column in that the partial differential equation (5.27) is insoluable due to symmetry since $(\theta_A)_p = -(\theta_B)_p$ and $(\theta_A)_{pm} = -(\theta_B)_{pm}$ and therefore the determinate of the partial differentials is zero i.e.

$$\det \begin{bmatrix} \dfrac{\partial \xi_1}{\partial (\theta_A)_p} & \dfrac{\partial \xi_1}{\partial (\theta_B)_p} \\[2ex] \dfrac{\partial \xi_2}{\partial (\theta_A)_p} & \dfrac{\partial \xi_2}{\partial (\theta_B)_p} \end{bmatrix} = 0 \tag{5.39}$$

However by making use of the symmetry it follows that:

$$\frac{\partial \xi_1}{\partial (\theta_A)_p} (\theta_A)_{pm} - \frac{\partial \xi_1}{\partial (\theta_B)_p} (\theta_A)_{pm} = -\xi_1 \tag{5.40}$$

Rearranging equation (5.40) yields an equation for $(\theta_A)_{pm}$:

$$(\theta_A)_{pm} = -\xi_1 \Bigg/ \left[\frac{\partial \xi_1}{\partial (\theta_A)_p} - \frac{\partial \xi_1}{\partial (\theta_B)_p} \right] \tag{5.41}$$

and $(\theta_B)_{pm}$ is given by:

$$(\theta_B)_{pm} = -(\theta_A)_{pm} \tag{5.42}$$

The proposals for the end slopes appropriate to the next iteration are given by equation (5.37). Before starting a new iteration by returning to calculate division point bending moments it is, however, necessary to adjust the proposed division point deflections $(y_r)_p$ through the application of equation (5.38) for the changes in end slope $(\theta_A)_{pm}$ and $(\theta_B)_{pm}$.

5.2.3.7 Modifications to Proposed Deflections

This procedure is only carried out when ξ_1 and ξ_2 are below the allowable limits and when the calculated and proposed division point deflections do not agree.

The modification procedure adopted is to take the previously calculated deflections as the proposals for the next iteration, i.e.:

$$(y_r)_{p,i+1} = (y_r)_{c,i} \tag{5.43}$$

It is, however, necessary to check the analysis is converging to a solution, since, if loads are specified which are beyond the capacity of the column, the calculated deflections will always exceed those proposed.

In order to carry out the check it is convenient to calculate the quantity H, defined as follows:

$$H = \sum_{r=0}^{n} \left| \xi_{yr} \right| \tag{5.44}$$

and compare it with H', the quantity calculated the previous time the deflections were modified.

If $H > H'$, a solution under the specified loading will normally not exist. Where $H < H'$, a solution may exist and a start can be made on the next iteration. A new iteration is begun by returning to calculate the division point bending moments.

5.2.3.8 Flow Diagram

Figure 5.9 gives the flow diagram illustrating the detailed sequence of the calculation for analysis under specified load.

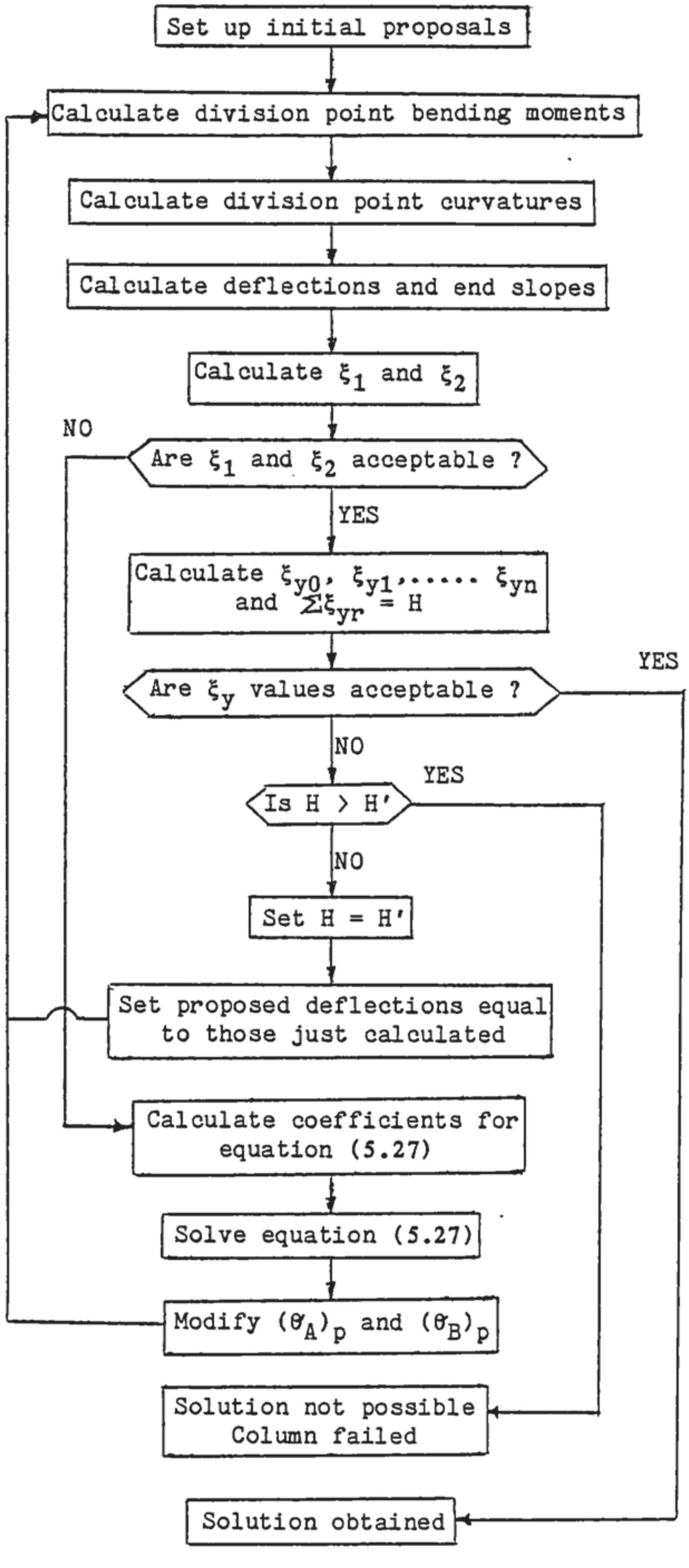

Figure 5.9 Flow diagram for analysis under specified load.

5.2.3.9 Accuracy and Convergence

Errors can arise on two counts: firstly from the idealizations made in the analysis, namely the idealization of the division point cross sections into elements in which the stresses are assumed to be uniform, and the assumption that the curvature varies linearly between division points, and secondly from the magnitudes of the incompatabilities allowed in the various iterative procedures. However, errors due to the idealization of the cross section and the assumption of linear variation of curvature will not seriously effect the overall analysis. These points are discussed in detail in Cranston (1967).

Values must be specified for the curvature calculation incompatabilities, denoted by $(\alpha)_{all}$ and $(\beta)_{all}$, incompatabilities in end rotation, denoted by $(\xi_1)_{all}$ and $(\xi_2)_{all}$, and incompatabilities in the division point deflections, denoted by $(\xi_y)_{all}$. To ensure accuracy of the response of the idealized cross section in the curvature calculation α_{all} and β_{all} may have to be 10^{-5} or 10^{-6} times the values of P and M respectively. Providing $(\xi_1)_{all}$ and $(\xi_2)_{all}$ are given a percentage value of the actual values of θ_A and θ_B errors will be less than that percentage.

It is necessary to ensure that the values selected for $(\xi_1)_{all}$ and $(\xi_2)_{all}$ are greater than the errors which arise from the inaccuracies tolerated in the curvature calculation. It is necessary, in turn, to ensure that the value selected for $(\xi_y)_{all}$ is greater than the errors which arise from the values selected for $(\xi_1)_{all}$ and $(\xi_2)_{all}$.

The allowable incompatabilities must not, of course, be smaller than the level of agreement numerically possible in the computer being used. The allowable values selected for the various incompatabilities in the computer program written by Cranston (1967) are below.

$(\alpha)_{all}$: 10^{-6} x maximum expected value of P

$(\beta)_{all}$: 10^{-6} x maximum expected value of M

$(\xi_1)_{all}$: 10^{-3} x maximum expected value of θ_A

$(\xi_2)_{all}$: 10^{-3} x maximum expected value of θ_B

$(\xi_y)_{all}$: 10^{-2} x maximum expected division point deflection.

The values chosen by Cranston are for the non fire situation. From experience it has been found that when applying the structural analysis to the fire situation the values for $(\alpha)_{all}$ and $(\beta)_{all}$ selected by Cranston were too fine. The most satisfactory results were obtained setting the latter incompatabilities as follows:

$(\alpha)_{all}$: 10^{-2} - 10^{-3} x maximum value of P

$(\beta)_{all}$: 10^{-2} - 10^{-3} x maximum value of M

The incompatabilities are read in as part of the initial data.

The convergence of the procedure to calculate the curvature and axial strain corresponding to a given P and M is dependent on the validity of equation (5.15) and the convergene of the procedure to give correct proposals for the end slopes is dependent on the validity of equation (5.27). Both these equations become approximate when the non-linear range is entered. If the stiffness of the section becomes very small or loads are proposed beyond the capacity of the section, the procedure will be unable to converge to a solution.

The convergence of the procedure to give correct proposals for division point deflections is dependent on the validity of the substitution equation (5.43). The procedure should converge to a solution quickly. However, it is possible to reach an unstable solution when the applied loads do not excite the mode of deflection associated with the minimum critical buckling load.

5.3 Axial Symmetry of Analysis

For uniaxial bending of the column, there is axial symmetry of the analysis and therefore only half the column section need be considered for the calculation of element temperatures (FIRES-T) and element stresses and strains (SAFE-RCC).

Consider Figure 5.10, elements X and X' are subject to the same temperature regime and the same bending stresses since the section is bent about the XX axis, thus the forces in the elements will be the same, (for a column exposed to heating on three sides as shown).

The following Chapter, Chapter 6, describes the model of restraint. Models of rotational restraint and axial restraint are presented in the Chapter.

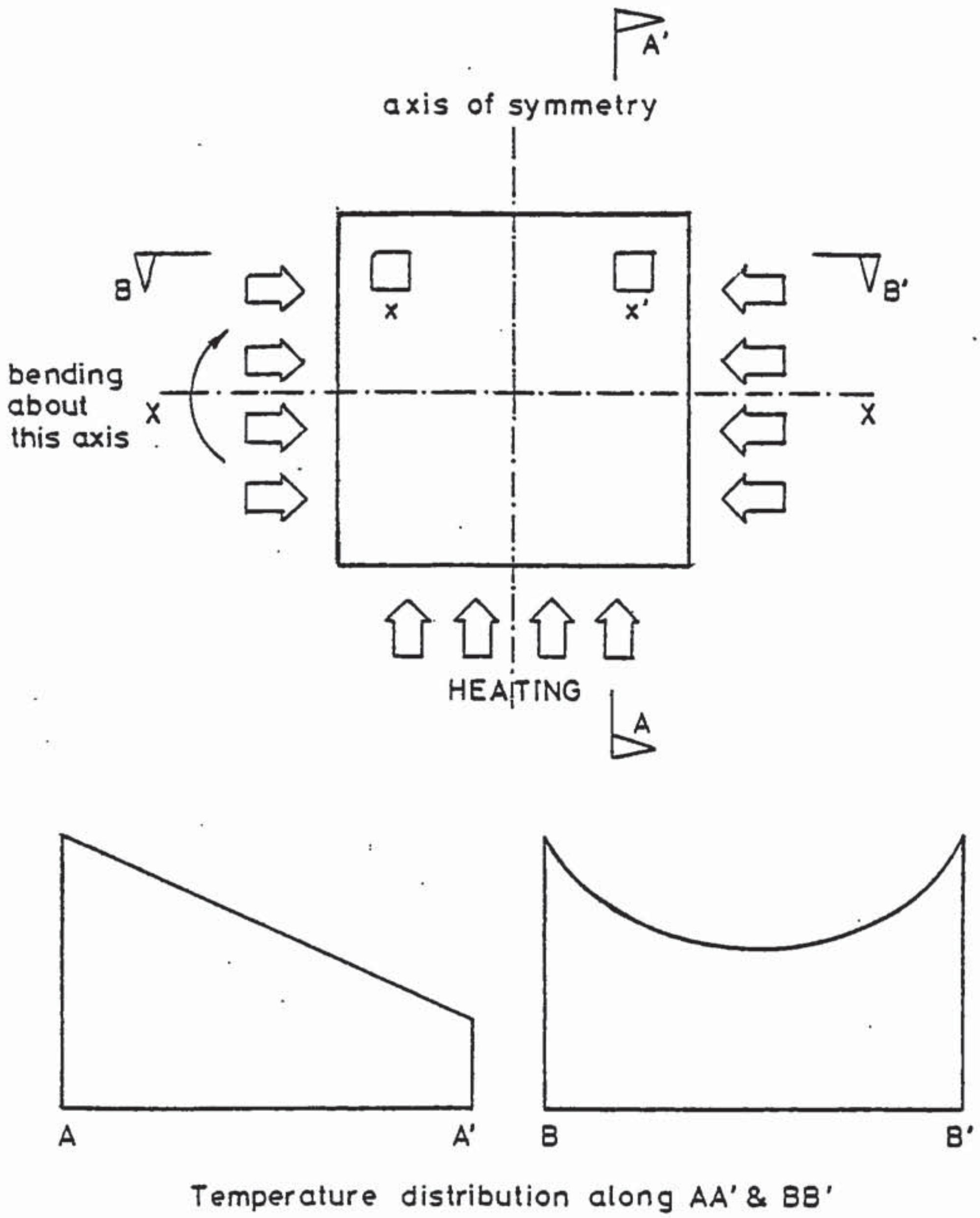

Figure 5.10 Symmetry of analysis for uniaxial bending of column heated on three sides.

CHAPTER 6

STRUCTURAL IDEALIZATION OF THE RESTRAINT SYSTEM

6.1 Introduction

Dougill (1972a, 1972b) suggested that axial restraint and rotational restraint should be evaluated separately for a realistic model of restraint and should not be considered in a combined parameter. The model of restraint incorporated in the computer program SAFE-RCC considers the axial restraint and rotational restraint as independent parameters.

6.2 Rotational Restraint

6.2.1 Moment-Rotation Relations

The rotational restraint afforded to the column is calculated from consideration of moment-rotation relationships and is based on the principle that the end slopes, or change in end slopes, of the column produce an induced restraining moment. The problem is to establish a moment-rotation relationship for the restraint system.

A typical moment-rotation relation, taken from Taylor (1974), for a reinforced concrete beam to column joint is presented in Figure 6.1 and shows the rotation θ increasing with the applied moment M. The actual moment-rotation diagram indicates only small deformations occurring prior to the concrete attaining the moment where the first crack occurs. At design load the deformations are larger but still nearly linear between M_C and M_D. As the plastic moment is approached much larger deformations occur and with the additional load a peak is reached after which the load cannot keep up with the displacements and the typical falling branch results. The falling branch behaviour may be due to material behaviour or inertia of the testing system or a combination of both. To simplify the analysis the curve can be idealized to a bi-linear relation.

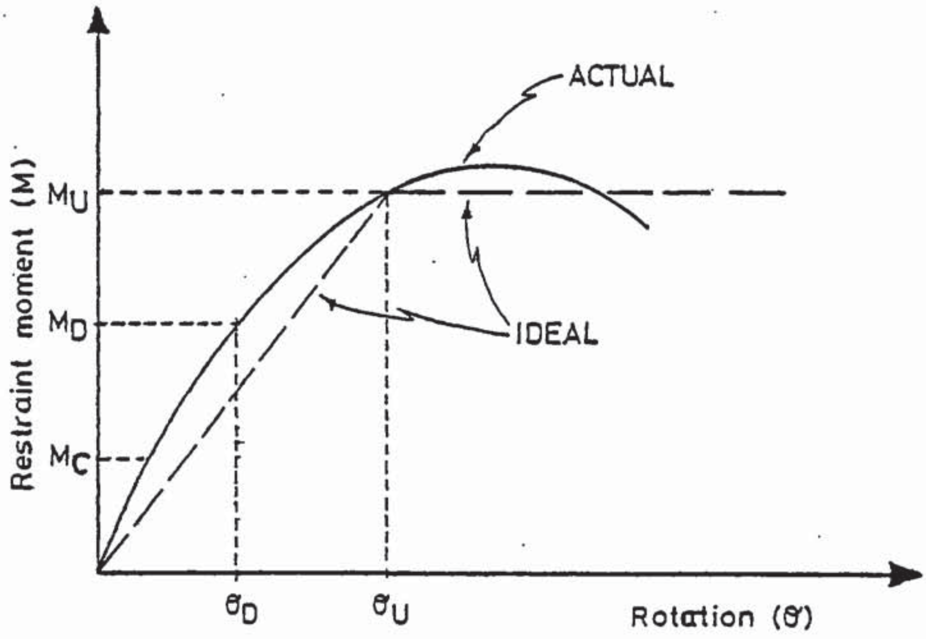

Figure 6.1 Typical moment-rotation relationship.

$M=0$ $\theta=0$
$M=M_C$ θ small - linear
$M=M_D$ $\theta=\theta_D$ - near linear
$M=M_U$ $\theta=\theta_U \rightarrow \infty$ hinge

(Taylor (1974))

The structural system idealization analysed in this research is shown in Figure 6.2. It is assumed that the column exposed to fire is an external column. From consideration of Figure 6.2 it can be seen that the combined moment-rotation relation for joint A, or joint B, is comprised from the moment-rotation characteristics for all the adjoining members at that joint. Hence the moment-rotation relation for the joint is more complex than that for the simple reinforced concrete beam to column joint described above and is determined from the consideration of slope deflection equations.

The stuctural analysis used by SAFE-RCC requires not only a resulting induced restraining moment for a particular end slope, or change in end slope, but also the gradient of the moment-rotation relation corresponding to the particular rotation.

6.2.2 Normal Rotational Restraint

Normal rotational restraint is a model that attempts to model realistic structural conditions of restraint and continuity, and as such is likely to produce values of restraint more likely to be encountered by a column in a real structure.

Previous researchers have only considered a limited model of restraint. The type of boundary conditions common to many analysis programs are either:

i) the use of constant linear spring models,

or ii) the imposition of fixed or pinned boundary conditions,

neither of which are likely to occur in a real structure.

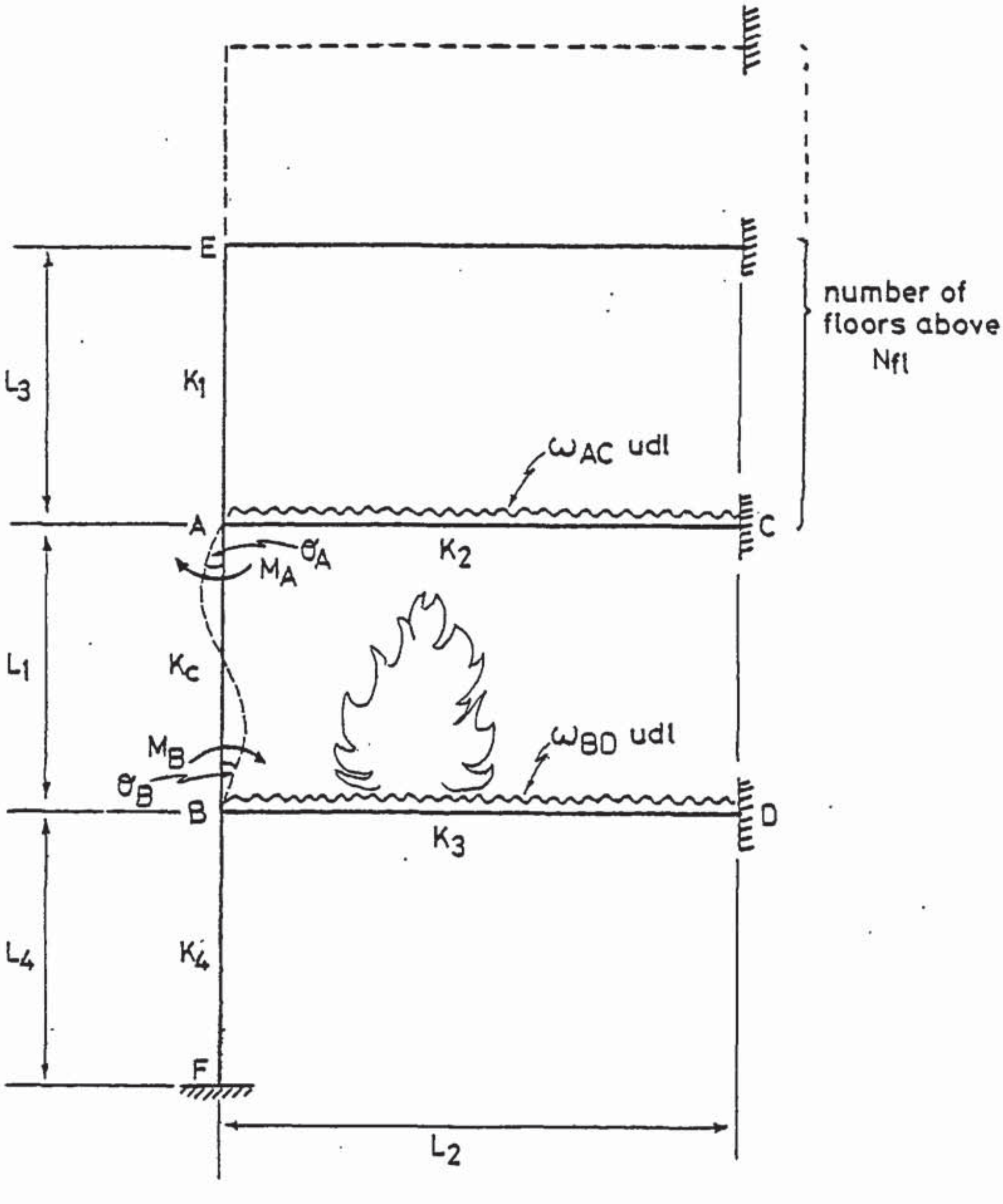

Figure 6.2 Structural system analysed.

SAFE-RCC allows the option of the restraint system being either isolated from the fire or affected by the fire. It will be the restraint beams (beams AC and BD, Figure 6.2) that will be exposed to the full effects of the fire, the columns above and below the column under analysis (columns AE and BF, Figure 6.2) are assumed not to be affected by the fire since they are relatively far removed from the fire and are insulated from the fire by the restraint beams.

The effect of temperature on the moment-rotation relation for a typical beam to column joint is for the ultimate restraining moment and slope of the moment-rotation relation to decrease with increasing temperature. A typical idealized curve has been plotted in Figure 6.3.

Therefore the column exposed to fire may be subject to moment-rotation relations composed of constant M-θ relations from the columns above and below not exposed to fire, and from variable M-θ relations from the beams exposed to fire.

The detailed slope deflection analysis of the structural system is presented in Appendix B. The basic moment-rotation relation for the structure at joint A is given by:

$$M_A = -\,(4K_1\theta_A + 4K_2\theta_A + M_{ac}) \qquad (6.1)$$

where: M_A is the moment induced in the column under analysis at joint A,

θ_A is the end slope at joint A,

M_{ac} is the fixed end moment = $\omega_{AC}L_2^2/12$

K_1 and K_2 are the stiffnesses of the adjoining members at joint A defined as EI/L,

ω_{AC}, L_2, K_1 and K_2 are defined in Figure 6.2.

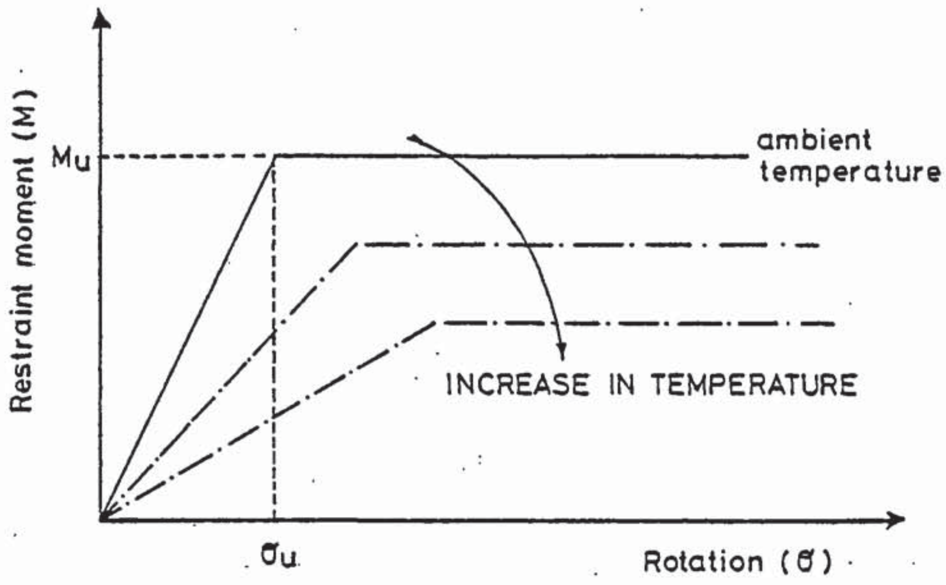

Figure 6.3 Variation of moment - rotation relationship with temperature.

The slope of the moment-rotation relation is given by:

$$\frac{dM_A}{d\theta_A} = -\ (4K_1 + 4K_2) \tag{6.2}$$

The axial load, P, acting on the column under analysis will also vary with the end slope and is calculated from the following equation:

$$P = \frac{\omega_{AC}L_2}{2} - \frac{6K_2\theta_A}{L_2} \tag{6.3}$$

The derivation of equation (6.3) is presented in Appendix B.

Similar equations can be derived for joint B. The basic moment-rotation relation for the structure at joint B is given by:

$$M_B = -\ (4K_3\theta_B + 4K_4\theta_B + M_{bd}) \tag{6.4}$$

where: M_B is the moment induced in the column under analysis at joint B,

θ_B is the slope at joint B,

M_{bd} is the fixed end moment = $\omega_{BD}L_2^2/12$

K_3 and K_4 are the stiffnesses of the adjoining members at joint B,

ω_{BD}, K_3 and K_4 are defined in Figure 6.2.

The slope of the moment-rotation relation at joint B is given by:

$$\frac{dM_B}{d\theta_B} = -\ (4K_3 + 4K_4) \tag{6.5}$$

The member stiffnesses, K, present in equations (6.1), (6.2), (6.3), (6.4) and (6.5) are determined from the equation:

$$K = EI/L \tag{6.6}$$

where: E is the initial tangent modulus of the concrete stress-strain relation,

I is the transformed second moment of area calculated according to Section 7.8,

L is the length of the member.

The initial tangent modulus of the concrete stress-strain relation used in this research, see Chapter 8, is given by:

$$E = \exp(1)\ \frac{\sigma_{max}}{\varepsilon_{max}} \tag{6.7}$$

where: σ_{max} is the temperature dependent concrete peak stress,

ε_{max} is the strain at peak stress.

Equation (6.6) can only be used for the calculation of restraint system member stiffness while the structure remains elastic, that is while no plastic hinges have formed.

6.2.2.1 Formation of Plastic Hinges

As the fire progresses and a resulting redistribution of moments occur due to decreasing member stiffness it is possible that a moment at a particular point in the structural system analysed will exceed the ultimate moment capacity of the section at that point. It is assumed that when a bending moment at a section reaches the ultimate moment capacity, Mu, failure does not occur but a hinge-like rotation takes place without any further increase of bending moment at that section.

Any formation of a plastic hinge as described above will affect the stiffness of the surrounding structure affording restraint to the column under analysis. At each time step during the analysis it is therefore necessary to check whether the current redistribution of moments results in the yield criterion being not satisfied at any point in the structure.

To simplify the analysis, hinges in the restraint beam will be assumed to occur at either end or midspan. This latter is not strictly correct as the exact hinge position will depend on the relative values of end moments. The error however, caused by this assumption will normally be small. The possible hinge positions are indicated in Figure 6.4. Once a plastic hinge has formed an appropriate plastic analysis is carried out using complimentary energy, as described in Section 6.2.2.4, to determine the stiffness of the remaining structure.

SAFE-RCC, as previously described, includes the option for a temperature dependent or temperature independent restraint system. If the temperature independent restraint system is present then the ultimate moment capacities of the restraint system sections remain constant throughout the duration of the fire. If the temperature dependent restraint system is present then the ultimate moment capacities of the restraint beam sections will vary as the fire temperature increases. Since there is an increase in concrete strength early in a fire the ultimate moment capacity will initially increase. As the concrete strength reduces with further increase in temperature there will be a subsequent reduction in the ultimate moment capacity of the section.

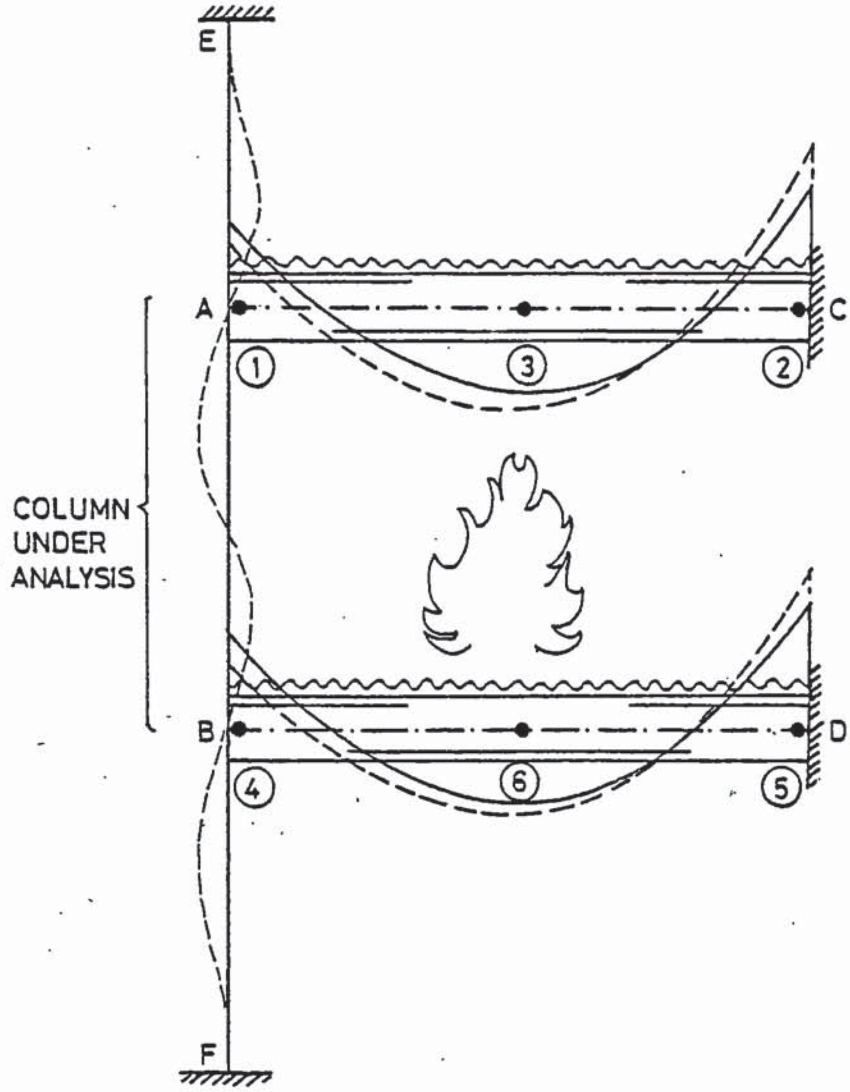

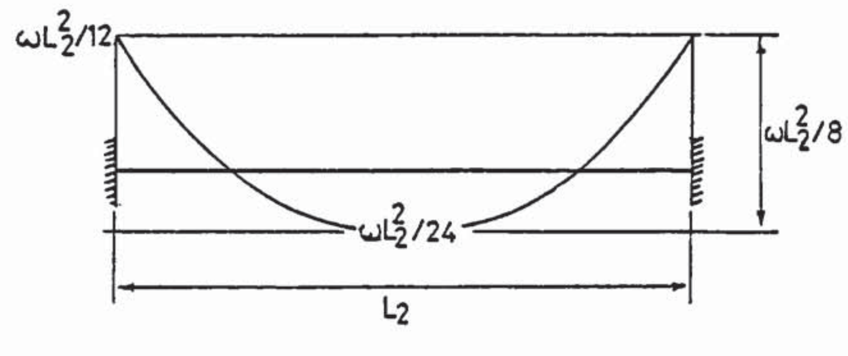

Figure 6.4 Redistribution of moments and most likely positions for formation of plastic hinges in restraint system.

When the temperature dependent restraint system is present the ultimate moment capacities of the restraint beam are calculated according to the auxillary analysis described in Section 6.2.2.5.

6.2.2.2 Order of Formation of Plastic Hinges

Consider the top restraint beam AC in Figure 6.4 and assume there is temperature dependent rotational restraint, that is the ultimate moment capacities of beam AC at positions 1, 2 and 3 vary with temperature. Since the tension steel is at the bottom at 3 and at the top at 2, the ultimate moment capacity at position 2 is likely to be greater than that at position 3 at any time in the analysis because degradation of steel strength will be more marked in the bottom steel due to the effects of the fire.

As the fire progresses the moment at position 1 is relieved due to the rotation at joint A which results in an increase in the moments at positions 3 and 2. Since the ultimate moment capacity at position 3 decreases faster than that at 2, a likely position for the formation of the first plastic hinge is at position 3.

However, at the start of the analysis position 2 carries more moment than position 3, $\nless \omega L_2^2/12$ and $\ngtr \omega L_2^2/24$ respectively. Because the ultimate moment capacity at position 2 is decreasing with increasing temperature (although slower than the rate of decrease of the ultimate moment capacity at position 3), the ultimate moment capacity could be exceeded at position 2 before the hinge is formed at position 3. It is therefore possible for the first plastic hinge to occur at either position 3 or 2.

The order of formation of plastic hinges in the top restraint beam AC is therefore either:

$$\boxed{\text{hinge 3}} \longrightarrow \boxed{\text{hinge 2}} \longrightarrow \boxed{\text{hinge 1}}$$

or $\boxed{\text{hinge 2}} \longrightarrow \boxed{\text{hinge 3}} \longrightarrow \boxed{\text{hinge 1}}$

Consider now the bottom restraint beam BD in Figure 6.4. As described previously all the ultimate moment capacities decrease with increased temperature. As the fire progresses the moment at position 4 decreases due to the rotation at joint B, therefore the moments at positions 5 and 6 must increase. Initially position 5 carries more moment than position 6 and the ultimate moment capacity at position 5 decreases faster than that at position 6 since the tension steel at the top of the beam is more exposed to the effects of the fire. Therefore the moment at position 5 will exceed the ultimate moment capacity at that position before the moment at position 6. Thus the first hinge will most likely form at position 5.

The order of formation of plastic hinges in the bottom restraint beam BD is therefore:

$$\boxed{\text{hinge 5}} \longrightarrow \boxed{\text{hinge 6}} \longrightarrow \boxed{\text{hinge 4}}$$

Depending on the current state of the formation of plastic hinges a relevant plastic anlaysis must be carried out in order to determine the stiffness of the remaining structure. The plastic analysis is decribed in Section 6.2.2.4.

6.2.2.3 Method to Check for First Formation of Plastic Hinge

The method of calculation described in this section is to check for the first formation of a plastic hinge either in the top restraint beam or bottom restraint beam. Therefore previous to the current redistribution of moments, the structural restraint system had remained elastic, and no formation of plastic hinges in the restraint beams had occurred.

During the analysis in this section and the plastic analysis described in section 6.2.2.4 the restraint system at each end of the column under analysis are considered independent of each other and therefore the restraint system at one end of the column may become plastic, with the formation of one or more plastic hinges, while the other remains elastic, without the formation of any plastic hinge.

6.2.2.3.1 Top Beam

From consideration of Figure 6.5 it can be seen that the total moments in the top restraint beam AC will be from the superposition of the moments due to rotation at joint A and the axial sway of the structural frame. Figure 6.6 shows the bending moment envelope at the start of the analysis before redistribution and the bending moment envelope after release due to the rotation of joint A.

From the assumption that the maximum sagging moment occurs at midspan the following equation can be written:

$$\left|M_3\right| = \frac{\omega L_2^2}{8} - \frac{(\left|M_1\right| + \left|M_2\right|)}{2} \tag{6.8}$$

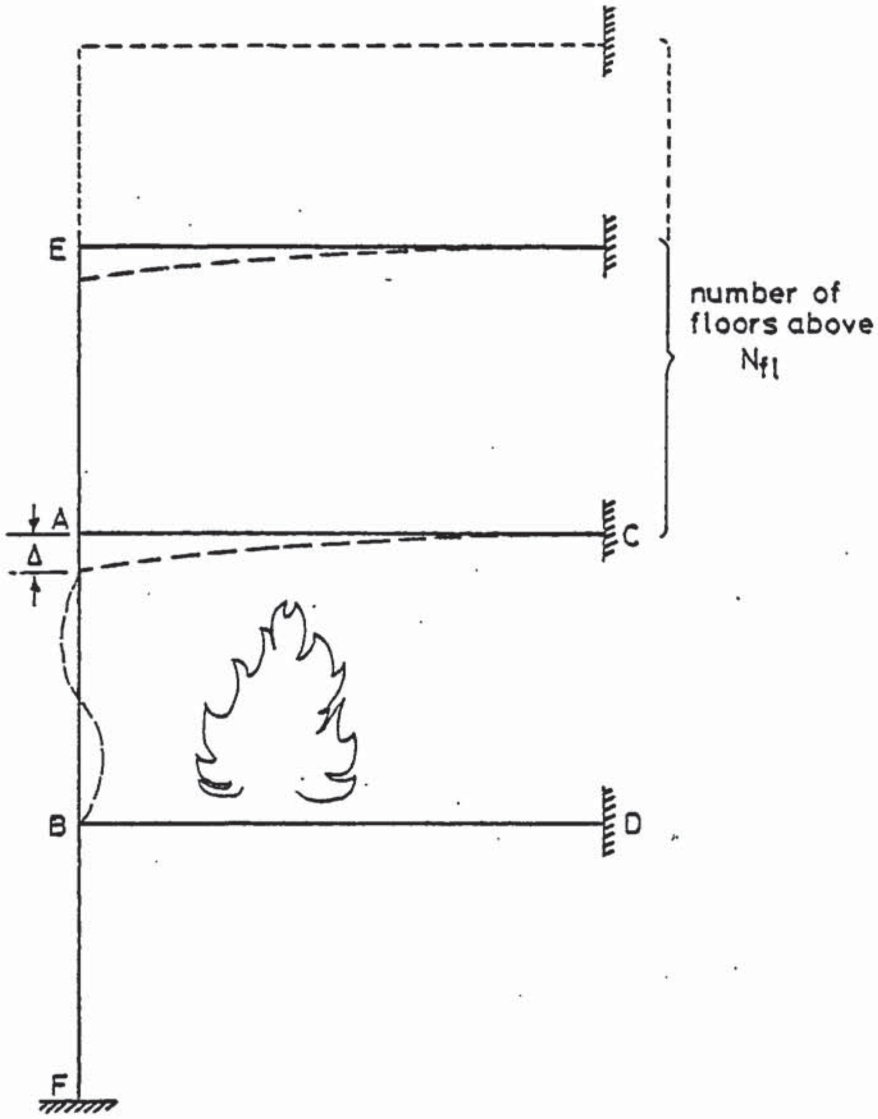

Figure 6.5 Structural system analysed showing rotation and axial sway of frame.

where: $|M_1|$, $|M_2|$ and $|M_3|$ are absolute values of the moments defined in Figure 6.6.

$M_1 \leqslant \omega L_2^2/12$

$M_2 \geqslant \omega L_2^2/12$

From the slope deflection equations for elastic response derived in Appendix B:

$$M_1 = 4K_2\theta_A + M_{ac}$$
$$M_2 = 2K_2\theta_A + M_{ca} \tag{6.9}$$

where: K_2 is the stiffness of the top restraint beam,

M_{ac} and M_{ca} are the fixed end moments.

Substituting equations (6.9) into (6.8) gives:

$$M_3 = \omega L_2^2/8 - (4K_2\theta_A + M_{ac} + 2K_2\theta_A + M_{ca})/2 \tag{6.10}$$

Figure 6.7 shows the moments in the top restraint beam due to the vertical sway of the frame above the column under analysis. From the sway analysis described in Appendix C using slope deflection equations M_1' and M_2' can be calculated for a known sway Δ (see Figure 6.5) and the moment at midspan M_3' can be found from linear interpolation. The sway Δ of the frame above, or the axial deformation of the column, is calculated according to the procedure described in Section 6.3.1.

From slope deflection equations (Appendix C):

$$M_1' = 4K_2\theta_A - 6N_{f1}K_2\Delta/L_2$$
$$M_2' = 2K_2\theta_A - 6N_{f1}K_2\Delta/L_2 \tag{6.11}$$

where: N_{f1} is the number of floors above the column exposed to fire.

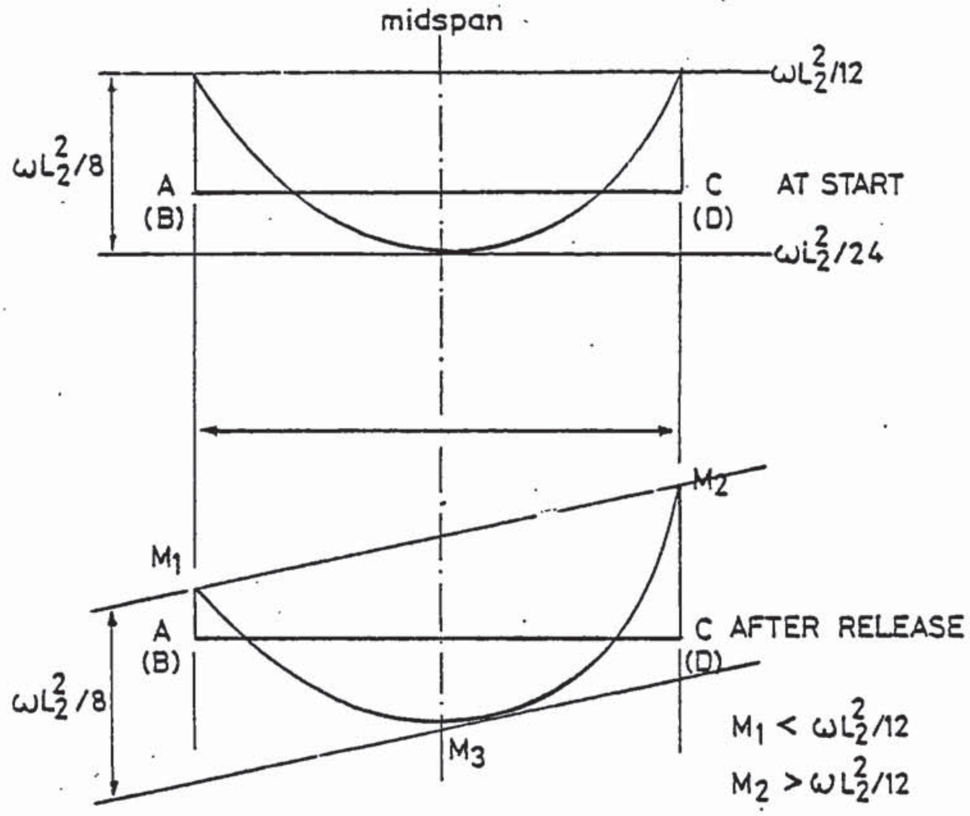

Figure 6.6 Bending moments in restraint beam due to rotation.

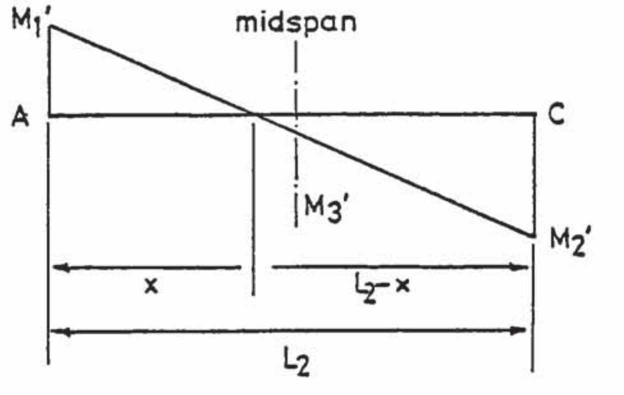

Figure 6.7 Bending moments in top restraint beam due to vertical sway of frame above column under analysis.

The sign convention for the axial deformation of the column, or sway Δ, is shown in Figure 6.8, Δ is positive for an increase in column length. See also Section 6.3.1.

From consideration of Figure 6.7 and using linear interpolation:

$$\frac{x}{|M_1'|} = \frac{L_2 - x}{|M_2'|} \tag{6.12}$$

rearranging equation (6.12) gives:

$$x = \frac{L_2 M_1'}{(|M_1'| + |M_2'|)} \tag{6.13}$$

Hence,

$$|M_3'| = |M_1'| \, (x - L_2/2)/x \qquad \text{if } x \geqslant L_2/2$$

$$\text{or} \qquad |M_3'| = |M_2'| \, (L_2/2 - x)/(L_2 - x) \qquad \text{if } x < L_2/2 \tag{6.14}$$

From the principle of superposition the total moment at any point in the top restraint beam is equal to the sum of the moments due to rotation and the moments due to vertical movement. If the sum of these moments at the three possible hinge positions is greater than the ultimate moment capacity at these points then a plastic hinge is said to have formed and no further increase in bending moment can occur at that position. Depending on where the first hinge occurs the appropriate plastic analysis must be followed to evaluate the new stiffness of the remaining structure.

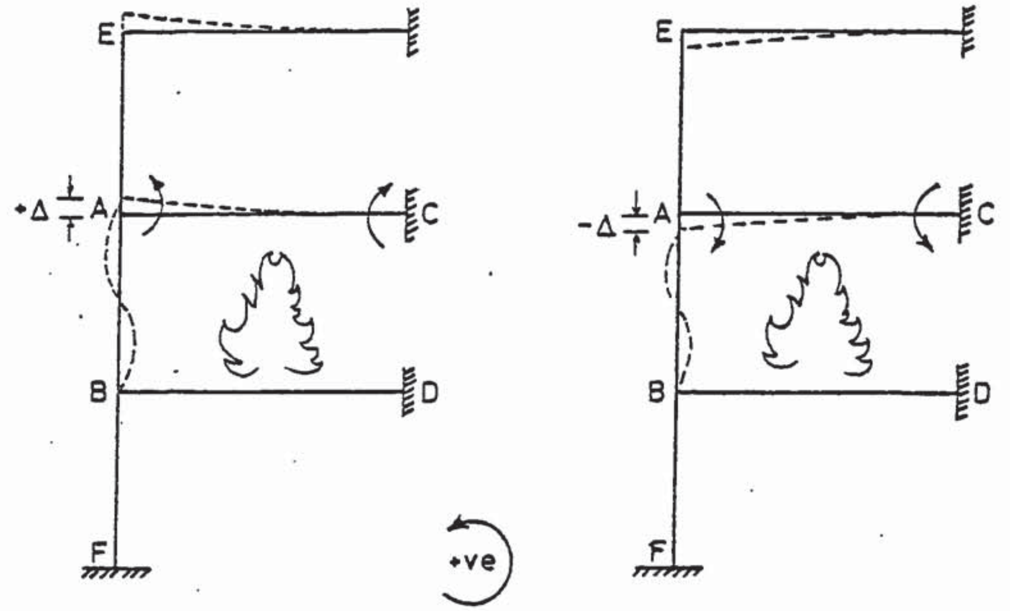

Figure 6.8 Sign convention for axial deformation of fire exposed column.

6.2.2.3.2 <u>Bottom Beam</u>

The moments in the bottom beam are due to rotation only since it is considered there is zero vertical movement at position B, see Figure 6.5.

Referring to Figure 6.6 and making the assumption that the maximum sagging moment occurs at midspan, equation (6.8) holds for the bottom beam. From the slope deflection equations for elastic response derived in Appendix B:

$$\begin{aligned} M_1 &= 4K_3\theta_B + M_{bd} \\ M_2 &= 2K_3\theta_B + M_{db} \end{aligned} \qquad (6.15)$$

where: K_3 is the stiffness of the bottom restraint beam,

M_{bd} and M_{db} are the fixed end moments.

Substituting equations (6.15) into (6.8) gives:

$$M_3 = \omega L_2^2/8 - (4K_3\theta_B + M_{bd} + 2K_3\theta_B + M_{db})/2 \qquad (6.16)$$

If the moments M_1, M_2 or M_3 exceed the ultimate moment capacity of the section at that point then a plastic hinge is said to have formed and no further increase in bending moment can occur at that position. Once a plastic hinge has formed the appropriate plastic analysis must be followed to determine the stiffness of the remaining structure.

6.2.2.4 Plastic Analysis

The top restraint system, that is the structural members and rest of the structure adjoining at column end A, and the bottom restraint system, that is the structural members and rest of the structure adjoining at column end B, are considered as two independent structural systems, and as such are analysed separately, see Figure 6.9.

The plastic analysis presented here is only carried out for a particular column end restraint system when and only when one or more plastic hinges have formed in that restraint system. The plastic analysis is carried out in order to determine the reduced stiffness of the structural members of the restraint system due to the formation of a plastic hinge.

Derivation of the plastic analysis is described in full in Appendix D. The analysis is based on complimentary energy theorem.

6.2.2.4.1 Restraint System at Column End A

As described in Section 6.2.2.2 and referring to Figure 6.10 there are two possible orders of formation of plastic hinges in the restraint beam adjoining column end A.

Consider first the order of hinge formation shown in Figure 6.10 and depicted by the route (a), (b), (d), (e).

For condition (a) the axial restraining force N is calculated according to the elastic theory described in Section 6.3.1.

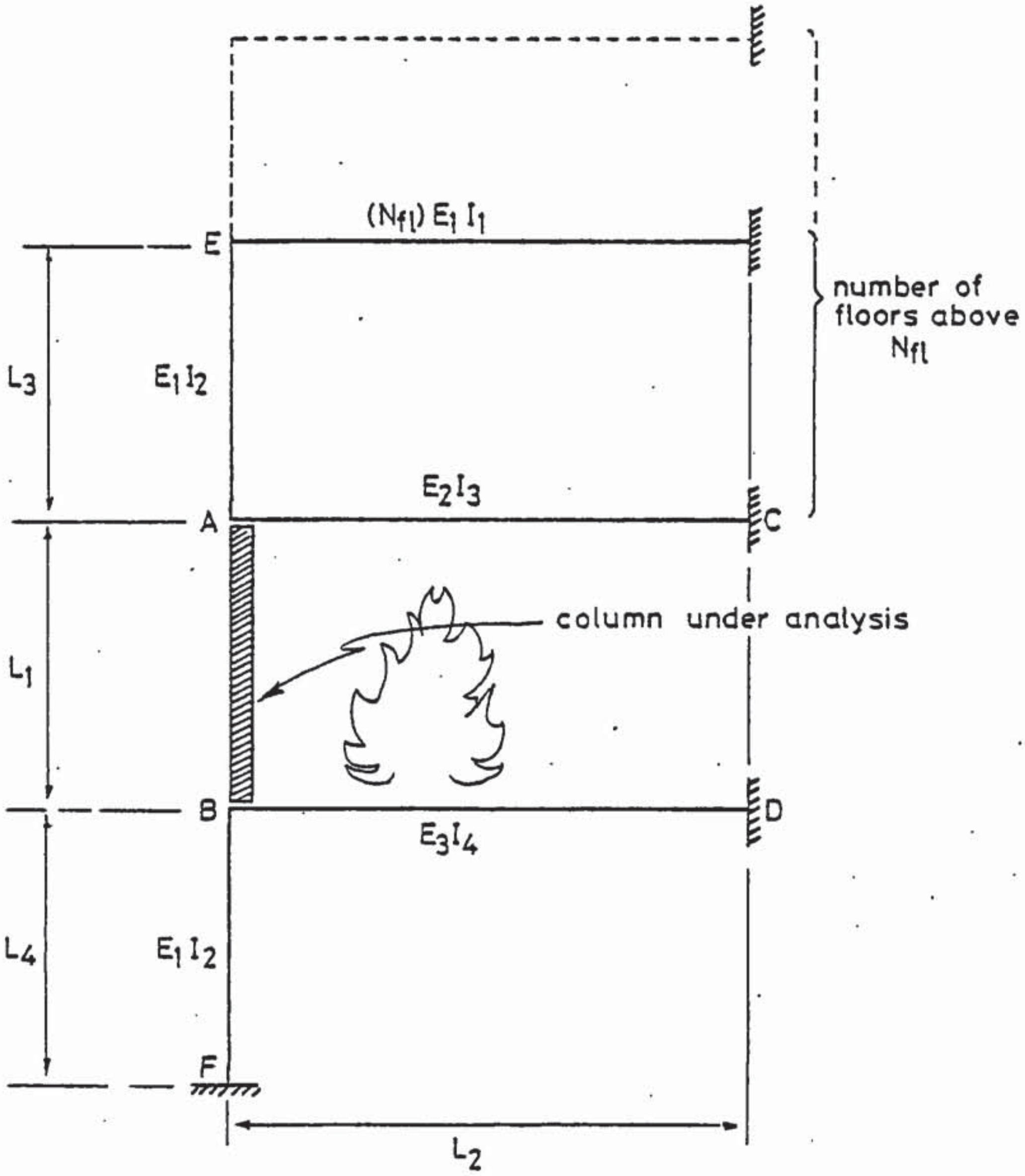

Figure 6.9 Structural restraint system for normal rotational restraint.

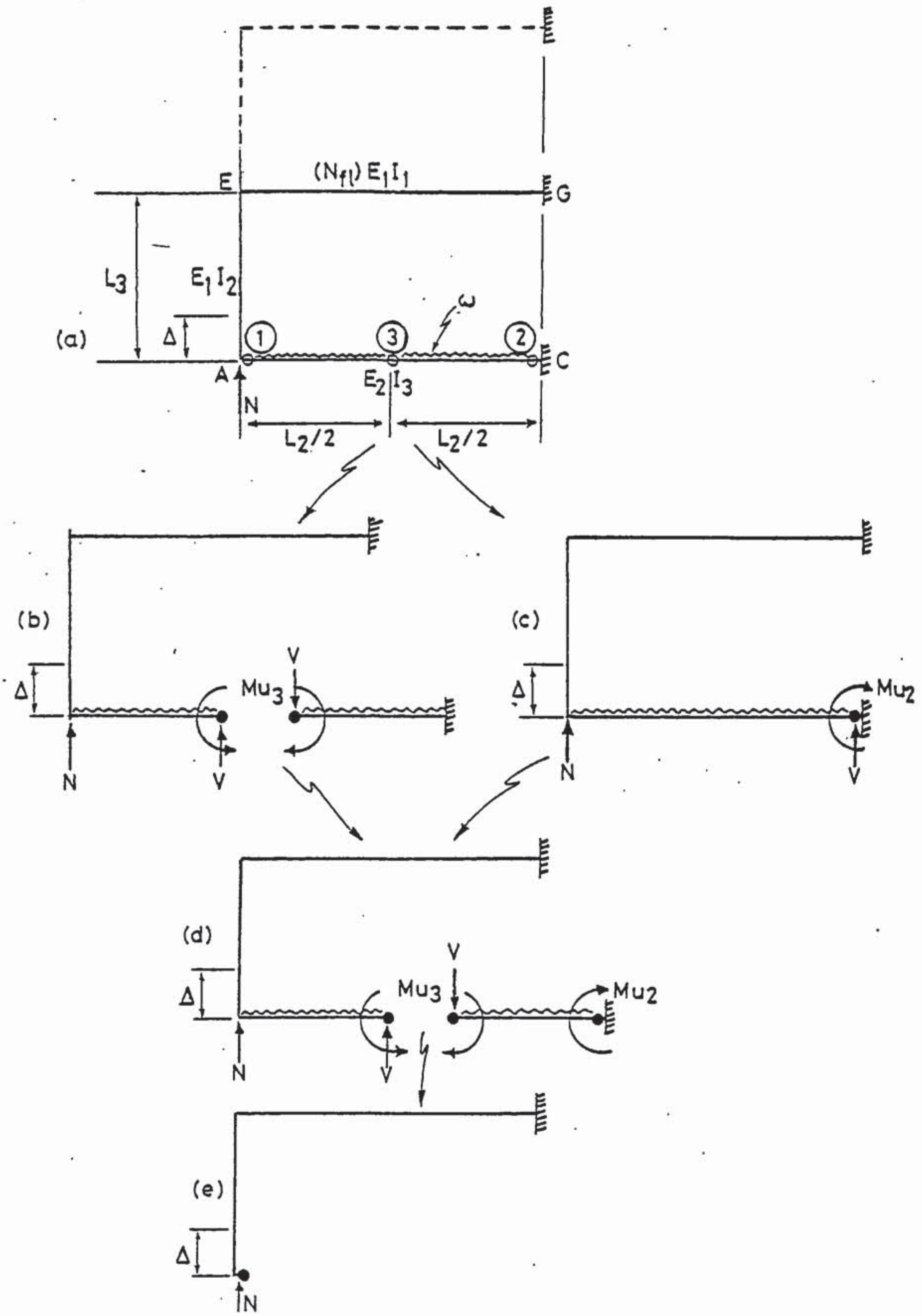

Figure 6.10 Permutations of order of plastic hinge formation considered in plastic analysis of restraint system at column end A.

For condition (b):

$$N = \frac{\Delta\left(\frac{N_{f1}E_1I_1}{E_2I_3} + \frac{3L_3I_1N_{f1}}{L_2I_2} + 1\right) + \omega\left(\frac{5L_2^4}{48E_2I_3} + \frac{L_2^3L_3}{4E_1I_2} + \frac{L_2^4}{16N_{f1}E_1I_1}\right) \ldots\ldots\ldots + Mu_3\left(\frac{2L_2L_3}{E_1I_2} + \frac{L_2^2}{2E_1I_1N_{f1}} + \frac{L_2^2}{2E_2I_3}\right)}{\frac{L_2^3}{3E_2I_3} + \frac{L_2^2L_3}{E_1I_2} + \frac{L_2^3}{4E_1I_1N_{f1}}} \qquad (6.17)$$

where: Δ is the change in chord length of the column exposed to fire,

N_{f1} is the number of floors above,

N is the axial restraining force,

L_2 and L_3 are member lengths defined in Figure 6.9,

E_1 and E_2 are current Young's Moduli defined in Figure 6.4,

ω is the uniformly distributed load,

Mu_3 is the ultimate moment at position 3 (see Figure 6.10).

$$V = \frac{-N\left(\frac{L_2^3}{12E_1I_1N_{f1}}\right) + \omega\left(\frac{L_2^3L_3}{16E_1I_2} + \frac{L_2^4}{24E_1I_1N_{f1}}\right) - Mu_3\left(\frac{L_2L_3}{2E_1I_2}\right)}{\frac{L_2^3}{12E_2I_3} + \frac{L_2^2L_3}{4E_1I_2} + \frac{L_2^3}{12E_1I_1N_{f1}}} \qquad (6.18)$$

where: V is the shear force shown in Figure 6.10 (b).

$$\theta_1 = \omega\left(\frac{L_2^3}{8E_1I_1N_{f1}} - \frac{L_3L_2^3}{8E_1I_2}\right) + V\left(\frac{L_2L_3}{2E_1I_2}\right) + Mu_3\left(\frac{L_3}{E_1I_2} + \frac{L_2}{E_1I_1N_{f1}}\right) \qquad (6.19)$$

where: θ_1 is the rotation at position 1.

The moment at position 1 is given by:

$$M_1 = \omega L_2^2/8 - Mu_3 - VL_2/2 \tag{6.20}$$

The effective reduced member stiffness K_2' of beam AC now becomes:

$$K_2' = 0.5M_1/\theta_1 \tag{6.21}$$

where: M_1 is calculated using equations (6.20), (6.18) and (6.17)

θ_1 is calculated using equations (6.19), (6.18) and (6.17),

0.5 is introduced to be consistent with Section 7.8.

For condition (d):

$$V = 2(Mu_2 + Mu_3 - \omega L_2^2/8)/L_2 \tag{6.22}$$

where: V is the shear force shown in Figure 6.10 (d),

Mu_2 is the ultimate moment at position 2.

$$N = \frac{3E_1I_1N_{f1}\Delta}{L_2^3} - 5L_2\omega/16 + V/4 - 3Mu_3/2L_2 \tag{6.23}$$

The effective reduced member stiffness of beam AC, K_2' is calculated using equation (6.21) where M_1 and θ_1 are now calculated using equations (6.20) and (6.22).

For condition (c):

The axial restraining force N is resisted by a structure equivalent to a cantilever:

$$N = 3E_1I_1N_{f1}\Delta/L_2^3 \tag{6.24}$$

The effective member stiffness of beam AC, K_2', is now zero.

Consider now the order of hinge formation shown in Figure 6.1(and depicted by the route (a), (c), (d), (e).

For condition (a) the axial restraining force N is calculatec according to the elastic theory described in Section 6.3.1.

For condition (c):

$$N = \frac{\omega\left(\frac{7L_2^4}{24E_2I_3} + \frac{L_2^3L_3}{E_1I_2} + \frac{L_2^4}{4E_1I_1N_{f1}}\right) - Mu_2\left(\frac{2L_2L_3}{E_1I_2} + \frac{L_2^2}{2E_1I_1N_{f1}} + \frac{L_2^2}{2E_2I_3}\right) \;\cdots\cdots\; + \Delta\left(\frac{6L_3I_1N_{f1}}{L_1I_2} + 2 + \frac{2E_1I_1N_{f1}}{E_2I_3}\right)}{\frac{2L_2^2L_3}{E_1I_2} + \frac{L_2^3}{2E_1I_1N_{f1}} + \frac{2L_2^3}{3E_2I_3}} \tag{6.25}$$

and,

$$V = -\,6E_1I_1N_{f1}\Delta/L_2^3 + 2N - \omega L_2/4 + 3Mu_2/L_2 \tag{6.26}$$

where: V is the shear force shown in Figure 6.10 (c).

$$\theta_1 = -\,\omega\left(\frac{L_2^2L_3}{2E_1I_2}\right) + V\left(\frac{L_3L_2}{E_1I_2} + \frac{L_2^2}{2E_1I_1N_{f1}}\right) - Mu_2\left(\frac{L_2}{E_1I_2} + \frac{L_2}{E_1I_1N_{f1}}\right) \tag{6.27}$$

The moment at position 1, M_1 is given by:

$$M_1 = \omega L_2^2/2 + Mu_2 - VL_2 \tag{6.28}$$

The effective reduced member stiffness of beam AC, K_2', is calculated using equation (6.21) where M_1 and θ_1 are calculated using equations (6.28), (6.29), (6.25) and (6.27).

The conditions (d) and (e) are calculated as described previously. After each stage of the plastic analysis described above the moments must be checked at positions 1, 2 and 3 to determine if they exceed the current ultimate moments at those points.

6.2.2.4.2 Restraint System at Column End B

As described previously in Section 6.2.2.2 and referring to Figure 6.11 there is only one order of formation of plastic hinges in the restraint beam adjoining column end B.

Condition (a) is the elastic stage, that is no plastic hinges have formed.

Condition (b):

$$V = \frac{\omega\left(\frac{L_2^4}{8E_3I_4} + \frac{L_2^3L_4}{2E_1I_2}\right) + Mu_5\left(\frac{L_2^2}{2E_3I_4} + \frac{L_2L_4}{E_1I_2}\right)}{\frac{L_2^3}{3E_3I_4} + \frac{L_2^2L_4}{E_1I_2}} \qquad (6.29)$$

where: V is the shear force shown in Figure 6.11 (b),

Mu_5 is the ultimate moment capacity at position 5,

L_2 and L_4 are member lengths defined in Figure 6.9,

E_1 and E_3 are current Young's Moduli defined in Figure 6.9.

$$\theta_4 = (VL_2L_4 - Mu_5L_4 - \omega L_2^2L_4/2)/E_1I_2 \qquad (6.30)$$

where: θ_4 is the rotation at position 4, see Figure 6.11.

The moment at position 4 is given by:

$$M_4 = \omega L_2^2/2 + Mu_5 - VL_2 \qquad (6.31)$$

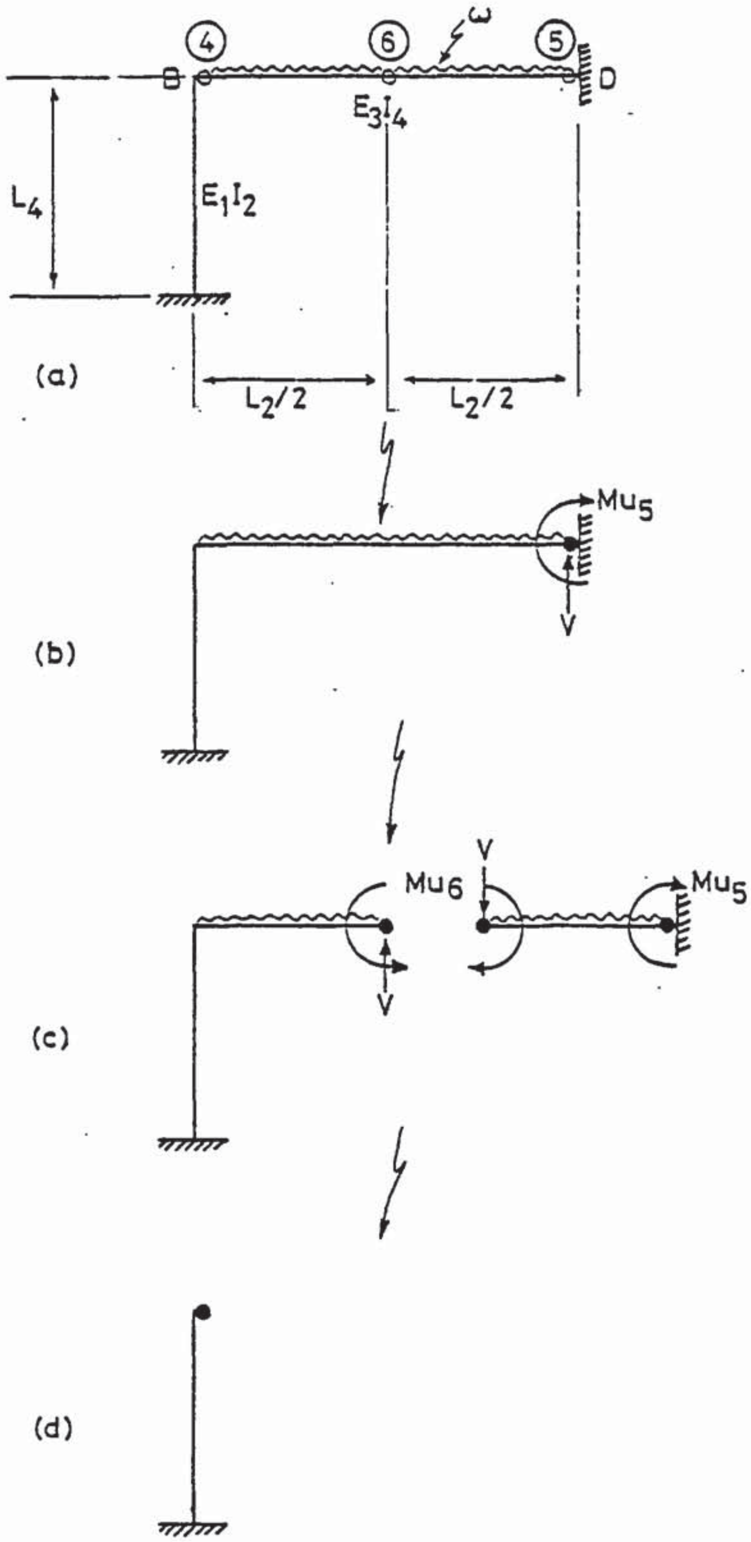

Figure 6.11 Order of formation of plastic hinges considered in plastic analysis of restraint system at column end B

The effective reduced member stiffness of beam BD, K_3' i calculated from:

$$K_3' = 0.5M_4/\theta_4 \qquad (6.32)$$

where: M_4 is calculated using equations (6.31) and (6.29),

θ_4 is calculated using equations (6.30) and (6.29).

For condition (c):

$$V = 2Mu_5/L_2 - \omega L_2/4 + 2Mu_6/L_2 \qquad (6.33)$$

where: V is the shear force defined in Figure 6.11 (c),

Mu_6 is the ultimate moment capacity at position 6.

The moment at position 4 is now given by:

$$M_4 = \omega L_2^2/8 - Mu_6 - VL_2/2 \qquad (6.34)$$

$$\theta_4 = \frac{VL_2L_4}{2E_1I_2} - \frac{\omega L_2^2L_4}{8E_1I_2} + \frac{Mu_6L_4}{E_1I_2} \qquad (6.35)$$

where: θ_4 is the rotation at position 4.

The effective reduced member stiffness of beam BD, K_3', is calculated using equation (6.32) where M_4 is calculated according to equation (6.34) and θ_4 is calculated using equations (6.35) and (6.33).

For condition (d):

The effective member stiffness of beam BD, K_3', is now zero.

After each stage in the analysis described above the moments must be checked at positions 4, 5 and 6 to determine whether any of them exceed the current ultimate moment capacity at those points.

6.2.2.4.3 Ultimate Rotations of Restraint System Columns

When all three hinges have formed in the restraint beam the effective stiffness of the beam is reduced to zero, as described previously, and further end rotation of the column exposed to fire is only restrained by the restraint system column (the column above or below the column exposed to fire).

A column hinge is considered to have formed when the ultimate permissible rotation of the restraint system column is reached, that is when the end slope of the column under analysis is greater than or equal to the ultimate rotation of the restraint system column. This ultimate rotation is determined by the equation:

$$\theta u_c = Mu_c / 4K_c \tag{6.36}$$

where: θu_c is the ultimate rotation of the restraint system column,

Mu_c is the ultimate moment capacity of the restraint system column allowing for the axial load present,

K_c is the stiffness of the restraint system column, K_1 or K_5.

Once a plastic hinge has formed in the restraint system column it effectively has a simply supported end. The stiffness K_c is therefore updated and taken as 3/4 times its original value.

6.2.2.5 Calculation of Ultimate Moment Capacity

The procedure described in this section calculates the ultimate moment capacity for the fire exposed restraint beam and is therefore only considered when the option is included in SAFE-RCC for the temperature dependent restraint system. The ultimate moment capacities of the restraint beam have to be calculated for the six positions shown in Figure 6.4.

In calculating the ultimate moment capacity it is necessary to find the maximum moment the section can withstand which will depend upon the temperature dependent concrete strength and steel reinforcing strength.

Since the concrete strength and steel reinforcing strength will vary with temperature, the first stage of the procedure is to carry out a thermal analysis of the restraint beam sections at the six positions shown in Figure 6.4 using the thermal analysis described in Chapter 4. In order to do this the sections must be discretized into a finite element mesh so that element temperatures can be calculated.

Having determined the elemental temperatures of the restraint beam section it is possible to evaluate the corresponding strength of the element which may be either concrete or steel.

In order to calculate the ultimate moment capacity it is assumed that the extreme concrete fibre will be loaded to an ultimate strain and on the basis of linear strain distribution across the section the strain in the steel can be calculated. It should be pointed out that only 'elastic' response is considered, that is no account is taken of thermal expansion, creep, transient strain and any degree of preload which must exist.

The idealized stress-strain relationship for concrete used in CP110 is shown in Figure 6.12. The graph gives a value of instantaneous modulus, maximum stress and maximum strain. The maximum stress is shown as $0.67f_{cu}/\gamma_m$. The 0.67 is introduced to allow for the difference in strength indicated by a cube crushing test and the strength of the concrete in a structure. γ_m is the partial safety factor for the material which takes account of the variation in the quality of the materials. The value for the safety factor γ_m suggested in the FIP/CEB Report (1978) for fire design is 1.3 for concrete. (In general the partial safety factor γ_m for concrete at ambient conditions is taken as 1.5).

For normal temperatures the value of limiting strain is taken as 0.0035. The FIP/CEB Report (1978) suggests that for temperatures above 500°C the limiting strain can be taken as 0.006. Therefore in order to determine the ultimate strain in the extreme concrete fibre it is assumed that the ultimate strain varies in a linear fashion between 0.0035 at 20°C and 0.006 at 500°C and can be represented by the following expression:

$$\varepsilon_u = 0.0035 + (0.0025/480)(T_{av} - 20) \qquad (6.37)$$

where: ε_u is the ultimate strain in the extreme concrete fibre,

T_{av} is the average temperature in the extreme concrete fibre.

For temperatures greater than 500°C $\varepsilon_u = 0.006$.

It is assumed that there is a linear strain profile across th section as shown in Figure 6.13. For equilibrium at any time th compressive force in the concrete and steel must be equal in magnitud to the tensile force in the steel, that is:

$$C = T \tag{6.38}$$

where: C is the compressive force in the concrete and compressioı steel (if present),

T is the tensile force in the steel.

From consideration of Figure 6.13 and using similar triangles the strain in the steel is given by:

$$\varepsilon_s = \varepsilon_u(d - x_{NA})/x_{NA} \tag{6.39}$$

where: ε_s is the strain in the tension steel,

d is the effective depth of the section,

x_{NA} is the depth of the neutral axis, see Figure 6.13.

For a steel strain of ε_s the corresponding steel stress σ_s can be found from the appropriate stress-strain relation described in Chapter 8, Section 8.2.2. The force in the tension steel is then calculated according to the following expression:

$$T = A_{st}\sigma_s \tag{6.40}$$

where: A_{st} is the area of tension steel.

The strain in each compressive element, $\varepsilon_{c,i}$ is given by:

$$\varepsilon_{c,i} = \varepsilon_u x_i/x_{NA} \tag{6.41}$$

where: x_i is the distance from the neutral axis to the centre of the element in the compressive zone.

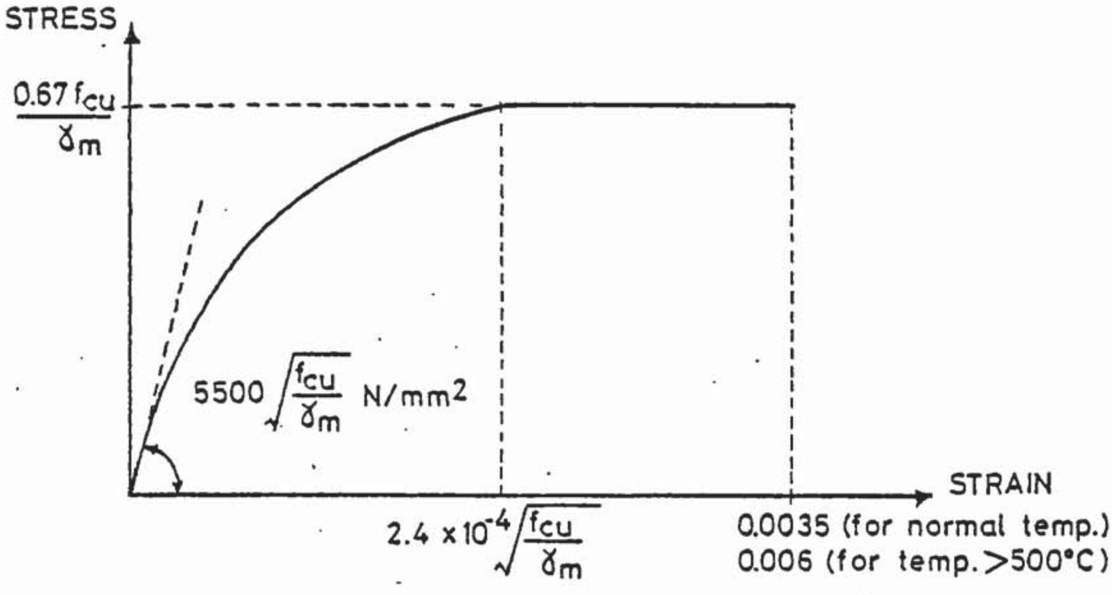

Figure 6.12 Idealized stress-strain relation for concrete used in CP 110.

For cylinder strength peak stress = $\frac{0.67 f_{cyl}}{0.8\gamma_m}$

since $f_{cyl} = 0.8 f_{cu}$

Note: f_{cu} in N/mm²

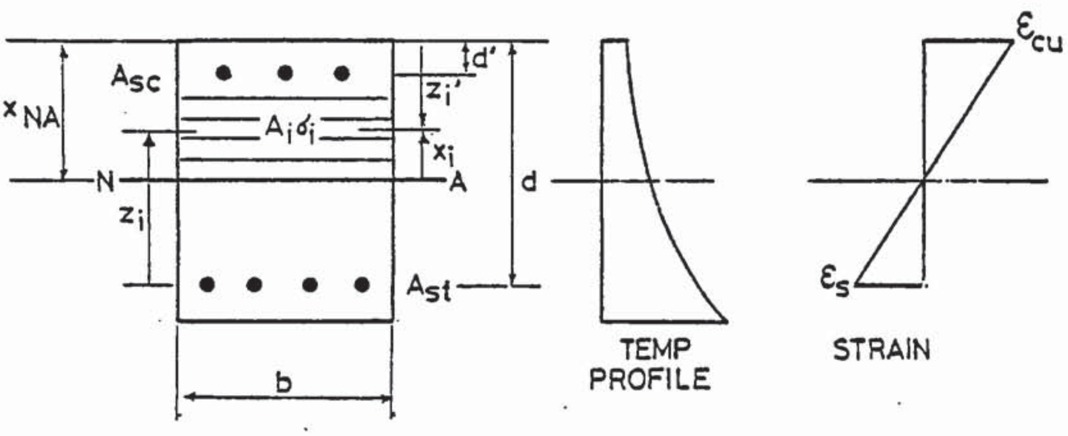

Figure 6.13 Strain profile across restraint beam section.

The stress $\sigma_{c,i}$ corresponding to the strain $\varepsilon_{c,i}$ can be found from th appropriate stress-strain relation described in Chapter 8.

The force in the concrete and steel in the compression zone i determined according to the following expression:

$$C = \sum A_{c,i}\sigma_{c,i} \qquad (6.42$$

where: $A_{c,i}$ is the area of the element in the compression zone,

$\sigma_{c,i}$ is the elemental stress.

In the calculation of C from equation (6.42) it is assumed tha the concrete takes compression only, therefore concrete elements ar ignored on the tension side of the neutral axis.

The depth of the neutral axis, x_{NA}, is found by an iterativ procedure whereby a proposal is first made for x_{NA} equal to 0.10d. I equation (6.38) is not satisfied after carrying out equations (6.39) to (6.42), the proposed value of x_{NA} is successively increased until the equilibrium equation (6.38) is satisfied. Once satisfied then the proposed value of x_{NA} is taken to be the actual value.

By taking moments about the tension steel the ultimate moment capacity of the section is given by:

$$Mu = \sum A_{c,i}\sigma_{c,i}z_i \qquad (6.43)$$

where: Mu is the ultimate moment capacity,

$A_{c,i}$ is the elemental area of concrete or compression steel,

z_i is the distance from the tension steel centroid to the centroid of the compression element, see Figure 6.13.

By taking moments about the extreme compression fibre th ultimate moment capacity of the section is given by:

$$Mu = A_{sc}\sigma_{sc}d' + \sum A_{c,i}z_i' - A_{st}\sigma_{st}d \qquad (6.44$$

where: A_{sc} is the area of compression steel,

A_{st} is the area of tension steel,

σ_{sc} is the stress in the compression steel,

σ_{st} is the stress in the tension steel,

z_i' is the distance from extreme compression fibre to th centroid of the compression element.

The ultimate moment capacity is taken as the lesser value of M from equations (6.43) and (6.44).

The stiffness of the restraint beam is calculated using th following equation:

$$K_{beam} = 0.5E_mI/L \qquad (6.45$$

where: E_m is the temperature dependent concrete initial tangen modulus corresponding to the mean section temperature,

I is the transformed second moment of area (see Section 7.8)

6.2.2.6 Complete Moment-Rotation Relation for Normal Rotational Restraint

The complete moment-rotation relation for normal rotationa restraint is shown in Figure 6.14.

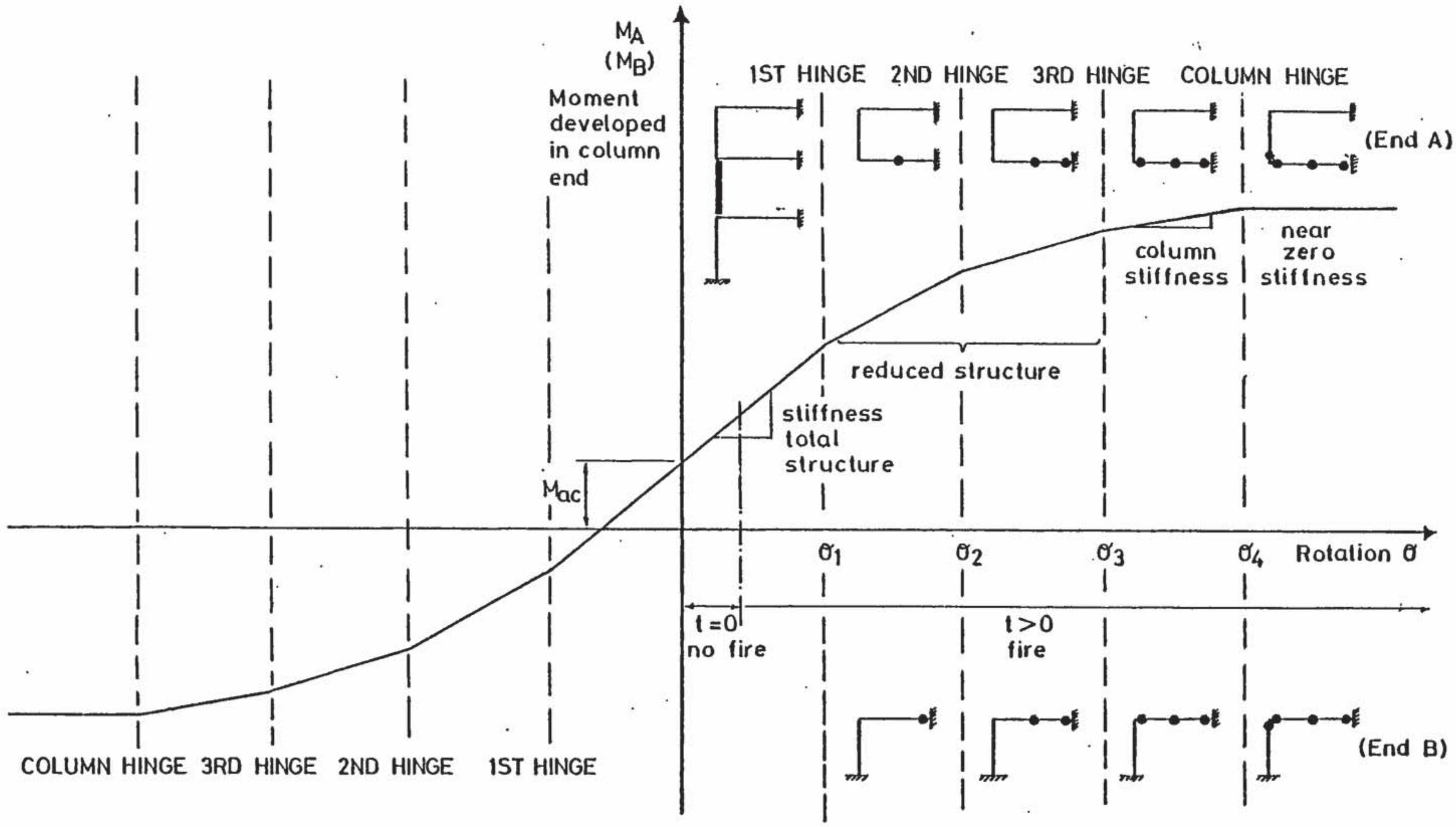

Figure 6.14 Complete moment-rotation relation for normal rotational restraint

6.2.3 Pin Ended Rotational Restraint

The moment-rotation relation corresponding to pin ended rotational restraint can be considered to be a relation of zero slope coincident with the rotation axis. Therefore whatever the value of end slope, or rotation, there is zero induced restraining moment, see Figure 6.15 (a). This is achieved by setting the value of the combined stiffness of the adjoining members at the column support shown in Figure B.1 Appendix B equal to zero, since the slope of the moment-rotation relation corresponds to the stiffness of the restraint members.

6.2.4 Fixed Rotational Restraint

The moment-rotation relation corresponding to fixed rotational restraint can be considered to be equivalent to a moment-rotation relation with a very steep slope, almost coincident with the restraint moment axis, see Figure 6.15 (b). The value of the slope of the relation for a fixed rotational restraint would tend towards infinity but for the purposes of calculation a slope of 10^{10} is assumed. Therefore the combined stiffness of the adjoining members at the column support as shown in Figure B.1 Appendix B are set to a value of 10^{10}. The model for fixed rotational restraint is therefore not ideally fixed but very stiff and as a result very small rotations can occur at the column supports.

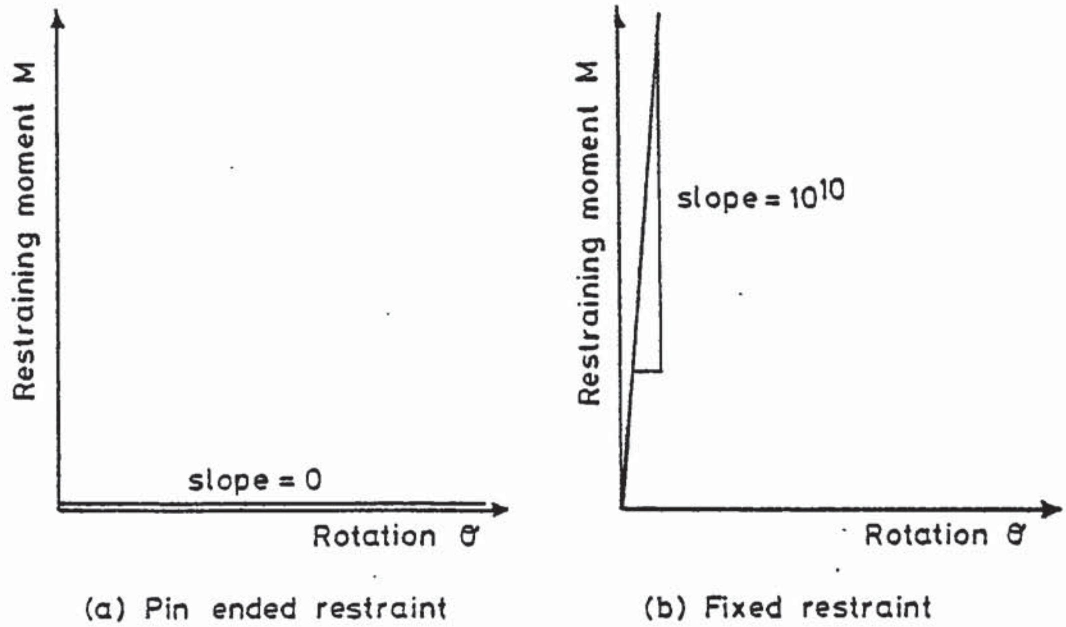

Figure 6.15 Moment - rotation relations used in the model of restraint for pin ended and fixed rotational restraint.

6.3 Axial Restraint

6.3.1 Normal Axial Restraint

Normal axial restraint is a model of axial restraint likely to be experienced by a column in a real structure. The analysis used in the model is based on the vertical movement of the bay above the column exposed to fire due to the chord shortening of that fire exposed column.

When the column is subject to a local fire the thermal expansion of the column is resisted by the axial restraint supplied by the surrounding structure inducing an additional load in the column. The restraint to the column is mainly due to the stiffness of the beams and floors and hence increases with the number of floors above.

Figure 6.16 shows the system to be analysed. For equilibrium at joint A the chord shortening (or lengthening) Δ due to the deflection of the fire exposed column must be equal to the vertical movement experienced by the frame GEAC. For small lateral deflections of the fire exposed column the chord length may in fact increase as a result of wedge effects at the end of the column due to geometry.

If the frame GEAC is turned through 90° it can be viewed to be equivalent to a portal frame experiencing a pure sway of Δ. The equivalent force N that would give a pure sway of Δ in the portal frame GEAC can therefore be calculated, and this force N must be equal to the axial restraining force, or thrust, experienced by the fire exposed column AB.

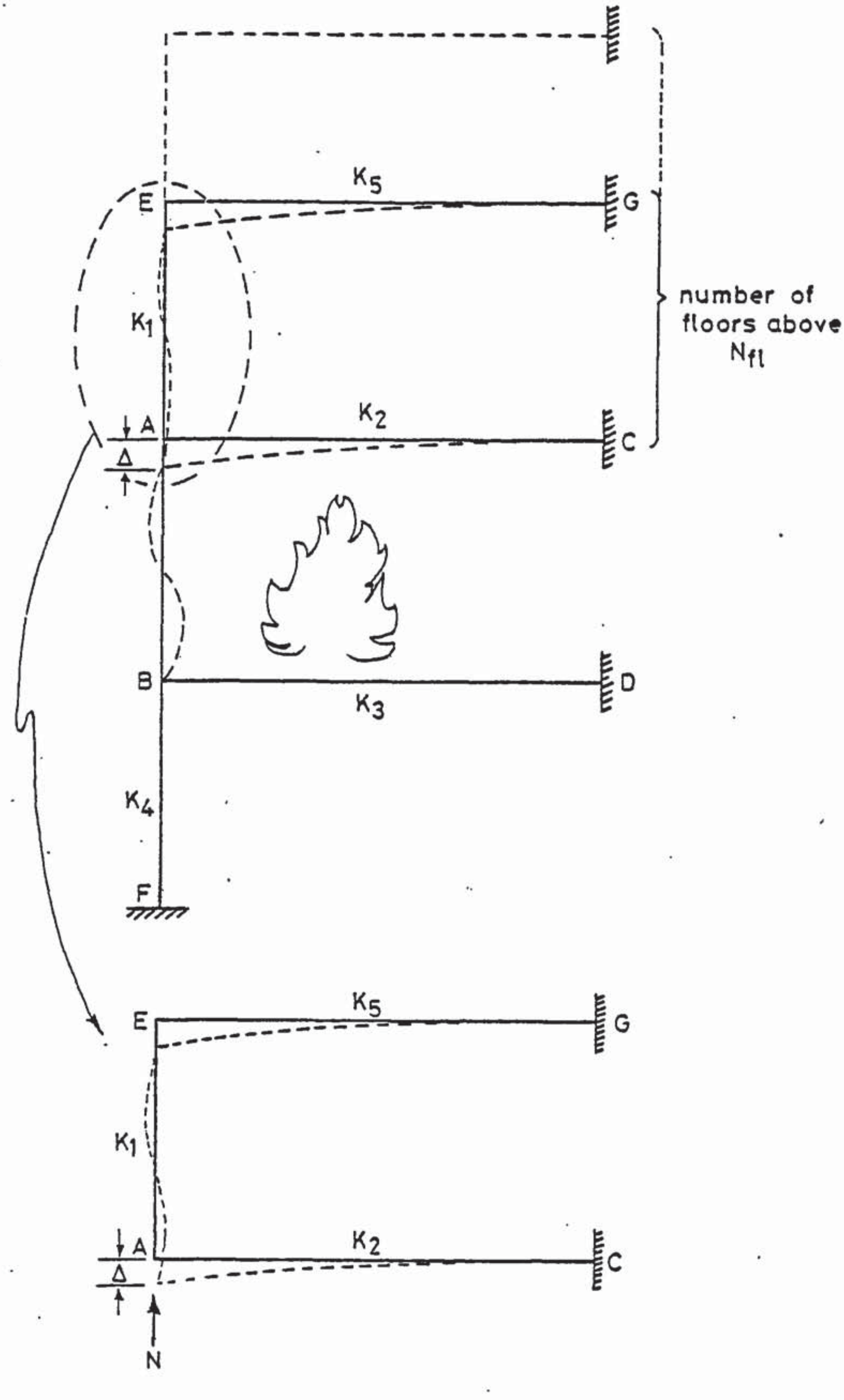

Figure 6.16 System analysed for axial restraint model.

The first stage in the analysis is to calculate the change in chord length of the fire exposed column due to the thermal axial expansion and the division point displacements calculated from the structural analysis described in Chapter 5. From consideration of Figure 6.17 it can be seen that the average total strain in segment l_i is represented by the following equation:

$$\varepsilon_{avtot,i} = (\varepsilon_{tot,i} + \varepsilon_{tot,i+1})/2 \tag{6.46}$$

where: $\varepsilon_{tot,i}$ is the average total strain at the cross section for division point i,

$\varepsilon_{tot,i+1}$ is the average total strain at the cross section for division point i+1,

$\varepsilon_{tot} = \varepsilon_{th} + \varepsilon_{\sigma} + \varepsilon_{tr} + \varepsilon_{cr}$ (total strain model Chapter 8)

The change in segment length is given by:

$$l_i(1 - \varepsilon_{avtot,i}) \tag{6.47}$$

where: l_i is the segment length.

The horizontal displacement Y_i of segment length end i relative to end i+1 is determined from:

$$Y_i = ((y_{i+1})_c - c_{i+1}) - ((y_i)_c - c_i) \tag{6.48}$$

where: $(y_{i+1})_c$ is the horizontal division point displacement, or division point deflections calculated from the structural analysis described in Chapter 5, for segment length end i+1,

c_{i+1} is the horizontal division point displacement of end i+1 under zero load,

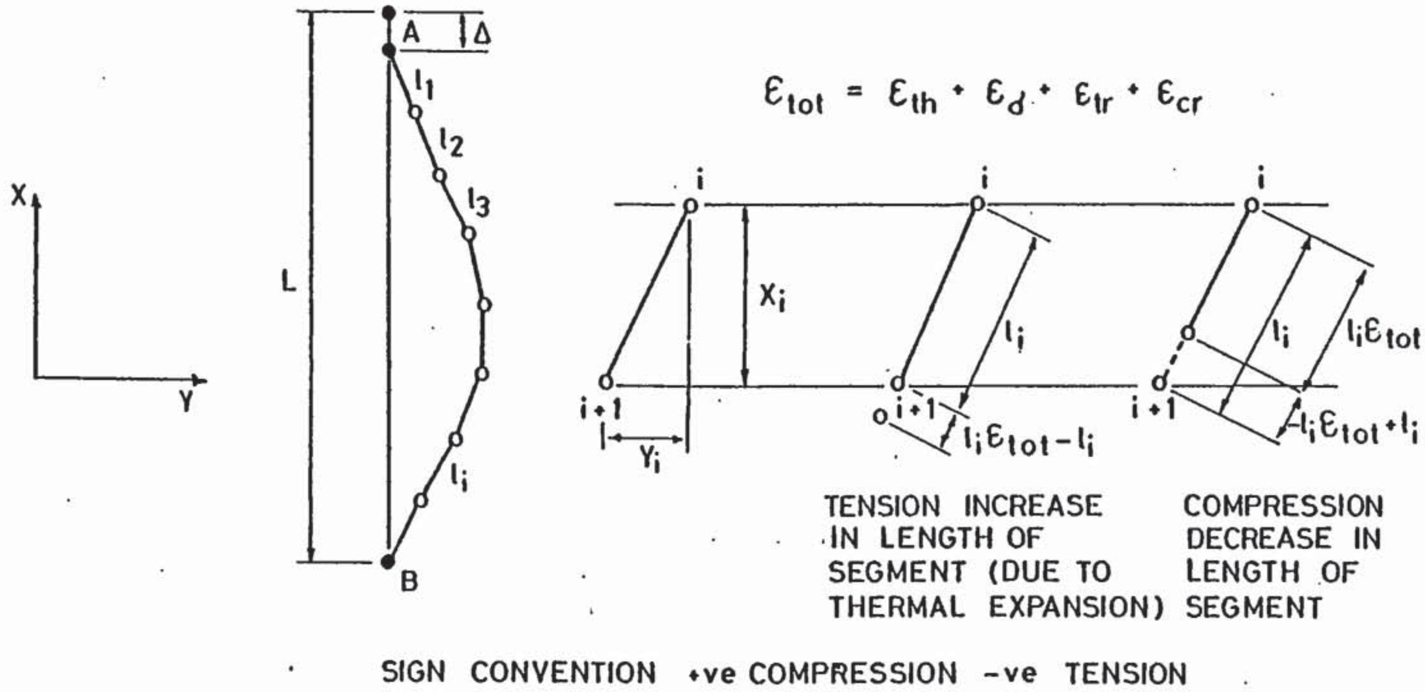

Figure 6.17 Change in chord length for axial deformation with consideration due to total strain (thermal expansion and loading).

$(y_i)_c$ is the horizontal division point displacement of segment length end i,

c_i is the horizontal division point displacement of segment length end i under zero load.

Applying Pythagoraus the vertical height X_i of segment length i see Figure 6.17, is calculated from:

$$X_i = ((l_i(1 - \varepsilon_{avtot,i}))^2 - (Y_i)^2)^{0.5} \tag{6.49}$$

and the vertical height of the deflected gusset lengths is given by:

$$G' = (g_A^2 - ((y_1)_c - c_1))^{0.5} + (g_B^2 - ((y_n)_c - c_n))^{0.5} \tag{6.50}$$

where: g_A and g_B are the gusset lengths at end A and B respectively.

The change in chord length Δ is therefore given by:

$$\Delta = G' - L + \sum_{i=1}^{i=n} X_i \tag{6.51}$$

where: L is the original chord length, or straight column length for the first time step,

n is the number of division points.

The change in chord length Δ produces a pure sway in the bay above the column under analysis, see Figure 6.16. The next stage in the analysis is to determine the force N that produces a pure sway Δ. It is now condusive to consult the moment-rotation analysis described in Section 6.2.2. Providing no plastic hinges have formed in the restraint system at column end A, the elastic slope deflection analysis described in full in Appendix C can be used to calculate the value of axial thrust N through the following equation:

$$N = \frac{12\Delta}{L_2^2}\left[\frac{K_2^2K_1/K_5 + K_2^2 + K_5K_1 + K_5K_2 + 3K_1^2K_2/K_5 + 3K_1^2 + 11K_1K_2}{4(K_1 + K_2)(K_1/K_5 + 1) - K_1^2/K_5}\right] \quad (6.52$$

where: K_1, K_2 and K_3 are the stiffnesses defined in Figure C.
Appendix C.

Note: the stiffness K_5 is adjusted for the number of floors above by multiplying by N_{f1}.

However, if plastic hinges have formed in the restraint system at end A then the axial thrust N must be calculated using the plastic analysis described in Section 6.2.2.4.1. Either equations (6.17) (6.23), (6.24) or (6.25) are used to calculate the axial thrust N depending on the position or positions of plastic hinges, see also Figue 6.10.

The total axial force acting on the column for the next time step of the structural analysis, Chapter 5, is determined from:

$$P_{i+1} = P_i + N \quad (6.53)$$

where: P_{i+1} is the axial force acting on the column under analysis for the next time step,
P_i is the current axial load.

Finally the chord length, the length between column supports A and B, must also be adjusted for the next time step through the application of the following expression:

$$L_{i+1} = L_i + \Delta \quad (6.54)$$

where: L_{i+1} is the chord length for the next time step,

L_i is the current chord length,

Δ is positive for an increase in length and negative for a decrease in length,

and the segment lengths are also adjusted from consideration of the total strain where:

$$l_i = (l_i)_o(1 - \varepsilon_{avtot,i}) \tag{6.55}$$

where: $(l_i)_o$ is the original segment length at the start of the analysis.

The adjusted values of P, L and segment lengths l_i from equations (6.53), (6.54) and (6.55) are used in the structural analysis, described in detail in Chapter 5, for the next time step.

6.3.2 Free Axial Expansion

With free axial expansion there is no restraint against axial deformation and the column is free to expand or contract without an induced restraining force. The chord length is, however, adjusted for axial deformation using equations (6.46), (6.47), (6.48), (6.49), (6.50), (6.51) and (6.55).

6.3.3 Fixed Axial Restraint

Fixed axial restraint is equivalent to a force-deflection relation with a very steep slope. Any attempted change in chord length will produce a very large restraining force since the very nature of an ideally fixed axial restraint means the chord length, the length between column supports, cannot change.

However, for the purposes of calculation a value of combined stiffness of the members adjoining joint A equal to 10^{10} is assumed. Therefore the model of fixed axial restraint is not ideally fixed but very stiff.

The change in column chord length is calculated from equations (6.46), (6.47), (6.48), (6.49), (6.50) and (6.51). The axial force, chord length, and segment lengths are then updated using equations (6.52) and (6.53), (6.54) and (6.55) respectively.

The following Chapter, Chapter 7, describes the system initialization. Various values must be proposed in order to achieve an equilibrium state that will act as the initial point for the structural anlaysis described in Chapter 5.

CHAPTER 7

SYSTEM INITIALIZATION

7.1 Introduction

This chapter deals with the calculation of the proposed values necessary for the initialization of the structural analysis described in Chapter 5. Proposed values must be calculated for moments, axial force, end slopes, curvatures, division point deflections and direct strain at the column axis for the start of the analysis only; subsequently values from the previous time step are used.

7.2 Calculation of Proposed End Slopes

The proposed end slopes for the structural system shown in Figure 7.1 are given by the following equations, derived in full in Appendix B using slope deflection equations:

$$(\theta_A)_p = -\frac{M_{ac}(4K_3 + 4K_4 + 4K_c) - 2K_cM_{bd}}{(4K_1 + 4K_2 + 4K_c)(4K_3 + 4K_4 + 4K_c) - 4K_c^2} \tag{7.1}$$

$$(\theta_B)_p = -\frac{M_{bd}(4K_1 + 4K_2 + 4K_c) - 2K_cM_{ac}}{(4K_1 + 4K_2 + 4K_c)(4K_3 + 4K_4 + 4K_c) - 4K_c^2} \tag{7.2}$$

where: M_{ac}, M_{bd}, K_1, K_2, K_3, K_4 and K_c are defined in Figure 7.1,

M_{ac} and M_{bd} are fixed end moments,

K_1, K_2, K_3, K_4 and K_c are member stiffnesses.

The numerical values of the fixed end moments are calculated according to the equations:

$$M_{ac} = \omega_{AC}L_2^2/12 \tag{7.3}$$

$$M_{bd} = \omega_{BD}L_2^2/12 \tag{7.4}$$

where: ω_{AC} is the uniformly distributed load on member AC,

ω_{BD} is the uniformly distributed load on member BD.

In the calculation of proposed end slopes for pinned rotation restraint the member stiffnesses are set to zero as follows:
If there is pinned rotational restraint at column end A then K_1 = and $K_2 = 0$. If there is pinned rotational restraint at column end then $K_3 = 0$ and $K_4 = 0$.

In the calculation of proposed end slopes for fixed rotationa restraint then the combined member stiffnesses are set to a value (10^{10} as decribed below:
If there is fixed rotational restraint at column end A the $K_1 + K_2 = 10^{10}$. If there is fixed rotational restraint at column er B then $K_3 + K_4 = 10^{10}$.

However, if there is pinned rotational restraint at both the enc of the column exposed to fire, as shown in Figure 7.2, the propose end slopes are calculated using the following formulae based c Macaulay's method and derived in full in Appendix E:

$$(\theta_A)_p = (M_A L_1/3 - M_B L_1/6)/EI \quad (7.5$$

$$(\theta_B)_p = (M_B L_1/3 - M_A L_1/6)/EI \quad (7.6$$

The end moments M_A and M_B are calculated using the equations:

$$M_A = - Pe \quad (7.7$$

$$M_B = Pe \quad (7.8$$

where: P is the axial force (entered as an item of data),

e is the eccentricity of the application of axial forc (entered as an item of data).

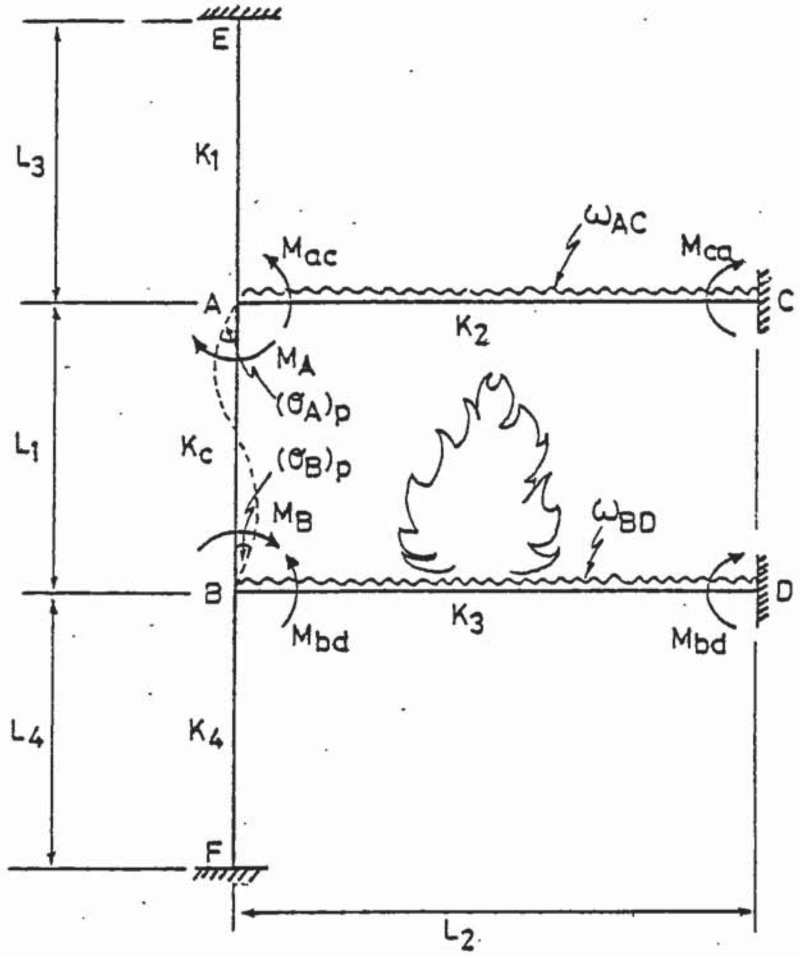

Figure 7.1 Structural system analysed

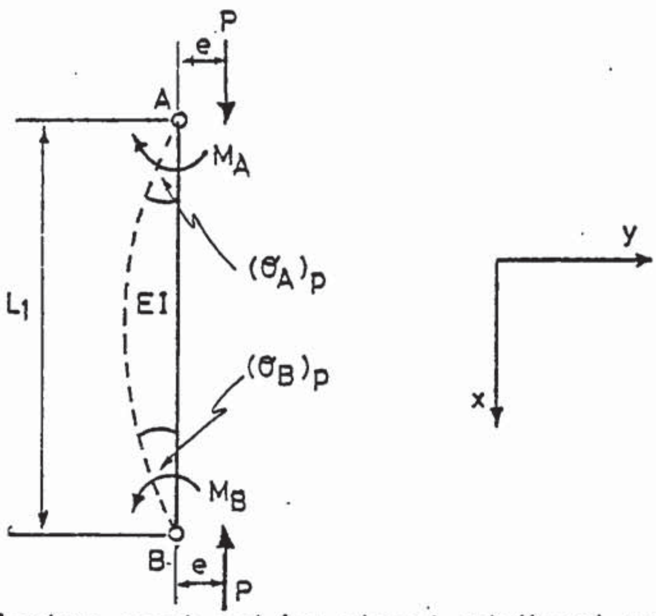

Figure 7.2 System analysed for pinned rotational restraint at both ends of the column exposed to fire.

7.3 Calculation of Proposed End Moments

The proposed end moments for the structural system shown i Figure 7.1 are calculated from the following equations derived i Appendix B from consideration of slope deflection equations:

$$M_A = K_c(4\theta_A + 2\theta_B) \tag{7.9}$$

$$M_B = K_c(4\theta_B + 2\theta_A) \tag{7.10}$$

However, if the column under anlaysis is pinned at both ends the the column end moments are calculated according to equations (7.7) an (7.8).

7.4 Calculation of Axial Force

The proposed value of axial force for the structural system show in Figure 7.1 is calculated from consideration of the shear due to th end moments in the beams. The following expression is derived i Appendix B:

$$P = \omega_{AC}L_2/2 - 6K_2\theta_A/L_2 \tag{7.11}$$

However, if the column under analysis is pinned at both ends th axial force P is entered as data.

7.5 Calculation of Proposed Division Point Deflections

The proposed division point deflections are calculated takin into consideration the column end moments and the axial forc eccentricities at each division point. The division point deflection are obtained from the following equation, derived in Appendix F:

$$(y_x)_p = -\frac{1}{EI\alpha^2}(M_A\cot\alpha L + \frac{M_B}{\sin\alpha L})\sin\alpha x + \frac{M_A}{EI\alpha^2}\cos\alpha x - \frac{M_A}{EI\alpha^2}$$

$$\ldots\ldots\ldots + (\frac{M_A + M_B}{EI\alpha^2})(\frac{x}{L}) \qquad (7.12)$$

where: $\alpha^2 = P/EI$,

x is the distance from end A to the division point,

L is the length of the column under analysis.

7.6 Calculation of Proposed Curvatures

The 'local' curvature of a column is expressed by the following equation:

$$\phi = 1/R \qquad (7.13)$$

where: R is the radius of the circle the deflected column would describe.

From the simple theory of bending:

$$M/EI = d^2y/dx^2 = 1/R \qquad (7.14)$$

where: d^2y/dx^2 is the rate of change of slope.

For simplicity it is assumed that the column is pin ended for the calculation of proposed curvatures. This will only produce a small error and furthermore the calculated values are only proposed values which will be automatically corrected by the structural analysis computer program SAFE-RCC as the analysis proceeds.

From Appendix E:

$$EId^2/dy^2 = (M_A + M_B)x/L - M_A \qquad (7.15)$$

Substituting equation (7.14) into (7.15) and rearranging give the following equation for the calculation of curvature:

$$1/R = ((M_A + M_B)x/L - M_A)/EI \qquad (7.16$$

7.7 Direct Strain at the Column Axis

The proposed value of the direct strain at the column axis fo each division point is assumed to be zero. This assumption i justified since at the initial stages of the fire axial strains ar low. Also bending strains will be more significant than direct axia strains in a column that is part of an overall structure of the typ shown in Figure 7.1. Furthermore the direct strain specified is onl a proposed value in order to start the structural analysis and will b adjusted by the structural analysis decribed in Chapter 5 to th correct value as the analysis proceeds.

7.8 Calculation of the Second Moment of Area

It is explicit in the structural analysis described in Chapter that the second moment of area of the column under analysis is base on the transformed section. For compatability within the moment rotation relations the second moment of area for all the members o the structural system analysed must also be calculated on the basis o a tranformed section in order to obtain a 'true' equilibrium conditio of end slopes and induced moments at each end of the column.

The uncracked transformed I value for the columns of th structural system is given by the equation (see Figure 7.3 (a)):

$$I_{uncrack} = bh^3/12 + (\alpha_e - 1)A_{sc}d_2^2 \qquad (7.17$$

where: b is the breadth of the column,

h is the overall depth of the column,

$\alpha_e = E_s/E_c$

E_s is the initial tangent modulus of the steel stress-strai relation for the average current temperature,

E_c is the initial tangent modulus of the concrete stress strain relation for the average current temperature,

A_{sc} is the area of steel,

d_2 is the distance between the centroid of the section and th centroid of the steel.

The uncracked transformed I value for the beams of the structura system is given by the equation (see Figure 7.3 (b)):

$$I_{uncrack} = bx^3/3 + b(h - x)^3/3 + (\alpha_e - 1)A_{sc}(x - d')^2 + (\alpha_e - 1)A_{st}(d-x)^2 \tag{7.18}$$

where:

$$x = \frac{bh^2 + \alpha_e(dA_{st} + d'A_{sc})}{bh + \alpha_e(A_{st} + A_{sc})} \tag{7.19}$$

b is the breadth of the beam,

h is the overall depth of the beam,

d is the effective depth,

A_{st} is the area of tension steel,

A_{sc} is the area of compression steel.

When the structural system is under load the member sections will crack resulting in a reduced I value. Cracking of the column under analysis will be increasingly significant as time proceeds due to the effects of the fire. Automatic consideration is taken of this within the structural analysis described in Chapter 5.

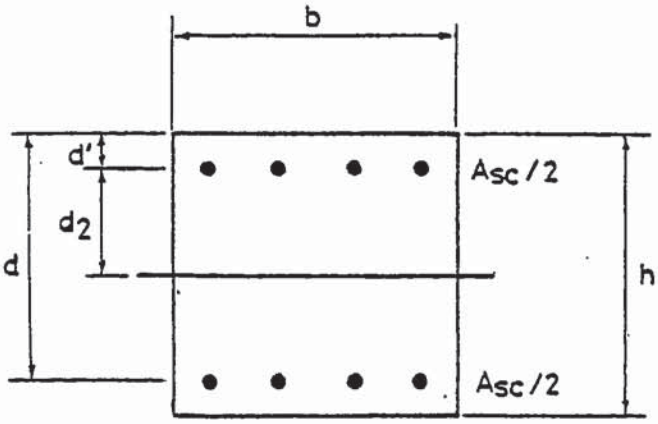

(a) Column section.

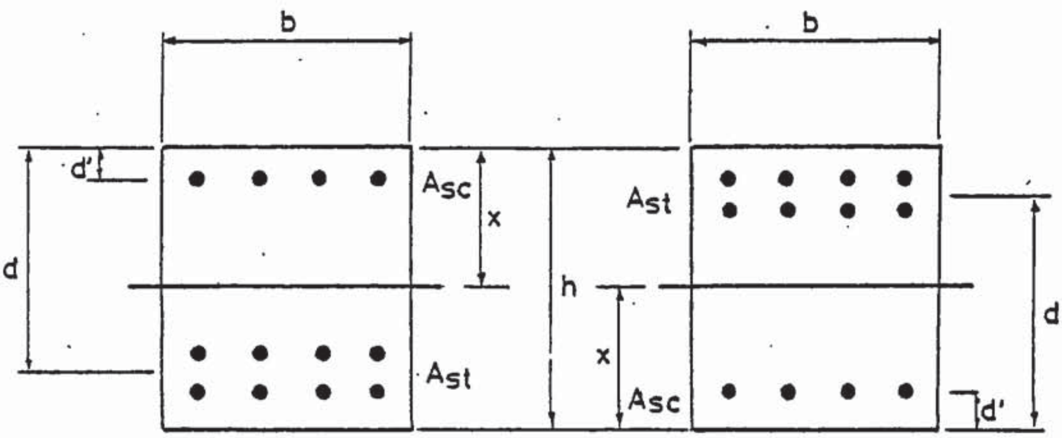

(b) Restraint beam section.

Figure 7.3 Typical sections of the structural system analysed.

However, it is assumed in this research that cracking of th columns above and below the column under analysis will not b significant since the columns primarily carry axial load and ar assumed to be remote from the effects of the fire. Therefore th uncracked I values for these columns are used throughout the analysis

Due to the fact that the restraint beams are moment carryin members cracking will be significant. In this research the assumptio is made that $I_{cracked}$ for the beams is equal to $0.5I_{uncracked}$. Th 0.5 is introduced to allow for cracking of the beam section. Althoug this is not strictly correct an assumption must be made since it i not possible to determine the $I_{cracked}$ value corresponding to th loaded section until a momant distribution has been carried out an conversely it is not possible to carry out a moment distribution whe the I value is unknown.

This assumption is supported by CP110 where it is suggested tha the stiffness of beams should be reduced to half the actual bea stiffness when analysing a structure by subframing. Although the 0. factor in CP110 is strictly there to allow for the assumption of en fixity in the beam remote from the column, the 0.5 will also tak account of cracking as a result of fire exposure.

The next Chapter is concerned with the description of th material behaviour models incorporated in the computer analysis.

CHAPTER 8

MATERIAL BEHAVIOUR MODELS

8.1 CONCRETE

8.1.1 Total Strain Model

The program requires the calculation of thermal strains as result of the fire environment. A computer orientated constitutiv model for concrete in compression, valid at transient hig temperatures, was presented in Anderberg and Thelandersson (1976) an is used here in the structural response program. Although th Anderberg and Thelandersson total strain model (1976) has some doub behind it, see Chapter 2, it is the only available model. The mode is based on the concept that the total strain ε can be separated int four components:

$$\varepsilon = \varepsilon_{th}(T) + \varepsilon_{\sigma}(\bar{\sigma},\sigma,T) + \varepsilon_{cr}(\sigma,T,t) + \varepsilon_{tr}(\sigma,T) \qquad (8.1$$

where: ε_{th} is the thermal strain, including shrinkage, measured o specimens under variable temperature,

ε_{σ} is the instantaneous, stress related strain, based o stress-strain relationships obtained under constant, stabilized temperature,

ε_{cr} is the creep strain or time dependent strain measured under constant stress and stabilized temperature.

ε_{tr} is the transient strain, accounting for the effect of temperature increase under stress, derived from tests under constant stress and variable temperature,

σ is the stress,

$\bar{\sigma}$ is the stress history,

T is the temperature,

t is the time.

8.1.2 Stress-Strain Model

The stress-strain relationship for both concrete and steel are temperature dependent and are modelled as a function of temperature dependent material paramaters. These temperature dependent material parameters are calculated for each elemental temperature using the procedure described in Section 8.3.

The stress-strain relationship for concrete is based on that developed by Baldwin and North (1973) on Furamura. The stress-strain curves for concrete under compression at high temperatures takes the form:

$$\frac{\sigma}{\sigma_{max}} = f\left(\frac{\varepsilon}{\varepsilon_{max}}\right) \tag{8.2}$$

where: f is a function independent of temperature,

σ_{max} and ε_{max} are the stress and strain at the peak of the curve for a given temperature, which are functions of temperature.

On plotting the normalized stress against normalized strain Baldwin and North developed the following expression to describe the stress-strain relationship for any temperature (see Figure 8.1):

$$\frac{\sigma}{\sigma_{max}} = \frac{\varepsilon}{\varepsilon_{max}} \exp\left(1 - \frac{\varepsilon}{\varepsilon_{max}}\right) \tag{8.3}$$

Therefore the stress-strain curve for concrete at high temperatures can be derived from the stress-strain relationship at room temperature together with the location of the maximum of the stress-strain curve at high temperatures, the compressive strength of the material.

It is common to assume σ_{max} to be approximately 80% of the actua cube strength. Both Forsén (1982) and Haksever and Anderberg (1982 use this approximation in models of structural behaviour.

The tangent modulus of elasticity is also required, which i equal to the gradient of the stress-strain curve for any given valu of strain, thus the modulus of elasticity can be found fro differentiation of the relationship with respect to strain.

$$\frac{d\sigma}{d\varepsilon} = E_t = \frac{\sigma_{max}}{\varepsilon_{max}} (\exp(1 - \frac{\varepsilon}{\varepsilon_{max}})(1 - \frac{\varepsilon}{\varepsilon_{max}})) \tag{8.4}$$

The model of the stress-strain relation in tension is relatively straight-forward, where the slope of the relation is equal to the initial slope of the stress-strain relation for compression and the concrete element is assumed to fail in tension once the ultimate tensile stress has been exceeded. This idealized stress-strain relationship in the tensile zone is essentially similar to that established by Anderberg (1976), (see Figure 8.2).

It has been demonstrated by researchers such as Hughes and Chapman (1966) that the Youngs modulus for concrete under tension does not significantly differ from that under compression. From equation (8.4) the initial tangent modulus of the stress-strain relation under compression, E_o or the slope of the stress-strain relation under tension is given by:

$$E_o = \frac{\sigma_{max}}{\varepsilon_{max}} \exp(1) \tag{8.5}$$

From CP110 the ultimate tensile stress can be determined from the following expression:

$$\sigma_u^t = 0.36 \sqrt{f_{cu}} \tag{8.6}$$

where: f_{cu} is the concrete cube strength in N/mm^2.

However, the tensile stresses in concrete contribute relatively insignificantly to the total load bearing capacity of a reinforced concrete column and therefore the importance of the tensile properties of concrete is relatively small for this research.

Unloading behaviour of the concrete in the stress-strain relation is idealized as a straight line with a slope equal to the instantaneous initial modulus, see Figure 8.2. As load is re-applied the stress-strain relation follows the linear behaviour until the original curve is reached. With further increase in load the relation follows the curve the relation would have described if unloading had not taken place.

Actual unloading-reloading behaviour of concrete is characterized by a hysteresis loop, however, tests have shown that with reloading the relation does return to the curve that would have been described had unloading and subsequent reloading not taken place, e.g. Furamura. Therefore concrete may be treated as a material obeying Prandtl's rules of plasticity.

If σ_i and ε_i are the current stress and strain respectively, and σ_{i-1} and ε_{i-1} are the stress and strain from the previous time step, where ε_i is less than ε_{i-1}, then the current state of stress, σ_i, is given by:

$$\sigma_i = \sigma_{i-1} - E_o(\varepsilon_{i-1} - \varepsilon_i) \tag{8.7}$$

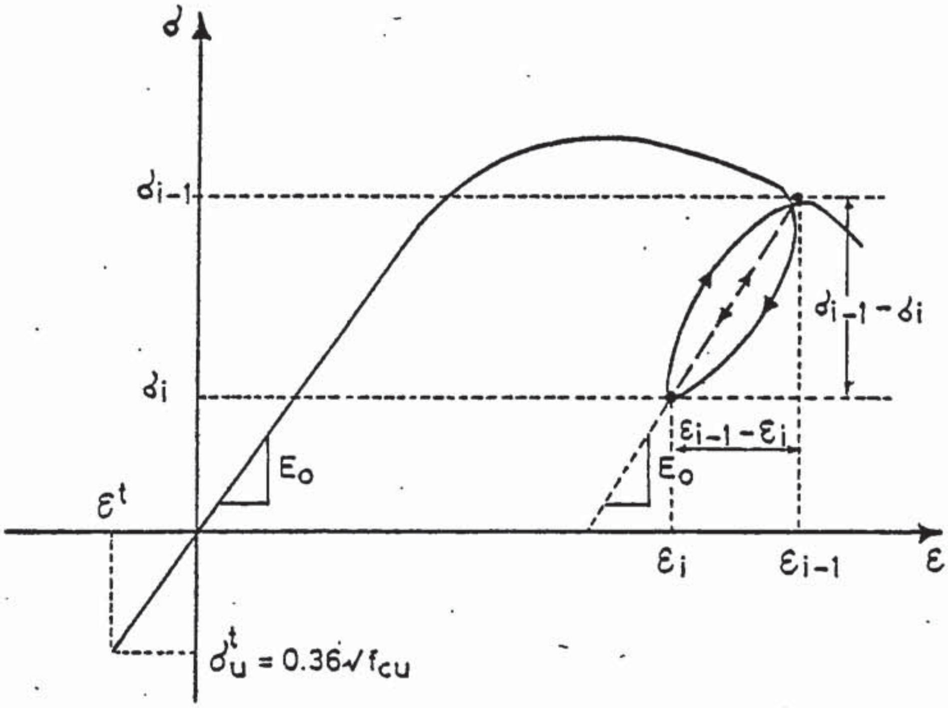

Figure 8.2 Idealized stress - stress relation showing tensile zone and unloading characteristics.

The ultimate strain is stress history dependent as well as temperature dependent. A theoretical quantification of the stress history dependence of ε_{max} with increasing temperature proposed by Anderberg and Thelandersson (1976) is used where:

$$\varepsilon_{max} = \max\left(\varepsilon_{max,o},\ \bar{\varepsilon}_{max} - \varepsilon_{tr}\right) \tag{8.8}$$

where: compressive strains are positive,

$\varepsilon_{max,o}$ is the value of strain corresponding to maximum stress at ambient conditions,

$\bar{\varepsilon}_{max}$ is the temperature dependent ε_{max} measured on specimens unloaded during heating,

ε_{tr} is the transient strain which represents the stress dependent component of strain.

A graphical interpretation of equation (8.8) is shown in Figure 8.3 for a typical variation of ε_{max}. The Figure illustrates that the maximum strain due to a prehistory of stress is always less than or equal to $\bar{\varepsilon}_{max}$ but not reduced to a value less than $\varepsilon_{max,o}$.

8.1.3 Thermal Strain

The thermal strain during heating is a simple function of temperature, directly given by the thermal expansion curve. Since drying shrinkage is included, the thermal expansion depends on the initial water content, rate of heating can be neglected. It can be assumed that the thermal expansion is fully reversible, although it is not quite in reality since the shrinkage is irrecoverable. Due to the irrecoverability of the shrinkage strain and due to the possibility that the structural response program may be used to determine the residual strength of a reinforced concrete column, the shrinkage strain will be modelled separately.

A constant value for the coefficient of thermal expansion of 12.5×10^{-6} deg^{-1}C is often used in calculation. Figure 8.4 shows the thermal expansion curve, including shrinkage, for quartzite aggregate derived by Anderberg (1976). Inspection of Figure 8.4 indicates that the thermal strain is considerably non-linear with respect to temperature. Forsén (1982) found that the experimental curve established by Anderberg (Figure 8.4) may be represented by the following two fourth degree polynomials:

$$\begin{aligned} \varepsilon_{th} &= -(a\tau^4 + b\tau^3 + c\tau^2 + d\tau + e) && \text{for } \tau \leqslant 6 \\ \varepsilon_{th} &= -(a'\tau^4 + b'\tau^3 + c'\tau^2 + d'\tau + e') && \text{for } \tau > 6 \end{aligned} \qquad (8.9)$$

where: $\tau = T/100$ (^oC)

$a = 0.02837$ $\qquad a' = 0.02102$

$b = -0.2447$ $\qquad b' = -0.4972$

$c = 0.7376$ $\qquad c' = 3.791$

$d = 0.3229$ $\qquad d' = -8.265$

$e = 0.09218$ $\qquad e' = 5.561$

Thermal strain is a negative strain component since tensile strains (expansion) are taken as negative in this research.

8.1.4 Transient Strain

Transient strains are those strains that cannot otherwise be accounted for due to the decomposition of the cement paste. They occur under compressive stresses as temperature increases, are essentially permanent, irrecoverable and only occur under first heating. Transient strains are temperature dependent and independent of time, see Figure 8.5. The model desribed here is that developed by Anderberg and Thelandersson (1976).

Anderberg and Thelandersson (1976) demonstrate:

$$\varepsilon_{tr} = \frac{\sigma}{\sigma_{max,o}} g(T) \qquad (8.10$$

where: g(T) is a function of temperature.

Inspection shows that g(T) is approximately proportional to ε_{th}, see Figure 8.6, hence:

$$\varepsilon_{tr} = -k_2 \frac{\sigma}{\sigma_{max,o}} \varepsilon_{th} \quad \text{for } 20^{o}C \leqslant T < 500^{o}C \qquad (8.11)$$

where: k_2 is a dimensionless constant varying with cement type.

Anderberg and Thelandersson (1976) found by means of linear regression that a value of k_2 equal to 2.35 best describes the quartzite concrete used in their tests. From investigation of the strain component ε_{tr} against the test series by Weigler and Fischer (1967) and Schneider (1976), Anderberg and Thelandersson (1976) demonstrated that good agreement was obtained if k_2 was given values of 2.0 and 1.8 respectively. The variation in the factor k_2 is assumed to be due to the different mix proportions used in the test series. A value of k_2 equal to 2.35 is used in this research.

For temperatures above 500^{o}C there is an accelerated effect on transient strains. Anderberg (1976) proposed the following expression for the incremental change in ε_{tr}:

$$\Delta\varepsilon_{tr} = 0.1 \times 10^{-3} \Delta T \sigma / \sigma_{max,o} \quad \text{for } 500^{o}C < T < 800^{o}C \qquad (8.12)$$

where: σ is the stress from the previous time increment,

$\sigma_{max,o}$ is the compressive ultimate strength at ambient conditions.

8.1.5 Creep Model

Anderberg and Thelandersson (1976) demonstrated that creep may t a good approximation be related between the actual applied stress ar the strength at the current temperature for primary and secondar phases of creep:

$$\varepsilon_{cr,3} = \frac{\sigma}{\sigma_{max}(T)} \phi_T(T) \qquad (8.13$$

where: $\varepsilon_{cr,3}$ is the 3 hour creep (see Figure 8.7),

σ is the applied stress,

$\sigma_{max}(T)$ is the strength at the current temperature.

From inspection Anderberg and Thelandersson (1976) found that th data fit well if:

$$\phi_T(T) = \beta_o e^{k_1(T-20)} \qquad (8.14)$$

where: β_o and k_1 are constants.

From regression analysis values of β_o and k_1 were found equal to 0.53×10^{-3} and 3.04×10^{-3} $deg^{-1}C$ respectively.

Equations (8.13) and (8.14) give an expression for the creep $\varepsilon_{cr,3}$ after 3 hours as affected by stress and temperature when the two parameters are held constant. Anderberg and Thelandersson (1976) expressed the influence of time with a power function as follows:

$$\varepsilon_{cr} = \varepsilon_{cr,3}\left[\frac{t}{t_r}\right]^p \qquad (8.15)$$

where: ε_{cr} is the creep after time t under constant stess an(
temperature,

$\varepsilon_{cr,3}$ is the creep after 3 hours under constant stess an(
temperature,

t is the time,

t_r is the reference time = 3 hours,

p is a dimensionless constant.

From analysis of results a reasonable estimate of p was found tc be 0.5.

According to equations (8.13), (8.14), and (8.15) the basic creep at constant temperature and stress is obtained from the following equation:

$$\varepsilon_{cr} = \beta_o \frac{\sigma}{\sigma_{max}(T)} \left[\frac{t}{t_r}\right]^p e^{k_1(T-20)} \tag{8.16}$$

Equation (8.16) expresses the creep verses time for any given combination of temperature and stress. For variable stress and temperature the strain hardening principle is used in order to describe the creep development. The creep is calculated incrementally for each time step throughout a time history, see Figure 8.8. Both stress and temperature are assumed to be constant during a time increment.

The principle of strain hardening is formulated according to the following procedure. It is assumed that the stress σ_i, the temperature T_i and the accumulated creep strain $\varepsilon_{cr,i}$ are known at the time t_i. The accumulated creep strain $\varepsilon_{cr,i+1}$ has now to be determined at a subsequent time $t_{i+1} = t_i + \Delta t_i$.

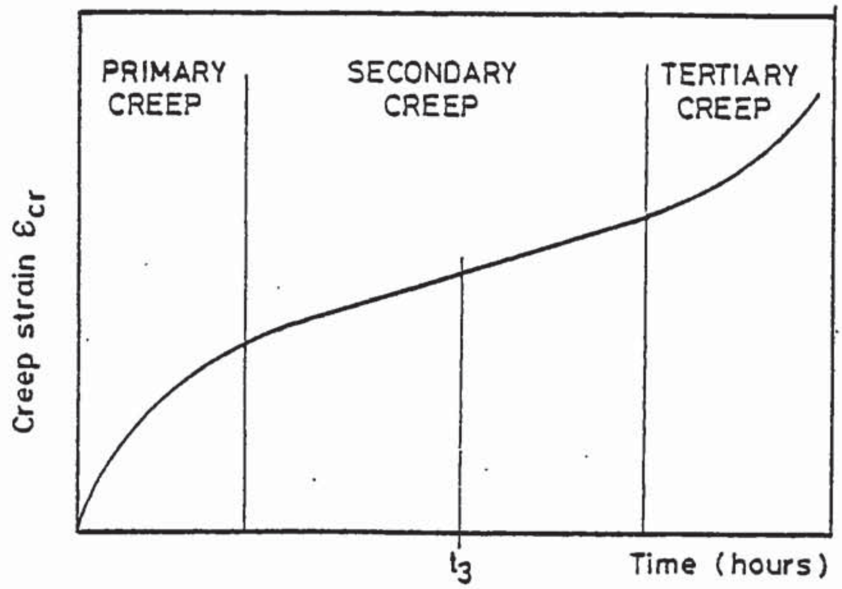

Figure 8.7 Phases of concrete creep.

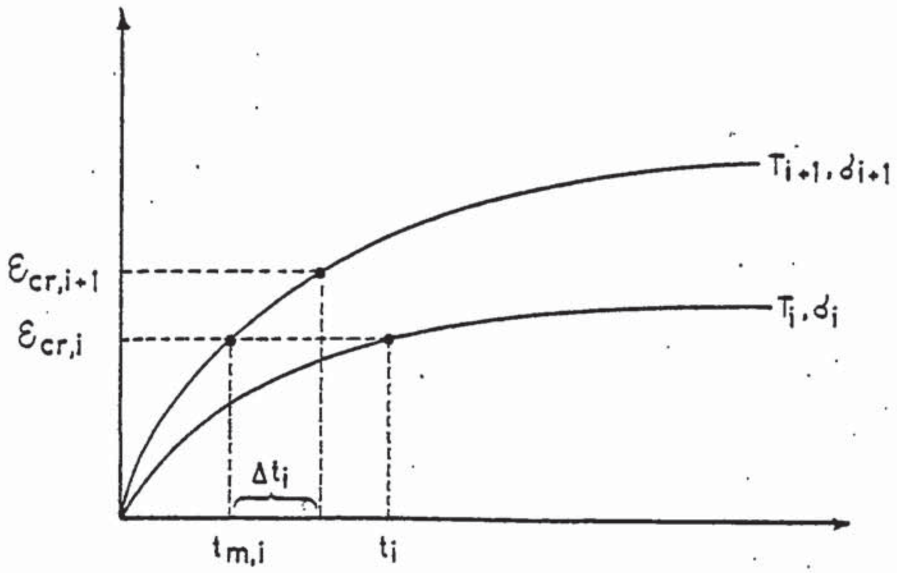

Figure 8.8 Strain hardening principle for temperature dependent concrete creep strain.

If the temperature T_{i+1} and the stress σ_{i+1} at time t_{i+1} are known, it is possible to calculate the material time $t_{m,i}$ that would give a creep strain equal to the accumulated value $\varepsilon_{cr,i}$ at a constant stress σ_{i+1} and constant temperature T_{i+1}. Substituting $t_{m,i}$ and the accumulated creep strain from the previous time step into equation (8.16) and rearranging yields the following expression:

$$t_{m,i} = t_r \left[\frac{\varepsilon_{cr,i}}{\beta_o \dfrac{\sigma_{i+1}}{\sigma_{max}(T_{i+1})} e^{k_1 (T_{i+1}-20)}} \right]^{\frac{1}{p}} \tag{8.17}$$

If the actual time increment Δt_i is added to the material time $t_{m,i}$ the following expression for the creep strain is obtained:

$$\varepsilon_{cr,i+1} = \beta_o \frac{\sigma_{i+1}}{\sigma_{max}(T_{i+1})} \left[\frac{t_{m,i} + \Delta t_i}{t_r} \right]^p e^{k_1 (T_{i+1}-20)} \tag{8.18}$$

However, the stress σ_{i+1} is unknown when the creep strain $\varepsilon_{cr,i+1}$ is evaluated, hence a simplification is made whereby the stress σ_i from the previous time step t_i is used. Provided the time increments are set sufficiently small when a rapid change in stress is expected, significant analytical errors caused by this simplification may be avoided. It should be noted that due to the use of material time at each time step, the true time is not explicitly used in the creep model, apart from at the very first time step when accumulated creep strain is zero.

It should be noted that no creep recovery is accounted for in the above mentioned model of creep, and no creep is considered to occur in tension since there is no available model and the stresses are low.

8.1.6 Shrinkage Strains

Shrinkage strain in concrete is due to moisture loss, it is an irreversible process and is highly temperature dependent. This temperature dependence dictates the total amount of shrinkage that may occur and the rate at which it occurs. The shrinkage model described here is taken from Becker and Bresler (1974). It is assumed that shrinkage continues in the concrete element until a temperature of 100°C is reached, which upon reaching all the remaining shrinkage is assumed to occur within the current time step. However, the total amount of shrinkage occurring within any time step cannot cause the cumulative shrinkage strain to exceed the total potential shrinkage for the temperature at that time step.

The shrinkage strain within a given time step is calculated from the following equations. The basic shrinkage model is:

$$\frac{d\varepsilon_{shr}}{dt} = a(T)(\varepsilon_{\infty}(T) - \varepsilon_{shr}) \tag{8.19}$$

where: ε_{shr} is the current cumulative shrinkage strain,

$\varepsilon_{\infty}(T)$ is the total potential shrinkage,

$a(T)$ is the rate constant.

$$a(T_i) = (0.001 + ((T_i - 20) \times 0.0125)^2 \tag{8.20}$$

$$\varepsilon_{\infty}(T_i) = 0.0005 \times (1 + (T_i - 20) \times 0.0125) \tag{8.21}$$

$$\partial\varepsilon_i{}^{shr} = a(T_i)(\varepsilon_{\infty}(T_i) - \varepsilon_{shr})\ \Delta t_i \tag{8.22}$$

where: $\partial\varepsilon^{shr}$ is the incremental shrinkage strain,

Δt is the time step.

The equations hold for the range of temperature 20 to 100°C and the maximum total shrinkage at 100°C is 0.001 mm/mm.

8.2 STEEL

8.2.1 Total Strain Model

The deformation process of steel at transient high temperatures can be described by three strain components, defined by the constitutive equation:

$$\varepsilon = \varepsilon_{th}(T) + \varepsilon_{\sigma}(\sigma,T) + \varepsilon_{cr}(\sigma,T,t) \qquad (8.23)$$

where: ε_{th} is the thermal strain,

ε_{σ} is the instantaneous, stress related strain based on stress relations obtained under constant, stabilized temperature,

ε_{cr} is the creep strain or time dependent strain.

8.2.2 Stress-Strain Model

The analytical description of the temperature dependent instantaneous stress-strain law for reinforcing steel is based on a bi linear stress-strain envelope determined by the modulus of elasticity, the yield stress and the strain hardening modulus (Becker and Bresler (1974)). The envelope is shown in Figure 8.9. The model includes the unloading path, determined by the current inelastic strain ε_o and the temperature dependent initial elasticity modulus E_s.

The envelope can be described using the three parameters:

$f_y(T)$ - the yield stress (temperature dependent),

$E_s(T)$ - the elastic modulus (temperature dependent),

E^* - the strain hardening modulus (temperature dependent).

The envelope is bounded by two parallel lines with a slope of E^*:

i) upper bound: $\sigma_u = f_y + E^*(\varepsilon - \varepsilon_y)$ (8.24)

ii) lower bound: $\sigma_l = -f_y + E^*(\varepsilon + \varepsilon_y)$ (8.25)

where: ε_y is the temperature dependent yield strain = f_y/E_s

A third line intercepts the axis at ε_o, with a slope of E_s:

iii) $\sigma_E = E_s(\varepsilon - \varepsilon_o)$ (8.26)

where: ε_o is calculated using stress-strain from previous time step:

$$\varepsilon_{o_{\text{for } i}} = \varepsilon_{i-1} - \sigma_{i-1}/E_s \tag{8.27}$$

From consideration of Figure 8.9, it can be seen that when $\sigma = \sigma_E$ the stress corresponding to the current strain $\varepsilon_\sigma = \varepsilon_i$ and the inelastic strain ε_o, with further loading the stress increases in accordance with the modulus E_s until the upper bound is reached. The upper bound has a reduced tangent modulus, the strain hardening modulus E^*, which has been taken equal to $E_s/20$. Failure of the steel is assumed to occur when the steel ruptures at a value of stress related strain equal to $10\varepsilon_y$. The stress-strain relation in compression is assumed to be the same as that in tension. No account is taken of the possibility of buckling of the reinforcement between the link supports.

The state of stress is determined from:

$$\begin{array}{ll} & \text{if } \sigma_E > \sigma_u \text{ then } \sigma = \sigma_u \\ \text{else} & \\ & \text{if } \sigma_E < \sigma_l \text{ then } \sigma = \sigma_l \\ \text{else} & \\ & \quad \sigma = \sigma_E \end{array} \tag{8.28}$$

8.2.3 Thermal Strain

The steel thermal strain is a function of the temperature dependent coefficient of thermal expansion and the temperature of the element. Determination of the thermal strain is achieved through the application of the expression:

$$\varepsilon_{th} = - \int_{20^{o}C}^{T} \alpha_s(T)\ dT \qquad (8.29)$$

where: α_s is the coefficient of expansion,
(temperature dependent)
T is the temperature.

ε_{th} is a negative strain component (expansion).

A constant value of $\alpha_s = 15.0 \times 10^{-6}\ {}^{o}C^{-1}$ is often used in calculation. However, Anderberg (1976) presented the following values for the steel type $K_s40\ \phi\ 10$:

$$\alpha_s\ (20^{o}C) = 12.0 \times 10^{-6}\ {}^{o}C^{-1}$$
$$\alpha_s\ (800^{o}C) = 20.0 \times 10^{-6}\ {}^{o}C^{-1}$$

A linear interpolation may be used to determine the value of α_s in the temperature range of 20°C to 800°C.

8.2.4 Creep Model

The model for creep in reinforcing steel is similar to that used in FIRES-RC, based on Harmathy's Comprehensive Creep Model (1970) with Dorn's Theta method (1954) for temperature variation. Only the primary and secondary phases of creep are considered. Creep in steel is considered to be a function of the current state of strain, and is primarily a function of the shear strain and is therefore assumed to be identical in both tension and compression.

The creep model for constant temperature and stress can b extended to variable temperatures by use of Dorn's Theta method an to variable stress by the use of a strain hardening rule. Usin Harmathy's formulation of creep (see Figure 8.10), the creep rate is constant in the domain of temperature compensated time, hence:

$$\frac{d\varepsilon_{cr}}{d\theta'} = Z \tag{8.30}$$

where: ε_{cr} is the creep strain,

θ' is the temperature compensated time,

Z is the Zener Holloman constant.

Harmathy (1970) has suggested that this relationship can be extended for use in both primary and secondary phases of creep with the following modification:

$$\frac{d\varepsilon_{cr}}{d\theta'} = Z \coth^2\left(\frac{\varepsilon_{cr}}{\varepsilon_{cro}}\right) \tag{8.31}$$

where: ε_{cro} is the y axis intercept of the secondary creep phase.

The temperature compensated time, θ', which combines temperature and time into one single parameter, can be calculated from the following expression:

$$\theta' = \int_o^t (\exp(-\Delta H/R(T + 273)))dt \tag{8.32}$$

where: ΔH is the activation energy of creep,

R is the gas constant.

Harmathy's (1974) computational algorithm follows, combining Dorn's Theta method and a strain hardening rule, which allows the computation of the incremental creep strain for varying stress and temperature:

$$\Delta\varepsilon_{cr} = Z(\sigma)\Delta\theta(T,\Delta t)\coth^2\left(\frac{\bar{\varepsilon}_{cr}}{\varepsilon_{cro}}\right) \tag{8.33}$$

where: $\Delta\theta(T,\Delta t) = \Delta t.e^{-\Delta H/R(T+273)}$

$\bar{\varepsilon}_{cr}$ is the accumulated (total) creep strain.

$Z(\sigma)$, $\Delta H/R$, ε_{cro} are constants varying with steel type.

Values of the coefficients for creep parameters Z, ε_{cro} and $\Delta H/R$ derived for different steels, are given in Appendix H.

The strain hardening rule combined in the Harmathy (1974) algorithm for the determination of creep strain in the steel for varying stress and temperature is applied in a way analagous to that for concrete, see Figure 8.8. It is assumed that the stress σ_i, the accumulated creep strain $\varepsilon_{cr,i}(\theta_i,\sigma_i)$ are known at the temperature compensated time θ_i. To evaluate the creep increment from θ_i to θ_{i+1} when the stress is σ_{i+1} a fictitious temperature compensated material time $\theta_{i,m}$ is introduced that would give the same creep $\varepsilon_{cr,i}$ at the stress σ_{i+1} as at σ_i. The incremental creep strain $\Delta\varepsilon_{cr,i}$ is then calculated for the temperature compensated time $\theta_{i+1} = \theta_{i,m} + \Delta\theta_i$ and the total strain is therefore given by $\varepsilon_{cr,i+1} = \varepsilon_{cr,i} + \Delta\varepsilon_{cr,i}$.

The current state of creep strain is given by the sum of the accumulated creep strain and the incremental creep strain for the current time step (or the accumulated creep strain for the next time step).

In the first time step where $\bar{\varepsilon}_{cr} = 0$, the hyperbolic cotange term tends towards infinity, thus the creep strain for the first tin step is calculated from the following equation as suggested t Harmathy (1967):

$$\Delta\varepsilon_{cr} = (3Z\theta\varepsilon_{cro}{}^{2})^{1/3} + Z\theta \quad (8.34$$

which provides a good approximation for strain values of ε_{cr} up t $0.5\varepsilon_{cro}$.

It should be noted that no model of creep recovery is accounte for in the above mentioned model of creep.

8.3 TEMPERATURE DEPENDENCE OF MATERIAL PARAMETERS

Many of the material paramaters are functions of temperature they include the coefficient of thermal expansion for steel, the yiel strength and elastic modulus of steel, and the stress and the strai corresponding to the maximum concrete stress. The temperatur dependent material parameters can be represented as linearly segmente curves, see Figure 8.11.

The temperature dependent material parameter is represented by a series of points and connecting lines where the y axis corresponds with the material parameter and the x axis temperature. The value of material property, f, for a given temperature T_i is given by:

$$f(T_i) = f(T_n) + (T_i - T_n)\, S_n \quad (8.35)$$

where: $T_n \leqslant T_i \leqslant T_{n+1}$,

S_n is the slope between points n and n+1.

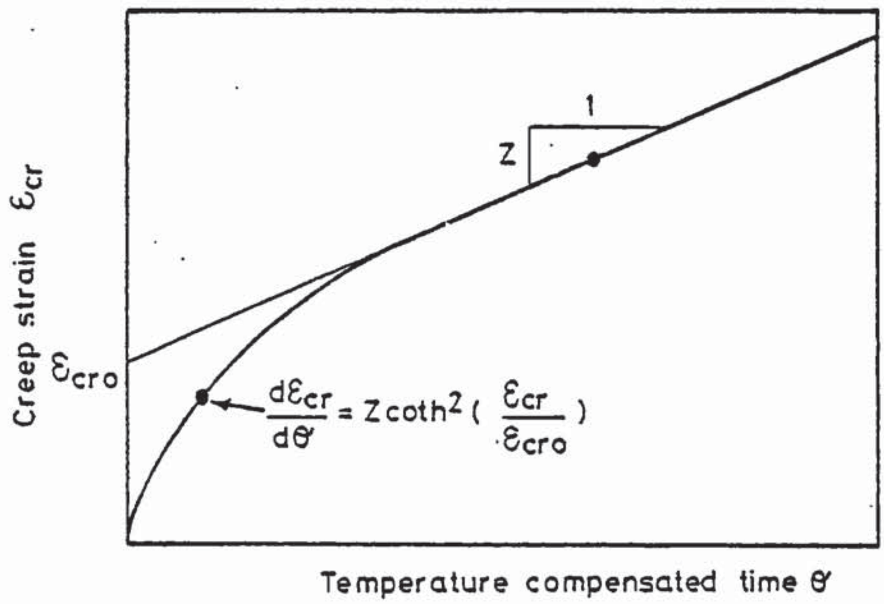

Figure 8.10 Harmathy's formulation of creep model.

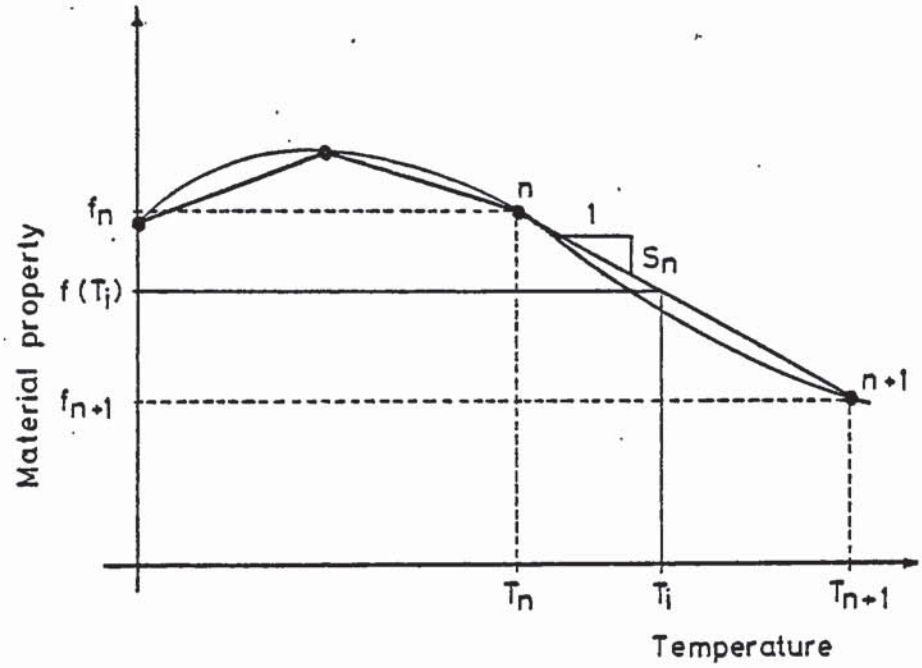

Figure 8.11 Linear segmented curve representation of material properties.

CHAPTER 9

DESCRIPTION OF COMPUTER PROGRAM (SAFE-RCC)

The computer model SAFE-RCC, Structural Analysis of Fire Exposed Reinforced Concrete Columns, is a non-linear structural analysis that has been developed as an analytical tool to study the fire response of reinforced concrete columns that are subject to restraint and continuity likely to be experienced in a total structure.

The computer program provides a description of the response in the form of printed output that includes the time history of lateral displacements, rate of deflection, axial deformation, end slopes, end moments, axial force, internal stresses and strains in the concrete and steel elements, and an indication of the current state of the concrete with respect to cracking. Crushing of the concrete does not strictly occur since a redistribution of stress occurs in the cross section after the attainment of a peak value.

The thermal response for the members of the structural system is evaluated using the computer program FIRES-T (Becker, Bizri and Bresler (1974)), which allows the use of up to four temperature-time fire curves and as many surface boundary conditions as are necessary to represent the fire exposure. It is assumed that the longitudinal thermal response is uniform throughout the structural member. Therefore each segment of the column under analysis is subject to the same temperature distributions.

Details of the finite element mesh for each structural cross section are passed directly over to SAFE-RCC from FIRES-T to ensure consistent cross sections in both the thermal analysis and the structural analysis.

The models of the mechanical properties, both of the concrete and the reinforcement, incorporated in SAFE-RCC take into account the variation due to temperature and stress dependence of transient strain, thermal strain, creep strain, and shrinkage strain. Material behaviour models that have been incorporated in SAFE-RCC to provide a description of material property are as realistic as possible. However, the material behaviour predicted by these proposed models is only as accurate as the analytical methods and numerical procedures contained therein, and for these reasons SAFE-RCC has been developed so that models of material behaviour may be easily interchanged.

The user should therefore be aware of the limitations of the proposed models, for example the sensitivity of the material models to the choice of coefficients such as the transient strain coefficients and the steel creep coefficients. If new material behaviour models are developed that are more accurate than the currently available models, the proposed models can be replaced.

The idealization of the support boundary conditions used in SAFE-RCC models continuity over the supports and allows for redistribution of moments to occur during the fire. Consideration is taken of column slenderness and second order effects due to the axial load eccentricity as a result of increasing lateral displacement.

In the current version of SAFE-RCC the geometric discretization is based as follows. The column under analysis can be segmented into a maximum of 20 segments, and the segment division points can be subdivided into a maximum of 150 concrete and steel finite elements which are directly passed over from FIRES-T. This corresponds to 300 elements for the whole cross section since only half the section is modelled due to the symmetry of the analysis.

Cross sections of the restraint system can be subdivided into maximum of 100 elements which are directly passed over from FIRES-T The 100 elements correspond to the half cross section for restrain members.

A maximum of 65 time steps can currently be employed in SAFE-RCC Choice of the time step size is at the discretion of the user However, numerical problems may arise, resulting in slow convergence if the time step increments, and thus also the temperature increments are set too large. This particularly applies in the beginning of th fire period where the fire curve is normally very steep.

It has been found from experience that it is most convenient t separate the fire period into time intervals. A time increment of : minutes during the steepest portion of the temperature-time curve, fo example the first half hour for the ISO 834 curve (see Figure 2.5) will yield acceptable convergence to a structural solution Thereafter the time increments may be increased quite significantl when the flatter portion of the curve is reached. However, it shoul be noted that time steps should be kept reasonably small near failur due to the fact that convergence difficulties may arise once more a the column approaches failure, and to enable the provision of a accurate description of the structural behaviour and determination o the corresponding fire performance.

SAFE-RCC is written in Fortran 77 and was developed on a CDC 760 Computer. However, every attempt has been made to develop a portable machine independent computer program. Due to the modelling of th temperature and time dependence a considerable storage space i required in SAFE-RCC.

The computer program in its present form requires a total o 147328 decimal words of memory. Array storage requires 72192 decima words of large core memory (LCM) stored in a named common block /LCM and 27008 decimal words of small core memory (SCM). 48128 decima words of large core memory are used for the input/output and jo supervisor requirements. Therefore a total of 120320 decimal words o large core memory is required. Since the maximum user LCM availabl on the CDC 7600 is 120832 (354000_8) decimal words, SAFE-RCC has bee dimensioned to the limit of the CDC 7600.

In the current version of SAFE-RCC the section temperatur profiles are assigned storage space in the central memory of th computer for every time step. This is not strictly necessary sinc only the current time step temperature profiles are required at an time during execution.

Larger jobs could be run using SAFE-RCC if the program wa restructured such that the section temperature profile information wa stored outside the program and only brought into central memory a required. However, information retrieval and storage from files use a significant portion of valuable real time which could otherwise b available for central processing time.

SAFE-RCC is likely to be used to model fire tests in excess o two hours, correspondingly requiring large central processing times It was therfore decided to remove the possibility of wastage of real time through information retrieval and storage from files by assignin storage in the central memory for all the information required for an program run.

The overall structure of the computer program SAFE-RCC is show in Figure 9.1. Individual elements of the program structure and th corresponding program subroutines are described in the followir Chapter, Chapter 10.

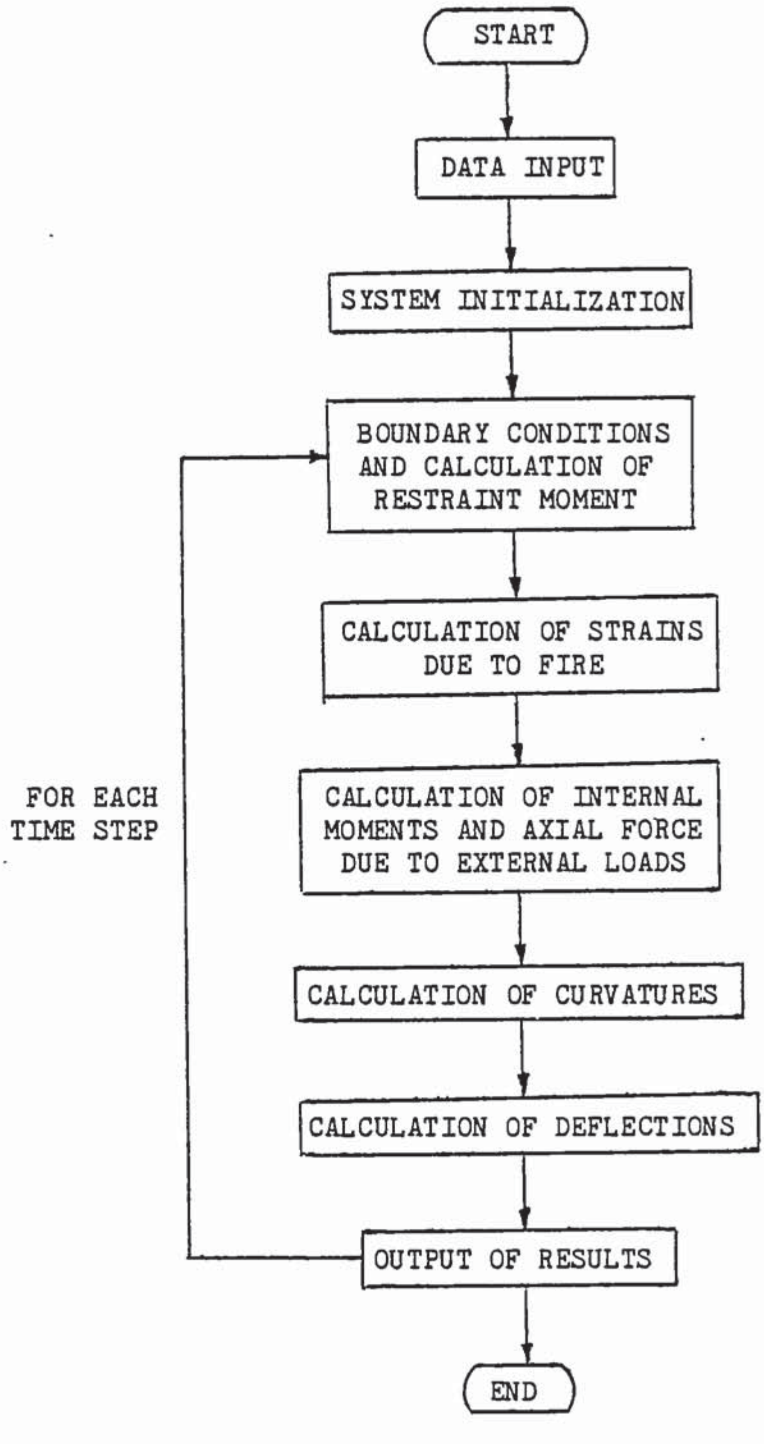

Figure 9.1 Macro flow diagram showing the structure of the computer program SAFE-RCC.

CHAPTER 10

STRUCTURE OF COMPUTER PROGRAM (SAFE-RCC)

10.1 Introduction

Chapter 9 concluded with a macro flow diagram showing the overall structure of the computer program SAFE-RCC. This Chapter will describe the individual elements of the program structure and the corresponding program subroutines.

SAFE-RCC is a hierarchically structured computer program as shown in Figure 10.1. Table 10.1 gives a list of the subroutines and their corresponding functions.

The main body of the computer program, SAFERCC, is the primary solution executor which controls the execution of the analysis and basically comprises of a series of Fortran call statements to the various subroutines that contain the analytical methods and numerical procedures. It is also concerned with the initialization of certain arrays and variables and inputs the data necessary for the determination of the array dimensions required for the particular program run. In this respect the program is semi-dynamically dimensioned in that only the portion of the arrays that are required for the run are initialized. The spare array space remains unitialized for the duration of the computer run.

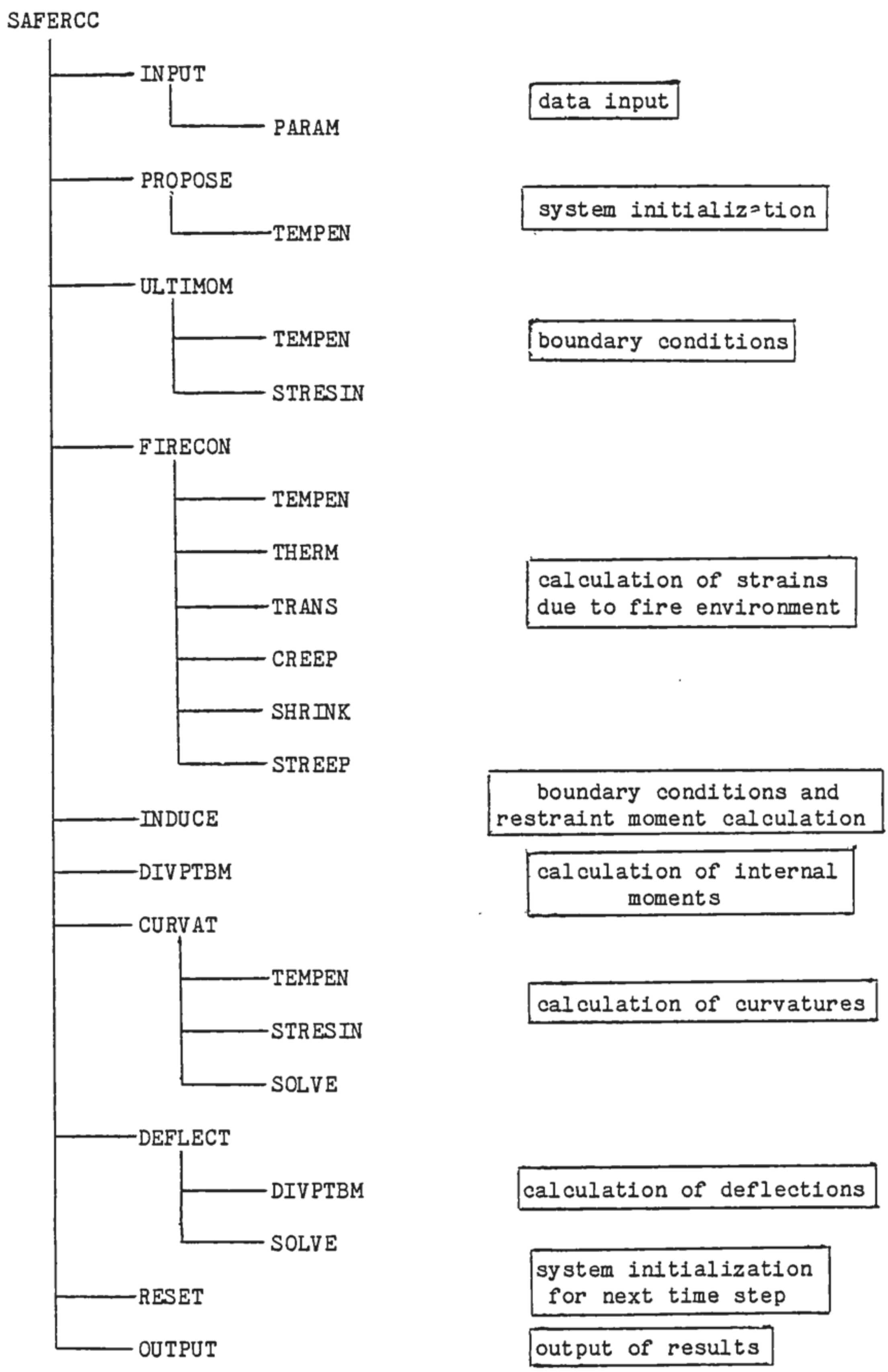

Figure 10.1 Hierarchical structure of SAFE-RCC

SUBROUTINE	FUNCTION
CREEP	calculates concrete creep strains
CURVAT	calculates division point curvatures
DEFLECT	calculates division point deflections
DIVPTBM	calculates division point bending moments
FIRECON	controls and selects the subroutines for the calculation of induced strains as a result of the fire environment
INDUCE	calculates induced restraining moment (column end moment) for given end slope
INPUT	inputs data
OUTPUT	outputs results of the analysis
PARAM	inputs ordered pairs of temperature and temperature dependent material properties
PROPOSE	calculates proposed values necessary to initialize structural analysis at start
RESET	initializes structural analysis for next time step
SAFERCC	primary solution executor
SHRINK	calculates concrete shrinkage strains
SOLVE	solves simultaneous equations
STREEP	calculates steel creep strain
STRESIN	stress-strain relationship for concrete and steel
TEMPEN	calculates temperature dependent material property for given temperature
THERM	calculates induced strains due to thermal expansion
TRANS	calculates induced transient strain
ULTIMOM	calculates ultimate moment capacity of restraint beam sections

Table 10.1 Table of subroutine functions.

10.2 Data Input

The majority of the data input is carried out by subroutine INPUT. Subroutine INPUT reads data from a file prepared by the user. A full description of the data file is given in Appendix A.

The temperature dependent material properties are modelled as linear segments. The description of these is accomplished through the entering of a series of eight ordered pairs of temperature-property values by subroutine PARAM. The ordered pairs of values then describe the nodes of the segments.

10.3 System Initialization

The system initialization is executed by subroutine PROPOSE. The initialization concerns the calculation of the proposed values necessary to initialize the structural response analysis. Proposed values must initially be calculated for the end moments, end slopes, axial force, curvatures, division point deflections and direct strain at the column axis. The theory behind the numerical procedures contained in subroutine PROPOSE is described in detail in Chapter 7.

Subroutine PROPOSE is only executed at the start of the analysis. Thereafter the system is initialized for the next time step through the execution of subroutine RESET. Subroutine RESET initializes the system for the following time step by setting the proposed values listed above (for the next time step) equal to the calculated values from the current time step.

10.4 Boundary Conditions and Calculation of Restraint Moment

The support boundary conditions common to many structural analysis programs are idealized through the use of linear springs. The structural response program SAFE-RCC includes a realistic model of restraint and continuity likely to be experienced by a column in a real structure, which allows for redistribution of moments to occur during the exposure to the fire.

The support boundary idealization employed in SAFE-RCC models a stage of linear restraint followed by a non-linear restraint due to changes in material properties and the stress-strain curve. As moment redistribution occurs the model will take into account the formation of plastic hinges. In addition SAFE-RCC includes the option of the restraint system being exposed to, or not being exposed to, the fire environment.

Axial restraint and rotational restraint are modelled independently. As well as modelling the support boundary conditions likely to be experienced in a real structure SAFE-RCC also models the support boundary conditions of fixed and pinned rotational restraint, and free axial expansion and fixed axial restraint.

Subroutine INDUCE is concerned with the rotational restraint aspects of the support boundary conditions, and calculates the restraint moment, or column end moment, due to an end slope for a given state of boundary conditions and structural loads.

For the linear (elastic) state of restraint the restraint moment is calculated according to the slope deflection analysis described in Section 6.2.2. For the non-linear (plastic) state of restraint due to the formation of plastic hinges, the restraint moment is calculated according to the same theory except that the plastic analysis described in Section 6.2.2.4 is applied to determine the reduced stiffness of the structural members of the restraint system.

If the option is included for the fire exposed restraint system the ultimate moment capacities of the restraint system sections will vary with the duration of the fire. Subroutine ULTIMOM calculates the current ultimate moment capacity of a section for a given temperature profile. The analytical procedure contained in subroutine ULTIMOM is described in detail in Section 6.2.2.5. Figure 10.2 shows the geometry and strain profiles assumed when calculating the ultimate moment capacity within subroutine ULTIMOM. A full glossary of computer terms used within SAFE-RCC is presented in Appendix I.

The axial restraint model for the support boundary condition for the elastic state of restraint is contained within subroutine DEFLECT. The axial restraint model calculates the axial restraint force for a given axial deformation and axial restraint boundary condition. The analytical method is described in detail in Section 6.3. When the plastic stage of restraint is entered the axial restraint force is calculated using the plastic analysis contained within subroutine INDUCE.

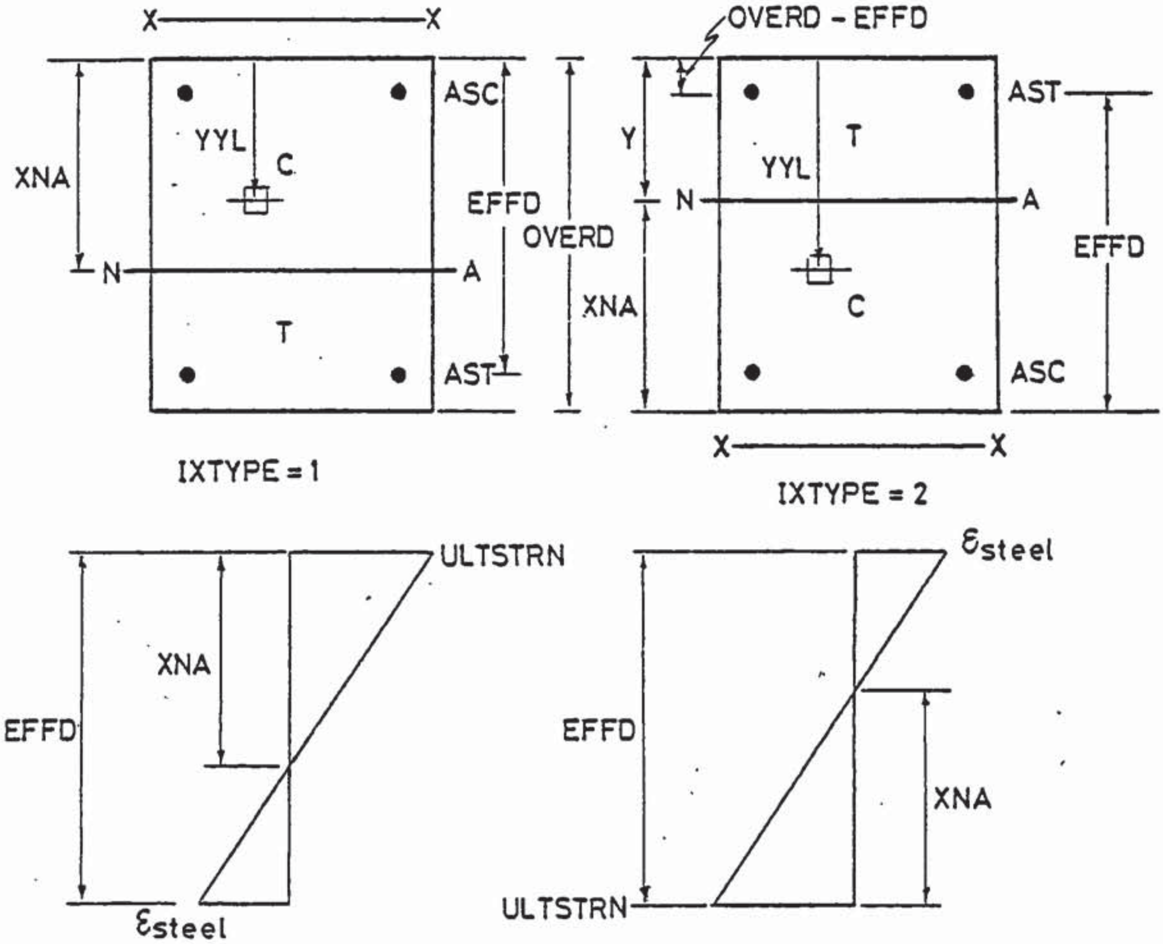

Figure 10.2 Geometry and strain profiles assumed for the calculation of ultimate moment capacities within subroutine ULTIMOM.

10.5 Calculation of Strains due to Fire

Material behaviour models are used to calculate the induced strains as a result of the fire environment. The material behaviour models are presented in detail in Chapter 8. Subroutine FIRECON controls and selects the appropriate subroutines containing the material behaviour models according to the material type.

10.5.1 Subroutine THERM

Subroutine THERM calculates the induced strains due to the thermal expansion.

Concrete thermal strains are calculated using the polynomial fit established by Forsén and presented in Section 8.1.3. SAFE-RCC has been developed to proceed with a structural response analysis starting with an initial temperature of 20°C and therefore the thermal strain model should predict a zero value of induced thermal strain at 20°C in order to satisfy compatability. For these reasons the value of thermal strain predicted by the Forsén polynomial fit at 20°C (1.8435×10^{-4} m/m) is subtracted from the current calculated value.

Steel thermal strain is calculated on the basis of the induced thermal strain being a function of the temperature dependent coefficient of thermal expansion and the elemental temperature, as presented in Section 8.2.3. Referring to Figure 10.3 the coefficient of thermal expansion is given by:

$$\alpha_s(T) = T_3 + (T_4 - T_3)(T - T_3)/(\alpha_4 - \alpha_3) \tag{10.1}$$

or

$$\alpha_s(T) = T_n + (T_{n+1} - T_n)(T - T_n)/(\alpha_{n+1} - \alpha_n) \quad \text{for } T_n < T < T_{n+1} \tag{10.2}$$

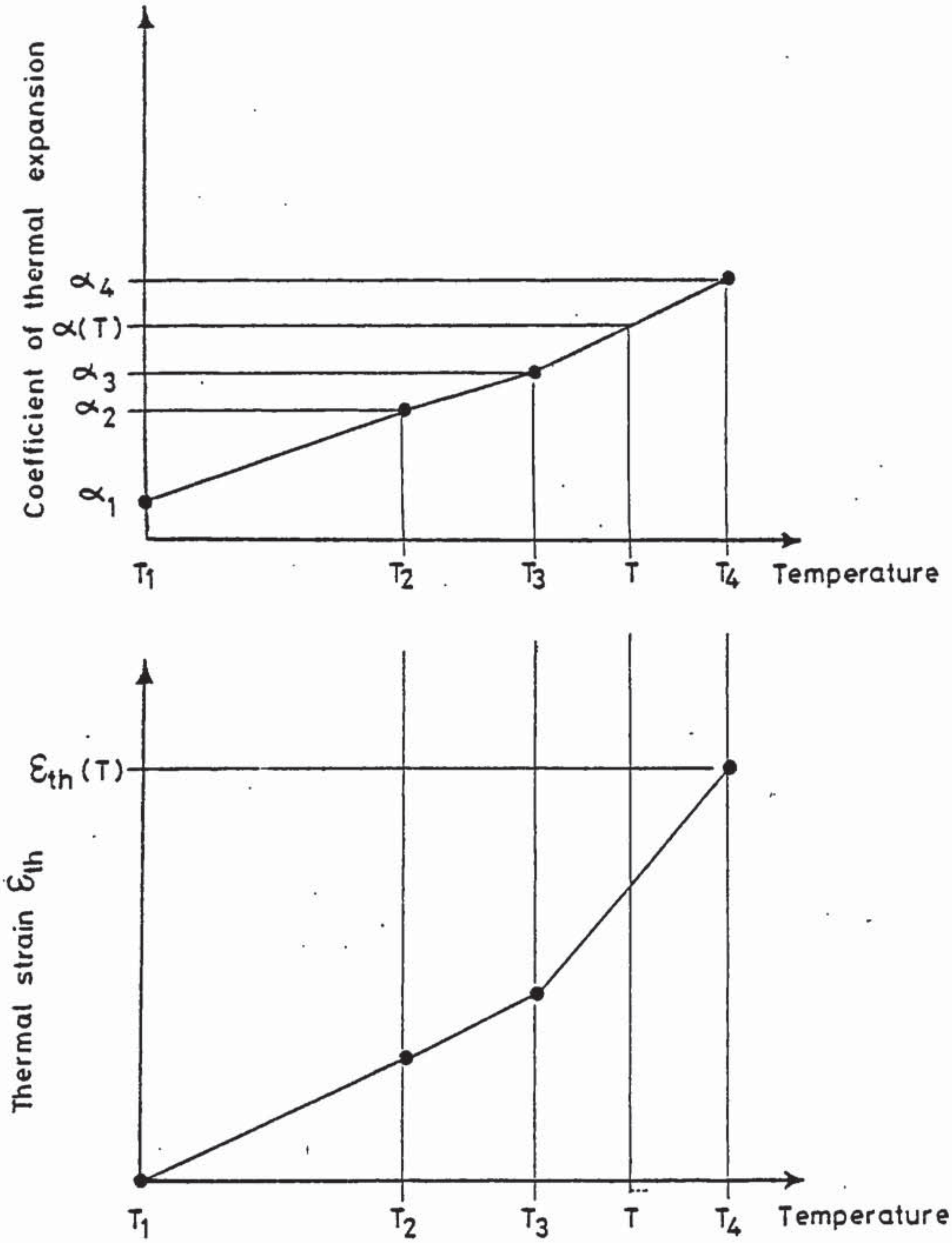

$$\alpha(T) = T_3 + \frac{T_4 - T_3}{\alpha_4 - \alpha_3}(T - T_3)$$

$$\varepsilon_{th} = \alpha_1(T_1 - 20) + \alpha_2(T_2 - T_1) + \alpha_3(T_3 - T_2) + \alpha(T)(T - T_3)$$

Figure 10.3 Calculation of steel thermal strain (subroutine THERM).

and the thermal strain is given by:

$$\varepsilon_{th}(T) = \alpha_1(T_1 - 20) + \alpha_2(T_2 - T_1) + \alpha_3(T_3 - T_2) + \alpha(T)(T - T_3) \tag{10.3}$$

or
$$\varepsilon_{th}(T) = \alpha_1(T_1 - 20) + \alpha_2(T_2 - T_1) + \dots\dots\dots + \alpha_n(T_n - T_{n-1}) + \alpha(T)(T - T_n) \quad \text{for } T_n < T < T_{n+1} \tag{10.4}$$

10.5.2 <u>Subroutine TRANS</u>

Subroutine TRANS calculates the induced transient strain in concrete elements using the Anderberg and Thelandersson (1976) model presented in Section 8.1.4. The transient strain is a function of the applied stress. Since the current stress state has yet to be determined, when calculating the fire strains the elemental stress from the previous time step is used. Providing time step increments are relatively small the errors caused by this assumption will be negligible.

For temperatures less than or equal to 500°C the transient strain is calculated using the expression:

$$\varepsilon_{tr} = - k_2 \varepsilon_{th} \sigma / \sigma_{max,o} \tag{10.5}$$

For temperatures greater than 500°C when there is an accelerated effect on transient strain the following equation is used:

$$\varepsilon_{tr} = (k_2 \times 7.10608 \times 10^{-3}) \sigma / \sigma_{max,o} + 0.1 \times 10^{-3} \times (T - 500) \sigma / \sigma_{max,o} \tag{10.6}$$

k_2 is set equal to 2.35 using the Fortran data statement. The value 7.10608×10^{-3} corresponds to the value of thermal strain predicted by the Forsén polynomial fit at 500°.

10.5.3 Subroutine CREEP

Subroutine CREEP calculates the induced creep strain in concrete elements from the Anderberg and Thelandersson (1976) model for primary and secondary creep presented in Section 8.1.5. The constants β_o, k_1, t_r, and p are assigned the values of 0.53×10^{-3}, 3.04×10^{-3}, 3.0 and 0.5 respectively through the use of the Fortran data statement. The concrete creep strain is a function of the current state of stress, since this has yet to be determined the creep strain is calculated using the stress from the previous time step. A strain hardening principle is employed to account for variable stress and temperature. No concrete creep strain is assumed to occur in tension.

10.5.4 Subroutine SHRINK

Subroutine SHRINK calculates the incremental concrete shrinkage strain during a time step. The shrinkage model is taken from Becker and Bresler (1974) and is presented in Section 8.1.6. The shrinkage strain is calculated incrementally for the temperature range of plus 20°C to 100°C. The maximum total shrinkage at 100°C is 0.001 m/m and upon reaching the temperature of 100°C all remaining shrinkage is assumed to occur. However, the shrinkage occuring at any time step may not exceed the total potential shrinkage.

10.5.5 Subroutine STREEP

Subroutine STREEP calculates the induced incremental strain due to creep in a steel element using the Harmathy (1970) comprehensive creep model with the Dorn (1954) Theta Method for temperature variation. A strain hardening principle is used to account for variation of stress. The model is presented in Section 8.2.4.

Values of the coefficients for creep parameters Z, ε_{cro} and $\Delta H/R$ derived for different steels are given in Appendix H. The coefficients employed in the current version of SAFE-RCC are for steel type Ks40 ϕ 10. The parameters Z and ε_{cro} are a function of the current state of stress, since this has yet to be determined the elemental stress from the previous time step is employed. Creep recovery is not accounted for in the model and is therefore assumed not to occur. The steel creep model is assumed to be identical in both tension and compression.

10.6 Calculation of Internal Moments and Axial Force due to External Loads

Subroutine DIVPTBM calculates the division point moments about the axis of the column due to the external loads. Account is taken of the second order effects due to axial load eccentricity at the division points as a result of the deflected column profile. The analytical procedure is described in Section 5.2.3.2.

For a pin ended column the external axial load is entered as an item of data. When the column is part of an overall structure the axial load is also in part calculated from the slope deflection equations (equation (6.3)) decribed in Section 6.2.2.

Internal variation of the axial force throughout the deflected column segment lengths is accounted for by vertical resolution at the division points. This procedure is contained within subroutine CURVAT.

10.7 Calculation of Curvatures

Subroutine CURVAT calculates the column curvature at each division point corresponding to the cross section loading. The numerical procedure is described in detail in Section 5.2.3.3. When equilibrium between the cross sectional column strength and applied loads can not be obtained failure is assumed to occur.

Contained within subroutine CURVAT is the Anderberg and Thelandersson (1976) total strain model and the corresponding stress and tangent modulus is determined through the application of subroutine STRESIN for each cross sectional element. The total strain model is presented in Sections 8.1.1 and 8.2.1. Subroutine CURVAT further contains the Anderberg (1976) model for the variation of maximum strain ε_{max} due to a prehistory of stress. The Anderberg (1976) model is described in Section 8.1.3.

The compatability equations, equation (5.13) are solved using subroutine SOLVE. Subroutine SOLVE solves a series of simultaneous equations written in matrix form using the numerical procedure of Gaussian Elimination.

10.7.1 Subroutine STRESIN

Subroutine STRESIN represents the stress-strain relationship for the column subslice be it concrete or steel.

The stress-strain relationship for concrete is modelled using the Baldwin and North (1973) representation for concrete in compression and a linear relation in tension. The model is presented in Section 8.1.2, however, it is convenient to discuss some additional features.

Consider Figure 10.4, in order to determine whether the linear unload relation should be followed, corresponding to 'true unloading', use is made of the following statement. If the stress predicted by the linear unload line (equation (8.7)) for a given state of strain yields a stress greater than the corresponding stress predicted by the Baldwin and North (1973) expression (equation (8.3)), the true state of stress is given by the Baldwin and North expression. If the latter is not the case then the true state of stress is that predicted by the linear unload relation.

Some typical stress-strain paths that are taken account of are shown in Figure 10.4. When the concrete has unloaded and cracked any state of strain less than the value of strain at which the linear unload relation crosses the strain axis of the stress-strain relation will predict zero stress. Subsequent reloading is assumed to continue from the point at which the linear unload line crosses the strain axis.

By virtue of the stress-strain relation it is not possible for any concrete element to crush when there is a solution to the analysis. The maximum stress attainable is σ_{max} for a corresponding strain ε_{max}, therefore any increase in strain beyond ε_{max} will give a smaller value of stress ($< \sigma_{max}$) due to the descending branch behaviour, or unloading behaviour, of the concrete stress-strain relation.

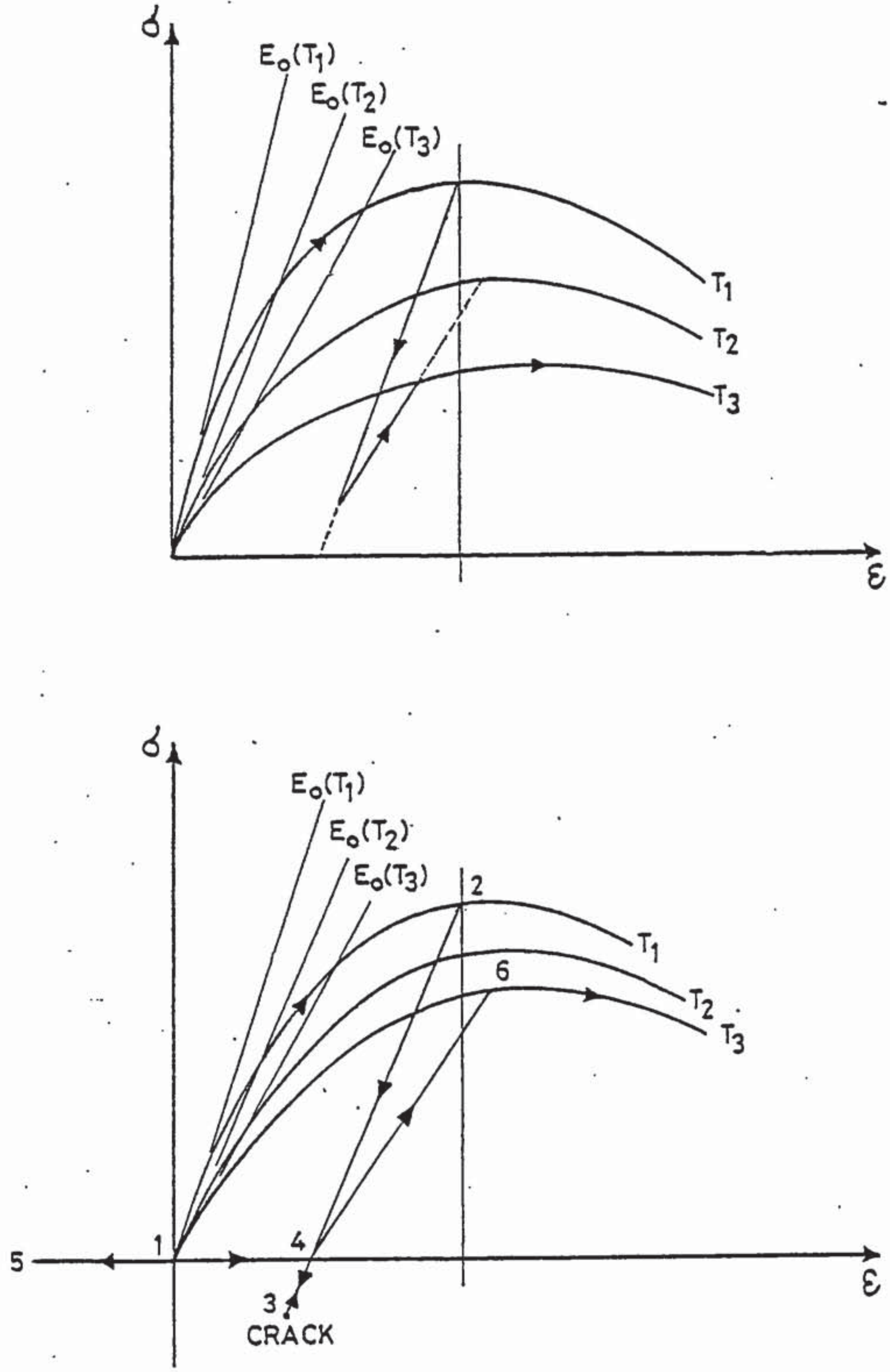

strain path: 1-2, 2-3, 3-4, 4-5, 5-4, 4-6, 6- previously uncracked
1-2, 2-4, 4-5, 5-4, 4-6, 6- . previously cracked

Figure 10.4 Examples of stress-strain path.

The consequences for the computer analysis are that if an element is strained beyond ε_{max} then the element must unload and the surrounding elements must take up the stress defeciency, which implies a shift in the neutral axis position. When many elements are strained into the descending branch portion of the stress-strain relation the neutral axis may shift right out of the section resulting in failure of the column.

A concrete tension failure flag is also employed within subroutine STRESIN to indicate whether any concrete element is cracked. A concrete element is considered to crack when it attains a tensile strain greater than the permissible tensile strain. When a concrete element is cracked it will no longer sustain any tensile strain and therefore a corresponding zero stress is predicted, the element may still however, be 'reloaded' into compression.

A bi-linear stress-strain relation is employed for steel where the stresses are computed on the basis of the permanent inelastic strain. The model for the steel stress-strain relation is presented in Section 8.2.2. Within subroutine STRESIN the steel strain hardening modulus has been set equal to one twentieth of the modulus of elasticity and the steel is assumed to rupture when strains greater than ten times the yield strain are attained. The relation is assumed to be identical in tension and compression.

The temperature dependent material properties, such as σ_{max}, ε_{max}, F_y and E_s, are calculated for a given temperature using subroutine TEMPEN. Subroutine TEMPEN represents the temperature dependent material properties as linear segments. The model is described in Section 8.3.

10.8 Calculation of Deflections

Subroutine DEFLECT calculates the division point deflections by double integration of the curvatures making allowance for any initial deflections. The procedure is described in detail in Sections 5.2.3.4 to 5.2.3.8. The partial differential equation (5.27) is solved using subroutine SOLVE. When division point deflections do not converge to a solution the column is assumed to have failed.

Calculation of the column axial deformation is also contained within subroutine DEFLECT. The axial deformation is calculated from the consideration of the average segment total strain as described in Section 6.3.1. If the column restraint system remains elastic, i.e. formation of plastic hinges has yet to occur, the resulting axial restraint force corresponding to the axial deformation is also calculated within subroutine DEFLECT according to the procedure described in Section 6.3.1. When the column restraint system is inelastic, i.e. plastic hinges have formed, the axial restraint force is calculated within subroutine INDUCE through the application of the plastic analysis described in Section 6.2.2.4.

The rate of deflection is also calculated within subroutine DEFLECT according to the equation:

$$\frac{d(y_r)_c}{dt} = \frac{\Delta(y_r)_c}{\Delta t} \leqslant \frac{L^2}{15b} \qquad (10.7)$$

where: $d(y_r)_c/dt$ is the rate of deflection,

$\Delta(y_r)_c$ is the change in deflection for the current time step,

Δt is the time interval for the current time step,

L is the column length,

b is the breadth of the column.

10.9 Output of Results

Subroutine OUTPUT outputs the results of the structural analysis in printed form. The printed output includes the time history of lateral displacements, rate of deflection, axial deformation, end slopes, end moments, axial force and internal stresses and strains in the concrete and steel elements.

Indication is given if any concrete element is cracked and a warning message is given if the rate of deflection exceeds the permissible rate. A statement of the type of column failure is also given with the corresponding failure time.

CHAPTER 11

PROVING TESTS

11.1 Introduction

In order to validate the computer model, i.e. to demonstrate that it is capable of reproducing the behaviour experienced by a real column in a fire, it is necessary to carry out a series of proving tests. This is achieved through a quantitative verification of the analytical method against some known test results.

It is equally necessary to validate the computer model against existing predictive methods. In this particular case the results used are those obtained by Forsén (1982) from CONFIRE. It should be realised that CONFIRE uses a flexibility approach, i.e. convergence is applied to the displacements and an out-of-balance load applied and the displacements recalculated until the error is acceptable (i.e. there is no indication of the final out-of-balance load), whereas SAFE-RCC uses a stiffness approach where the loads are tested for convergence and the resultant deflections calculated. It is, therefore, to be expected that the two programs whilst necessarily predicting the same trends will not necessarily give exactly identical numerical solutions. This is due partially to the choice of values in the convergence criteria.

The actual tests to which the analytical method is compared were performed at the Swedish National Testing Institute in Boras, Sweden according to ISO 834 (1975) and were reported in Haksever and Anderberg (1982). The reinforced concrete columns, loaded concentrically and eccentrically, were tested exposed to heating from three sides.

11.2 Testing Procedure

The test arrangement is illustrated in Figure 11.1. The reinforced concrete test columns were placed at the opening of a vertical furnace such that they were exposed to heating on three sides and were loaded either concentrically or eccentrically by means of a hydraulic system. The furnace measured 3 x 1.8 x 3 m^3 and lightweight concrete walls were used to close the test furnace.

The columns were 2 m in length and measured 200 mm by 200 mm. For steel reinforcement 8 16 mm diameter bars of grade Ks 40 (hot rolled steel) were employed with a yield stress of 453 N/mm^2. 6mm diameter stirrups of grade Ps 50 were placed at 200 mm centres at mid-height and 100 mm centres at the ends of the column. The concrete used for the three test columns had a cube strength of about 46 N/mm^2 at the testing age of 110 days.

11.3 Thermal Response

In order to predict the thermal response of the cross section of the column test specimens FIRES-T was employed. The thermal properties and values of parameters used in the calculation are shown in Tables 11.1 to 11.7. A schematic diagram indicating the boundary conditions and material types used in the FIRES-T run is shown in Figure 11.2.

Concrete Thermal Conductivity (Anderberg (1976))		
Temp. (^oC)	Value (W/m^oC)(J/sm^oC)	Value (J/hm^oC)
20	1.8	6480
100	1.3	4680
225	1.2	4320
380	1.2	4320
600	0.95	3420
900	0.90	3240
1000	0.82	2950

Table 11.1 Values of thermal conductivity for quartzite concrete used in calculation.

Concrete Specific Heat (Harmathy (1970))	
Temp. (^oC)	Value (J/kg^oC)
20	850
200	1100
400	1250
1000	1300

Table 11.2 Values of specific heat for quartzite concrete used in calculation.

Concrete Density
Constant value 2400 kg/m^3

Table 11.3 Value of density for quartzite concrete used in calculation.

Steel Thermal Conductivity (Malhotra (1982))		
Temp.(^{o}C)	Value ($W/m^{o}C$)($J/sm^{o}C$)	Value ($J/hm^{o}C$)
20	50.0	180000
200	47.5	171000
800	37.5	135000
1000	37.5	135000

Table 11.4 Values of thermal conductivity for steel Ks 40 used in calculation.

Steel Specific Heat (Malhotra (1982))	
Temp.(^{o}C)	Value ($J/kg^{o}C$)
20	475
700	775
900	650
1000	650

Table 11.5 Values of specific heat for steel Ks 40 used in calculation.

Steel Density
Constant value 7850 kg/m^3

Table 11.6 Value of density for steel Ks 40 used in calculation

Parameter	Value
Convection factor (A) fire exposed face	3600 $J/hm^2K^{1.33}$
Convection power (N) fire exposed face	1.33
Convection factor (A) cool face	7920 $J/hm^2K^{1.25}$
Convection power (N) cool face	1.25
View factor (V)	0.5
Absorption (a) fire exposed face	0.9
Fire emissivity (ε_f) fire exposed face	0.7
Absorption (a) cool face	1.0
Fire emissivity (ε_f) cool face	0.9
Surface emissivity (ε_s)	0.9
Resultant emissivity (ε_r)	0.65
Stefan-Boltzmann const. (σ)	2.04×10^{-4} J/hm^2K^4

Table 11.7 Values of concrete parameters for non-linear heat flow equation. (See Section 4.7).

The predicted and measured temperatures are illustrated in Figure 11.3. The full line curves in Figure 11.3 give the measured temperatures at six different locations at the mid-section of the column as a function of time. Calculated temperatures obtained by Forsén (1982) using TASEF-2 (Wickström (1979)) are also given. Forsén (1982) only presented calculated temperatures for three of the thermocouple locations. Although reasonable agreement is obtained between measured and calculated temperatures for the locations plotted it is unknown how the remaining half compared.

Agreement between measured and calculated temperatures using FIRES-T is reasonable over the majority of the section. Temperatures at point 1 exhibit most disagreement. This could, however, be due to the thermocouple at this point measuring the furnace temperature, rather than the surface of the column, during the test. The calculated temperatures at this point correspond to the surface temperature. The main reason for the discrepancy between calculated and measured temperatures is probably explained by the fact that FIRES-T does not consider moisture content which means the capillary moisture transport is neglected in the program, and may also account for the variation at thermocouples 5 and 6 where substantial moisture may still be present.

The predicted temperatures are then used as data for the structural response program SAFE-RCC.

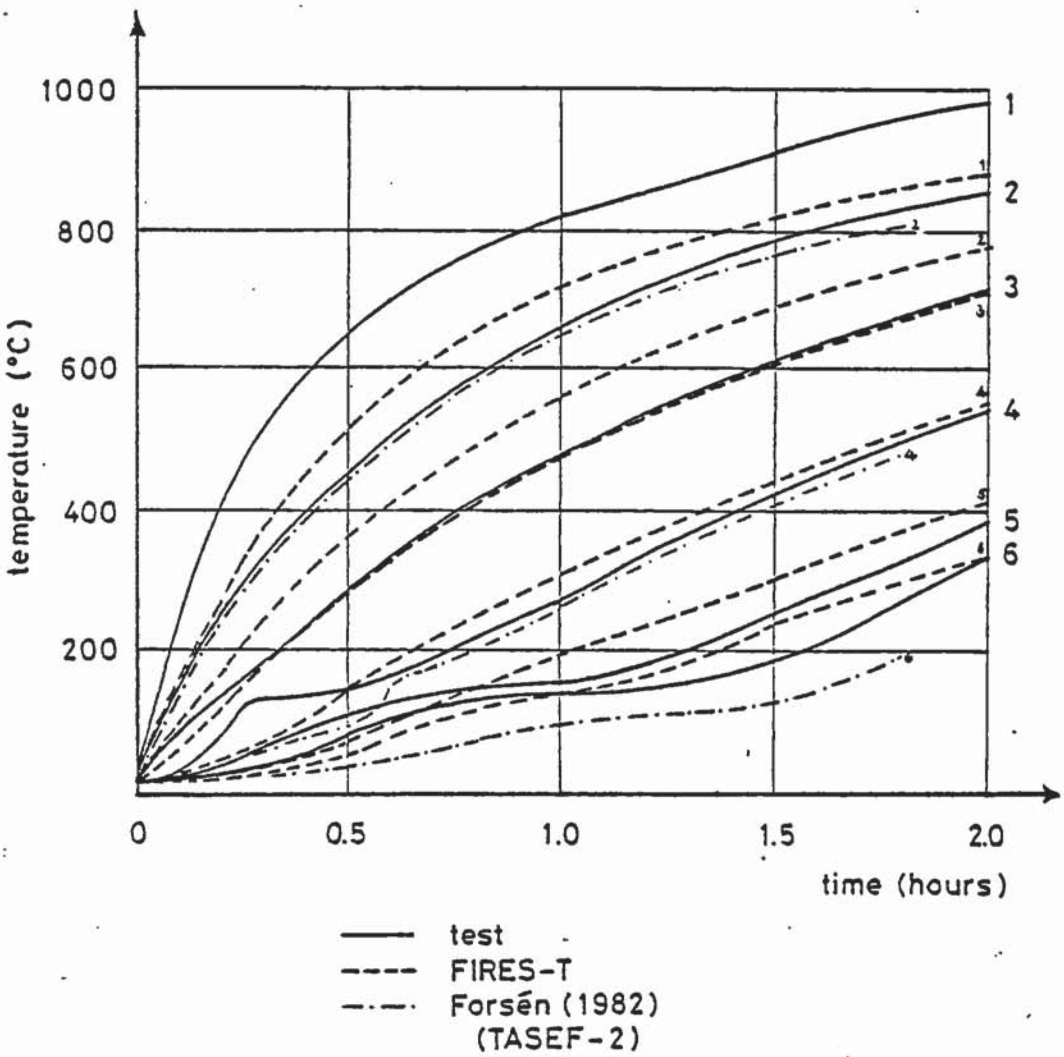

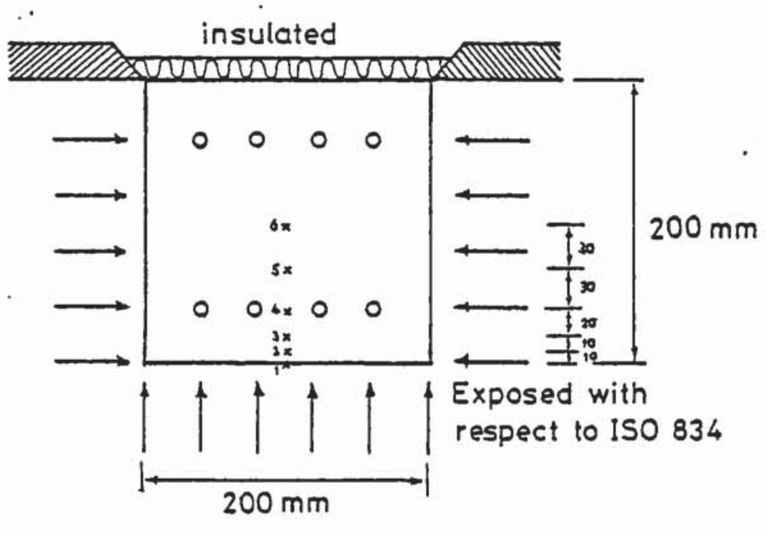

Figure 11.3 Measured and predicted temperatures at mid-section of the column.

11.4 Structural Response

Three columns were tested, one loaded concentrically and two loaded eccentrically. Column SL1 was concentrically loaded to 900 KN which corresponded to approximately 46% of the ultimate load at ordinary conditions. Column SL2 was loaded to 600 KN with an eccentricity of 60 mm directed away from the furnace. This represented about 63% of the ultimate load at ordinary conditions. Finally column SL3 was loaded to 300 KN with an eccentricity of 60 mm directed towards the furnace, which corresponded to approximately 31% of the ultimate load at ambient conditions.

In order to predict the structural response using SAFE-RCC the two metre column was divided into 10 equal segments. The 11 segment division points were further subdivided into 116 elements for the half section (232 elements for the whole section due to symmetry). For the first 48 minutes the time step increments were set to 3 minutes, thereafter the time step increments were increased to 6 minutes. The structural response program employs a force and deflection compatability analysis. The material data for the concrete and reinforcing steel used to predict the structural response are presented in Tables 11.8 to 11.12. The concrete maximum stress at ambient conditions was set to 36.8 N/mm^2 (0.8 x 46 N/mm^2).

The mid-point deflection and axial deformation that occurred during the test for column SL1 are shown in Figure 11.4 by the full line curves, where the initial deflection and contraction were 0.05 mm and 1.6 mm respectively. The test column will show initial deflection due either to concrete variability across the section, the reinforcement being not absolutely symmetric, the applied loading being not absolutely concentric, or to a lack of column straightness.

Temp. (^{o}C)	Proportionate loss of strength (Anderberg (1976))	σ_{max} (N/mm^2)
20	1.0	36.8
135	1.02	37.54
265	0.95	34.96
400	0.95	34.96
450	0.75	27.6
500	0.55	20.24
650	0.35	12.88
960	0.05	1.84

Table 11.8 Variation of maximum concrete stress with temperature.

Temp. (^{o}C)	ε_{max} (Anderberg and Thelandersson (1976))
20	0.0024
100	0.0030
200	0.00325
300	0.0036
400	0.0044
500	0.0055
600	0.0070
960	0.0142

Table 11.9 Variation of concrete strain at maximum stress with temperature.

Steel coefficient of thermal expansion
Constant value 15.0×10^{-6}

Table 11.10 Value of steel coefficient of thermal expansion used in calculation

Temp. (^{o}C)	Proportionate loss of strength (Crook (1980))*	Yield strength f_y (N/mm^2)
20	1.0	453.0
100	0.96	434.9
200	0.83	376.0
300	0.82	371.5
400	0.75	339.75
500	0.59	267.25
600	0.37	167.6
700	0.21	95.15

Table 11.11 Variation of steel yield strength with temperature.

* Crook (1980) proportionate loss of strength for 25 mm diameter unisteel bars (hot rolled steel, yield strength 557.5 N/mm^2) is applied to 16 mm diameter bars of grade Ks 40 (hot rolled steel, yield strength 453 N/mm^2).

Temp. (^{o}C)	Proportionate loss (Anderberg (1976))	Elastic Modulus E_s (KN/mm^2)
20	1.0	210.0
100	1.0	210.0
200	0.98	205.8
300	0.89	186.9
400	0.77	161.7
500	0.62	130.2
600	0.40	84.0
700	0.15	31.5

Table 11.12 Variation of steel elastic modulus with temperature.

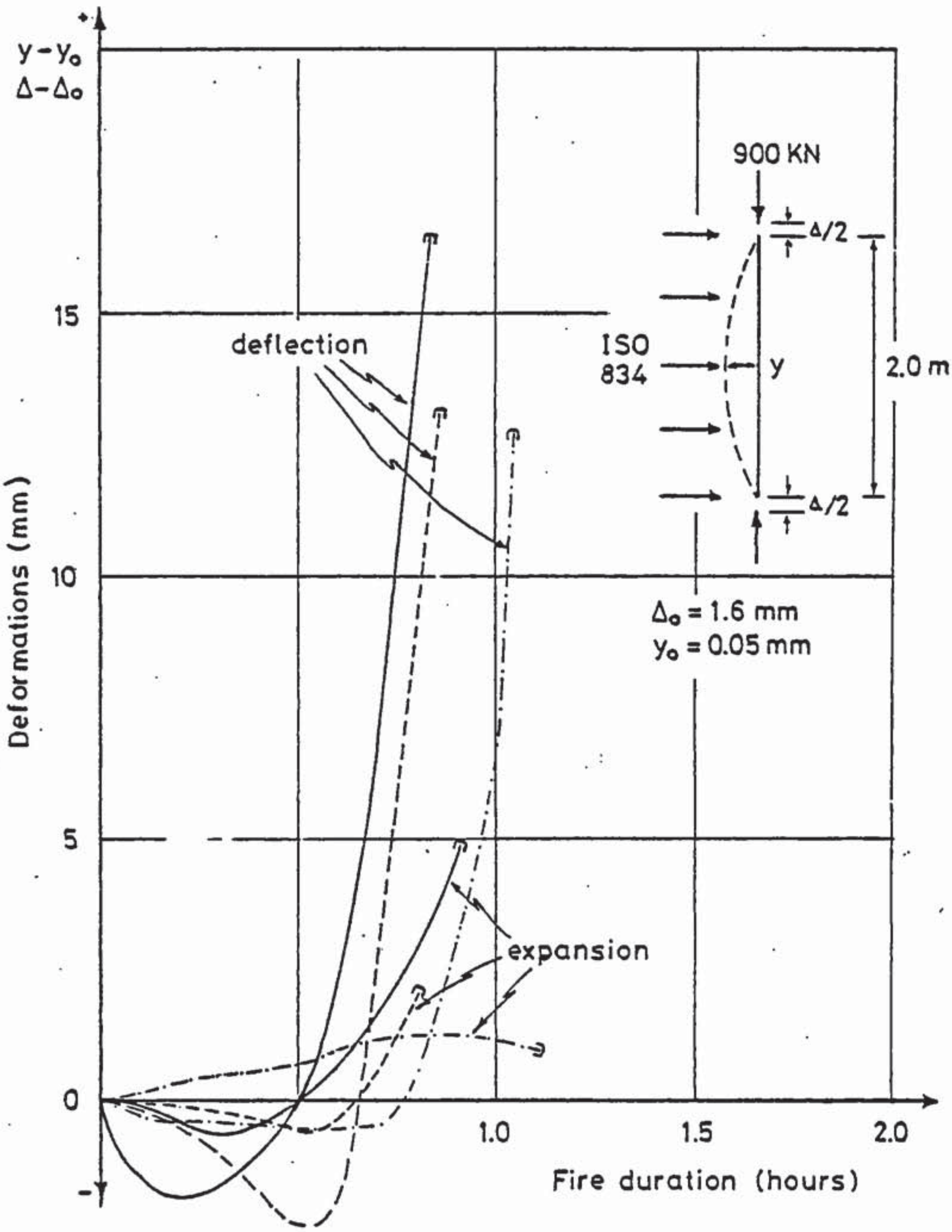

Positive y: deflection towards fire
Positive Δ: expansion
——— test
- - - - - - SAFE-RCC
-·-·-·- Haksever (1980)
(Haksever & Anderberg (1982))

Figure 11.4 Measured and predicted behaviour of a reinforced concrete column (SL1) axially loaded to 900 KN in a fire.

Haksever and Anderberg (1982) comment that the column exploded after 52 minutes in the test due to high moisture content but estimate, however, that failure was imminent. The explosive failure is most likely due to spalling as a result of the high values of concrete cover to main reinforcement employed in the test columns. The estimated failure time is about 60-65 minutes.

The predicted mid-point deflection and axial deformation are also shown in Figure 11.4, by the dashed line curves. Calculated values for the initial deflection and column contraction are 0.0 mm and 1.1 mm respectively. The failure time predicted by the structural response program is 51 minutes. As can be seen from Figure 11.4 the predicted curves and curves as a result of the test are relatively close together. In both test and calculation the deflection was initially towards the furnace and then changed sign. However, the predicted deflections appear to lag behind the test deflections, probably due to shortcomings in the material behaviour models.

The test and the predicted axial deformation both show a small axial elongation during the first stages of the fire, then increased column shortening occurs with increased deflection. However, the predicted axial deformations are smaller than the test deformations.

Despite the discrepancies the predicted structural response from SAFE-RCC is acceptable for column SL1.

Forsén (1982) does not present a comparison between tested and predicted deformations for column SL1, possibly due to the fact that difficulties may have been encountered in applying the large displacement analysis incorporated in CONFIRE to the axially loaded test case.

Haksever and Anderberg (1982), however, do present a comparison between tested and predicted deformations for column SL1. The calculated deformations were predicted using a computer program, based on a stiffness method, that was developed by Haksever (1980). The results are plotted in Figure 11.4. As can be seen from the Figure, SAFE-RCC gives a significantly better prediction for the deformation behaviour of the column.

The mid-point deflection and axial deformation that occurred during the test for column SL2 are shown in Figure 11.5 by the full line curves. Initial mid-point deflection and column shortening were 6.4 mm and 1.1 mm respectively. Due to an unintended support failure the test measurements were stopped after 30 minutes, however, a comparison is still of interest. The test estimated failure time was 55 minutes.

The predicted mid-point deflection and axial deformation for column SL2 using SAFE-RCC is given by the dashed line curve in Figure 11.5, where the initial deflection and column shortening were predicted to be 5.49 mm and 0.68 mm respectively. As can be seen from the Figure the predicted time of failure was 39 minutes. Agreement between the predicted and tested deformations is generally quite good, especially for the mid-point deflection, although the predicted axial deformation is about 50% of the measured deformation.

The predicted response from CONFIRE is also shown in Figure 11.5. Despite the difference between analysis approach of SAFE-RCC and CONFIRE the two predicted responses compare well. Predicted failure times are in agreement, although SAFE-RCC predicts a larger mid-point deflection at the time of failure.

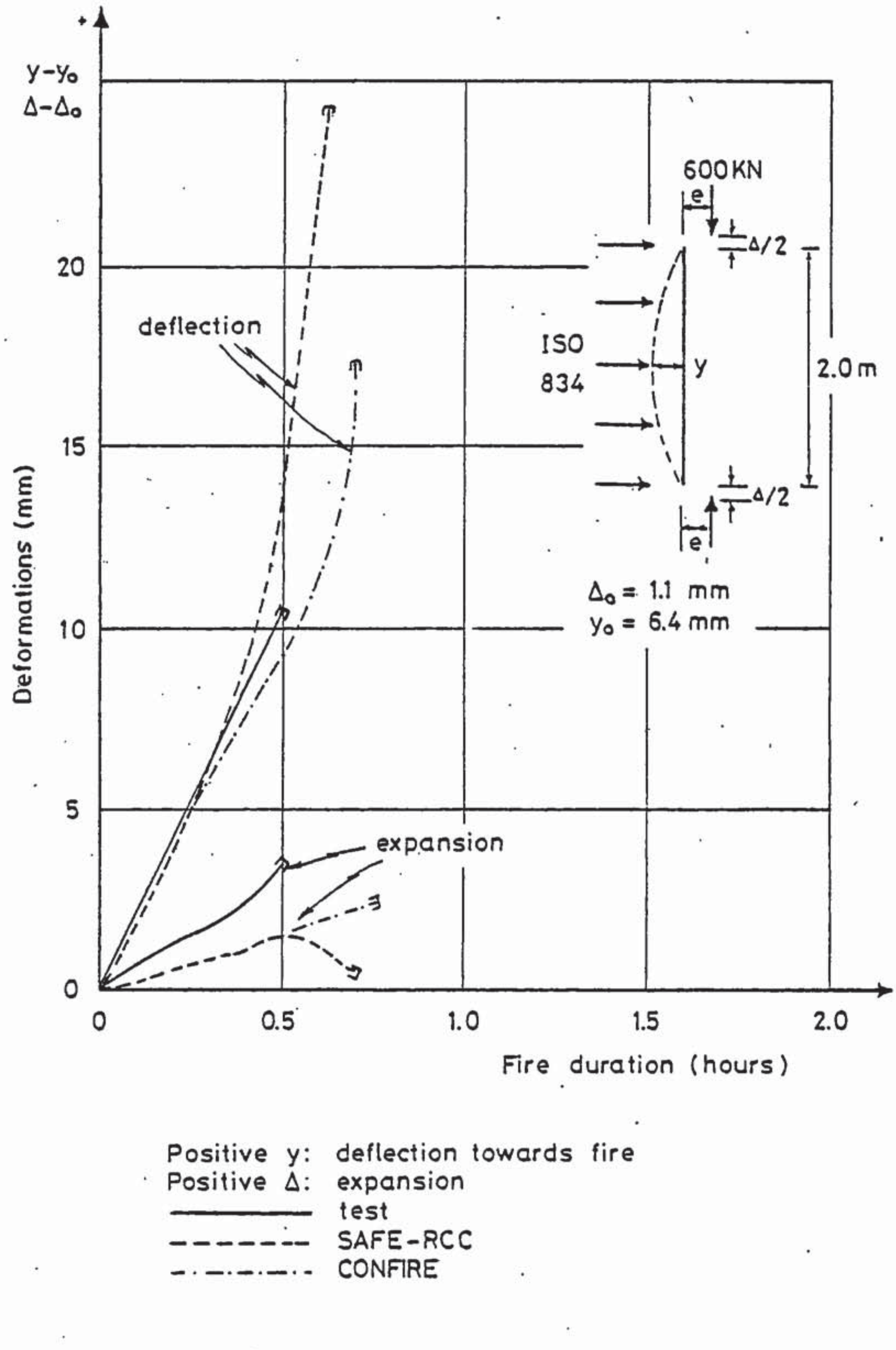

Figure 11.5 Measured and predicted behaviour of a reinforced concrete column (SL2) in a fire, eccentrically loaded to 600 kN.

The test mid-point deflection and axial deformation for column SL3 are shown by the full line curves in Figure 11.6, where the initial mid-point deflection and column shortening were 2.7 mm and 0.5mm repectively. The dashed line curves indicate the predicted deformations using SAFE-RCC. Initial mid-point deflection and column contraction were predicted to be 2.05 mm and 0.29 mm respectively.

The initial movement of mid-point deflection towards the column furnace during the first 30 minutes of the test is not predicted and the mid-point deflections differ somewhat during the middle stages of the fire. However, during the later stages of the fire agreement is much improved and the final deflections are in good agreement.

During the first 30 minutes axial deformations compare well, but after this time the predicted expansion is greater than that which occurred during the test. This difference is probably mainly due to the discrepancy between test and predicted deflections, however, the correct trend of axial deformation during the fire test is predicted.

For column SL3 the predicted and test deformations are only qualitatively in agreement. However, the predicted behaviour by SAFE-RCC does agree with that predicted by Forsén (1982) using CONFIRE. Both the computer programs make certain similar assumptions, e.g. that concrete creep is evaluated for moisture free concrete and that a limited validity concrete shrinkage model is taken (i.e. a combined coefficient with thermal expansion).

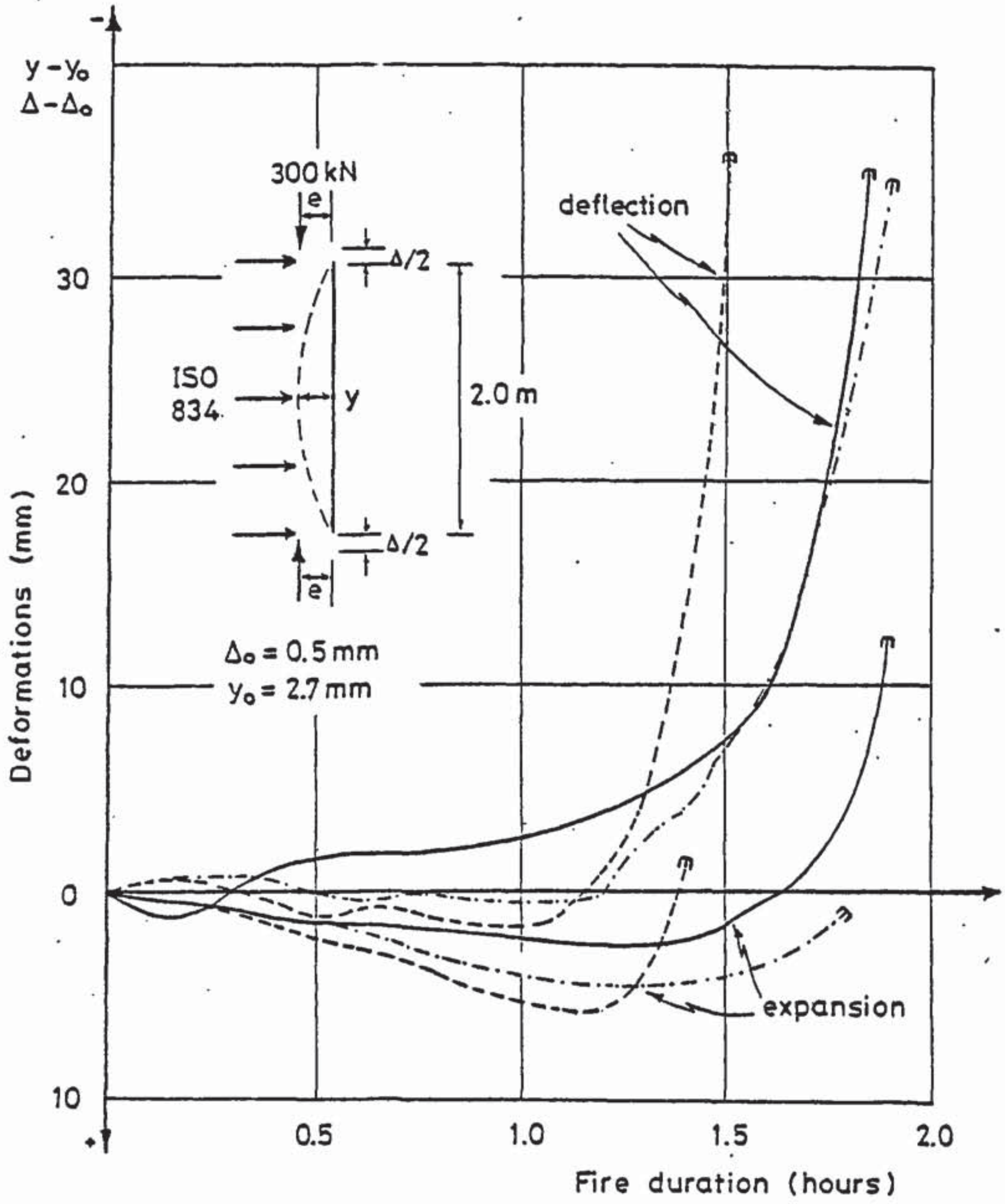

Positive y: deflection towards fire
Positive Δ: expansion
——— test
- - - - SAFE-RCC
-·-·-· CONFIRE

Figure 11.6 Measured and predicted behaviour of a reinforced concrete column (SL3) in a fire, eccentrically loaded to 300 kN.

It should, as a result, be realised that in this test the concrete compression face is exposed to the full effects of the fire and thus any problems due to lack of consideration of moisture transport will be exacerbated. Since the tension face of the column, where moisture can easily escape due to the presence of cracks, is away from the exposed face, the moisture transport escape length will be large. Thus full qualitative comparison between test and computer prediction cannot be expected. It is, however, gratifying to observe that, in general, predictions made by both CONFIRE and SAFE-RCC are in good agreement in this case, thus validating SAFE-RCC.

It should be noted that moisture transport effects will be far less marked for column SL2 since the tension face, where cracks provide an easy moisture escape route, is directly exposed to the fire, hence moisture content will be reduced very quickly. An intermediate state will exist for column SL1.

It is thereby noted that in order to obtain a very good correlation between observed and predicted measurements, materials (and, possibly, thermal) models will have to be developed which allow for the effect of moisture transport. This will obviously make the solution to any problem very complex, and may lead to the situation whereby the thermal and structural analyses may not be able to be uncoupled as they are at present.

SAFE-RCC and CONFIRE are based on similar structural idealizations and incorporate similar material behaviour models, although SAFE-RCC provides a better model of the concrete stress-strain behaviour. CONFIRE is based on a flexibility approach while SAFE-RCC is based on a stiffness approach.

Therefore similar but not identical results must be expected which is as it turned out and is therefore good.

Both the computer analyses are based on a number of basic premises concerning the structural idealization which may not hold for the real test column. All the cross sections are assumed to be identical with exactly placed reinforcement and no local strength variation throughout the column. No initial curvature has been considered, neither has any temperature variation along the column axis. It has also been assumed that moisture transport has no effect on material or thermal properties. With these basic premises in mind complete agreement cannot be expected between the test and predicted deformations. However, it can be expected that the overall trends should exhibit agreement. This does indeed occur and therefore SAFE-RCC, in its present state (and also CONFIRE) may be taken as giving reasonable predicative results when compared to actual test conditions.

Thus, despite the complexity of the problem and the assumptions made in the determination of the variation of the test column material properties with temperature and the shortcomings in the material behaviour models, for example the concept that the current state of strain is a function of the stress state from the previous time step, it can be concluded that the structural response program SAFE-RCC gives a generally good prediction for the behaviour of a column in a fire test.

CHAPTER 12

APPLICATION OF SAFE-RCC TO SOME STRUCTURAL SYSTEMS

12.1 Introduction

Having established in the previous Chapter that the structural response program SAFE-RCC may be taken as giving reasonable predicative results for isolated columns in a standard furnace test, it seems reasonable to assume that, subject to the availability of any experimental results to the contrary, the computer program should give reasonable predicative results for columns that are part of a total structure.

In this manner a series of computer runs were performed to attempt to provide a description for the type of behaviour experienced by some fire exposed reinforced concrete columns that are part of a total structure. The aim of the investigation was to determine the fire performance for some columns while varying the stiffness of the restraint system.

The stiffness of the restraint system was varied in two ways, namely variation in the stiffness due to the height of the structure above and variation in the stiffness of the restraint beams that adjoin the column ends. The stiffness of the structure above was altered by adjusting the number of floors above and the stiffness of the restraint beams was varied by adjusting the restraint beam length.

Throughout the modifications to the restraint system the cross section dimensions for the structural members remained constant. The length of the fire exposed columns was also adjusted so that the performance of short and slender columns could be compared.

12.2 Structural Systems Analysed

The structural systems analysed are shown in Figure 12.1. A programme of three test series was undertaken, summarized in Table 12.1. Firstly in test series 1 the number of floors above was varied while holding the column length and restraint beam length constant. In test series 2 the column length was varied while holding the restraint beam length and number of floors above constant. Finally in test series 3 the restraint beam length was varied while holding the column length and number of floors above constant. The structural system corresponding to a 6 m column, 16 m restraint beam and 3 floors above was common to each test series in order to allow direct comparison of results.

For each of the structural systems analysed, all column cross sections measured 400 mm by 400 mm and the restraint beam sections measured 400 mm by 800 mm. Concrete cover to main reinforcement was taken to be 40 mm corresponding to a 2 hour fire resistance in accordance with CP110. Each fire exposed column was divided into segment lengths of 400 mm and rigid gusset lengths of 400 mm were employed at the column ends, corresponding to half the restraint beam depth.

Full design calculations were carried out for each case using a design concrete cube strength of 40 N/mm^2 and a steel yield strength of 460 N/mm^2. Some sample design calculations, for the common test case with a 6 m column, 16 m restraint beam and 3 floors above, are presented in Appendix J.

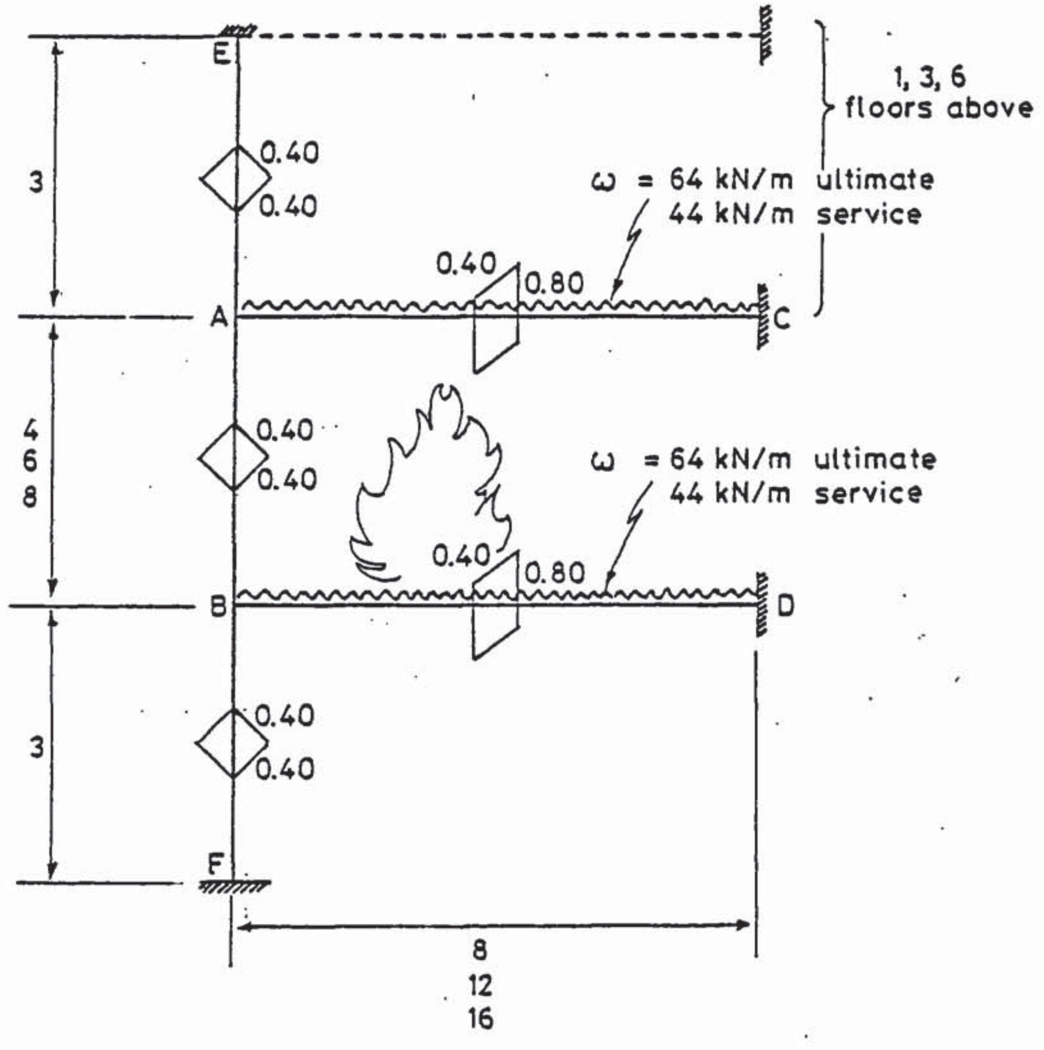

Figure 12.1 Structural systems analysed for test series.

TEST SERIES	STRUCTURAL SYSTEM	COLUMN LENGTH (m)	RESTRAINT BEAM LENGTH (m)	NUMBER OF FLOORS ABOVE	FIRE RESISTANCE (hours)
1	1	6	16	1	4.0
	2 *	6	16	3	2.9
	3	6	16	6	4.0
2	4	4	16	3	4.0
	2 *	6	16	3	2.9
	5	8	16	3	3.7
3	6	6	8	3	1.0
	7	6	12	3	0.65
	2 *	6	16	3	2.9

Table 12.1 Summary of test series showing variation in the restraint system and column length.

* Common structural system

Design calculations according to CP110 include material partial safety factors (γ_m) for the concrete and steel strengths. In order to be consistent with the calculated moment capacities of the structural cross sections from the computer program SAFE-RCC (which does not consider partial safety factors) the ultimate moment capacities of the restraint system members, which must be entered as part of the data file for SAFE-RCC, must be factored up using an equivalent cube strength of $1.5 \times 40 = 60\ N/mm^2$. The cross sections are designed, however, according to CP110 taking due consideration of the material partial safety factors.

The structural cross sections that resulted from the design calculations and employed in the test series are shown in Figure 12.2. A finite element mesh for each different cross section was constructed, a sample mesh is shown in Figure 12.3, to be employed in the thermal analysis (FIRES-T) and the structural analysis (SAFE-RCC). In constructing the finite element meshes every effort was made to keep the element meshes similar over the majority of the cross section. Obviously at the position of the reinforcement the mesh varied depending on the amount and position of the steel reinforcement.

The thermal properties for the concrete and steel used to predict the thermal response of the cross sections and the material data used to predict the structural response were taken to be the same as those used for the proving tests described in Chapter 11.

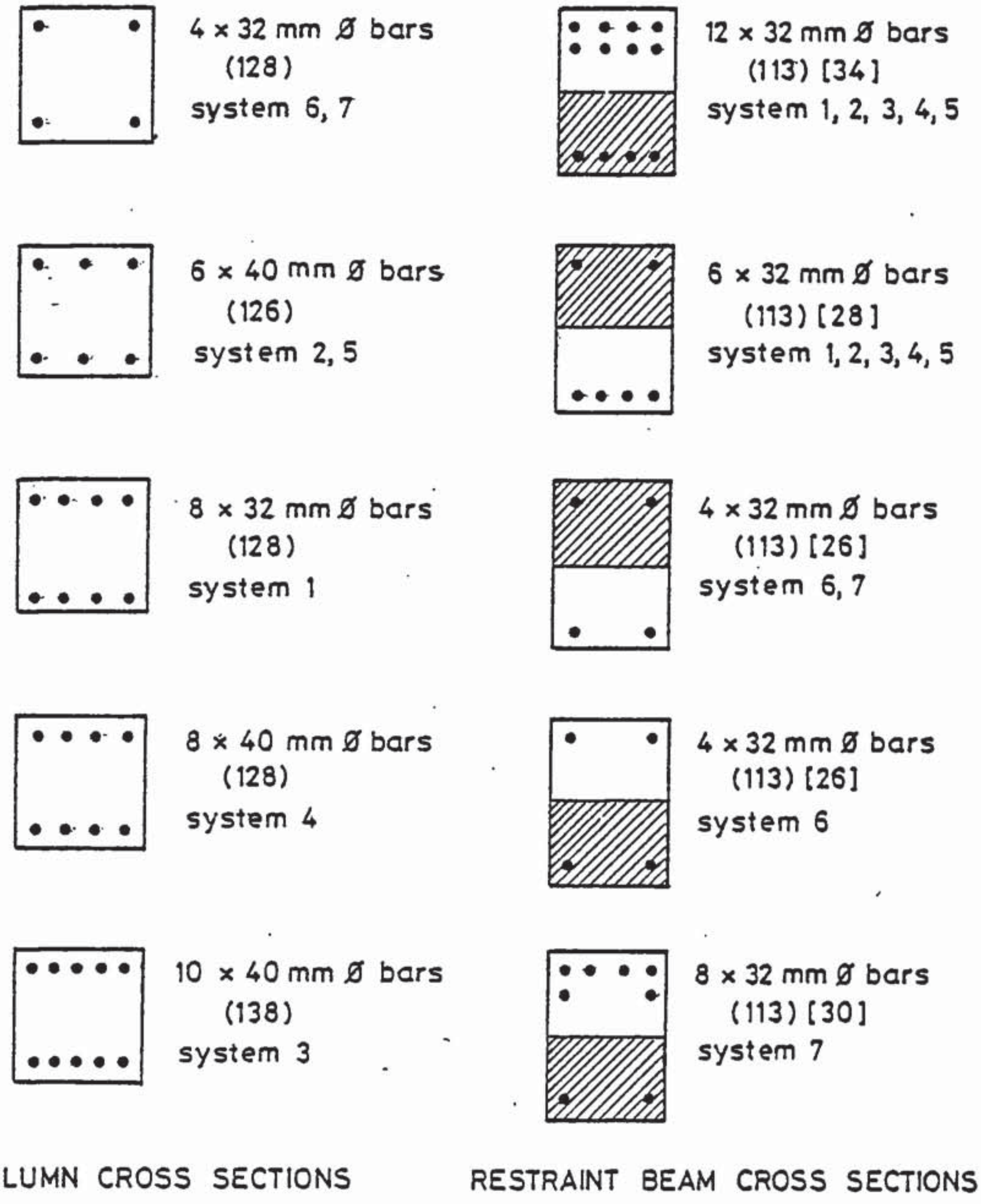

Figure 12.2 Structural cross sections employed in the thermal and structural analyses.

Numbers in ( ) refer to the number of finite elements.
Numbers in [ ] refer to the number of layers.
System number refers to the structural system number (see Table 12.1).

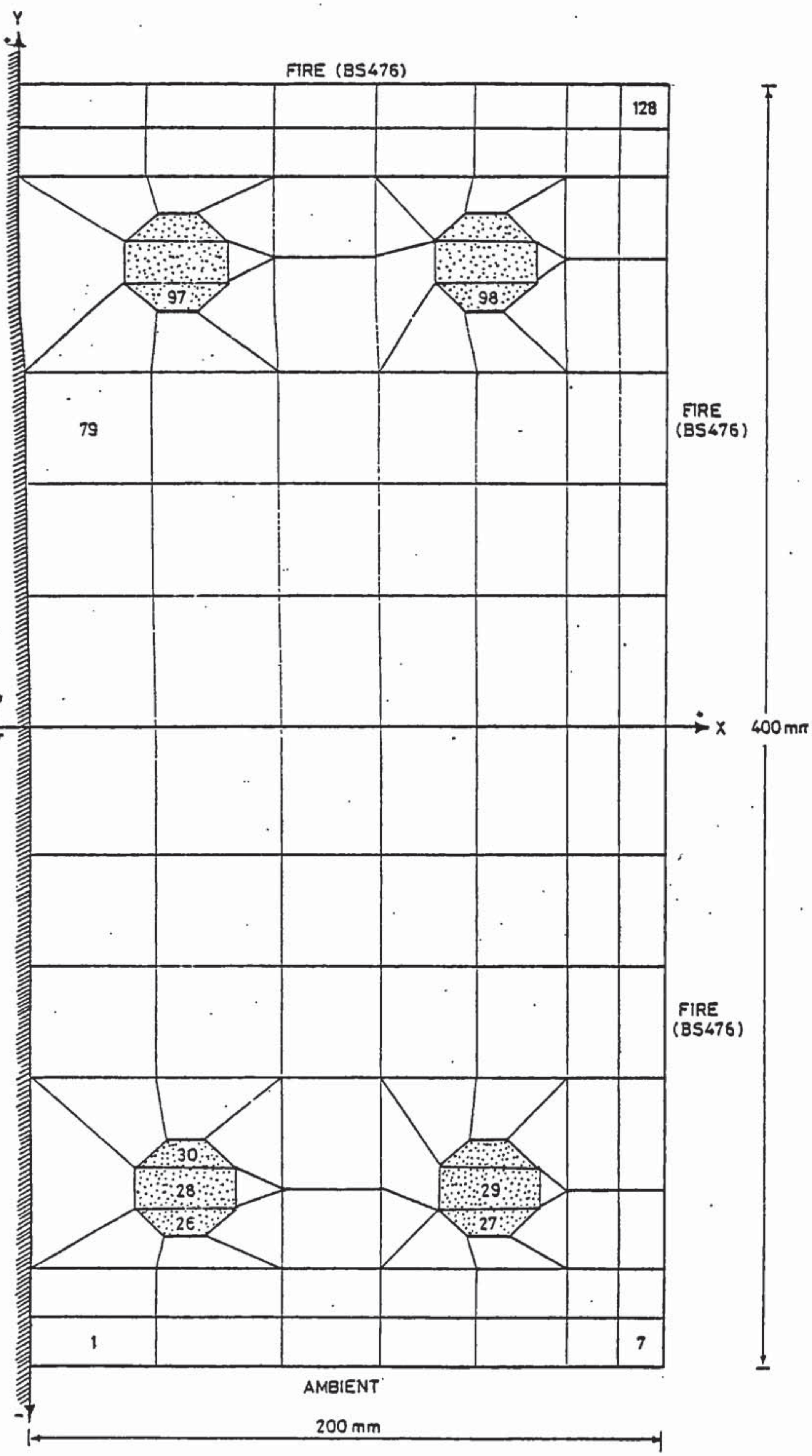

Figure 12.3 Example of finite element mesh for column cross section (8 × 32 mm diameter bars).

In determining the thermal response of the cross sections it was assumed that the column was heated from three sides according to the standard fire exposure (BS476), the top restraint beam was exposed to a standard fire on the bottom three faces while the bottom restraint beam was exposed to heating only to the top surface, as shown in Figure 12.4.

12.3 Discussion of Results

The results of the structural analysis using SAFE-RCC will now be discussed in some detail. A typical sample of computer output for one of the structural systems analysed is given in Table 12.2.

The computer test runs were set to simulate a maximum of four hours fire exposure. Four hours was used as an end point since after this time a standard furnace test would be terminated and the fire exposed columns can be said to have satisfied the fire resistance requirement, and in any case the columns were designed for a two hour fire resistance. The duration for which each test run resisted the fire exposure is shown in Table 12.1.

The fire resistance for the majority of the structural systems exceeded the design requirement of 2 hours. Three of the structural systems had not failed after 4 hours. However, two structural systems did not attain the design fire resistance. The structural system with an 8 m restraint beam and the structural system with a 12 m restraint beam failed after 1.0 and 0.65 hours respectively.

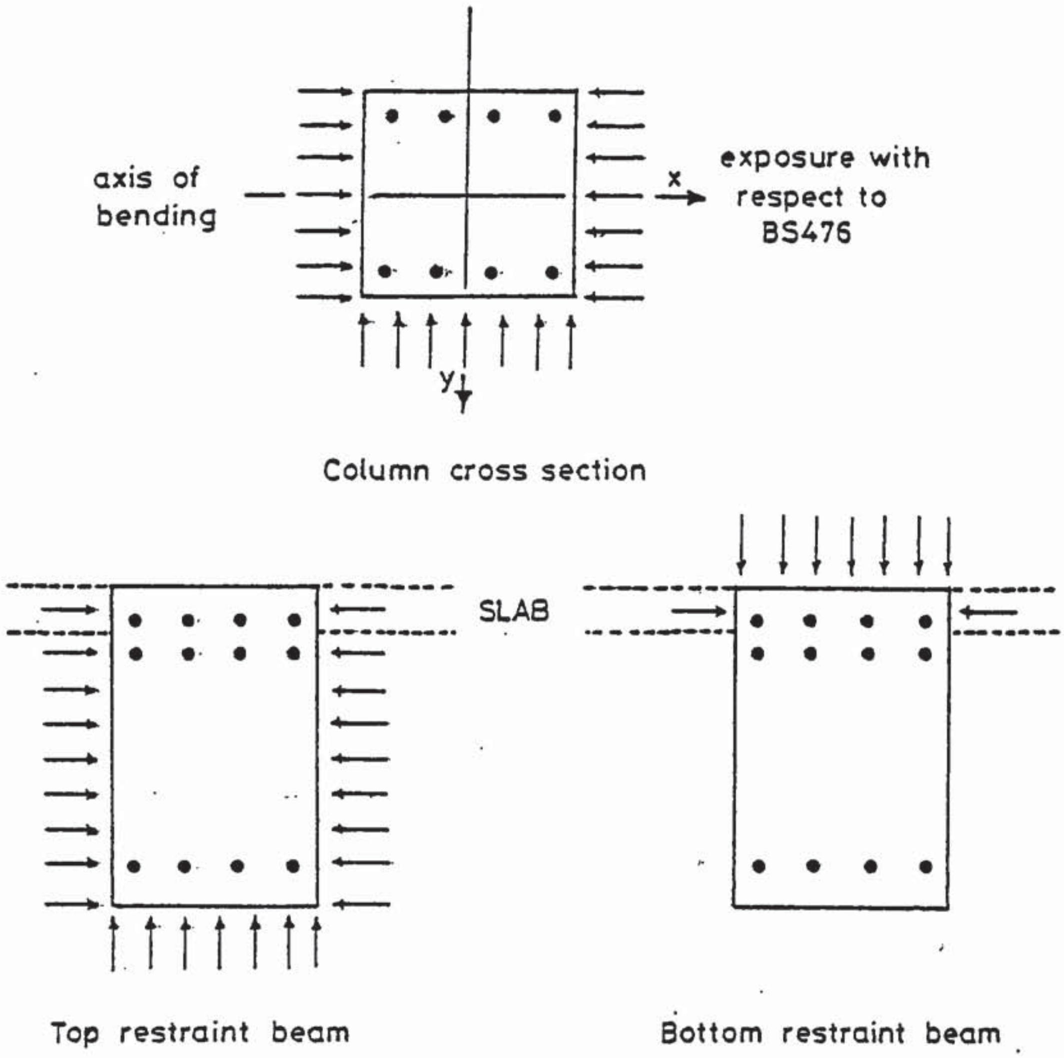

Figure 12.4 Diagram depicting exposure conditions for the cross sections of the structural system.

Table 12.2 Sample computer output

```
********************************************************************************************

   SSSSSS     AAAAAA    FFFFFFFF  EEEEEEEE              RRRRRRR    CCCCCC     CCCCCC
  SSSSSSSS   AAAAAAAA   FFFFFFFF  EEEEEEEE              RRRRRRRR  CCCCCCCC   CCCCCCCC
  SS     S   AA    AA   FF        EE                    RR    RR  CC      C  CC      C
  SS         AA    AA   FF        EE                    RR    RR  CC         CC
  SSSSSSS    AA    AA   FFFFF     EEEEE       ======    RRRRRRRR  CC         CC
   SSSSSSS   AAAAAAAA   FFFFF     EEEEE       ======    RRRRRRR   CC         CC
        SS   AAAAAAAA   FF        EE                    RR RR     CC         CC
  S     SS   AA    AA   FF        EE                    RR  RR    CC      C  CC      C
  SSSSSSSS   AA    AA   FF        EEEEEEEE              RR   RR   CCCCCCCC   CCCCCCCC
   SSSSSS    AA    AA   FF        EEEEEEEE              RR    RR   CCCCCC     CCCCCC


                        MODEL OF THE STRUCTURAL BEHAVIOUR
                        OF A REINFORCED CONCRETE COLUMN
                        EXPOSED TO A FIRE ENVIRONMENT


********************************************************************************************

                        - - - TITLE OF RUN - - -

££££ COLUMN 4M RESTRAINT BEAM 16M 3 FLOORS ABOVE ££££                          00003455

********************************************************************************************


********************************************************************************************

    SAFE-RCC - STRUCTURAL ANALYSIS OF FIRE EXPOSED REINFORCED CONCRETE COLUMNS

£££ COLUMN 4M RESTRAINT BEAM 16M 3 FLOORS ABOVE ££££                           00003455

    INFORMATION RELEVANT TO ANALYSIS PROCEDURE

********************************************************************************************

. . . . COLUMN DETAILS . . . .

BREADTH X DEPTH =    .400 X    .400 M
COLUMN LENGTH           =  4.000 M
GUSSET LENGTHS - END A =    .400 M
               - END B =    .400 M
NUMBER OF SEGMENT LENGTHS =   8
NUMBER OF ELEMENTS OF COLUMN CROSS SECTION = 128


. . . . END FORCES . . . .

AXIAL FORCE      =     1742.24 KN
MOMENTS - END A =     -377.02 KNM
        - END B =     -377.02 KNM


SECOND ORDER EFFECTS INCLUDED


SHRINKAGE MODEL NOT INCLUDED


. . . . RESTRAINT CONDITIONS . . . .

END A - NORMAL ROTATIONAL RESTRAINT
        NORMAL AXIAL RESTRAINT
        TEMPERATURE DEPENDENT RESTRAINT SYSTEM

END B - NORMAL ROTATIONAL RESTRAINT
        TEMPERATURE DEPENDENT RESTRAINT SYSTEM

ROTATIONAL RESTRAINT - LENGTH OF MEMBER = 16.000 M
                       EFFECTIVE DEPTH X BREADTH =    .755 X    .400 M
                       OVERALL DEPTH =    .800 M

AXIAL RESTRAINT - NUMBER OF FLOORS ABOVE =    3
```

. . . . CONVERGENCE CRITERIA . . . .

PERMISSIBLE NUMBER OF EQUILLIBRIUM ITERATIONS = 20

```
ALLOWABLE INCOMPATABILITIES - ALPHA =14.000000
                              BETA = 4.500000
                              E1 =  .000400
                              E2 =  .000400
                              EYA =  .000200
```

NUMBER OF TIME STEPS = 34

. . . . PROPOSED VALUES . . . .

```
ENDSLOPE - END A = -.00206
         - END B = -.00206
```

PROPOSED STIFFNESSES OF RESTRAINT SYSTEM

```
COLUMN ABOVE =    40691.21
BEAM AT JOINT A =   27505.17
COLUMN BELOW =    40691.21
BEAM AT JOINT B =   27505.17
```

DIVISION POINT DEFLECTIONS UNDER ZERO LOAD

DIVN	DEFLEC	DIVN	DEFLEC	DIVN	DEFLEC	DIVN	DEFLEC	DIVN	DEFLEC	DIVN	DEFLE
1	.00000	2	.00000	3	.00000	4	.00000	5	.00000	6	.00000
7	.00000	8	.00000	9	.00000						

DIVISION POINT DEFLECTIONS UNDER LOAD

DIVN	DEFLEC	DIVN	DEFLEC	DIVN	DEFLEC	DIVN	DEFLEC	DIVN	DEFLEC	DIVN	DEFLE
1	-.00060	2	-.00080	3	-.00070	4	-.00040	5	.00000	6	.00040
7	.00070	8	.00080	9	.00060						

DIVISION POINT CURVATURES

DIVN	CURVAT	DIVN	CURVAT	DIVN	CURVAT	DIVN	CURVAT	DIVN	CURVAT	DIVN	CURVA
1	.00247	2	.00185	3	.00124	4	.00062	5	.00000	6	-.00062
7	-.00124	8	-.00185	9	-.00247						

```
*****************************************************************************************

    SAFE-RCC - STRUCTURAL ANALYSIS OF FIRE EXPOSED REINFORCED CONCRETE COLUMNS

 £££ COLUMN 4M RESTRAINT BEAM 16M 3 FLOORS ABOVE ££££                      00003455

    INITIAL TIME IS    .000                               TIME STEP =     1

*****************************************************************************************


 --------- END MOMENTS AND ROTATIONS --------

     END A - TOTAL END MOMENT =      -154.68
             END ROTATION = -.00183

     END B - TOTAL END MOMENT =      -154.68
             END ROTATION = -.00183


 --------- AXIAL DEFORMATION ---------------

     TOTAL AXIAL FORCE = 1736.44004 KN
     COLUMN CHORD LENGTH =  3.9993356 M
     CHANGE IN CHORD LENGTH =  -.0006644 M


 --------- ULTIMATE MOMENT CAPACITIES ---------

     BEAMA 1   BEAMA 3   BEAMA 2   BEAMB 4   BEAMB 6   BEAMB 5

     2372.72   1253.02   2372.72   2372.72   1253.02   2372.72

 STIFFNESSES OF RESTRAINT SYSTEM

 COLUMN ABOVE =    40691.21
 BEAM AT JOINT A =    27505.17
 COLUMN BELOW =    40691.21
 BEAM AT JOINT B =    27505.17


 ----------------------- DIVISION POINT DEFLECTIONS ---------------------------

 DIVN    DEFLEC     DIVN    DEFLEC     DIVN    DEFLEC     DIVN    DEFLEC     DIVN    DEFLEC     DIVN    DEFLEC

  1    -.00073       2    -.00112       3    -.00100       4    -.00057       5     .00000       6     .00057
  7     .00100       8     .00112       9     .00073


 ----------------------- RATE OF DEFLECTION ----------------------------------

 DIVN     RATE      DIVN     RATE      DIVN     RATE      DIVN     RATE      DIVN     RATE      DIVN     RATE

  1      .0000       2      .0000       3      .0000       4      .0000       5      .0000       6      .0000
  7      .0000       8      .0000       9      .0000
```

. . . . DIVISION POINT 1 . . . .

---------------------- ELEMENTAL STRESSES AND STRAINS ----------------------

ELEM	TOTAL STRAIN	STRESS STRAIN	STRESS	ELEM	TOTAL STRAIN	STRESS STRAIN	STRESS	ELEM	TOTAL STRAIN	STRESS STRAIN	STRESS
1	-781.	-781.	CRACKED	2	-781.	-781.	CRACKED	3	-781.	-781.	CRACKED
4	-781.	-781.	CRACKED	5	-781.	-781.	CRACKED	6	-781.	-781.	CRACKED
7	-781.	-781.	CRACKED	8	-709.	-709.	CRACKED	9	-709.	-709.	CRACKED
10	-709.	-709.	CRACKED	11	-709.	-709.	CRACKED	12	-709.	-709.	CRACKED
13	-709.	-709.	CRACKED	14	-709.	-709.	CRACKED	15	-529.	-529.	CRACKED
16	-634.	-634.	CRACKED	17	-648.	-648.	CRACKED	18	-604.	-604.	CRACKED
19	-613.	-613.	CRACKED	20	-598.	-598.	CRACKED	21	-634.	-634.	CRACKED
22	-648.	-648.	CRACKED	23	-604.	-604.	CRACKED	24	-613.	-613.	CRACKED
25	-613.	-613.	CRACKED	26	-595.	-595.	-125.03	27	-595.	-595.	-125.03
28	-529.	-529.	-111.17	29	-529.	-529.	-111.17	30	-463.	-463.	-97.31
31	-463.	-463.	-97.31	32	-537.	-537.	CRACKED	33	-537.	-537.	CRACKED
34	-424.	-424.	CRACKED	35	-411.	-411.	CRACKED	36	-466.	-466.	CRACKED
37	-469.	-469.	CRACKED	38	-499.	-499.	CRACKED	39	-424.	-424.	CRACKED
40	-411.	-411.	CRACKED	41	-466.	-466.	CRACKED	42	-469.	-469.	CRACKED
43	-469.	-469.	CRACKED	44	-302.	-302.	CRACKED	45	-302.	-302.	CRACKED
46	-302.	-302.	CRACKED	47	-302.	-302.	CRACKED	48	-302.	-302.	CRACKED
49	-302.	-302.	CRACKED	50	-302.	-302.	CRACKED	51	-134.	-134.	CRACKED
52	-134.	-134.	CRACKED	53	-134.	-134.	CRACKED	54	-134.	-134.	CRACKED
55	-134.	-134.	CRACKED	56	-134.	-134.	CRACKED	57	-134.	-134.	CRACKED
58	46.	46.	1.89	59	46.	46.	1.89	60	46.	46.	1.89
61	46.	46.	1.89	62	46.	46.	1.89	63	46.	46.	1.89
64	46.	46.	1.89	65	238.	238.	8.99	66	238.	238.	8.99
67	238.	238.	8.99	68	238.	238.	8.99	69	238.	238.	8.99
70	238.	238.	8.99	71	238.	238.	8.99	72	418.	418.	14.63
73	418.	418.	14.63	74	418.	418.	14.63	75	418.	418.	14.63
76	418.	418.	14.63	77	418.	418.	14.63	78	418.	418.	14.63
79	586.	586.	19.13	80	586.	586.	19.13	81	586.	586.	19.13
82	586.	586.	19.13	83	586.	586.	19.13	84	586.	586.	19.13
85	586.	586.	19.13	86	814.	814.	24.16	87	709.	709.	21.99
88	695.	695.	21.68	89	751.	751.	22.88	90	754.	754.	22.95
91	784.	784.	23.56	92	709.	709.	21.99	93	695.	695.	21.68
94	751.	751.	22.88	95	754.	754.	22.95	96	754.	754.	22.95
97	748.	748.	157.00	98	748.	748.	157.00	99	814.	814.	170.86
100	814.	814.	170.86	101	880.	880.	184.72	102	880.	880.	184.72
103	822.	822.	24.32	104	822.	822.	24.32	105	919.	919.	26.11
106	932.	932.	26.35	107	889.	889.	25.58	108	898.	898.	25.74
109	882.	882.	25.46	110	919.	919.	26.11	111	932.	932.	26.35
112	889.	889.	25.58	113	898.	898.	25.74	114	898.	898.	25.74
115	993.	993.	27.37	116	993.	993.	27.37	117	993.	993.	27.37
118	993.	993.	27.37	119	993.	993.	27.37	120	993.	993.	27.37
121	993.	993.	27.37	122	1065.	1065.	28.49	123	1065.	1065.	28.49
124	1065.	1065.	28.49	125	1065.	1065.	28.49	126	1065.	1065.	28.49
127	1065.	1065.	28.49	128	1065.	1065.	28.49				

. . . . DIVISION POINT 5 . . . .

---------------------- ELEMENTAL STRESSES AND STRAINS ----------------------

ELEM	TOTAL STRAIN	STRESS STRAIN	STRESS	ELEM	TOTAL STRAIN	STRESS STRAIN	STRESS	ELEM	TOTAL STRAIN	STRESS STRAIN	STRESS
1	223.	223.	8.47	2	223.	223.	8.47	3	223.	223.	8.47
4	223.	223.	8.47	5	223.	223.	8.47	6	223.	223.	8.47
7	223.	223.	8.47	8	223.	223.	8.47	9	223.	223.	8.47
10	223.	223.	8.47	11	223.	223.	8.47	12	223.	223.	8.47
13	223.	223.	8.47	14	223.	223.	8.47	15	223.	223.	8.47
16	223.	223.	8.47	17	223.	223.	8.47	18	223.	223.	8.47
19	223.	223.	8.47	20	223.	223.	8.47	21	223.	223.	8.47
22	223.	223.	8.47	23	223.	223.	8.47	24	223.	223.	8.47
25	223.	223.	8.47	26	223.	223.	46.86	27	223.	223.	46.86
28	223.	223.	46.86	29	223.	223.	46.86	30	223.	223.	46.86
31	223.	223.	46.86	32	223.	223.	8.47	33	223.	223.	8.47
34	223.	223.	8.47	35	223.	223.	8.47	36	223.	223.	8.47
37	223.	223.	8.47	38	223.	223.	8.47	39	223.	223.	8.47
40	223.	223.	8.47	41	223.	223.	8.47	42	223.	223.	8.47
43	223.	223.	8.47	44	223.	223.	8.47	45	223.	223.	8.47
46	223.	223.	8.47	47	223.	223.	8.47	48	223.	223.	8.47
49	223.	223.	8.47	50	223.	223.	8.47	51	223.	223.	8.47
52	223.	223.	8.47	53	223.	223.	8.47	54	223.	223.	8.47
55	223.	223.	8.47	56	223.	223.	8.47	57	223.	223.	8.47
58	223.	223.	8.47	59	223.	223.	8.47	60	223.	223.	8.47
61	223.	223.	8.47	62	223.	223.	8.47	63	223.	223.	8.47
64	223.	223.	8.47	65	223.	223.	8.47	66	223.	223.	8.47
67	223.	223.	8.47	68	223.	223.	8.47	69	223.	223.	8.47
70	223.	223.	8.47	71	223.	223.	8.47	72	223.	223.	8.47
73	223.	223.	8.47	74	223.	223.	8.47	75	223.	223.	8.47
76	223.	223.	8.47	77	223.	223.	8.47	78	223.	223.	8.47
79	223.	223.	8.47	80	223.	223.	8.47	81	223.	223.	8.47
82	223.	223.	8.47	83	223.	223.	8.47	84	223.	223.	8.47
85	223.	223.	8.47	86	223.	223.	8.47	87	223.	223.	8.47
88	223.	223.	8.47	89	223.	223.	8.47	90	223.	223.	8.47
91	223.	223.	8.47	92	223.	223.	8.47	93	223.	223.	8.47
94	223.	223.	8.47	95	223.	223.	8.47	96	223.	223.	8.47
97	223.	223.	46.86	98	223.	223.	46.86	99	223.	223.	46.86
100	223.	223.	46.86	101	223.	223.	46.86	102	223.	223.	46.86
103	223.	223.	8.47	104	223.	223.	8.47	105	223.	223.	8.47
106	223.	223.	8.47	107	223.	223.	8.47	108	223.	223.	8.47
109	223.	223.	8.47	110	223.	223.	8.47	111	223.	223.	8.47
112	223.	223.	8.47	113	223.	223.	8.47	114	223.	223.	8.47
115	223.	223.	8.47	116	223.	223.	8.47	117	223.	223.	8.47
118	223.	223.	8.47	119	223.	223.	8.47	120	223.	223.	8.47
121	223.	223.	8.47	122	223.	223.	8.47	123	223.	223.	8.47
124	223.	223.	8.47	125	223.	223.	8.47	126	223.	223.	8.47
127	223.	223.	8.47	128	223.	223.	8.47				

. . . . . DIVISION POINT 9 . . . . .

---------------------- ELEMENTAL STRESSES AND STRAINS ----------------------

ELEM	TOTAL STRAIN	STRESS STRAIN	STRESS	ELEM	TOTAL STRAIN	STRESS STRAIN	STRESS	ELEM	TOTAL STRAIN	STRESS STRAIN	STRESS
1	1065.	1065.	28.49	2	1065.	1065.	28.49	3	1065.	1065.	28.49
4	1065.	1065.	28.49	5	1065.	1065.	28.49	6	1065.	1065.	28.49
7	1065.	1065.	28.49	8	993.	993.	27.37	9	993.	993.	27.37
10	993.	993.	27.37	11	993.	993.	27.37	12	993.	993.	27.37
13	993.	993.	27.37	14	993.	993.	27.37	15	814.	814.	24.16
16	919.	919.	26.11	17	932.	932.	26.35	18	889.	889.	25.58
19	898.	898.	25.74	20	882.	882.	25.46	21	919.	919.	26.11
22	932.	932.	26.35	23	889.	889.	25.58	24	898.	898.	25.74
25	898.	898.	25.74	26	880.	880.	184.72	27	880.	880.	184.72
28	814.	814.	170.86	29	814.	814.	170.86	30	748.	748.	157.00
31	748.	748.	157.00	32	822.	822.	24.32	33	822.	822.	24.32
34	709.	709.	21.99	35	695.	695.	21.68	36	751.	751.	22.88
37	754.	754.	22.95	38	784.	784.	23.56	39	709.	709.	21.99
40	695.	695.	21.68	41	751.	751.	22.88	42	754.	754.	22.95
43	754.	754.	22.95	44	586.	586.	19.13	45	586.	586.	19.13
46	586.	586.	19.13	47	586.	586.	19.13	48	586.	586.	19.13
49	586.	586.	19.13	50	586.	586.	19.13	51	418.	418.	14.63
52	418.	418.	14.63	53	418.	418.	14.63	54	418.	418.	14.63
55	418.	418.	14.63	56	418.	418.	14.63	57	418.	418.	14.63
58	238.	238.	8.99	59	238.	238.	8.99	60	238.	238.	8.99
61	238.	238.	8.99	62	238.	238.	8.99	63	238.	238.	8.99
64	238.	238.	8.99	65	46.	46.	1.89	66	46.	46.	1.89
67	46.	46.	1.89	68	46.	46.	1.89	69	46.	46.	1.89
70	46.	46.	1.89	71	46.	46.	1.89	72	-134.	-134.	CRACKED
73	-134.	-134.	CRACKED	74	-134.	-134.	CRACKED	75	-134.	-134.	CRACKED
76	-134.	-134.	CRACKED	77	-134.	-134.	CRACKED	78	-134.	-134.	CRACKED
79	-302.	-302.	CRACKED	80	-302.	-302.	CRACKED	81	-302.	-302.	CRACKED
82	-302.	-302.	CRACKED	83	-302.	-302.	CRACKED	84	-302.	-302.	CRACKED
85	-302.	-302.	CRACKED	86	-529.	-529.	CRACKED	87	-424.	-424.	CRACKED
88	-411.	-411.	CRACKED	89	-466.	-466.	CRACKED	90	-469.	-469.	CRACKED
91	-499.	-499.	CRACKED	92	-424.	-424.	CRACKED	93	-411.	-411.	CRACKED
94	-466.	-466.	CRACKED	95	-469.	-469.	CRACKED	96	-469.	-469.	CRACKED
97	-463.	-463.	-97.31	98	-463.	-463.	-97.31	99	-529.	-529.	-111.17
100	-529.	-529.	-111.17	101	-595.	-595.	-125.03	102	-595.	-595.	-125.03
103	-537.	-537.	CRACKED	104	-537.	-537.	CRACKED	105	-634.	-634.	CRACKED
106	-648.	-648.	CRACKED	107	-604.	-604.	CRACKED	108	-613.	-613.	CRACKED
109	-598.	-598.	CRACKED	110	-634.	-634.	CRACKED	111	-648.	-648.	CRACKED
112	-604.	-604.	CRACKED	113	-613.	-613.	CRACKED	114	-613.	-613.	CRACKED
115	-709.	-709.	CRACKED	116	-709.	-709.	CRACKED	117	-709.	-709.	CRACKED
118	-709.	-709.	CRACKED	119	-709.	-709.	CRACKED	120	-709.	-709.	CRACKED
121	-709.	-709.	CRACKED	122	-781.	-781.	CRACKED	123	-781.	-781.	CRACKED
124	-781.	-781.	CRACKED	125	-781.	-781.	CRACKED	126	-781.	-781.	CRACKED
127	-781.	-781.	CRACKED	128	-781.	-781.	CRACKED				

```
*****************************************************************************

    SAFE-RCC - STRUCTURAL ANALYSIS OF FIRE EXPOSED REINFORCED CONCRETE COLUMNS

£££ COLUMN 4M RESTRAINT BEAM 16M 3 FLOORS ABOVE ££££                 00003455

    TIME =   .4000 HOURS                                 TIME STEP =    9

*****************************************************************************


--------- END MOMENTS AND ROTATIONS --------

    END A - TOTAL END MOMENT =     -424.02
            END ROTATION = -.00158

    END B - TOTAL END MOMENT =     -300.75
            END ROTATION = -.00274


--------- AXIAL DEFORMATION ----------------

    TOTAL AXIAL FORCE = 1739.75457 KN
    COLUMN CHORD LENGTH =  4.0000156 M
    CHANGE IN CHORD LENGTH =   .0000156 M


--------- ULTIMATE MOMENT CAPACITIES ---------

    BEAMA 1   BEAMA 3   BEAMA 2   BEAMB 4   BEAMB 6   BEAMB 5

    2178.53   1386.39   2178.53   2313.34   1256.16   2313.34

STIFFNESSES OF RESTRAINT SYSTEM

COLUMN ABOVE =    40691.21
BEAM AT JOINT A =    24519.92
COLUMN BELOW =    40691.21
BEAM AT JOINT B =    26389.11


----------------------- DIVISION POINT DEFLECTIONS --------------------------

DIVN   DEFLEC    DIVN   DEFLEC    DIVN   DEFLEC    DIVN   DEFLEC    DIVN   DEFLEC    DIVN   DEFLEC

 1    -.00063     2    -.00087     3    -.00055     4     .00010     5     .00084     6     .00148
 7     .00186     8     .00180     9     .00109


----------------------- RATE OF DEFLECTION ----------------------------------

DIVN   RATE      DIVN   RATE      DIVN   RATE      DIVN   RATE      DIVN   RATE      DIVN   RATE

 1     .0031      2     .0059      3     .0070      4     .0033      5     .0083      6     .0085
 7     .0076      8     .0056      9     .0029
```

. . . . DIVISION POINT 1 . . . .

---------------------- ELEMENTAL STRESSES AND STRAINS ----------------------

ELEM	TOTAL STRAIN	STRESS STRAIN	STRESS	ELEM	TOTAL STRAIN	STRESS STRAIN	STRESS	ELEM	TOTAL STRAIN	STRESS STRAIN	STRESS
1	-1130.	-1128.	CRACKED	2	-1130.	-1120.	CRACKED	3	-1130.	-1093.	CRACKED
4	-1130.	-1001.	CRACKED	5	-1130.	-512.	CRACKED	6	-1130.	-48.	CRACKED
7	-1130.	1812.	33.34	8	-1045.	-1042.	CRACKED	9	-1045.	-1034.	CRACKED
10	-1045.	-1001.	CRACKED	11	-1045.	-904.	CRACKED	12	-1045.	-438.	CRACKED
13	-1045.	-489.	CRACKED	14	-1045.	14.	.00	15	-831.	-828.	CRACKED
16	-956.	-952.	CRACKED	17	-972.	-963.	CRACKED	18	-920.	-906.	CRACKED
19	-931.	-870.	CRACKED	20	-913.	-767.	CRACKED	21	-956.	-761.	CRACKED
22	-972.	-549.	CRACKED	23	-920.	-304.	CRACKED	24	-931.	-35.	CRACKED
25	-931.	-2124.	CRACKED	26	-910.	-894.	-187.69	27	-910.	-397.	-83.33
28	-831.	-815.	-171.25	29	-831.	-318.	-66.76	30	-753.	-737.	-154.83
31	-753.	-240.	-50.41	32	-841.	-829.	CRACKED	33	-841.	-349.	CRACKED
34	-707.	-703.	CRACKED	35	-690.	-682.	CRACKED	36	-756.	-743.	CRACKED
37	-760.	-699.	CRACKED	38	-796.	-627.	CRACKED	39	-707.	-511.	CRACKED
40	-690.	-269.	CRACKED	41	-756.	-143.	CRACKED	42	-760.	940.	22.29
43	-760.	2168.	34.21	44	-561.	-559.	CRACKED	45	-561.	-551.	CRACKED
46	-561.	-518.	CRACKED	47	-561.	-414.	CRACKED	48	-561.	21.	.73
49	-561.	-410.	CRACKED	50	-561.	-3199.	CRACKED	51	-362.	-360.	CRACKED
52	-362.	-353.	CRACKED	53	-362.	-326.	CRACKED	54	-362.	-218.	CRACKED
55	-362.	109.	3.85	56	-362.	1420.	28.65	57	-362.	-886.	CRACKED
58	-148.	-154.	CRACKED	59	-148.	-147.	CRACKED	60	-148.	-120.	CRACKED
61	-148.	-25.	-1.02	62	-148.	205.	7.26	63	-148.	1294.	28.96
64	-148.	-3958.	CRACKED	65	79.	43.	.82	66	79.	48.	1.01
67	79.	65.	1.77	68	79.	120.	4.10	69	79.	287.	10.03
70	79.	-772.	CRACKED	71	79.	-2729.	CRACKED	72	293.	230.	6.75
73	293.	232.	6.85	74	293.	240.	7.20	75	293.	267.	8.35
76	293.	387.	13.23	77	293.	-1754.	CRACKED	78	293.	2995.	34.31
79	492.	403.	11.49	80	492.	404.	11.52	81	492.	405.	11.57
82	492.	413.	11.88	83	492.	493.	15.25	84	492.	1554.	33.40
85	492.	-335.	CRACKED	86	762.	608.	15.54	87	638.	517.	13.93
88	621.	504.	13.69	89	687.	552.	14.56	90	691.	554.	14.59
91	727.	587.	15.31	92	638.	526.	14.33	93	621.	556.	15.84
94	687.	586.	15.96	95	691.	437.	5.92	96	691.	137.	.00
97	684.	1188.	249.56	98	684.	1590.	333.92	99	762.	1292.	271.42
100	762.	1689.	354.71	101	840.	1405.	295.11	102	840.	1795.	377.04
103	772.	612.	15.55	104	772.	647.	17.00	105	887.	714.	17.52
106	903.	723.	17.59	107	851.	679.	16.79	108	862.	702.	17.55
109	844.	697.	17.67	110	887.	684.	16.23	111	903.	362.	2.39
112	851.	327.	1.98	113	862.	-145.	CRACKED	114	862.	-1141.	CRACKED
115	975.	491.	4.47	116	975.	422.	1.50	117	975.	417.	1.19
118	975.	363.	.00	119	975.	-153.	CRACKED	120	975.	-1881.	CRACKED
121	975.	-2263.	CRACKED	122	1061.	-575.	CRACKED	123	1061.	-620.	CRACKED
124	1061.	-619.	CRACKED	125	1061.	-694.	CRACKED	126	1061.	-1014.	CRACKED
127	1061.	-4370.	CRACKED	128	1061.	4807.	18.90				

. . . . DIVISION POINT 5 . . . .

---------------------- ELEMENTAL STRESSES AND STRAINS ----------------------

ELEM	TOTAL STRAIN	STRESS STRAIN	STRESS	ELEM	TOTAL STRAIN	STRESS STRAIN	STRESS	ELEM	TOTAL STRAIN	STRESS STRAIN	STRESS
1	129.	98.	3.25	2	129.	104.	3.49	3	129.	123.	4.30
4	129.	175.	6.44	5	129.	313.	11.07	6	129.	1111.	28.88
7	129.	-4046.	CRACKED	8	120.	89.	2.88	9	120.	95.	3.15
10	120.	119.	4.14	11	120.	173.	6.40	12	120.	314.	11.09
13	120.	1066.	28.20	14	120.	-2918.	CRACKED	15	96.	67.	1.98
16	110.	81.	2.55	17	112.	86.	2.77	18	106.	85.	2.72
19	107.	119.	4.16	20	105.	166.	6.08	21	110.	191.	7.06
22	112.	266.	9.51	23	106.	311.	10.98	24	107.	901.	25.60
25	107.	-838.	CRACKED	26	105.	120.	25.30	27	105.	617.	129.66
28	96.	112.	23.49	29	96.	609.	127.97	30	87.	103.	21.64
31	87.	600.	126.06	32	97.	75.	2.32	33	97.	278.	9.87
34	82.	54.	1.44	35	81.	56.	1.54	36	88.	68.	2.01
37	88.	103.	3.50	38	92.	168.	6.15	39	82.	174.	6.41
40	81.	253.	9.03	41	88.	304.	10.72	42	88.	655.	20.63
43	88.	247.	3.48	44	66.	37.	.72	45	66.	44.	1.02
46	66.	71.	2.16	47	66.	138.	4.96	48	66.	299.	10.52
49	66.	381.	13.43	50	66.	-4545.	CRACKED	51	44.	15.	-.18
52	44.	22.	.09	53	44.	46.	1.12	54	44.	121.	4.25
55	44.	298.	10.45	56	44.	119.	2.38	57	44.	-2642.	CRACKED
58	21.	-8.	-1.15	59	21.	-1.	-.86	60	21.	24.	.22
61	21.	104.	3.57	62	21.	290.	10.17	63	21.	-161.	CRACKED
64	21.	-3830.	CRACKED	65	-4.	-31.	-2.10	66	-4.	-25.	-1.86
67	-4.	3.	-.65	68	-4.	87.	2.88	69	-4.	281.	9.83
70	-4.	-402.	CRACKED	71	-4.	-2768.	CRACKED	72	-28.	-46.	CRACKED
73	-28.	-40.	CRACKED	74	-28.	-17.	-1.47	75	-28.	77.	2.47
76	-28.	274.	9.56	77	-28.	-606.	CRACKED	78	-28.	-4703.	CRACKED
79	-50.	-33.	-2.11	80	-50.	-20.	-1.55	81	-50.	-2.	-.77
82	-50.	97.	3.31	83	-50.	271.	9.47	84	-50.	-783.	CRACKED
85	-50.	-4854.	CRACKED	86	-80.	151.	5.41	87	-66.	60.	1.79
88	-64.	70.	2.19	89	-72.	94.	3.16	90	-72.	102.	3.49
91	-76.	181.	6.44	92	-66.	177.	6.33	93	-64.	257.	8.93
94	-72.	264.	9.31	95	-72.	-1075.	CRACKED	96	-72.	1693.	33.11
97	-71.	433.	91.03	98	-71.	835.	175.39	99	-80.	451.	94.64
100	-80.	847.	177.92	101	-88.	477.	100.07	102	-88.	867.	182.00
103	-81.	120.	4.20	104	-81.	264.	9.33	105	-93.	235.	8.18
106	-95.	242.	8.43	107	-90.	200.	7.03	108	-91.	255.	8.89
109	-89.	257.	8.94	110	-93.	250.	8.72	111	-95.	151.	4.05
112	-90.	150.	4.01	113	-91.	-2121.	CRACKED	114	-91.	2742.	34.64
115	-103.	-834.	CRACKED	116	-103.	-997.	CRACKED	117	-103.	-1100.	CRACKED
118	-103.	-1251.	CRACKED	119	-103.	-2175.	CRACKED	120	-103.	-3119.	CRACKED
121	-103.	537.	6.15	122	-113.	2261.	34.90	123	-113.	2415.	34.96
124	-113.	2436.	34.96	125	-113.	2861.	34.89	126	-113.	526.	10.24
127	-113.	[illegible]	[illegible]	128	-113.	[illegible]	[illegible]				

. . . . DIVISION POINT 9 . . . .

---------------------- ELEMENTAL STRESSES AND STRAINS ----------------------

ELEM	TOTAL STRAIN	STRESS STRAIN	STRESS	ELEM	TOTAL STRAIN	STRESS STRAIN	STRESS	ELEM	TOTAL STRAIN	STRESS STRAIN	STRESS
1	964.	833.	18.81	2	964.	831.	18.71	3	964.	823.	18.38
4	964.	807.	17.71	5	964.	849.	19.45	6	964.	298.	.00
7	964.	-2641.	CRACKED	8	883.	759.	17.58	9	883.	757.	17.50
10	883.	750.	17.21	11	883.	740.	16.76	12	883.	789.	18.84
13	883.	326.	.00	14	883.	-1794.	CRACKED	15	682.	574.	14.18
16	800.	681.	16.22	17	815.	694.	16.44	18	766.	649.	15.60
19	776.	654.	15.58	20	759.	639.	15.28	21	800.	673.	15.84
22	815.	714.	17.21	23	766.	700.	17.71	24	776.	450.	5.34
25	776.	-1163.	CRACKED	26	756.	772.	162.05	27	756.	1269.	266.41
28	682.	698.	146.53	29	682.	1195.	251.01	30	608.	624.	130.98
31	608.	1121.	235.40	32	691.	582.	14.33	33	691.	633.	16.43
34	564.	468.	11.96	35	549.	455.	11.68	36	611.	511.	12.89
37	615.	517.	13.08	38	648.	553.	13.95	39	564.	494.	13.01
40	549.	522.	14.44	41	611.	589.	16.14	42	615.	1884.	34.33
43	615.	-929.	CRACKED	44	427.	345.	9.09	45	427.	347.	9.19
46	427.	356.	9.58	47	427.	382.	10.68	48	427.	467.	14.16
49	427.	1028.	27.66	50	427.	66.	.00	51	239.	179.	4.69
52	239.	183.	4.86	53	239.	198.	5.50	54	239.	245.	7.51
55	239.	354.	11.96	56	239.	-1450.	CRACKED	57	239.	-2058.	CRACKED
58	37.	5.	-.73	59	37.	11.	-.47	60	37.	35.	.55
61	37.	108.	3.65	62	37.	260.	9.34	63	37.	169.	4.65
64	37.	-2235.	CRACKED	65	-177.	-180.	CRACKED	66	-177.	-174.	CRACKED
67	-177.	-146.	CRACKED	68	-177.	-42.	-1.69	69	-177.	177.	6.26
70	-177.	262.	6.65	71	-177.	-3889.	CRACKED	72	-379.	-366.	CRACKED
73	-379.	-359.	CRACKED	74	-379.	-331.	CRACKED	75	-379.	-223.	CRACKED
76	-379.	70.	2.21	77	-379.	227.	6.15	78	-379.	-968.	CRACKED
79	-567.	-513.	CRACKED	80	-567.	-496.	CRACKED	81	-567.	-473.	CRACKED
82	-567.	-358.	CRACKED	83	-567.	117.	3.88	84	-567.	-340.	CRACKED
85	-567.	-2544.	CRACKED	86	-822.	-481.	CRACKED	87	-704.	-535.	CRACKED
88	-689.	-507.	CRACKED	89	-751.	-526.	CRACKED	90	-755.	-516.	CRACKED
91	-788.	-391.	CRACKED	92	-704.	-326.	CRACKED	93	-689.	-65.	CRACKED
94	-751.	108.	3.53	95	-755.	-145.	CRACKED	96	-755.	1967.	34.32
97	-748.	-243.	-51.13	98	-748.	158.	33.23	99	-822.	-292.	-61.23
100	-822.	105.	22.06	101	-896.	-331.	-69.51	102	-896.	59.	12.42
103	-831.	-552.	CRACKED	104	-831.	-44.	CRACKED	105	-940.	-343.	CRACKED
106	-955.	-307.	CRACKED	107	-906.	-441.	CRACKED	108	-916.	-205.	CRACKED
109	-899.	-209.	CRACKED	110	-940.	-84.	CRACKED	111	-955.	131.	4.19
112	-906.	194.	6.05	113	-916.	430.	14.32	114	-916.	-1009.	CRACKED
115	-1023.	-483.	CRACKED	116	-1023.	-57.	CRACKED	117	-1023.	-7.	CRACKED
118	-1023.	237.	7.28	119	-1023.	-1799.	CRACKED	120	-1023.	-4215.	CRACKED
121	-1023.	1680.	31.09	122	-1104.	-2935.	CRACKED	123	-1104.	-3404.	CRACKED
124	-1104.	-3450.	CRACKED	125	-1104.	-4203.	CRACKED	126	-1104.	-1442.	CRACKED
127	-1104.	269.	4.80	128	-1104.	1191.	13.79				

```
*******************************************************************************
    SAFE-RCC - STRUCTURAL ANALYSIS OF FIRE EXPOSED REINFORCED CONCRETE COLUMNS
£££ COLUMN 4M RESTRAINT BEAM 16M 3 FLOORS ABOVE ££££                  00003455
    TIME =   .7000 HOURS                                   TIME STEP =   15
*******************************************************************************
```

--------- END MOMENTS AND ROTATIONS --------

```
    END A - TOTAL END MOMENT =     -438.42
            END ROTATION = -.00213

    END B - TOTAL END MOMENT =     -161.56
            END ROTATION = -.00309
```

--------- AXIAL DEFORMATION ---------------

```
    TOTAL AXIAL FORCE = 1738.76414 KN
    COLUMN CHORD LENGTH =  4.0013118 M
    CHANGE IN CHORD LENGTH =   .0013118 M
```

--------- ULTIMATE MOMENT CAPACITIES ---------

BEAMA 1	BEAMA 3	BEAMA 2	BEAMB 4	BEAMB 6	BEAMB 5
2176.21	1378.55	2176.21	2330.20	1263.55	2330.20

STIFFNESSES OF RESTRAINT SYSTEM

```
COLUMN ABOVE =    40691.21
BEAM AT JOINT A =    23010.82
COLUMN BELOW =    40691.21
BEAM AT JOINT B =    25712.64
```

---------------------- DIVISION POINT DEFLECTIONS --------------------------

DIVN	DEFLEC	DIVN	DEFLEC	DIVN	DEFLEC	DIVN	DEFLEC	DIVN	DEFLEC	DIVN	DEFLEC
1	-.00085	2	-.00126	3	-.00096	4	-.00021	5	.00071	6	.00155
7	.00206	8	.00202	9	.00124						

---------------------- RATE OF DEFLECTION ----------------------------------

DIVN	RATE	DIVN	RATE	DIVN	RATE	DIVN	RATE	DIVN	RATE	DIVN	RATE
1	.0013	2	.0018	3	.0015	4	.0002	5	.0009	6	.0016
7	.0019	8	.0020	9	.0013						

. . . . DIVISION POINT 1 . . . . .

---------------------- ELEMENTAL STRESSES AND STRAINS ----------------------

ELEM	TOTAL STRAIN	STRESS STRAIN	STRESS	ELEM	TOTAL STRAIN	STRESS STRAIN	STRESS	ELEM	TOTAL STRAIN	STRESS STRAIN	STRESS
1	-1492.	-1478.	CRACKED	2	-1492.	-1448.	CRACKED	3	-1492.	-1357.	CRACKED
4	-1492.	-1107.	CRACKED	5	-1492.	-160.	CRACKED	6	-1492.	-3092.	CRACKED
7	-1492.	-4280.	CRACKED	8	-1402.	-1386.	CRACKED	9	-1402.	-1354.	CRACKED
10	-1402.	-1244.	CRACKED	11	-1402.	-965.	CRACKED	12	-1402.	-107.	CRACKED
13	-1402.	-2959.	CRACKED	14	-1402.	-7808.	CRACKED	15	-1175.	-1154.	CRACKED
16	-1308.	-1284.	CRACKED	17	-1325.	-1284.	CRACKED	18	-1270.	-1211.	CRACKED
19	-1281.	-1073.	CRACKED	20	-1262.	-792.	CRACKED	21	-1308.	-709.	CRACKED
22	-1325.	-219.	CRACKED	23	-1270.	162.	5.05	24	-1281.	-1804.	CRACKED
25	-1281.	4997.	27.58	26	-1259.	-1179.	-247.59	27	-1259.	-26.	-5.36
28	-1175.	-1096.	-230.14	29	-1175.	60.	12.53	30	-1092.	-1013.	-212.70
31	-1092.	143.	30.04	32	-1186.	-1133.	CRACKED	33	-1186.	-56.	CRACKED
34	-1043.	-1019.	CRACKED	35	-1026.	-984.	CRACKED	36	-1096.	-1037.	CRACKED
37	-1100.	-889.	CRACKED	38	-1138.	-603.	CRACKED	39	-1043.	-431.	CRACKED
40	-1026.	-74.	CRACKED	41	-1096.	-267.	CRACKED	42	-1100.	-910.	CRACKED
43	-1100.	-3549.	CRACKED	44	-889.	-874.	CRACKED	45	-889.	-841.	CRACKED
46	-889.	-727.	CRACKED	47	-889.	-412.	CRACKED	48	-889.	-416.	CRACKED
49	-889.	-3188.	CRACKED	50	-889.	-336.	CRACKED	51	-677.	-664.	CRACKED
52	-677.	-634.	CRACKED	53	-677.	-535.	CRACKED	54	-677.	-212.	CRACKED
55	-677.	-313.	CRACKED	56	-677.	-1309.	CRACKED	57	-677.	-6525.	CRACKED
58	-451.	-443.	CRACKED	59	-451.	-414.	CRACKED	60	-451.	-317.	CRACKED
61	-451.	-4.	-.26	62	-451.	-1245.	CRACKED	63	-451.	-1129.	CRACKED
64	-451.	-939.	CRACKED	65	-209.	-223.	CRACKED	66	-209.	-195.	CRACKED
67	-209.	-99.	CRACKED	68	-209.	175.	6.00	69	-209.	-371.	CRACKED
70	-209.	2696.	34.85	71	-209.	312.	.00	72	17.	11.	.00
73	17.	39.	.00	74	17.	113.	1.99	75	17.	314.	9.89
76	17.	315.	6.34	77	17.	-474.	CRACKED	78	17.	-2270.	CRACKED
79	228.	321.	7.85	80	228.	362.	9.43	81	228.	410.	11.29
82	228.	384.	10.28	83	228.	183.	.00	84	228.	-1082.	CRACKED
85	228.	-3379.	CRACKED	86	515.	325.	3.12	87	383.	540.	14.40
88	366.	517.	13.77	89	436.	482.	11.21	90	440.	419.	8.26
91	477.	550.	13.73	92	383.	-51.	CRACKED	93	366.	357.	5.54
94	436.	82.	.00	95	440.	-1816.	CRACKED	96	440.	-2761.	CRACKED
97	432.	1703.	357.60	98	432.	2613.	403.60	99	515.	1828.	383.83
100	515.	2729.	403.58	101	598.	1965.	412.48	102	598.	2854.	403.29
103	525.	388.	5.34	104	525.	-1.	CRACKED	105	647.	542.	7.85
106	665.	413.	3.47	107	610.	-8.	CRACKED	108	621.	137.	.00
109	602.	158.	.00	110	647.	-2061.	CRACKED	111	665.	-377.	CRACKED
112	610.	-433.	CRACKED	113	621.	-3740.	CRACKED	114	621.	249.	.00
115	742.	-1408.	CRACKED	116	742.	-1541.	CRACKED	117	742.	-1593.	CRACKED
118	742.	-2256.	CRACKED	119	742.	-3631.	CRACKED	120	742.	700.	5.61
121	742.	5879.	16.39	122	832.	-3513.	CRACKED	123	832.	-3064.	CRACKED
124	832.	-4073.	CRACKED	125	832.	-3265.	CRACKED	126	832.	4644.	18.78
127	832.	9843.	4.42	128	832.	4818.	.00				

. . . . DIVISION POINT 5 . . . .

ELEMENTAL STRESSES AND STRAINS

ELEM	TOTAL STRAIN	STRESS STRAIN	STRESS	ELEM	TOTAL STRAIN	STRESS STRAIN	STRESS	ELEM	TOTAL STRAIN	STRESS STRAIN	STRESS
1	-327.	-347.	CRACKED	2	-327.	-318.	CRACKED	3	-327.	-228.	CRACKED
4	-327.	-77.	CRACKED	5	-327.	131.	1.89	6	-327.	-1200.	CRACKED
7	-327.	-1750.	CRACKED	8	-336.	-353.	CRACKED	9	-336.	-322.	CRACKED
10	-336.	-216.	CRACKED	11	-336.	-53.	CRACKED	12	-336.	146.	1.86
13	-336.	-1068.	CRACKED	14	-336.	-131.	CRACKED	15	-358.	-370.	CRACKED
16	-345.	-355.	CRACKED	17	-344.	-336.	CRACKED	18	-349.	-324.	CRACKED
19	-348.	-189.	CRACKED	20	-350.	-40.	CRACKED	21	-345.	0.	-.77
22	-344.	330.	11.05	23	-349.	158.	2.98	24	-348.	-661.	CRACKED
25	-348.	-5420.	CRACKED	26	-350.	-271.	-56.82	27	-350.	883.	185.41
28	-358.	-279.	-58.52	29	-358.	877.	184.15	30	-366.	-287.	-60.21
31	-366.	869.	182.52	32	-357.	-337.	CRACKED	33	-357.	-59.	CRACKED
34	-371.	-379.	CRACKED	35	-373.	-364.	CRACKED	36	-366.	-339.	CRACKED
37	-365.	-193.	CRACKED	38	-362.	5.	-.30	39	-371.	1.	-.59
40	-373.	194.	6.59	41	-366.	974.	23.51	42	-365.	14.	.00
43	-365.	-3836.	CRACKED	44	-386.	-402.	CRACKED	45	-386.	-371.	CRACKED
46	-386.	-262.	CRACKED	47	-386.	-18.	CRACKED	48	-386.	-1247.	CRACKED
49	-386.	-1981.	CRACKED	50	-386.	-1806.	CRACKED	51	-407.	-424.	CRACKED
52	-407.	-394.	CRACKED	53	-407.	-298.	CRACKED	54	-407.	-61.	CRACKED
55	-407.	952.	23.60	56	-407.	-2210.	CRACKED	57	-407.	206.	.00
58	-429.	-445.	CRACKED	59	-429.	-415.	CRACKED	60	-429.	-319.	CRACKED
61	-429.	-67.	CRACKED	62	-429.	-1231.	CRACKED	63	-429.	-2988.	CRACKED
64	-429.	-958.	CRACKED	65	-452.	-457.	CRACKED	66	-452.	-429.	CRACKED
67	-452.	-330.	CRACKED	68	-452.	-68.	CRACKED	69	-452.	-913.	CRACKED
70	-452.	-3588.	CRACKED	71	-452.	114.	.00	72	-474.	-441.	CRACKED
73	-474.	-409.	CRACKED	74	-474.	-313.	CRACKED	75	-474.	-49.	CRACKED
76	-474.	-648.	CRACKED	77	-474.	-4641.	CRACKED	78	-474.	-1802.	CRACKED
79	-495.	-325.	CRACKED	80	-495.	-257.	CRACKED	81	-495.	-165.	CRACKED
82	-495.	19.	.35	83	-495.	-271.	CRACKED	84	-495.	2606.	34.48
85	-495.	-1934.	CRACKED	86	-522.	-140.	CRACKED	87	-510.	13.	.05
88	-508.	23.	.46	89	-515.	15.	.20	90	-515.	-7.	-.79
91	-519.	-484.	CRACKED	92	-510.	-392.	CRACKED	93	-508.	69.	.86
94	-515.	-1210.	CRACKED	95	-515.	76.	.00	96	-515.	-2390.	CRACKED
97	-514.	757.	158.87	98	-514.	1667.	349.18	99	-522.	790.	165.99
100	-522.	1691.	354.20	101	-531.	836.	175.53	102	-531.	1725.	361.31
103	-523.	-51.	CRACKED	104	-523.	-434.	CRACKED	105	-535.	96.	1.91
106	-537.	-29.	CRACKED	107	-532.	-569.	CRACKED	108	-533.	-143.	CRACKED
109	-531.	73.	.79	110	-535.	-1454.	CRACKED	111	-537.	-505.	CRACKED
112	-532.	-535.	CRACKED	113	-533.	-728.	CRACKED	114	-533.	-2485.	CRACKED
115	-544.	119.	.00	116	-544.	-17.	CRACKED	117	-544.	-26.	CRACKED
118	-544.	-123.	CRACKED	119	-544.	-806.	CRACKED	120	-544.	-746.	CRACKED
121	-544.	-1208.	CRACKED	122	-553.	-3205.	CRACKED	123	-553.	-3174.	CRACKED
124	-553.	-3070.	CRACKED	125	-553.	-2969.	CRACKED	126	-553.	-2714.	CRACKED
127	-553.	3570.	18.54	128	-553.	2033.	.00				

. . . . DIVISION POINT 9 . . . .

------------------------ ELEMENTAL STRESSES AND STRAINS ------------------------

ELEM	TOTAL STRAIN	STRESS STRAIN	STRESS	ELEM	TOTAL STRAIN	STRESS STRAIN	STRESS	ELEM	TOTAL STRAIN	STRESS STRAIN	STRESS
1	645.	508.	5.27	2	645.	523.	5.91	3	645.	559.	7.47
4	645.	610.	9.51	5	645.	67.	.00	6	645.	-2179.	CRACKED
7	645.	-208.	CRACKED	8	554.	427.	3.80	9	554.	445.	4.57
10	554.	493.	6.62	11	554.	546.	8.70	12	554.	24.	.00
13	554.	-2347.	CRACKED	14	554.	6474.	20.97	15	328.	230.	-.11
16	460.	348.	2.39	17	478.	374.	3.15	18	423.	337.	2.69
19	434.	415.	5.77	20	415.	446.	7.31	21	460.	476.	7.58
22	478.	-265.	CRACKED	23	423.	27.	.00	24	434.	-1779.	CRACKED
25	434.	1509.	3.78	26	411.	491.	103.08	27	411.	1644.	345.31
28	328.	408.	85.67	29	328.	1564.	328.34	30	246.	325.	68.26
31	246.	1481.	310.99	32	339.	261.	1.08	33	339.	-832.	CRACKED
34	197.	117.	.00	35	179.	118.	.00	36	249.	191.	-.30
37	253.	279.	3.40	38	291.	358.	5.93	39	197.	289.	4.54
40	179.	-140.	CRACKED	41	249.	85.	.00	42	253.	-1180.	CRACKED
43	253.	2631.	28.30	44	42.	-30.	CRACKED	45	42.	2.	.00
46	42.	97.	-.88	47	42.	198.	3.29	48	42.	1463.	29.59
49	42.	-490.	CRACKED	50	42.	-3765.	CRACKED	51	-169.	-218.	CRACKED
52	-169.	-190.	CRACKED	53	-169.	-97.	CRACKED	54	-169.	72.	.72
55	-169.	-883.	CRACKED	56	-169.	-324.	CRACKED	57	-169.	833.	3.33
58	-395.	-415.	CRACKED	59	-395.	-386.	CRACKED	60	-395.	-290.	CRACKED
61	-395.	-46.	CRACKED	62	-395.	60.	.00	63	-395.	-2011.	CRACKED
64	-395.	654.	.40	65	-636.	-617.	CRACKED	66	-636.	-588.	CRACKED
67	-636.	-490.	CRACKED	68	-636.	-166.	CRACKED	69	-636.	-409.	CRACKED
70	-636.	-1409.	CRACKED	71	-636.	-1018.	CRACKED	72	-862.	-797.	CRACKED
73	-862.	-765.	CRACKED	74	-862.	-664.	CRACKED	75	-862.	-336.	CRACKED
76	-862.	-907.	CRACKED	77	-862.	-1312.	CRACKED	78	-862.	-6245.	CRACKED
79	-1072.	-866.	CRACKED	80	-1072.	-802.	CRACKED	81	-1072.	-707.	CRACKED
82	-1072.	-353.	CRACKED	83	-1072.	240.	8.06	84	-1072.	-3472.	CRACKED
85	-1072.	315.	3.38	86	-1359.	-387.	CRACKED	87	-1227.	-669.	CRACKED
88	-1210.	-604.	CRACKED	89	-1280.	-517.	CRACKED	90	-1283.	-481.	CRACKED
91	-1321.	-75.	CRACKED	92	-1227.	-60.	CRACKED	93	-1210.	-276.	CRACKED
94	-1280.	814.	19.66	95	-1283.	-2261.	CRACKED	96	-1283.	-3482.	CRACKED
97	-1276.	-5.	-1.00	98	-1276.	906.	189.35	99	-1359.	-46.	-9.58
100	-1359.	855.	178.67	101	-1442.	-75.	-15.75	102	-1442.	814.	170.09
103	-1369.	-499.	CRACKED	104	-1369.	-677.	CRACKED	105	-1491.	-216.	CRACKED
106	-1508.	-254.	CRACKED	107	-1453.	-193.	CRACKED	108	-1464.	284.	8.38
109	-1445.	317.	9.27	110	-1491.	-542.	CRACKED	111	-1508.	-481.	CRACKED
112	-1453.	-709.	CRACKED	113	-1464.	2404.	33.48	114	-1464.	-6016.	CRACKED
115	-1585.	-2907.	CRACKED	116	-1585.	-612.	CRACKED	117	-1585.	-3269.	CRACKED
118	-1585.	-2281.	CRACKED	119	-1585.	-551.	CRACKED	120	-1585.	-1962.	CRACKED
121	-1585.	-1543.	CRACKED	122	-1675.	-532.	CRACKED	123	-1675.	-881.	CRACKED
124	-1675.	-755.	CRACKED	125	-1675.	-1297.	CRACKED	126	-1675.	-6787.	CRACKED
127	-1675.	-2953.	CRACKED	128	-1675.	-385.	CRACKED				

End of sample computer output

In designing the fire exposed columns for the previous systems only minimum steel was required so 4 32 mm diameter bars were placed at the corners of the column. The steel nearest to the fire, which represented half the reinforcement, will be exposed to heating from two sides of the column (see Figure 12.4) and will therefore rapidly lose its strength. The columns have to resist a moment during the fire exposure, however, the design Code of Practice (CP110) for the fire situation is based on fire tests for columns with axial load only. It is therefore noted that care should be taken when detailing columns for minimum reinforcement when subject to a moment and likely to be exposed to fire, or perhaps more seriously CP110 in its present form should not be applied to moment carrying columns with only minimum reinforcement and subject to possible fire exposure. A similar comment applies to BS8110.

It is most likely that the fire resistance of the columns with minimum reinforcement could be increased if a greater number of steel bars with an equivalent area to 4 32 mm diameter bars (for example 8 25 mm diameter bars) were employed. In this way while two of the steel bars would still be exposed to heating from two sides, the majority of the steel area would retain its strength for a longer period of time. This is the case with the column cross sections for the other structural systems analysed where more than four steel bars were employed in each case.

At no time during any of the computer simulations did the rate of deflection exceed the allowable value of $L^2/15b$, neither did any plastic hinges form in the restraint system members.

However, in some preliminary runs, problems were encountered with the upper limit for the iteration to find the neutral axis depth at midspan in the top restraint beam, since it was most likely that the strength of the tension reinforcement was reducing to near zero and that a plastic hinge of zero resistance moment was imminent.

The aim of test series 1 was to determine the effect of varying the number of floors above, or axial restraint, on the fire performance of the exposed column. The fire exposed column was 6 m in length and was slender.

Figure 12.5 shows the variation of end slope with the time of exposure for test series 1, and the variation of column end moments with time is illustrated in Figure 12.6. The trends for variation of end slope are very similar in each case. With the increased height of the structure the magnitude of variation in end slope appears to increase which is expected due to the higher axial load.

A significant observation is that the curves for the endslopes at column ends A and B cross each other at roughly the same point in time for each test case. Referring to figure 12.6 this cross over point corresponds to the time at which the value of end moments for ends A and B change sign and also cross each other. The plot for end moments in Figure 12.6 also shows some further interesting traits and are very similar in each case. Variation of column end moment at end B follows the same unload line and reversal of moment. The magnitude of this moment with a change in sign increases with the number of floors above, and the maximum value attained in each case occurs at the same point in time.

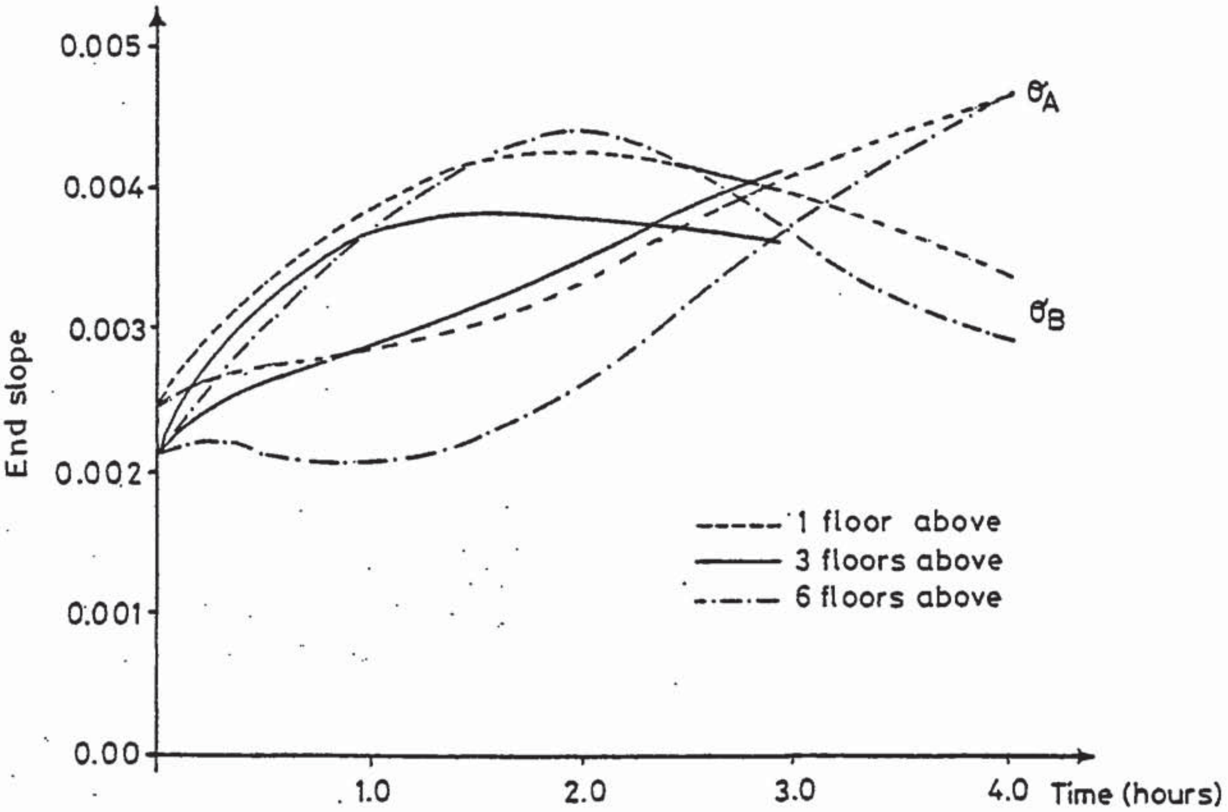

Figure 12.5 Variation of column end slope with time for test series 1.

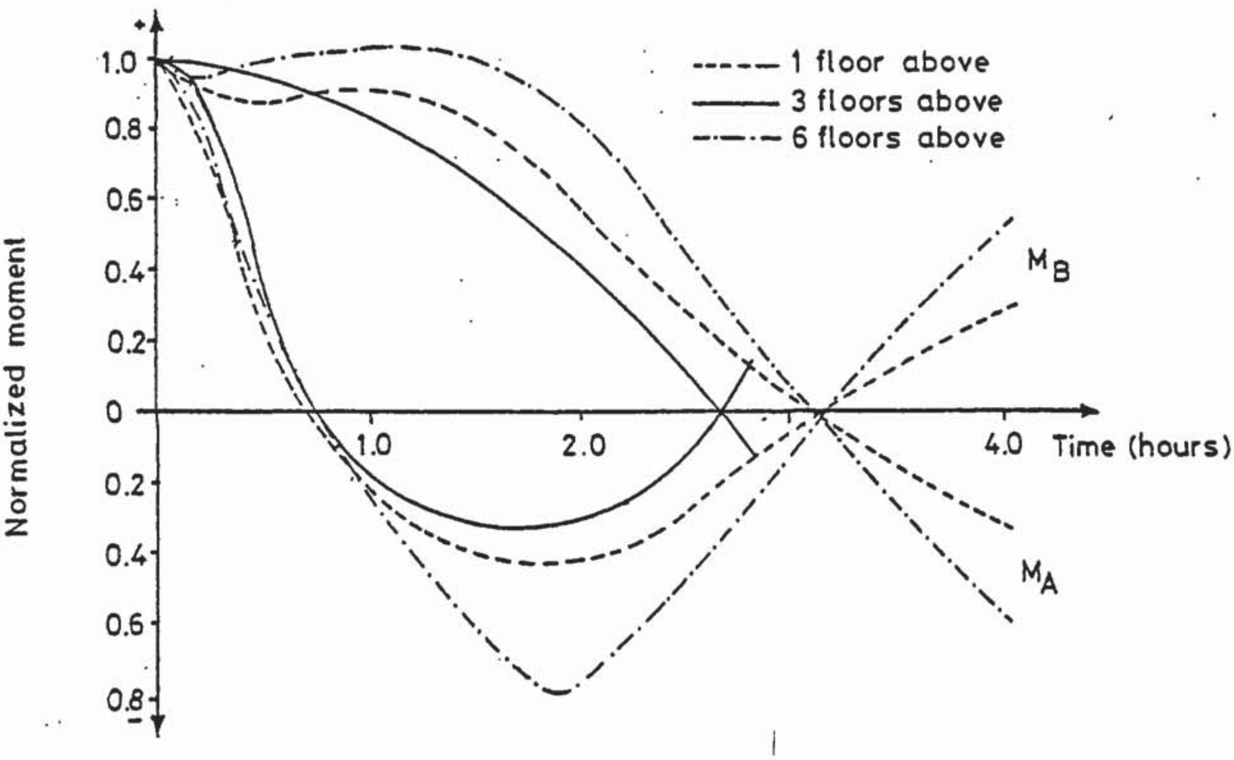

Figure 12.6 Variation of column end moment with time for test series 1.

Figure 12.7 shows the axial deformation of the fire exposed column plotted against time for test series 1. As can be seen from the Figure an expansion occurs in each test. The maximum expansion and rate of increase in expansion decrease with the number of floors above. This result is to be expected due to the increased stiffness and axial load acting on the column with an increase in floors above. In each case the maximum expansion occurs at the same time of 2 hours.

The lateral deflection responses for the columns in test series 1 exhibited no significant differences. The number of floors above, or the stiffness of the structure above, the fire exposed column appeared not to influence the deflection response. A typical deflection response, in this case the deflection profiles for the column with 6 floors above, is shown in Figure 12.8. Deflection profiles are plotted for the time periods 0.0, 0.5, 1.0, 2.0, 3.0 and 4.0 hours.

Referring to Figure 12.8 it can be seen that initially, at time zero, the column is bent into symmetrical double curvature. For exposure up to 2.0 hours the deflections (away from the fire) for the upper half of the column decrease in value, while the deflections for the lower half of the column (towards the fire) increase in value. After 2.0 hours a reversal in the behaviour occurs where the deflections for the upper half increase away from the fire and the deflections, towards the fire, for the lower half decrease.

Throughout the duration of the computer simulations for test series 1 the axial load remained sensibly constant for each test case.

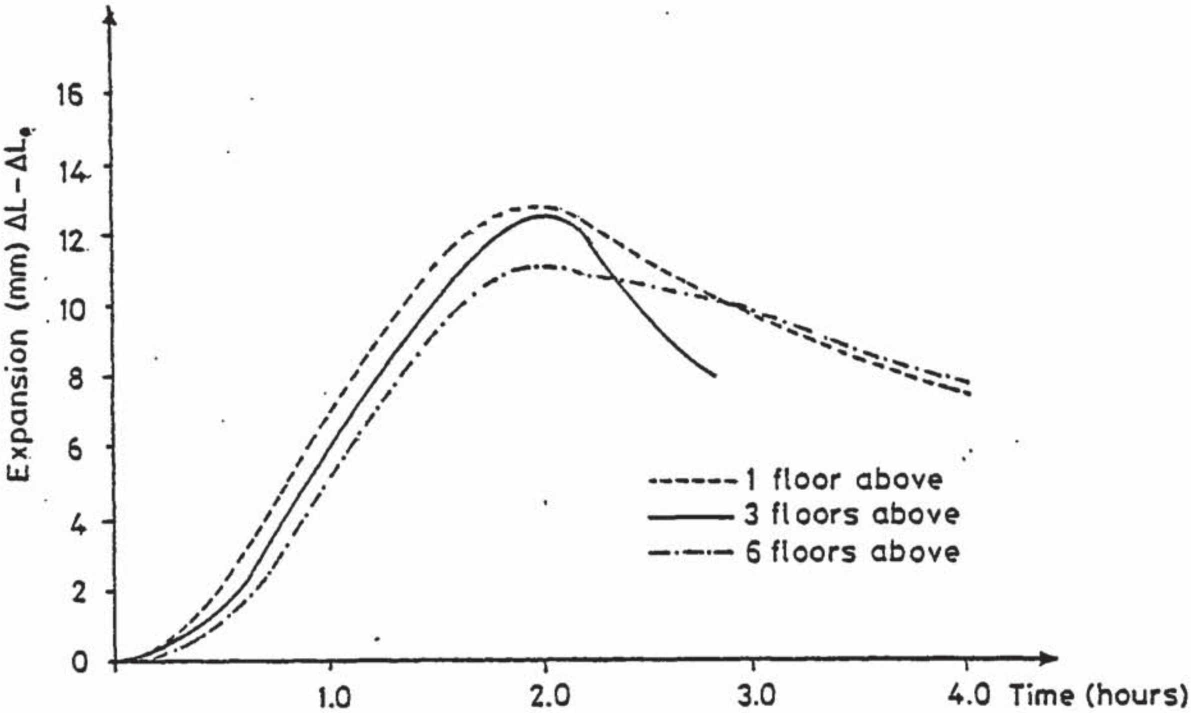

Figure 12.7 Expansion of column plotted against time for test series 1.

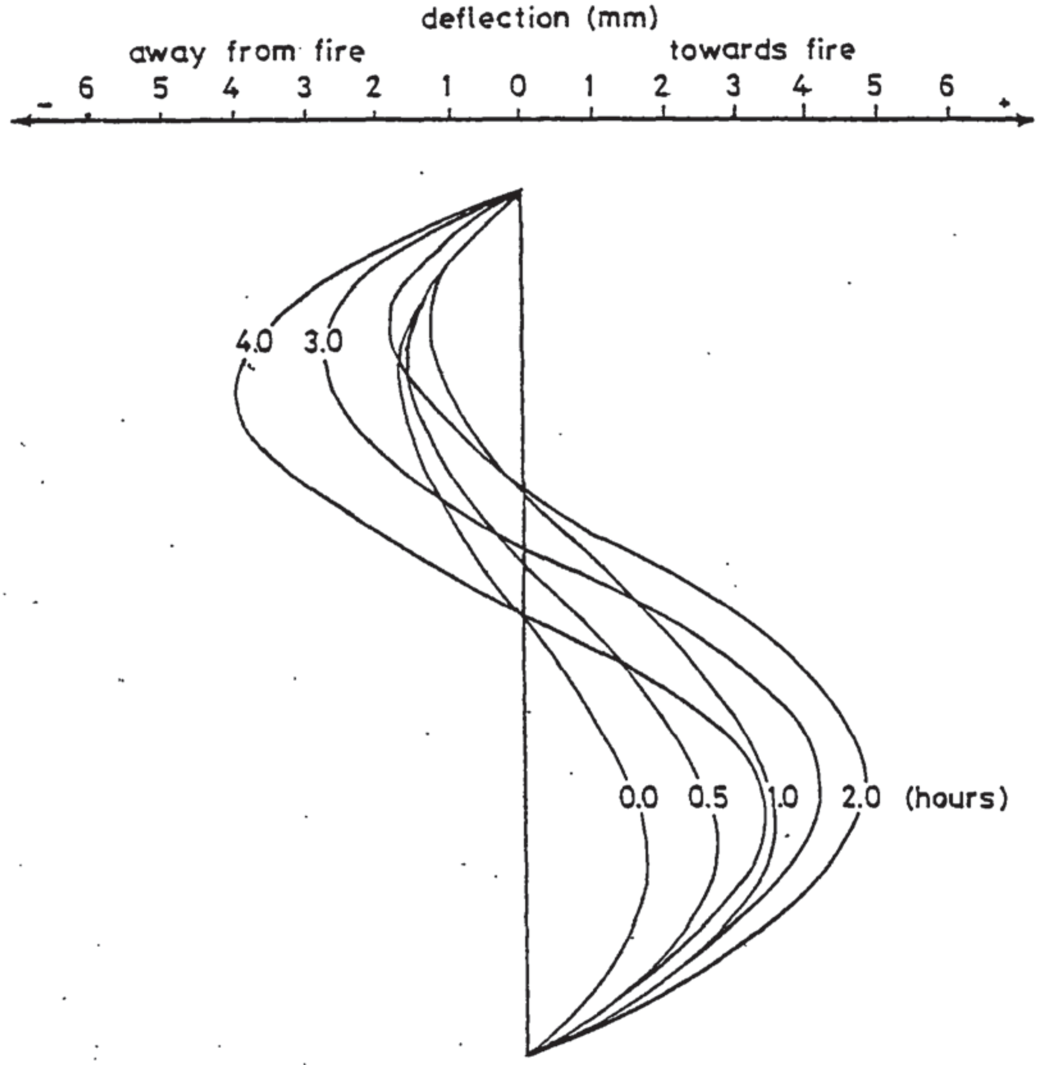

Figure 12.8 Deflected profile for typical column from test series 1 at various times during expose to fire.

The aim of test series 2 was to determine the effect, if any, on the fire performance of a column due to variation in the fire exposed column length. Column lengths of 4 m, 6 m and 8 m were considered. The 4 m column was classed as short, the 6m column classed just slender and the 8 m column slender.

The variation of end slope with time for test series 2 is illustrated in Figure 12.9, and are very similar in each case. The point at which the curves for the slopes at end A and B cross each other are almost coincident for each different column length, and occur at the point at which the curves describing the moments, plotted in Figure 12.10, cross each other and change sign. From consideration of Figure 12.10 it appears that the magnitude of the reversal of moment at end B increases with the height of the column.

Figure 12.11 illustrates the axial deformation of the fire exposed columns for test series 2. The maximum expansion and rate of increase in expansion increase with the length of the column and again the maximum value of expansion is attained at the same point in time of 2 hours.

For test series 2 the deflection response did show a difference in behaviour. The 4 m and 6 m column exhibited a similar response to that reported in test series 1, only the 4 m column showed smaller deflections than the 6 m column. However, the 8 m column did not exhibit the reversal in deflection described in test series 1. The deflection profile of the lower column half continued to increase (towards the fire) with the duration of the computer simulation. The deflection profiles for the 4 m and 6 m column are plotted in Figure 12.12.

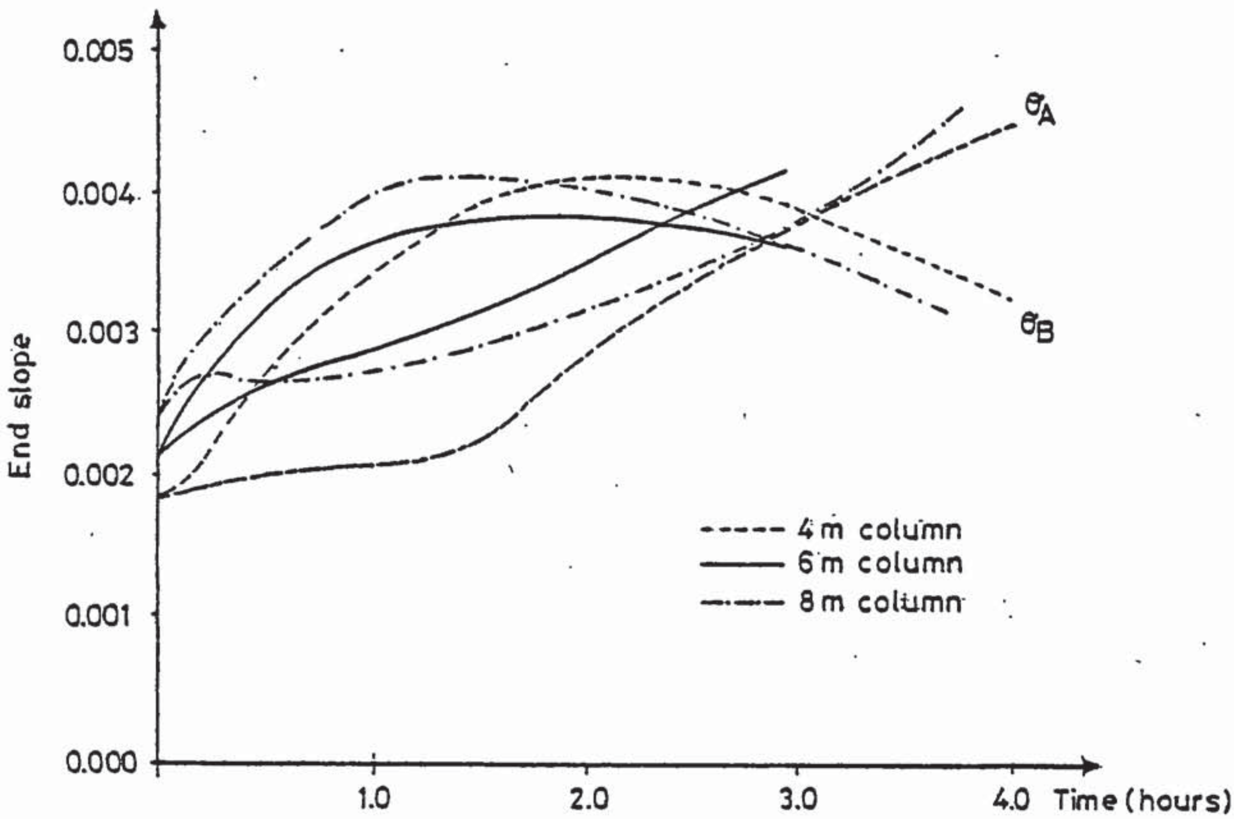

Figure 12.9 Variation of column end slope with time for test series 2.

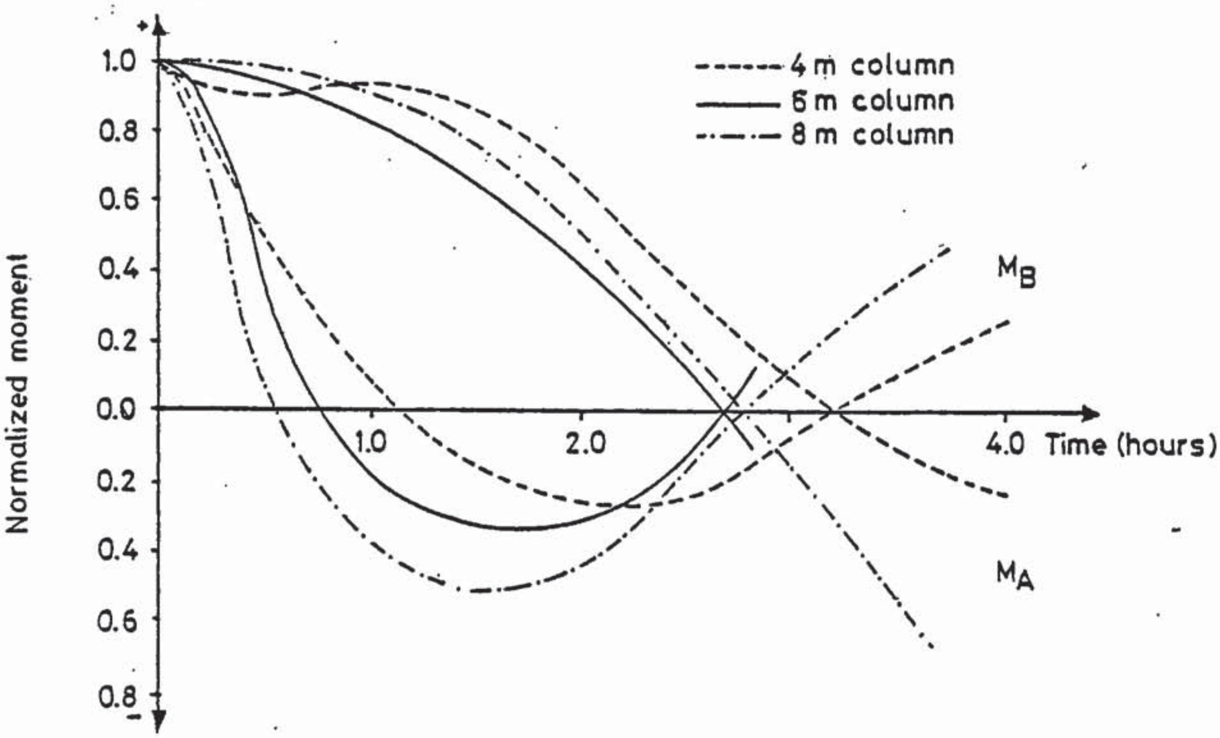

Figure 12.10 Variation of column end moment with time for test series 2.

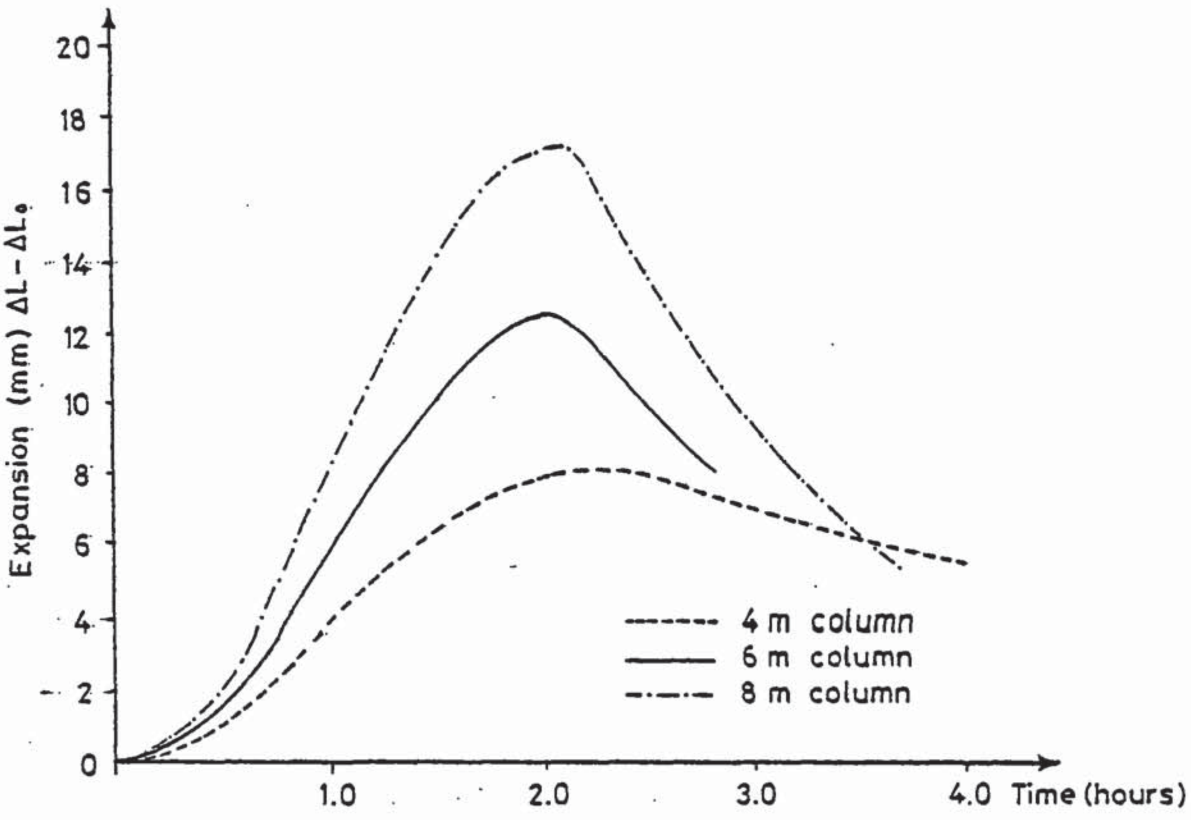

Figure 12.11 Expansion of column plotted against time for test series 2.

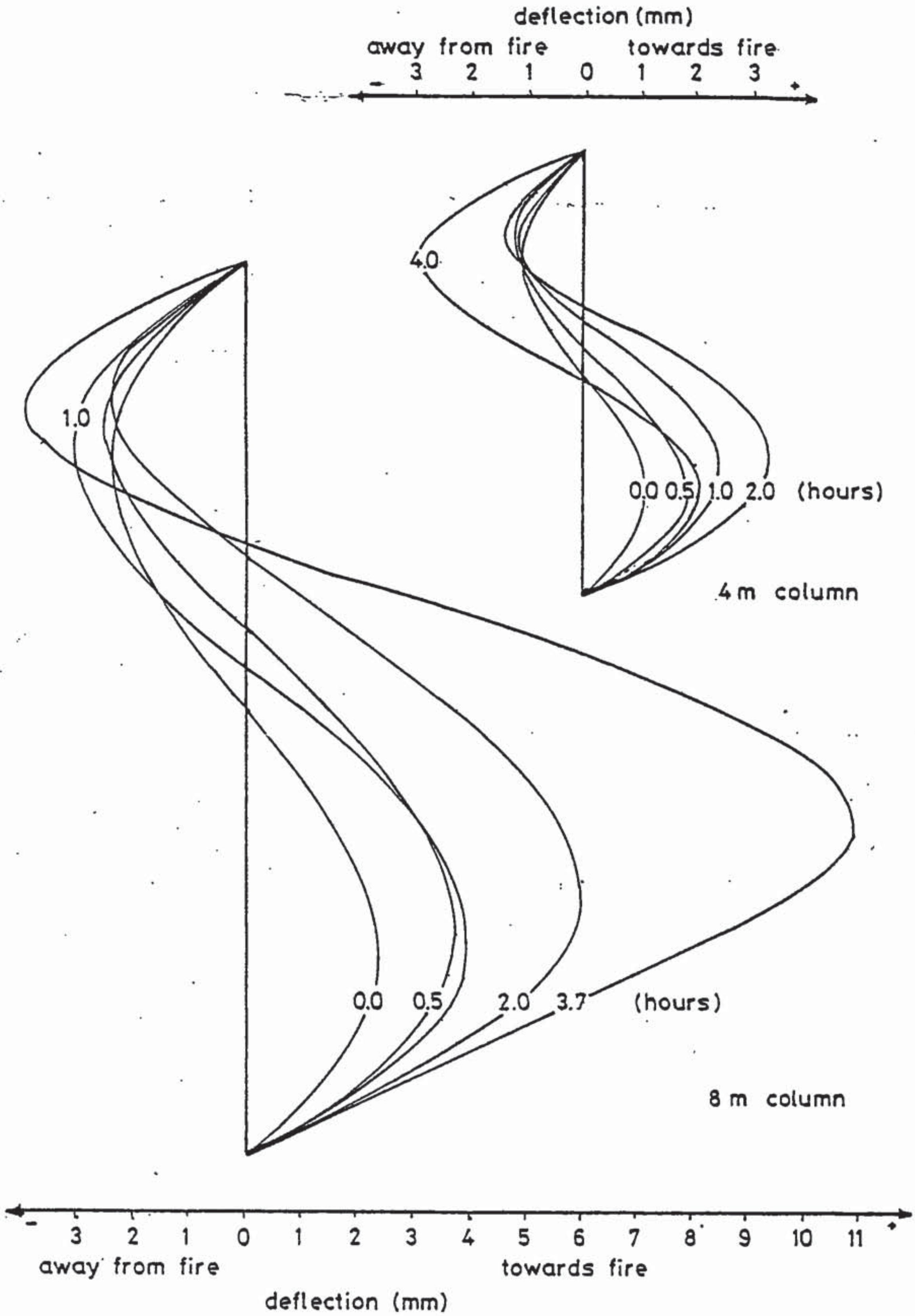

Figure 12.12 Deflection profiles for 8 m column and 4 m column at various times during exposure to fire for test series 2.

Throughout the duration of the computer simulation for test series 2 the axial load remained sensibly constant.

The aim of test series 3 was to determine the effect of adjusting the stiffness of the restraint system by adjusting the length of the restraint beam members. Unfortunately comparison is difficult due to the early failure of the structural systems with the 8 m and 12 m restraint beams.

Adjusting the length of the restraint beam members will markedly effect the rotational restraint afforded to the fire exposed column. This will have the effect of changing the stiffness or flexibility of the restraint system. Despite the early failure of the columns it is apparent from Figure 12.13 that as the restraint beam is shortened, and hence the rotational restraint becomes increasingly stiff relative to the fire exposed column, the rate of reversal of moment at column end B becomes more rapid. This could have contributed to the early failure times since the moment reversal at end B at failure for the 8 m restraint beam test case is of a magnitude greater than the moment at ambient conditions.

Figure 12.14 illustrates the axial deformation experienced by the fire exposed column in test series 3. The figure appears to indicate that axial deformation increases with a shorter restraint beam length. This is probably due to the fact that the moment applied at the ends of the column will decrease with the decrease in restraint beam length since the fixed end moments on these beams will be smaller and the mode of deflection will not be excited as markedly as that corresponding to the longer restraint beam. Hence the expansion will not be counteracted by the lateral deflection of the column.

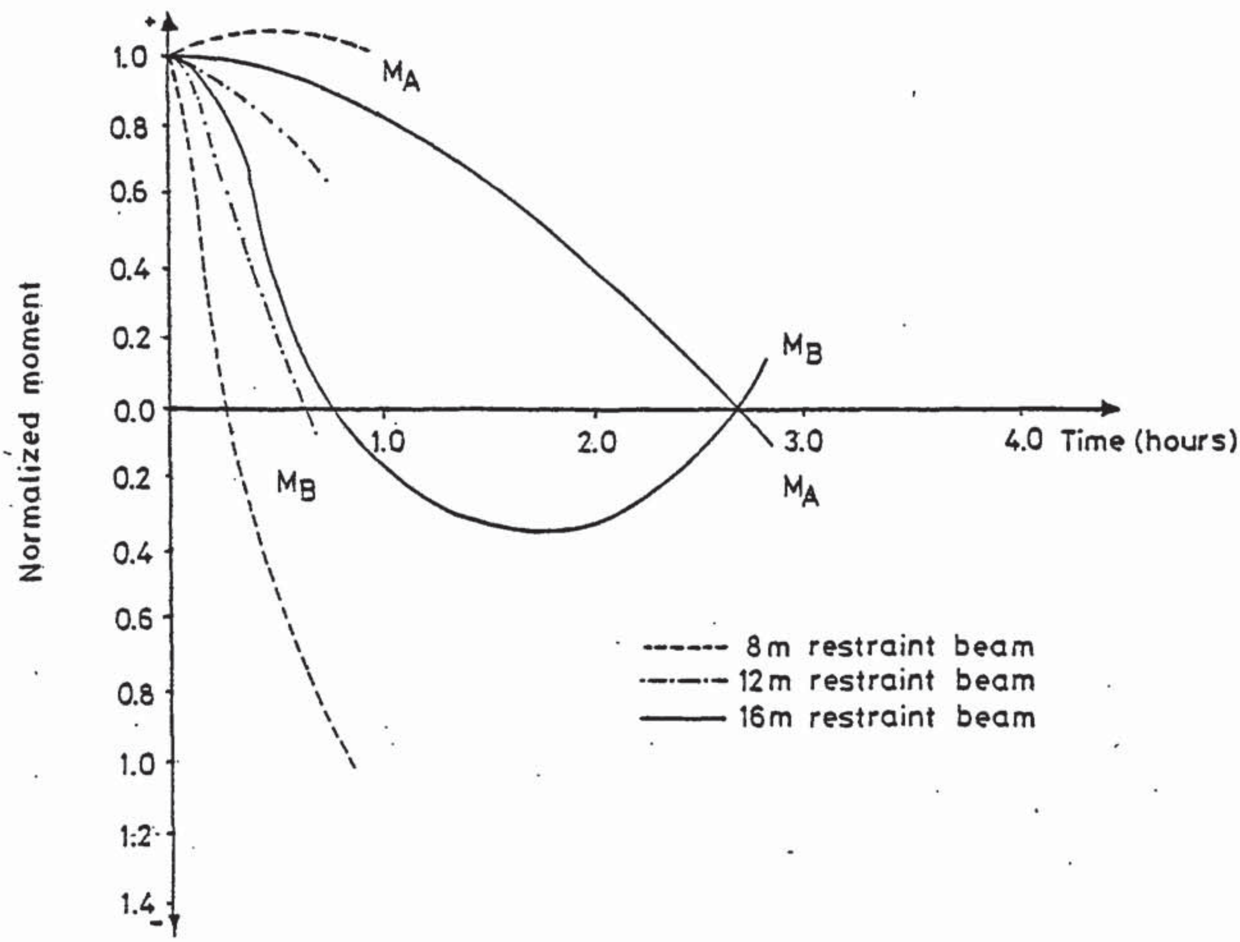

Figure 12.13 Variation of column end moment with time for test series 3.

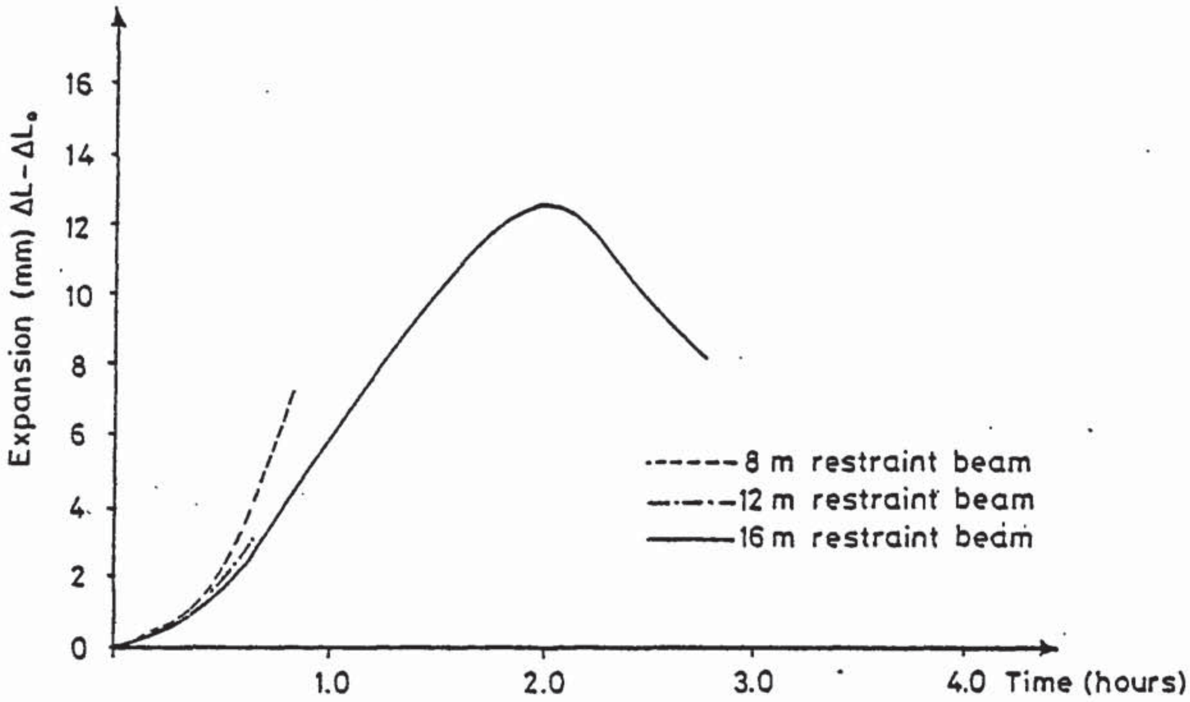

Figure 12.14 Expansion of column plotted against time for test series 3.

The lateral deflection for the test case with 8 m and 16 m restraint beams are plotted in Figure 12.15. As can be seen from the Figure the deflections are less pronounced than those for the previous test series, although the overall trend of behaviour is the same as that described in test series 1.

Test series 3 was the only test series to indicate any variation in magnitude of the axial force with time, athough only very slight. A small increase was recorded with time for the fire exposed column with the 8 m restraint beam. The 8 m restraint beam represented the stiffest restraint out of all the test series, and hence column expansion is most likely to produce an induced restraining force for this case. The variation of axial force for test series 3 is shown in Figure 12.16. It can be seen that the induced restraint force increases the axial load on the column with the increased stiffness of the restraint beam, or decrease in restraint beam length.

It should be pointed out that overdesign, for example it being not possible to place exactly the required amount of reinforcement, will effect the results. This could explain the anomalies in the results where a short and slender column lasts longer than an intermediate column (test series 2) and where columns supporting 1 floor above and 6 floors above last longer than the column supporting 3 floors above (test series 1).

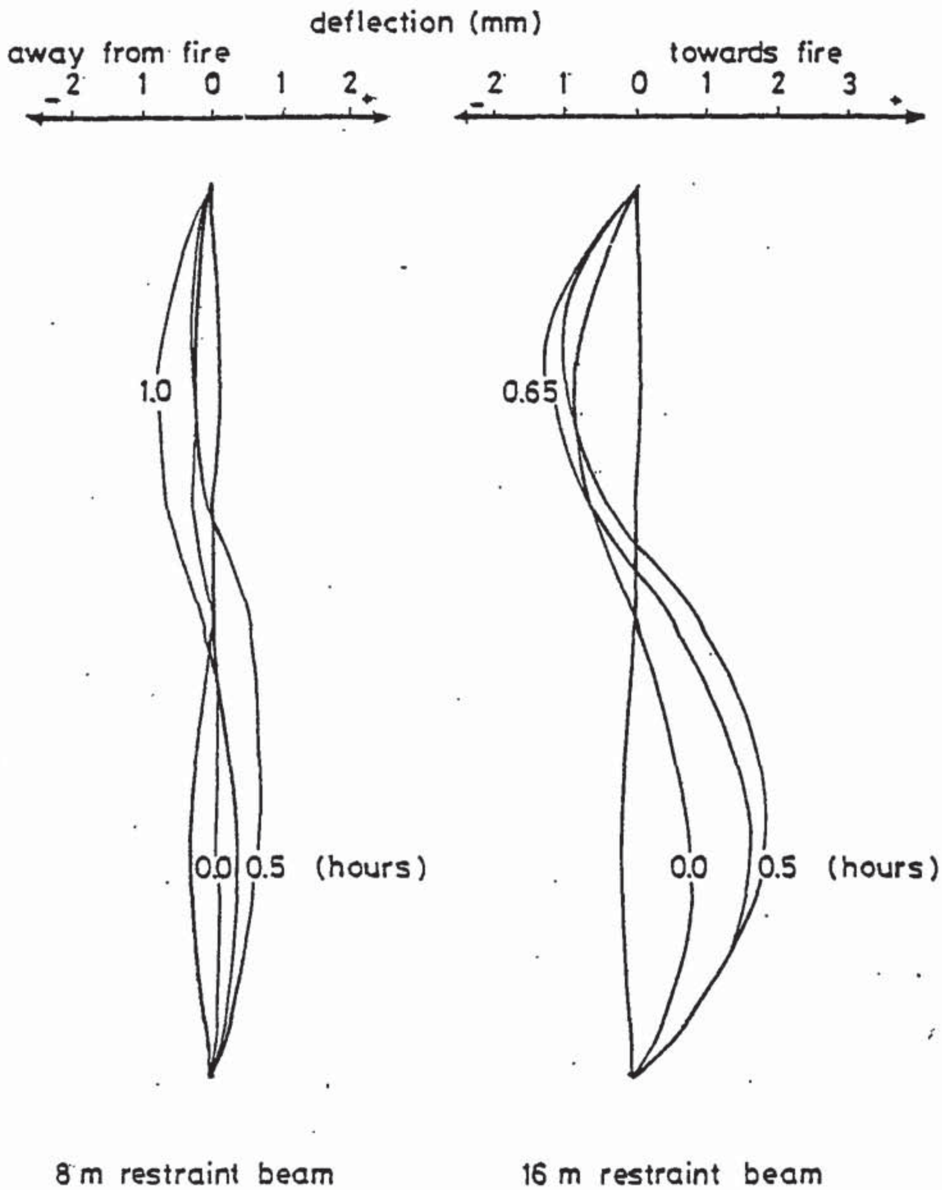

Figure 12.15 Deflection profiles for test series 3 at various times during exposure to fire.

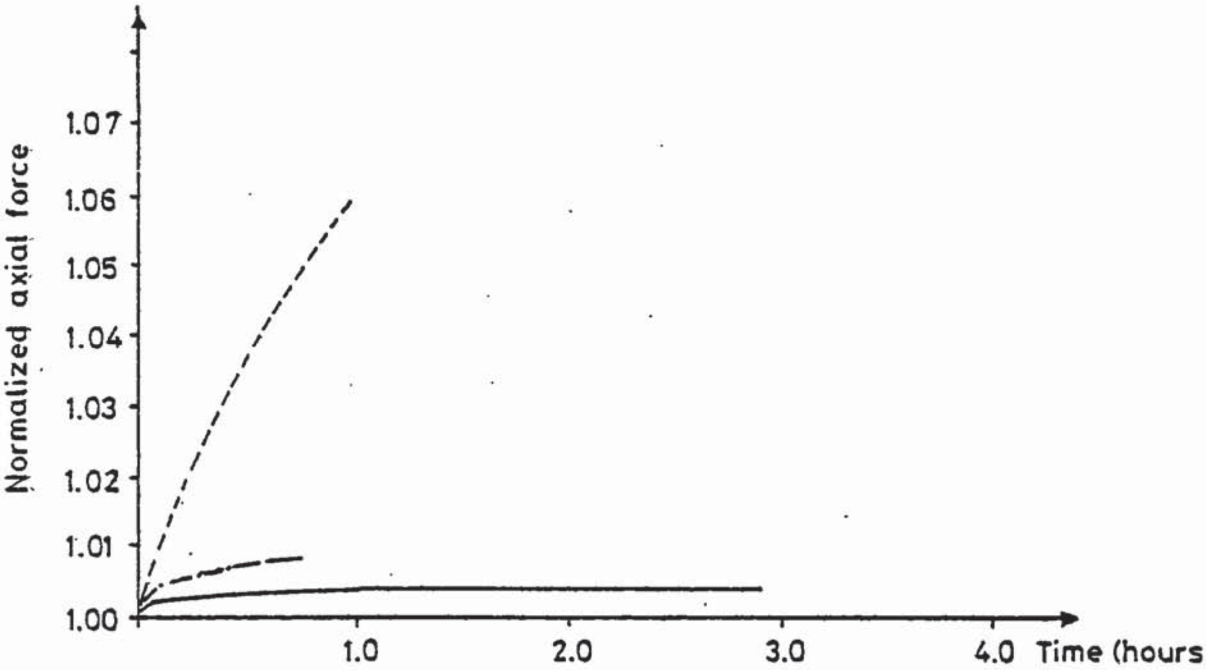

Figure 12.16 Variation of axial force with time for test series 3.

The intention of the computer simulations reported in this chapter was to demonstrate the application of the structural response program SAFE-RCC to some structural systems. It would be necessary to perform a large number of runs to gain any complete insight into the overall effect of altering the structural restraint and relative column stiffness, but such results as have been presented seem to indicate that the effects of restraint and stiffness may well be inter-related. The results described previously have shown that SAFE-RCC is capable of sensibly predicting the behaviour for a column that is part of a total structure.

CHAPTER 13

CONCLUSIONS

Computer simulation can offer a number of advantages in the study of structural response to fire. Models can be used which take into account the interaction between the structural elements exposed to fire together with the effect of the fire on the elements individually, thus allowing for the effects of restraint and continuity.

It is possible to model fire exposure more realistically by accounting for the amount and type of combustibles (or fire load), ventilation, and containment, than by specifying an arbitrary temperature-time curve such as the standard fire (BS476). In addition to evaluating deflections, and capacity to support design loads, it is possible to calculate local stresses, internal cracking in concrete or yielding in steel reinforcement, together with the redistribution of internal forces during the fire exposure. Probably the only way to assess structural performance in a fire is by computational methods since fire tests will be extremely difficult and costly to carry out.

However, there are limitations and uncertainties in the use of such techniques, the most important concerning the assumed behaviour of the constituent materials - steel and concrete. Much work still needs to be done in determining material properties for both concrete and steel at elevated temperatures in a form which is readily usable in analysis.

In order to determine thermal strain, stress related strain, creep strain and transient strain, a series of different testing regimes are required. However, currently, there is no standardization of test method. Therefore it is most important to take care in comparing test data from different sources. Purkiss (1986) discusses these points in some detail.

The recently published RILEM reports (Schneider (1985) and Anderberg (1985)) on material behaviour at elevated temperatures appear to consolidate the current position.

The aim behind the study of the mechanical properties of a material is to establish a constitutive law that governs the behaviour of the material. At present the only computer orientated constitutive model available for concrete is that developed by Anderberg and Thelandersson (1976), the limitations and uncertainties of which have been previously described.

The analytical method reported in this thesis has been shown to simulate well the structural response of columns exposed to the standard test condition, and has been further demonstrated to sensibly predict the behaviour experienced by a column that is part of a total structure.

Computer simulation using SAFE-RCC could be used to determine the fire response of a complete test series of columns that are part of a total structure. The fire performance of slender columns could be compared with that for short and intermediate columns. The importance of the relative stiffness of the adjoining members at the column ends could be investigated, as well as the importance of the height of the structure, or the stiffness of the structure, above. This type of study would allow the comparison of the fire performance of columns that are part of flexible or stiff structures.

The computer program SAFE-RCC also lends itself ideally to an extensive parameter study which could be carried out at a reasonable cost. The importance of various material parameters could be fully determined, for example the importance of the thermal expansion and transient strain, the importance of the values of Young's Modulus for concrete and steel, the values of concrete peak stress and peak strain or the yield strength of the reinforcing steel, to name but a few. The program could also be used to determine the importance of computational parameters such as the magnitudes of the values of incompatabilities on the convergence of the structural solution, or the importance of geometrical effects such as second order effects.

Future modifications to SAFE-RCC include the alteration of the program to store only the current section temperature profiles in the central memory of the computer instead of the section temperature profiles for each time step. This would allow an increase in the number of elements into which the column section and the restraint beam sections can currently be discretized, and also allow for the provision of a larger number of column division points if required.

It is also possible that when a better understanding is available on the effect of moisture (or moisture transport) on the material properties of concrete, the current mode in which the thermal analysis and the structural analysis are completely decoupled may no longer be appropriate and that provision may have to be made for the two analyses to be run in harness with interactive feed-back on each time step of, say, local moisture content.

Alternatively the thermal response and structural response could be no longer uncoupled as they are at present but contained in a single computer program, although this major modification would require much further storage. This would allow account to be taken of the breakdown of the finite element mesh common to the thermal and structural analysis due to the phenomenon of spalling once the mechanism of this phenomenon is completely understood, which is not currently the case.

In its present form the structural response program SAFE-RCC is still a research tool. It is important to establish a series of results that may give the structural engineer some better feel for the behaviour of complete structures or substructures in a fire environment since it will neither be possible nor realistic to expect the engineer in routine design work to have access to a computer program such as SAFE-RCC. Only in the case of non-routine structural design will it be necessary to employ the techniques described in this thesis. Thus it should be possible using the type of program described in this thesis to produce guidelines for the structural engineer to enable a better understanding to be obtained and thus enable more realistic design procedures to be adopted on reinforced concrete columns in fires.

APPENDIX A

INSTRUCTIONS FOR THE USE OF SAFE-RCC

SAFE-RCC is a non-linear structural analysis that has been developed as an analytical tool to study the fire response of reinforced concrete columns that are subject to restraint and continuity likely to be experienced in a total structure. The structural system is shown in Figure A.1. SAFE-RCC is also capable of modelling columns with pinned or fixed rotational restraint and free axial expansion or fixed axial restraint.

The reinforced concrete column to be analysed is idealized through a substructuring process into segments and the segment division point cross sections are modelled through further discretization into subslices. SAFE-RCC includes the option of the restraint beam members being exposed to, or not being exposed to, the fire environment. If the option for the fire exposed restraint beam members is included then their cross sections are also discretized into subslices. The geometric idealization is shown in Figure A.2.

Prior to running SAFE-RCC the modified version of FIRES-T, listed in Appendix L, must be used to produce the thermal histories of the structural cross sections of the structural system. For the user instructions for FIRES-T refer to the user manual in FIRES-T (Becker, Bizri and Bresler (1974)) and Section 4.8 in this thesis. As well as producing the thermal histories of the structural cross sections in a format compatable with SAFE-RCC, the modified version of FIRES-T also produces details of the finite element mesh in a format compatable with SAFE-RCC.

The structured input data for SAFE-RCC is now described in detail.

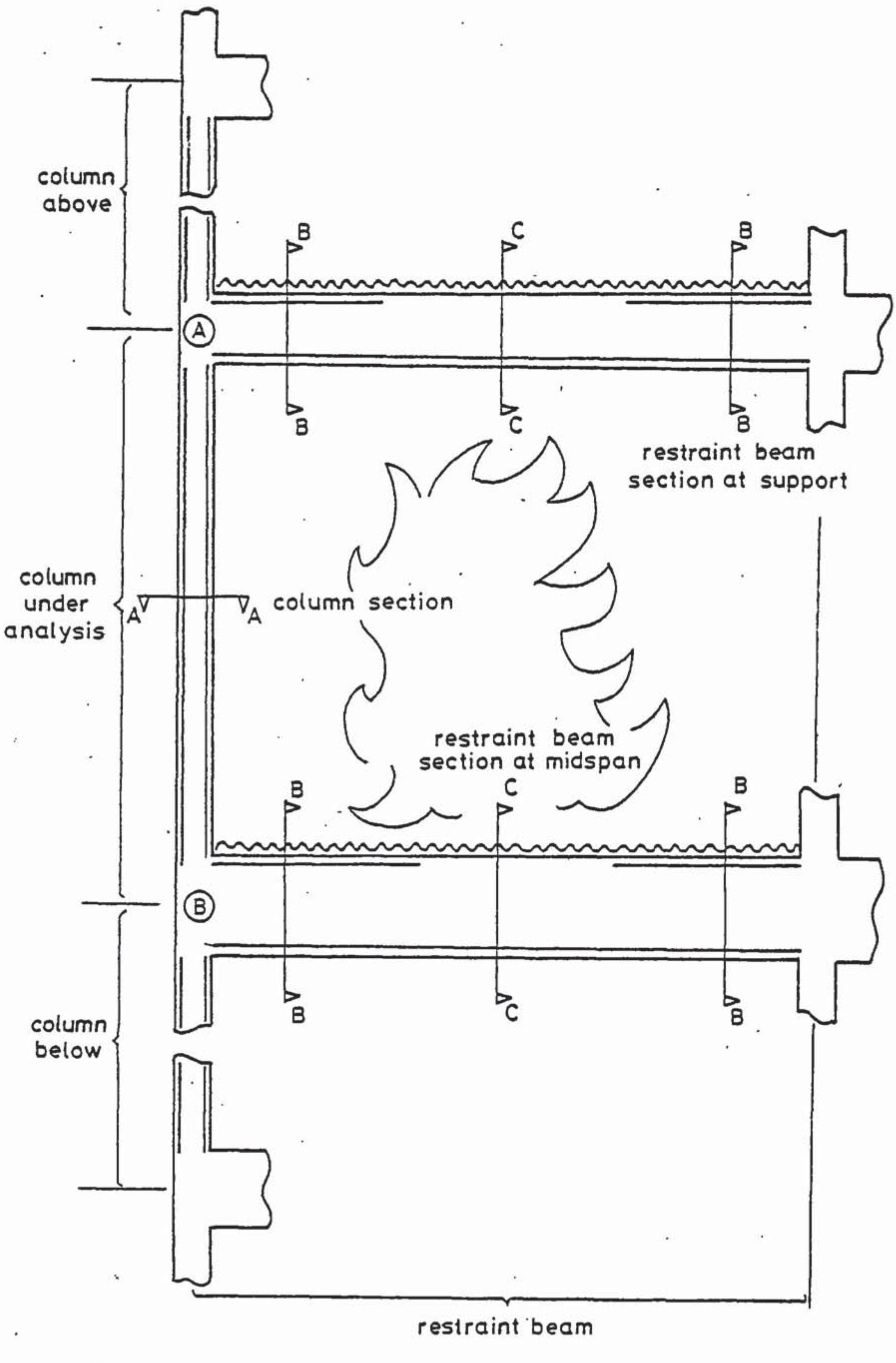

Figure A.1 Structural system.

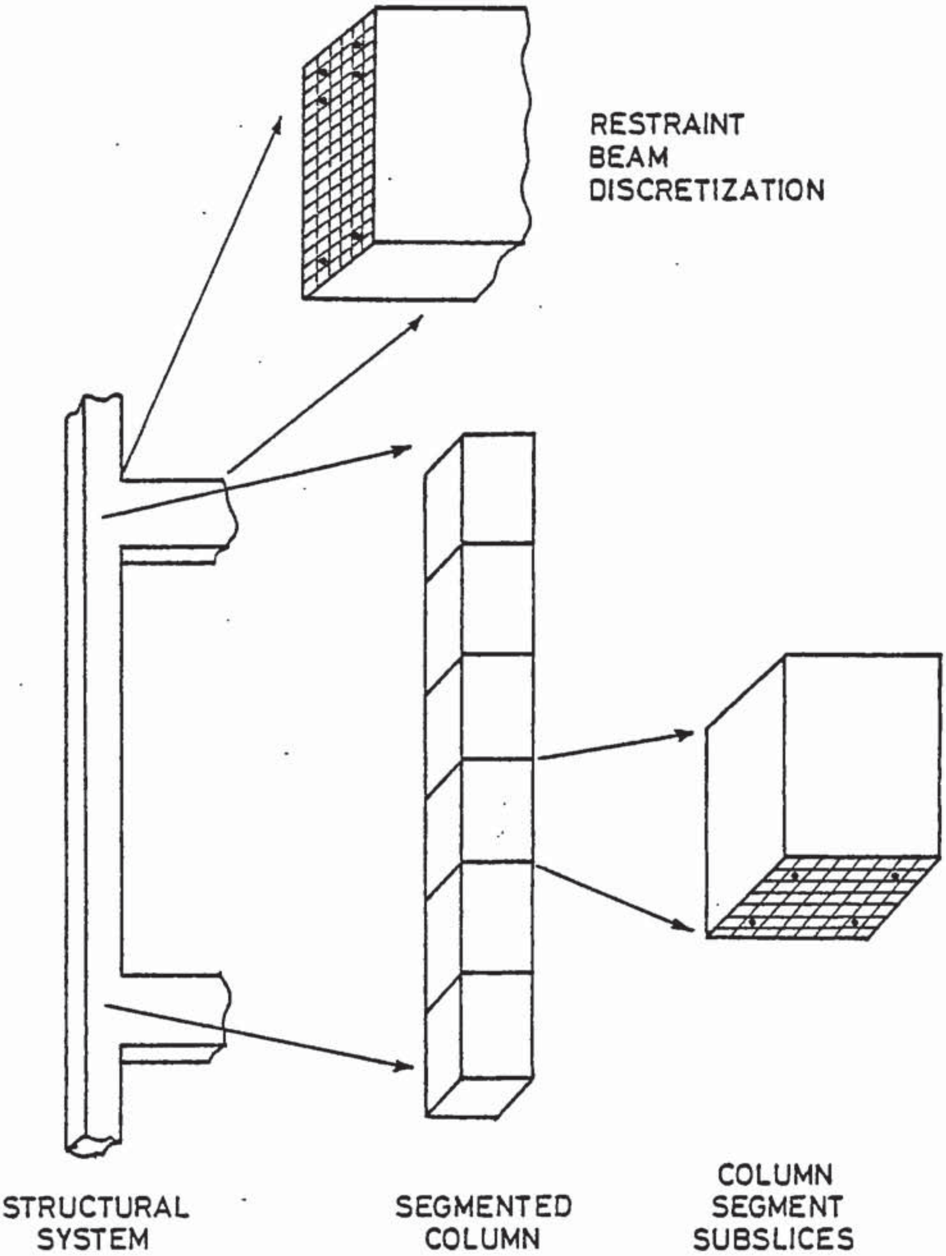

Figure A.2 Geometric idealization of structural system.

INPUT INSTRUCTIONS

Units of the data input are assumed to be metres (m), kilo Newtons (kN), hours (h) and degrees Centigrade (^{o}C) unless otherwise stated.

(01) TITLE CARD

(80A1)

The first line of data is to contain an appropriate title which will be used in the labelling of output.

(02) DEBUG OPTION

(I4)

The debug option facilitates the tracing of errors, for example due to the incorrect entry of data, in the form of producing additional printed output. If the debug option is selected there is two levels of 'debug':

0 - no debug option,

1 - input file is listed in full,

2 - input file is listed in full, interim output is printed showing the solution path of the analysis for each time step, and values of the fire strain components are printed for each time step.

(03) NUMBER OF SEGMENT LENGTHS

(I4)

SAFE-RCC is dimensioned for a maximum of 20 division points, therefore a maximum of 19 column segments can be employed.

(04) NUMBER OF ELEMENTS OF COLUMN CROSS SECTION

(I4)

The maximum number of column division point cross section elements that can be employed is 150. Due to the symmetry of the analysis only half of the column section is discretized, and therefore 150 elements corresponds to 300 elements for the whole cross section.

(05) NUMBER OF ELEMENTS OF RESTRAINT SYSTEM BEAM CROSS SECTION AT MIDSPAN

(I4)

A maximum of 100 elements can be employed for the restraint beam cross section at support. If the column restraint system is not exposed to fire enter zero.

(06) NUMBER OF ELEMENTS OF RESTRAINT SYSTEM BEAM CROSS SECTION AT SUPPORT

(I4)

A maximum of 100 elements can be employed for the restraint beam cross section at midspan. If the column restraint system is not exposed to fire enter zero.

(07) NUMBER OF TIME STEPS

(I4)

The number of time steps includes the initial time step, normally at time zero. The maximum number of time steps is 65.

(08) SECOND ORDER EFFECT OPTION

(I4)

0 - no second order effects

1 - second order effects included

(09) SHRINKAGE MODEL OPTION

(I4)

0 - shrinkage model not included

1 - shrinkage model included

(10) ROTATIONAL RESTRAINT FOR COLUMN END A AND B

(2I2)

0 - pinned rotational restraint

1 - normal rotational restraint

2 - fixed rotational restraint

COLUMNS

1 - 2 option end A

3 - 4 option end B

(11) AXIAL RESTRAINT

(I4)

0 - free axial expansion

1 - normal axial restraint

2 - fixed axial restraint

note: normal axial restraint can only be considered if the normal rotational restraint option is included.

(12) OPTION FOR TEMPERATURE DEPENDENT RESTRAINT SYSTEM END A AND B (2I2)

Temperature dependent restraint system means the column restraint system is also exposed to the fire.

0 - temperature independent restraint system

1 - temperature dependent restraint system

COLUMNS

1 - 2 option column end A

3 - 4 option column end B

(13) COLUMN LENGTH, GUSSET LENGTH END A AND GUSSET LENGTH END B (F6.3,1X,F6.3,1X,F6.3)

COLUMNS

1 - 6 column length

8 - 13 gusset length end A

15 - 20 gusset length end B

(14) COLUMN BREADTH AND COLUMN DEPTH (F6.3,1X,F6.3)

COLUMNS

1 - 6 column breadth

8 - 13 column depth

(15) COVER + HALF BAR DIAMETER AND AREA OF STEEL FOR COLUMN (F6.4,1X,F7.1)

COLUMNS

1 - 6 cover to column reinforcement + half bar diameter (m)

8 - 14 area of steel reinforcement for column (mm^2)

(16) SEGMENT LENGTHS

(I4,3X,F6.3)

Segment lengths are entered in sequential order for segments 1 to the number of segments.

COLUMNS

1 - 4 column segment number

8 - 13 segment length

(17) AXIAL LOAD AND ECCENTRICITY

If the column has pinned rotational restraint at both ends the axial force and eccentricity are entered as follows:

(F7.2,1X,F6.4)

COLUMNS

1 - 7 axial load

9 - 14 axial load eccentricity

If the column is part of a structure then the axial load due to the dead load of the structure above is entered in the format:

(F7.2)

IF THE FIRE EXPOSED COLUMN IS NOT PART OF A TOTAL STRUCTURE THE DATA INPUT (18) TO (23) IS NOT ENTERED. DATA INPUT IS CONTINUED FROM (24). DATA INPUT (18) TO (23) IS ENTERED IF THERE IS NORMAL ROTATIONAL RESTRAINT.

(18) UNIFORMLY DISTRIBUTED LOADS ENDS A AND B

(F6.2,1X,F6.2)

If the fire exposed column is part of a structure then values for the uniformly distributed loads on the restraint beams adjoining column ends A and B are entered.

COLUMNS

1 - 6 uniformly distributed load on restraint beam at end A

8 - 13 uniformly distributed load on restraint beam at end B

(19) LENGTH OF COLUMN ABOVE AND BELOW

(F6.3,1X,F6.3)

The lengths of the column above and below the column under analysis are entered if the fire exposed column is part of a total structure.

COLUMNS

1 - 6 length of column above

8 - 13 length of column below

(20) COVER + HALF BAR DIAMETER AND AREA OF STEEL FOR COLUMN ABOVE AND BELOW COLUMN UNDER ANALYSIS

(F6.4,1X,F7.1,1X,F6.4,1X,F7.1)

If the column is part of a total structure the concrete cover to the steel reinforcement + half the steel bar diameter and the area of steel is entered for the column above and below.

COLUMNS

1 - 6 cover + half bar diameter for column above (m)

8 - 14 area of steel for column above (mm^2)

16 - 21 cover + half bar diameter for column below (m)

23 - 29 area of steel for column below (mm^2)

(21) AREAS OF TENSION STEEL AND COMPRESSION STEEL AT SUPPORT AND MIDSPAN OF RESTRAINT BEAM SECTIONS

(F7.1,1X,F7.1,1X,F7.1,1X,F7.1)

If the fire exposed column is part of a total structure the areas of the tension steel and compression steel at support and midspan of the restraint beam sections are entered. It is assumed that the restraint beams are of the same design at column end A and end B.

COLUMNS

1 - 7	area of tension steel at support (mm^2)
9 - 15	area of compression steel at support (mm^2)
17 - 23	area of tension steel at midspan (mm^2)
25 - 31	area of compression steel at midspan (mm^2)

(22) EFFECTIVE DEPTH, BREADTH, OVERALL DEPTH AND LENGTH OF COLUMN RESTRAINT BEAM AND NUMBER OF FLOORS ABOVE

(F6.3,1X,F6.3,1X,F6.3,1X,F6.3,1X,I2)

If the fire exposed column is part of a total structure the effective depth, breadth, overall depth and length of the restraint beam, and the number of floors above are entered.

COLUMNS

1 - 6	effective depth of restraint beam
8 - 13	breadth of restraint beam
15 - 20	overall depth of restraint beam
22 - 27	length of restraint beam
29 - 30	number of floors above column under analysis

(23) ULTIMATE MOMENT CAPACITIES AT AMBIENT TEMPERATURES FOR COLUMNS AND RESTRAINT BEAMS AT COLUMN END A AND B

(F7.2,1X,F7.2,1X,F7.2,1X,F7.2,1X,F7.2,1X,F7.2)

The ultimate moment capacities at ambient temperature are only entered if the column under analysis is part of a total structure.

COLUMNS

1 - 7	ultimate moment capacity column above
9 - 15	ultimate moment capacity column below
17 - 23	ultimate moment capacity top beam at midspan
25 - 31	ultimate moment capacity top beam at support
33 - 39	ultimate moment capacity bottom beam at midspan
41 - 47	ultimate moment capacity bottom beam at support

(24) PERMISSIBLE NUMBER OF ITERATIONS AND ALLOWABLE INCOMPATABILITIES (I3,1X,5F9.6)

COLUMNS

1 - 2	permissible number of equilibrium iterations
4 - 12	allowable incompatability in axial force
13 - 21	allowable incompatability in bending moment
22 - 30	allowable incompatability in end slope column end A
31 - 39	allowable incompatability in end slope column end B
40 - 48	allowable incompatability in division point deflections

Note: from experience it has been found that a satisfactory permissible number of equilibrium iterations is 20.

(25) INITIAL DIVISION POINT DEFLECTIONS UNDER ZERO LOAD

(I4,3X,F6.4)

Initial division point deflections under zero load are entered in sequential order for division point 1 to the number of division points.

COLUMNS

1 - 4 division point number

8 - 12 division point deflection under zero load

(26) ELEMENTAL CENTROID COORDINATES, ELEMENTAL AREAS AND MATERIAL TYPE OF COLUMN CROSS SECTION

(I4,1X,F7.5,1X,F10.8,1X,I4)

The elemental centroid coordinates, elemental areas and material type represent the details of the finite element mesh and are produced from the modified version of FIRES-T included in this thesis.

The centroid coordinates, areas and material types are entered in sequential order for column element 1 to the number of column elements. The material type designations for SAFE-RCC are:

1 - concrete

2 - steel

COLUMNS

1 - 4 element number

6 - 12 elemental centroid coordinate

14 - 23 elemental area

25 - 28 material type

The finite element mesh data input format is designed to be compatible with the filed output option of the modified version of FIRES-T.

IF THE TEMPERATURE DEPENDENT RESTRAINT SYSTEM, OR FIRE EXPOSED RESTRAINT SYSTEM, IS NOT INCLUDED CONTINUE DATA INPUT FROM (29).

(27) ELEMENTAL CENTROID COORDINATES, ELEMENTAL AREAS AND MATERIAL TYPE OF RESTRAINT BEAM CROSS SECTION AT MIDSPAN

(I4,1X,F7.5,1X,F10.8,1X,I4)

The details of the finite element mesh for the restraint beams at midspan are only included if either of the restraint beams are exposed to fire. Cross sections for the top and bottom restraint beams are assumed to be identical, however, the sections can be exposed to the fire environment from different sides. The details are entered in sequential order for midspan element 1 to the number of elements at midspan.

COLUMNS	
1 - 4	element number
6 - 12	elemental centroid coordinate
14 - 23	elemental area
25 - 28	material type

(28) ELEMENTAL CENTROID COORDINATES, ELEMENTAL AREAS AND MATERIAL TYPE OF RESTRAINT BEAM CROSS SECTION AT SUPPORT

(I4,1X,F7.5,1X,F10.8,1X,I4)

The details of the finite element mesh for the restraint beam at support are only included if either of the restraint beams are exposed to fire. Cross sections for the top and bottom restraint beams are assumed to be identical, however, the sections can be exposed to the fire environment from different sides. The details are entered in sequential order for support element 1 to the number of elements at support in a similar manner to that described in data input (27).

(29) TEMPERATURE DEPENDENT MATERIAL PARAMETERS

4(F6.2,E12.8)

The temperature dependent material parameters are represented as linear segments. Eight ordered pairs of temperature-value are entered to represent the nodes of the linear segments. Values of temperature and material property must be entered in the order of:

COEFFICIENT OF STEEL THERMAL EXPANSION	(8 values)
CONCRETE STRAIN AT PEAK STRESS	(8 values)
CONCRETE PEAK STRESS	(8 values)
STEEL YIELD STRESS	(8 values)
STEEL ELASTIC MODULUS	(8 values)

The eight ordered pairs of temperature-value for each of the above material parameters are entered four to a line in the format described below.

COLUMNS	
1 - 6	temperature 1
7 - 18	material property 1
19 - 24	temperature 2
25 - 36	material property 2
37 - 42	temperature 3
43 - 54	material property 3
55 - 60	temperature 4
61 - 72	material property 4
1 - 6	temperature 5
7 - 18	material property 5
.	
.	
61 - 72	material property 8

(30) INITIAL TIME

(F7.3)

Time at start of analysis (normally 0.00 hours).

(31) INITIAL TEMPERATURE OF COLUMN

(F6.2)

Initial temperature of column under analysis (normally 20°C).

(32) TIME AND ELEMENTAL TEMPERATURES OF COLUMN

(F7.3)

6(I4,1X,F6.2)

The time history of elemental temperatures are produced from the modified version of FIRES-T. The elemental temperatures are entered in sequential order for column element 1 to the number of column elements for time step 2 to the number of time steps.

COLUMNS

1 - 7 time of exposure to fire

1 - 4 element number

6 - 11 elemental temperature

12 - 15 element number

17 - 22 elemental temperature

.

.

56 - 59 element number

61 - 66 elemental temperature

1 - 4 elemental number

.

.

up to the number of elements

The procedure is then repeated for each time step up to the number of time steps.

The temperature data input format is designed to be compatible with the filed output option of the modified version of FIRES-T.

IF THE TEMPERATURE DEPENDENT RESTRAINT SYSTEM OPTION IS NOT INCLUDED THEN NO FURTHER DATA INPUT IS REQUIRED.

(33) INITIAL TEMPERATURE OF TOP RESTRAINT BEAM

(F6.2)

Initial temperature of restraint beam is normally 20°C.

(34) ELEMENTAL TEMPERATURES OF TOP RESTRAINT BEAM AT MIDSPAN

6(I4,1X,F6.2)

The time history of elemental temperatures are produced from the modified version of FIRES-T. The elemental temperatures are entered in sequential order for midspan top restraint beam element 1 to the number of elements.

COLUMNS

1 - 4 element number

6 - 11 elemental temperature

12 - 15 element number

17 - 22 elemental temperature

•

56 - 59 element number

61 - 66 elemental temperature

1 - 4 element number

•

up to the number of elements

The procedure is then repeated for each time step up to the number of time steps.

The temperature data input format is designed to be compatible with the filed output option of the modified version of FIRES-T.

(35) ELEMENTAL TEMPERATURES OF TOP RESTRAINT BEAM AT SUPPORT

6(I4,1X,F6.2)

The temperatures are entered in a similar manner to (34).

(36) INITIAL TEMPERATURE OF BOTTOM RESTRAINT BEAM

(F6.2)

Initial temperature of restraint beam is normally 20°C.

(37) ELEMENTAL TEMPERATURES OF BOTTOM RESTRAINT BEAM AT MIDSPAN

6(I4,1X,F6.2)

The temperatures are entered in a similar manner to (34).

(38) ELEMENTAL TEMPERATURES OF BOTTOM RESTRAINT BEAM AT SUPPORT

6(I4,1X,F6.2)

The temperatures are entered in a similar manner to (34).

NOTES

RUNNING FIRES-T

Some discussion on the running of the modified version of FIRES-T is given in Section 4.7. For full user instructions to run the modified version of FIRES-T the user manual for FIRES-T (Becker, Bizri and Bresler (1974)) should be consulted. Some additional information with regard to the modifications to FIRES-T made to make the program compatible with SAFE-RCC are given in Section 4.8.

ORIGIN OF COORDINATE AXIS

The origin of the coordinate axis must be considered when constructing the finite element mesh for the column sections and the restraint beam sections, for the preliminary FIRES-T run. Details of the finite element mesh in the form of element centroid coordinates, elemental areas and material type are then written to a data file in a format compatible with SAFE-RCC.

The origin of the coordinate axis for the column under analysis must coincide with the longitudinal axis of the column. Only half the section is divided into finite elements due to the symmetry of the analysis. The origin of the coordinate axis for the restraint beam sections must coincide with the top edge of the restraint beam. Again only half the section is divided into a finite element mesh due to the symmetry of the analysis. See Figure A.3.

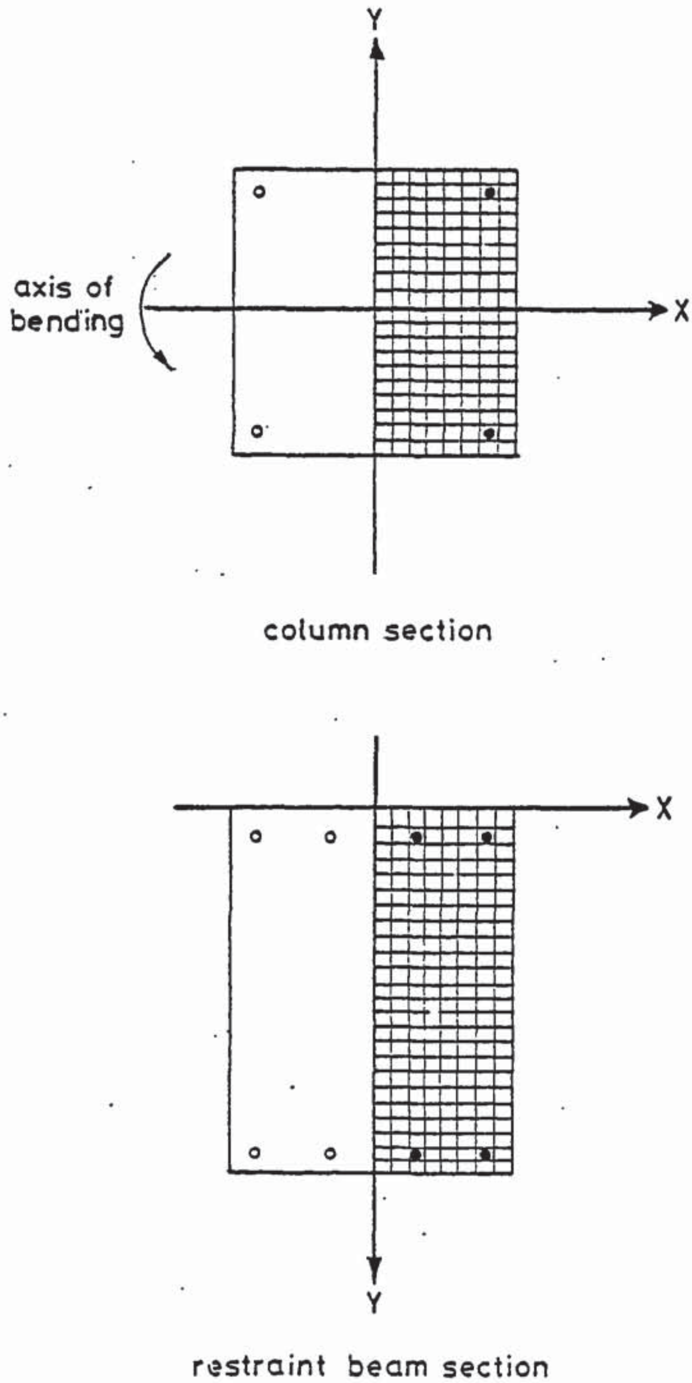

Figure A.3 Origin of coordinate axis for column sections and restraint beam sections.

REPRESENTATION OF STEEL REINFORCEMENT

Since the finite element mesh can only be constructed from triangles, squares, trapezia and quadrilaterals, a round steel reinforcement cross section has to be approximated.

The average centroid coordinate of the steel finite elements for a particular steel bar cross section must coincide with the centroidal distance of the steel bar from the axis of bending for the real column for an accurate structural analysis. If an equivalent area square section is used with its centroid at the centroid of the round steel bar, the concrete cover to the steel and the perimeter length of the steel element may be significantly in error. A satisfactory approximation is obtained using an octahedral equivalent area steel section. This gives a good approximation to the perimeter length of the steel cross section and a good approximation for the depth of concrete cover for coincident centroids. See Figure A.4.

An octahedral equivalent area steel section is therefore best used for the cross section idealization of the column, however, an equivalent area square steel section is accurate enough for the restraint beam sections.

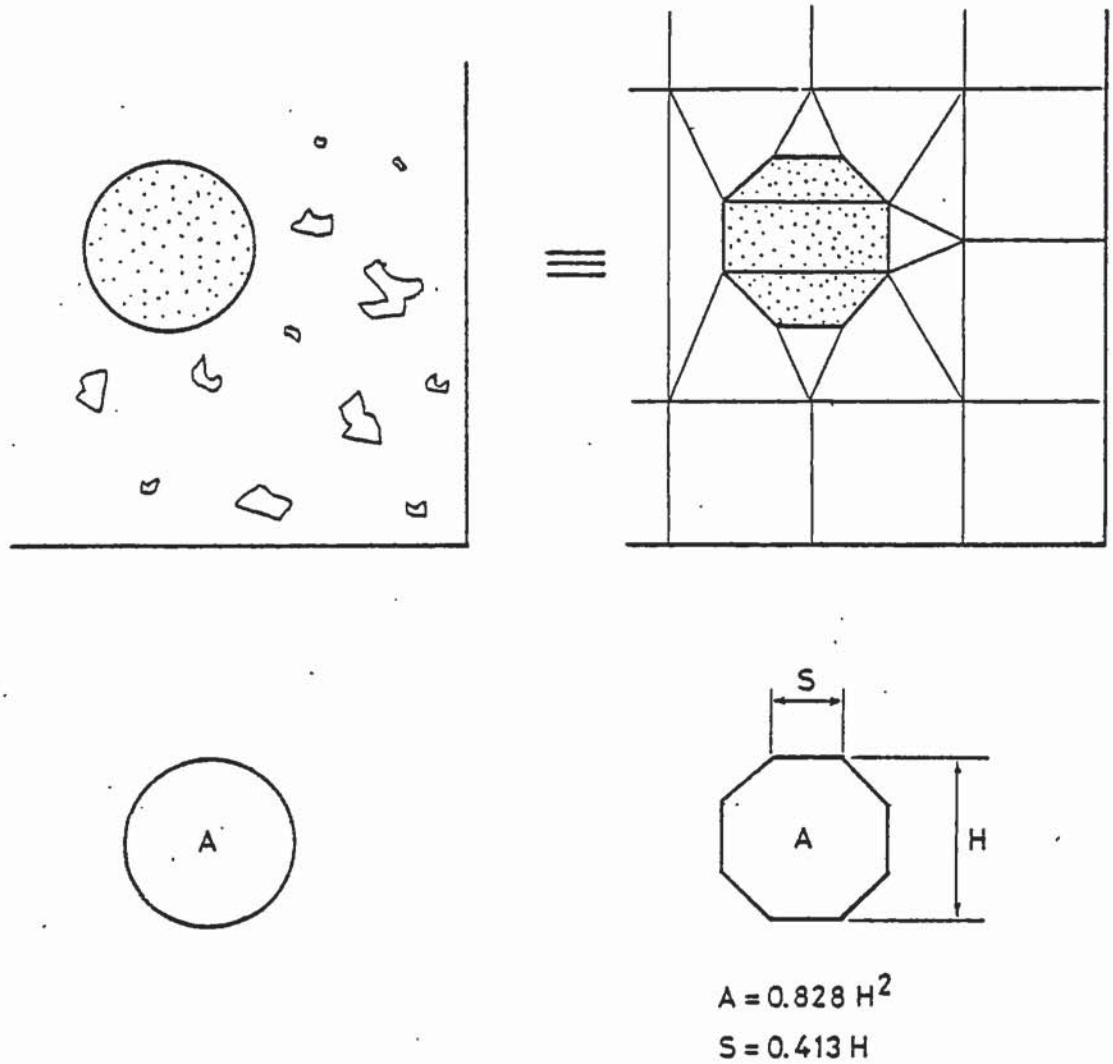

Figure A.4 Represention of steel reinforcement for column cross sections.

SAMPLE DATA INPUT FILE

Presented in the following pages is a sample data input file. The data input file is that corresponding to the structural system shown in Figure A.5. The dimensions of the members of the structural system and details of the reinforcement are given in the Figure. The fire exposed column is divided into 13 segments and the segment division points are further subdivided into 128 elements. The finite element mesh for the column cross section is drawn in Figure A.6. The fire exposure is considered to be similar to that for the structural systems described in Chapter 12 and the thermal and structural material properties are taken to be similar to those described in Chapter 11.

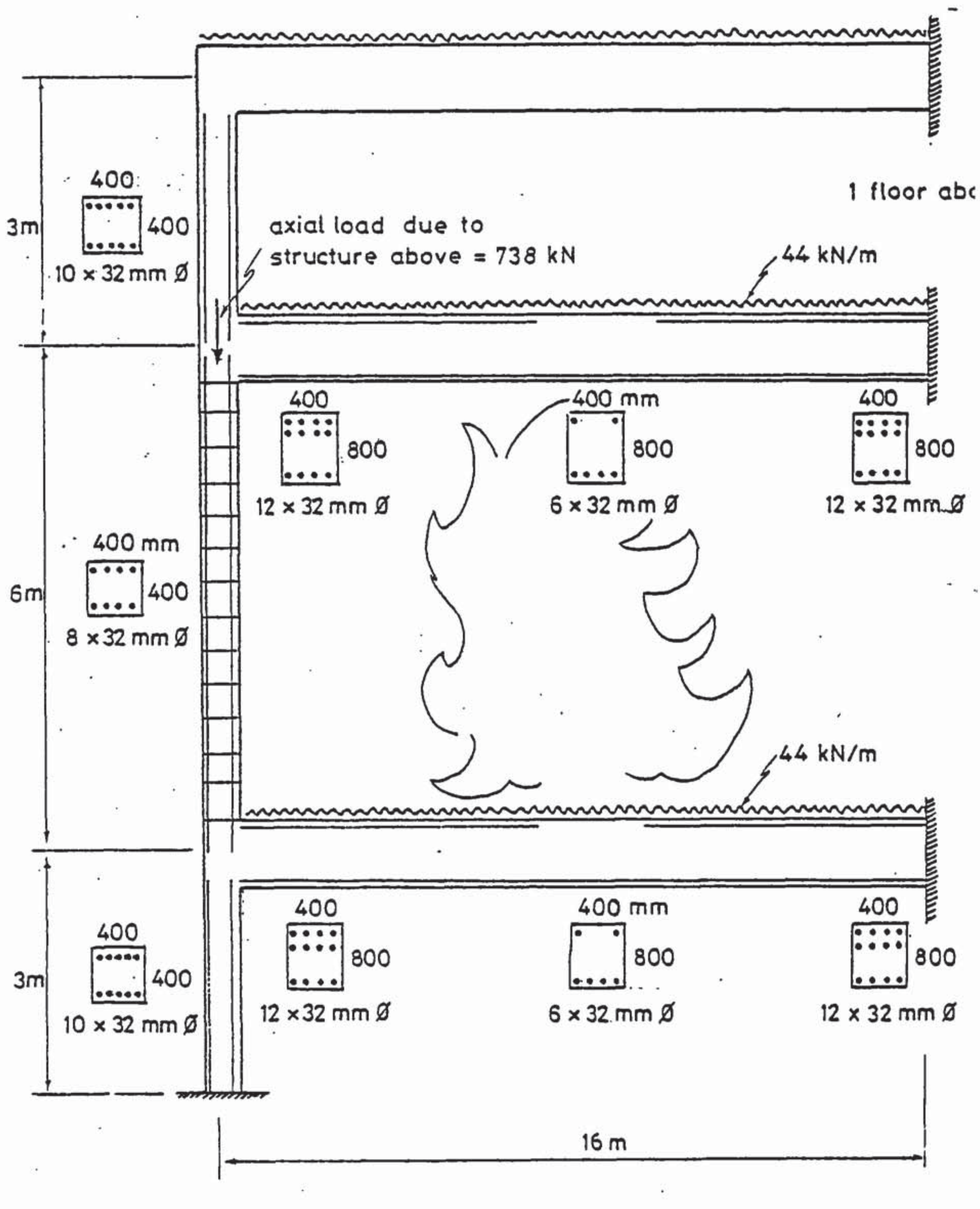

Figure A.5 Sample structural system.

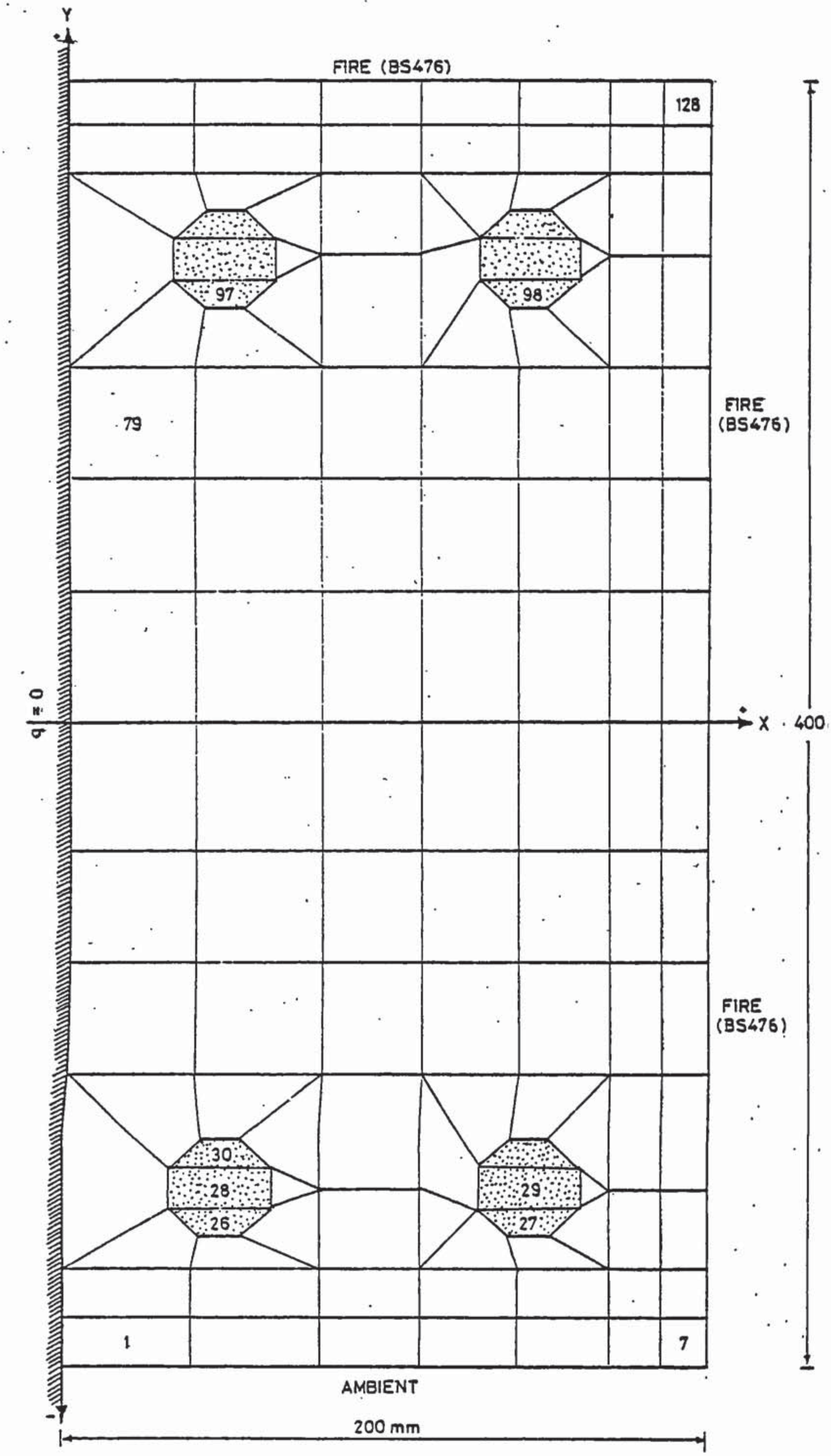

Figure A.6 Example of finite element mesh for column cross section (8 x 32 mm diameter bars).

```
££££ COLUMN 6M RESTRAINT BEAM 16M 1 FLOOR ABOVE ££££
   0
  13
 128
  28
  34
  34
   1
   0
 1 1
   1
 1 1
6.0       0.400   0.400
0.400     0.400
.0560     6434.0
   1      0.400
   2      0.400
   3      0.400
   4      0.400
   5      0.400
   6      0.400
   7      0.400
   8      0.400
   9      0.400
  10      0.400
  11      0.400
  12      0.400
  13      0.400
738.0
44.0      44.0
3.0       3.0
.0560     8042.0   .0560   8042.0
6434.0    3217.0   3217.0  1608.0
0.755     0.400    0.800  16.0      1
730.0     730.0    785.0  1570.0     785.0    1570.0
20   7.500       4.500    0.0004    0.0004    0.0002
   1   0.0
   2   0.0
   3   0.0
   4   0.0
   5   0.0
   6   0.0
   7   0.0
   8   0.0
   9   0.0
  10   0.0
  11   0.0
  12   0.0
  13   0.0
  14   0.0
   1 -.19250   .00060000      1
   2 -.19350   .00060000      1
   3 -.19350   .00045000      1
   4 -.19350   .00045000      1
```

```
   9 -.17750   .00060000      1
  10 -.17750   .00045000      1
  11 -.17750   .00045000      1
  12 -.17750   .00045000      1
  13 -.17750   .00022500      1
  14 -.17750   .00022500      1
  15 -.14300   .00110111      1
  16 -.16350   .00044611      1
  17 -.16479   .00027537      1
  18 -.15625   .00036979      1
  19 -.15750   .00075000      1
  20 -.15515   .00023021      1
  21 -.16250   .00032998      1
  22 -.16479   .00022329      1
  23 -.15625   .00026735      1
  24 -.15750   .00037500      1
  25 -.15750   .00037500      1
  26 -.15501   .00020142      2
  27 -.15501   .00020142      2
  28 -.14400   .00040111      2
  29 -.14400   .00040111      2
  30 -.13299   .00020142      2
  31 -.13299   .00020142      2
  32 -.14433   .00010564      1
  33 -.14433   .00006703      1
  34 -.12150   .00064270      1
  35 -.11921   .00048685      1
  36 -.13025   .00048047      1
  37 -.12750   .00105000      1
  38 -.13575   .00044081      1
  39 -.12150   .00048658      1
  40 -.11921   .00039477      1
  41 -.13025   .00035603      1
  42 -.12750   .00052500      1
  43 -.12750   .00052500      1
  44 -.09250   .00140000      1
  45 -.09250   .00140000      1
  46 -.09250   .00105000      1
  47 -.09250   .00105000      1
  48 -.09250   .00105000      1
  49 -.09250   .00052500      1
  50 -.09250   .00052500      1
  51 -.05750   .00140000      1
  52 -.05750   .00140000      1
  53 -.05750   .00105000      1
  54 -.05750   .00105000      1
  55 -.05750   .00105000      1
  56 -.05750   .00052500      1
  57 -.05750   .00052500      1
  58 -.02000   .00160000      1
  59 -.02000   .00160000      1
  60 -.02000   .00120000      1
  61 -.02000   .00120000      1
  62 -.02000   .00120000      1
  63 -.02000   .00060000      1
```

67	.02000	.00120000	1
68	.02000	.00120000	1
69	.02000	.00120000	1
70	.02000	.00060000	1
71	.02000	.00060000	1
72	.05750	.00140000	1
73	.05750	.00140000	1
74	.05750	.00105000	1
75	.05750	.00105000	1
76	.05750	.00105000	1
77	.05750	.00052500	1
78	.05750	.00052500	1
79	.09250	.00140000	1
80	.09250	.00140000	1
81	.09250	.00105000	1
82	.09250	.00105000	1
83	.09250	.00105000	1
84	.09250	.00052500	1
85	.09250	.00052500	1
86	.14200	.00118111	1
87	.12150	.00064270	1
88	.11921	.00048685	1
89	.13025	.00048847	1
90	.12750	.00105000	1
91	.13575	.00044081	1
92	.12150	.00048658	1
93	.11921	.00039477	1
94	.13025	.00035603	1
95	.12750	.00052500	1
96	.12750	.00052500	1
97	.13299	.00020142	2
98	.13299	.00020142	2
99	.14400	.00040111	2
100	.14400	.00040111	2
101	.15501	.00020142	2
102	.15501	.00020142	2
103	.14433	.00010564	1
104	.14433	.00006703	1
105	.16250	.00044611	1
106	.16479	.00027537	1
107	.15625	.00036979	1
108	.15750	.00075000	1
109	.15515	.00023021	1
110	.16250	.00032798	1
111	.16479	.00022329	1
112	.15625	.00026735	1
113	.15750	.00037500	1
114	.15750	.00037500	1
115	.17750	.00060000	1
116	.17750	.00060000	1
117	.17750	.00045000	1
118	.17750	.00045000	1
119	.17750	.00045000	1
120	.17750	.00022500	1
121	.17750	.00022500	1

125	.19250	.00045000	1
126	.19250	.00045000	1
127	.19250	.00022500	1
128	.19250	.00022500	1
1	.79000	.00400000	1
2	.76909	.00436400	1
3	.74400	.00095914	1
4	.74400	.00080429	2
5	.74400	.00191827	1
6	.74400	.00080429	2
7	.74400	.00118602	1
8	.71471	.00596400	1
9	.68000	.00800000	1
10	.64000	.00800000	1
11	.60000	.00800000	1
12	.55000	.01200000	1
13	.49000	.01200000	1
14	.43000	.01200000	1
15	.37000	.01200000	1
16	.31000	.01200000	1
17	.26000	.00800000	1
18	.22000	.00800000	1
19	.18000	.00800000	1
20	.16709	.00188634	1
21	.14709	.00384486	1
22	.12000	.00567200	1
23	.08000	.00712000	1
24	.05600	.00368170	1
25	.05600	.00080429	2
26	.05600	.00118602	1
27	.03071	.00436400	1
28	.01000	.00400000	1
1	.79000	.00400000	1
2	.76909	.00436400	1
3	.74400	.00095914	1
4	.74400	.00080429	2
5	.74400	.00191827	1
6	.74400	.00080429	2
7	.74400	.00118602	1
8	.71471	.00596400	1
9	.68000	.00800000	1
10	.64000	.00800000	1
11	.60000	.00800000	1
12	.55000	.01200000	1
13	.49000	.01200000	1
14	.43000	.01200000	1
15	.37000	.01200000	1
16	.31000	.01200000	1
17	.26000	.00800000	1
18	.22000	.00800000	1
19	.18000	.00800000	1
20	.16709	.00188634	1
21	.14709	.00384486	1
22	.12000	.00095914	1
23	.12000	.00080429	2
24	.12000	.00191827	1

```
 27  .08000   .00712000     1
 28  .05600   .00095914     1
 29  .05600   .00080429     2
 30  .05600   .00191827     1
 31  .05600   .00080429     2
 32  .05600   .00110602     1
 33  .03091   .00436400     1
 34  .01000   .00400100     1
 20.0   15.0E-6      100.0   15.0E 6     200.0   15.0E-6      300.0   15.0E-6
400.0   15.0E-6      500.0   15.0E-6     600.0   15.0E-6      700.0   15.0E-6
 20.0    0.24E-2     100.0    0.30E-2    300.0    0.325E-2    400.0    0.36E-2
500.0    0.44E-2     600.0    0.55E-2    700.0    0.70E-2     960.0    1.42E-2
 20.0    0.3600E+5   100.0    0.3754E+5  300.0    0.3496E+5   400.0    0.3496E+5
500.0    0.2760E+5   600.0    0.2024E+5  700.0    0.1280E+5   960.0    0.0184E+5
 20.0    0.4530E+6   100.0    0.4348E+6  200.0    0.3760E+6   300.0    0.3715E+6
400.0    0.3398E+6   500.0    0.2673E+6  600.0    0.1676E+6   700.0    0.09513E+6
 20.0    0.2100E+9   100.0    0.2100E+9  200.0    0.2058E+9   300.0    0.1869E+9
400.0    0.1617E+9   500.0    0.1302E+9  600.0    0.0840E+9   700.0    0.0315E+9
 0.0
 20.0
  .050
   1  20.00    2  20.01    3  20.04    4  20.32    5  22.76    6  32.20
   7  63.91    8  20.00    9  20.01   10  20.05   11  20.31   12  22.69
  13  31.76   14  59.08   15  20.00   16  20.00   17  20.00   18  20.01
  19  20.07   20  20.32   21  20.52   22  21.72   23  22.93   24  31.22
  25  56.09   26  20.00   27  20.85   28  20.00   29  20.85   30  20.00
  31  20.04   32  20.01   33  22.37   34  20.00   35  20.00   36  20.01
  37  20.07   38  20.41   39  20.52   40  21.65   41  22.85   42  30.90
  43  56.31   44  20.00   45  20.01   46  20.04   47  20.31   48  22.50
  49  30.69   50  56.22   51  20.00   52  20.00   53  20.04   54  20.31
  55  22.53   56  30.72   57  56.21   58  20.00   59  20.00   60  20.04
  61  20.31   62  22.54   63  30.72   64  56.22   65  20.00   66  20.00
  67  20.04   68  20.32   69  22.54   70  30.72   71  56.22   72  20.01
  73  20.01   74  20.04   75  20.32   76  22.54   77  30.72   78  56.22
  79  20.06   80  20.07   81  20.09   82  20.36   83  22.56   84  30.73
  85  56.35   86  21.27   87  20.43   88  20.43   89  20.57   90  20.44
  91  20.99   92  20.92   93  22.04   94  23.35   95  31.19   96  56.57
  97  20.76   98  21.54   99  20.85  100  21.63  101  20.99  102  21.76
 103  20.79  104  23.06  105  22.65  106  23.03  107  21.83  108  22.73
 109  22.37  110  23.11  111  24.54  112  24.56  113  33.36  114  58.64
 115  30.60  116  31.03  117  30.88  118  31.24  119  33.30  120  41.08
 121  66 01  122  56.19  123  56.30  124  56.31  125  56.55  126  58.51
 127  65.91  128  89.86
  .100
   1  20.00    2  20.03    3  20.18    4  21.20    5  28.36    6  50.60
   7 114.37    8  20.00    9  20.03   10  20.22   11  21.21   12  28.22
  13  50.6?   14 107 23   15  20.00   16  20.01   17  20.02   18  20.04
  19  20.3?   20  21 25   21  21.98   22  25.53   23  28.87   24  48.85
```

* * * portion of input data omitted * * *

```
2.500
   1   68 70    2   91    1         8          (          7
   7  710.77    8   73.59    9   98.09   10  154.51   11  140.97   12  370.79
  13  540.79   14  771.12   15   81.68   16  13.25    17   96.10   18  109.35
  19  174.32   20  262.79   21  301.33   22  349.32   23  412.52   24  566.18
  25  773.72   26   91.13   27  350.03   28   91.27   29  350.70   30   91.40
  31  351.31   32  105.67   33  395.59   34   65.75   35  101.95   36  113.69
  37  183.63   38  288.52   39  315.75   40  394.93   41  429.20   42  594.30
  43  791.80   44   81.51   45  113.99   46  161.62   47  286.04   48  447.45
  49  628.00   50  806.89   51   84.17   52  117.57   53  184.13   54  290.21
  55  459.58   56  642.21   57  814.19   58   92.01   59  125.08   60  190.98
  61  296.59   62  465.59   63  647.07   64  816.51   65  111.74   66  143.70
  67  207.36   68  309.67   69  474.97   70  653.23   71  619.42   72  151.86
  73  181.95   74  241.05   75  336.44   76  493.79   77  665.18   78  824.91
  79  227.68   80  257.49   81  304.37   82  390.44   83  531.32   84  604.84
  85  833.55   86  407.41   87  343.85   88  357.62   89  392.70   90  406.82
  91  501.16   92  495.16   93  560.92   94  606.83   95  708.16   96  845.68
  97  408.76   98  566.30   99  412.45  100  568.56  101  416.51  102  571.19
 103  420.43  104  600.24  105  474.49  106  484.38  107  461.48  108  535.15
 109  565.15  110  603.38  111  634.64  112  637.27  113  755.64  114  870.55
 115  621.42  116  633.04  117  672.40  118  762.03  119  752.09  120  827.30
 121  902.95  122  804.12  123  810.21  124  817.86  125  841.83  126  868.56
 127  903.42  128  938.21
20.0
   1   54.51    2   29.08    3   21.04    4   20.97    5   21.31    6   22.25
   7   38.72    8   23.67    9   24.10   10   24.08   11   24.08   12   24.00
  13   24.08   14   24.08   15   24.08   16   24.08   17   24.08   18   24.07
  19   24.07   20   20.00   21   25.03   22   23.25   23   22.45   24   20.05
  25   20.51   26   25.30   27   20.17   28   20.05
   1   97.80    2   43.53    3   23.56    4   23.35    5   24.43    6   27.21
   7   64.81    8   29.37    9   30.05   10   29.92   11   29.91   12   29.91
  13   29.91   14   29.91   15   29.91   16   29.91   17   29.91   18   29.91
  19   29.90   20   20.02   21   33.24   22   27.88   23   25.92   24   20.19
  25   21.62   26   32.77   27   20.56   28   20.20
   1  143.80    2   60.69    3   27.48    4   37.10    5   29.22    6   34.44
   7   94.68    8   36.54    9   37.14   10   36.80   11   36.77   12   36.76
  13   36.76   14   36.76   15   36.76   16   36.76   17   36.76   18   36.76
  19   36.75   20   20.05   21   40.72   22   33.33   23   29.97   24   20.47
  25   23.30   26   41.43   27   21.17   28   20.48
   1  188.94    2   79.73    3   34.64    4   32.07    5   35.46    6   43.43
   7  126.52    8   44.82    9   44.98   10   44.31   11   44.23   12   44.22
  13   44.22   14   44.22   15   44.22   16   44.22   17   44.21   18   44.21
  19   44.19   20   20.10   21   49.95   22   39.25   23   34.38   24   20.74
  25   25.47   26   50.73   27   21.98   28   20.91
   1  231.88    2   99.94    3   38.84    4   38.09    5   42.92    6   54.06
   7  158.86    8   53.94    9   53.32   10   52.18   11   52.02   12   52.00
  13   52.00   14   52.00   15   53.00   16   52.00   17   51.98   18   51.98
  19   51.96   20   20 20   21   59.59   22   45.47   23   39.01   24   21.15
  25   28.02   26   60.33   27   27.95   28   21.50
```

* * * portion of input data omitted * * *

```
         10        20        30        40        50        60        70
19 263.68  20  72.71  21 310.89  22 223.05  23 185.73  24  81.37
25 191.70  26 291.24  27 102.31  28  89.34
 1 796.50   2 584.71   3 384.55   4 386.84   5 436.31   6 535.66
 7 725.14   8 417.92   9 356.43  10 309.36  11 289.10  12 280.48
13 277.19  14 276.39  15 276.08  16 275.44  17 274.00  18 272.95
19 271.01  20  77.04  21 318.80  22 229.41  23 191.35  24  85.26
25 198.29  26 297.37  27 106.33  28  92.82
 1 806.60   2 597.23   3 396.83   4 399.21   5 449.58   6 558.31
 7 736.35   8 430.41   9 367.75  10 319.10  11 297.77  12 288.51
13 284.90  14 284.02  15 283.67  16 202.98  17 281.44  18 280.38
19 278.30  20  81.43  21 326.51  22 235.66  23 196.87  24  89.14
25 204.66  26 303.24  27 110.28  28  96.24
 1 816.23   2 609.29   3 408.75   4 411.20   5 462.45   6 564.49
 7 747.13   8 442.55   9 378.82  10 328.71  11 306.33  12 296.43
13 292.50  14 291.52  15 291.13  16 290.39  17 288.76  18 287.52
19 205.25  20  85.88  21 334.04  22 241.79  23 202.28  24  93.02
25 210.82  26 308.86  27 114.18  28  99.58
 1  54.51   2  29.00   3  21.04   4  20.97   5  21.31   6  22.25
 7  38.72   8  23.67   9  24.10  10  24.08  11  24.08  12  24.08
13  24.08  14  24.08  15  24.08  16  24.08  17  24.08  18  24.07
19  24.07  20  20.00  21  24.95  22  20.00  23  20.00  24  20.24
25  21.17  26  37.44  27  22.43  28  20.00  29  20.00  30  20.11
31  20.51  32  25.29  33  20.17  34  20.05
 1  97.80   2  43.53   3  23.56   4  23.35   5  24.43   6  27.21
 7  64.81   8  29.37   9  30.05  10  29.92  11  29.91  12  29.91
13  29.91  14  29.91  15  29.91  16  29.91  17  29.91  18  29.90
19  29.88  20  20.02  21  32.01  22  20.01  23  20.02  24  20.02
25  23.63  26  60.07  27  25.86  28  20.01  29  20.02  30  20.39
31  21.61  32  32.73  33  20.56  34  20.20
 1 143.80   2  60.69   3  27.48   4  27.10   5  29.22   6  34.44
 7  94.60   8  36.54   9  37.14  10  36.80  11  36.77  12  36.76
13  36.76  14  36.76  15  36.76  16  36.76  17  36.76  18  36.75
19  36.71  20  20.06  21  40.28  22  20.03  23  20.06  24  21.75
25  27.20  26  87.11  27  29.88  28  20.02  29  20.04  30  20.85
31  23.29  32  41.33  33  21.17  34  20.48
 1 180.94   2  79.73   3  32.64   4  32.07   5  35.46   6  43.43
 7 126.52   8  44.82   9  44.98  10  44.31  11  44.23  12  44.22
13  44.22  14  44.22  15  44.22  16  44.22  17  44.21  18  44.20
19  44.13  20  20.14  21  49.27  22  20.07  23  20.14  24  22.97
25  31.59  26 114.68  27  34.26  28  20.05  29  20.10  30  21.49
31  25.46  32  50.56  33  21.98  34  20.91
 1 231.88   2  99.94   3  30.84   4  30.09   5  42.92   6  54.06
 7 158.86   8  53.94   9  53.32  10  52.18  11  52.02  12  52.00
13  52.00  14  52.00  15  52.00  16  52.00  17  51.98  18  51.98
19  51.87  20  20.26  21  50.64  22  20.14  23  20.26  24  24.47
25  36.70  26 142.58  27  38.87  28  20.11  29  20.19  30  22.30
31  28.82  32  6J.11  33  22.96  34  21.51
 1 272.27   2 120.65   3  45.83   4  44.89   5  51.31   6  65.97
 7 198.78   8  63.67   9  61.99  10  60.24  11  59.98  12  59.95
13  59.94  14  59.94  15  59.94  16  57.94  17  59.91  18  59.90
```

* * * portion of input data omitted * * *

```
         10        20        30        40        50        60        70
19 248.51  20  69 43  21 284.77  22  40 00  23   7 51  24 134 88
25 2 0.1    2 5              8           5            0       0 9 .04
31 181.21  32 279.26  33  97.54  34  84.59
 1 774.71   2 558.11   3 356.80   4 340.85   5 408.41   6 504.78
 7 701.26   8 391.83   9 333.09  10 289.45  11 271.44  12 264.08
13 261.37  14 260.75  15 260.53  16 260.07  17 258.94  18 258.39
19 256.15  20  73.89  21 294.93  22  63.07  23  71.74  24 141.13
25 289.77  26 588.23  27 184.39  28  57.21  29  62.02  30 183.96
31 188.54  32 286.21  33 102.00  34  88.44
 1 785.89   2 571.68   3 371.88   4 374.06   5 422.60   6 520.49
 7 713.45   8 405.06   9 344.88  10 299.48  11 280.33  12 272.34
13 269.34  14 268.65  15 268.39  16 267.89  17 266.68  18 266.04
19 263.63  20  78.41  21 302.85  22  67.80  23  76.03  24 147.31
25 299.00  26 597.96  27 190.38  28  60.59  29  65.59  30 108.83
31 195.62  32 292.83  33 106.39  34  92.21
 1 796.50   2 584.71   3 384.55   4 386.84   5 436.31   6 535.66
 7 725.14   8 417.92   9 356.43  10 309.36  11 289.10  12 280.48
13 277.19  14 276.40  15 274.11  16 275.57  17 274.28  18 273.55
19 270.95  20  82.98  21 310.54  22  71.78  23  80.36  24 153.42
25 307.90  26 607.21  27 194.25  28  64.01  29  69.19  30 113.65
31 202.45  32 299.14  33 110.72  34  95.92
 1 806.60   2 597.23   3 394.83   4 399.21   5 449.58   6 550.31
 7 736.35   8 430.41   9 367.75  10 319.10  11 297.77  12 288.51
13 284.91  14 284.03  15 283.70  16 283.11  17 281.74  18 280.91
19 278.12  20  87.60  21 318.02  22  75.81  23  84.72  24 159.47
25 316.55  26 616.00  27 202.01  28  67.47  29  72.83  30 118.43
31 209.06  32 305.20  33 114.98  34  99.56
 1 816.23   2 609.29   3 408.75   4 411.20   5 462.45   6 564.49
 7 747.13   8 442.55   9 370.82  10 328.71  11 306.33  12 296.43
13 292.51  14 291.53  15 291.17  16 290.53  17 289.08  18 288.15
19 285.16  20  92.20  21 325.32  22  79.98  23  89.16  24 165.46
25 324.97  26 624.39  27 207.68  28  70.97  29  76.49  30 123.16
31 215.45  32 311.00  33 119.17  34 103.13
20.0
 1  20.00   2  20.00   3  20.00   4  20.00   5  20.00   6  20.00
 7  20.00   8  20.00   9  20.00  10  20.00  11  20.00  12  20.00
13  20.00  14  20.00  15  20.00  16  20.00  17  20.00  18  20.00
19  20.00  20  20.00  21  20.02  22  20.11  23  21.08  24  21.20
25  21.74  26  33.47  27  29.13  28  54.51
 1  20.00   2  20.00   3  20.00   4  20.00   5  20.00   6  20.00
 7  20.00   8  20.00   9  20.00  10  20.00  11  20.00  12  20.00
13  20.00  14  20.00  15  20.00  16  20.00  17  20.00  18  20.00
19  20.01  20  20.01  21  20.09  22  20.41  23  23.04  24  24.07
25  25.64  26  52.37  27  43.74  28  97.79
 1  20.00   2  20.00   3  20.00   4  20.00   5  20.00   6  20.00
 7  20.00   8  20.00   9  20.00  10  20.00  11  20.00  12  20.00
13  20.00  14  20.00  15  20.00  16  20.00  17  20.00  18  20.00
19  20.03  20  20.05  21  20.24  22  20.92  23  25.81  24  28.49
25  31.41  26  74.12  27  61.17  28 143.81
 1  20.00   2  20.00   3  20.00   4  20.00   5  20.00   6  20.00
```

* * * portion of input data omitted * * *

19	52.86	20	73.70	21	88.52	22	135.02	23	251.43	24	350.86
25	403.57	26	570.88	27	546.02	28	761.11				
1	20.00	2	20.00	3	20.00	4	20.00	5	20.00	6	20.00
7	20.00	8	20.00	9	20.00	10	20.00	11	20.00	12	20.00
13	20.02	14	20.12	15	20.54	16	22.22	17	26.33	18	35.50
19	55.82	20	78.46	21	93.58	22	142.34	23	261.74	24	363.30
25	416.43	26	590.50	27	558.95	28	772.31				
1	20.00	2	20.00	3	20.00	4	20.00	5	20.00	6	20.00
7	20.00	8	20.00	9	20.00	10	20.00	11	20.00	12	20.01
13	20.03	14	20.15	15	20.65	16	22.58	17	27.17	18	37.13
19	58.82	20	83.31	21	98.63	22	149.60	23	271.73	24	375.26
25	428.67	26	601.49	27	571.26	28	702.91				
1	20.00	2	20.00	3	20.00	4	20.00	5	20.00	6	20.00
7	20.00	8	20.00	9	20.00	10	20.00	11	20.00	12	20.01
13	20.04	14	20.18	15	20.77	16	22.97	17	28.05	18	38.80
19	61.86	20	88.22	21	103.67	22	156.76	23	281.41	24	386.77
25	440.33	26	611.88	27	582.99	28	792.95				
1	20.00	2	20.00	3	20.00	4	20.00	5	20.00	6	20.00
7	20.00	8	20.00	9	20.00	10	20.00	11	20.00	12	20.01
13	20.05	14	20.22	15	20.91	16	23.39	17	28.97	18	40.51
19	64.94	20	93.17	21	108.68	22	163.81	23	290.80	24	397.83
25	451.70	26	621.70	27	594.17	28	802.49				
1	20.00	2	20.00	3	20.00	4	20.00	5	20.00	6	20.00
7	20.00	8	20.00	9	20.00	10	20.00	11	20.00	12	20.01
13	20.06	14	20.27	15	21.06	16	23.84	17	29.93	18	42.27
19	68.06	20	98.16	21	113.66	22	170.76	23	299.88	24	408.48
25	462.20	26	631.83	27	604.89	28	811.58				
1	20.00	2	20.00	3	20.00	4	20.00	5	20.00	6	20.00
7	20.00	8	20.00	9	20.00	10	20.00	11	20.00	12	20.00
13	20.00	14	20.00	15	20.00	16	20.00	17	20.00	18	20.00
19	20.00	20	20.01	21	20.05	22	20.03	23	20.03	24	20.06
25	20.17	26	20.33	27	21.14	28	21.02	29	20.93	30	21.18
31	21.74	32	33.46	33	28.91	34	54.47				
1	20.00	2	20.00	3	20.00	4	20.00	5	20.00	6	20.00
7	20.00	8	20.00	9	20.00	10	20.00	11	20.00	12	20.00
13	20.00	14	20.00	15	20.00	16	20.00	17	20.00	18	20.00
19	20.02	20	20.06	21	20.18	22	20.13	23	20.14	24	20.26
25	20.40	26	21.09	27	23.25	28	23.47	29	23.21	30	24.02
31	25.62	32	52.34	33	42.99	34	97.64				
1	20.00	2	20.00	3	20.00	4	20.00	5	20.00	6	20.00
7	20.00	8	20.00	9	20.00	10	20.00	11	20.00	12	20.00
13	20.00	14	20.00	15	20.00	16	20.00	17	20.00	18	20.01
19	20.07	20	20.18	21	20.45	22	20.36	23	20.37	24	20.65
25	21.37	26	22.28	27	24.24	28	27.30	29	26.81	30	28.38
31	31.35	32	74.06	33	59.62	34	143.45				
1	20.00	2	20.00	3	20.00	4	20.00	5	20.00	6	20.00
7	20.00	8	20.00	9	20.00	10	20.00	11	20.00	12	20.00
13	20.00	14	20.00	15	20.00	16	20.00	17	20.00	18	20.02
19	20.15	20	20.38	21	20.88	22	20.75	23	20.77	24	21.28
25	22.40	26	23.88	27	29.99	28	32.34	29	31.59	30	34.07
31	38.59	32	97.29	33	78.04	34	188.35				
1	20.00	2	20.00	3	20.00	4	20.00	5	20.00	6	20.00

* * * portion of input data omitted * * *

19	49.41	20	74.72	21	84.80	22	98.13	23	97.54	24	108.18
25	126.69	26	120	2	8 1	28	27 .44	29	470.94	30	293.97
31	336.69	32	518.55	33	455.21	34	697.07				
1	20.00	2	20.00	3	20.00	4	20.00	5	20.00	6	20.00
7	20.00	8	20.00	9	20.00	10	20.00	11	20.00	12	20.00
13	20.01	14	20.06	15	20.33	16	21.56	17	24.96	18	33.18
19	52.85	20	80.63	21	90.92	22	106.03	23	105.30	24	116.28
25	134.72	26	127.59	27	219.44	28	287.55	29	285.17	30	308.53
31	351.93	32	533.16	33	470.38	34	710.82				
1	20.00	2	20.00	3	20.00	4	20.00	5	20.00	6	20.00
7	20.00	8	20.00	9	20.00	10	20.00	11	20.00	12	20.00
13	20.02	14	20.08	15	20.42	16	21.90	17	25.81	18	34.97
19	56.36	20	86.62	21	97.06	22	113.96	23	113.11	24	124.38
25	143.26	26	134.59	27	230.34	28	301.18	29	298.81	30	322.45
31	366.36	32	546.81	33	484.81	34	723.78				
1	20.00	2	20.00	3	20.00	4	20.00	5	20.00	6	20.00
7	20.00	8	20.00	9	20.00	10	20.00	11	20.00	12	20.00
13	20.02	14	20.11	15	20.52	16	22.27	17	26.73	18	36.03
19	59.92	20	92.67	21	103.20	22	121.89	23	120.94	24	132.43
25	151.66	26	141.44	27	240.90	28	314.12	29	311.93	30	335.78
31	380.04	32	559.59	33	490.54	34	736.03				
1	20.00	2	20.00	3	20.00	4	20.00	5	20.00	6	20.00
7	20.00	8	20.00	9	20.00	10	20.00	11	20.00	12	20.01
13	20.03	14	20.14	15	20.64	16	22.68	17	27.70	18	38.75
19	63.54	20	98.76	21	109.33	22	129.81	23	128.77	24	140.43
25	159.93	26	148.12	27	251.12	28	326.64	29	324.51	30	348.53
31	393.01	32	571.59	33	511.63	34	747.62				
1	20.00	2	20.00	3	20.00	4	20.00	5	20.00	6	20.00
7	20.00	8	20.00	9	20.00	10	20.00	11	20.00	12	20.01
13	20.04	14	20.18	15	20.78	16	23.12	17	28.72	18	40.73
19	67.23	20	104.87	21	115.43	22	137.71	23	136.57	24	148.36
25	168.02	26	154.63	27	261.02	28	330.71	29	336.62	30	360.75
31	405.31	32	582.91	33	524.12	34	758.62				
1	20.00	2	20.00	3	20.00	4	20.00	5	20.00	6	20.00
7	20.00	8	20.00	9	20.00	10	20.00	11	20.00	12	20.01
13	20.05	14	20.22	15	20.93	16	23.60	17	29.80	18	42.76
19	70.98	20	111.00	21	121.51	22	145.57	23	144.35	24	156.21
25	175.93	26	160.95	27	270.61	28	350.33	29	348.25	30	372.46
31	416.99	32	593.58	33	536.04	34	769.06				
1	20.00	2	20.00	3	20.00	4	20.00	5	20.00	6	20.00
7	20.00	8	20.00	9	20.00	10	20.00	11	20.00	12	20.01
13	20.06	14	20.27	15	21.10	16	24.11	17	30.92	18	44.84
19	74.76	20	117.15	21	127.56	22	153.43	23	152.12	24	163.97
25	183.66	26	167.10	27	279.89	28	361.50	29	359.40	30	383.67
31	428.11	32	603.69	33	547.43	34	778.98				
1	20.00	2	20.00	3	20.00	4	20.00	5	20.00	6	20.00
7	20.00	8	20.00	9	20.00	10	20.00	11	20.00	12	20.02
13	20.00	14	20.32	15	21.28	16	24.66	17	32.08	18	46.96
19	78.58	20	123.31	21	133.57	22	161.26	23	159.84	24	171.64
25	191.23	26	173.08	27	288.89	28	372.25	29	370.13	30	394.43
31	438.73	32	613.25	33	558.32	34	788.42				
1	20.00	2	20.00	3	20.00	4	20.00	5	20.00	6	20.00
7	20.00	8	20.00	9	20.00	10	20.00	11	20.01	12	20.02
13	20.09	14	20.39	15	21.48	16	25.23	17	33.29	18	49.12
19	82.42	20	129.46	21	[illegible]	22	167.04	23	167.48	24	179.21
25	198.62	26	178.91	27	297.62	28	382.61	29	380.45	30	404.78
31	448.91	32	622.32	33	568.74	34	797.42				

APPENDIX B

Slope Deflection Analysis of Structural Analysis System

Consider Figure B.1, if θ_A is the slope at joint A and θ_B is the slope at joint B from slope deflection equations it follows:

$$M_{AE} = 4K_1\theta_A \tag{B.1}$$

$$M_{AC} = 4K_2\theta_A + M_{ac} \tag{B.2}$$

$$M_{AB} = 4K_c\theta_A + 2K_c\theta_B \tag{B.3}$$

where: M_{ac} is the fixed end moment = $\omega_{AC}L_2^2/12$.

From equilibrium at joint A:

$$M_{AE} + M_{AC} + M_{AB} = 0 \tag{B.4}$$

therefore,

$$\theta_A(4K_1 + 4K_2 + 4K_c) + 2K_c\theta_B + M_{ac} = 0 \tag{B.5}$$

A similar set of equations can be written for joint B giving:

$$\theta_B(4K_3 + 4K_4 + 4K_c) + 2K_c\theta_A + M_{bd} = 0 \tag{B.6}$$

rewriting equations (B.5) and (B.6) in matrix form gives:

$$\begin{bmatrix} 4K_1 + 4K_2 + 4K_c & 2K_c \\ 2K_c & 4K_3 + 4K_4 + 4K_c \end{bmatrix} \begin{bmatrix} \theta_A \\ \theta_B \end{bmatrix} + \begin{bmatrix} M_{ac} \\ M_{bd} \end{bmatrix} = 0 \tag{B.7}$$

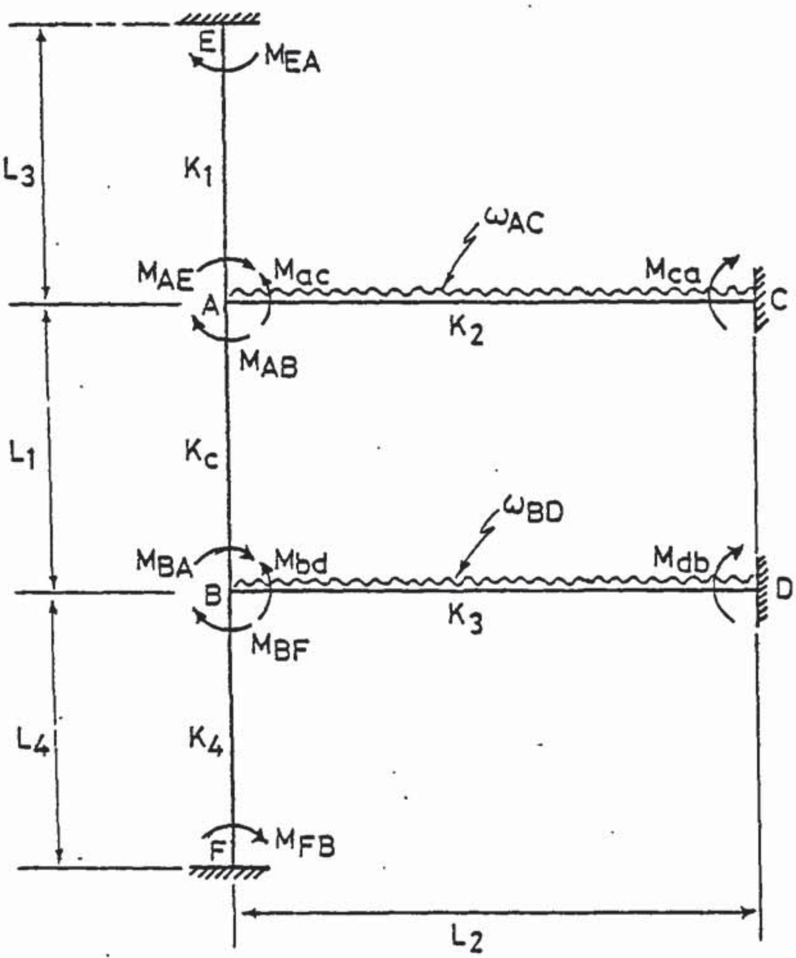

Figure B.1 Slope deflection analysis of structural system

$K = EI/L$

+ve Anticlockwise moments are positive

Solving for θ_A and θ_B using matrix algebra equation (B.7) becomes:

$$\begin{bmatrix} \theta_A \\ \\ \theta_B \end{bmatrix} = -\frac{1}{\Delta} \begin{bmatrix} 4K_3 + 4K_4 + 4K_c & -2K_c \\ \\ -2K_c & 4K_1 + 4K_2 + 4K_c \end{bmatrix} \begin{bmatrix} M_{ac} \\ \\ M_{bd} \end{bmatrix} \tag{B.8}$$

where: $\Delta = (4K_1 + 4K_2 + 4K_c)(4K_3 + 4K_4 + 4K_c) - 4K_c^2$

hence,

$$\theta_A = -\frac{M_{ac}(4K_3 + 4K_4 + 4K_c) - 2K_cM_{bd}}{(4K_1 + 4K_2 + 4K_c)(4K_3 + 4K_4 + 4K_c) - 4K_c^2}$$

$$\theta_B = -\frac{M_{bd}(4K_1 + 4K_2 + 4K_c) - 2K_cM_{ac}}{(4K_1 + 4K_2 + 4K_c)(4K_3 + 4K_4 + 4K_c) - 4K_c^2} \tag{B.9}$$

From consideration of joint equilibrium, rearranging equation (B.4) gives:

$$M_{AB} = -(M_{AC} + M_{AE}) \tag{B.10}$$

Substituting for M_{AC} and M_{AE} from equations (B.1) and (B.2):

$$M_{AB} = -(4K_1\theta_A + 4K_2\theta_A + M_{ac}) \tag{B.11}$$

Equation (B.11) represents the basic moment-rotation relation for the structure at joint A. A similar equation can be written for joint B. The slope of the moment-rotation relation is given by:

$$\frac{dM_{AB}}{d\theta_A} = -(4K_1 + 4K_2) \tag{B.12}$$

The axial load P on the column under analysis, or the reaction at A, is determined as follows:

Taking moments about C yields the equation:

$$P = \omega_{AC}L_2/2 - (M_{AC} + M_{CA})/L_2 \tag{B.13}$$

and from the slope deflection equations:

$$M_{AC} = 4K_2\theta_A + M_{ac} \tag{B.2}$$

$$M_{CA} = 2K_2\theta_A + M_{ca} \tag{B.14}$$

Substituting for M_{AC} and M_{CA} into equation (B.13) gives:

$$P = \omega_{AC}L_2/2 - (6K_2\theta_A + M_{ac} + M_{ca})/L_2 \tag{B.15}$$

However, for a uniformly distributed load $M_{ca} = - M_{ac}$, and therefore:

$$P = \omega_{AC}L_2/2 - 6K_2\theta_A/L_2 \tag{B.16}$$

APPENDIX C

Elastic Analysis for Pure Sway of Portal Frame

Consider Figure C.1. It is assumed that the axial deformation of the structural system is equivalent to the pure sway of a portal frame. From slope deflection equations:

$$M_{AC} = 4K_2\theta_A - 6K_2\Delta/L_2 \quad \text{(C.1)}$$

$$M_{CA} = 2K_2\theta_A - 6K_2\Delta/L_2 \quad \text{(C.2)}$$

$$M_{AE} = 4K_1\theta_A + 2K_1\theta_E \quad \text{(C.3)}$$

$$M_{EG} = 4K_5\theta_E - 6K_5\Delta/L_2 \quad \text{(C.4)}$$

$$M_{EA} = 2K_1\theta_A + 4K_1\theta_E \quad \text{(C.5)}$$

where: θ_A and θ_E are the joint rotations at A and E respectively,

K_1, K_2 and K_5 are the member stiffnesses shown in Figure C.1,

K_5 is adjusted for the number of floors above by multiplying by the number of floors above.

For joint equilibrium $M_{AC} + M_{AE} = 0$ and $M_{EA} + M_{EG} = 0$, hence:

$$4(K_1 + K_2)\theta_A + 2K_1\theta_E = 6K_2\Delta/L_2 \quad \text{(C.6)}$$

$$4(K_1 + K_5)\theta_E + 2K_1\theta_A = 6K_5\Delta/L_2 \quad \text{(C.7)}$$

Solving equations (C.6) and (C.7) gives:

$$\theta_A = \frac{6\Delta K_2(K_1 + K_5)/L_2 - 3\Delta K_5K_1/L_2}{4(K_1 + K_2)(K_1 + K_5) - K_1^2} \quad \text{(C.8)}$$

$$\theta_E = \frac{6\Delta K_5(K_1 + K_2)/L_2 - 3\Delta K_1K_2/L_2}{4(K_1 + K_2)(K_1 + K_5) - K_1^2} \quad \text{(C.9)}$$

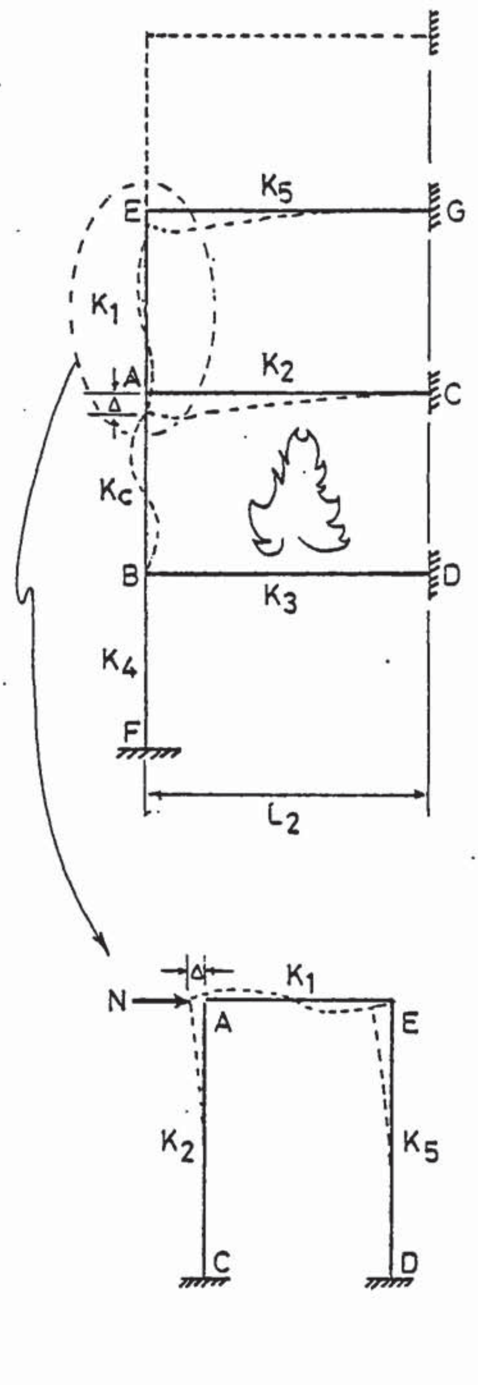

Figure C.1 Axial deformation of structural system.

For sway equilibrium:

$$(M_{CA} + M_{AC} + M_{EA} + M_{GE}) + NL_2 = 0 \tag{C.10}$$

hence,

$$2K_2\theta_A - 6\Delta K_2/L_2 + 4K_2\theta_A - 6\Delta K_2/L_2 + 2K_5\theta_E - 6\Delta K_5/L_2 + 4K_5\theta_E$$

$$\ldots\ldots\ldots - 6\Delta K_5/L_2 + NL_2 = 0 \tag{C.11}$$

Simplifying equation (C.11) gives:

$$6K_2\theta_A + 6K_5\theta_E - 12\Delta(K_1 + K_5)/L_2 + NL_2 = 0 \tag{C.12}$$

Substituting for θ_A and θ_E into equation (C.12) and rearranging yields the following equation:

$$N = \frac{12\Delta}{L_2^{\,2}}\left[\frac{K_2^2K_1/K_5 + K_2^2 + K_5K_1 + K_5K_2 + 3K_1^2K_2/K_5 + 3K_1^2 + 11K_1K_2}{4(K_1 + K_2)(K_1/K_5 + 1) - K_1^{\,2}/K_5}\right] \tag{C.13}$$

APPENDIX D

Plastic Analysis of Restraint System

D.1 Restraint System Column End A

Figure D.1 shows the frames analysed after formation of plastic hinges. Reference will be made to Case (a), Case (b), Case (c) and Case (d) which refer to Figure D.1 (a), Figure D.1 (b), (c) and (d) respectively.

D.1.1 Case (a)

From complimentary energy:

$$\Delta = \int m_0 m_1 ds/EI \tag{D.1}$$

$$\delta = \int m_0 m_2 ds/EI \tag{D.2}$$

$$\theta_1 = \int m_0 m_3 ds/EI \tag{D.3}$$

In the calculation of the rotation θ the force N due to sway is neglected since the slope deflection analysis described in Appendix B considers the sway to be zero. This is a small error as rotations due to sway are likely to be very small.

From consideration of Figure D.2 it can be seen that equation (D.1) can be expanded to:

$$\Delta = \int((m_0)_N m_1 + (m_0)_\omega m_1 + (m_0)_V m_1 + (m_0)_{Mu_3} m_1)ds/EI \tag{D.4}$$

Evaluating equation (D.4):

$$\Delta = (NL_2^3/3 - 5\omega L_2^4/48 + VL_2^3/12 - Mu_3 L_2^2/2)/N_{f1}E_1I_1 \tag{D.5}$$

where: N_{f1} is the number of floors above the column under analysis.

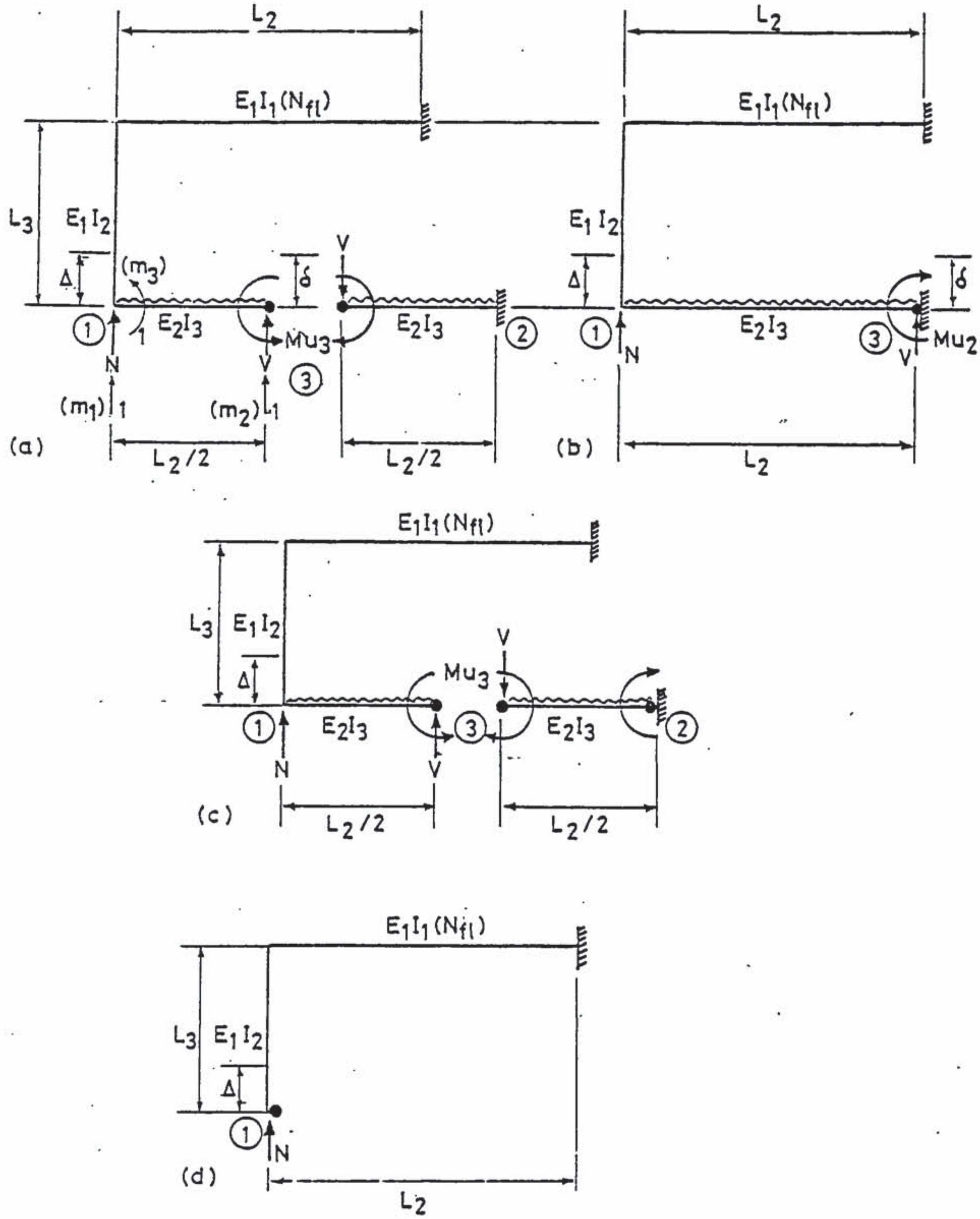

Figure D.1 Frames analysed for plastic analysis of restraint system column end A.

Rearranging:

$$N = 3N_{f1}\Delta E_1 I_1/L_2^3 + 5\omega L_2/16 - V/4 + 3Mu_3/2L_2 \qquad \text{(D.6)}$$

From consideration of Figure D.2 it can be seen that equation (D.2) can be expanded to:

$$\delta = \int((m_0)_N m_2 + (m_0)_\omega m_2 + (m_0)_V m_2 + (m_0)_{Mu_3} m_2)ds/EI \qquad \text{(D.7)}$$

Evaluating equation (D.7):

$$\delta = -\frac{NL_2^3}{12E_1I_1N_{f1}} - \omega\left(\frac{L_2^4}{128E_2I_3} + \frac{L_2^3L_3}{16E_1I_2} + \frac{L_2^4}{24E_1I_1N_{f1}}\right)$$
$$+ V\left(\frac{L_2^3}{24E_2I_3} + \frac{L_2^2L_3}{4E_1I_2} + \frac{L_2^3}{12E_1I_1N_{f1}}\right) + Mu_3\left(\frac{L_2^2}{8E_2I_3} + \frac{L_2L_3}{2E_1I_2}\right) \qquad \text{(D.8)}$$

A cantilever analysis is now carried out on the remaining structure, see Figure D.3. From standard deflection cases:

$$\delta = -\frac{VL_2^3}{24E_2I_3} - \frac{\omega L_2^4}{128E_2I_3} + \frac{Mu_3L_2^2}{8E_2I_3} \qquad \text{(D.9)}$$

Equating equations (D.8) and (D.9) yields the following equation:

$$V = \frac{-\dfrac{NL_2^3}{12E_1I_1N_{f1}} + \omega\left(\dfrac{L_2^3L_3}{16E_1I_2} + \dfrac{L_2^4}{24E_1I_1N_{f1}}\right) - \dfrac{Mu_3L_2L_3}{2E_1I_2}}{\dfrac{L_2^3}{12E_2I_3} + \dfrac{L_2^2L_3}{4E_1I_2} + \dfrac{L_2^3}{12E_1I_1N_{f1}}} \qquad \text{(D.10)}$$

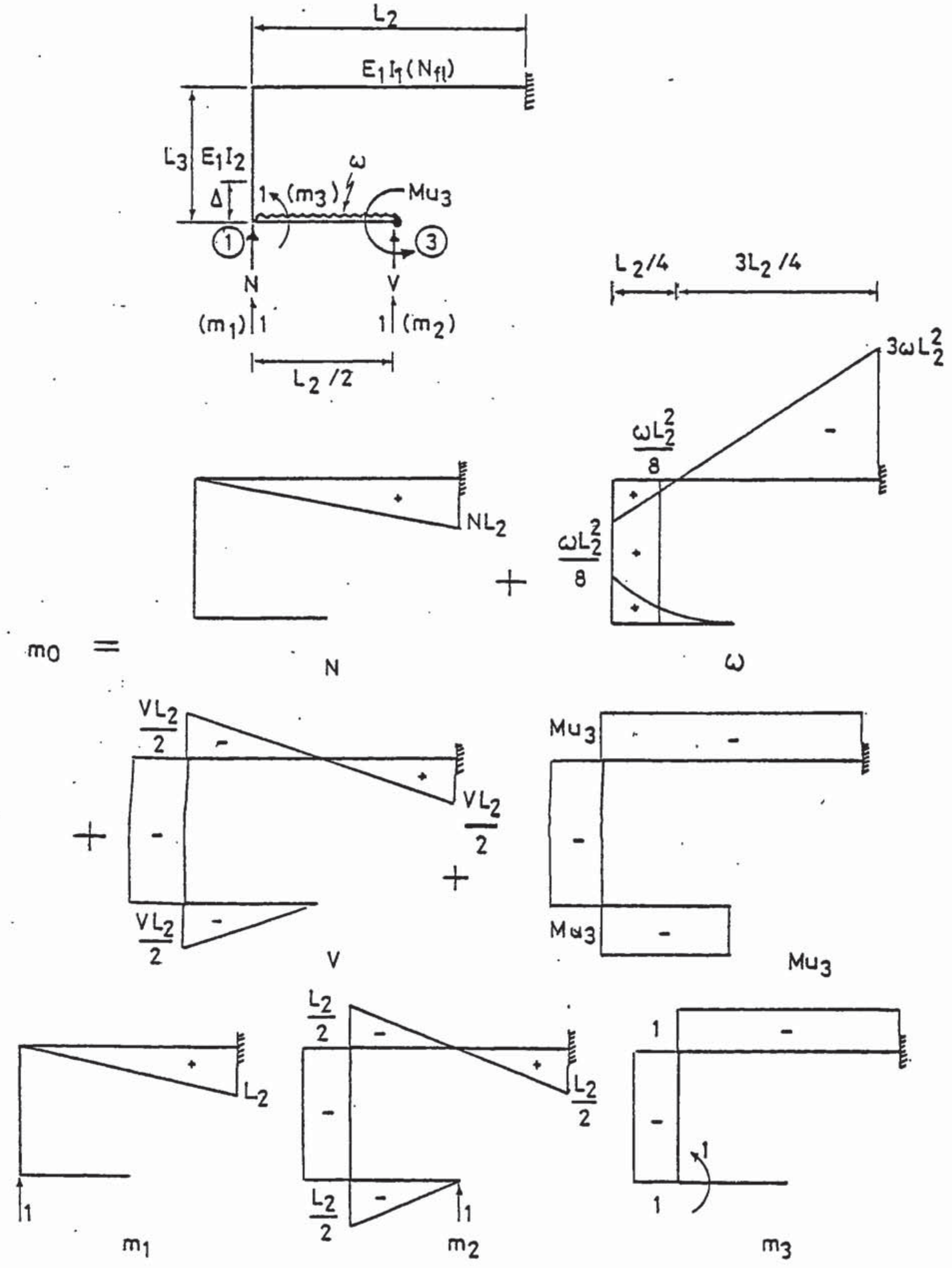

Figure D.2 Complimentary energy analysis Case (a).

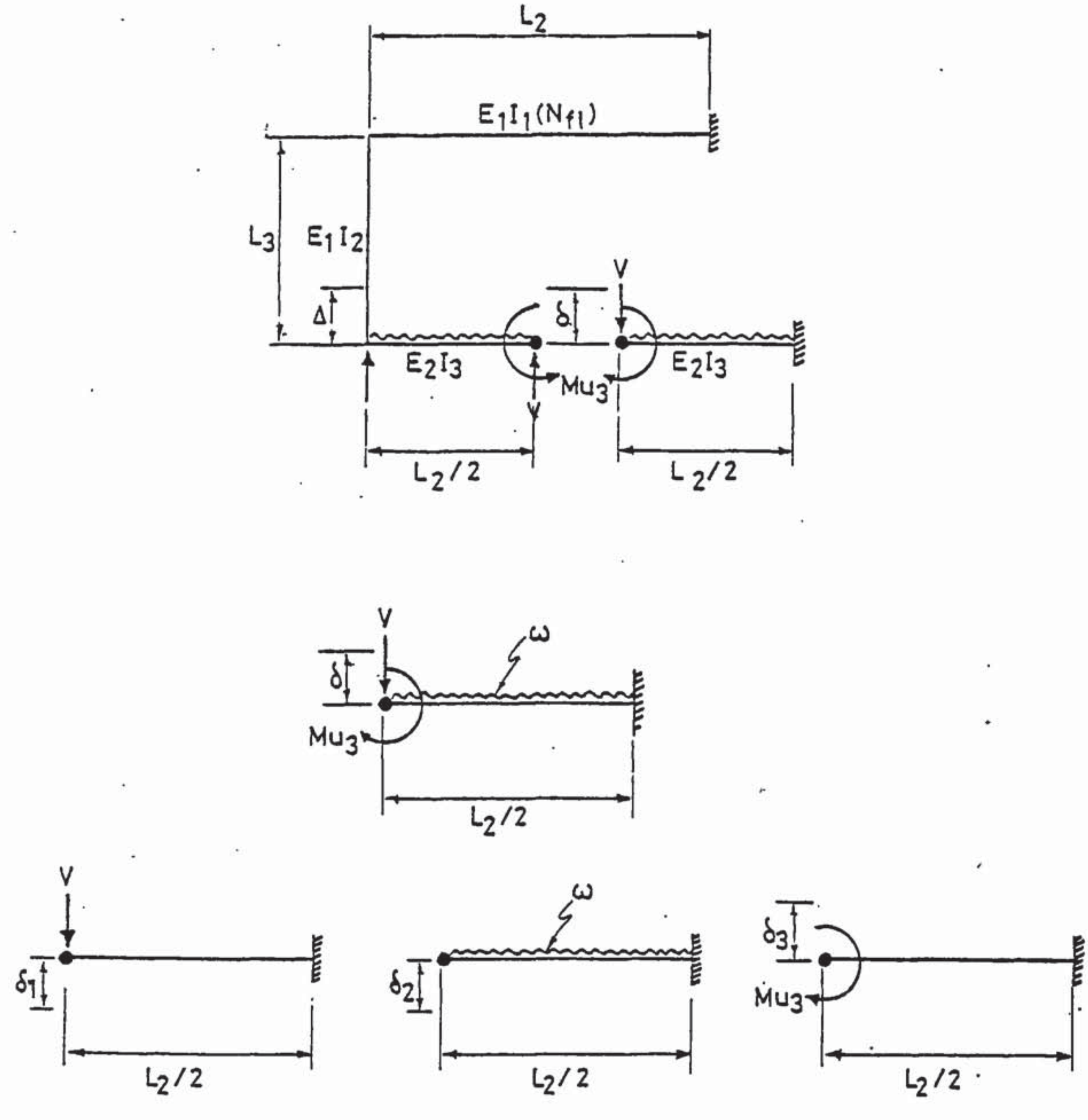

$$\delta = -\delta_1 - \delta_2 + \delta_3$$

$$\delta = -\frac{VL_2^3}{24E_2I_3} - \frac{\omega L_2^4}{128E_2I_3} + \frac{Mu_3L_2^2}{8E_2I_3}$$

Figure D.3 Cantilever analysis for Case (a).

Substituting equation (D.10) into equation (D.6) gives:

$$N = \frac{\Delta\left(\frac{N_{f1}E_1I_1}{E_2I_3} + \frac{3L_3I_1N_{f1}}{L_2I_2} + 1\right) + \omega\left(\frac{5L_2^4}{48E_2I_3} + \frac{L_2^3L_3}{4E_1I_2} + \frac{L_2^4}{16N_{f1}E_1I_1}\right) \cdots\cdots + Mu_3\left(\frac{2L_2L_3}{E_1I_2} + \frac{L_2^2}{2E_1I_1N_{f1}} + \frac{L_2^2}{2E_2I_3}\right)}{\frac{L_2^3}{3E_2I_3} + \frac{L_2L_3^2}{E_1I_2} + \frac{L_2^3}{4E_1I_1N_{f1}}} \qquad \text{(D.11)}$$

From consideration of Figure D.2 it can be seen that equation (D.3) can be expanded to:

$$\theta'_1 = \int(\cancel{(m_0)_N m_3} + (m_0)_\omega m_3 + (m_0)_V m_3 + (m_0)_{Mu_3} m_3)\,ds/EI \qquad \text{(D.12)}$$

consider no sway for calculation of rotation

Evaluating equation (D.12):

$$\theta'_1 = \omega\left(\frac{L_2^3}{8E_1I_1N_{f1}} - \frac{L_2^2L_3}{8E_1I_2}\right) + \frac{VL_2L_3}{2E_1I_2} + Mu_3\left(\frac{L_3}{E_1I_2} + \frac{L_2}{E_1I_1N_{f1}}\right) \qquad \text{(D.13)}$$

Substituting for V from equations (D.10) and (D.11) will yield θ'_1.

From statics the moment at position 1 is given by:

$$M_1 = - Mu_3 + \omega L_2^2/8 - VL_2/2 \qquad \text{(D.14)}$$

If $M_1 > Mu_1$ then a further hinge has formed and the plastic analysis Case (d) must be followed, where Mu_1 is the ultimate moment capacity at position 1 (see Figure D.1).

The effective reduced member stiffness of the beam segment 1 2 (originally K_2) is determined from the following:

$$K_2' = 0.5M_1/\theta_1 \tag{D.15}$$

The moment at position 2 of the equivalent cantilever segment is given by:

$$M_2 = -\ Mu_3 + VL_2/2 + \omega L_2^2/8 \tag{D.16}$$

If $M_2 > Mu_2$ then a further hinge has formed and the plastic analysis Case (c) must be followed, where Mu_2 is the ultimate moment capacity at position 2 (see Figure D.1).

D.1.2 <u>Case (c)</u>

From complimentary energy:

$$\Delta = \int m_0 m_1 ds/EI \tag{D.17}$$

$$\delta = \int m_0 m_2 ds/EI = 0 \tag{D.18}$$

$$\theta_1 = \int m_0 m_3 ds/EI \tag{D.19}$$

From consideration of Figure D.4 it can be seen that equation (D.17) can be expanded to:

$$\Delta = \int((m_0)_N m_1 + (m_0)_\omega m_1 + (m_0)_V m_1 + (m_0)_{Mu_2})ds/EI \tag{D.20}$$

evaluating equation (D.20):

$$\Delta = (NL_2^3/3 - \omega L_2^4/12 - VL_2^3/6 + Mu_2 L_2^2/2)/E_1 I_1 N_{f1} \tag{D.21}$$

rearranging for V:

$$V = -\ 6E_1 I_1 N_{f1}\Delta/L_2^3 + 2N - \omega L_2/4 + 3Mu_2/L_2 \tag{D.22}$$

From consideration of Figure D.4 it can be seen that equation (D.18) can be expanded to:

$$0 = \int((m_0)_N m_2 + (m_0)_\omega m_2 + (m_0)_V m_2 + (m_0)_{Mu_2} m_2)ds/EI \tag{D.23}$$

Evaluating equation (D.23):

$$0 = -\frac{NL_2^3}{6E_1I_1N_{f1}} - \omega\left(\frac{L_2^4}{8E_2I_3} + \frac{L_2^3L_3}{2E_1I_2} + \frac{L_2^4}{12E_1I_1N_{f1}}\right) + V\left(\frac{L_2^2L_3}{E_1I_2} + \frac{L_2^3}{3E_1I_1N_{f1}} + \frac{L_2^3}{3E_2I_3}\right) - Mu_2\left(\frac{L_2^2}{2E_2I_3} + \frac{L_2L_3}{E_1I_2} + \frac{L_2^2}{2E_1I_1N_{f1}}\right) \tag{D.24}$$

Substituting for V from equation (D.22) into equation (D.24) and rearranging gives the following equation:

$$N = \frac{\omega\left(\frac{7L_2^4}{24E_2I_3} + \frac{L_2^3L_3}{E_1I_2} + \frac{L_2^4}{4E_1I_1N_{f1}}\right) - Mu_2\left(\frac{2L_2L_3}{E_1I_2} + \frac{L_2^2}{2E_1I_1N_{f1}} + \frac{L_2^2}{2E_2I_3}\right) \ldots\ldots\ldots + \Delta\left(\frac{6L_3I_1N_{f1}}{L_1I_2} + 2 + \frac{2E_1I_1N_{f1}}{E_2I_3}\right)}{\frac{2L_2^2L_3}{E_1I_2} + \frac{L_2^3}{2E_1I_1N_{f1}} + \frac{2L_2^3}{3E_2I_3}} \tag{D.25}$$

From consideration of Figure D.4 it can be seen that equation (D.19) can be expanded to:

$$\theta_1 = \int((m_0)_\omega m_3 + (m_0)_V m_3 + (m_0)_{Mu_2} m_3)ds/EI \tag{D.26}$$

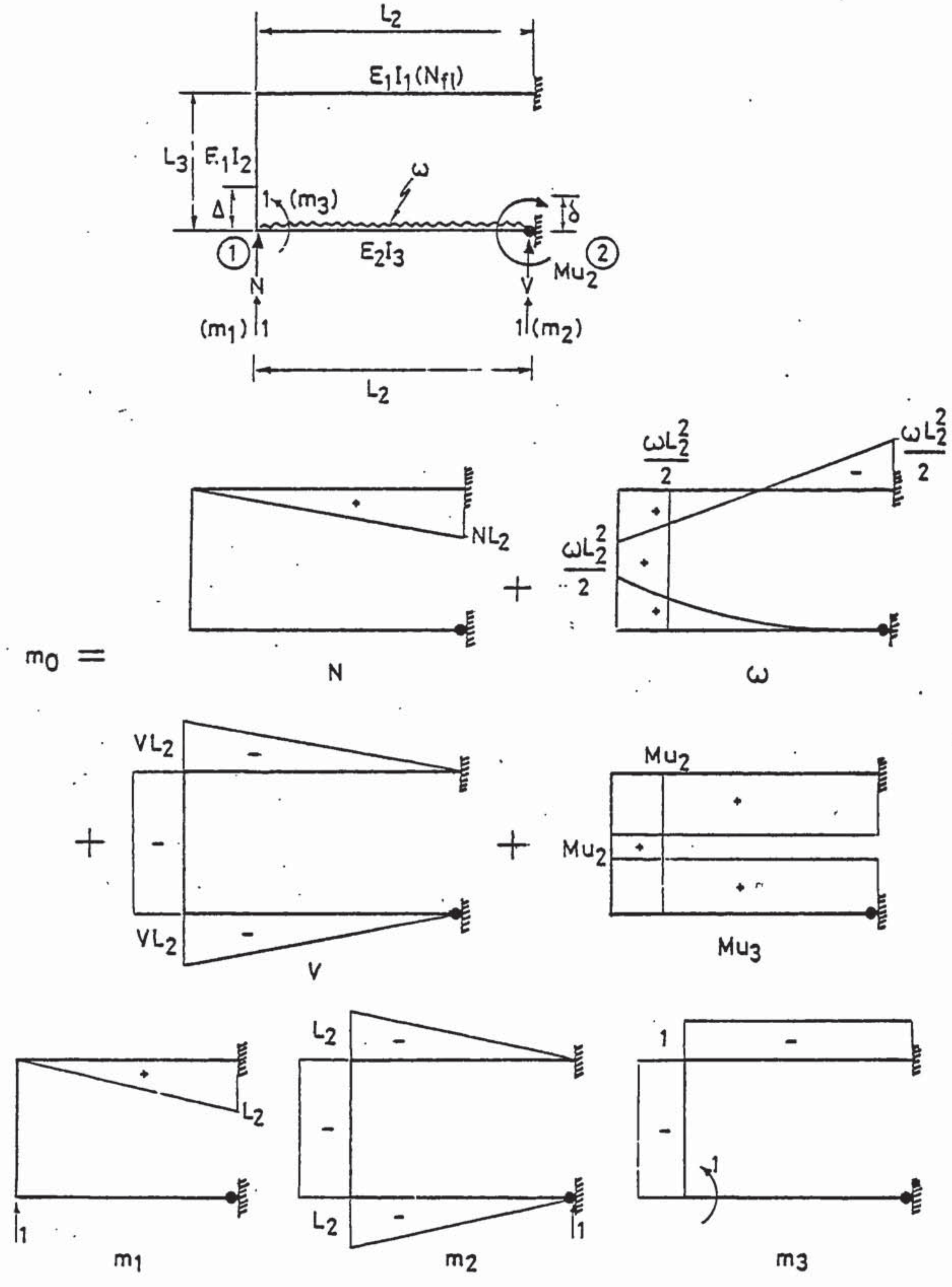

Figure D.4 Complimentary energy analysis Case (b).

Evaluating equation (D.26):

$$\theta_1 = -\omega\left(\frac{L_2^2 L_3}{2E_1I_2}\right) + V\left(\frac{L_2L_3}{E_1I_2} + \frac{L_2^2}{2E_1I_1N_{f1}}\right) - Mu_2\left(\frac{L_2}{E_1I_2} + \frac{L_2}{E_1I_1N_{f1}}\right) \tag{D.27}$$

The moment at position 1 using statics is given by:

$$M_1 = \omega L_2^2/2 + Mu_2 - VL_2 \tag{D.28}$$

The effective reduced member stiffness of the beam segment 1 2 (originally K_2) is determined using equation (D.15) only M_1 and θ_1 are from equations (D.27) and (D.26) respectively.

The moment at position 3 using statics is given by:

$$M_3 = \omega L_2^2/8 + Mu_2 - VL_2/2 \tag{D.29}$$

If $M_3 > Mu_3$ then a further hinge has formed and the plastic analysis Case (c) must be followed, where Mu_3 is the ultimate moment capacity at position 3.

D.1.3 Case (c)

The complimentary energy analysis described in Case (a) is repeated, however, from consideration of Figure D.5 it can be seen that the equivalent cantilever from Case (a) now has an extra hinge and is therefore equivalent to a simply supported beam.

From simple beam analysis (taking moments about position 2):

$$V = 2(Mu_2 + Mu_3 - \omega L_2^2/8)/L_2 \tag{D.30}$$

Substituting for V from equation (D.30) into equation (D.6) gives:

$$N = \frac{3E_1I_1N_{f1}\Delta}{L_2^{\,3}} + \frac{5L_2\omega}{16} + \frac{1}{2L_2}(Mu_2 + Mu_3 - \omega L_2^2/8) + \frac{3Mu_3}{2L_2} \qquad (D.31)$$

The effective reduced member stiffness of the beam segment is calculated according to equations (D.15). M_1 is also checked to see whether it exceeds Mu_1 as previously described, using equation (D.14).

D.1.4 Case (d)

From consideration of Figure D.6 it can be seen that the axial force N is resisted by a structure equivalent to a cantilever. From the standard deflection case:

$$\Delta = \frac{NL_2^3}{3E_1I_1N_{f1}} \qquad (D.32)$$

and rearranging:

$$N = 3E_1I_1N_{f1}\Delta/L_2^3 \qquad (D.33)$$

The effective stiffness of the original beam AC (beam segment 1 3 2) is now zero:

$$K_2' = 0 \qquad (D.34)$$

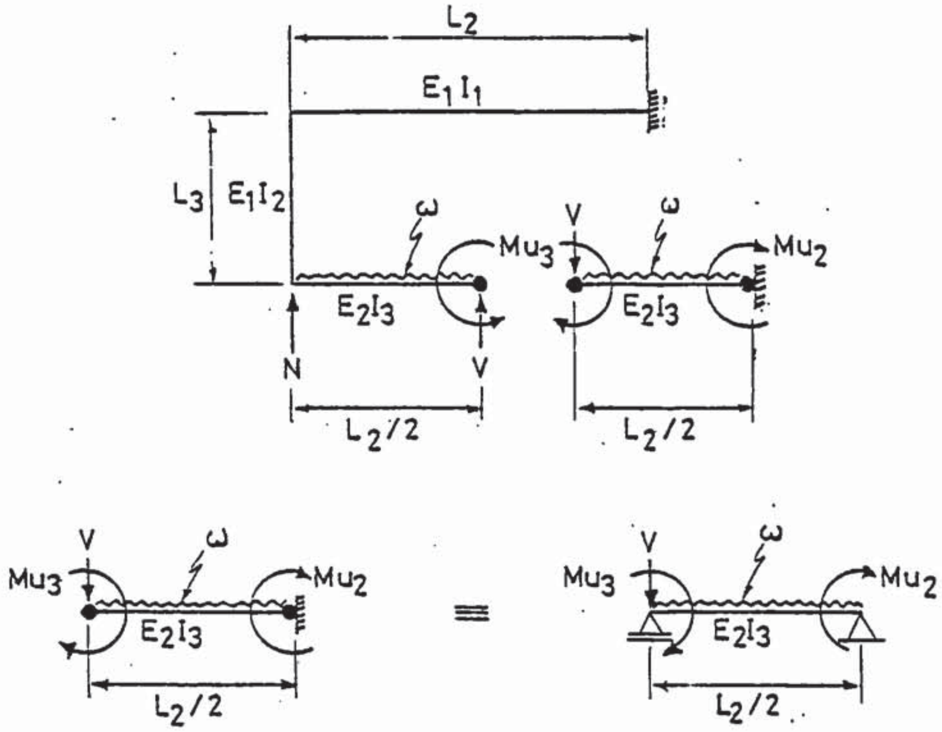

Figure D.5 Simple beam analysis for Case (c).

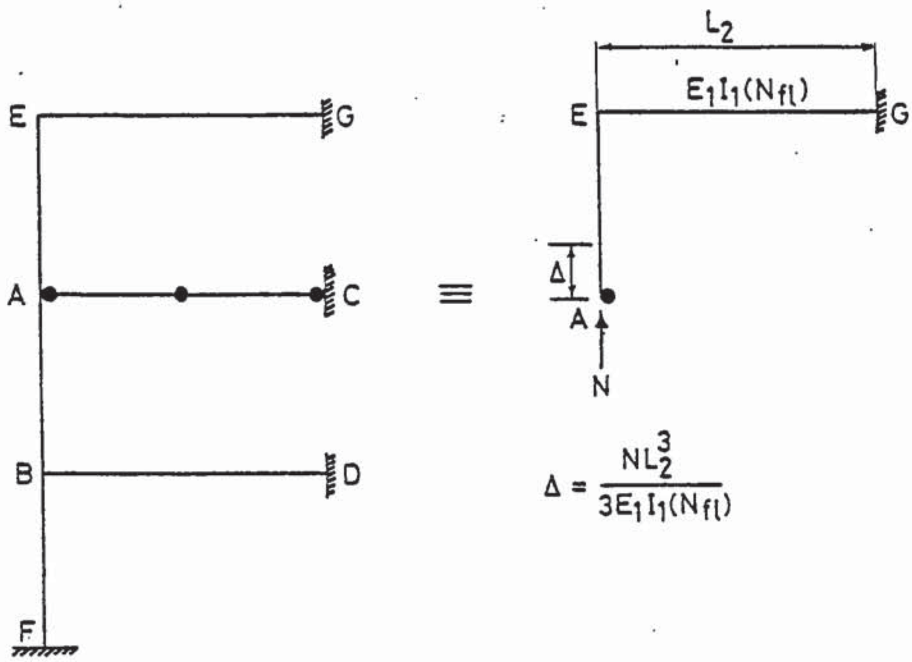

Figure D.6 Equivalent cantilever analysis for Case (d).

D.2 Restraint System Column End B

Figure D.7 shows the frames analysed after formation of plastic hinges in the restraint system at column end B. Reference will be made to Case (e), Case (f) and Case (g) which refer to Figure D.7 (e), (f) and (g) respectively.

D.2.1 Case (e)

From complimentary energy:

$$\delta = \int m_0 m_1 ds/EI = 0 \tag{D.35}$$

$$\theta_4 = \int m_0 m_2 ds/EI \tag{D.36}$$

From consideration of Figure D.8 it can be seen that equation (D.35) can be expanded to:

$$\delta = 0 = \int((m_0)_\omega m_1 + (m_0)_V m_1 + (m_0)_{Mu_5} m_1) ds/EI \tag{D.37}$$

Evaluating equation (D.37):

$$0 = -\omega\left(\frac{L_2^4}{8E_3I_4} + \frac{L_2^3L_4}{2E_1I_2}\right) + V\left(\frac{L_2^3}{3E_3I_4} + \frac{L_2^2L_4}{E_1I_2}\right) - Mu_5\left(\frac{L_2^2}{2E_3I_4} + \frac{L_2L_4}{E_1I_2}\right) \tag{D.38}$$

rearranging for V gives:

$$V = \frac{\omega\left(\frac{L_2^4}{8E_3I_4} + \frac{L_2^3L_4}{2E_1I_2}\right) + Mu_5\left(\frac{L_2^2}{2E_3I_4} + \frac{L_2L_4}{E_1I_2}\right)}{\frac{L_2^3}{3E_3I_4} + \frac{L_2^2L_4}{E_1I_2}} \tag{D.39}$$

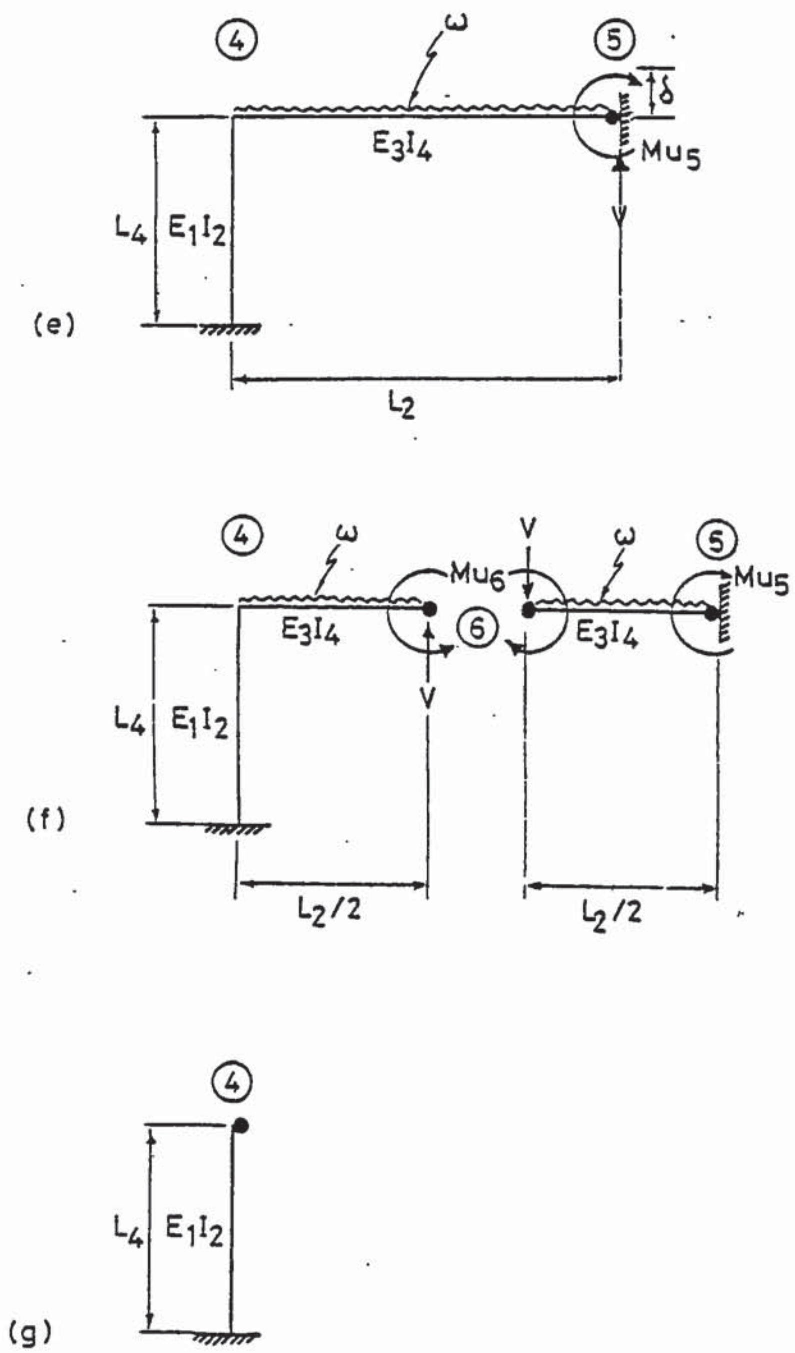

Figure D.7 Frames analysed for plastic analysis of restraint system column end B.

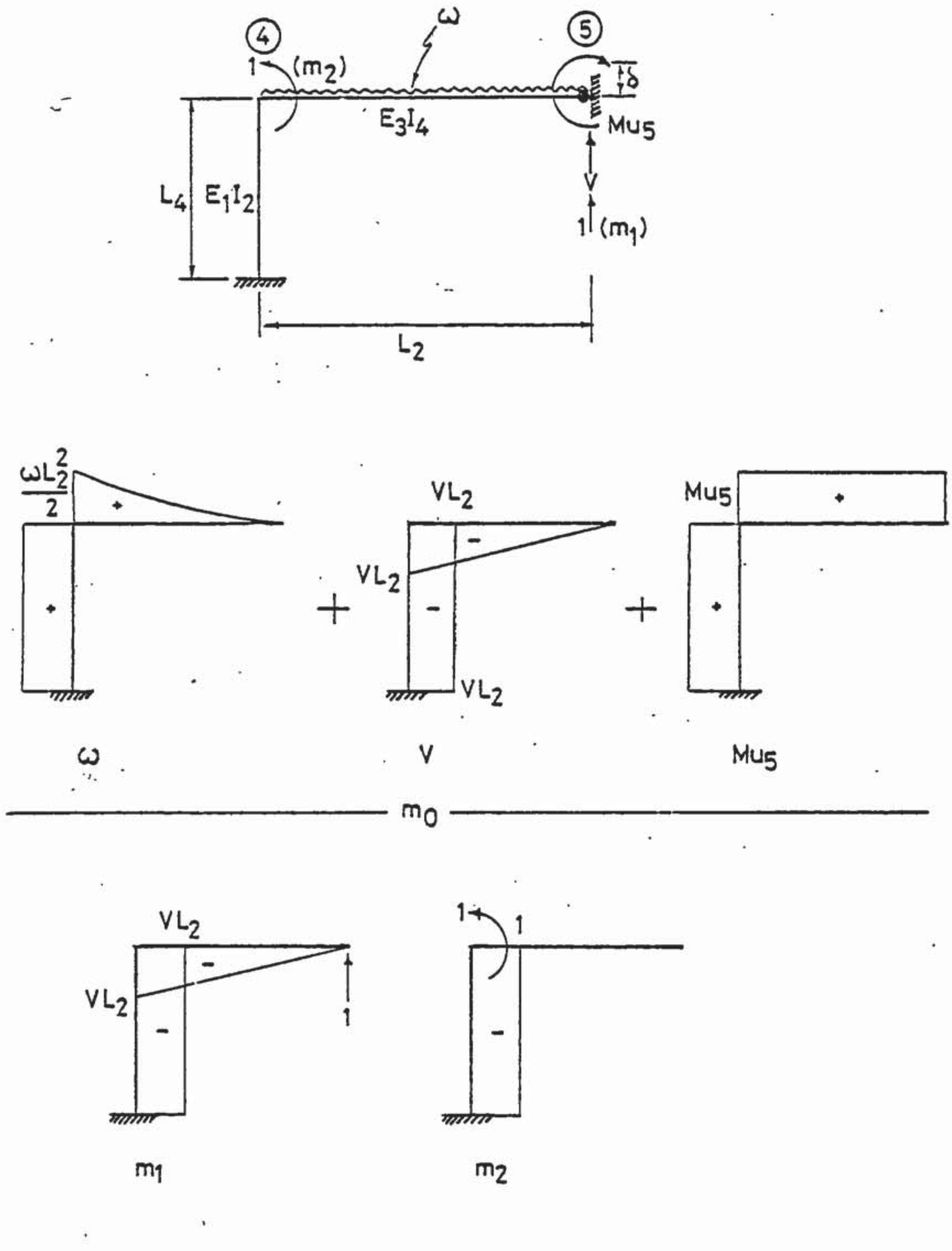

Figure D.8 Complimentary energy analysis Case (e).

From consideration of Figure D.8 it can be seen that equation (D.36) can be expanded to:

$$\theta_4 = \int((m_0)_{\omega}m_2 + (m_0)_V m_2 + (m_0)_{Mu_5}m_2)ds/EI \tag{D.40}$$

Evaluating equation (D.40):

$$\theta_4 = (VL_2L_4 - Mu_5L_4 - \omega L_2^2L_4/2)/E_1I_2 \tag{D.41}$$

Substituting for V from equation (D.39) will yield θ_4.

The moment at position 4 using statics is given by:

$$M_4 = \omega L_2^2/2 + Mu_5 - VL_2 \tag{D.42}$$

The moment at midspan, postion 6, using statics is given by:

$$M_6 = \omega L_2^2/8 + Mu_5 - VL_2/2 \tag{D.43}$$

If $M_6 > Mu_6$ then the plastic analysis described in Case (f) must be followed, where Mu_6 is the ultimate moment capacity at position 6.

The reduced effective stiffness of the beam segment 4 5 (originally K_3) is determined from:

$$K_3' = 0.5M_4/\theta_4 \tag{D.44}$$

D.2.2 <u>Case (f)</u>

From consideration of Figure D.9 it can be seen that V can be found from statics alone:

$$V = 2Mu_5/L_2 - \omega L_2/4 - 2Mu_6/L_2 \tag{D.45}$$

The moment at position 4 using statics is given by:

$$M_4 = \omega L_2^2/8 - Mu_6 - VL_2/2 \tag{D.46}$$

If $M_4 > Mu_4$ then the plastic analysis described in Case (g) must be followed, where Mu_4 is the ultimate moment capacity at position 4.

Consider now Figure D.10. From complimentary energy:

$$\theta_4 = \int m_0 m_1 ds/EI \tag{D.47}$$

Equation (D.47) can be expanded to:

$$\theta_4 = \int((m_0)_\omega m_1 + (m_0)_V m_1 + (m_0)_{Mu_6} m_1)ds/EI \tag{D.48}$$

Evaluating equation (D.48):

$$\theta_4 = \frac{VL_2L_4}{2E_1I_2} - \frac{\omega L_2^2L_4}{8E_1I_2} + \frac{Mu_6L_4}{E_1I_2} \tag{D.49}$$

The reduced effective stiffness of the beam segment 4 6 (originally K_3) is determined using equation (D.44) only M_4 and θ_4 are taken from equations (D.46) and (D.47) respectively.

D.2.3 Case (g)

With three hinges in the restraint beam BD (4 6 5) the effective stiffness of the beam (originally K_3) is now zero:

$$K_3' = 0 \tag{D.50}$$

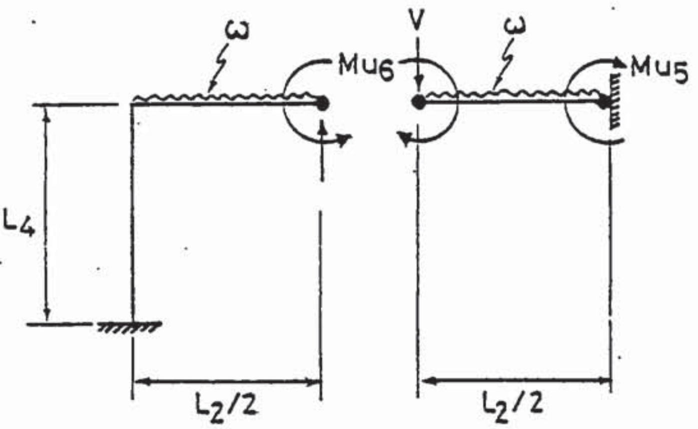

Figure D.9 Static analysis Case (f).

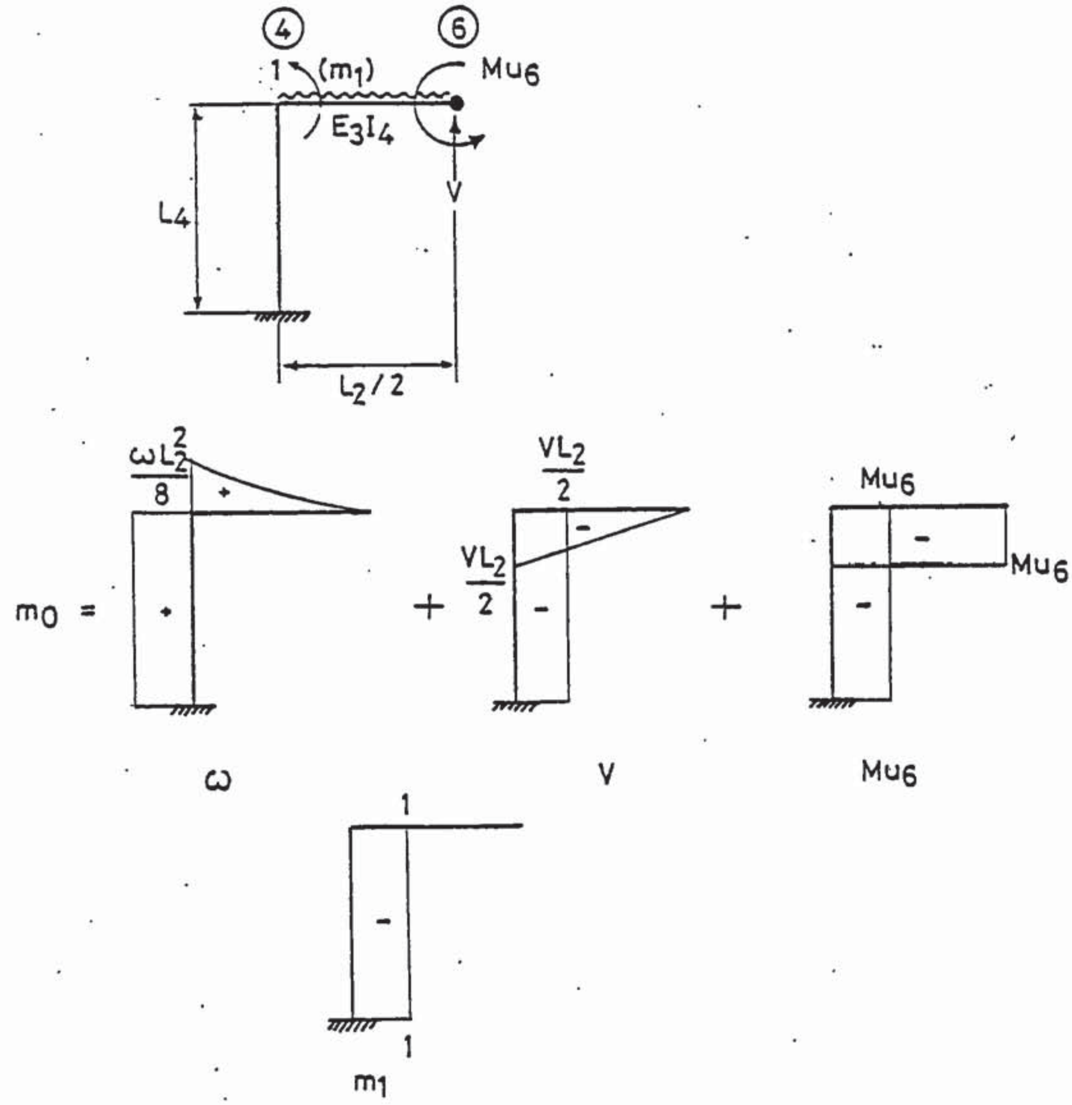

Figure D.10 Complimentary energy analysis Case (f).

APPENDIX E

Analysis of Pin Ended Column using Macaulay Method

Consider the pinned column element shown in Figure E.1 loaded by moments at its ends. Using Macaulay's method an expression can be obtained for the rotations in terms of the end moments:

$$M(x) = M_A - Vx \tag{E.1}$$

$$V = (M_A + M_B)/L \tag{E.2}$$

$$EId^2y/dx^2 = -M(x) = Vx - M_A \tag{E.3}$$

If the equation (E.3) is integrated once an expression for the slope can be obtained:

$$EIdy/dx = Vx^2/2 - M_Ax + A \tag{E.4}$$

Integrating again gives an expression for the deflections:

$$EIy = Vx^3/6 - M_Ax^2/2 + Ax + B \tag{E.5}$$

The arbitrary constants A and B are found using the boundary conditions y = 0 when x = 0 and x = L. The equation for slope therefore becomes:

$$\theta_{(x)} = (-M_Ax + (M_A + M_B)x^2/2L + M_AL/2 - (M_A + M_B)/6L)/EI \qquad (E.6)$$

The slope at the ends of the column are obtained by substituting x = 0 and x = L in equation (E.6):

$$\theta_A = (M_AL/3 - M_BL/6)/EI \qquad (E.6)$$

$$\theta_B = (M_BL/3 - M_AL/6)/EI \qquad (E.7)$$

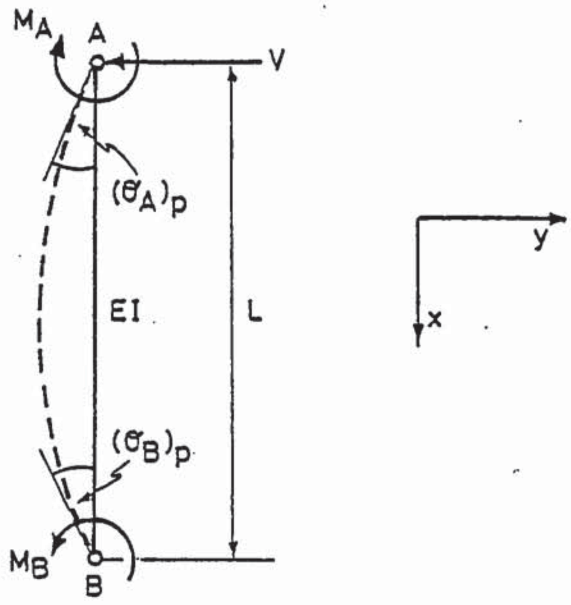

Figure E.1 Pin ended column element.

APPENDIX F

Lateral Deflections due to Column End Moments and Axial Force Eccentricities

The lateral column deflections are calculated from the solution of the differential equation below:

$$EId^2y/dx^2 = -M - Py \tag{F.1}$$

or rearranging equation (F.2) gives:

$$d^2y/dx^2 + Py/EI = -M/EI \tag{F.2}$$

From consideration of Figure F.1 it can be seen that:

$$M = M_A - (M_A + M_B)x/L \tag{F.3}$$

where: L is the length of the column.

Substituting equation (F.3) into equation (F.2) gives rise to the following equation:

$$d^2y/dx^2 + Py/EI = -(M_A - (M_A + M_B)x/L)/EI \tag{F.4}$$

the solution of which is:

$$y = A\sin\alpha x + B\cos\alpha x - M_A/EI\alpha^2 + (M_A + M_B)x/EI\alpha^2L \tag{F.5}$$

Using the boundary conditions y = 0 at x = 0 and x = L gives:

$$B = M_A/EI\alpha^2 \tag{F.6}$$

$$A = -M_A(\cot\alpha L)/EI\alpha^2 - M_B/(\sin\alpha L)EI\alpha^2 \tag{F.7}$$

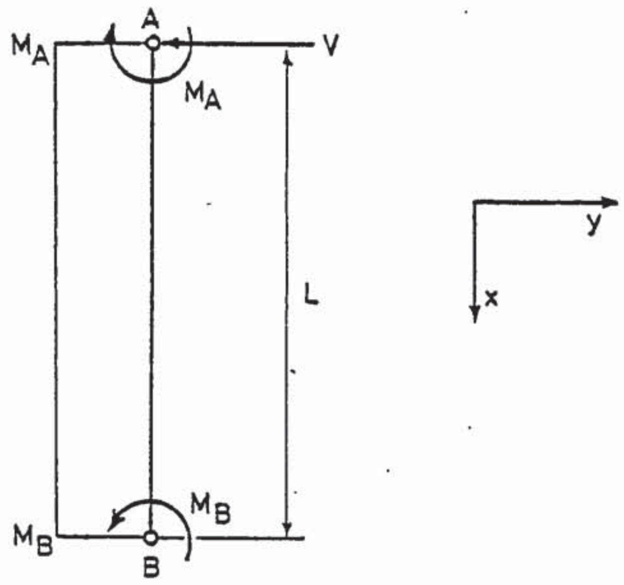

$V = (M_A + M_B)/L$

Figure F.1 Column system analysed for calculation of lateral deflections.

The complete equation for the determination of lateral deflections is:

$$y = -\frac{1}{EI\alpha^2}(M_A \cot\alpha L + \frac{M_B}{\sin\alpha L})\sin\alpha x + \frac{M_A}{EI\alpha^2}\cos\alpha x - \frac{M_A}{EI\alpha^2}$$

$$\text{........} + (\frac{M_A + M_B}{EI\alpha^2})(\frac{x}{L}) \qquad \text{(F.8)}$$

where: $\alpha^2 = P/EI$.

APPENDIX G

Change in Division Point Deflections Corresponding to a Change in End Slope

Consider the pinned column element shown in Figure G.1 loaded by one moment at its end. Using Macaulay's method an expression can be obtained for the change in division point deflections corresponding to a change in end slope:

$$M(x) = M_A - Vx \qquad (G.1)$$

$$V = M_A/L \qquad (G.2)$$

$$EId^2y/dx^2 = -M(x) = Vx - M_A \qquad (G.3)$$

If the equation (G.3) is integrated once an expression for the slope can be obtained:

$$EIdy/dx = Vx^2 - M_Ax + A \qquad (G.4)$$

Integrating again gives an expression for the deflections:

$$EIy = Vx^3/6 - M_Ax^2 + Ax + B \qquad (G.5)$$

The arbitrary constants A and B are found using the boundary conditions y = 0 when x = 0 and x = L. The equations for deflections and slopes become:

$$y_{(X)} = (M_Ax^3/6L - M_Ax^2/2 + M_ALx/3)/EI \qquad (G.6)$$

$$dy/dx \text{ or } \theta_{(x)} = (M_Ax^2/2L - M_Ax + M_AL/3)EI \qquad (G.7)$$

The slope at the ends of the column are obtained by substituting x = 0 and x = L into equation (G.7):

$$\theta_A = M_AL/3EI \qquad (G.8)$$

$$\theta_B = - M_AL/6EI \qquad (G.9)$$

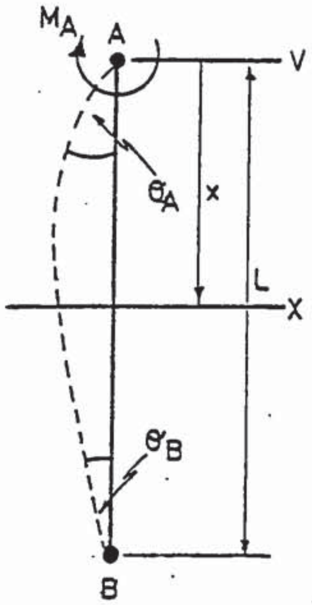

Figure G.1 Pin ended column element.

Rearranging equation (G.8) gives:

$$M_A = 3\theta_A EI/L \tag{G.10}$$

and rearranging equation (G.7) gives:

$$y = M_A(x^3/6L - x^2/2 + Lx/3)/EI \tag{G.11}$$

Substituting equation (G.10) into (G.11) yields the expression:

$$y_{(x)} = 3\theta_A(x^3/6L - x^2/2 + Lx/3)/L \tag{G.12}$$

and the change in deflections corresponding to a change in end slope are obtained from the equation:

$$\partial y_{(x)} = 3\partial\theta_A(x^3/6L - x^2/2 + Lx/3)/L \tag{G.13}$$

APPENDIX H

Steel Creep Paramters

The creep parameters employed in equations (8.28) to (8.32) may be expressed as follows:

$$Z = A\sigma^{B} \qquad \text{for } \sigma \leqslant \bar{\sigma} \tag{H.1}$$

$$Z \text{ in hours}^{-1}$$

$$Z = Ce^{D\sigma} \qquad \text{for } \sigma > \bar{\sigma} \tag{H.2}$$

$$\varepsilon_{cro} = E\sigma^{F} \tag{H.3}$$

where: σ is the steel stress in N/mm^2,

A, B, C, D, E, F and $\bar{\sigma}$ are empirical constants.

The terms A to F and σ as well as the $\Delta H/R$ term are defined in Table G.1 for several reinforcing steels. The values for K_s40 ∅ 10, K_s40 ∅ 8 and K_s60 ∅ 8 steels are from Anderberg (1978), and for ASTM A421 and A36 steels are from Harmathy and Stanzack (1970).

STEEL TYPE	Ks40 ∅ 10	Ks40 ∅ 8	Ks60 ∅ 8	ASTM A421	ASTM A36
A	6.96×10^{10}	4.58×10^{7}	5.11×10^{7}	1.95×10^{8}	3.27×10^{12}
B	4.70	4.72	2.93	8.0	4.7
C	2.58×10^{18}	7.5×10^{14}	1.59×10^{16}	8.21×10^{13}	1.23×10^{16}
D	0.0443	0.512	0.0313	0.0145	0.1392
E	2.85×10^{-8}	3.39×10^{-7}	2.06×10^{-6}	9.26×10^{-5}	3.02×10^{-5}
F	1.037	0.531	0.439	0.67	1.75
$\bar{\sigma}$	84	90	90	172	104
$\Delta H/R$	45000	40000	40000	30560	38900

Ks40 = 40kgf/cm^2 where 1kgf/cm^2 = 9.81 N/mm^2

A421 = 50×10^3 lb/in^2 = 350 N/mm^2

A36 = 42.5×10^3 lb/in^2 = 300 N/mm^2

Table H.1 Empirical constants used in equations (H.1) to (H.3) for several reinforcing steels.

APPENDIX I

GLOSSARY OF COMPUTER NOTATION

A(150)	column elemental areas
AID(2,2,20)	cross sectional stiffness matrix for each division point
AL(100)	restraint beam section elemental areas
ALPHA	allowable axial force incompatability
ALPHA1	modular ratio
ALPHA2	modular ratio
ALROD	allowable rate of deflection
AM(2,2)	current sectional stiffness
AMBEC	initial concrete modulus of elasticity at ambient conditions
AMBTEMP	ambient temperature
AMID(100)	restraint beam section elemental areas at midspan
AMULT1	ultimate moment capacity at position 1 for restraint beam A
AMULT2	ultimate moment capacity at position 2 for restraint beam A
AMULT3	ultimate moment capacity at position 3 for restraint beam A
ASC	area of compression steel
ASCAB	area of steel in column above
ASCMID	area of compression steel in restraint beam at midspan
ASCOL	area of steel in column under analysis
ASCOW	area of steel in column below
ASCSUP	area of compression steel in restraint beam at support
ASUP(100)	restraint beam section elemental areas at support
AST	area of tension steel

AT(150,65) /LCM/ *	column section elemental temperatures for each time step
ATL(100)	current restraint beam section elemental temperatures
ATMIDA(100,65) /LCM/	section elemental temperatures of restraint beam A at midspan
ATMIDB(100,65) /LCM/	section elemental temperatures of restraint beam B at midspan
ATSUPA(100,65) /LCM/	section elemental temperatures of restraint beam A at support
ATSUPB(100,65) /LCM/	section elemental temperatures of restraint beam B at support
B	breadth of restraint beam
BC	breadth of column
BETA	allowable incompatability in moments
BMULT1	ultimate moment capacity at position 1 for restraint beam B
BMULT2	ultimate moment capacity at position 2 for restraint beam B
BMULT3	ultimate moment capacity at position 3 for restraint beam B
C(20)	division point deflections under zero load
CIS(20)	change in slope at division points
COLAB	length of column above
COLLEN	length of column under analysis
COLOW	length of column below
CS(150,20) /LCM/	accumulated elemental shrinkage strain
CTES	steel coefficient of thermal expansion
CURP(20)	proposed curvatures
CURV(20)	calculated curvatures

---

* /LCM/ denotes the array is stored in large core memory

DC	depth of column
DCOL	axial deformation
DCURV(20)	change in curvature
DIFF(2,2)	partial differentials
DMR(20)	change in division point bending moments
D1	concrete cover + half bar diameter for column above
D2	concrete cover + half bar diameter for column under analysis
D3	concrete cover + half bar diameter for column below
EBEAMA1	average elastic modulus of restraint beam A at position 1
EBEAMA3	average elastic modulus of restraint beam A at position 3
EBEAMB1	average elastic modulus of restraint beam B at position 1
EBEAMB3	average elastic modulus of restraint beam B at position 3
ECCEN	axial load eccentricity
ECREEP	elemental creep strain
EFFD	effective depth of restraint beam section
EM	peak strain
EMUO	peak strain at ambient conditions
EO(150,20) /LCM/	strain from previous time step
ESHRIN	elemental shrinkage strain
ET(150,20) /LCM/	creep strain from previous time step for concrete elements or cumulative incremental creep strain for steel elements
ETHERM	elemental thermal strain

ETRANS	elemental transient strain
EYA	allowable incompatability in division point deflections
EYC(20)	calculated incompatabilities in division point deflections
E1	allowable incompatability in end slope A
E2	allowable incompatability in end slope B
FEMA	fixed end moment at column end A
FEMB	fixed end moment at column end B
FIRSTRN(150,20) /LCM/	total elemental fire strains
GA	gusset length end A
GB	gusset length end B
GUS	vertical height of deflected gusset lengths
H1	calculated maximum incompatability in deflections from previous time step
IBUG	debug option
IC	system iteration counter
IDIVPT	number of division points
IPLASA1	plastic hinge indicator for restraint beam A at position 1
IPLASA2	plastic hinge indicator for restraint beam A at position 2
IPLASA3	plastic hinge indicator for restraint beam A at position 3
IPLASB1	plastic hinge indicator for restraint beam B at position 1
IPLASB2	plastic hinge indicator for restraint beam B at position 2
IPLASB3	plastic hinge indicator for restraint beam B at position 3
IPLCOLA	plastic hinge indicator for column above
IPLCOLB	plastic hinge indicator for column below

IRESTA	option for temperature dependent restraint system end A
IRESTB	option for temperature dependent restraint system end B
ISECO	option for second order effects
ISHIN	option for shrinkage model
IT	indicator for new iteration or column failure
ITF(150,20) /LCM/	indicator for elemental tensile failure
ITFC(150,20) /LCM/	indicator for elemental tensile failure for current iteration
ITITLE(80)	title of computer job run
ITYRAXA	option for type of axial restraint
ITYROTA	option for type of rotational restraint column end A
ITYROTB	option for type of rotational restraint column end B
IXTYPE	restraint beam cross section type
MLTYPE(100)	material type for restraint beam elements
MMTYPE(150)	material type for column elements
MTYPE	element material type
MTYPMID(100)	material type for restraint beam elements at midspan
MTYPSUP(100)	material type for restraint beam elements at support
NFILE	device number for filed output
NFL	number of floors above column under analysis
NIN	device number for data input
NOUT	device number for printed output
NUMEL	number of column elements

NUMMID	number of restraint beam elements at midspan
NUMSEG	number of column segments
NUMSUP	number of restraint beam elements at support
NUMTIM	number of time steps
OVERD	overall depth of restraint beam section
P	axial load
PAB	axial load from structure above
PYC(20)	division point deflections calculated from previous time step
RC(100)	convergence array
ROD(20)	rate of deflection
RSL	length of restraint beam
SCUO	concrete strength at ambient conditions
SEGLEN(20)	column segment lengths
SLEG(20)	column segment lengths at start of analysis
SLOA	calculated end slope end A
SLOB	calculated end slope end B
SLOP	end slope
SLOPA	proposed end slope end A
SLOPB	proposed end slope end B
SLOPE1	slope of moment-rotation relation end A
SLOPE2	slope of moment-rotation relation end B
SM	concrete peak stress
SO(150,20) /LCM/	elemental stress from previous time step
STRAIN(150,20) /LCM/	elemental stress related strain
STRAP(20)	direct strain at column axis

STRESS(150,20) /LCM/	elemental stress
STRNCR(150,20)	elemental creep strains
STRNSH(150)	elemental shrinkage strains
STRNTH(150)	elemental thermal strains
STRNTR(150,20)	elemental transient strains
TEMP	elemental temperature
TEMPEM(8)	temperature values corresponding to concrete peak strain values
TEMPES(8)	temperature values corresponding to steel coefficient of thermal expansion values
TEMPFY(8)	temperature values corresponding to steel yield stress values
TEMPI	initial temperature of column
TEMPILA	initial temperature of restraint beam end A
TEMPILB	initial temperature of restraint beam end B
TEMPMOD(8)	temperature values corresponding to steel elasticity modulus
TEMPSM(8)	temperature values corresponding to concrete peak stress values
TENSTR(150,20) /LCM/	value of strain giving zero stress on unload line
TIME(65)	time elapsed at each time step
TOTSTRN(150,20) /LCM/	total elemental strain
TR(150,20) /LCM/	transient strain history
UDLA	uniformly distributed load on restraint beam at column end A
UDLB	uniformly distributed load on restraint beam at column end B
ULTSTRN	ultimate permissible concrete strain
VALEM(8)	values of concrete peak strain

VALES(8)	values of steel coefficient of thermal expansion
VALFY(8)	values of steel yield stress
VALMOD(8)	values of steel elasticity modulus
VALSM(8)	values of concrete peak stress
XNA	depth to neutral axis from extreme compression fibre
YC(20)	calculated division point deflections
YP(20)	proposed division point deflections
YT(20)	store for division point deflections
YY(150)	distance of column elemental centroids from centroid of section
YYL(100)	distance of restraint beam elemental centroids from reference point
YYMID(100)	distance of restraint beam elemental centroids from top of beam at midspan
YYSUP(100)	distance of restraint beam elemental centroids from top of beam at support
ZI	second moment of area of section
ZIC	second moment of area of column section under analysis
ZIMID	second moment of area of restraint beam section at midspan
ZINC(2,1)	values of incompatabilities
ZISUP	second moment of area of restraint beam section at support
ZI1	second moment of area of column above
ZI2	second moment of area of restraint beam at column end A
ZI3	second moment of area of restraint beam at column end B
ZI4	second moment of area of column below
ZK1	stiffness of column above

COMPUTER NOTATION (Cont.)

ZK2	stiffness of restraint beam column end A
ZK3	stiffness of restraint beam column end B
ZK4	stiffness of column below
ZMA	column end moment at A
ZMB	column end moment at B
ZMR(20)	division point bending moments
ZMUBS2	ultimate moment capacity for section of restraint beam end A with bottom steel
ZMUBS3	ultimate moment capacity for section of restraint beam end B with bottom steel
ZMUTS2	ultimate moment capacity for section of restraint beam end A with top steel
ZMUTS3	ultimate moment capacity for section of restraint beam end B with top steel
ZMU1	ultimate moment capacity of column above
ZMU4	ultimate moment capacity of column below

APPENDIX J

Sample Design Calculations

The following sample design calculations are for the structural system with a 6 m column exposed to fire, 16 m restraint beam and 3 floors above, see Chapter 12.

Assume 6 m frame spacing.

Total ultimate load = 1.4 x dead load + 1.6 x live load

Approximate dead weight due to columns:

$$0.40 \times 0.40 \times 2400 \times 9.81 / 1000 = 3.75 \text{ kN/m} \qquad \text{(dead load)}$$

Approximate dead weight due to beam and slab:

$$(\underbrace{(0.40 \times 0.80)}_{\text{beam}} + \underbrace{(0.15 \times 6)}_{\text{slab}}) \times 2400 \times 9.81 / 1000 = 29 \text{ kN/m} \quad \text{(dead load)}$$

Live load for general office use from BS6399 $= 2.5 \text{ kN/m}^2$

$= 2.5 \times 6 = 15 \text{ kN/m}$

Ultimate load on restraint beam span:

$$1.4 \times 29 + 1.6 \times 15 = 64 \text{ kN/m}$$

Working load on restraint beam span:

$$29 + 15 = 44 \text{ kN/m}$$

Column size: 400 x 400 mm

Restraint beam size: 400 x 800 mm

Use $f_{cu} = 40 \text{ N/mm}^2$

$f_y = 460 \text{ N/mm}^2$ (use 425 N/mm^2 design graphs from CP110)

Design caclulations are carried out for live + dead ultimate load on both bottom and top restraint beams, and then checked against the condition of live + dead ultimate load on the top restraint beam and only dead ultimate load on the bottom restraint beam, see Figure J.1.

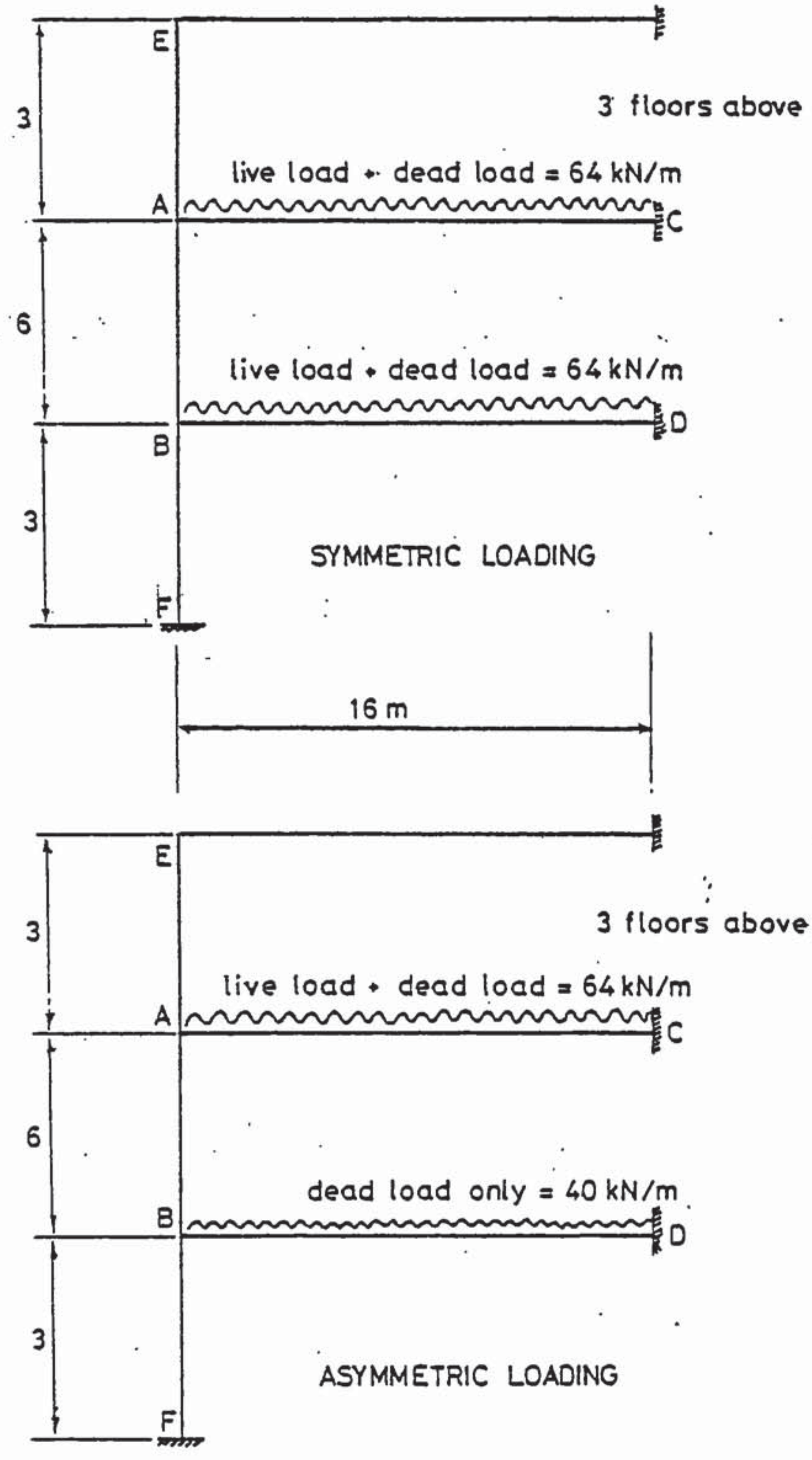

Figure J.1 Loading on structural system considered in design calculations.

Stiffnesses

$$\text{Column AB} = \frac{0.4 \times 0.4^3}{12} \times \frac{E}{6} = 3.55555 \times 10^{-4}E$$

$$\text{Column AE} = \frac{0.4 \times 0.4^3}{12} \times \frac{E}{3} = 7.11111 \times 10^{-4}E$$

$$\text{Column BF} = \frac{0.4 \times 0.4^3}{12} \times \frac{E}{3} = 7.11111 \times 10^{-4}E$$

$$\text{Beam AC} = \frac{0.4 \times 0.8^3}{12} \times \frac{E}{16} = 10.66666 \times 10^{-4}E$$

$$\text{Beam BD} = \frac{0.4 \times 0.8^3}{12} \times \frac{E}{16} = 10.66666 \times 10^{-4}E$$

Assume under working load restraint beam is cracked therefore take half the stiffness as an approximation.

$$K_{AC} = K_{BD} = 5.33333 \times 10^{-4}$$

Column Design

Effective Length (CP110)

$$\alpha_{c,min} = \frac{(3.55555 \times 10^{-4} + 7.11111 \times 10^{-4})}{5.33333 \times 10^{-4}} = 2.0$$

l_e = lesser of $6(0.7 + 0.05(2 + 2)) = 5.4$

or $6(0.85 + (0.005 \times 2)) = \underline{5.16}$

$l_e/b = 5.16/0.4 = 12.9 > 12$ therefore column is slender

Fixed end moment on beam for symmetrical loading:

$$M_{ac} = M_{ca} = M_{bd} = M_{db} = 64 \times 16^2 / 12 = 1356 \text{ kNm}$$

From equation (B.9) $\theta_A = -191953.49/E$

$\theta_B = -191953.49/E$

From equation (B.3) $M_A = -409$ kNm

$M_B = -409$ kNm

Axial load due to shear of moments from equation (B.16) = 38 kN

Dead weight of columns = 1.4 x ((3 x 3) + 6) x 3.75 = 78.75 kN

Dead weight of restraint beams and slabs for floors above:

(3 + 1) x 1.4 x 29 x 16 / 2 = 1299.2 kN

TOTAL DEAD LOAD = 1299.2 + 78.75 = 1377.95 kN

Live load (3 floors above - allowable reduction factor 20% (BS6399))

0.8 x (3 + 1) x 1.6 x 15 x 16 / 2 = 614.4 kN

TOTAL AXIAL LOAD = 1377.95 + 614.4 + 38 = 2030 kN

Additional moment (CP110) for slender column K = 1:

$$M_{add} = \frac{2030 \times 0.4}{1750}\left[\frac{5.16}{0.4}\right]^2\left[1 - 0.0035\frac{5.16}{0.4}\right] = 74\text{kNm}$$

TOTAL MOMENT = 409 + 74 = 483 kNm

Design Chart 84 (CP110)

$M_t/bh^2 = 483 \times 10^6 / 400^3 = 7.55$

and $N/bh = 2030 \times 10^3 / 400^2 = 12.69$

gives $100A_s/bd = 5.2$

therefore $A_s = 5.2 \times 400 \times 4 = 8320 \text{ mm}^2$

Factor K (CP110)

$N_{uz} = 0.45 \times 40 \times 400 \times 400 + 0.75 \times 425 \times 8320 = 5532000$ N

$N = 2030 \times 10^3$ N

$$N_{bal} = 0.45 \times 40 \left[1 - \frac{\sqrt{40}}{3 \times 17.6}\right]\frac{7}{11} \times 0.9 \times 400 \times 400 = 1451877.5$$

$$K = \frac{5532000 - 2030 \times 10^3}{5532000 - 1451877.5} = 0.86$$

Adjust additional moment $M_{add} = 0.86 \times 74 = 64$kNm

TOTAL MOMENT = 409 + 64 + 473 kNm

Design Chart 84 (CP110)

$M_t/bh^2 = 473 \times 10^6 / 400^3 = 7.4$ and $N/bh = 12.69$

gives $100A_s/bd$ 4.75

therefore $A_s = 4.75 \times 400 \times 4 = 7600 \text{ mm}^2$

Factor K (CP110)

$$N_{uz} = 0.45 \times 40 \times 400 \times 400 + 0.75 \times 425 \times 7600 = 5302500 \text{ N}$$

$$K = \frac{5302500 - 2030 \times 10^3}{5302500 - 1451877.5} = 0.85 \quad \text{(previously 0.86)}$$

therefore use steel area 7600 mm^2

Use 6 x 40 mm diameter bars (steel area 7540 mm^2)

Note that 7540 < 7600 this is acceptable since f_y of 460 N/mm^2 will be used and design graphs are based on f_y of 425 N/mm^2.

Design of Restraint Beam

From equation (B.2) $M_{AC} = 965$ kNm

From equation (B.14) $M_{CA} = 1570$ kNm

from equation (6.8) moment at midspan = 785 kNm

Beam Design at Supports

Use design moment of 1570 kNm

Effective depth = depth - cover - steel diameter/2

Assuming a bar diameter of 32 mm and the cover 40 mm:

effective depth = 800 - 40 - 15 = 745 mm

Hence $M/bd^2 = 1570 \times 10^6 / 400 \times 745^2 = 7.07$

Design Chart 39 (CP110) (doubly reinforced beam)

for $100A_s'/bd$ (compression steel) = 0.5 and $M/bd^2 = 7.07$

$100A_s/bd$ (tension steel) = 2.50

Therefore compression steel A_s' = $0.5 \times 400 \times 7.45$ = $1490\ mm^2$

try 2 x 32 mm diameter bars ($1608\ mm^2$)

tension steel As = $2.5 \times 400 \times 7.45$ = $7540\ mm^2$

try 6 x 40 mm diameter bars ($7540\ mm^2$)

Beam Design at Midspan

Design moment = 785 kNm

$M/bd^2 = 785 \times 10^6 / 400 \times 745^2 = 3.53$

Design Chart 3 (CP110) (Singly reinforced beams)

$100A_s/bd = 1.07$ hence $A_s = 1.07 \times 400 \times 7.45 = 3188\ mm^2$

use 4 x 32 mm diameter bars ($3217\ mm^2$)

Redesign Beam at Support

Now redesign beam at support for 4 x 32 mm diameter bars for compression steel:

$100A_s'/bd = 100 \times 3217 / 400 \times 7.45 = 1.08$

Design Chart 39 (CP110)

$M/bd^2 = 7.07$ and $100A_s' = 1.08$ gives $100A_s/bd = 2.1$

therefore $A_s = 2.1 \times 400 \times 7.45 = 6258\ mm^2$

use 8 x 32 mm diameter bars ($6434\ mm^2$)

Hence at support use 8 x 32 mm dia. bars for tension reinforcement
and 4 x 32 mm dia. bars for compresn. reinforcement
at midspan use 4 x 32 mm dia. bars for tension reinforcement
and 2 x 32 mm dia. bars for compresn. reinforcement
(to support shear links)

Now check design for asymmetric loading i.e. live load and dead load on the top restraint beam and dead load only on the bottom restraint beam.

Fixed end moment beam AC: $M_{ac} = M_{ca} = 64 \times 16^2 / 12 = 1365$ kNm

Fixed end moment beam BD: $M_{bd} = M_{db} = 1.4 \times 29 \times 16^2 / 12$

$= 866$kNm

From equation (B.9) $\theta_A = -200724.98/E$

$\theta_B = -113099.99/E$

From equation (B.3) $M_A = -366$ kNm

$M_B = -304$ kNm

Column Design

For asymmetric loading M_A and M_B are less than M_A and M_B for symmetric loading. Dead load and live load acting on the fire exposed column is the same as that for the symmetric loading. Hence the column design from the symmetrical loading is acceptable.

Restraint Beam Design

From equation (B.2) $M_{AC} = 937$ kNm $M_{BD} = 625$ kNm (956 kNm)

From equation (B.14) $M_{CA} = 1579$ kNm $M_{DB} = 986$ kNm (1570 kNm)

From equation (6.8) $M_{mid} = 790$ kNm $M_{mid} = 494$ kNm (785 kNm)

The majority of the moments calculated above for the restraint beam corresponding to asymmetric loading are less than those calculated for symmetric loading (shown in parentheses). The moments that are greater in value exhibit only a small increase which will be covered by the fact that the area of steel actually used is greater than that directly calculated from the moments. Therefore the restraint beam design for the symmetric loading is acceptable.

APPENDIX K

The following listing is the operational version of the computer program SAFE-RCC as of October, 1985. Although the program has been tested, no warranty is made regarding its accuracy or reliability, and no responsibility is assumed in this respect.

```
      PROGRAM SAFERCC(INPUT,OUTPUT,TAPE1=INPUT,TAPE2=OUTPUT)
C
C     ****************************************
C     *                                      *
C     * SAFE-RCC                             *
C     *                                      *
C     * STRUCTURAL ANALYSIS OF FIRE EXPOSED  *
C     * REINFORCED CONCRETE COLUMNS          *
C     *                                      *
C     ****************************************
C
      COMMON /CONTROL/ NIN,NOUT,NFILE,ITITLE(80)
      COMMON /LCM/ AT(150,65),STRAIN(150,20),
     .             STRESS(150,20),ITFC(150,20),EO(150,20),
     .             ET(150,20),ITF(150,20),CS(150,20),SO(150,20),
     .             TOTSTRN(150,20),TR(150,20),TENSTR(150,20),
     .             ATMIDA(100,65),ATMIDB(100,65),
     .             ATSUPA(100,65),ATSUPB(100,65),
     .             FIRSTRN(150,20)
      LEVEL 2,/LCM/
C
      DIMENSION SEGLEN (20),C(20),YP(20),STRAP(20),CURP(20),
     .          PYC(20),ROD(20),YY(150),A(150),HMTYPE(150),
     .          VALES(8),VALEM(8),VALSM(8),VALFY(8),
     .          VALMOD(8),TEMPES(8),TEMPEM(8),TEMPSM(8),
     .          TEMPFY(8),TEMPMOD(8),TIME(70),MLTYPE(100),YYL(100),
     .          AL(100),ATL(100),FN(8),TN(8),RC(100),AMID(100),
     .          ZMR(20),AM(2,2),ZINC(2,1),CURV(20),ASUP(100),
     .          CIS(20),SLEG(20),SLOP(20),YYMID(100),YYSUP(100),
     .          MTYPMID(100),MTYPSUP(100),
     .          YT(20),YC(20),DMR(20),CH(2,1),DCURV(20),
     .          STRNTH(150),STRNTR(150,20),STRNCR(150,20),STRNSH(150),
     .          DIFF(2,2),EYC(20),AID(2,2,20)
C
C     CONTROL SEGMENT OF PROGRAM CALLS SUBROUTINES AS
C     REQUIRED AND READS DATA NECCESSARY FOR THE
C     DIMENSION OF ARRAYS
C
      NIN=1
      NOUT=2
      NFILE=6
C
      READ (NIN,275) ITITLE
C
C     DEBUG OPTION
C
C     - 0 NO DEBUG OPTION
C     - 1 LOW LEVEL DEBUG OPTION
C     - 2 HIGH LEVEL DEBUG OPTION
C
      READ (NIN,285) IBUG
C
C     NUMBER OF SEGMENT LENGTHS
C
      READ (NIN,285) NUMSEG
C
C     NUMBER OF DIVISION POINTS
C
      IDIVPT=NUMSEG+1
C
C     NUMBER OF ELEMENTS OF COLUMN CROSS SECTION
C
      READ (NIN,285) NUMEL
C
C     NUMBER OF LAYERS OF RESTRAINT SYSTEM CROSS SECTION
C     AT MIDSPAN
C
      READ (NIN,285) NUMMID
C
C     NUMBER OF LAYERS OF RESTRAINT SYSTEM CROSS SECTION
C     AT SUPPORT
C
      READ (NIN,285) NUMSUP
C
C     NUMBER OF TIME STEPS INCLUDING INITIAL TIME
C
      READ (NIN,285) NUMTIM
C
      WRITE (NOUT,300)
      WRITE (NOUT,310)
      WRITE (NOUT,320)
      WRITE (NOUT,325)
      WRITE (NOUT,330)
      WRITE (NOUT,335)
      WRITE (NOUT,340)
      WRITE (NOUT,345)
      WRITE (NOUT,350)
      WRITE (NOUT,360)
      WRITE (NOUT,370)
      WRITE (NOUT,380)
      WRITE (NOUT,390)
      WRITE (NOUT,310)
      WRITE (NOUT,400) ITITLE
      WRITE (NOUT,310)
C
C     INPUT ISECO
C
C     1 FOR SECOND ORDER EFFECTS
C     0 FOR NO SECOND ORDER EFFECTS
C
      READ (NIN,285) ISECO
C
C     INPUT ISHIN
C
C     - 1 FOR SHRINKAGE MODEL
C     - 0 FOR NO SHRINKAGE
C
      READ (NIN,285) ISHIN
C
C     INPUT ITYROTA, ITYROTB - FOR END A AND B
C
```

```
C     - 0 FOR PINNED ROTATIONAL RESTRAINT
C     - 1 FOR NORMAL ROTATIONAL RESTRAINT
C     - 2 FOR FIXED ROTATIONAL RESTRAINT
C
      READ (NIN,290) ITYROTA,ITYROTB
C
C     INPUT ITYRAXA
C
C     - 0 FOR FREE AXIAL EXPANSION
C     - 1 FOR NORMAL AXIAL RESTRAINT
C     - 2 FOR FIXED AXIAL RESTRAINT
C
      READ (NIN,285) ITYRAXA
C
C     INPUT IRESTA, IRESTB - FOR END A AND END B
C
C     - 1 FOR TEMPERATURE DEPENDENT RESTRAINT SYSTEM
C     - 0 FOR TEMPERATURE INDEPENDENT RESTRAINT SYSTEM
C
      READ (NIN,290) IRESTA,IRESTB
C
C     TRANSFER INPUT OF DATA TO SUBROUTINE INPUT
C
      CALL INPUT (COLLEN,GA,GB,BC,DC,SEGLEN,PAB,ECCEN,C,
     .            UDLA,UDLB,YY,A,MMTYPE,NIT,ALPHA,BETA,E1,E2,
     .            EYA,TIME,VALES,VALEM,VALSM,VALFY,
     .            VALMOD,TEMPES,TEMPEM,TEMPSM,
     .            TEMPFY,TEMPMOD,D2,ASCOL,
     .            D1,ASCAB,D3,ASCOW,
     .            ASTSUP,ASCSUP,ASTMID,ASCMID,
     .            NUMMID,YYMID,AMID,MTYPMID,
     .            NUMSUP,YYSUP,ASUP,MTYPSUP,
     .            EFFD,B,OVERD,ITYROTA,ITYROTB,
     .            IRESTA,IRESTB,ITYRAXA,COLAB,COLOW,
     .            ZMU1,ZMUBS2,ZMUTS2,ZMU4,ZMUBS3,ZMUTS3,
     .            TEMPI,TEMPILA,TEMPILB,
     .            NFL,RSL,NUMSEG,NUMEL,IDIVPT,NUMTIM)
C
C     DEBUG OPTION
C
      IF (IBUG.EQ.0) GOTO 175
C
      WRITE (NOUT,900)
      WRITE (NOUT,275) ITITLE
      WRITE (NOUT,920) IBUG
      WRITE (NOUT,920) NUMSEG
      WRITE (NOUT,920) NUMEL
      WRITE (NOUT,920) NUMMID
      WRITE (NOUT,920) NUMSUP
      WRITE (NOUT,920) NUMTIM
      WRITE (NOUT,920) ISECO
      WRITE (NOUT,920) ISHIN
      WRITE (NOUT,930) ITYROTA,ITYROTB
      WRITE (NOUT,920) ITYRAXA
      WRITE (NOUT,930) IRESTA,IRESTB
      WRITE (NOUT,940) COLLEN,GA,GB
      WRITE (NOUT,950) BC,DC
      WRITE (NOUT,955) D2,ASCOL
      DO 100 I=1,NUMSEG
  100 WRITE (NOUT,960) I,SEGLEN(I)
      IF (ITYROTA.EQ.0.AND.ITYROTB.EQ.0) GOTO 105
      GOTO 110
  105 WRITE (NOUT,970) PAB,ECCEN
      GOTO 130
  110 WRITE (NOUT,980) PAB
      IF (ITYROTA.EQ.2.AND.ITYROTB.EQ.2) GOTO 130
      WRITE (NOUT,990) UDLA,UDLB
      WRITE (NOUT,950) COLAB,COLOW
      WRITE (NOUT,965) D1,ASCAB,D3,ASCOW
      WRITE (NOUT,975) ASTSUP,ASCSUP,ASTMID,ASCMID
      WRITE (NOUT,1030) EFFD,B,OVERD,RSL,NFL
      WRITE (NOUT,1020) ZMU1,ZMU4,ZMUBS2,ZMUTS2,ZMUBS3,ZMUTS3
  130 WRITE (NOUT,1040) NIT,ALPHA,BETA,E1,E2,EYA
      DO 135 I=1,IDIVPT
  135 WRITE (NOUT,1050) I,C(I)
      DO 140 I=1,NUMEL
  140 WRITE (NOUT,1060) I,YY(I),A(I),MMTYPE(I)
      IF (IRESTA.NE.1.AND.IRESTB.NE.1) GOTO 150
      DO 145 I=1,NUMMID
  145 WRITE (NOUT,1060) I,YYMID(I),AMID(I),MTYPMID(I)
      DO 146 I=1,NUMSUP
  146 WRITE (NOUT,1060) I,YYSUP(I),ASUP(I),MTYPSUP(I)
  150 WRITE (NOUT,1070) (TEMPES(I),VALES(I),I=1,8)
      WRITE (NOUT,1070) (TEMPEM(I),VALEM(I),I=1,8)
      WRITE (NOUT,1070) (TEMPSM(I),VALSM(I),I=1,8)
      WRITE (NOUT,1070) (TEMPFY(I),VALFY(I),I=1,8)
      WRITE (NOUT,1070) (TEMPMOD(I),VALMOD(I),I=1,8)
      WRITE (NOUT,1080) TIME(1)
      WRITE (NOUT,985) TEMPI
      DO 155 I=2,NUMTIM
      WRITE (NOUT,1080) TIME(I)
  155 WRITE (NOUT,1090) (J,AT(J,I),J=1,NUMEL)
      IF (IRESTA.NE.1) GOTO 165
      WRITE (NOUT,985) TEMPILA
      DO 160 I=2,NUMTIM
  160 WRITE (NOUT,1090) (J,ATMIDA(J,I),J=1,NUMMID)
      DO 161 I=2,NUMTIM
  161 WRITE (NOUT,1090) (J,ATSUPA(J,I),J=1,NUMSUP)
  165 IF (IRESTB.NE.1) GOTO 175
      WRITE (NOUT,985) TEMPILB
      DO 170 I=2,NUMTIM
  170 WRITE (NOUT,1090) (J,ATMIDB(J,I),J=1,NUMMID)
      DO 171 I=2,NUMTIM
  171 WRITE (NOUT,1090) (J,ATSUPB(J,I),J=1,NUMSUP)
C
  175 CONTINUE
C
C     CALCULATE PROPOSED VALUES TO START ANALYSIS
C
      CALL PROPOSE (ITYROTA,ITYROTB,TEMPEM,VALEM,TEMPSM,VALSM,
     .              BC,DC,COLLEN,COLAB,COLOW,B,OVERD,RSL,
     .              UDLA,UDLB,PAB,ECCEN,GA,IDIVPT,YP,CURP,
```

```
     .          [illegible],STIRRP,SLOPE1,SLOPE2,
     .          FEMA,FEMB,AMBEC,EFFD,ZI1,ZI2,ZI3,ZI4,
     .          ASCAB,D1,ASCOW,D3,
     .          ASTSUP,ASCSUP,ASTMID,ASCMID,
     .          TEMPMOD,VALMOD,TEMPFY,VALFY,ASCOL,D2,
     .          SLOPA,SLOPB,ZMA,ZMB,P,SEGLEN,NUMSEG,C)
C
      WRITE (NOUT,410)
      WRITE (NOUT,310)
      WRITE (NOUT,420)
      WRITE (NOUT,275) ITITLE
      WRITE (NOUT,430)
      WRITE (NOUT,310)
      WRITE (NOUT,435)
      WRITE (NOUT,455) BC,DC
      WRITE (NOUT,445) COLLEN
      WRITE (NOUT,465) GA
      WRITE (NOUT,475) GB
      WRITE (NOUT,440) NUMSEG
      WRITE (NOUT,450) NUMEL
      WRITE (NOUT,470)
      WRITE (NOUT,480) P
      IF (ITYROTA.EQ.0.AND.ITYROTB.EQ.0) WRITE (NOUT,485) ECCEN
      WRITE (NOUT,490) ZMA
      WRITE (NOUT,500) ZMB
      IF (ISECO.EQ.1) WRITE (NOUT,505)
      IF (ISHIN.EQ.1) WRITE (NOUT,510)
      IF (ISECO.EQ.0) WRITE (NOUT,520)
      IF (ISHIN.EQ.0) WRITE (NOUT,530)
      WRITE (NOUT,540)
      IF (ITYROTA.EQ.0) WRITE (NOUT,550)
      IF (ITYROTA.EQ.1) WRITE (NOUT,560)
      IF (ITYROTA.EQ.2) WRITE (NOUT,570)
      IF (ITYRAXA.EQ.0) WRITE (NOUT,580)
      IF (ITYRAXA.EQ.1) WRITE (NOUT,590)
      IF (ITYRAXA.EQ.2) WRITE (NOUT,600)
      IF (IRESTA.EQ.1) WRITE (NOUT,610)
      IF (IRESTA.EQ.0) WRITE (NOUT,620)
      IF (ITYROTB.EQ.0) WRITE (NOUT,650)
      IF (ITYROTB.EQ.1) WRITE (NOUT,660)
      IF (ITYROTB.EQ.2) WRITE (NOUT,670)
      IF (IRESTB.EQ.1) WRITE (NOUT,610)
      IF (IRESTB.EQ.0) WRITE (NOUT,620)
      IF (IRESTA.EQ.1.OR.IRESTB.EQ.1) WRITE (NOUT,740) RSL
      IF (IRESTA.EQ.1.OR.IRESTB.EQ.1) WRITE (NOUT,750) EFFD,B
      IF (IRESTA.EQ.1.OR.IRESTB.EQ.1) WRITE (NOUT,760) OVERD
      IF (ITYRAXA.EQ.1) WRITE (NOUT,770) NFL
      WRITE (NOUT,680)
      WRITE (NOUT,685) NIT
      WRITE (NOUT,690) ALPHA
      WRITE (NOUT,700) BETA
      WRITE (NOUT,710) E1
      WRITE (NOUT,720) E2
      WRITE (NOUT,730) EYA
      WRITE (NOUT,460) NUMTIM
      WRITE (NOUT,800)
      WRITE (NOUT,810) SLOPA
      WRITE (NOUT,820) SLOPB
      IF (ITYROTA.EQ.1.OR.ITYROTB.EQ.1) WRITE (NOUT,2000)
      IF (ITYROTA.NE.1) GOTO 180
      WRITE (NOUT,2010) ZK1
      WRITE (NOUT,2020) ZK2
  180 IF (ITYROTB.NE.1) GOTO 185
      WRITE (NOUT,2030) ZK4
      WRITE (NOUT,2040) ZK3
  185 CONTINUE
      WRITE (NOUT,830)
      WRITE (NOUT,840)
      WRITE (NOUT,850) (I,C(I),I=1,IDIVPT)
      WRITE (NOUT,860)
      WRITE (NOUT,840)
      WRITE (NOUT,850) (I,YP(I),I=1,IDIVPT)
      WRITE (NOUT,870)
      WRITE (NOUT,880)
      WRITE (NOUT,850) (I,CURP(I),I=1,IDIVPT)
C
C     INITIALIZE PLASTIC HINGES
C
      IPLASA1=0
      IPLASA2=0
      IPLASA3=0
      IPLASB1=0
      IPLASB2=0
      IPLASB3=0
      IPLCOLA=0
      IPLCOLB=0
      DCOL=0.0
C
C     INITIALIZE STRESS AND STRAIN HISTORIES
C
      DO 190 I=1,IDIVPT
      DO 190 J=1,NUMEL
      FIRSTRN(J,I)=0.0
      EO(J,I)=0.0
      SO(J,I)=0.0
      ET(J,I)=0.0
      CS(J,I)=0.0
      TR(J,I)=0.0
      ITF(J,I)=0
      STRNTR(J,I)=0.0
      STRNCR(J,I)=0.0
      TENSTR(J,I)=0.0
  190 CONTINUE
      DO 195 I=1,NUMEL
      STRNTH(I)=0.0
      STRNSH(I)=0.0
  195 CONTINUE
C
C     CALCULATE CONCRETE STRAIN AT PEAK STRESS
C     UNDER AMBIENT CONDITIONS
C
      MTYPE=1
```

```
      AMBTEMP=20.0
      CALL TEMPEN (MTYPE,AMBTEMP,TEMPEM,VALEM,EMUO)
C
C     CALCULATE CONCRETE COMPRESSIVE ULTIMATE
C     STRENGTH UNDER AMBIENT CONDITIONS
C
      CALL TEMPEN (MTYPE,AMBTEMP,TEMPSM,VALSM,SCUO)
C
C     CARRY OUT A FULL STRUCTURAL ANALYSIS FOR EACH
C     TIME STEP OF COLUMN EXPOSED TO FIRE
C
      DO 270 NUM=1,NUMTIM
C
C     IC - ITERATION COUNT
C
      IC=1
C
      IF (IBUG.EQ.2) WRITE (NOUT,3000) NUM
C
C     DETERMINE ULTIMATE MOMENTS OF RESTRAINT SYSTEM
C
C     RESTRAINT BEAM AT COLUMN JOINT A
C
      IF (ITYROTA.NE.1) GOTO 220
      IF (IRESTA.EQ.1) GOTO 200
      AMULT1=ZMUTS2
      AMULT2=ZMUTS2
      AMULT3=ZMUBS2
      GOTO 220
C
C     ULTIMATE MOMENT AT SUPPORT
C
  200 DO 210 I=1,NUMSUP
  210 ATL(I)=ATSUPA(I,NUM)
      IF (IBUG.EQ.2) WRITE (NOUT,3010)
C
      CALL ULTIMOM (IBUG,B,EFFD,OVERD,NUMSUP,MTYPSUP,2,YYSUP,ASUP,RC,
     .              AMULT1,ATL,TEMPFY,VALFY,TEMPMOD,VALMOD,
     .              TEMPSM,VALSM,TEMPEM,VALEM,EBEAMA1,ALPHA1)
C
C     ULTIMATE MOMENT AT MIDSPAN
C
      DO 215 I=1,NUMMID
  215 ATL(I)=ATMIDA(I,NUM)
      CALL ULTIMOM (IBUG,B,EFFD,OVERD,NUMMID,MTYPMID,1,YYMID,AMID,RC,
     .              AMULT3,ATL,TEMPFY,VALFY,TEMPMOD,VALMOD,
     .              TEMPSM,VALSM,TEMPEM,VALEM,EBEAMA3,ALPHA3)
      AMULT2=AMULT1
C
C     CALCULATE STIFFNESS OR RESTRAINT BEAM
C
      IF (IPLASA1.EQ.1) GOTO 219
      IF (IPLASA2.EQ.1) GOTO 219
      IF (IPLASA3.EQ.1) GOTO 219
      DD=OVERD-EFFD
      X=(B*(OVERD**2)/2)+(ALPHA1*((EFFD*ASTSUP)+(ASCSUP*DD)))
      X=X/((B*OVERD)+(ALPHA1*(ASTSUP+ASCSUP)))
      ZI=B*((X**3)+((OVERD-X)**3))/3
      ZI=ZI+(ALPHA1-1.0)*((ASCSUP*((X-DD)**2))+(ASTSUP*((EFFD-X)**2)))
      ZISUP=ZI
      X=(B*(OVERD**2)/2)+(ALPHA3*((EFFD*ASTMID)+(ASCMID*DD)))
      X=X/((B*OVERD)+(ALPHA3*(ASTMID+ASCMID)))
      ZI=B*((X**3)+((OVERD-X)**3))/3
      ZI=ZI+(ALPHA3-1.0)*((ASCMID*((X-DD)**2))+(ASTMID*((EFFD-X)**2)))
      ZIMID=ZI
      ZI2=(2*ZISUP+ZIMID)/3
      ZK2=0.5*ZI2*((2*EBEAMA1)+EBEAMA3)/(3*RSL)
  219 CONTINUE
      IF (IBUG.EQ.2) WRITE (NOUT,3020) ZK2
C
C     RESTRAINT BEAM AT COLUMN JOINT B
C
  220 IF (ITYROTB.NE.1) GOTO 250
      IF (IRESTB.EQ.1) GOTO 230
      BMULT1=ZMUTS3
      BMULT2=ZMUTS3
      BMULT3=ZMUBS3
      GOTO 250
C
C     ULTIMATE MOMENT AT SUPPORT
C
  230 DO 240 I=1,NUMSUP
  240 ATL(I)=ATSUPB(I,NUM)
      IF (IBUG.EQ.2) WRITE (NOUT,3030)
C
      CALL ULTIMOM (IBUG,B,EFFD,OVERD,NUMSUP,MTYPSUP,2,YYSUP,ASUP,RC,
     .              BMULT1,ATL,TEMPFY,VALFY,TEMPMOD,VALMOD,
     .              TEMPSM,VALSM,TEMPEM,VALEM,EBEAMB1,ALPHA1)
C
C     ULTIMATE MOMENT AT MIDSPAN
C
      DO 245 I=1,NUMMID
  245 ATL(I)=ATMIDB(I,NUM)
C
      CALL ULTIMOM (IBUG,B,EFFD,OVERD,NUMMID,MTYPMID,1,YYMID,AMID,RC,
     .              BMULT3,ATL,TEMPFY,VALFY,TEMPMOD,VALMOD,
     .              TEMPSM,VALSM,TEMPEM,VALEM,EBEAMB3,ALPHA3)
      BMULT2=BMULT1
C
C     CALCULATE STIFFNESS OF RESTRAINT BEAM
C
      IF (IPLASB1.EQ.1) GOTO 249
      IF (IPLASB2.EQ.1) GOTO 249
      IF (IPLASB3.EQ.1) GOTO 249
      DD=OVERD-EFFD
      X=(B*(OVERD**2)/2)+(ALPHA1*((EFFD*ASTSUP)+(ASCSUP*DD)))
      X=X/((B*OVERD)+(ALPHA1*(ASTSUP+ASCSUP)))
      ZI=B*((X**3)+((OVERD-X)**3))/3
      ZI=ZI+(ALPHA1-1.0)*((ASCSUP*((X-DD)**2))+(ASTSUP*((EFFD-X)**2)))
      ZISUP=ZI
      X=(B*(OVERD**2)/2)+(ALPHA3*((EFFD*ASTMID)+(ASCMID*DD)))
      X=X/((B*OVERD)+(ALPHA3*(ASTMID+ASCMID)))
```

```
      ZI=B*((X**3)+((OVERD-X)**3))/3
      ZI=ZI+(ALPHA3-1.0)*((ASCMID*((X-DD)**2))+(ASTMID*((EFFD-X)**2)))
      ZIMID=ZI
      ZI3=(2*ZI3UP+ZIMID)/3
      ZK3=0.5*ZI3*((2*EBEAMB1)+EBEAMB3)/(3*RSL)
  249 CONTINUE
      IF (IBUG.EQ.2) WRITE (NOUT,3020) ZK3
C
  250 CONTINUE
      IF (NUM.EQ.1) GOTO 265
C
C     CALCULATE STRAINS DUE TO FIRE FROM MATERIAL BEHAVIOUR MODELS
C
      DO 255 LEM=1,NUMEL
C
C     CALCULATE TEMPERATURE DEPENDENT MATERIAL PARAMETERS
C
      TEMP=AT(LEM,NUM)
      MTYPE=MMTYPE(LEM)
      IF (MTYPE.EQ.2) GOTO 252
C
C     CALCULATE MAXIMUM CONCRETE STRESS
C
      CALL TEMPEN (MTYPE,TEMP,TEMPSM,VALSM,SM)
C
C     CALCULATE INDUCED STRAINS AS A RESULT OF FIRE ENVIRONMENT
C
  252 DO 255 IDIV=1,IDIVPT
C
      CALL FIRECON (NUM,IDIV,MTYPE,TEMP,LEM,SM,TEMPES,VALES,
     .              NUMEL,STRNTH,STRNTR,STRNCR,STRNSH,
     .              TIME,ISHIN,SCUO,NUMTIM,IDIVPT)
C
  255 CONTINUE
C
  260 CONTINUE
C
C     CHANGES IN ENDSLOPES INDUCE CHANGES IN COLUMN END MOMENTS
C     AND CHANGES IN MOMENTS IN THE RESTRAINT SYSTEMS
C
      CALL INDUCE (NUM,1,ITYROTA,IRESTA,ZMA,SLOPE1,SLOPA,
     .             FEMA,ZK1,ZK2,UDLA,RSL,NFL,DCOL,
     .             ZMU1,AMBEC,
     .             IPLASA1,IPLASA2,ZI1,ZI2,ZI3,ZI4,
     .             IPLASA3,PAB,COLAB,COLOW,
     .             EBEAMA1,EBEAMA3,IPLCOLA,
     .             AMULT1,AMULT2,AMULT3)
C
      IF (IBUG.NE.2) GOTO 262
      WRITE (NOUT,3040)
      WRITE (NOUT,3020) ZK2
      WRITE (NOUT,3050) SLOPA
      WRITE (NOUT,3060) ZMA
  262 CONTINUE
C
      CALL INDUCE (NUM,2,ITYROTB,IRESTB,ZMB,SLOPE2,SLOPB,
     .             FEMB,ZK4,ZK3,UDLB,RSL,NFL,DCOL,
     .             ZMU4,AMBEC,
     .             IPLASB1,IPLASB2,ZI1,ZI2,ZI3,ZI4,
     .             IPLASB3,PAB,COLAB,COLOW,
     .             EBEAMB1,EBEAMB3,IPLCOLB,
     .             BMULT1,BMULT2,BMULT3)
C
      IF (IBUG.NE.2) GOTO 263
      WRITE (NOUT,3070)
      WRITE (NOUT,3020) ZK3
      WRITE (NOUT,3050) SLOPB
      WRITE (NOUT,3060) ZMB
  263 CONTINUE
C
C     CALCULATE AXIAL FORCE
C
      IF (ITYROTA.EQ.0.AND.ITYROTB.EQ.0) GOTO 265
      IF (ITYROTA.EQ.2.AND.ITYROTB.EQ.2) GOTO 265
      P=(UDLA*RSL/2)-(6*ZK2*SLOPA/RSL)+PAB
C
  265 CONTINUE
C
C     CALCULATION OF DIVISION POINT BENDING MOMENTS
C
      CALL DIVPTBM (ISECO,SEGLEN,ZMA,P,YP,ZMB,GA,COLLEN,ZMR,
     .              NUMSEG,IDIVPT)
C
C     CALCULATION OF CURVATURES
C
      IF (IBUG.EQ.2) WRITE (NOUT,3080)
C
      CALL CURVAT (IT,NIT,NUM,MMTYPE,STRAP,CURP,YY,YP,GA,SEGLEN,A,P,
     .             ZMR,ALPHA,BETA,CURV,AID,TIME,VALEM,
     .             VALSM,VALFY,VALMOD,TEMPEM,TEMPSM,
     .             TEMPFY,TEMPMOD,EMUO,
     .             NUMSEG,NUMEL,IDIVPT,NUMTIM)
C
      IF (IT.EQ.5HFAILD) GOTO 267
C
C     CALCULATION OF DEFLECTIONS
C
      IF (IBUG.EQ.2) WRITE (NOUT,3090)
C
      CALL DEFLECT (IBUG,NUM,SEGLEN,C,GA,GB,SLOPA,CURV,
     .              COLLEN,SLOPB,E1,E2,YP,EYA,YC,SLOA,SLOB,
     .              IT,AID,CIS,SLOP,DMR,DCURV,SLOPE1,SLOPE2,
     .              EYC,NFL,ZI2,RSL,DSEGSM,GUS,H1,
     .              ITYRAXA,ZK1,ZK2,AMBEC,P,DC,ECCEN,
     .              IC,SLEG,ISECO,ITYROTA,ITYROTB,YT,
     .              ALROD,PYC,ROD,TIME,NUMTIM,DCOL,
     .              IPLASA2,IPLASA3,IPLASB2,IPLASB3,
     .              NUMSEG,NUMEL,IDIVPT)
C
      IF (IBUG.EQ.2) WRITE (NOUT,3100) SLOPA,SLOPB
C
      IF (IT.EQ.5HFAILD) GOTO 267
```

```
      IF (IT.EQ.5HNEWIT) GOTO 260
C
C     SET PROPOSED DEFLECTIONS AND END SLOPES EQUAL TO
C     CALCULATED DEFLECTIONS AND END SLOPES FROM PREVIOUS
C     TIME STEP
C
  267 CALL RESET (YP,YC,SLOPA,SLOPB,SLOA,SLOB,
     .              IDIVPT,NUMEL,MMTYPE)
C
C     OUTPUT RESULTS OF STRUCTURAL ANALYSIS
C
      CALL OUTPUT (IT,NUM,TIME,ZMA,ZMB,SLOPA,SLOPB,YC,SLEG,GA,GB,
     .             ROD,ALROD,ITYROTA,ITYROTB,ZK1,ZK2,ZK4,ZK3,
     .             STRNTH,STRNTR,STRNCR,STRNSH,IBUG,
     .             AMULT1,AMULT2,AMULT3,BMULT1,BMULT2,BMULT3,
     .             IPLCOLA,IPLCOLB,
     .             IPLASA1,IPLASA2,IPLASA3,IPLASB1,IPLASB2,IPLASB3,
     .             DSEGSM,GUS,P,NUMSEG,NUMEL,IDIVPT,NUMTIM)
C
      IF (IT.EQ.5HFAILD) STOP
  270 CONTINUE
C
      WRITE (NOUT,295)
C
      STOP
C
  275 FORMAT (80A1)
  285 FORMAT (I4)
  290 FORMAT (2I2)
  295 FORMAT(////37H    PROGRAM TERMINATED - JOB COMPLETED)
  300 FORMAT (1H1,5(/))
  310 FORMAT (85H *****************************************************
     .******************************)
  320 FORMAT (///5X,6HSSSSSS,4X,6HAAAAAA,3X,8HFFFFFFFF,2X,8HEEEEEEEE,12X
     .,7HRRRRRRR,4X,6HCCCCCC,4X,6HCCCCCC)
  325 FORMAT (4X,8HSSSSSSSS,2X,8HAAAAAAAA,2X,8HFFFFFFFF,2X,8HEEEEEEEE,12
     .X,8HRRRRRRRR,2X,8HCCCCCCCC,2X,8HCCCCCCCC)
  330 FORMAT (4X,2HSS,5X,1HS,2X,2HAA,4X,2HAA,2X,2HFF,8X,2HEE,18X,2HRR,4X
     .,2HRR,2X,2HCC,5X,1HC,2X,2HCC,5X,1HC)
  335 FORMAT (4X,2HSS,8X,2HAA,4X,2HAA,2X,2HFF,8X,2HEE,18X,2HRR,4X,2HRR,2
     .X,2HCC,8X,2HCC)
  340 FORMAT (4X,7HSSSSSSS,3X,2HAA,4X,2HAA,2X,5HFFFFF,5X,5HEEEEE,6X,6H==
     .====,3X,8HRRRRRRRR,2X,2HCC,8X,2HCC)
  345 FORMAT (5X,7HSSSSSSS,2X,8HAAAAAAAA,2X,5HFFFFF,5X,5HEEEEE,6X,6H====
     .==,3X,7HRRRRRRR,3X,2HCC,8X,2HCC)
  350 FORMAT (10X,2HSS,2X,8HAAAAAAAA,2X,2HFF,8X,2HEE,18X,2HRR,1X,2HRR,5X
     .,2HCC,8X,2HCC)
  360 FORMAT (4X,1HS,5X,2HSS,2X,2HAA,4X,2HAA,2X,2HFF,8X,2HEE,18X,2HRR,2X
     .,2HRR,4X,2HCC,5X,1HC,2X,2HCC,5X,1HC)
  370 FORMAT (4X,8HSSSSSSSS,2X,2HAA,4X,2HAA,2X,2HFF,8X,8HEEEEEEEE,12X,2H
     .RR,3X,2HRR,3X,8HCCCCCCCC,2X,8HCCCCCCCC)
  380 FORMAT (5X,6HSSSSSS,3X,2HAA,4X,2HAA,2X,2HFF,8X,8HEEEEEEEE,12X,2HRR
     .,4X,2HRR,3X,6HCCCCCC,4X,6HCCCCCC)
  390 FORMAT (///23X,33HMODEL OF THE STRUCTURAL BEHAVIOUR,/23X,31HOF A R
     .EINFORCED CONCRETE COLUMN,/23X,29HEXPOSED TO A FIRE ENVIRONMENT,//
     ../)
  400 FORMAT (//23X,24H- - - TITLE OF RUN - - -,//1X,80A1//)
  410 FORMAT (6(/))
  420 FORMAT (/5X,74HSAFE-RCC - STRUCTURAL ANALYSIS OF FIRE EXPOSED REIN
     .FORCED CONCRETE COLUMNS,/)
  430 FORMAT (/5X,42HINFORMATION RELEVANT TO ANALYSIS PROCEDURE,/)
  435 FORMAT (//1X,30H. . . . COLUMN DETAILS . . . .)
  440 FORMAT (1X,27HNUMBER OF SEGMENT LENGTHS =,I4)
  445 FORMAT (1X,13HCOLUMN LENGTH,10X,2H= ,F6.3,2H M)
  450 FORMAT (1X,44HNUMBER OF ELEMENTS OF COLUMN CROSS SECTION =,I4)
  455 FORMAT (/1X,18HBREADTH X DEPTH = ,F6.3,3H X ,F6.3,2H M)
  460 FORMAT (//1X,22HNUMBER OF TIME STEPS =,I4)
  465 FORMAT (1X,25HGUSSET LENGTHS - END A = ,F6.3,2H M)
  470 FORMAT (//1X,26H. . . . END FORCES . . . .)
  475 FORMAT (16X,10H- END B = ,F6.3,2H M)
  480 FORMAT (/1X,11HAXIAL FORCE,5X,2H= ,F10.2,3H KN)
  485 FORMAT (1X,12HECCENTRICITY,4X,2H= ,4X,F6.4,2H M)
  490 FORMAT (1X,18HMOMENTS - END A = ,F10.2,4H KNM)
  500 FORMAT (9X,10H- END B = ,F10.2,4H KNM)
  505 FORMAT (//1X,29HSECOND ORDER EFFECTS INCLUDED)
  510 FORMAT (//1X,24HSHRINKAGE MODEL INCLUDED)
  520 FORMAT (//1X,33HSECOND ORDER EFFECTS NOT INCLUDED)
  530 FORMAT (//1X,28HSHRINKAGE MODEL NOT INCLUDED)
  540 FORMAT (//1X,36H. . . . RESTRAINT CONDITIONS . . . .)
  550 FORMAT (/1X,35HEND A - PINNED ROTATIONAL RESTRAINT)
  560 FORMAT (/1X,35HEND A - NORMAL ROTATIONAL RESTRAINT)
  570 FORMAT (/1X,34HEND A - FIXED ROTATIONAL RESTRAINT)
  580 FORMAT (9X,20HFREE AXIAL EXPANSION)
  590 FORMAT (9X,22HNORMAL AXIAL RESTRAINT)
  600 FORMAT (9X,21HFIXED AXIAL RESTRAINT)
  610 FORMAT (9X,38HTEMPERATURE DEPENDENT RESTRAINT SYSTEM)
  620 FORMAT (9X,40HTEMPERATURE INDEPENDENT RESTRAINT SYSTEM)
  650 FORMAT (/1X,35HEND B - PINNED ROTATIONAL RESTRAINT)
  660 FORMAT (/1X,35HEND B - NORMAL ROTATIONAL RESTRAINT)
  670 FORMAT (/1X,34HEND B - FIXED ROTATIONAL RESTRAINT)
  680 FORMAT (//1X,36H. . . . CONVERGENCE CRITERIA . . . .)
  685 FORMAT (//1X,48HPERMISSIBLE NUMBER OF EQUILLIBRIUM ITERATIONS = ,I
     .2)
  690 FORMAT (//1X,37HALLOWABLE INCOMPATABILITIES - ALPHA =,F9.6)
  700 FORMAT (31X,6HBETA =,F9.6)
  710 FORMAT (31X,4HE1 =,F9.6)
  720 FORMAT (31X,4HE2 =,F9.6)
  730 FORMAT (31X,5HEYA =,F9.6)
  740 FORMAT (/1X,42HROTATIONAL RESTRAINT - LENGTH OF MEMBER = ,F6.3,2H
     .M)
  750 FORMAT (24X,28HEFFECTIVE DEPTH X BREADTH = ,F6.3,3H X ,F6.3,2H M)
  760 FORMAT (24X,16HOVERALL DEPTH = ,F6.3,2H M)
  770 FORMAT (/1X,43HAXIAL RESTRAINT - NUMBER OF FLOORS ABOVE = ,I4)
  800 FORMAT (//1X,31H. . . . PROPOSED VALUES . . . .)
  810 FORMAT (//1X,19HENDSLOPE - END A = ,F7.5)
  820 FORMAT (10X,10H- END B = ,F7.5)
  830 FORMAT (//1X,42HDIVISION POINT DEFLECTIONS UNDER ZERO LOAD)
  840 FORMAT (//1X,4HDIVN,3X,6HDEFLEC,3X,4HDIVN,3X,6HDEFLEC,3X,4HDIVN,3X
     .,6HDEFLEC,3X,4HDIVN,3X,6HDEFLEC,3X,4HDIVN,3X,6HDEFLEC,3X,4HDIVN,3X
     .,6HDEFLEC,/)
  850 FORMAT (6(I3,3X,F7.5,3X))
  860 FORMAT (//1X,37HDIVISION POINT DEFLECTIONS UNDER LOAD)
```

```
  870 FORMAT (//1X, 25HDIVISION POINT CURVATURES)
  880 FORMAT (//1X, 4HDIVN,3X,6HCURVAT,3X,4HDIVN,3X,6HCURVAT,3X,4HDIVN,3X
     .,6HCURVAT,3X, 4HDIVN,3X,6HCURVAT,3X,4HDIVN,3X,6HCURVAT,3X,4HDIVN,3X
     .,6HCURVAT,/)
  900 FORMAT (/1X,24HDATA FILE (DEBUG OPTION),/)
  920 FORMAT (1X,I4)
  930 FORMAT (1X,2I2)
  940 FORMAT (1X,F6.3,1X,F6.3,1X,F6.3)
  950 FORMAT (1X,F6.3,1X,F6.3)
  955 FORMAT (1X,F6.4,1X,6PF7.1)
  960 FORMAT (1X,I4,3X,F6.3)
  965 FORMAT (1X,F6.4,1X,6PF7.1,1X,F6.4,1X,6PF7.1)
  970 FORMAT (1X,F7.2,1X,F6.4)
  975 FORMAT (1X,6PF7.1,1X,6PF7.1,1X,6PF7.1,1X,6PF7.1)
  980 FORMAT (1X,F7.2)
  985 FORMAT (1X,F6.2)
  990 FORMAT (1X,F6.2,1X,F6.2)
 1020 FORMAT (1X,F7.2,1X,F7.2,1X,F7.2,1X,F7.2,1X,F7.2,1X,F7.2)
 1030 FORMAT (1X,F6.3,1X,F6.3,1X,F6.3,1X,F6.3,1X,I2)
 1040 FORMAT (1X,I3,1X,5F9.6)
 1050 FORMAT (1X,I4,3X,F6.4)
 1060 FORMAT (1X,I4,1X,F7.5,1X,F10.8,1X,I4)
 1070 FORMAT (1X,4(F6.2,E15.8))
 1080 FORMAT (1X,F7.3)
 1090 FORMAT (1X,6(I4,1X,F6.2))
 2000 FORMAT (//1X, 40HPROPOSED STIFFNESSES OF RESTRAINT SYSTEM,//)
 2010 FORMAT (1X,15HCOLUMN ABOVE = ,F10.2)
 2020 FORMAT (1X,18HBEAM AT JOINT A = ,F10.2)
 2030 FORMAT (1X,15HCOLUMN BELOW = ,F10.2)
 2040 FORMAT (1X,18HBEAM AT JOINT B = ,F10.2)
 3000 FORMAT (///1X,17HTIME STEP NUMBER ,I3)
 3010 FORMAT (/1X,24HSUBROUTINE ULTIMOM END A)
 3020 FORMAT (/1X,27HRESTRAINT BEAM STIFFNESS = ,F10.2)
 3030 FORMAT (/1X,24HSUBROUTINE ULTIMOM END B)
 3040 FORMAT (/1X,23HSUBROUTINE INDUCE END A)
 3050 FORMAT (/1X,11HENDSLOPE = ,F7.5)
 3060 FORMAT (/1X,13HEND MOMENT = ,F10.2)
 3070 FORMAT (/1X,23HSUBROUTINE INDUCE END B)
 3080 FORMAT (/1X,17HSUBROUTINE CURVAT)
 3090 FORMAT (/1X,18HSUBROUTINE DEFLECT)
 3100 FORMAT (/1X,13HENDSLOPE A = ,F7.5,14H ENDSLOPE B = ,F7.5)
C
      END
```

```
C
C
      SUBROUTINE INPUT (COLLEN,GA,GB,BC,DC,SEGLEN,PAB,ECCEN,C,
     .                  UDLA,UDLB,YY,A,MMTYPE,NIT,ALPHA,
     .                  BETA,E1,E2,EYA,TIME,VALES,
     .                  VALEM,VALSM,VALFY,VALMOD,
     .                  TEMPES,TEMPEM,TEMPSM,TEMPFY,
     .                  TEMPMOD,D2,ASCOL,
     .                  D1,ASCAB,D3,ASCOW,
     .                  ASTSUP,ASCSUP,ASTMID,ASCMID,
     .                  NUMMID,YYMID,AMID,MTYPMID,
     .                  NUMSUP,YYSUP,ASUP,MTYPSUP,
     .                  EFFD,B,OVERD,ITYROTA,ITYROTB,
     .                  IRESTA,IRESTB,ITYRAXA,COLAB,COLOW,
     .                  ZMU1,ZMUBS2,ZMUTS2,ZMU4,ZMUBS3,ZMUTS3,
     .                  TEMPI,TEMPILA,TEMPILB,
     .                  NFL,RSL,NUMSEG,NUMEL,IDIVPT,NUMTIM)
C
      COMMON /CONTROL/ NIN,NOUT,NFILE,ITITLE(80)
      COMMON /LCM/ AT(150,65),STRAIN(150,20),
     .             STRESS(150,20),ITFC(150,20),EO(150,20),
     .             ET(150,20),ITF(150,20),CS(150,20),SO(150,20),
     .             TOTSTRN(150,20),TR(150,20),TENSTR(150,20),
     .             ATMIDA(100,65),ATMIDB(100,65),
     .             ATSUPA(100,65),ATSUPB(100,65),
     .             FIRSTRN(150,20)
      LEVEL 2,/LCM/
      DIMENSION SEGLEN(NUMSEG),C(IDIVPT),
     .          YY(NUMEL),A(NUMEL),MMTYPE(NUMEL),
     .          VALES(8),VALEM(8),VALSM(8),VALFY(8),
     .          VALMOD(8),TEMPES(8),TEMPEM(8),
     .          TEMPSM(8),TEMPFY(8),TEMPMOD(8),TIME(NUMTIM),
     .          YYMID(NUMMID),YYSUP(NUMSUP),AMID(NUMMID),ASUP(NUMSUP),
     .          MTYPMID(NUMMID),MTYPSUP(NUMSUP)
C
C     SUBROUTINE INPUT INPUTS ALL THE NECCESSARY DATA IN
C     ORDER TO CARRY OUT A FULL STRUCTURAL ANALYSIS
C
C     INPUT COLUMN LENGTH, COLLEN, AND GUSSET LENGTHS
C
      READ (NIN,300) COLLEN,GA,GB
C
C     INPUT COLUMN BREADTH, BC, AND EFFECTIVE DEPTH, DC
C
      READ (NIN,310) BC,DC
C
C     INPUT COVER+HALF BAR DIA AND AREA OF STEEL IN MM**2
C
      READ (NIN,315) D2,ASCOL
      ASCOL=ASCOL*1E-6
C
C     INPUT SEGMENT LENGTHS
C
      DO 110 I=1,NUMSEG
      READ (NIN,320) J,SEGLEN(I)
  110 CONTINUE
```

```
C
      IF (ITYROTA.EQ.0.AND.ITYROTB.EQ.0) GOTO 115
      GOTO 120
C
C     INPUT AXIAL LOAD AND ECCENTRICITY
C
  115 READ (NIN,330) PAB,ECCEN
      GOTO 150
C
C     INPUT AXIAL LOAD FROM STRUCTURE ABOVE
C
  120 READ (NIN,335) PAB
C
      IF (ITYROTA.EQ.2.AND.ITYROTB.EQ.2) GOTO 150
C
C     INPUT UDL AT COLUMN SUPPORTS JOINT A AND JOINT B
C
      READ (NIN,350) UDLA,UDLB
C
C     INPUT LENGTHS OF COLUMN ABOVE AND
C     BELOW COLUMN UNDER ANALYSIS
C
      READ (NIN,310) COLAB,COLOW
C
C     INPUT COVER+HALF BAR DIA AND AREA OF STEEL IN MM**2
C     FOR COLUMNS ABOVE AND BELOW COLUMN UNDER ANALYSIS
C
      READ (NIN,450) D1,ASCAB,D3,ASCOW
C
C     INPUT AREAS OF TENSION STEEL AND COMPRESSION STEEL
C
C     AT SUPPORT AND MIDSPAN OF RESTRAINT BEAM SECTIONS
C
      READ (NIN,460) ASTSUP,ASCSUP,ASTMID,ASCMID
      ASCAB=ASCAB*1E-6
      ASCOW=ASCOW*1E-6
      ASTSUP=ASTSUP*1E-6
      ASCSUP=ASCSUP*1E-6
      ASTMID=ASTMID*1E-6
      ASCMID=ASCMID*1E-6
C
C     INPUT EFFECTIVE DEPTH, BREADTH, OVERALL DEPTH
C     LENGTH OF COLUMN TEMPERATURE DEPENDENT
C     RESTRAINT SYSTEM AND NUMBER OF FLOORS ABOVE
C
      READ (NIN,380) EFFD,B,OVERD,RSL,NFL
C
C     INPUT ULTIMATE MOMENTS FOR COLUMN AND ADJOINING
C     BEAM ABOVE AND BELOW COLUMN UNDER ANALYSIS
C
C     ZMU1 - ULTIMATE MOMENT COLUMN ABOVE
C     ZMU4 - ULTIMATE MOMENT COLUMN BELOW
C     ZMUBS2 - ULTIMATE MOMENT TOP BEAM, BOTTOM TENSION STEEL
C     ZMUTS2 - ULTIMATE MOMENT TOP BEAM, TOP TENSION STEEL
C     ZMUBS3 - ULTIMATE MOMENT BOTTOM BEAM, BOTTOM TENSION STEEL
C     ZMUTS3 - ULTIMATE MOMENT BOTTOM BEAM, TOP TENSION STEEL
C
      READ (NIN,440) ZMU1,ZMU4,ZMUBS2,ZMUTS2,ZMUBS3,ZMUTS3
C
  150 CONTINUE
C
C     INPUT ALLOWABLE INCOMPATABILITIES
C
      READ (NIN,390) NIT,ALPHA,BETA,E1,E2,EYA
C
C     INPUT INITIAL DIVISION POINT DEFLECTIONS UNDER ZERO LOAD
C
      DO 160 I=1,IDIVPT
      READ (NIN,400) J,C(I)
  160 CONTINUE
C
C     INPUT ELEMENTAL CENTROID COORDINATES
C     ELEMENTAL AREAS AND MATERIAL TYPE OF
C     COLUMN CROSS SECTION
C
      DO 170 I=1,NUMEL
      READ (NIN,410) J,YY(I),A(I),MMTYPE(I)
  170 CONTINUE
C
      IF (IRESTA.NE.1.AND.IRESTB.NE.1) GOTO 190
C
C     INPUT ELEMENTAL LAYER CENTROID COORDINATES
C     LAYER AREA AND MATERIAL TYPE OF RESTRAINT
C     BEAM CROSS SECTION AT MIDSPAN
C
      DO 180 I=1,NUMMID
      READ (NIN,410) J,YYMID(I),AMID(I),MTYPMID(I)
  180 CONTINUE
C
C     INPUT ELEMENTAL LAYER CENTROID COORDINATES
C     LAYER AREA AND MATERIAL TYPE OF RESTRAINT
C     BEAM CROSS SECTION AT SUPPORT
C
      DO 185 I=1,NUMSUP
      READ (NIN,410) J,YYSUP(I),ASUP(I),MTYPSUP(I)
  185 CONTINUE
  190 CONTINUE
C
C     INPUT VALUES FOR TEMPERATURE DEPENDENT MATERIAL PARAMETERS
C
C     INPUT STEEL COEFFICIENT THERMAL EXPANSION VALUES
C
      CALL PARAM (VALES,TEMPES)
C
C     INPUT CONCRETE STRAIN VALUES AT PEAK STRESS FOR GIVEN TEMP.
C
      CALL PARAM (VALEM,TEMPEM)
C
C     INPUT PEAK CONCRETE STRESS VALUES FOR GIVEN TEMP.
C
      CALL PARAM (VALSM,TEMPSM)
C
```

```
C     INPUT STEEL YIELD STRESS VALUES
C
      CALL PARAM (VALFY,TEMPFY)
C
C     INPUT STEEL ELASTIC MODULUS VALUES
C
      CALL PARAM (VALMOD,TEMPMOD)
C
C     INPUT TIME STEP AND ELEMENTAL TEMPERATURES
C     OF COLUMN CROSS SECTION
C
C     INITIAL TEMPERATURE
C
      READ (NIN,340) TIME(1)
      READ (NIN,420) TEMPI
      DO 200 I=1,NUMEL
  200 AT(I,1)=TEMPI
C
      DO 210 I=2,NUMTIM
      READ (NIN,340) TIME(I)
      READ (NIN,430) (K,AT(J,I),J=1,NUMEL)
  210 CONTINUE
C
      IF (IRESTA.EQ.1.OR.IRESTB.EQ.1) GOTO 220
      GOTO 280
  220 CONTINUE
C
C     INPUT ELEMENTAL LAYER TEMPERATURES OF RESTRAINT SYSTEM
C
C     RESTRAINT BEAM AT JOINT A
C
C     INITIAL TEMPERATURE
C
      IF (IRESTA.NE.1) GOTO 250
      READ (NIN,420) TEMPILA
      DO 230 I=1,NUMMID
  230 ATMIDA(I,1)=TEMPILA
      DO 235 I=1,NUMSUP
  235 ATSUPA(I,1)=TEMPILA
C
C     LAYER TEMPERATURES OF RESTRAINT BEAM SECTION
C     AT MIDSPAN
C
      DO 240 I=2,NUMTIM
      READ (NIN,430) (K,ATMIDA(J,I),J=1,NUMMID)
  240 CONTINUE
C
C     LAYER TEMPERATURE OF RESTRAINT BEAM SECTION
C     AT SUPPORT
C
      DO 245 I=2,NUMTIM
      READ (NIN,430) (K,ATSUPA(J,I),J=1,NUMSUP)
  245 CONTINUE
C
C     RESTRAINT BEAM AT JOINT A
C
C     INITIAL TEMPERATURE
C
  250 IF (IRESTB.NE.1) GOTO 280
      READ (NIN,420) TEMPILB
      DO 260 I=1,NUMMID
  260 ATMIDB(I,1)=TEMPILB
      DO 265 I=1,NUMSUP
  265 ATSUPB(I,1)=TEMPILB
C
C     LAYER TEMPERATURES OF RESTRAINT BEAM SECTION
C     AT MIDSPAN
C
      DO 270 I=2,NUMTIM
      READ (NIN,430) (K,ATMIDB(J,I),J=1,NUMMID)
  270 CONTINUE
C
C     LAYER TEMPERATURE OF RESTRAINT BEAM SECTION
C     AT SUPPORT
C
      DO 275 I=2,NUMTIM
  275 READ (NIN,430) (K,ATSUPB(J,I),J=1,NUMSUP)
  280 CONTINUE
C
      RETURN
C
  300 FORMAT (F6.3,1X,F6.3,1X,F6.3)
  310 FORMAT (F6.3,1X,F6.3)
  315 FORMAT (F6.4,1X,F7.1)
  320 FORMAT (I4,3X,F6.3)
  330 FORMAT (F7.2,1X,F6.4)
  335 FORMAT (F7.2)
  340 FORMAT (F7.3)
  350 FORMAT (F6.2,1X,F6.2)
  380 FORMAT (F6.3,1X,F6.3,1X,F6.3,1X,F6.3,1X,I2)
  390 FORMAT (I3,1X,5F9.6)
  400 FORMAT (I4,3X,F6.4)
  410 FORMAT (I4,1X,F7.5,1X,F10.8,1X,I4)
  420 FORMAT (F6.2)
  430 FORMAT (6(I4,1X,F6.2))
  440 FORMAT (F7.2,1X,F7.2,1X,F7.2,1X,F7.2,1X,F7.2,1X,F7.2)
  450 FORMAT (F6.4,1X,F7.1,1X,F6.4,1X,F7.1)
  460 FORMAT (F7.1,1X,F7.1,1X,F7.1,1X,F7.1)
C
      END
```

```
C
C
      SUBROUTINE PARAM (FN,TN)
C
C     SUBROUTINE PARAM INPUTS VALUES OF TEMPERATURE
C     DEPENDENT MATERIAL PARAMETERS FOR GIVEN
C     TEMPERATURES
C
      COMMON /CONTROL/ NIN,NOUT,NFILE,ITITLE(80)
      DIMENSION FN(8),TN(8)
C
      READ (NIN,200) (TN(I),FN(I),I=1,8)
C
      RETURN
C
  200 FORMAT (4(F6.2,E12.8))
C
      END
```



```
C
C
      SUBROUTINE PROPOSE (ITYROTA,ITYROTB,TEMPEM,VALEM,TEMPSM,VALSM,
     .                    BC,DC,COLLEN,COLAB,COLOW,B,OVERD,RSL,
     .                    UDLA,UDLB,PAB,ECCEN,GA,IDIVPT,YP,CURP,
     .                    ZK1,ZK2,ZK4,ZK3,STRAP,SLOPE1,SLOPE2,
     .                    FEMA,FEMB,AMBEC,EFFD,ZI1,ZI2,ZI3,ZI4,
     .                    ASCAB,D1,ASCOW,D3,
     .                    ASTSUP,ASCSUP,ASTMID,ASCMID,
     .                    TEMPMOD,VALMOD,TEMPFY,VALFY,ASCOL,D2,
     .                    SLOPA,SLOPB,ZMA,ZMB,P,SEGLEN,NUMSEG,C)
C
      COMMON /CONTROL/ NIN,NOUT,NFILE,ITITLE(80)
      DIMENSION TEMPEM(8),VALEM(8),TEMPSM(8),VALSM(8),YP(IDIVPT),
     .          TEMPMOD(8),VALMOD(8),TEMPFY(8),VALFY(8),
     .          CURP(IDIVPT),STRAP(IDIVPT),C(IDIVPT),SEGLEN(NUMSEG)
C
C     SUBROUTINE PROPOSE CALCULATES THE PROPOSED VALUES FOR
C     ENDSLOPES, SLOPA AND SLOPB, DIVISION POINT DEFLECTIONS
C     YP(I), CURVATURES, CURP(I), AND DIRECT STRAIN AT THE
C     COLUMN AXIS, STRAP(I)
C
C     CALCULATE MEMBER STIFFNESSES OF STRUCTURAL SYSTEM
C
      AVTEM=20.0
      MTYPE=1
      CALL TEMPEN (MTYPE,AVTEM,TEMPEM,VALEM,EM)
      CALL TEMPEN (MTYPE,AVTEM,TEMPSM,VALSM,SM)
      AMBEC=EXP(1.0)*SM/EM
      MTYPE=2
      CALL TEMPEN (MTYPE,AVTEM,TEMPMOD,VALMOD,AMBES)
      CALL TEMPEN (MTYPE,AVTEM,TEMPFY,VALFY,FY)
      ALPHA=AMBES/AMBEC
C
C     NORMAL ROTATIONAL RESTRAINT, FIXED ROTATIONAL
C     RESTRAINT AND PINNED ROTATIONAL RESTRAINT
C
      ZIC=(BC*(DC**3)/12)+(ALPHA-1.0)*ASCOL*(((0.5*DC)-D2)**2)
      ZKC=AMBEC*ZIC/COLLEN
      IF (ITYROTA.EQ.0) GOTO 100
      IF (ITYROTA.EQ.2) GOTO 100
      ZI1=(BC*(DC**3)/12)+(ALPHA-1.0)*ASCAB*(((0.5*DC)-D1)**2)
      ZK1=AMBEC*ZI1/COLAB
      DD=OVERD-EFFD
      X=(B*(OVERD**2)/2)+(ALPHA*((EFFD*ASTSUP)+(ASCSUP*DD)))
      X=X/((B*OVERD)+(ALPHA*(ASTSUP+ASCSUP)))
      ZI=B*((X**3)+((OVERD-X)**3))/3
      ZISUP=ZI+(ALPHA-1.0)*((ASCSUP*((X-DD)**2))+(ASTSUP*((EFFD-X)**2)))
      X=(B*(OVERD**2)/2)+(ALPHA*((EFFD*ASTMID)+(ASCMID*DD)))
      X=X/((B*OVERD)+(ALPHA*(ASTMID+ASCMID)))
      ZI=B*((X**3)+((OVERD-X)**3;)/3
      ZIMID=ZI+(ALPHA-1.0)*((ASCMID*((X-DD)**2))+(ASTMID*((EFFD-X)**2)))
      ZI2=(2*ZISUP+ZIMID)/3
      ZK2=0.5*AMBEC*ZI2/RSL
      GOTO 110
  100 ZK1=(10**10)/2
```

```
      IF (ITYROTA.EQ.0) ZK1=0.0
      ZK2=ZK1
  110 IF (ITYROTB.EQ.0) GOTO 120
      IF (ITYROTB.EQ.2) GOTO 120
      ZI4=(BC*(DC**3)/12)+(ALPHA-1.0)*ASCOW*(((0.5*DC)-D3)**2)
      ZK4=AMBEC*ZI4/COLOW
      DD=OVERD-EFFD
      X=(B*(OVERD**2)/2)+(ALPHA*((EFFD*ASTSUP)+(ASCSUP*DD)))
      X=X/((B*OVERD)+(ALPHA*(ASTSUP+ASCSUP)))
      ZI=B*((X**3)+((OVERD-X)**3))/3
      ZISUP=ZI+(ALPHA-1.0)*((ASCSUP*((X-DD)**2))+(ASTSUP*((EFFD-X)**2)))
      X=(B*(OVERD**2)/2)+(ALPHA*((EFFD*ASTMID)+(ASCMID*DD)))
      X=X/((B*OVERD)+(ALPHA*(ASTMID+ASCMID)))
      ZI=B*((X**3)+((OVERD-X)**3))/3
      ZIMID=ZI+(ALPHA-1.0)*((ASCMID*((X-DD)**2))+(ASTMID*((EFFD-X)**2)))
      ZI3=(2*ZISUP+ZIMID)/3
      ZK3=0.5*AMBEC*ZI3/RSL
      GOTO 130
  120 ZK4=(10**10)/2
      IF (ITYROTB.EQ.0) ZK4=0.0
      ZK3=ZK4
  130 CONTINUE
C
C     CALCULATE PROPOSED ENSLOPES WITHOUT CONSIDERATION
C     OF SECOND ORDER EFFECT OF
C     AXIAL LOAD * DIVISION POINT DEFLECTIONS
C
      IF (ITYROTA.EQ.0.AND.ITYROTB.EQ.0) GOTO 140
      IF (ITYROTA.EQ.2.AND.ITYROTB.EQ.2) GOTO 135
C
C     CALCULATE FIXED END MOMENTS AT JOINT A AND B
C
      FEMA=UDLA*(RSL**2)/12
      FEMB=UDLB*(RSL**2)/12
C
      SUMKA=ZK1+ZK2+ZKC
      SUMKB=ZK4+ZK3+ZKC
      TOP=FEMA*4*SUMKB-(2*ZKC*FEMB)
      BOT=16*SUMKA*SUMKB-((ZKC**2)*4)
      SLOPA=-(TOP/BOT)
C
      TOP=FEMB*4*SUMKA-(2*FEMA*ZKC)
      SLOPB=-(TOP/BOT)
C
C     SLOPE OF MOMENT-ROTATION RELATION
C
      SLOPE1=-4*(ZK1+ZK2)
      SLOPE2=-4*(ZK4+ZK3)
C
C     CALCULATE END MOMENTS AND AXIAL FORCE DUE TO SHEAR
C     OF MOMENTS FOR PROPOSED ENDSLOPES
C
      ZMA=2*ZKC*(2*SLOPA+SLOPB)
      ZMB=2*ZKC*(2*SLOPB+SLOPA)
C
      PSH=(UDLA*RSL/2)-(6*ZK2*SLOPA/RSL)
C
C     TOTAL AXIAL LOAD
C     AXIAL LOAD FROM STRUCTURE ABOVE + SHEAR FROM MOMENTS
C
      P=PSH+PAB
C
      GOTO 150
C
C     FIXED ROTATIONAL RESTRAINT AT BOTH ENDS
C
  135 FEMA=0.0
      FEMB=0.0
      SLOPA=0.0
      SLOPB=0.0
      ZMA=0.0
      ZMB=0.0
C
C     SLOPE OF THE MOMENT-ROTATION RELATION
C
      SLOPE1=-4*(ZK1+ZK2)
      SLOPE2=-4*(ZK4+ZK3)
C
C     AXIAL LOAD
C
      P=PAB
C
      GOTO 150
  140 CONTINUE
C
C     PINNED ROTATIONAL RESTRAINT BOTH ENDS
C
C     CALCULATE END MOMENTS
C
      ZMA=-ECCEN*PAB
      ZMB=-ZMA
      P=PAB
C
C     CALCULATE ENDSLOPES
C
      EI=AMBEC*ZIC
      VAL=COLLEN/(3*EI)
      SLOPA=VAL*(ZMA-ZMB/2)
      SLOPB=VAL*(ZMB-ZMA/2)
C
C     SLOPE OF MOMENT ROTATION RELATION
C
      SLOPE1=0.0
      SLOPE2=0.0
  150 CONTINUE
C
C     CALCULATE PROPOSED DEFLECTIONS
C
      EI=AMBEC*ZIC
      AL2=P/EI
      AL=SQRT(AL2)
      DO 180 I=1,IDIVPT
```

```
      X=GA
      IF (I.EQ.1) GOTO 170
      DO 160 J=1,I
      IF (J.EQ.1) GOTO 160
      X=X+SEGLEN(J-1)
  160 CONTINUE
  170 CONTINUE
C
      VAL1=AL*COLLEN
      VAL2=AL*X
      VAL=-((ZMA/TAN(VAL1))+(ZMB/SIN(VAL1)))*SIN(VAL2)
      VAL=VAL+ZMA*COS(VAL2)-ZMA+(ZMA+ZMB)*(X/COLLEN)
      YP(I)=VAL/P
  180 CONTINUE
C
C     CALCULATE CURVATURES
C
      DO 190 I=1,IDIVPT
      IF (I.EQ.1) GOTO 185
      X=X+SEGLEN(I-1)
      GOTO 190
  185 X=GA
  190 CURP(I)=(((ZMA+ZMB)*X/COLLEN)-ZMA)/EI
C
C     SET PROPOSED DIRECT STRAIN AT COLUMN AXIS TO ZERO AND
C     ADJUST PROPOSED DEFLECTIONS FOR DEFORMATION UNDER ZERO LOAD
C
      DO 290 I=1,IDIVPT
      STRAP(I)=0.0
      YP(I)=YP(I)+C(I)
  290 CONTINUE
C
      RETURN
C
      END
C
C
      SUBROUTINE INDUCE (NUM,IBM,ITYROT,IREST,ZM,SLOPE,SLOP,
     .                   FEM,ZKCOLM,ZKBEAM,UDL,RSL,NFL,DCOL,
     .                   ZMUCOLM,AMBEC,
     .                   IPLAST1,IPLAST2,ZI1,ZI2,ZI3,ZI4,
     .                   IPLAST3,PAB,COLAB,COLOW,
     .                   EBEAM1,EBEAM3,IPLCOL,
     .                   ZMULT1,ZMULT2,ZMULT3)
C
C
C     SUBROUTINE INDUCE CALCULATES THE CHANGES INDUCED IN MOMENTS
C     IN THE RESTRAINT SYSTEMS AND COLUMN END MOMENTS
C     FROM CONSIDERATION OF RESTRAINING MOMENT-END ROTATION
C     RELATIONS FOR CHANGES IN ENDSLOPES.
C     WHEN HINGES FORM IN THE RESTRAINING STRUCTURE THE STIFFNESS
C     OF THE REMAINING STRUCTURE IS CALCULATED USING A PLASTIC
C     ANALYSIS FROM COMPLEMENTARY ENERGY
C
C     IBM - 1 FOR TOP BEAM
C           2 FOR BOTTOM BEAM
C
      SLOPE=0.0
C
C     CHECK TYPE OF ROTATIONAL RESTRAINT
C
      IF (ITYROT.EQ.0) GOTO 420
      IF (ITYROT.EQ.2) GOTO 400
C
C     CHECK FOR PREVIOUS FORMATION OF PLASTIC HINGE
C
      IF (IPLAST2.EQ.1.OR.IPLAST3.EQ.1) GOTO 135
C
C     CHECK FOR CURRENT FORMATION OF PLASTIC HINGE
C
C     CALCULATE MOMENTS IN RESTRAINT SYSTEM
C
C     MOMENTS DUE TO ROTATION
C
      VAL=2*ZKBEAM*SLOP
      ZMR1=ABS(2*VAL+FEM)
      ZMR2=ABS(VAL-FEM)
      ZMR3=(UDL*(RSL**2)/8)-((ZMR1+ZMR2)/2)
C
C     MOMENTS DUE TO SWAY
C
      ZMS1=0.0
      ZMS2=0.0
      ZMS3=0.0
      IF (NUM.EQ.1) GOTO 130
      IF (IBM.NE.1) GOTO 130
      VAL1=6*REAL(NFL)*DCOL*ZKBEAM/RSL
      ZMS1=ABS(2*VAL+VAL1)
      ZMS2=ABS(VAL+VAL1)
C
      X=RSL*ZMS1/(ZMS1+ZMS2)
```

```
      XL=RSL/2
      IF (X.LT.XL) GOTO 110
      IF (X.GT.XL) GOTO 120
      ZMS3=0.0
      GOTO 130
  110 ZMS3=ZMS2*(XL-X)/(RSL-X)
      GOTO 130
  120 ZMS3=ZMS1*(X-XL)/X
C
C     PRINCIPLE OF SUPERPOSITION FOR ELASTICITY
C
  130 ZM1=ZMR1+ZMS1
      ZM2=ZMR2+ZMS2
      ZM3=ZMR3+ZMS3
      GOTO 170
  135 IF (IPLAST2.EQ.1.OR.IPLAST3.EQ.1) GOTO 240
  170 CONTINUE
C
C     CHECK CALCULATED MOMENTS DUE TO STRUCTURAL AND FIRE LOAD
C     DO NOT EXCEED THE ULTIMATE MOMENTS OF THE SECTION
C
      IF (IBM.EQ.2) GOTO 180
      IF (ABS(ZM2).GT.ABS(ZMULT2)) IPLAST2=1
      IF (ABS(ZM3).GT.ABS(ZMULT3)) IPLAST3=1
      GOTO 190
  180 IF (ABS(ZM2).GT.ABS(ZMULT2)) IPLAST2=1
C
  190 IF (IPLAST2.EQ.1.OR.IPLAST3.EQ.1) GOTO 240
C
      PN=0.0
C
      GOTO 400
C
C     PLASTIC ANALYSIS TO DETERMINE STIFFNESS OF REMAINING STRUCTURE
C     AND INDUCED AXIAL FORCE DUE TO AXIAL RESTRAINT
C
  240 IF (IBM.EQ.2) GOTO 310
C
C     DETERMINE YOUNGS MODULUS AND SECOND MOMENT AREA FOR MEMBERS
C
      ZIBEAM=ZI2
      ZICOLAB=ZI1
      EBEAM=AMREC
      ECOLAB=EBEAM
      IF (IREST.EQ.1) GOTO 250
      EIBEAMA=EBEAM*ZIBEAM
      GOTO 260
  250 EIBEAMA=ZIBEAM*((2*EBEAM1)+EBEAM3)/3
C
  260 IF (IPLAST3.EQ.1) GOTO 270
      IF (IPLAST2.EQ.1) GOTO 300
C
  270 IF (IPLAST2.EQ.1) GOTO 280
      FN1=REAL(NFL)*EBEAM*ZIBEAM/EIBEAMA
      FN2=3*REAL(NFL)*ZIBEAM*COLAB/(RSL*ZICOLAB)
      PN=DCOL*(FN1+FN2+1)
      FN1=5*(RSL**4)/(48*EIBEAMA)
      FN2=(RSL**3)*COLAB/(4*ECOLAB*ZICOLAB)
      FN3=(RSL**4)/(16*REAL(NFL)*EBEAM*ZIBEAM)
      PN=PN+UDL*(FN1+FN2+FN3)
      FN1=(RSL**2)/(2*EIBEAMA)
      FN2=(RSL**2)/(2*REAL(NFL)*EBEAM*ZIBEAM)
      FN3=2*RSL*COLAB/(ECOLAB*ZICOLAB)
      PN=PN+ZMULT3*(FN1+FN2+FN3)
      FN1=(RSL**2)*COLAB/(ECOLAB*ZICOLAB)
      FN2=(RSL**3)/(4*REAL(NFL)*EBEAM*ZIBEAM)
      FN3=(RSL**3)/(3*EIBEAMA)
      PN=PN/(FN1+FN2+FN3)
C
      V=-PN*(RSL**3)/(12*REAL(NFL)*EBEAM*ZIBEAM)
      FN2=(RSL**3)*COLAB/(16*ECOLAB*ZICOLAB)
      FN3=(RSL**4)/(24*REAL(NFL)*EBEAM*ZIBEAM)
      V=V+UDL*(FN2+FN3)
      FN2=RSL*COLAB/(2*ECOLAB*ZICOLAB)
      V=V-ZMULT3*FN2
      FN1=(RSL**2)*COLAB/(4*ECOLAB*ZICOLAB)
      FN2=(RSL**3)/(12*REAL(NFL)*EBEAM*ZIBEAM)
      FN3=(RSL**3)/(12*EIBEAMA)
      V=V/(FN1+FN2+FN3)
C
C     CHECK CALCULATED MOMENTS DO NOT EXCEED ULTIMATE MOMENTS
C
      ZM1=-ZMULT3+UDL*(RSL**2)/8-V*RSL/2
      ZM2=-ZMULT3+UDL*(RSL**2)/8+V*RSL/2
C
      IF (ABS(ZM2).GT.ABS(ZMULT2)) IPLAST2=1
      IF (IPLAST2.EQ.1) GOTO 260
C
C     CALCULATE STIFFNESS OF REMAINING RESTRAINT BEAM
C
      ROT1=V*RSL*COLAB/(2*ECOLAB*ZICOLAB)
      FN1=COLAB/(ECOLAB*ZICOLAB)
      FN2=RSL/(REAL(NFL)*EBEAM*ZIBEAM)
      ROT1=ROT1+ZMULT3*(FN1+FN2)
      FN1=(RSL**3)/(8*REAL(NFL)*ZICOLOW)
      V=V/(FN1+FN2)
C
C     CHECK CALCULATED MOMENTS DO NOT EXCEED ULTIMATE MOMENTS
C
      ZM1=UDL*(RSL**2)/2+ZMULT2-V*RSL
      ZM3=UDL*(RSL**2)/8+ZMULT2-V*RSL/2
C
      IF (ABS(ZM3).GT.ABS(ZMULT3)) IPLAST3=1
      IF (IPLAST3.EQ.1) GOTO 330
C
C     CALCULATE STIFFNESS OF REMAINING RESTRAINT BEAM
C
      ROT1=V*RSL*COLOW-ZMULT2*COLOW
      ROT1=ROT1-UDL*COLOW*(RSL**2)/2
      ROT1=ROT1/(ECOLOW*ZICOLOW)
C
      ZKBEAM=0.5*ABS(ZM1/ROT1)
```

```
      GOTO 400
C
  340 IF (IPLAST1.EQ.1) GOTO 350
C
      PN=0.0
      V=2*ZMULT2/RSL-UDL*RSL/4+2*ZMULT3/RSL
C
C     CHECK CALCULATED MOMENTS DO NOT EXCEED ULTIMATE MOMENTS
C
      ZM1=UDL*(RSL**2)/8-ZMULT3-V*RSL/2
C
      IF (ABS(ZM1).GT.ABS(ZMULT1)) IPLAST1=1
      IF (IPLAST1.EQ.1) GOTO 330
C
C     CALCULATE STIFFNESS OF REMAINING RESTRAINT BEAM
C
      ROT1=-UDL*(RSL**2)/8+V*RSL/2+ZMULT3
      ROT1=ROT1*COLOW/(ECOLOW*ZICOLOW)
C
      ZKBEAM=0.5*ABS(ZM1/ROT1)
      GOTO 400
C
  350 PN=0.0
      ZKBEAM=0.0
      GOTO 400
C
  400 CONTINUE
C
C     MOMENT-ROTATION RELATION FOR REMAINING STRUCTURE
C     USING SLOPE DEFLECTION EQUATIONS
C
      ZMBEAM=(4*ZKBEAM*SLOP)+FEM
      ZMCOLM=4*ZKCOLM*SLOP
      ZKCOL=ZKCOLM
      IF (ITYROT.EQ.2) GOTO 410
      SLOPUB=ZMUCOLM/(4*ZKCOLM)
      IF (ABS(SLOP).LT.SLOPUB) GOTO 410
      ZMCOLM=ZMUCOLM
      ZKCOL=3*ZKCOLM/4
      IPLCOL=1
C
  410 ZM=-(ZMBEAM+ZMCOLM)
C
C     SLOPE OF MOMENT-ROTATION RELATION
C
      SLOPE=-4*(ZKCOL+ZKBEAM)
C
C     CORRECT AXIAL FORCE
C
      IF (ITYROT.EQ.2) GOTO 420
      IF (DCOL.EQ.0.0) GOTO 420
      IF (PN.EQ.0.0) GOTO 420
      PN=SIGN(PN,DCOL)
      PAB=PAB+PN
C
```



```
C
      RETURN
C
      END



C
C
      SUBROUTINE ULTIMOM (IBUG,B,EFFD,OVERD,NUMLAY,MLTYPE,IXTYPE,YYL,
     .                    AL,RC,ZMU,ATL,TEMPFY,VALFY,TEMPMOD,VALMOD,
     .                    TEMPSM,VALSM,TEMPEM,VALEM,EBEAM,ALPHA)
C
      COMMON /CONTROL/ NIN,NOUT,NFILE,ITITLE(80)
      DIMENSION MLTYPE(NUMLAY),YYL(NUMLAY),AL(NUMLAY),ATL(NUMLAY),
     .          RC(100),TEMPFY(8),VALFY(8),TEMPMOD(8),VALMOD(8),
     .          TEMPSM(8),VALSM(8),TEMPEM(8),VALEM(8)
C
C     SUBROUTINE ULTIMOM CALCULATES THE ULTIMATE MOMENT FOR THE
C     FIRE EXPOSED STRUCTURAL CROSS SECTIONS OF THE RESTRAINT SYSTEM
C
C     IXTYPE - 1 FOR CROSS SECTION WITH BOTTOM TENSION STEEL
C            - 2 FOR CROSS SECTION WITH TOP TENSION STEEL
C
C     ASSUME DEPTH OF NEUTRAL AXIS
C
      IL=0
      DO 180 LL=3,99,1
      IL=IL+1
      VALU=REAL(LL-1)/100
      XNA=EFFD*VALU
C
C     DETERMINE AVERAGE TEMPERATURE OF EXTREME CONCRETE FIBRE
C
      AVTC=0.0
      ICO=0
      IF (IXTYPE.EQ.2) GOTO 80
      EFC=YYL(1)
      GOTO 90
   80 EFC=YYL(NUMLAY)
   90 DO 100 I=1,NUMLAY
      IF (YYL(I).NE.EFC) GOTO 100
      AVTC=AVTC+ATL(I)
      ICO=ICO+1
  100 CONTINUE
      AVTC=AVTC/ICO
C
C     DETERMINE ULTIMATE CONCRETE STRAIN FROM ASSUMPTION
C     ULTIMATE STRAIN VARIES BETWEEN 0.0035 AT 20 DEG C
C     AND 0.006 AT 500 DEG C.  FOR TEMPERATURES GREATER
C     THAN 500 DEG C ULTIMATE STRAIN IS EQUAL TO 0.006
C
      ULTSTRN=0.0035+(0.0025/480)*(AVTC-20)
      IF (AVTC.GT.500) ULTSTRN=0.006
```

```
C     CALCULATE TENSILE FORCE IN STEEL
C
      T=0.0
      AVEST=0.0
      AST=0.0
      IST=0
      Y=OVERD-XNA
      DO 130 I=1,NUMLAY
      VAL=YYL(I)
      IF (MLTYPE(I).NE.2) GOTO 130
      IF (IXTYPE.EQ.2) GOTO 110
      IF (VAL.LE.XNA) GOTO 130
      GOTO 120
  110 IF (VAL.GE.Y) GOTO 130
  120 TEMP=ATL(I)
      AST=AST+AL(I)
      IST=IST+1
      MTYPE=MLTYPE(I)
      CALL TEMPEN (MTYPE,TEMP,TEMPFY,VALFY,FY)
      CALL TEMPEN (MTYPE,TEMP,TEMPMOD,VALMOD,EMOD)
      EY=FY/EMOD
      STRNRS=ULTSTRN*((EFFD/XNA)-1)
      I1=0
      S2=0.0
      S3=0.0
      ETEN=0.0
      CALL STRESIN (MTYPE,EM,SM,EY,FY,ETJ,ETEN,
     .              I1,STRNRS,S2,S3,STRSRS)
C
      T=T+2*STRSRS*AL(I)
C
      AVEST=AVEST+EMOD
C
  130 CONTINUE
C
C     CALCULATE AVERAGE YOUNGS MODULUS STEEL
C
      AVEST=AVEST/IST
C
C     CALCULATE COMPRESSIVE FORCE IN CONCRETE AND STEEL
C
C     CALCULATE STRAINS AT CENTRE OF EACH LAYER
C
      C=0.0
      ZMU1=0.0
      ZMU2=0.0
      AVEC=0.0
      AVESC=0.0
      ASC=0.0
      ICO=0
      IST=0
      DO 170 I=1,NUMLAY
      VAL=YYL(I)
      IF (IXTYPE.EQ.2) GOTO 140
      IF (VAL.GE.XNA) GOTO 170
      ---- ---
  140 IF (VAL.LE.Y) GOTO 170
C
      STRNRS=ULTSTRN*(VAL-(OVERD-XNA))/XNA
      GOTO 155
C
  150 STRNRS=ULTSTRN*(XNA-VAL)/XNA
C
  155 TEMP=ATL(I)
      MTYPE=MLTYPE(I)
      IF (MTYPE.EQ.1) ICO=ICO+1
      IF (MTYPE.EQ.2) IST=IST+1
      IF (MTYPE.EQ.2) GOTO 156
C
C     CALCULATE CONCRETE TEMPERATURE DEPENDENT MATERIAL PARAMETERS
C
C     CONCRETE STRAIN AT MAXIMUM STRESS
C
      CALL TEMPEN (MTYPE,TEMP,TEMPEM,VALEM,EM)
C
C     MAXIMUM CONCRETE STRESS
C
      CALL TEMPEN (MTYPE,TEMP,TEMPSM,VALSM,SM)
      GOTO 157
C
C     CALCULATE STEEL TEMPERATURE DEPENDENT MATERIAL PARAMETERS
C
C     STEEL ELASTIC MODULUS
C
  156 CALL TEMPEN (MTYPE,TEMP,TEMPMOD,VALMOD,EMOD)
C
C     STEEL YIELD STRESS
C
      CALL TEMPEN (MTYPE,TEMP,TEMPFY,VALFY,FY)
C
      EY=FY/EMOD
C
C     CALCULATE STRESS AT CENTRE OF COMPRESSION ELEMENT
C
  157 I1=0
      S2=0.0
      S3=0.0
      ETEN=0.0
C
      CALL STRESIN (MTYPE,EM,SM,EY,FY,ETJ,ETEN,
     .              I1,STRNRS,S2,S3,STRSRS)
C
      VAL1=AL(I)
      C=C+2*VAL1*STRSRS
C
      IF (MTYPE.EQ.1) AVEC=AVEC+(EXP(1.0)*SM/EM)
      IF (MTYPE.EQ.2) AVESC=AVESC+EMOD
      IF (MTYPE.EQ.2) ASC=ASC+VAL1
C
C     CALCULATE ULTIMATE MOMENT - MOMENTS ABOUT STEEL
C
```

```
C
      ZMU1=ZMU1+2*VAL1*STRSRS*(EFFD-VAL)
      ZMU2=ZMU2+2*VAL1*STRSRS*VAL
      GOTO 170
  160 ZMU1=ZMU1+2*VAL1*STRSRS*(VAL-OVERD+EFFD)
      ZMU2=ZMU2+2*VAL1*STRSRS*(OVERD-VAL)
C
  170 CONTINUE
C
      ZMU2=ZMU2-T*EFFD
C
C     CALCULATE AVERAGE YOUNGS MODULUS CONCRETE
C     AND COMPRESSION STEEL
C
      AVEC=AVEC/ICO
      IF (IST.GT.0) AVESC=AVESC/IST
C
C     DETERMINE LESSER ULTIMATE MOMENT
C
      IF (ABS(ZMU1).LE.ABS(ZMU2)) ZMU=ABS(ZMU1)
      IF (ABS(ZMU2).LT.ABS(ZMU1)) ZMU=ABS(ZMU2)
C
C     CALCULATE AVERAGE YOUNGS MODULUS OF SECTION
C
      EBEAM=AVEC
C
C     CALCULATE ALPHA = ESTEEL / ECONCRETE
C
      ALPHA=AVEST/AVEC
C
      RC(IL)=C-T
      IF (IL.EQ.1) GOTO 180
      R=RC(IL)/RC(IL-1)
      IF (R.LT.0.0) GOTO 190
  180 CONTINUE
      GOTO 200
  190 CONTINUE
C
      IF (IBUG.NE.2) GOTO 195
      IF (IXTYPE.EQ.1) WRITE (NOUT,310)
      IF (IXTYPE.EQ.2) WRITE (NOUT,320)
      WRITE (NOUT,330) XNA
      WRITE (NOUT,340) AST
      WRITE (NOUT,350) ASC
      WRITE (NOUT,360) ABS(ZMU1)
      WRITE (NOUT,370) ABS(ZMU2)
  195 CONTINUE
C
      RETURN
C
  200 WRITE (NOUT,300)
      STOP
C
  300 FORMAT (////50H . . . EQUILIBRIUM UNSATISFIED IN RESTRAINT SYSTEM)
  310 FORMAT (///1X,24HCROSS SECTION AT MIDSPAN)
  330 FORMAT (/1X,24HDEPTH TO NEUTRAL AXIS = ,F6.4,2H M)
  340 FORMAT (/1X,24HAREA OF TENSION STEEL = ,6PF8.2,6H MM**2)
  350 FORMAT (/1X,28HAREA OF COMPRESSION STEEL = ,6PF8.2,6H MM**2)
  360 FORMAT (/1X,7HZMU1 = ,F7.2)
  370 FORMAT (/1X,7HZMU2 = ,F7.2)
C
      END
C
C
      SUBROUTINE DIVPTBM (ISECO,SEGLEN,ZMA,P,YP,ZMB,GA,COLLEN,ZMR,
     *                    NUMSEG,IDIVPT)
C
      COMMON /CONTROL/ NIN,NOUT,NFILE,ITITLE(80)
      DIMENSION ZMR(IDIVPT),SEGLEN(NUMSEG),YP(IDIVPT)
C
C     SUBROUTINE DIVPTBM CALCULATES THE DIVISION POINT
C     BENDING MOMENTS ABOUT THE AXIS OF THE COLUMN
C
      DO 140 I=1,IDIVPT
      SUM=0.0
      IF (GA.EQ.0.0) GOTO 105
      SUM=SQRT((GA**2)-(YP(1)**2))
  105 IF (I.EQ.1) GOTO 115
      DO 110 J=1,I
      IF (J.EQ.1) GOTO 110
      OP=(YP(J))-(YP(J-1))
      SUM=SUM+SQRT((SEGLEN(J-1)**2)-(OP**2))
  110 CONTINUE
  115 CONTINUE
C
      IF (ISECO.EQ.1) GOTO 120
      SECORD=0.0
      GOTO 130
C
C     CALCULATE SECOND ORDER EFFECTS
C
  120 SECORD=P*YP(I)
C
  130 ZMR(I)=-(ZMA+SECORD)+((ZMA+ZMB)*SUM/COLLEN)
C
  140 CONTINUE
C
      RETURN
C
      END
```

```
C
C
      SUBROUTINE CURVAT (IT,NIT,NUM,MMTYPE,STRAP,CURP,YY,YP,GA,SEGLEN,
     .                   A,P,ZMR,ALPHA,BETA,CURV,AID,TIME,
     .                   VALEM,VALSM,VALFY,VALMOD,
     .                   TEMPEM,TEMPSM,TEMPFY,TEMPMOD,EMUO,
     .                   NUMSEG,NUMEL,IDIVPT,NUMTIM)
C
      COMMON /CONTROL/ NIN,NOUT,NFILE,ITITLE(80)
      COMMON /LCM/ AT(150,65),STRAIN(150,20),
     .             STRESS(150,20),ITFC(150,20),EO(150,20),
     .             ET(150,20),ITF(150,20),CS(150,20),SO(150,20),
     .             TOTSTRN(150,20),TR(150,20),TENSTR(150,20),
     .             ATMIDA(100,65),ATMIDB(100,65),
     .             ATSUPA(100,65),ATSUPB(100,65),
     .             FIRSTRN(150,20)
      LEVEL 2,/LCM/
      DIMENSION STRAP(IDIVPT),YP(IDIVPT),CURP(IDIVPT),
     .          YY(NUMEL),AM(2,2),ZINC(2,1),A(NUMEL),
     .          ZMR(IDIVPT),SEGLEN(NUMSEG),CURV(IDIVPT),
     .          MMTYPE(NUMEL),TIME(NUMTIM),
     .          VALEM(8),VALSM(8),VALFY(8),
     .          VALMOD(8),AID(2,2,IDIVPT),
     .          TEMPEM(8),TEMPSM(8),TEMPFY(8),TEMPMOD(8)
C
C     SUBROUTINE CURVAT CALCULATES THE CURVATURE AT EACH
C     DIVISION POINT CORRESPONDING TO THE LOADING
C
C     EO - STRAIN FROM PREVIOUS TIME STEP
C     SO - STRESS FROM PREVIOUS TIME STEP
C     TR - TRANSIENT STRAIN HISTORY
C     ITF - ACTUAL INDICATOR FOR TENSILE FAILURE OF ELEMENT
C     ITFC - CURRENT INDICATOR FOR TENSILE FAILURE OF ELEMENT
C     TENSTR - VALUE OF STRAIN GIVING ZERO STRESS ON UNLOAD LINE
C
      DO 190 IDIV=1,IDIVPT
      ICON=0
C
  100 SUM1=0.0
      SUM2=0.0
      SUM3=0.0
      SUM4=0.0
      SUM5=0.0
      ICON=ICON+1
C
C     WHERE - SUM1 = SUM OF STRAIN RELATED STRESS * AREA
C             SUM2 = SUM OF STRAIN RELATED STRESS * AREA
C                    * ORDINATE
C             SUM3 = SUM OF TANGENT MODULUS * AREA
C             SUM4 = SUM OF TANGENT MODULUS * AREA
C                    * ORDINATE
C             SUM5 = SUM OF TANGENT MODULUS * AREA
C                    * ORDINATE**2
C
      DO 130 LEM=1,NUMEL
C     SET CURRENT INDICATOR FOR TENSILE FAILURE OF ELEMENT
C
      ITFC(LEM,IDIV)=ITF(LEM,IDIV)
C
C     CALCULATE TEMPERATURE DEPENDENT MATERIAL PARAMETERS
C
      TEMP=AT(LEM,NUM)
      MTYPE=MMTYPE(LEM)
      IF (MTYPE.EQ.2) GOTO 110
C
C     CALCULATE CONCRETE STRAIN AT PEAK STRESS
C
      CALL TEMPEN (MTYPE,TEMP,TEMPEM,VALEM,EM1)
C
C     CALCULATE CONCRETE STRAIN AT PEAK STRESS
C     FOR PREHISTORY OF STRESS
C
      EM2=EM1-TR(LEM,IDIV)
      EM=AMAX1(EMUO,EM2)
C
C     CALCULATE PEAK CONCRETE STRESS
C
      CALL TEMPEN (MTYPE,TEMP,TEMPSM,VALSM,SM)
      GOTO 120
C
C     CALCULATE YIELD STRESS STEEL
C
  110 CALL TEMPEN (MTYPE,TEMP,TEMPFY,VALFY,FY)
C
C     CALCULATE ELASTIC MODULUS STEEL
C
      CALL TEMPEN (MTYPE,TEMP,TEMPMOD,VALMOD,EMOD)
      EY=FY/EMOD
C
  120 TOTSTRN(LEM,IDIV)=STRAP(IDIV)+(CURP(IDIV)*YY(LEM))
C
C     ANDERBERG AND THELANDERSON TOTAL STRAIN MODEL
C
      STRAIN(LEM,IDIV)=TOTSTRN(LEM,IDIV)-FIRSTRN(LEM,IDIV)
C
C     CORRESPONDING STRESS FOUND BY INTERPOLATION OF STRESS-
C     STRAIN RELATIONSHIP ALONG WITH CORRESPONDING VALUE OF
C     TANGENT MODULUS
C
      I1=ITFC(LEM,IDIV)
      S1=STRAIN(LEM,IDIV)
      S2=EO(LEM,IDIV)
      S3=SO(LEM,IDIV)
      ETEN=TENSTR(LEM,IDIV)
C
      CALL STRESIN (MTYPE,EM,SM,EY,FY,ETJ,ETEN,
     .              I1,S1,S2,S3,S4)
      ITFC(LEM,IDIV)=I1
      TENSTR(LEM,IDIV)=ETEN
C
```

```
C
      VAL1=STRESS(LEM,IDIV)
      VAL2=A(LEM)
      VAL3=YY(LEM)
      VAL4=VAL1*VAL2*2
      VAL5=VAL4*VAL3
      VAL6=ETJ*VAL2*2
      VAL7=VAL6*VAL3
      VAL8=VAL7*VAL3
      SUM1=SUM1+VAL4
      SUM2=SUM2+VAL5
      SUM3=SUM3+VAL6
      SUM4=SUM4+VAL7
      SUM5=SUM5+VAL8
C
  130 CONTINUE
C
C     CALCULATED AXIAL FORCE AND DIVISION POINT MOMENT
C
      PC=SUM1
      ZMC=SUM2
C
C     CHECK INCOMPATABILITIES ARE BELOW ALLOWABLE LIMITS
C
C     ADJUST AXIAL FORCE FOR SEGMENT DISPLACEMENT
C
      IF (IDIV.GT.1) GOTO 140
      OP=YP(IDIV)
      IF (GA.EQ.0.0) GOTO 160
      ADJ=SQRT(ABS((GA**2)-(OP**2)))
      GOTO 150
  140 OP=(YP(IDIV))-(YP(IDIV-1))
      ADJ=SQRT(ABS((SEGLEN(IDIV-1)**2)-(OP**2)))
  150 IF (ADJ.EQ.0.0) GOTO 160
      CAN=COS(OP*3.1415927/(ADJ*180))
      GOTO 170
  160 CAN=1.0
C
  170 AA=PC-(P*CAN)
      BB=ZMC-ZMR(IDIV)
      IF (ABS(AA).LE.ALPHA.AND.ABS(BB).LE.BETA) GOTO 180
C
C     MODIFICATIONS TO STRAP(IDIV) AND CURP(IDIV)
C     MUST REDUCE AA AND BB TO ZERO ON NEXT ITERATION
C
      AM(1,1)=SUM3
      AM(2,1)=SUM4
      AM(1,2)=SUM4
      AM(2,2)=SUM5
C
      ZINC(1,1)=-AA
      ZINC(2,1)=-BB
C
C     SOLVE FOR MODIFIED VALUES OF ALPHA AND BETA
C
C
C     THE SUM OF PROPOSED VALUES OF DIRECT STRAIN
C     AND CURVATURE FOR CURRENT ITERATION AND
C     MODIFIED VALUES OF DIRECT STRAIN AND CURVATURE
C     ARE THE VALUES USED FOR THE NEXT ITERATION
C
      STRAP(IDIV)=STRAP(IDIV)+ZINC(1,1)
      CURP(IDIV)=CURP(IDIV)+ZINC(2,1)
C
      IF (ICON.GT.NIT) GOTO 290
      GOTO 100
C
  180 CURV(IDIV)=CURP(IDIV)
C
      AID(1,1,IDIV)=SUM3
      AID(2,1,IDIV)=SUM4
      AID(1,2,IDIV)=SUM4
      AID(2,2,IDIV)=SUM5
C
  190 CONTINUE
C
      RETURN
C
  290 WRITE (NOUT,320) IDIV
      WRITE (NOUT,330) TIME(NUM)
      IT=5HFAILD
      RETURN
C
C
  320 FORMAT (///1X,32HCOLUMN FAILED AT DIVISION POINT ,I2,28H - EQUILLI
     .BRIUM NOT ACHIEVED)
  330 FORMAT (/1X,18HTIME AT FAILURE = ,F7.4,6H HOURS)
C
      END
```

```
C
C
      SUBROUTINE TEMPEN (MTYPE,TEMP,TEMPER,VALUE,COEFF)
C
C     SUBROUTINE TEMPEN CALCULATES THE TEMPERATURE
C     DEPENDENT MATERIAL PARAMETERS
C
C     THE TEMPERATURE DEPENDENT MATERIAL PARAMETER IS
C     REPRESENTED BY A SERIES OF POINTS AND CONNECTING
C     LINES WHERE THE Y AXIS IS THE MATERIAL PARAMETER
C     AND THE X AXIS TEMPERATURE. VALUE OF MATERIAL
C     PROPERTY, COEFF, FOR A GIVEN TEMP TI IS -
C
C     COEFF=VALUE(TN)+(TI+TN)*SN
C
C     WHERE - TN .LE. TI .LE. TN+1
C             SN = SLOPE BETWEEN POINTS N AND N+1
C
      COMMON /CONTROL/ NIN,NOUT,NFILE,ITITLE(80)
      DIMENSION TEMPER(8),VALUE(8)
C
      DO 120 I=1,8
      TEMP1=TEMPER(I)
      VAL1=VALUE(I)
      IF (TEMP.LT.TEMP1) GOTO 130
      IF (TEMP.EQ.TEMP1) GOTO 140
  120 CONTINUE
      WRITE (NOUT,200)
      IF (MTYPE.EQ.2) GOTO 125
      WRITE (NOUT,210) TEMP
      STOP
  125 WRITE (NOUT,220) TEMP
      STOP
  130 IF (I.GT.1) GOTO 135
      SN=VAL1/TEMP1
      COEFF=VAL1+SN*(TEMP-TEMP1)
C
      RETURN
C
  135 TEMP2=TEMPER(I-1)
      VAL2=VALUE(I-1)
      SN=(VAL1-VAL2)/(TEMP1-TEMP2)
      COEFF=VAL2+((TEMP-TEMP2)*SN)
C
      RETURN
C
  140 COEFF=VAL1
C
      RETURN
C
  200 FORMAT (////50H   TEMPERATURE EXCEEDS RANGE OF MATERIAL PARAMETER)
  210 FORMAT (//1X,30HCONCRETE ELEMENT - TEMPERATURE,F7.2,6H DEG C)
  220 FORMAT (//1X,27HSTEEL ELEMENT - TEMPERATURE,F7.2,5HDEG C)
C
      END
```

```
C
      SUBROUTINE FIRECON (NUM,IDIV,MTYPE,TEMP,LEM,SM,TEMPES,VALES,
     .                    NUMEL,STRNTH,STRNTR,STRNCR,STRNSH,
     .                    TIME,ISHIN,SCUO,NUMTIM,IDIVPT)
C
      COMMON /CONTROL/ NIN,NOUT,NFILE,ITITLE(80)
      COMMON /LCM/ AT(150,65),STRAIN(150,20),
     .             STRESS(150,20),ITFC(150,20),EO(150,20),
     .             ET(150,20),ITF(150,20),CS(150,20),SO(150,20),
     .             TOTSTRN(150,20),TR(150,20),TENSTR(150,20),
     .             ATMIDA(100,65),ATMIDB(100,65),
     .             ATSUPA(100,65),ATSUPB(100,65),
     .             FIRSTRN(150,20)
      LEVEL 2,/LCM/
      DIMENSION TIME(NUMTIM),TEMPES(8),VALES(8),
     .        STRNTR(150,20),STRNCR(150,20),
     .        STRNTH(NUMEL),STRNSH(NUMEL)
C
C     SUBROUTINE FIRECON CONTROLS AND SELECTS SUBROUTINES
C     FOR THE CALCULATION OF INDUCED STRAINS AS A RESULT
C     OF THE FIRE ENVIRONMENT
C
C     CHECK MATERIAL TYPE
C
      IF (MTYPE.EQ.2) GOTO 110
C
C     CONCRETE MODELS
C
C     CALCULATE THERMAL STRAINS IN CONCRETE ELEMENT
C
      CALL THERM (MTYPE,TEMP,TEMPES,VALES,ETHERM)
C
C     CALCULATE TRANSIENT STRAINS IN CONCRETE ELEMENT
C
      CALL TRANS (IDIV,TEMP,LEM,ETHERM,ETRANS,SCUO)
      IF (ETRANS.EQ.0.0) ETRANS=STRNTR(LEM,IDIV)
C
C     CALCULATE CREEP STRAINS IN CONCRETE ELEMENT
C
      CALL CREEP (NUM,IDIV,TEMP,LEM,TIME,NUMTIM,SM,ECREEP)
C
C     CALCULATE SHRINKAGE STRAINS IN CONCRETE ELEMENT
C
      IF (ISHIN.EQ.0) GOTO 115
      CALL SHRINK (NUM,LEM,IDIV,TIME,TEMP,NUMTIM)
      ESHRIN=CS(LEM,IDIV)
C
      GOTO 120
  110 CONTINUE
C
C     STEEL MODELS
C
C     CALCULATE THERMAL STRAIN IN STEEL ELEMENT
C
      CALL THERM (MTYPE,TEMP,TEMPES,VALES,ETHERM)
```

```
C     CALCULATE CREEP STRAIN IN STEEL ELEMENT
C
      CALL STREEP (NUM,TEMP,LEM,IDIV,TIME,NUMTIM)
      ECREEP=ET(LEM,IDIV)
C
      ETRANS=0.0
  115 CONTINUE
      ESHRIN=0.0
C
  120 CONTINUE
C
C     TOTAL INDUCED STRAIN DUE TO FIRE ENVIRONMENT
C
      FIRSTRN(LEM,IDIV)=ETHERM+ETRANS+ECREEP+ESHRIN
C
      STRNTH(LEM)=ETHERM
      STRNTR(LEM,IDIV)=ETRANS
      STRNCR(LEM,IDIV)=ECREEP
      STRNSH(LEM)=ESHRIN
      RETURN
C
      END
```

```
C
C
      SUBROUTINE THERM (MTYPE,TEMP,TEMPES,VALES,ETH)
C
      COMMON /CONTROL/ NIN,NOUT,NFILE,ITITLE(80)
      DIMENSION TEMPES(8),VALES(8)
      DATA A1,B1,C1,D1,E1 /0.02837,-0.2447,0.7376,0.3229,0.09218/
      DATA A2,B2,C2,D2,E2 /0.02102,-0.4972,3.791,-8.265,5.561/
C
C     SUBROUTINE THERM CALCULATES THE INDUCED STRAINS
C     DUE TO THERMAL EXPANSION
C
      IF (MTYPE.EQ.2) GOTO 200
C
C     CONCRETE THERMAL EXPANSION MODEL USING
C     ANDERBERG VARIATION AND FORSEN POLYNOMIAL FIT
C
      T=TEMP/100.0
      IF (T.GE.6.0) GOTO 100
C
      A=A1
      B=B1
      C=C1
      D=D1
      E=E1
      GOTO 110
  100 A=A2
      B=B2
      C=C2
      D=D2
      E=E2
C
  110 ETH=A*(T**4)+B*(T**3)+C*(T**2)+D*T+E
      ETH=-(ETH*1E-3)+1.8435E-4
C
      RETURN
C
  200 CONTINUE
C
C     STEEL THERMAL EXPANSION MODEL
C     THERMAL STRAIN IS A FUNCTION OF THE TEMPERATURE
C     DEPENDENT COEFFICIENT OF THERMAL EXPANSION AND
C     THE TEMPERATURE
C
C     CTE - COEFFICIENT OF THERMAL EXPANSION
C           (TEMPERATURE DEPENDENT)
C     TEMP - TEMPERATURE OF ELEMENT
C     ETH - STRAIN DUE TO THERMAL EXPANSION
C
      ETH=0.0
      DO 220 I=1,8
      TEMP1=TEMPES(I)
      VAL1=VALES(I)
      IF (I.EQ.1) GOTO 205
      TEMP2=TEMPES(I-1)
```

```
  205 IF (TEMP.LE.TEMP1) GOTO 230
      IF (I.GT.1) GOTO 210
      CTE=VAL1
      ETH=CTE*(TEMP1-20.0)
      GOTO 220
  210 CTE=VAL1
      ETH=ETH+CTE*(TEMP1-TEMP2)
  220 CONTINUE
C
      WRITE (NOUT,300)
      STOP
C
  230 IF (I.GT.1) GOTO 240
      CTE=VAL1
      ETH=CTE*(TEMP-20.0)
      GOTO 250
  240 SN=(VAL1-VAL2)/(TEMP1-TEMP2)
      CTE=VAL2+SN*(TEMP-TEMP2)
      ETH=ETH+CTE*(TEMP-TEMP2)
  250 CONTINUE
C
      ETH=-ETH
C
      RETURN
C
  300 FORMAT (////67HTEMPERATURE EXCEEDS RANGE OF STEEL COEFFICIENT OF T
     .HERMAL EXPANSION)
C
      END
```



```
C
C
      SUBROUTINE TRANS (IDIV,TEMP,LEM,ETH,ETR,SCUO)
C
      COMMON /CONTROL/ NIN,NOUT,NFILE,ITITLE(80)
      COMMON /LCM/ AT(150,65),STRAIN(150,20),
     .             STRESS(150,20),ITFC(150,20),EO(150,20),
     .             ET(150,20),ITF(150,20),CS(150,20),SO(150,20),
     .             TOTSTRN(150,20),TR(150,20),TENSTR(150,20),
     .             ATMIDA(100,65),ATMIDB(100,65),
     .             ATSUPA(100,65),ATSUPB(100,65),
     .             FIRSTRN(150,20)
      LEVEL 2,/LCM/
      DATA C2 /2.35/
C
C     SUBROUTINE TRANS CALCULATES THE INDUCED TRANSIENT
C     STRAIN WHERE THE TRANSIENT STRAIN IS CONSIDERED
C     TO BE A FUNCTION OF THE COEFFICIENT OF THERMAL
C     EXPANSION
C
C     C2 - A CONSTANT VARYING WITH CEMENT TYPE
C          IN THE RANGE OF 1.8 TO 2.35
C     ETH - STRAIN DUE TO THERMAL EXPANSION
C     SCUO - COMPRESSIVE ULTIMATE STRENGTH OF
C            CONCRETE AT AMBIENT CONDITIONS
C     SO(LEM,IDIV) - STRESS IN ELEMENT FROM
C                    PREVIOUS TIME INCREMENT
C     TR(LEM,IDIV) - TRANSIENT STRAIN HISTORY
C     ETR - TRANSIENT STRAIN
C
C     FOR TEMPERATURES LESS THAN OR EQUAL TO 500 DEG.C
C
      ETR=0.0
      IF (SO(LEM,IDIV).LT.0.0) RETURN
      IF (TEMP.GT.500.0) GOTO 110
C
      ETR=-C2*SO(LEM,IDIV)*ETH/SCUO
C
      GOTO 120
  110 CONTINUE
C
C     ABOVE 500 DEG.C ACCELERATED EFFECT ON TRANSIENT STRAIN
C
      ETR=C2*SO(LEM,IDIV)*7.10608E-3/SCUO
      ETR=ETR+0.1E-3*(TEMP-500.0)*SO(LEM,IDIV)/SCUO
C
  120 CONTINUE
C
C     SET TRANSIENT STRAIN HISTORY
C
      TR(LEM,IDIV)=ETR
C
      RETURN
C
      END
```

```
C
C
      SUBROUTINE CREEP (NUM,IDIV,TEMP,LEM,TIME,NUMTIM,SM,ECR)
C
      COMMON /CONTROL/ NIN,NOUT,NFILE,ITITLE(80)
      COMMON /LCM/ AT(150,65),STRAIN(150,20),
     .             STRESS(150,20),ITFC(150,20),EO(150,20),
     .             ET(150,20),ITF(150,20),CS(150,20),SO(150,20),
     .             TOTSTRN(150,20),TR(150,20),TENSTR(150,20),
     .             ATMIDA(100,65),ATMIDB(100,65),
     .             ATSUPA(100,65),ATSUPB(100,65),
     .             FIRSTRN(150,20)
      LEVEL 2,/LCM/
      DIMENSION TIME(NUMTIM)
      DATA BETAO,ZK1,T3,P /0.53E-3,3.04E-3,3.0,0.5/
C
C     SUBROUTINE CREEP CALCULATES THE INDUCED CREEP STRAIN
C     IN THE CONCRETE ELEMENT FROM ANDERBERG AND
C     THELANDERSON MODEL FOR PRIMARY AND SECONDARY CREEP
C
C     SO(LEM,IDIV) - STRESS FROM PREVIOUS TIME STEP
C     ET(LEM,IDIV) - CREEP STRAIN FROM PREVIOUS TIME STEP
C     BETO - CONSTANT DEPENDING ON CONCRETE TYPE
C     K1 - CONSTANT DEPENDING ON CONCRETE TYPE
C     T3 - 3 HOUR TIME, SECONDARY CREEP PHASE
C     SM - ULTIMATE CONCRETE STRENGTH AT CURRENT TEMPERATURE
C     P - DIMENSIONLESS CONSTANT
C     ECR - INDUCED STRAIN DUE TO CREEP
C
      IF (SO(LEM,IDIV).GT.0.0) GOTO 100
      ECR=ET(LEM,IDIV)
      RETURN
C
  100 CONTINUE
C
C     CALCULATE TIME INCREMENT
C
      DTIME=TIME(NUM)-TIME(NUM-1)
C
C     CALCULATE CREEP STRAIN USING STRAIN HARDENING PRINCIPLE
C
C
C     CALCULATE MATERIAL TIME
C
      X1=SO(LEM,IDIV)/SM
      X2=EXP(ZK1*(TEMP-20.0))
      IF (NUM.GT.2) GOTO 110
      TM=0.0
      GOTO 120
  110 TM=T3*((ET(LEM,IDIV)/(BETAO*X1*X2))**(1/P))
C
  120 X3=((TM+DTIME)/T3)**P
      ECR=BETAO*X1*X2*X3
C
      ET(LEM,IDIV)=ECR
C
      RETURN
C
      END
C
C
      SUBROUTINE SHRINK (NUM,LEM,IDIV,TIME,TEMP,NUMTIM)
C
      COMMON /CONTROL/ NIN,NOUT,NFILE,ITITLE(80)
      COMMON /LCM/ AT(150,65),STRAIN(150,20),
     .             STRESS(150,20),ITFC(150,20),EO(150,20),
     .             ET(150,20),ITF(150,20),CS(150,20),SO(150,20),
     .             TOTSTRN(150,20),TR(150,20),TENSTR(150,20),
     .             ATMIDA(100,65),ATMIDB(100,65),
     .             ATSUPA(100,65),ATSUPB(100,65),
     .             FIRSTRN(150,20)
      LEVEL 2,/LCM/
      DIMENSION TIME(NUMTIM)
C
C     SUBROUTINE SHRINK CALCULATES THE CHANGE IN SHRINKAGE
C     STRAIN DURING A TIME STEP. THE INCREMENTAL SHRINKAGE
C     STRAIN IS CALCULATED FROM THE FOLLOWING FORMULA AND
C     IS CONSIDERED TO BE IRRECOVERABLE
C
C     INCREMENTAL STRAIN = ESHR = A(T)*(SMAX(T)-CS)*DTIME
C
C     A - SHRINKAGE RATE CONSTANT
C     SMAX - MAXIMUM POSSIBLE SHRINKAGE
C     CS - CUMALITIVE SHRINKAGE FROM PREVIOUS TIME STEP
C
C     CHECK TO SEE IF MAXIMUM SHRINKAGE HAS ALREADY OCCURRED
C
      IF (TEMP.LE.20.0) GOTO 100
      IF (CS(LEM,IDIV)-0.001) 110,100,100
C
  100 ESHR=0.0
      RETURN
C
C     CHECK TO SEE IF SUBSLICE TEMPERATURE HAS EXCEEDED 100 C
C
  110 IF (TEMP-100.0) 130,130,120
C
C     IF TEMPERATURE HAS EXCEEDED 100 C THEN ALL SHRINKAGE MUST OCCUR
C
  120 ESHR=0.001-CS(LEM,IDIV)
      CS(LEM,IDIV)=0.001
      RETURN
C
C     CALCULATE A AND SMAX
C
  130 SMAX=TEMP-20.0
      SMAX=0.0125*SMAX
      A=SMAX*SMAX
      A=A+0.001
```

```
      SMAX=0.0005*SMAX
C
C     CHECK TO SEE IF CS HAS ALREADY EXCEEDED SMAX
C
      IF (CS(LEM,IDIV)-SMAX) 140,160,160
C
C     CALCULATE INCREMENTAL SHRINKAGE STRAIN
C
  140 DTIME=TIME(NUM)-TIME(NUM-1)
      ESHR=A*(SMAX-CS(LEM,IDIV))*DTIME
      CS(LEM,IDIV)=CS(LEM,IDIV)+ESHR
C
C     CHECK TO SEE THAT CS DOES NOT EXCEED SMAX
C
      IF (CS(LEM,IDIV)-SMAX) 160,160,150
C
C     CORRECT ESHR IF CS HAS EXCEEDED SMAX
C
  150 ESHR=SMAX-(CS(LEM,IDIV)-ESHR)
      CS(LEM,IDIV)=SMAX
C
  160 RETURN
C
      END
```

```
C
C
      SUBROUTINE STREEP (NUM,TEMP,LEM,IDIV,TIME,NUMTIM)
C
      COMMON /CONTROL/ NIN,NOUT,NFILE,ITITLE(80)
      COMMON /LCM/ AT(150,65),STRAIN(150,20),
     .             STRESS(150,20),ITFC(150,20),EO(150,20),
     .             ET(150,20),ITF(150,20),CS(150,20),SO(150,20),
     .             TOTSTRN(150,20),TR(150,20),TENSTR(150,20),
     .             ATMIDA(100,65),ATMIDB(100,65),
     .             ATSUPA(100,65),ATSUPB(100,65),
     .             FIRSTRN(150,20)
      LEVEL 2,/LCM/
      DIMENSION TIME(NUMTIM)
C
C     SUBROUTINE STREEP CALCULATES THE INDUCED INCREMENTAL STRAIN DUE
C     TO CREEP IN THE STEEL ELEMENT USING HARMATHY'S
C     COMPREHENSIVE CREEP MODEL, WITH DORNS THETA METHOD
C     FOR TEMPERATURE VARIATION
C
C     Z - ZENER-HOLLOMAN CONSTANT
C         (STRESS DEPENDENT)
C     DT - CHANGE IN TEMPERATURE COMPENSATED TIME
C     ET - CUMALATIVE (TOTAL) CREEP STRAIN
C     ETO - INTERCEPT OF LINEAR PORTION OF CREEP CURVE
C
C     COEFFICIENTS FOR CALCULATION FROM ANDERBERG (1978)
C     FOR KS 40 DIA 10 STEEL
C
C
C     DETERMINE SIGN AND NORMALISE STRESS TO POSITIVE NUMBER
C
      SIGN=1.0
      S=SO(LEM,IDIV)/1000
      IF (S) 110,100,120
  100 RETURN
  110 SIGN=-1.0
      S=SIGN*S
  120 CONTINUE
C
C     CREEP STRAIN IS CALCULATED FOR ALL TEMPERATURES
C
C     CALCULATE INTERCEPT ETO
C
      ETO=S**1.037
      ETO=ETO*2.85E-8
C
C     CALCULATE EXPONENT OF DTHETA TERM
C
      A=TEMP+273.0
      A=-45000/A
      DT=TIME(NUM)-TIME(NUM-1)
C
      IF (S-84) 150,150,160
C
```

```
C
  150 S=S**4.7
      S=S*6.96E10
      A=EXP(A)
      ZT=S*A*DT
      GOTO 170
C
C     CALCULATE Z*DTHETA TERM (ZT) FOR STRESSES GREATER THAN 84 N/MM**2
C
  160 S=0.0433*S
      S=EXP(S)*2.58E18
      A=EXP(A)
      ZT=S*A*DT
C
  170 CONTINUE
      IF (ET(LEM,IDIV)) 190,180,190
C
C     IF ET=0.0 THEN START CREEP CALCULATIONS WITH
C     ET=(3*ZT*ETO*ETO)**0.333333+ZT
C
  180 CONTINUE
      ECR=3.0*ZT*ETO*ETO
      ECR=ECR**0.33333333333
      ECR=ECR+ZT
      GOTO 220
C
  190 CONTINUE
C
C     CALCULATE INCREMENTAL CREEP STRAIN
C
      SIN=1.0
      IF (ET(LEM,IDIV)) 200,210,210
  200 SIN=-1.0
  210 CONTINUE
      A=SIN*ET(LEM,IDIV)/ETO
      A=SIN*CTNH(A)
      ECR=ZT*A*A
C
  220 CONTINUE
C
C     CHANGE INCREMENTAL CREEP STRAIN TO PROPER SIGN
C
      ECR=SIGN*ECR
      ET(LEM,IDIV)=ET(LEM,IDIV)+ECR
C
      RETURN
C
      END
```



```
C
C
      SUBROUTINE STRESIN (MTYPE,EM,SM,EY,FY,ETJ,ETEN,
     .                    ITF,STRAIN,EO,SO,STRESS)
C
      COMMON /CONTROL/ NIN,NOUT,NFILE,ITITLE(80)
C
C     SUBROUTINE STRESIN REPRESENTS THE STRESS-STRAIN
C     RELATIONSHIP FOR THE COLUMN SUBSLICE BE IT
C     CONCRETE OR STEEL
C
C     CHECK MATERIAL TYPE - 1 FOR CONCRETE
C                           2 FOR STEEL
C
      IF (MTYPE.EQ.2) GOTO 150
C
C     STRESS-STRAIN RELATIONSHIP FOR CONCRETE USING
C     BALDWIN AND NORTH REPRESENTATION FOR CONCRETE
C     IN COMPRESSION AND A LINEAR UNLOAD RELATION
C
C     EY - YIELD STRAIN
C     EO - STRAIN FROM PREVIOUS TIME STEP
C     SO - STRESS FROM PREVIOUS TIME STEP
C     EM - STRAIN AT MAXIMUM STRESS FOR GIVEN TEMPERATURE
C     SM - MAXIMUM STRESS FOR GIVEN TEMPERATURE
C     ET - STRAIN CORRESPONDING TO TENSION FAILURE OF ELEMENT
C     ITF - INDICATOR FOR TENSION FAILURE OF ELEMENT
C     ETEN - VALUE OF STRAIN GIVING ZERO STRESS ON UNLOAD LINE
C     STRAIN - STRAIN IN CONCRETE ELEMENT
C
C     CALCULATE STRESS
C
C     CHECK FOR TENSION FAILURE OF CONCRETE ELEMENT
C
      IF (ITF.EQ.1.AND.STRAIN.LT.0.0) GOTO 130
      IF (ITF.EQ.1) GOTO 100
      FT=-0.36*31.622777*SQRT(SM)
C
C     INITIAL TANGENT MODULUS
C
      ETJ=(SM/EM)*EXP(1.0)
C
      ET=FT/ETJ
      ETEN=EO-(SO/ETJ)
      IF (STRAIN.LE.ET) GOTO 130
C
      STRESS=SO-ETJ*(EO-STRAIN)
      IF (STRESS.LE.FT) GOTO 130
      GOTO 110
C
  100 IF (STRAIN.LT.ETEN) GOTO 130
      ETJ=(SM/EM)*EXP(1.0)
      STRESS=SO-ETJ*(EO-STRAIN)
      IF (STRESS.LT.0.0) GOTO 130
      ETEN=EO-(SO/ETJ)
```

```
C
C     CHECK WHETHER UNLOAD LINE HAS INTERSECTED
C     BALDWIN AND NORTH COMPRESSION RELATION
C
  110 CONTINUE
      AE=STRAIN/EM
      AX=1-AE
      STRESSC=AE*EXP(AX)*SM
C
      IF (STRESS.GE.STRESSC) GOTO 120
      GOTO 140
C
  120 STRESS=STRESSC
C
C     CALCULATE YOUNGS TANGENTAL MODULUS BY DIFFERENTIATING
C     FUNCTION FOR STRESS WITH RESPECT TO STRAIN
C
      ETJ=(SM/EM)*EXP(AX)*AX
      GOTO 140
C
  130 STRESS=0.0
      ETJ=0.0
      ITF=1
C
  140 CONTINUE
C
      RETURN
C
  150 CONTINUE
C
C     STRESS-STRAIN RELATIONSHIP FOR STEEL
C
C     BILINEAR STRESS-STRAIN LAW, STRESSES ARE COMPUTED ON
C     THE BASIS OF THE PERMANENT INELASTIC STRAIN (EPL)
C
C     FY - YIELD STRESS
C     EY - YIELD STRAIN
C     EPL - INELASTIC DEFORMATION
C     EO - STRAIN FROM PREVIOUS TIME STEP
C     SO - STRESS FROM PREVIOUS TIME STEP
C     ITF - INDICATOR FOR REINFORCING FAILURE
C     EST - MODULUS OF ELASTICITY
C     ESTAR - STRAIN HARDENING MODULUS
C     STRAIN - STRAIN IN STEEL
C              PERMANENT INELASTIC STRAIN
C
C     CALCULATE PERMANENT DEFORMATION USING STRESS-STRAIN
C     FROM PREVIOUS TIME STEP
C
C     CALCULATE MODULUS ELASTICITY, EST
C
      EST=FY/EY
C
C
C     CALCULATE INELASTIC DEFORMATION
C
      EPL=EO-SO/EST
C
C     CALCULATE STRESS FROM SHIFTED ORIGIN
C
      SE=EST*(STRAIN-EPL)
C
C     CALCULATE UPPER BOUND OF STRESS-STRAIN ENVELOPE
C
      SU=FY+ESTAR*(STRAIN-EY)
C
C     CALCULATE LOWER BOUND OF STRESS-STRAIN ENVELOPE
C
      SL=-FY+ESTAR*(STRAIN+EY)
C
C     CALCULATE STRESS
C
      IF (SE.GT.SU) STRESS=SU
      IF (SE.LT.SL) STRESS=SL
      IF (SE.LE.SU.AND.SE.GE.SL) STRESS=SE
C
C     SET APPROPIATE TANGENT MODULUS
C
      IF (SE.GT.SU) ETJ=ESTAR
      IF (SE.LT.SL) ETJ=ESTAR
      IF (SE.LE.SU.AND.SE.GE.SL) ETJ=EST
C
      EYRUP=10*EY
      IF (ABS(STRAIN).GE.EYRUP) ITF=2
C
      RETURN
C
      END
```

```
C
C
      SUBROUTINE SOLVE (N,M,S,W)
C
      DIMENSION S(N,N),W(N,M)
C
C     SUBROUTINE SOLVE SOLVES SX=W
C     PUTTING X IN W
C     COEFF.MATRIX IS S(N,N)
C     R.H.S.MATRIX IS W(N,M)
C
C     *****ELIMINATION*****
C
      N1=N-1
      DO 120 K=1,N1
      K1=K+1
      DO 120 I=K1,N
      P=S(I,K)/S(K,K)
      S(I,K)=0
      DO 110 J=K1,N
      S(I,J)=S(I,J)-P*S(K,J)
  110 CONTINUE
      DO 120 L=1,M
      W(I,L)=W(I,L)-P*W(K,L)
  120 CONTINUE
C
C     *****BACK SUBSTITUTION*****
C
      DO 130 L=1,M
      W(N,L)=W(N,L)/S(N,N)
  130 CONTINUE
      DO 150 I1=1,N1
      I=N1-I1+1
      J1=I+1
      DO 150 L=1,M
      SM=0
      DO 140 J=J1,N
      SM=SM+S(I,J)*W(J,L)
  140 CONTINUE
      W(I,L)=(W(I,L)-SM)/S(I,I)
  150 CONTINUE
C
      RETURN
C
      END
```



```
C
C
      SUBROUTINE DEFLECT (IBUG,NUM,SEGLEN,C,GA,GB,SLOPA,
     .                    CURV,COLLEN,SLOPB,E1,E2,YP,EYA,YC,
     .                    SLOA,SLOB,IT,AID,CIS,SLOP,
     .                    DMR,DCURV,SLOPE1,SLOPE2,EYC,
     .                    NFL,ZI2,RSL,DSEGSM,GUS,H1,
     .                    ITYRAXA,ZK1,ZK2,AMBEC,P,DC,ECCEN,
     .                    IC,SLEG,ISECO,ITYROTA,ITYROTB,YT,
     .                    ALROD,PYC,ROD,TIME,NUMTIM,DCOL,
     .                    IPLASA2,IPLASA3,IPLASB2,IPLASB3,
     .                    NUMSEG,NUMEL,IDIVPT)
C
      COMMON /CONTROL/ NIN,NOUT,NFILE,ITITLE(80)
      COMMON /LCM/ AT(150,65),STRAIN(150,20),
     .             STRESS(150,20),ITFC(150,20),EO(150,20),
     .             ET(150,20),ITF(150,20),CS(150,20),SO(150,20),
     .             TOTSTRN(150,20),TR(150,20),TENSTR(150,20),
     .             ATMIDA(100,65),ATMIDB(100,65),
     .             ATSUPA(100,65),ATSUPB(100,65),
     .             FIRSTRN(150,20)
      LEVEL 2,/LCM/
      DIMENSION CIS(IDIVPT),SEGLEN(NUMSEG),C(IDIVPT),SLOP(IDIVPT),
     .          CURV(IDIVPT),SLEG(NUMSEG),YP(IDIVPT),YC(IDIVPT),
     .          DMR(IDIVPT),CH(2,1),AM(2,2),DCURV(IDIVPT),
     .          DIFF(2,2),EYC(IDIVPT),PYC(IDIVPT),ROD(IDIVPT),
     .          AID(2,2,IDIVPT),TIME(NUMTIM),YT(IDIVPT)
C
C     SUBROUTINE DEFLECT CALCULATES THE DEFLECTIONS
C     OF THE DIVISION POINTS BY DOUBLE INTERGRATION
C     OF THE CURVATURES, MAKING ALLOWANCE FOR ANY
C     INITIAL DEFLECTIONS
C
C     CALCULATE CHANGES IN SLOPE, CIS(I),
C     DUE TO INITIAL DEFLECTIONS
C
      IT=5H
      IF (NUM.GT.1.) GOTO 235
      IF (C(2).EQ.0.AND.C(1).EQ.0) GOTO 105
      IF (SEGLEN(1).NE.0) GOTO 110
  105 SL2=0.0
      GOTO 120
  110 SL2=(C(2)-C(1))/SEGLEN(1)
  120 IF (C(1).EQ.0.0) GOTO 125
      IF (GA.NE.0) GOTO 130
  125 SL1=0.0
      GOTO 140
  130 SL1=C(1)/GA
  140 CIS(1)=SL2-SL1
      IF (C(IDIVPT).EQ.0.0) GOTO 145
      IF (GB.NE.0) GOTO 150
  145 SL4=0.0
      GOTO 160
  150 SL4=-C(IDIVPT)/GB
  160 IF (C(IDIVPT).EQ.0.0.AND.C(IDIVPT-1).EQ.0.0) GOTO 165
```

```
  165 SL3=0.0
      GOTO 180
  170 SL3=(C(IDIVPT)-C(IDIVPT-1))/SEGLEN(NUMSEG)
  180 CIS(IDIVPT)=SL4-SL3
      L=IDIVPT-1
      DO 230 I=2,L
      IF (C(I+1).EQ.0.0.AND.C(I).EQ.0.0) GOTO 185
      IF (SEGLEN(I).NE.0.0) GOTO 190
  185 SL6=0.0
      GOTO 200
  190 SL6=(C(I+1)-C(I))/SEGLEN(I)
  200 IF (C(I).EQ.0.0.AND.C(I-1).EQ.0.0) GOTO 205
      IF (SEGLEN(I-1).NE.0.0) GOTO 210
  205 SL5=0.0
      GOTO 220
  210 SL5=(C(I)-C(I-1))/SEGLEN(I-1)
  220 CIS(I)=SL6-SL5
  230 CONTINUE
  235 CONTINUE
C
C     CALCULATE PROVISIONAL SLOPES, SLOP(I), AND DEFLECTIONS
C     YC(I), ON THE ASSUMPTION CURVATURE VARIES LINEARLY
C     BETWEEN DIVISION POINTS
C
      SLOP(1)=SLOPA+CIS(1)
      YC(1)=SLOPA*GA
      DO 240 I=2,IDIVPT
      SL7=SLOP(I-1)+CIS(I)
      SL8=(CURV(I-1)+CURV(I))*SEGLEN(I-1)/2.0
      SLOP(I)=SL7+SL8
      DE1=YC(I-1)+(SLOP(I-1)*SEGLEN(I-1))
      DE2=(SEGLEN(I-1)**2)*(2*CURV(I-1)+CURV(I))/6.0
      YC(I)=DE1+DE2
  240 CONTINUE
C
C     CALCULATE DEFLECTION OF END B, YB
C
      YB=YC(IDIVPT)+(SLOP(IDIVPT)*GB)
C
C     CORRECT DEFLECTIONS OF DIVISION POINTS
C     FOR NON ZERO END SLOPE B, TO GIVE
C     CALCULATED DEFLECTIONS
C
      DO 260 I=1,IDIVPT
      SUML=0.0
      IF (GA.EQ.0.0) GOTO 245
      SUML=SQRT((GA**2)-(YP(1)**2))
  245 DO 250 J=1,I
      IF (J.EQ.1) GOTO 250
      OP=(YP(J))-(YP(J-1))
      SUML=SUML+SQRT((SEGLEN(J-1)**2)-(OP**2))
  250 CONTINUE
      YC(I)=YC(I)-((YB*SUML)/COLLEN)
  260 CONTINUE
C
      SLOA=SLOPA-(YB/COLLEN)
      SLOB=SLOP(IDIVPT)-(YB/COLLEN)
C
C     CHECK INCOMPATABILITIES IN END SLOPES
C     EC1/2 - CALCULATED INCOMPATABILITY
C     E1/2  - ALLOWABLE INCOMPATABILITY
C
      EC1=SLOA-SLOPA
      EC2=SLOB-SLOPB
C
      IF (ABS(EC1).GT.E1.OR.ABS(EC2).GT.E2) GOTO 450
C
C     CHECK INCOMPATABILITIES IN DEFLECTIONS
C
C     EYC(I) - CALCULATED INCOMPATABILITY
C     EYA    - ALLOWABLE INCOMPATABILITY
C
      DO 270 I=1,IDIVPT
      EYC(I)=YC(I)-YP(I)
      IF (ABS(EYC(I)).GT.EYA) GOTO 410
  270 CONTINUE
C
C     VALID SOLUTION OBTAINED
C
C     CHECK RATE OF DEFLECTION
C
      IF (NUM.GT.1) GOTO 290
      ALROD=(COLLEN**2)/(15*DC)
      DO 280 I=1,IDIVPT
      ROD(I)=0.0
  280 PYC(I)=YC(I)
      GOTO 310
C
  290 DO 300 I=1,IDIVPT
      ROD(I)=ABS(ABS(YC(I))-ABS(PYC(I)))/(TIME(NUM)-TIME(NUM-1))
  300 PYC(I)=YC(I)
  310 CONTINUE
C
C     AXIAL DEFORMATION
C
C     CALCULATE CHORD SHORTENING DUE TO DIV PT DISPLACEMENTS
C
      DSEGSM=0.0
      DO 330 I=1,NUMSEG
C
C     AVERAGE STRAIN IN SEGMENT
C
      AVS=0.0
      DO 320 J=1,NUMEL
      AVS=AVS+((TOTSTRN(J,I)+TOTSTRN(J,I+1))/2)
  320 CONTINUE
      AVS=AVS/NUMEL
      IF (NUM.EQ.1) SLEG(I)=SEGLEN(I)
      SEG=((SLEG(I)*(1-AVS))**2)-(((YC(I+1)-C(I+1))-(YC(I)-C(I)))**2)
```

```
      DSEGSM=DSEGSM+DSEG
      SEGLEN(I)=SLEG(I)*(1-AVS)
  330 CONTINUE
C
C     CHANGE IN CHORD LENGTH
C
      GUS=0.0
      IF (GA.EQ.0.0.AND.GB.EQ.0.0) GOTO 340
      GUS=SQRT((GA**2)-((YC(1)-C(1))**2))
      GUS=GUS+SQRT((GB**2)-((YC(IDIVPT)-C(IDIVPT))**2))
C
  340 DCOL=-COLLEN+DSEGSM+GUS
C
C     CHECK TYPE OF AXIAL RESTRAINT
C
      IF (ITYRAXA.EQ.0) GOTO 370
      IF (ITYRAXA.EQ.2) GOTO 350
C
C     CHECK FOR FORMATION OF PLASTIC HINGE
C
      FORCE=0.0
      IF (IPLASA2.EQ.1.OR.IPLASA3.EQ.1) GOTO 400
      IF (IPLASB2.EQ.1.OR.IPLASB3.EQ.1) GOTO 400
C
C     CALCULATE STIFFNESS OF FLOORS ABOVE
C
      ZK5=REAL(NFL)*AMBEC*ZI2/RSL
C
  350 IF (ITYRAXA.EQ.2) ZK5=10**5
C
C     CALCULATE FORCE ON COLUMN FOR ELASTIC SWAY OF DCOL
C
      TOP=(ZK1*(ZK2**2))/ZK5+ZK2**2+ZK5*ZK2
      TOP=TOP+ZK5*ZK1+3*ZK2*(ZK1**2)/ZK5+3*(ZK1**2)
      TOP=TOP+11*ZK2*ZK1
      BOT=4*(ZK2+ZK1)*(1+ZK1/ZK5)-(ZK1**2)/ZK5
      FORCE=12*TOP*DCOL/(BOT*(RSL**2))
      GOTO 400
C
C     FREE AXIAL EXPANSION
C
  370 FORCE=0.0
C
  400 CONTINUE
C
C     CALCULATE TOTAL FORCE ON COLUMN
C
      P=P+FORCE
C
C     ADJUST COLUMN LENGTH FOR AXIAL DEFORMATION
C
      COLLEN=DSEGSM+GUS
C
      RETURN
C
C
  410 H=0.0
      IF (IBUG.EQ.2) WRITE (NOUT,570)
      DO 420 J=1,IDIVPT
      H=H+ABS(YC(J)-YP(J))
  420 CONTINUE
      IF (IC.EQ.1) GOTO 430
      IF (H.GT.H1) GOTO 530
C
C     SET PROPOSALS FOR DEFLECTIONS FOR NEXT
C     ITERATION EQUAL TO THOSE JUST CALCULATED
C
  430 DO 440 J=1,IDIVPT
      YP(J)=YC(J)
  440 CONTINUE
      IT=5HNEWIT
      IC=IC+1
      H1=H
      IF (IBUG.EQ.2) WRITE (NOUT,580)
C
      RETURN
C
  450 CONTINUE
      IF (IBUG.EQ.2) WRITE (NOUT,560)
C
C     MODIFICATIONS TO PROPOSED END SLOPES
C     DUE TO INCOMPATABILITY
C
C     CONSIDER THE EFFECTS OF A SMALL INDEPENDENT
C     CHANGE IN THE PROPOSED END SLOPES, DEL1, DEL2
C
      DEL1=0.001*SLOPA
      IF (SLOPA.EQ.0.0) DEL1=0.001*SLOA
      DEL2=0.001*SLOPB
      IF (SLOPB.EQ.0.0) DEL2=0.001*SLOB
      DMA=DEL1*SLOPE1
      DMB=0.0
      DP=0.0
      IF (ITYROTA.EQ.1) DP=-6*DEL1*ZK2/RSL
      PD=DP
      ID=1
C
  460 CONTINUE
C
C     FOR A COLUMN WITH PINNED ROTATIONAL RESTRAINT AT BOTH
C     ENDS CONSIDER THE EFFECTS OF A SMALL INDEPENDENT
C     CHANGE IN ENDSLOPE ON THE DIVISION POINT DEFLECTIONS
C
      IF (ITYROTA.NE.0.OR.ITYROTB.NE.0) GOTO 480
      SIGN=-1.0
      IF (ID.EQ.0) GOTO 461
      SIGN=1.0
      IF (ECCEN.NE.0.0) GOTO 461
      DEL1=0.001*SLOA
      DEL2=0.001*SLOB
```

```
      DO 475 I=1,IDIVPT
      YT(I)=YP(I)
      X=0.0
      IF (GA.EQ.0.0) GOTO 462
      X=SQRT((GA**2)-(YT(1)**2))
  462 IF (I.EQ.1) GOTO 470
      DO 465 J=1,I
      IF (J.EQ.1) GOTO 465
      OP=YT(J)-YT(J-1)
      X=X+SQRT((SEGLEN(J-1)**2)-(OP**2))
  465 CONTINUE
  470 CONTINUE
      IF (ID.EQ.0) X=-X+COLLEN
      DEL=DEL1
      IF (ID.EQ.0) DEL=DEL2
      DYP=((X**3)/(6*COLLEN))-((X**2)/2)+(COLLEN*X/3)
      YP(I)=3*SIGN*DYP*DEL/COLLEN
  475 CONTINUE
C
C     CHANGES IN LOADING AT EACH DIVISION POINT
C
  480 CALL DIVPTBM (ISECO,SEGLEN,DMA,PD,YP,DMB,GA,COLLEN,
     .              DMR,NUMSEG,IDIVPT)
C
C     FIND REQUIRED CHANGE IN CURVATURE, DCURV(I)
C
      DO 485 I=1,IDIVPT
      CH(1,1)=DP
      CH(2,1)=DMR(I)
C
      AM(1,1)=AID(1,1,I)
      AM(2,1)=AID(2,1,I)
      AM(1,2)=AID(1,2,I)
      AM(2,2)=AID(2,2,I)
C
      CALL SOLVE (2,1,AM,CH)
C
C     CHANGED CURVATURES
C
      DCURV(I)=CH(2,1)+CURV(I)
C
      IF (ITYROTA.EQ.0.AND.ITYROTB.EQ.0) YP(I)=YT(I)
  485 CONTINUE
C
C     RECALCULATE DEFLECTIONS AND END SLOPES
C     BASED ON CHANGED CURVATURES
C
      SLOP(1)=SLOPA+CIS(1)
      YC(1)=SLOPA*GA
      DO 490 I=2,IDIVPT
      SL11=SLOP(I-1)+CIS(I)
      SL12=(DCURV(I-1)+DCURV(I))*SEGLEN(I-1)/2.0
      SLOP(I)=SL11+SL12
      DE3=YC(I-1)+(SLOP(I-1)*SEGLEN(I-1))
      DE4=(SEGLEN(I-1)**2)*(2*DCURV(I-1)+DCURV(I))/6.0
  490 CONTINUE
C
C     CALCULATE NEW DEFLECTION OF END B, YB
C
      YB=YC(IDIVPT)+(SLOP(IDIVPT)*GB)
C
C     CORRECT DEFLECTION FOR NON ZERO END SLOPE B
C
      DO 510 I=1,IDIVPT
      SUML=0.0
      IF (GA.EQ.0.0) GOTO 495
      SUML=SQRT((GA**2)-(YP(1)**2))
  495 DO 500 J=1,I
      IF (J.EQ.1) GOTO 500
      OP=(YP(J))-(YP(J-1))
      SUML=SUML+SQRT((SEGLEN(J-1)**2)-(OP**2))
  500 CONTINUE
      YC(I)=YC(I)-(YB*SUML/COLLEN)
  510 CONTINUE
C
C     CALCULATE END SLOPES, SLOA, SLOB
C
      SLOA=SLOPA-(YB/COLLEN)
      SLOB=SLOP(IDIVPT)-(YB/COLLEN)
C
      IF (ID.EQ.0) GOTO 520
C
C     CALCULATE INCOMPATABILITIES
C
      ED11=SLOA-(SLOPA+DEL1)
      ED21=SLOB-SLOPB
C
C     CALCULATE DIFFERENTIALS
C
      DIFF(1,1)=(ED11-EC1)/DEL1
      DIFF(2,1)=(ED21-EC2)/DEL1
C
      DMA=0.0
      ID=0
      DMB=DEL2*SLOPE2
      DP=0.0
      PD=DP
      GOTO 460
C
C     CALCULATE INCOMPATABILITIES
C
  520 ED12=SLOA-SLOPA
      ED22=SLOB-(SLOPB+DEL2)
C
C     CALCULATE DIFFERENTIALS
C
      DIFF(1,2)=(ED12-EC1)/DEL2
      DIFF(2,2)=(ED22-EC2)/DEL2
C
      CH(1,1)=-EC1
```

```
C
C     SOLVE FOR MODIFIED END SLOPES
C
C     FOR COLUMN WITH PINNED ROTATIONAL
C     RESTRAINT AT BOTH ENDS
C
      IF (ITYROTA.NE.0.OR.ITYROTB.NE.0) GOTO 521
      IF (SLOA.NE.-SLOB) GOTO 521
      CH(1,1)=-EC1/(DIFF(1,1)-DIFF(1,2))
      CH(2,1)=-CH(1,1)
      GOTO 522
C
C     FOR ANY OTHER COLUMN
C
  521 CALL SOLVE (2,1,DIFF,CH)
C
  522 SLOPA=SLOPA+CH(1,1)
      SLOPB=SLOPB+CH(2,1)
C
C     FOR COLUMNS WITH PINNED ROTATIONAL RESTRAINT AT BOTH
C     ENDS ADJUST PROPOSED DIVISION POINT DEFLECTIONS
C
      IF (ITYROTA.NE.0.OR.ITYROTB.NE.0) GOTO 527
      DO 526 I=1,IDIVPT
      X=0.0
      IF (GA.EQ.0.0) GOTO 523
      X=SQRT((GA**2)-(YT(1)**2))
  523 IF (I.EQ.1) GOTO 525
      DO 524 J=1,I
      IF (J.EQ.1) GOTO 524
      OP=YP(J)-YP(J-1)
      X=X+SQRT((SEGLEN(J-1)**2)-(OP**2))
  524 CONTINUE
  525 CONTINUE
      W=COLLEN-X
      DYPA=((X**3)/(6*COLLEN))-((X**2)/2)+(COLLEN*X/3)
      DYPA=3*DYPA*CH(1,1)/COLLEN
      DYPB=((W**3)/(6*COLLEN))-((W**2)/2)+(COLLEN*W/3)
      DYPB=-3*DYPB*CH(2,1)/COLLEN
      YP(I)=YP(I)+DYPA+DYPB
  526 CONTINUE
  527 CONTINUE
C
      IT=5HNEWIT
      GOTO 540
  530 CONTINUE
      WRITE (NOUT,550)
      IT=5HFAILD
  540 CONTINUE
C
      RETURN
C
  550 FORMAT (////60H   COLUMN FAILED - DEFLECTIONS DO NOT CONVERGE TO A
     . SOLUTION)
  560 FORMAT (1X,36HMODIFICATIONS TO PROPOSED END SLOPES)
  580 FORMAT (1X,37HMODIFICTIONS TO PROPOSED DEFLECTIONS)
C
      END



C
C
      SUBROUTINE RESET (YP,YC,SLOPA,SLOPB,SLOA,SLOB,
                        IDIVPT,NUMEL,MMTYPE)
C
      COMMON /CONTROL/ NIN,NOUT,NFILE,ITITLE(80)
      COMMON /LCM/ AT(150,65),STRAIN(150,20),
                   STRESS(150,20),ITFC(150,20),EO(150,20),
                   ET(150,20),ITF(150,20),CS(150,20),SO(150,20),
                   TOTSTRN(150,20),TR(150,20),TENSTR(150,20),
                   ATMIDA(100,65),ATMIDB(100,65),
                   ATSUPA(100,65),ATSUPB(100,65),
                   FIRSTRN(150,20)
      LEVEL 2,/LCM/
      DIMENSION YP(IDIVPT),YC(IDIVPT),MMTYPE(NUMEL)
C
C     SUBROUTINE RESET RESETS THE PROPOSED DEFLECTIONS
C     AND PROPOSED END SLOPES EQUAL TO THE CALCULATED
C     DEFLECTIONS AND END SLOPES FOR THE PREVIOUS TIME
C     STEP THUS ACCELERATING CONVERGENCE
C
C     RESET DEFLECTIONS
C
      DO 110 I=1,IDIVPT
      YP(I)=YC(I)
  110 CONTINUE
C
C     RESET ENDSLOPES
C
      SLOPA=SLOA
      SLOPB=SLOB
C
C     ESTABLISH STRESS AND STRAIN HISTORIES FOR COLUMN
C     AND SET INDICATOR FOR TENSION FAILURE OF ELEMENT
C
C     CONCRETE
C
C     EO - STRAIN FROM PREVIOUS TIME STEP
C     SO - STRESS FROM PREVIOUS TIME STEP
C     ITF - ACTUAL INDICATOR OF TENSION FAILURE
C     ITFC - CURRENT INDICATOR OF TENSION FAILURE
C     TENSTR - VALUE OF STRAIN GIVING ZERO STRESS ON UNLOAD LINE
C
      DO 180 IDIV=1,IDIVPT
      DO 180 I=1,NUMEL
      IF (MMTYPE(I).EQ.2) GOTO 170
      ITF(I,IDIV)=ITFC(I,IDIV)
      EO(I,IDIV)=STRAIN(I,IDIV)
      SO(I,IDIV)=STRESS(I,IDIV)
```

```
      GOTO 180
  150 IF (TENSTR(I,IDIV).GE.STRAIN(I,IDIV)) EO(I,IDIV)=TENSTR(I,IDIV)
      GOTO 180
C
C     STEEL
C
C     EO - STRAIN FROM PREVIOUS TIME STEP
C     SO - STRESS FROM PREVIOUS TIME STEP
C     ITFC - INDICATOR FOR REINFORCEMENT FAILURE
C
  170 SO(I,IDIV)=STRESS(I,IDIV)
      EO(I,IDIV)=STRAIN(I,IDIV)
C
C     CHECK FOR STEEL REINFORCEMENT FAILURE
C
      IF (ITFC(I,DIV).EQ.2) GOTO 200
  180 CONTINUE
C
      RETURN
C
  200 WRITE (NOUT,300) IDIV
      RETURN
C
  300 FORMAT (///1X,61HCOLUMN FAILED DUE TO REINFORCEMENT FAILURE AT DIV
     .ISION POINT, I2)
C
      END
```

```
C
C
      SUBROUTINE OUTPUT (IT,NUM,TIME,ZMA,ZMB,SLOPA,SLOPB,YC,SLEG,GA,GB,
     .                   ROD,ALROD,ITYROTA,ITYROTB,ZK1,ZK2,ZK4,ZK3,
     .                   STRNTH,STRNTR,STRNCR,STRNSH,IBUG,
     .                   AMULT1,AMULT2,AMULT3,BMULT1,BMULT2,BMULT3,
     .                   IPLCOLA,IPLCOLB,
     .                   IPLASA1,IPLASA2,IPLASA3,IPLASB1,IPLASB2,
     .                   IPLASB3,DSEG,GUS,P,NUMSEG,NUMEL,IDIVPT,NUMTIM)
C
      COMMON /CONTROL/ NIN,NOUT,NFILE,ITITLE(80)
      COMMON /LCH/ AT(150,65),STRAIN(150,20),
     .             STRESS(150,20),ITFC(150,20),EO(150,20),
     .             ET(150,20),ITF(150,20),CS(150,20),SO(150,20),
     .             TOTSTRN(150,20),TR(150,20),TENSTR(150,20),
     .             ATMIDA(100,65),ATMIDB(100,65),
     .             ATSUPA(100,65),ATSUPB(100,65),
     .             FIRSTRN(150,20)
      LEVEL 2,/LCH/
      CHARACTER*7 CHAR(150)
      DIMENSION YC(IDIVPT),TIME(NUMTIM),SLEG(NUMSEG),ROD(IDIVPT),
     .          STRNTR(150,20),STRNCR(150,20),
     .          STRNTH(NUMEL),STRNSH(NUMEL)
C
C     SUBROUTINE OUTPUT OUTPUTS THE RESULTS OF THE
C     STRUCTURAL ANALYSIS
C
      WRITE (NOUT,300)
      WRITE (NOUT,310)
      WRITE (NOUT,320)
      WRITE (NOUT,330) ITITLE
      IF (NUM.EQ.1) WRITE (NOUT,340) TIME(NUM),NUM
      IF (NUM.GT.1) WRITE (NOUT,350) TIME(NUM),NUM
      WRITE (NOUT,310)
      IF (IT.EQ.5HFAILD) WRITE (NOUT,830)
      WRITE (NOUT,360)
      WRITE (NOUT,370) ZMA
      WRITE (NOUT,380) SLOPA
      WRITE (NOUT,390) ZMB
      WRITE (NOUT,380) SLOPB
      WRITE (NOUT,490)
      DCL=0.0
      DO 100 I=1,NUMSEG
  100 DCL=DCL+SLEG(I)
      CL=DSEG+GUS
      DCL=-DCL-GA-GB+CL
      WRITE (NOUT,495) P
      WRITE (NOUT,500) CL
      WRITE (NOUT,510) DCL
      IF (ITYROTA.NE.1.AND.ITYROTB.NE.1) GOTO 102
      WRITE (NOUT,700)
      WRITE (NOUT,710)
      WRITE (NOUT,720) AMULT1,AMULT3,AMULT2,BMULT1,BMULT3,BMULT2
      IF (ITYROTA.EQ.1.OR.ITYROTB.EQ.1) WRITE (NOUT,730)
      IF (ITYROTA.NE.1) GOTO 101
      WRITE (NOUT,740) ZK1
```

```
      WRITE (NOUT,750) ZK2
  101 IF (ITYROTB.NE.1) GOTO 102
      WRITE (NOUT,760) ZK4
      WRITE (NOUT,770) ZK3
  102 CONTINUE
      IF (IPLASA1.EQ.1) WRITE (NOUT,560)
      IF (IPLASA2.EQ.1) WRITE (NOUT,570)
      IF (IPLASA3.EQ.1) WRITE (NOUT,580)
      IF (IPLASB1.EQ.1) WRITE (NOUT,590)
      IF (IPLASB2.EQ.1) WRITE (NOUT,600)
      IF (IPLASB3.EQ.1) WRITE (NOUT,610)
      IF (IPLCOLA.EQ.1) WRITE (NOUT,620)
      IF (IPLCOLB.EQ.1) WRITE (NOUT,630)
      IF (IBUG.NE.2) GOTO 106
      WRITE (NOUT,810)
      DO 105 J=1.IDIVPT
      WRITE (NOUT,395) J
      WRITE (NOUT,820)
      WRITE (NOUT,800) (I,STRNTH(I),STRNTR(I,J),STRNCR(I,J),STRNSH(I),
     .I=1,NUMEL)
  105 CONTINUE
  106 CONTINUE
      DO 200 K=1,IDIVPT
      DO 120 J=1,NUMEL
      IF (ITF(J,K).EQ.0) GOTO 110
      IF (STRAIN(J,K).GE.0.0) GOTO 110
      CHAR(J)='CRACKED'
      GOTO 120
  110 WRITE (CHAR(J),290) STRESS(J,K)
  120 CONTINUE
      WRITE(NOUT,395) K
      WRITE (NOUT,400)
      WRITE (NOUT,430)
      WRITE (NOUT,410)
      WRITE (NOUT,420) (I,TOTSTRN(I,K),STRAIN(I,K),CHAR(I),
     .I=1,NUMEL)
  200 CONTINUE
      WRITE (NOUT,450)
      WRITE (NOUT,460)
      WRITE (NOUT,470) (I,YC(I),I=1,IDIVPT)
      WRITE (NOUT,530)
      WRITE (NOUT,540)
      WRITE (NOUT,550) (I,ROD(I),I=1,IDIVPT)
      DO 210 I=1,IDIVPT
      IF (ROD(I).GE.ALROD) WRITE (NOUT,520) I
  210 CONTINUE
      IF (IT.EQ.5HFAILD) WRITE (NOUT,840)
C
  290 FORMAT (-3PF7.2)
  300 FORMAT (1H1,5(/))
  310 FORMAT (80H ****************************************************
     .**************************)
  320 FORMAT (/5X,74HSAFE-RCC - STRUCTURAL ANALYSIS OF FIRE EXPOSED REIN
     .FORCED CONCRETE COLUMNS,/)
  330 FORMAT (80A1)
  340 FORMAT (/5X,15HINITIAL TIME IS,F7.3,30X,12HTIME STEP = ,I4,/)
  350 FORMAT (/5X,7HTIME = ,F7.4,6H HOURS,32X,12HTIME STEP = ,I4,/)
  360 FORMAT (///1X,44H--------- END MOMENTS AND ROTATIONS --------)
  370 FORMAT (//5X,27HEND A - TOTAL END MOMENT = ,F10.2)
  380 FORMAT (13X,15HEND ROTATION = ,F7.5)
  390 FORMAT (/5X,27HEND B - TOTAL END MOMENT = ,F10.2)
  395 FORMAT (///23X,23H. . . . DIVISION POINT ,I2,8H . . . .)
  400 FORMAT (///1X,78H---------------------- ELEMENTAL STRESSES AND ST
     .RAINS -----------------------)
  410 FORMAT (1X,4HELEM,3X,6HSTRAIN,3X,6HSTRAIN,3X,6HSTRESS,8X,4HELEM,3X
     .,6HSTRAIN,3X,6HSTRAIN,3X,6HSTRESS,8X,4HELEM,3X,6HSTRAIN,3X,6HSTRAI
     .N,3X,6HSTRESS,/)
  420 FORMAT (3(I4,3X,6PF7.0,2X,6PF7.0,2X,A7,7X))
  430 FORMAT (//8X,5HTOTAL,4X,6HSTRESS,24X,5HTOTAL,4X,6HSTRESS,24X,5HTOT
     .AL,4X,6HSTRESS)
  450 FORMAT (///1X,78H---------------------- DIVISION POINT DEFLECTION
     .S ---------------------------)
  460 FORMAT (//1X,4HDIVN,3X,6HDEFLEC,3X,4HDIVN,3X,6HDEFLEC,3X,4HDIVN,3X
     .,6HDEFLEC,3X,4HDIVN,3X,6HDEFLEC,3X,4HDIVN,3X,6HDEFLEC,3X,4HDIVN,3X
     .,6HDEFLEC,/)
  470 FORMAT (6(I3,3X,F7.5,3X))
  490 FORMAT (///1X,44H--------- AXIAL DEFORMATION ---------------)
  495 FORMAT (//5X,20HTOTAL AXIAL FORCE = ,F10.5,3H KN)
  500 FORMAT (5X,22HCOLUMN CHORD LENGTH = ,F10.7,2H M)
  510 FORMAT (5X,25HCHANGE IN CHORD LENGTH = ,F10.7,2H M)
  520 FORMAT (/1X,47HWARNING - RATE OF DEFLECTION AT DIVISION POINT ,I2,
     .22H EXCEEDS (L**2)/(15*D))
  530 FORMAT (///1X,78H---------------------- RATE OF DEFLECTION ------
     .----------------------------)
  540 FORMAT (//1X,4HDIVN,3X,6H RATE ,3X,4HDIVN,3X,6H RATE ,3X,4HDIVN,3X
     .,6H RATE ,3X,4HDIVN,3X,6H RATE ,3X,4HDIVN,3X,6H RATE ,3X,4HDIVN,3X
     .,6H RATE ,/)
  550 FORMAT (6(I3,3X,F7.4,3X))
  560 FORMAT (///1X,64H. . . . PLASTIC HINGE FORMED IN TOP RESTRAINT BEA
     .M AT POSITION 1)
  570 FORMAT (///1X,64H. . . . PLASTIC HINGE FORMED IN TOP RESTRAINT BEA
     .M AT POSITION 2)
  580 FORMAT (///1X,64H. . . . PLASTIC HINGE FORMED IN TOP RESTRAINT BEA
     .M AT POSITION 3)
  590 FORMAT (///1X,67H. . . . PLASTIC HINGE FORMED IN BOTTOM RESTRAINT
     .BEAM AT POSITION 1)
  600 FORMAT (///1X,67H. . . . PLASTIC HINGE FORMED IN BOTTOM RESTRAINT
     .BEAM AT POSITION 2)
  610 FORMAT (///1X,67H. . . . PLASTIC HINGE FORMED IN BOTTOM RESTRAINT
     .BEAM AT POSITION 3)
  620 FORMAT (///1X,44H. . . . PLASTIC HINGE FORMED IN COLUMN ABOVE)
  630 FORMAT (///1X,44H. . . . PLASTIC HINGE FORMED IN COLUMN BELOW)
  700 FORMAT (///1X,46H--------- ULTIMATE MOMENT CAPACITIES ---------)
  710 FORMAT (//5X,7HBEAMA 1,2X,7HBEAMA 3,2X,7HBEAMA 2,2X,7HBEAMB 4,2X,7
     .HBEAMB 6,2X,7HBEAMB 5,/)
  720 FORMAT (5X,F7.2,2X,F7.2,2X,F7.2,2X,F7.2,2X,F7.2,2X,F7.2)
  730 FORMAT (//1X,31HSTIFFNESSES OF RESTRAINT SYSTEM,//)
  740 FORMAT (1X,15HCOLUMN ABOVE = ,F10.2)
  750 FORMAT (1X,18HBEAM AT JOINT A = ,F10.2)
  760 FORMAT (1X,15HCOLUMN BELOW = ,F10.2)
```

```
  770 FORMAT (1X,18HBEAM AT JOINT B = ,F10.2)
  800 FORMAT (2(I4,2X,E10.3,E10.3,E10.3,E10.3,4X))
  810 FORMAT (///30X,12HFIRE STRAINS)
  820 FORMAT (//1X,4HELEM,2X,7HTHERMAL,3X,9HTRANSIENT,2X,5HCREEP,3X,9HSH
     .RINKAGE,5X,4HELEM,2X,7HTHERMAL,3X,9HTRANSIENT,2X,5HCREEP,3X,9HSHRI
     .NKAGE,/)
  830 FORMAT (///,10X,28HSITUATION AT TIME OF FAILURE)
  840 FORMAT (///,1X,34HPROGRAM TERMINATED - COLUMN FAILED)
C
      RETURN
C
      END
```

```
C
C
      FUNCTION CTNH(X)
C
C     FUNCTION CTNH(X) CALCULATES AN APPROXIMATE
C     VALUE OF THE HYPERBOLIC COTANGENT OF X
C
      IF (X-0.2) 100,100,110
C
C     IF X IS LESS THAN 0.2 THEN CTNH IS EQUAL TO 1/X
C
  100 CTNH=1.0/X
      RETURN
C
  110 IF (X-2.0) 120,130,130
C
C     IF X IS GREATER THAN 0.2 AND LESS THAN 2.0 A
C     SERIES EXPANSION IS USED IN APPROXIMATING CTNH
C
  120 ST=1.0
      SB=X
      A=X
      A=A*X
      ST=0.5*A+ST
      A=A*X
      SB=0.1667*A+SB
      A=A*X
      ST=0.0417*A+ST
      A=A*X
      SB=0.00834*A+SB
      A=A*X
      ST=0.00139*A+ST
      A=A*X
      SB=0.000185*A+SB
      CTNH=ST/SB
      RETURN
C
C     IF X IS GREATER THAN 2.0 THEN CTNH=1.0
C
  130 CTNH=1.0
C
      RETURN
C
      END
```

APPENDIX L

The following is a listing of the modified version of the computer program FIRES-T, originally developed by Becker, Bizri and Bresler (1973).

```
      PROGRAM FIREST(INPUT,OUTPUT,RESULT,TAPE1=INPUT,
     .TAPE2=OUTPUT,TAPE6=RESULT)
C     *************
C     *           *
C     *  FIRES-T  *
C     *           *
C     *************
C
      COMMON /CONTROL/ ITITLE(80),IREAD(80),NIN,NOUT,NPUNCH,NUMNP,
     .                 NUMEL,MBAND,NMAT,NUMFBC,NBCMAT,NBCTYP
      COMMON C(20000)
      NIN=1
      NOUT=2
      NPUNCH=6
      NUMFBC=0
      READ (NIN,160) ITITLE
      WRITE (NOUT,170)
      WRITE (NOUT,180)
      WRITE (NOUT,190)
      WRITE (NOUT,210)
      WRITE (NOUT,200)
      WRITE (NOUT,200)
      WRITE (NOUT,220)
      WRITE (NOUT,230)
      WRITE (NOUT,240)
      WRITE (NOUT,250)
      WRITE (NOUT,260)
      WRITE (NOUT,270)
      WRITE (NOUT,280)
      WRITE (NOUT,290)
      WRITE (NOUT,180)
      WRITE (NOUT,300) ITITLE
      WRITE (NOUT,180)
C
      READ (NIN,310) IREAD
      IF (IREAD(1).NE.16B) GOTO 150
      N=1
      NUMNP=NUMBER(N)
      IF (NUMNP.LE.0) GOTO 150
      NTBC=NUMBER(N)
      IF (NTBC.GT.NUMNP) GOTO 150
      N1=1
      N2=N1+NUMNP
      N3=N2+NUMNP
      ND1=N3+NUMNP
      ND2=ND1+NUMNP
      ND3=ND2+NUMNP
      ND4=ND3+NUMNP
      ND5=ND4+NUMNP
      N4=ND5+NUMNP
      CALL NODE (C(N1),C(N2),C(N3),C(ND1),NTBC)
      READ (NIN,310) IREAD
      IF (IREAD(1).NE.5B) GOTO 150
      N=1
      NUMEL=NUMBER(N)
      IF (NUMEL.LE.0) GOTO 150
      N5=N4+5*NUMEL
      N6=N5+NUMEL
      N=4*NUMEL
      NS1=N6+N
      NS2=NS1+N
      NS3=NS2+N
      NS5=NS3+N
      NS6=NS5+N
      NS9=NS6+N
      N7=NS9+N
      CALL ELEMENT (C(N1),C(N2),C(N4),C(N5),C(N6),C(NS1),
     .              C(NS2),C(NS3),C(NS5),C(NS6),C(NS9))
      READ (NIN,310) IREAD
      IF (IREAD(1).NE.15B) GOTO 150
      N=1
      NMAT=NUMBER(N)
      IF (NMAT.EQ.0) GOTO 150
      N8=N7+6*NMAT
      CALL MATRIAL (C(N5),C(N7),C(N8),N)
      N9=N8+N
      READ (NIN,310) IREAD
      N=1
      IF (IREAD(1).NE.6B) GOTO 130
      NUMFBC=NUMBER(N)
      NBCMAT=NUMBER(N)
      IF (NUMFBC.EQ.0.OR.NBCMAT.EQ.0) GOTO 150
      READ (NIN,310) IREAD
      IF (IREAD(1).NE.14B) GOTO 110
      NBCTYP=10HLINEAR BC
      N10=N9+2*NBCMAT
      GOTO 120
  110 IF (IREAD(1).NE.16B) GOTO 150
      NBCTYP=10HNON-LIN BC
      N10=N9+NBCMAT
  120 CONTINUE
      CALL FIREMAT (C(N9),C(N10),N)
      N11=N10+N
      N12=N11+NUMFBC
      N13=N12+NUMFBC
      N14=N13+NUMFBC
      N15=N14+NUMFBC
      N16=N15+NUMFBC
      CALL FIREBC (C(N1),C(N2),C(N3),C(N11),C(N12),C(N13),
     .             C(N14),C(N15))
      GOTO 140
  130 CONTINUE
      N10=N9+1
      N11=N10+1
      N12=N11+1
      N13=N12+1
      N14=N13+1
      N15=N14+1
      N16=N15+1
  140 CONTINUE
```

```
      N17=N16+NUMNP
      N18=N17+NUMNP
      N19=N18+NUMNP
      N20=N19+NUMEL
      NTOTAL=N20+NUMNP*MBAND
      READ (NIN,310) IREAD
      IF (IREAD(1).NE.3B) GOTO 150
      CALL CONVERG (NTOTAL)
      CALL HEATFLO (C(N1),C(N2),C(N3),C(N4),C(N5),C(N6),C(N7),
     .              C(N8),C(N9),C(N10),C(N11),C(N12),C(N13),C(N14),
     .              C(N15),C(N16),C(N17),C(N18),C(N19),C(N20),
     .              NUMNP,C(NS1),C(NS2),C(NS3),C(NS5),C(NS6),
     .              C(NS9),C(ND1),C(ND2),C(ND3),C(ND4),C(ND5))
  150 CONTINUE
      WRITE (NOUT,320) IREAD
  160 FORMAT (80A1)
  170 FORMAT (1H6,13(/))
  180 FORMAT (80H *********************************************************
     .************************)
  190 FORMAT (///7X,49HFFFFFFFFF   I   RRRRRRRRR   EEEEEEEEE   SSSSSSSSS
     .,9X,9HTTTTTTTTT)
  200 FORMAT (7X,1HF,11X,1HI,3X,1HR,7X,1HR,3X,1HE,11X,1HS,21X,1HT)
  210 FORMAT (7X,1HF,11X,1HI,3X,1HR,7X,1HR,3X,1HE,11X,1HS,7X,1HS,13X,1HT
     .)
  220 FORMAT (7X,56HFFFFFF      I   RRRRRRRRR   EEEEEE      SSSSSSSSS
     .====,6X,1HT)
  230 FORMAT (7X,1HF,11X,1HI,3X,1HR,2X,1HR,8X,1HE,19X,1HS,13X,1HT)
  240 FORMAT (7X,1HF,11X,1HI,3X,1HR,3X,1HR,7X,1HE,19X,1HS,13X,1HT)
  250 FORMAT (7X,1HF,11X,1HI,3X,1HR,4X,1HR,6X,1HE,19X,1HS,13X,1HT)
  260 FORMAT (7X,1HF,11X,1HI,3X,1HR,5X,1HR,5X,1HE,19X,1HS,13X,1HT)
  270 FORMAT (7X,1HF,11X,1HI,3X,1HR,6X,1HR,4X,1HE,11X,1HS,7X,1HS,13X,1HT
     .)
  280 FORMAT (7X,1HF,11X,1HI,3X,1HR,7X,1HR,3X,9HEEEEEEEEE,3X,9HSSSSSSSSS
     .,13X,1HT///)
  290 FORMAT (16X,46HA THERMAL ANALYZER FOR TWO DIMENSIONAL SOLIDS,,/16X
     .,46HWITH TEMPERATURE DEPENDANT THERMAL PROPERTIES,,/16X,31HSUBJECT
     .ED TO A FIRE ENVIROMENT,///)
  300 FORMAT (///20X,24H- - - TITLE OF RUN - - -,//1X,80A1///)
  310 FORMAT (80R1)
  320 FORMAT (6(/),45H - - - PROGRAM TERMINATED - INPUT ERROR - - -,1X
     .,80R1)
      STOP
      END
C
C
      SUBROUTINE NODE (X,Y,KODE,ID,NTBC)
C
      COMMON /CONTROL/ ITITLE(80),IREAD(80),NIN,NOUT,NPUNCH,NUMNP,
     .                 NUMEL,MBAND,NMAT,NUMFBC,NBCMAT,NBCTYP
      DIMENSION X(1),Y(1),KODE(1),ID(1)
      WRITE (NOUT,200)
      WRITE (NOUT,210)
      WRITE (NOUT,220) ITITLE
      WRITE (NOUT,230)
      WRITE (NOUT,210)
      WRITE (NOUT,240) NUMNP
      WRITE (NOUT,250)
      DO 110 I=1,NUMNP
  110 KODE(I)=4HFLOW
      L=1
  120 READ (NIN,260) N,X(N),Y(N)
      IF (N.GE.L) GOTO 140
  130 WRITE (NOUT,270) N,X(N),Y(N)
      STOP
  140 IF (N.EQ.L) GOTO 160
      IF (L.EQ.1) GOTO 130
      DIFF=N+1-L
      DX=(X(N)-X(L-1))/DIFF
      DY=(Y(N)-Y(L-1))/DIFF
  150 X(L)=X(L-1)+DX
      Y(L)=Y(L-1)+DY
      L=L+1
      IF (N.GT.L) GOTO 150
  160 L=L+1
      IF (N.LT.NUMNP) GOTO 120
      IF (N.NE.NUMNP) GOTO 130
      IF (NTBC.EQ.0) GOTO 180
      READ (NIN,280) (ID(I),I=1,NTBC)
      DO 170 I=1,NTBC
      J=ID(I)
      IF (J.LE.0.OR.J.GT.NUMNP) GOTO 190
  170 KODE(J)=4HTEMP
  180 WRITE (NOUT,290) (I,X(I),Y(I),KODE(I),I=1,NUMNP)
      RETURN
  190 WRITE (NOUT,300)
      STOP
  200 FORMAT (1H6,5(/))
  210 FORMAT (80H *********************************************************
     .************************)
  220 FORMAT (/5X,49HFIRES-T  -  FIRE RESPONSE OF STRUCTURES - THERMAL,/
     ./5X,80A1)
  230 FORMAT (/5X,46HGEOMETRIC DESCRIPTION OF SYSTEM TO BE ANALYZED,/)
  240 FORMAT (//,20H    . . . . THERE ARE ,I5,22H,NODAL POINTS . . . . )
  250 FORMAT (//,7H  NODAL,11X,11HCOORDINATES,13X,8HBOUNDARY,/,7H  POINT
     .,10X,1HX,14X,1HY,9X,9HCONDITION,/)
  260 FORMAT (I5,2E10.0)
  270 FORMAT (5(/),51H  - - - PROGRAM TERMINATED - NODE INPUT ERROR - -
     .-,//1X,I5,2F10.4)
  280 FORMAT (16I5)
  290 FORMAT (I7,2F15.4,8X,A4)
  300 FORMAT (5(/),33H  - - - PROGRAM TERMINATED - - - ,/,47H  ERROR IN
     .TEMPERATURE BOUNDARY CONDITION INPUT)
      END
C
C
      SUBROUTINE ELEMENT (X,Y,LM,MMTYPE,XLAM,SS1,SS2,SS3,SS5,SS6,SS9)
C
      COMMON /CONTROL/ ITITLE(80),IREAD(80),NIN,NOUT,NPUNCH,NUMNP,
     .                 NUMEL,MBAND,NMAT,NUMFBC,NBCMAT,NBCTYP
      DIMENSION X(1),Y(1),LM(5,1),MMTYPE(1),XLAM(4,1),SS1(4,1),
     .          SS2(4,1),SS3(4,1),SS5(4,1),SS6(4,1),SS9(4,1)
      WRITE (NOUT,250) NUMEL
```

```
      WRITE (NOUT,260)
      MBAND=0
      NUM=0
      DO 240 N=1,NUMEL
      IF (NUM-N) 110,120,120
  110 READ (NIN,270) NUM,K1,K2,K3,K4,MTYPE
      IF (NUM.GT.NUMEL) GOTO 150
      IF (N.EQ.1) GOTO 140
  120 DO 130 I=1,4
  130 LM(I,N)=LM(I,N-1)+1
      MMTYPE(N)=MMTYPE(N-1)
  140 IF (NUM-N) 150,160,170
  150 CONTINUE
      WRITE (NOUT,280) NUM,K1,K2,K3,K4,MTYPE
      STOP
  160 CONTINUE
      LM(1,N)=K1
      LM(2,N)=K2
      LM(3,N)=K3
      LM(4,N)=K4
      MMTYPE(N)=MTYPE
  170 CONTINUE
      I=LM(1,N)
      J=LM(2,N)
      K=LM(3,N)
      L=LM(4,N)
      LM(5,N)=I
      IF (K.EQ.L) GOTO 180
      XX=(X(I)+X(J)+X(K)+X(L))/4.0
      YY=(Y(I)+Y(J)+Y(K)+Y(L))/4.0
      GOTO 190
  180 XX=(X(I)+X(J)+X(K))/3.0
      YY=(Y(I)+Y(J)+Y(K))/3.0
  190 CONTINUE
      DO 210 K=1,4
      I=LM(K,N)
      J=LM(K+1,N)
      IF (I-J) 200,210,200
  200 AJ=X(J)-X(I)
      AK=XX-X(I)
      BJ=Y(J)-Y(I)
      BK=YY-Y(I)
      C=BJ-BK
      DX=AK-AJ
      XLAM(K,N)=AJ*BK-AK*BJ
      SS1(K,N)=C**2+DX**2
      SS2(K,N)=BK*C-AK*DX
      SS3(K,N)=-BJ*C+AJ*DX
      SS5(K,N)=BK**2+AK**2
      SS6(K,N)=-BJ*BK-AJ*AK
      SS9(K,N)=BJ**2+AJ**2
  210 CONTINUE
      DO 230 L=1,4
      I=LM(L,N)
      DO 230 M=1,4
      J=LM(M,N)-I+1
```



```
      IF (MBAND-J) 220,230,230
  220 MBAND=J
  230 CONTINUE
  240 CONTINUE
      WRITE (NOUT,290) (I,(LM(J,I),J=1,4),MMTYPE(I),I=1,NUMEL)
      WRITE (NOUT,300) MBAND
      RETURN
  250 FORMAT (6(/),20H   . . . . THERE ARE ,I5,18H ELEMENTS . . . . ,//)
  260 FORMAT (2X,7HELEMENT,10X,14HNODAL LOCATION,11X,8HMATERIAL/2X,6HNUM
     .BER,10X,1HI,6X,1HJ,6X,1HK,6X,1HL,5X,4HTYPE/)
  270 FORMAT (6I5)
  280 FORMAT (5(/),50H   - - - - PROGRAM TERMINATED - ELEMENT INPUT ERROR
     ../1X,6I5)
  290 FORMAT (I8,4X,4I7,I8)
  300 FORMAT (///,31H     . . . MAXIMUM BANDWIDTH IS ,I4,6H . . .)
      END
C
C
      SUBROUTINE MATRIAL (MMTYPE,MATL,XYS,NSTORE)
C
      COMMON /CONTROL/ ITITLE(80),IREAD(80),NIN,NOUT,NPUNCH,NUMNP,
     .                 NUMEL,MBAND,NMAT,NUMFBC,NBCMAT,NBCTYP
      DIMENSION MMTYPE(1),MATL(1),XYS(1)
      NSTORE=1
      WRITE (NOUT,150)
      WRITE (NOUT,160)
      WRITE (NOUT,170) ITITLE
      WRITE (NOUT,180) NMAT
      WRITE (NOUT,160)
      DO 110 I=1,NUMEL
      IF (MMTYPE(I).GT.NMAT) GOTO 120
  110 CONTINUE
      GOTO 130
  120 WRITE (NOUT,190) I,MMTYPE(I),NMAT
      STOP
  130 CONTINUE
      DO 140 M=1,NMAT
      WRITE (NOUT,200) M
      READ (NIN,210) MK,MCP,MD
      MS=(M-1)*6
      WRITE (NOUT,220)
      MATL(MS+1)=NSTORE
      MATL(MS+2)=MK
      CALL MATIN (MK,XYS(NSTORE),XYS(NSTORE+MK),XYS(NSTORE+MK+MK))
      NSTORE=NSTORE+3*MK
      IF (MK.EQ.0) NSTORE=NSTORE+1
      WRITE (NOUT,230)
      MATL(MS+3)=NSTORE
      MATL(MS+4)=MCP
      CALL MATIN (MCP,XYS(NSTORE),XYS(NSTORE+MCP),XYS(NSTORE+MCP+MCP))
      NSTORE=NSTORE+3*MCP
      IF (MCP.EQ.0) NSTORE=NSTORE+1
      WRITE (NOUT,240)
      MATL(MS+5)=NSTORE
      MATL(MS+6)=MD
      CALL MATIN (MD,XYS(NSTORE),XYS(NSTORE+MD),XYS(NSTORE+MD+MD))
```

```
      NSTORE=NSTORE+3*MD
      IF (MD.EQ.0) NSTORE=NSTORE+1
  140 CONTINUE
      RETURN
  150 FORMAT (1H6,5(/))
  160 FORMAT (80H ***********************************************************
     .*************************)
  170 FORMAT (/5X,49HFIRES-T  -  FIRE RESPONSE OF STRUCTURES - THERMAL,/
     ./5X,80A1)
  180 FORMAT (/5X,43HTHERMAL PROPERTIES OF SYSTEM TO BE ANALYZED,//,5X,1
     .0HTHERE ARE ,I3,20H DIFFERENT MATERIALS,/)
  190 FORMAT (5(/),32H  - - - PROGRAM TERMINATED - - -,/,17H  ELEMENT NO
     .MBER ,I5,24H HAS A MATERIAL TYPE OF ,I5,22H WHICH IS GREATER THAN,
     ./,24H  THE INTENDED INPUT OF ,I5,10H MATERIALS)
  200 FORMAT (////,26H  . . . . MATERIAL NUMBER ,I4,9H  . . . .)
  210 FORMAT (3I5)
  220 FORMAT (//7X,25H . . . CONDUCTIVITY . . .)
  230 FORMAT (//7X,25H . . . SPECFIC HEAT . . .)
  240 FORMAT (//7X,20H . . . DENSITY . . .)
      END
C
C
      SUBROUTINE FIREMAT (MAT,FXYS,NSTORE)
C
      COMMON /CONTROL/ ITITLE(80),IREAD(80),NIN,NOUT,NPUNCH,NUMNP,
     .                 NUMEL,MBAND,NMAT,NUMFBC,NBCMAT,NBCTYP
      DIMENSION MAT(1),FXYS(1)
      WRITE (NOUT,140)
      WRITE (NOUT,150)
      WRITE (NOUT,160) ITITLE
      IF (NBCTYP.EQ.10HLINEAR BC ) GOTO 120
      WRITE (NOUT,170)
      WRITE (NOUT,150)
      WRITE (NOUT,180)
      READ (NIN,190) SB,TSHIFT
      WRITE (NOUT,200) SB,TSHIFT
      WRITE (NOUT,210)
      FXYS(1)=SB
      FXYS(2)=TSHIFT
      NSTORE=3
      DO 110 I=1,NBCMAT
      MAT(I)=NSTORE
      READ (NIN,190) A,P,V,AB,EF,ES
      WRITE (NOUT,220) I,A,P,V,AB,EF,ES
      FXYS(NSTORE)=A
      FXYS(NSTORE+1)=P
      FXYS(NSTORE+2)=V
      FXYS(NSTORE+3)=AB
      FXYS(NSTORE+4)=EF
      FXYS(NSTORE+5)=ES
      NSTORE=NSTORE+6
  110 CONTINUE
      RETURN
  120 CONTINUE
      WRITE (NOUT,230)
      WRITE (NOUT,150)
      WRITE (NOUT,240)
      NSTORE=1
      DO 130 I=1,NBCMAT
      WRITE (NOUT,250) I
      READ (NIN,260) K
      MS=(I-1)*2
      MAT(MS+1)=NSTORE
      MAT(MS+2)=K
      CALL MATIN (K,FXYS(NSTORE),FXYS(NSTORE+K),FXYS(NSTORE+K+K))
      NSTORE=NSTORE+3*K
      IF (K.EQ.0) NSTORE=NSTORE+1
  130 CONTINUE
      RETURN
  140 FORMAT (1H6,5(/))
  150 FORMAT (80H ***********************************************************
     .*************************)
  160 FORMAT (/5X,49HFIRES-T  -  FIRE RESPONSE OF STRUCTURES - THERMAL,/
     ./5X,80A1)
  170 FORMAT (/5X,34HNON-LINEAR FIRE BOUNDARY CONDITION,/)
  180 FORMAT (//9X,64HQ = A*(TF-TS)**N + SB*V*(AB*EF*(TF-TSHIFT)**4-ES*(
     .TS+TSHIFT)**4))
  190 FORMAT (8E10.0)
  200 FORMAT (//10X,5HWHERE/15X,28HTF - PSEUDO FIRE TEMPERATURE,/15X,24H
     .TS - SURFACE TEMPERATURE,/15X,33HSB - STEFAN BOLTZMANN CONSTANT =
     .,E12.4/15X,47HTSHIFT - SHIFT TO ABSOLUTE TEMPERATURE SCALE = ,F8.1
     ./10X,3HAND)
  210 FORMAT (//4X,76HMATERIAL  CONVECTION  CONVECTION    VIEW     ABSOR
     .BTION  FIRE          SURFACE,/3X,42H NUMBER    FACTOR       POWER
     .     FACTOR,16X,22HEMISSIVITY  EMISSIVITY,/17X,3H(A),9X,3H(N),9X,3H
     .(V),9X,4H(AB),8X,4H(EF),8X,4H(ES))
  220 FORMAT (/I9,6F12.3)
  230 FORMAT (15X,30HLINEAR FIRE BOUNDARY CONDITION,/)
  240 FORMAT (//9X,16HQ = H(T)*(TF-TS)//10X,5HWHERE,/15X,31HH(T) - HEAT
     .TRANSFER COEFFICENT,/15X,28HTF - PSEUDO FIRE TEMPERATURE,/15X,24HT
     .S - SURFACE TEMPERATURE,/15X,33HT - AVERAGE TEMPERATURE (TF+TS)/2,
     .//)
  250 FORMAT (//,25H   . . . MATERIAL NUMBER ,I4,6H . . .)
  260 FORMAT (I5)
      END
C
C
      SUBROUTINE FIREBC (X,Y,KODE,LI,LJ,LMAT,LFIRE,XL)
C
      COMMON /CONTROL/ ITITLE(80),IREAD(80),NIN,NOUT,NPUNCH,NUMNP,
     .                 NUMEL,MBAND,NMAT,NUMFBC,NBCMAT,NBCTYP
      DIMENSION X(1), Y(1), KODE(1), LI(1), LJ(1), LMAT(1),
     .          LFIRE(1), XL(1)
      WRITE (NOUT,160) NUMFBC
      READ (NIN,170) (LI(I),LJ(I),LMAT(I),LFIRE(I),I=1,NUMFBC)
      DO 110 I=1,NUMFBC
      IF (LMAT(I).GT.NBCMAT) GOTO 120
      II=LI(I)
      JJ=LJ(I)
      IF (KODE(II).EQ.4HTEMP.OR.KODE(JJ).EQ.4HTEMP) GOTO 120
  110 CONTINUE
      GOTO 130
```

```
120 CONTINUE
    WRITE (NOUT,180) I,LI(I),LJ(I),LMAT(I),LFIRE(I)
    STOP
130 CONTINUE
    DO 140 I=1,NUMFBC
    II=LI(I)
    JJ=LJ(I)
    DX=X(II)-X(JJ)
    DY=Y(II)-Y(JJ)
    D=DX*DX+DY*DY
    XL(I)=SQRT(D)
140 CONTINUE
    WRITE (NOUT,190)
    WRITE (NOUT,200) (I,LI(I),LJ(I),LMAT(I),LFIRE(I),XL(I),I=1,NUMFBC)
    DO 150 I=1,NUMFBC

150 XL(I)=0.5*XL(I)
    RETURN
160 FORMAT (////,21H   . . . . THERE ARE ,I4,52H SURFACE ELEMENTS DIRE
   .CTLY EXPOSED TO A FIRE . . . .)
170 FORMAT (16I5)
180 FORMAT (5(/),54H  - - - PROGRAM TERMINATED - FIRE BC INPUT ERROR -
   . - -,1X,5I5)
190 FORMAT (//9X,47HDESCRIPTION OF SURFACE DIRECTLY EXPOSED TO FIRE,/4
   .X,6HFIREBC.6X,12HNODE TO NODE,4X,8HMATERIAL,4X,4HFIRE,7X,6HLENGTH/
   .4X,7HSURFACE,6X,1HI,7X,1HJ,6X,4HTYPE,8X,4HTYPE/)
200 FORMAT (I8,2X,2I8,I9,I11,F14.3)
    END
C
C
    SUBROUTINE CONVERG (NTOTAL)
C
    COMMON /CONTROL/ ITITLE(80),IREAD(80),NIN,NOUT,NPUNCH,NUMNP,
   .                 NUMEL,MBAND,NMAT,NUMFBC,NBCMAT,NBCTYP
    COMMON /CONRG/ NCONV,CONV,BETA,NCONU,CONU,ALPHA
    WRITE (NOUT,120)
    WRITE (NOUT,130)
    WRITE (NOUT,140) ITITLE
    WRITE (NOUT,150)
    WRITE (NOUT,130)
    WRITE (NOUT,160)
    READ (NIN,170) NCONV,CONV,BETA,NCONU,CONU,ALPHA
    IF (NCONU.EQ.0) GOTO 110
    WRITE (NOUT,180) CONU,NCONU,ALPHA
110 CONTINUE
    WRITE (NOUT,190) CONV,NCONV,BETA
    CONV=CONV*0.50
    CONU=CONU*0.50
    WRITE (NOUT,200) NTOTAL,NTOTAL
    RETURN
120 FORMAT (1H6,5(/))
130 FORMAT (80H ***********************************************************
   .**************************)
140 FORMAT (/5X,49HFIRES-T  -  FIRE RESPONSE OF STRUCTURES - THERMAL,/
   ./5X,80A1)
150 FORMAT (/5X,46HINFORMATION RELEVANT TO THE ANALYSIS PROCEDURE,/)
160 FORMAT (////38H  . . . . CONVERGENCE CRITERIA . . . .)
170 FORMAT (I5,2F10.0,I5,2F10.0)
180 FORMAT (//40H  CONVERGENCE CRITERIA FOR ENTIRE SYSTEM,/,23H    PER
   .MISSIBLE ERROR =,F10.5/,34H    MAXIMUM NUMBER OF ITERATIONS =,I5/,
   .12H     ALPHA =,F10.4)
190 FORMAT (//,46H  CONVERGENCE CRITERIA FOR BOUNDARY CONDITIONS,/,24H
   .     PERMISSABLE ERROR =,F10.5/,35H     MAXIMUM NUMBER OF ITERATIO
   .NS =,I5,11H     BETA =,F10.4)
200 FORMAT (////,54H  . . . . STORAGE REQUIREMENT FOR BLANK COMMON . .
   . . . .,//5X,20HSIZE BLANK COMMON = ,I10,10H (DECIMAL),/23X,5H=    ,O
   .7,8H (OCTAL))
    END
C
C
    SUBROUTINE HEATFLO (X,Y,KODE,LM,MMTYPE,XLAM,MATL,XYS,MAT,FXYS,LI,L
   .J,LMAT,LFIRE,XL,Q,T,B,AT,A,NP,SS1,SS2,SS3,SS5,SS6,SS9,D,MA,T1,T2,T
   .3)
C
    COMMON /CONTROL/ ITITLE(80),IREAD(80),NIN,NOUT,NPUNCH,NUMNP,
   .                NUMEL,MBAND,NMAT,NUMFBC,NBCMAT,NBCTYP
    COMMON /CONRG/ NCONV,CONV,BETA,NCONU,CONU,ALPHA
    DIMENSION X(1), Y(1), KODE(1), LM(5,1), MMTYPE(1),XLAM(4,1),
   .          MATL(1), XYS(1), MAT(1), FXYS(1), LI(1), LJ(1),
   .          LMAT(1), LFIRE(1), XL(1), Q(1), T(1), B(1), AT(1),
   .          A(NP,1), SS1(4,1), SS2(4,1), SS3(4,1), SS5(4,1),
   .          SS6(4,1), SS9(4,1), D(1), MA(1), T1(1), T2(1), T3(1)
    DIMENSION TFIRE(4)
    IP1=0
    IP2=0
    SDT=0.0
    DS=0.0
    READ (NIN,450) IA,MDT,TIME,TEMP,JP
    WRITE (NOUT,460)
    WRITE (NOUT,470)
    WRITE (NOUT,480) ITITLE
    IF (IA.NE.4HSTEP) GOTO 140
    WRITE (NOUT,490) MDT,TIME
    WRITE (NOUT,470)
    IF (TEMP.NE.0.0) GOTO 110
    READ (NIN,500) (T(I),I,NUMNP)
    GOTO 130
110 DO 120 I=1,NUMNP
120 T(I)=TEMP
130 CALL PROUT (4,T,AT,T1,B,MAIN,NCON,1)
    GOTO 150
140 CONTINUE
    WRITE (NOUT,510) IA,MDT,TIME,TEMP,JP
    STOP
150 CONTINUE
160 READ (NIN,520) IA,NDT,DT,ITOF,TFIRE(1),TFIRE(2),TFIRE(3),TFIRE(4),
   .I1,I2,I6
    MAIN=0
    MDT=MDT+1
    IF (NDT.EQ.MDT.AND.IA.EQ.4HSTEP) GOTO 190
    WRITE (NOUT,530)
170 WRITE (NOUT,540) IA,NDT,DT,ITOF,TFIRE(1),TFIRE(2),TFIRE(3),TFIRE(4
```

```
     .),I1,I2,I6
      STOP
  180 WRITE (NOUT,550)
      GOTO 170
  190 IF (DT) 200,210,220
  200 WRITE (NOUT,560)
      STOP
  210 IF (DS.EQ.0.0) GOTO 180
      DT=DS
      GOTO 230
  220 DS=DT
  230 CONTINUE
      TIME=TIME+DT
      WRITE (NOUT,460)
      WRITE (NOUT,470)
      WRITE (NOUT,480) ITITLE
      WRITE (NOUT,570) NDT,TIME,DT
      WRITE (NOUT,470)
      WRITE (NOUT,580) ITOF
      IF (NUMFBC.EQ.0) GOTO 240
      WRITE (NOUT,590) (I,TFIRE(I),I=1,4)
  240 CONTINUE
      DT2=1./DT
  250 MAIN=MAIN+1
      DO 260 N=1,NUMNP
  260 T1(N)=T(N)
      IF (I6.NE.0) CALL PROUT (1,T,AT,T1,B,MAIN,NCON,I1,LM)
      DO 270 N=1,NUMEL
      SCALE=0.333333333333333
      LL1=LM(1,N)
      LL2=LM(2,N)
      LL3=LM(3,N)
      ATS=T(LL1)+T(LL2)+T(LL3)
      LL4=LM(4,N)
      IF (LL3.EQ.LL4) GOTO 270
      ATS=ATS+T(LL4)
      SCALE=0.2500
  270 AT(N)=SCALE*ATS
      CALL HCONDC (MMTYPE,LM,SS1,SS2,SS3,SS5,SS6,SS9,AT,A,NUMNP,XLAM,MAT
     .L,XYS)
      DO 280 I=1,NUMNP
  280 B(I)=0.0
      CALL HATEMP (ITOF,D,KODE,B,A,NUMNP,MAIN,T3,Q)
      CALL HCAP (MMTYPE,Q,AT,XLAM,LM,MATL,XYS)
      DO 300 N=1,NUMNP
      IF (KODE(N).EQ.4HTEMP) GOTO 300
      IF (Q(N)) 290,300,290
  290 A(N,1)=A(N,1)+Q(N)*DT2
  300 CONTINUE
      CALL MSYM (1,B,MA,A,NUMNP)
      IF (MAIN.NE.1) GOTO 320
      DO 310 II=1,NUMNP
      IF (KODE(II).EQ.4HTEMP) GOTO 310
      T2(II)=Q(II)*T(II)*DT2
  310 CONTINUE
  320 DO 330 II=1,NUMNP
      IF (KODE(II).EQ.4HTEMP) GOTO 330
      B(II)=B(II)+T2(II)
  330 Q(II)=B(II)
      NCON=0
      IF (NUMFBC.EQ.0) GOTO 350
  340 CONTINUE
      CALL FIRE (LI,LJ,LMAT,LFIRE,XL,MAT,FXYS,T,TFIRE,B)
      NCON=NCON+1
  350 CALL MSYM (2,B,MA,A,NUMNP)
      IF (NUMFBC.EQ.0) GOTO 405
      IF (NCONV.EQ.0) GOTO 405
      IF (I6.NE.0) CALL PROUT (2,T,AT,T1,B,MAIN,NCON,I1,LM)
      DO 360 N=1,NUMNP
      DX=ABS(B(N)-T(N))
      DY=CONV*ABS(B(N)+T(N))
      IF (DX.GT.DY) GOTO 380
  360 CONTINUE
  405 DO 370 N=1,NUMNP
  370 T(N)=B(N)
      GOTO 400
  380 IF (NCON.GT.NCONV) CALL PROUT (3,T,AT,T1,B,MAIN,NCON,I1,LM)
      DO 390 JJ=1,NUMNP
      DX=B(JJ)-T(JJ)
      T(JJ)=B(JJ)+BETA*DX
  390 B(JJ)=Q(JJ)
      GOTO 340
  400 IF (NCONU.EQ.0) GOTO 440
      DO 410 N=1,NUMNP
      DX=ABS(T(N)-T1(N))
      DY=CONU*ABS(T(N)+T1(N))
      IF (DX.GT.DY) GOTO 420
  410 CONTINUE
      GOTO 440
  420 IF (MAIN.GT.NCONU) CALL PROUT (3,T,AT,T1,B,MAIN,NCON,I1,LM)
      DO 430 N=1,NUMNP
      DX=T(N)-T1(N)
  430 T(N)=T(N)+ALPHA*DX
      GOTO 250
  440 CONTINUE
      IF (I1.NE.0) CALL PROUT (4,T,AT,T1,B,MAIN,NCON,I1,LM)
      IF (I2.NE.0) CALL PUOUT (I1,I2,T,AT,LM,X,Y,MMTYPE,TIME,IP1,IP2,D,T
     .3,JP)
      GOTO 160
  450 FORMAT (A4,I6,2F10.0,2X,A3)
  460 FORMAT (1H6,5(/))
  470 FORMAT (80H *********************************************************
     .***********************)
  480 FORMAT (/5X,49HFIRES-T  -  FIRE RESPONSE OF STRUCTURES - THERMAL,/
     ./5X,80A1)
  490 FORMAT (/5X,27HINITIAL SEQUENCE NUMBER IS ,I4,25H AND THE INITIAL
     .TIME IS ,F8.2/)
  500 FORMAT (7(4X,F6.1))
  510 FORMAT (5(/),69H - - - - PROGRAM TERMINATED - ERROR IN INITIAL TIM
     .E STEP CARD - - - -,//1X,A4,I6,2F10.2,2X,A3)
  520 FORMAT (A4,I6,F10.0,I5,4F10.0,3I5)
  530 FORMAT (///,43H  TIME STEP CARD OUT OF SEQUENCE - CARD NO.,I5/,12H
```

```
     . INPUT CARD)
  540 FORMAT (//,57H  - - - - PROGRAM TERMINATED - TIME STEP CARD WAS -
     .- - -,//1X,A4,I6,F10.2,I5,4F10.2,3I5)
  550 FORMAT (///,30H  NO TIME INTERVAL ESTABLISHED)
  560 FORMAT (///,36H  PROGRAM TERMINATED - JOB COMPLETED)
  570 FORMAT (/5X,17HTIME STEP NUMBER ,I4,8H - TIME ,F7.3,13H - TIME STE
     .P ,F7.3/)
  580 FORMAT (/5X,50H NUMBER OF NON-ZERO FLOW OR TEMPERATURE CONDITIONS,
     .I5)

  590 FORMAT (/5X,24H FIRE BOUNDARY CONDITION,/7X,4(5HFIRE(,I1,4H) = ,F7
     ..1,2X))
      END
C
C
      SUBROUTINE MSYM (KKK,B,MA,A,NP)
C
      COMMON /CONTROL/ ITITLE(80),IREAD(80),NIN,NOUT,NPUNCH,NUMNP,
     .                 NUMEL,MBAND,NMAT,NUMFBC,NBCMAT,NBCTYP
      DIMENSION B(1), MA(1), A(NP,1)
      NEQ=NUMNP
      GOTO (110,170), KKK
  110 NEQQ=NEQ-1
      DO 160 N=1,NEQQ
      M=MBAND
      DO 120 I=2,MBAND
      IF (A(N,M).NE.0) GOTO 130
  120 M=M-1
  130 MA(N)=M
      I=N
      DO 150 L=2,M
      I=I+1
      CC=A(N,L)/A(N,1)
      IF (CC.EQ.0) GOTO 150
      J=0
      DO 140 K=L,M
      J=J+1
  140 A(I,J)=A(I,J)-CC*A(N,K)
      A(N,L)=CC
  150 CONTINUE
  160 CONTINUE
      GOTO 220
  170 DO 190 N=1,NEQQ
      CC=B(N)
      IF (CC.EQ.0) GOTO 190
      M=MA(N)
      I=N
      DO 180 L=2,M
      I=I+1
  180 B(I)=B(I)-CC*A(N,L)
      B(N)=CC/A(N,1)
  190 CONTINUE
      B(NEQ)=B(NEQ)/A(NEQ,1)
      NN=NEQ
      DO 210 N=1,NEQQ
      NN=NN-1
      M=MA(NN)
      I=NN
      DO 200 K=2,M
      I=I+1
  200 B(NN)=B(NN)-A(NN,K)*B(I)
  210 CONTINUE
  220 RETURN
      END
C
C
      SUBROUTINE HCONDC (MMTYPE,LM,SS1,SS2,SS3,SS5,SS6,SS9,AT,A,NP,XLAM,
     .MATL,XYS)
C
      COMMON /CONTROL/ ITITLE(80),IREAD(80),NIN,NOUT,NPUNCH,NUMNP,
     .                 NUMEL,MBAND,NMAT,NUMFBC,NBCMAT,NBCTYP
      DIMENSION MMTYPE(1), LM(5,1), SS1(4,1), SS2(4,1), SS3(4,1),
     .          SS5(4,1),SS6(4,1), SS9(4,1), AT(1), A(NP,1), XLAM(4,1),
     .          MATL(1), XYS(1)
      DIMENSION E(3,3), S(5,5), IX(3)
      MB=MBAND*NUMNP
      DO 110 I=1,MB
  110 A(I,1)=0.0
      DO 210 N=1,NUMEL
      DO 120 I=1,5
      DO 120 J=1,5
  120 S(I,J)=0.0
      TEMP=AT(N)
      MS=MMTYPE(N)
      MS=(MS-1)*6
      J=MATL(MS+1)
      K=MATL(MS+2)
      COND=VMAT(K,XYS(J),XYS(J+K),XYS(J+K+K),TEMP,10H    K(T)    )
      DO 170 K=1,4
      IK=LM(K,N)
      JK=LM(K+1,N)
      IF (IK-JK) 130,170,130
  130 E(1,1)=SS1(K,N)
      E(1,2)=SS2(K,N)
      E(1,3)=SS3(K,N)
      E(2,1)=SS2(K,N)
      E(2,2)=SS5(K,N)
      E(2,3)=SS6(K,N)
      E(3,1)=SS3(K,N)
      E(3,2)=SS6(K,N)
      E(3,3)=SS9(K,N)
      COMM=0.5*COND/XLAM(K,N)
      IX(1)=K
      IX(2)=K+1
      IF (K-4) 150,140,150
  140 IX(2)=1
  150 IX(3)=5
      DO 160 I=1,3
      II=IX(I)
      DO 160 J=1,3
      JJ=IX(J)
  160 S(II,JJ)=S(II,JJ)+E(I,J)*COMM
```

```
170 CONTINUE
    DO 180 I=1,4
    DO 180 J=1,4
180 S(I,J)=S(I,J)-S(I,5)*S(J,5)/S(5,5)
    DO 200 L=1,4
    I=LM(L,N)
    DO 200 M=1,4
    J=LM(M,N)-I+1
    IF (J) 200,200,190
190 A(I,J)=A(I,J)+S(L,M)
200 CONTINUE
210 CONTINUE
    RETURN
    END
C
C
    SUBROUTINE HATEMP (ITOF,D,KODE,B,A,NP,MAIN,FT,J)
C
    COMMON /CONTROL/ ITITLE(80),IREAD(80),NIN,NOUT,NPUNCH,NUMNP,
   .                 NUMEL,MBAND,NMAT,NUMFBC,NBCMAT,NBCTYP
    DIMENSION D(1), KODE(1), B(1), A(NP,1), FT(1), J(1)
    IF (MAIN.NE.1) GOTO 130
    DO 110 I=1,NUMNP
110 D(I)=0.0
    IF (ITOF.EQ.0) GOTO 130
    WRITE (NOUT,200)
    READ (NIN,210) (J(I),FT(I),I=1,ITOF)
    WRITE (NOUT,220)
    DO 120 I=1,ITOF
    II=J(I)
    D(II)=FT(I)
    JJ=KODE(II)
    WRITE (NOUT,230) II,JJ,D(II)
120 CONTINUE
130 DO 190 N=1,NUMNP
    B(N)=B(N)+D(N)
    IF (KODE(N).EQ.4HFLOW) GOTO 190
    DO 180 M=2,MBAND
    K=N-M+1
    IF (K) 150,150,140
140 B(K)=B(K)-A(K,M)*D(N)
    A(K,M)=0.0
150 L=N+M-1
    IF (NUMNP-L) 170,160,160
160 B(L)=B(L)-A(N,M)*D(N)
170 A(N,M)=0.0
180 CONTINUE
    A(N,1)=1.0
    B(N)=D(N)
190 CONTINUE
    RETURN
200 FORMAT (//5X,64HVALUES OF TEMPERATURES OR FLOWS FOR NON-ZERO BOUND
   .ARY CONDITIONS)
210 FORMAT (5(I5,F10.2))
220 FORMAT (/,8H    NODE,7X,4HTYPE,10X,5HVALUE)
230 FORMAT (I8,7X,A4,5X,F10.2)
```



```
    END
C
C
    SUBROUTINE HCAP (MMTYPE,Q,AT,XLAM,LM,MATL,XYS)
C
    COMMON /CONTROL/ ITITLE(80),IREAD(80),NIN,NOUT,NPUNCH,NUMNP,
   .                 NUMEL,MBAND,NMAT,NUMFBC,NBCMAT,NBCTYP
    DIMENSION MMTYPE(1), Q(1), AT(1), XLAM(4,1),LM(5,1),
   .          MATL(1), XYS(1)
    DO 110 I=1,NUMNP
110 Q(I)=0.0
    DO 140 N=1,NUMEL
    TEMP=AT(N)
    MS=MMTYPE(N)
    MS=(MS-1)*6
    J=MATL(MS+3)
    K=MATL(MS+4)
    SPHT=VMAT(K,XYS(J),XYS(J+K),XYS(J+K+K),TEMP,10H   CP(T)  )
    J=MATL(MS+5)
    K=MATL(MS+6)
    DENS=VMAT(K,XYS(J),XYS(J+K),XYS(J+K+K),TEMP,10H    D(T)  )
    DO 130 K=1,4
    IK=LM(K,N)
    JK=LM(K+1,N)
    IF (IK-JK) 120,130,120
120 CONTINUE
    QSTORE=0.25*XLAM(K,N)*SPHT*DENS
    Q(IK)=Q(IK)+QSTORE
    Q(JK)=Q(JK)+QSTORE
130 CONTINUE
140 CONTINUE
    RETURN
    END
C
C
    SUBROUTINE FIRE (LI,LJ,LMAT,LFIRE,XL,MAT,FXYS,T,TFIRE,B)
C
    COMMON /CONTROL/ ITITLE(80),IREAD(80),NIN,NOUT,NPUNCH,NUMNP,
   .                 NUMEL,MBAND,NMAT,NUMFBC,NBCMAT,NBCTYP
    DIMENSION LI(1), LJ(1), LMAT(1), LFIRE(1), XL(1), MAT(1),
   .          FXYS(1), T(1), TFIRE(1), TF4(4), B(1)
    IF (NBCTYP.EQ.10HLINEAR BC ) GOTO 120
    SB=FXYS(1)
    TSHIFT=FXYS(2)
    DO 110 I=1,4
    TF=TFIRE(I)+TSHIFT
    TF=TF*TF
    TF4(I)=TF*TF
110 CONTINUE
120 CONTINUE
    DO 180 N=1,NUMFBC
    I=LI(N)
    J=LJ(N)
    M=LMAT(N)
    LF=LFIRE(N)
    TF=TFIRE(LF)
```

```
      TS=0.5*(T(I)+T(J))
      DT=TF-TS
      IF (NBCTYP.EQ.10HNON-LIN BC) GOTO 130
      M=(M-1)*2
      JJ=MAT(M+1)
      K=MAT(M+2)
      TA=0.5*(TF+TS)
      H=VMAT(K,FXYS(JJ),FXYS(JJ+K),FXYS(JJ+K+K),TA,10H  H(T)     )
      Q=XL(N)*H*DT
      GOTO 170
  130 CONTINUE
      K=MAT(M)
      A=FXYS(K)
      QC=0.0
      IF (A.EQ.0) GOTO 150
      P=FXYS(K+1)
      IF (P.EQ.1.0) GOTO 140
      SIGN=1.0
      IF (DT.LT.0) SIGN=-1.0
      DT=SIGN*DT
      QC=SIGN*A*DT**P
      GOTO 150
  140 QC=A*DT
  150 V=FXYS(K+2)
      QR=0.0
      IF (V.EQ.0) GOTO 160
      TS=TS+TSHIFT
      TS=TS*TS
      TS=TS*TS
      AB=FXYS(K+3)
      EF=FXYS(K+4)
      ES=FXYS(K+5)
      QR=SB*V*(AB*EF*TF4(LF)-ES*TS)
  160 Q=XL(N)*(QC+QR)
  170 B(I)=B(I)+Q
      B(J)=B(J)+Q
  180 CONTINUE
      RETURN
      END
C
C
      SUBROUTINE PROUT (K,T,AT,T1,B,MAIN,NCON,I1,LM)
C
      COMMON /CONTROL/ ITITLE(80),IREAD(80),NIN,NOUT,NPUNCH,NUMNP,
     .                 NUMEL,MBAND,NMAT,NUMFBC,NBCMAT,NBCTYP
      DIMENSION T(1), AT(1), T1(1), B(1),LM(5,1)
      GOTO (110,120,130,140), K
  110 CONTINUE
      WRITE (NOUT,200) MAIN
      WRITE (NOUT,290) (N,T(N),N=1,NUMNP)
      RETURN
  120 CONTINUE
      WRITE (NOUT,210) NCON
      WRITE (NOUT,290) (N,B(N),N=1,NUMNP)
      RETURN
  130 CONTINUE
      WRITE (NOUT,220)
      WRITE (NOUT,230) MAIN,NCON
      WRITE (NOUT,240)
      WRITE (NOUT,290) (N,T1(N),N=1,NUMNP)
      WRITE (NOUT,250)
      WRITE (NOUT,290) (N,T(N),N=1,NUMNP)
      WRITE (NOUT,260)
      WRITE (NOUT,290) (N,B(N),N=1,NUMNP)
      STOP
  140 CONTINUE
      IF (I1.EQ.1.OR.I1.EQ.3) GOTO 150
      GOTO 160
  150 CONTINUE
      WRITE (NOUT,270)
      WRITE (NOUT,280)
      WRITE (NOUT,290) (N,T(N),N=1,NUMNP)
  160 CONTINUE
      IF (I1.EQ.2.OR.I1.EQ.3) GOTO 170
      GOTO 190
  170 WRITE (NOUT,300)
      WRITE (NOUT,280)
      DO 180 JI=1,NUMEL
      SCALE=0.33333333333
      IL1=LM(1,JI)
      IL2=LM(2,JI)
      IL3=LM(3,JI)
      ATS=T(IL1)+T(IL2)+T(IL3)
      IL4=LM(4,JI)
      IF (IL3.EQ.IL4) GOTO 180
      SCALE=0.25000
      ATS=ATS+T(IL4)
  180 AT(JI)=ATS*SCALE
      WRITE (NOUT,290) (N,AT(N),N=1,NUMEL)
  190 CONTINUE
      RETURN
  200 FORMAT (/,62H  NODAL POINT TEMPERATURES AT BEGINNING OF SYSTEM CYC
     .LE NUMBER,I6/)
  210 FORMAT (/,40H  NODAL POINT TEMPERATURE FOR B.C. CYCLE,I5/)
  220 FORMAT (//,20H  PROGRAM TERMINATED,/,59H  CONVERGENCE NOT OBTAINED
     . IN REQUIRED NUMBER OF ITERATIONS)
  230 FORMAT (/,15H  SYSTEM CYCLE ,I5,16H AND B.C. CYCLE ,I5)
  240 FORMAT (//,33H  SYSTEM NODAL POINT TEMPERATURES)
  250 FORMAT (//,53H  NODAL POINT TEMPERATURES AT BEGINNING OF B.C. CYCL
     .E)
  260 FORMAT (//,47H  NODAL POINT TEMPERATURES AT END OF B.C. CYCLE)
  270 FORMAT (/,54H------------ NODAL POINT TEMPERATURES -------------
     .-/)
  280 FORMAT (/1X,4(16H     N      TEMP. ))
  290 FORMAT (4(I6,F10.2))
  300 FORMAT (//,53H ------------ TEMPERATURE OF ELEMENTS -----------
     .-/)
      END
```

```
C
C
      SUBROUTINE PUOUT (I1,I2,T,AT,LM,X,Y,MMTYPE,TIME,IP1,IP2,XX,YY,JP)
C
C     SUBROUTINE PUOUT WRITES THE TEMPERATURE DISTRIBUTIONS THAT
C     RESULT FROM THE ANALYSIS INTO A FILE IN A FORMAT COMPATIBLE
C     WITH THE STRUCTURAL RESPONSE PROGRAM SAFE-RCC
C
      COMMON /CONTROL/ ITITLE(80),IREAD(80),NIN,NOUT,NPUNCH,NUMNP,
     .                NUMEL,MBAND,NMAT,NUMFBC,NBCMAT,NBCTYP
      DIMENSION T(1), AT(1), LM(5,1), X(1), Y(1),
     .          MMTYPE(1), XX(1), YY(1), NL(3),A(1000),
     .            ATL(100),YYL(100),AL(100),MLTYPE(100)
      NP=NPUNCH
      DO 100 I=1,100
      AL(I)=0.0
  100 CONTINUE
      IF (I2.EQ.1) GOTO 110
      IF (I2.EQ.2) GOTO 335
      GOTO 405
C
C     FILE DATA FOR COLUMN CROSS SECTION
C
C     WRITING ELEMENT DATA
C
  110 WRITE (NOUT,430) TIME
      IF (IP2.NE.0) GOTO 170
      WRITE (NP,435) ITITLE
      WRITE (NP,440) NUMEL
C
C     WRITE THE ELEMENTS CENTROID COORDINATES DURING THE FIRST
C     REQUEST FOR ELEMENTAL DATA
C
C     CALCULATE THE CENTROIDS OF EACH ELEMENT
C
      DO 130 I=1,NUMEL
      J=LM(1,I)
      K=LM(2,I)
      M=LM(3,I)
      N=LM(4,I)
      IF (M.EQ.N) GOTO 120
      XX(I)=(X(J)+X(K)+X(M)+X(N))/4.0
      YY(I)=(Y(J)+Y(K)+Y(M)+Y(N))/4.0
      GOTO 130
  120 XX(I)=(X(J)+X(K)+X(M))/3.0
      YY(I)=(Y(J)+Y(K)+Y(M))/3.0
  130 CONTINUE
C
C     CALCULATE AREAS OF ELEMENTS
C
      DO 150 I=1,NUMEL
      J=LM(1,I)
      K=LM(2,I)
      M=LM(3,I)
      N=LM(4,I)
      IF (M.EQ.N) GOTO 140
      A(I)=(X(N)-X(J))*(Y(J)+Y(N))+(X(M)-X(N))*(Y(M)+Y(N))
      A(I)=A(I)+(X(J)-X(K))*(Y(J)+Y(K))+(X(K)-X(M))*(Y(K)+Y(M))
      A(I)=ABS(A(I)/2)
      GOTO 150
  140 A(I)=X(K)*Y(M)-X(M)*Y(K)+X(M)*Y(J)-X(J)*Y(M)+X(J)*Y(K)-X(K)*Y(J)
      A(I)=ABS(A(I)*0.5)
  150 CONTINUE
C
      DO 160 I=1,NUMEL
      IP2=IP2+1
  160 WRITE (NP,410) I,YY(I),A(I),MMTYPE(I)
  170 CONTINUE
C
C     WRITE TIME OF EXPOSURE TO FIRE
C
      WRITE (NP,450) TIME
C
C     WRITING ELEMENT TEMPERATURES
C
C     CALCULATE AVERAGE ELEMENT TEMPERATURES
C
      DO 310 I=1,NUMEL
      J=LM(1,I)
      K=LM(2,I)
      M=LM(3,I)
      N=LM(4,I)
      IF (M.EQ.N) GOTO 300
      AT(I)=(T(J)+T(K)+T(M)+T(N))/4.0
      GOTO 310
  300 CONTINUE
      AT(I)=(T(J)+T(K)+T(M))/3.0
  310 CONTINUE
      IP2=IP2+1
      WRITE (NP,420) (I,AT(I),I=1,NUMEL)
  330 CONTINUE
      GOTO 405
C
  335 CONTINUE
C
C     FILE DATA FOR COLUMN RESTRAINT SYSTEM
C
      WRITE (NOUT,460) TIME
C
C     CALCULATE ELEMENT CENTROID COORDINATES,
C     AREAS AND TEMPERATURES
C
      ILAY=1
      NEL=0
      AV=0
      DO 390 I=1,NUMEL
      J=LM(1,I)
      K=LM(2,I)
      M=LM(3,I)
      N=LM(4,I)
      NEL=NEL+1
      IF (M.EQ.N) GOTO 340
```

```
      YY(I)=(Y(J)+Y(K)+Y(M)+Y(N))/4.0
      A(I)=(X(N)-X(J))*(Y(J)+Y(N))+(X(M)-X(N))*(Y(M)+Y(N))
      A(I)=A(I)+(X(J)-X(K))*(Y(J)+Y(K))+(X(K)-X(M))*(Y(K)+Y(M))
      A(I)=ABS(A(I)/2)
      AT(I)=(T(J)+T(K)+T(M)+T(N))/4.0
      GOTO 350
  340 A(I)=X(K)*Y(M)-X(M)*Y(K)+X(M)*Y(J)-X(J)*Y(M)+X(J)*Y(K)-X(K)*Y(J)
      A(I)=ABS(A(I)*0.5)
      AT(I)=(T(J)+T(K)+T(M))/3.0
      YY(I)=(Y(J)+Y(K)+Y(M))/3.0
      GOTO 370
C
C     CALCULATE LAYER CENTROID COORDINATES,
C     AREAS AND TEMPERATURES
C
  350 IF (I.EQ.1) GOTO 360
      IF (MMTYPE(I-1).EQ.2) GOTO 380
      IF (MMTYPE(I).EQ.2) GOTO 380
      IF (YY(I).EQ.YYL(ILAY)) GOTO 370
      GOTO 380
  360 YYL(ILAY)=YY(I)
  370 AL(ILAY)=AL(ILAY)+A(I)
      AV=AV+AT(I)
      IF (I.EQ.NUMEL) ATL(ILAY)=AV/NEL
      MLTYPE(ILAY)=MMTYPE(I)
      GOTO 390
  380 ATL(ILAY)=AV/(NEL-1)
      AV=0
      NEL=1
      ILAY=ILAY+1
      GOTO 360
  390 CONTINUE
C
C     WRITE LAYER AREAS AND CENTROID COORDINATES
C     AND MATERIAL TYPE
C
      IF (IP2.NE.0) GOTO 398
      WRITE (NP,435) ITITLE
      WRITE (NP,440) ILAY
      DO 395 I=1,ILAY
      IP2=IP2+1
      WRITE (NP,410) I,YYL(I),AL(I),MLTYPE(I)
  395 CONTINUE
  398 CONTINUE
C
C     WRITE LAYER TEMPERATURES
C
      WRITE (NP,420) (I,ATL(I),I=1,ILAY)
  405 CONTINUE
C
      RETURN
C
  410 FORMAT (I4,1X,F7.5,1X,F10.8,1X,I4)
  420 FORMAT (6(I4,1X,F6.2))
  430 FORMAT (////35H . . WRITING ELEMENT DATA FOR TIME ,F7.3)
  435 FORMAT (80A1)
  440 FORMAT (I4)
  450 FORMAT (F7.3)
  460 FORMAT (////33H . . WRITING LAYER DATA FOR TIME ,F7.3)
C
      END
C
C
      SUBROUTINE MATIN (K,X,Y,S)
C
      COMMON /CONTROL/ ITITLE(80),IREAD(80),NIN,NOUT,NPUNCH,NUMNP,
     .                 NUMEL,MBAND,NMAT,NUMFBC,NBCMAT,NBCTYP
      DIMENSION X(1), Y(1), S(1)
      IF (K.NE.0) GOTO 110
      READ (NIN,150) X(1)
      WRITE (NOUT,160) X(1)
      RETURN
  110 CONTINUE
      IF (K.EQ.1.OR.K.LT.0) GOTO 140
      READ (NIN,150) (X(I),Y(I),I=1,K)
      M=K-1
      DO 120 I=1,M
  120 S(I)=(Y(I+1)-Y(I))/(X(I+1)-X(I))
      WRITE (NOUT,170)
      DO 130 I=1,M
      WRITE (NOUT,180) I,X(I),Y(I)
      WRITE (NOUT,190) S(I)
  130 CONTINUE
      WRITE (NOUT,180) K,X(K),Y(K)
      RETURN
  140 WRITE (NOUT,200) K
      STOP
  150 FORMAT (8E10.0)
  160 FORMAT (/,39H  MATERIAL PARAMETER OF CONSTANT VALUE ,G11.3)
  170 FORMAT (/5X,19HNODE    TEMPERATURE,6X,5HVALUE,7X,5HSLOPE,/)
  180 FORMAT (I9,F13.1,6X,G11.3)
  190 FORMAT (39X,G11.3)
  200 FORMAT (///,44H  ------------PROGRAM TERMINATED-----------,/,14H
     .  INPUT ERROR,/,23H   CONTROL CONSTANT IS ,I5,22H AND IT MUST BE E
     .ITHER,/,34H   0 OR GREATER THAN OR EQUAL TO 2)
      END
C
C
      FUNCTION VMAT (K,X,Y,S,T,NAME)
C
      COMMON /CONTROL/ ITITLE(80),IREAD(80),NIN,NOUT,NPUNCH,NUMNP,
     .                 NUMEL,MBAND,NMAT,NUMFBC,NBCMAT,NBCTYP
      DIMENSION X(1), Y(1), S(1)
      IF (K.NE.0) GOTO 110
      VMAT=X(1)
      RETURN
  110 I=0
  120 I=I+1
      IF (I.GT.K) GOTO 150
      IF (T-X(I)) 140,130,120
  130 VMAT=Y(I)
      RETURN
```

```
  140 IF (I.EQ.1) GOTO 150
      VMAT=Y(I-1)+S(I-1)*(T-X(I-1))
      RETURN
  150 WRITE (NOUT,160) NAME,T,X(1),X(K)
      STOP
  160 FORMAT (///,48H  -------------PROGRAM TERMINATED---------------,/,
     .50H    BOUNDS OF CURVE DESCRIBING MATERIAL PARAMETER ,A10,19H HAVE
     . BEEN EXCEEDED,/,23H   THE TEMPERATURE WAS ,F10.3,20H THE LOWER BO
     .UND IS ,F10.3,24H AND THE UPPER BOUND IS ,F10.3)
      END
C
C
      FUNCTION NUMBER(I)
C
      COMMON /CONTROL/ ITITLE(80),IREAD(80),NIN,NOUT,NPUNCH,NUMNP,
     .                 NUMEL,MBAND,NMAT,MUMFBC,NBCMAT,NBCTYP
      K=0
  110 J=IREAD(I)
      IF (J.EQ.56B) GOTO 120
      IF (J.GT.32B) GOTO 140
      I=I+1
      IF (I.EQ.81) GOTO 130
      GOTO 110
  120 I=I+1
      J=IREAD(I)
      IF (J.EQ.55B.OR.J.EQ.56B) GOTO 130
      IF (J.LT.33B.OR.J.GT.44B) GOTO 140
      J=J-33B
      K=K*10+J
      GOTO 120
  130 NUMBER=K
      RETURN
  140 CONTINUE
      WRITE (NOUT,150) IREAD
      STOP
  150 FORMAT (///,33H - - - PROGRAM TERMINATED - - - -,//,13H  INPUT ERR
     .OR,/1X,80R1)
      END
```

LIST OF REFERENCES

Abrams H S (1970) — Compressive Strength of Concrete at Temperatures of $1600^{o}F$. ACI, SP25, 15pp.

Åldstedt D E (1975) — Nonlinear Analysis of Reinforced Concrete Frames. Division of Structural Mechanics, Norwegian Institute of Technology. Repcrt no. 75-1, Trondheim.

Allen D E (1974)
Lie T T — Further Studies of the Fire Resistance of Reinforced Concrete Columns. Technical paper no. 416, Division of Building Research, Ottawa.

Anderberg Y (1976) — Fire Exposed Hyperstatic Concrete Structures - An experimental and theoretical study. Lund Institute of Technology, Bulletin 55.

Anderberg Y (1978) — Armeringsstahls Mekaniskan Egenskaper vid Hoga Temperaturer, Division of Structural Mechanics and Concrete Construction, Bulletin 61, Lund Institute of Technology, Lund, Sweden.

Anderberg Y (1983) — Predicted Fire Behaviour of Steels and Concrete Structures. Three Decades of Structural Fire Safety (BRE).

Anderberg Y (1985) — Behaviour of Steel at High Temperatures. Editor Anderberg, Pub. Lund Institute of Technology.

Anderberg Y (1978)
Pettersson O
Thelandersson S — Deformation Characteristics of Concrete and Steel at Transient High Temperature Conditions. Appendix A. pp. 40-60 of FIP/CEB Report.

Anderberg Y (1976)
Thelandersson S — Stress and Deformation Characteristics of Concrete at High Temperatures. 2 Experimental Investigation and Material Behaviour Model. Lund Institute of Technology, Bulletin 54.

Baldwin R (1973)
North M A — A Stress-strain Relationship for Concrete at High Temperatures. Building Research Establishment, Fire Research Station. Magazine of Concrete Research: Vol. 25, No. 85.

Bali A (1984) — The Transient Behaviour of Plain Concrete at Elevated Temperatures. PhD Thesis, University of Aston.

Bandyopadhyay B (1975) — Computer Analysis of Skeletal Structures with Special Reference to Deterioration due to Fire. PhD Thesis, University of London.

Bazant Z P (1978)
Panula L — Practical Prediction of Time Dependent Deformations of Concrete. Part I - Shrinkage and Part II - Basic Creep. Matériaux et Construction,Vol. 11, No. 65, pp. 307 - 328. Part III - Drying Creep and Part IV - Temperature Effect on Basic Creep. Matériaux et Construction, Vol. 11, No. 66, pp. 415 - 434. Part V - Temperature Effect on Drying Creep and Part VI Cyclic Creep, Non Linearity and Statistical Scatter. Matériaux et Construction, Vol. 12, No. 69, pp. 169 - 183.

Becker J (1974)
Bizri H
Bresler B — FIRES-T. A computer program for the Fire Response of Structures - Thermal. Fire Research Group, University of California, Berkeley. Report no. UCB FRG 74-1.

Becker J (1974)
Bresler B — FIRES-RC. A computer program for the Fire Response of Structures - Reinforced Concrete frames. Fire Research group, University of California, Berkeley. Report no. UCB FRG 74-3.

Becker W (1970)
Stanke J — Brandversuche an Stahlbetonfetigstützen, Deutscher Ausschuss für Stahlbeton. Heft 215, Berlin.

Bresler B (1983)
Iding R — Fire Response of Prestressed Concrete Members. Fire Safety of Concrete Structures, American Concrete Institute, Editor M S Abrams, Publiction SP80.

Bizri H (1973) — Structural Capacity of Reinforced Concrete Columns Subject to Fire Induced Thermal Gradients. Structural Engineering Laboratory. Report No. 73-1. University of California, Berkeley.

Bletzacker R W (1960) Effect of Structural Restraint on the fire Resistance of Protected Steel Beam Floors and Roof Assemblies. Ohio University, Report no. REs 246/266, pp. 130.

BS476 Part 8: Fire Tests on Building Materials and Structures. BSI, 15 pp. 1972.

BS476 Parts 20, 21 and 22: Fire Tests on Building Materials and Structures. BSI, to be published (1985).

BS5268 The Structural Use of Timber, Part 4, Section 4.1, Method for Calculating Fire Resistance of Timber Members, 1978.

BS5628 Part 1: Structural Use of Masonary-Unreinforced, BSI, London, 1978.

BS5950 Structural Use of Steelwork in Building. Part 4, to be published (1985).

BS6399 Design Loading for Buildings. Part 1: Code of Practice for dead and imposed loads, 1984.

BS8110 The Structural Use of Concrete. 1985.

Building Regulations No. 1676. Building and Buildings, HMSO, 1976.

Carlson et al (1961) A Review of Studies of the Effects of Restraint on the Fire Resistance of Prestressed Concrete. Proceedings, Symposium on Fire Resistance of Prestressed Concrete, Research Department Bulletin 206, PCA.

CEB (1982) Design of Concrete Structures for Fire Resistance. Preliminary Draft of an Appendix to the CEB/FIP Model Code, Bulletin d'information No. 145, Paris.

Clarke J H (1960) Method of Assessing Probable Fire Endurance of Load Bearing Columns. Proc. ACI Vol.31 pp. 12-23.

Collette Y (1976) Études de propiétés du béton soumis à des températures élevées. Group de Travail, Comportement du Matériaux Béton en Fonction de la Température, Bruxelles.

CP110 Part 1: The Structural Use of Concrete. BSI, 154 pp London, 1972.

Cranston W B (1967) A Computer Method for the Analysis of Restrained Columns. TRA Report 402.

Cranston W B (1972) Analysis and Design of Reinforced Concrete Columns. Cement and Concrete Association. Research Report No. 20.

Crook N (1980) The Elevated Temperature Properties of Reinforced Concrete. PhD Thesis University of Aston.

Cruz C R (1966) Elastic Properties of Concrete at High Temperatures. PCA Research and Development Laboratories.

Cruz C R (1968) Apparatus for Measuring Creep at High Temperatures. Journal PCA, Vol. 10, No. 3, pp. 36-42.

Cruz C R (1981)
Gillen M Thermal Expansion of Portland Cement Paste, Mortar and Concrete at High Temperatures. PCA. Fire and Materials, Vol. 4, No. 2.

Diedrichs U (1981)
Schneider U Bond Strength at High Temperatures. Technical University of Brunswick. Magazine of Concrete Research, Vol. 33, No. 115.

Dorn J E (1954) Some Fundamental Experiments on High Temperature Creep. Journal of the Mechanics and Physics of Solids Vol. 3, No.2, pp. 85-116.

Dougill J W (1966) Relevance of the Established Method of Structural Fire Testing to Reinforced Concrete. Applied Materials Research, Vol. 5, No. 4, pp. 235-240.

Dougill J W (1972a) Modes of Failure of Concrete Panels Exposed to High Temperatures. Magazine of Concrete Research, Vol. 24, No. 79, pp.71-76.

Dougill J W (1972b) — Conditions for Instability in Restrained Concrete Panels Exposed to Fire. Magazine of Concrete Research, Vol. 24, No. 80, pp. 139-148.

Dougill J W (1983) — Materials Dominated Aspects for Structural Fire Resistance of Concrete Structures. Fire Safety of Concrete Structures. Editor S Abrams. Publication SP-80. American Concrete Institute, Detroit.

FIP/CEB (1978) — Report on Methods of Assessment of the Fire Resistance of Concrete Structural Members, C and CA, No. 15-393, 91 pp.

Fire Grading of Buildings (1946) — Part 1: General Principles and Structural Precautions, Ministry of Public Buildings and Works, Post War Building Studies, No. 20, HMSO.

Fischer R (1970) — Über das Verhalten von Zementmörtel und Beton bei höhreren Temperaturen Deutscher Ausschuss für Stahlbeton (DAS) Heft 214, Berlin, pp.60-128.

Forsén N E (1982) — A Theoretical Study of the Fire Resistance of Concrete Structures. FCB-SINTEFF, Trondheim.

Freudenthal A M (1958) Roll F — Creep and Creep Recovery under High Compressive Stress. Journal of the American Concrete Institute, Vol. 54, No. 12, pp1111-1142.

Furamura F (1966) — The Stress-strain Curve of Concrete at High Temperatures- I. Paper no. 7004 for the Annual Meeting of the Architectural Institute of Japan. (In Japanese, copy held by the Fire Research Station Library, ref. D17CT67 23.1966). Summary (also in Japanese but with three figures) printed in extra number of Transactions of the Architectural Institute of Japan. (Summaries of Technical papers of Annual Meeting of AIJ).

Gillen M (1981) — Short Term Creep of Concrete at Elevated Temperatures. Fire Research Dept. PCA, Fire and Materials, Vol. 5, No. 4.

Gross H (1973) Computer Aided Thermal Creep Analysis of Concrete Continua. PhD Thesis, University of London.

Haksever A (1977) Zur Frage Des Trag -und Verformungs- verhaltens ebener Stahlbetonrahmen im Brandfall. Insitute für Baustoffkunde und Stahlbetonbau der Technischen Univerität Braunschweig. Heft 35, Braunschweig.

Haksever A (1980) Ein Rechenmodell zur Beschreibung des Verhaltens von Gesambtbauwerken und Bauwerksabschnitten im Brandfall, Sonderforschungsbereich 148 'Brandverhalten von Bauteilen', Bericht 1978 - 1980, A1/2 - 1, Technische Universität Braunschweig.

Haksever A (1982) Anderberg Y Comparison between Measured and Computed Structural Response of some Reinforced Concrete Columns in a Fire. Lund Institute of Technology and Technical University Braunschweig. Fire Safety Journal, 4, pp. 293-297, (1981/1982).

Haksever A (1982) Haβ R Traglast von Druckgleidern mit vereinfachter Bugelbewehrung unter Feuerangriff. Technische Universität Braunschweig Institut fur Baustoffe, Massivbau und Brandschutz. Deutscher Auschuss für Stahlbeton, Heft 332, pp. 50-75.

Harada T (1949) Thermal Character of Concrete. Transactions AIJ. Vol. 39, 1949, pp. 66-71, Vol. 42, 1951, Vol. 44, 1952, pp. 1-8, Vol. 45, 1952, pp. 1-6, Vol. 46, 1953, pp. 1-10.

Harada T (1953) Variation of Concrete Strength and Elasticity under High Temperatures. Trans. AIJ, No. 47, 1953, pp.11-18, No. 48, 1954, pp. 1-9, No.56, 1957, pp.1-7.

Harmathy T Z (1970) Thermal Properties of Concrete at Elevated Temperatures. National Research Council of Canada. ASTM Journal of Materials, pp. 47-74, Ottawa.

Harmathy T Z (1966)
Berndt J E

Hydrated Portland Cement and Lightweight Concrete at Elevated Temperatures. Proc. ACI, Vol. 63, pp. 93-111.

Harmathy T Z (1970)
Stanzack W W

Elevated Temperature Tensile and Creep Properties of some Structural and Prestressing Steels in Fire Test Performance. ASTM Spec. Tech. Pubn. STP 464, pp. 186-208.

Harmathy T Z (1974)

Creep Deflection of Beams. ASCE National Structural Engineering Meeting Preprint 2216, 25pp.

Hertz K (1982)

The Anchorage Capacity of Reinforcing Bars at Normal and High Temperatures. Technical University of Denmark. Magazine of Concrete Research, Vol. 34, No. 121.

Holmes M (1982)
Anchor R D
Cook G M E
Crook R N

The Effects of Elevated Temperatures on the Strength Properties of Reinforcing and Prestressing Steels. Journal IStructE, Vol. 60B, No.1.

Hughes B P (1966)
Chapman G P

The Deformation of Concrete and Micro-concrete in Compression and Tension with Particular Reference to Aggregate size. Magazine of Concrete Research, Vol. 18, No. 54.

Hull W A (1918)

Behaviour of Reinforced Columns under Fire Test. Proc. ACI, Vol. 14, 1919, pp.89-103, Vol. 16, 1920, pp. 20-45.

Iding R (1977)
Bresler B
Nizammuddin Z

FIRES-RC II, A computer program for the Fire Response of Structures - Reinforced Concrete frames. Report no. UCB FRG 77-8, Fire Research Group, University of California, Berkeley.

Iding R (1977)
Bresler B
Nizamuddin Z

FIRES-T3. A Computer Program for the Fire Response of Structures-Thermal-3-Dimensional Version. Report No. UCB-FRG 77-15, Fire Research Group, University of California, Berkeley.

Ingberg S H (1921)
Griffin H K
Robinson W C
Wilson R E

Fire Tests on Building Columns. US Bureau of Standards, Technical paper no. 184, pp. 375.

ISO 834 — Fire Resistance Tests - Elements of Building Construction, International Standards Organization, 1975.

Issen L A (1970)
Gustaferro A H
Carlson CC — Fire Tests of Concrete Members, an Improved Method of Estimating Thermal Restraint Forces. ASTM STP 464, pp. 153-165.

Joint Report — Fire Resistance of Concrete Structures. Institution of Structural Engineers and the Concrete Society, 59 pp. 1975.

Law M (1983a) — A Basis for the Design of Fire Protection of Building Structures. Journal IStructE, Vol. 61A, No. 1.

Law M (1983b) — Fire Exposure of Building Structures- A Review of Experiments. Three Decades of Structural Fire Safety (BRE).

Lea F C (1920) — Effects of Temperature on some of the Properties of Materials. Engineering, Vol. 110, pp. 293-298.

Lie T T (1983) — A Procedure to Calculate Fire Resistance of Structural Members. Division of Building Research, National Research Council, Canada, Ottawa. Three Decades of Structural Fire Safety (BRE).

Lie T T (1972)
Allen D E — Calculation of the Fire Resistance of Reinforced Concrete Columns. Division of Building Research, National Research Council. Technical paper no. 378, Ottawa.

Lie T T (1984)
Lin T D
Allen D E
Abrams M S — Fire Resistance of Reinforced Concrete Columns. National Research Council Canada, Division of Building Research.

Lie T T (1972)
Harmathy T Z — A Numerical Procedure to Calculate the Temperature of Protected Steel Columns Exposed to Fire. Division of Building Research Council, Canada. Technical paper no. NRC 12535.

Malhotra H L (1956) — The Effect of Temperature on the Compressive Strength of Concrete. Magazine of Concrete Research, Vol. 8, No. 23, pp. 85-94.

Malhotra H L (1982) — Design of Fire Resisting Structures Surrey University Press, pp. 226.

Maréchal J C (1969) — Le fluage du béton en fonction de la température, Matériaux et Constructions, Vol. 2, No. 8 pp. 111-115.

Maréchal J C (1970a) — Fluage du béton en fonction de la température, Annales de l'Institut Technique du Bâtiment et Travaux Publiques, Vol. 23, no. 266, pp. 12-24.

Maréchal J C (1970b) — Contribution a l'étude des propriétés thermiques du béton, Annales de l'Institut Technique du Bâtiment et Travaux Publiques, Vol. 23, No. 274, pp. 123-146.

Maréchal J C (1970c) — Fluage du béton en fonction de la température - Complements expérimentaux, Matériaux et Constructions, Vol. 3, No.18, pp. 395-406.

Mukaddam M (1974) — Creep Analysis of Concrete at Elevated Temperature. Journal of the American Concrete Institute, Vol. 71, pp. 72-79.

Morley P D (1980)
Royles R — The Influence of High Temperature on the Bond in Reinforced Concrete. Fire Safety Journal 2, pp. 243-255, 1979/80.

Odeen (1968) — Fire Resistance of Prestressed Concrete Double T Units. Acta Polytechnica Scandinavia Ci 48, Stockholm.

Odeen K (1972)
Nordstrom A — Thermal Properties of Concrete at High Temperatures. Cement och Betong, Stockholm.

Pettersson O (1976)
Magnusson S
Thor T — Fire Engineering Design of Steel Structures. Division of Structural Mechanics and Concrete Construction Lund Institute of Technology, Swedish Institute of Steel Construction, Stockholm, Sweden, Pub. 50.

Philleo R (1958) — Some Physical Properties of Concrete at High Temperature. Proc. ACI Vol. 54, pp. 857-864.

Purkiss J A (1972) A Study of the Behaviour of Concrete Heated to High Temperatures under Restraint or Compressive Loading. PhD Thesis, University of London.

Purkiss J A (1986) Material Behaviour at Elevated Temperatures. Paper to be presented at 'Design of Structures against Fire', University of Aston, April 1986 (to be published).

Reichel V (1978) How Fire Effects Steel to Concrete Bond. Building Research and Practice.

Schneider U (1976) Behaviour of Concrete under Thermal Steady State and Non-Steady State Conditions. Fire and Materials, Vol. 1, No. 3, pp.103-115.

Schneider U (1985) Behaviour of Concrete at High Temperatures. Editor Schneider. Pub. Gesamthochschule Kassel.

Seekamp H (1964), Becker W, Struck W. Brandversuche an Stahlbetonfertigsäulen. Deutscher Asschuss für Stahlbeton Vol. 64, Berlin, pp. 34.

Selvaggio S L (1963), Carlson C C. Effect of Restraint on Fire Resistance of Prestressed Concrete. Fire Test Methods (1962), ASTM STP 344, pp. 1-25, Research Dept. Bulletin 164, PCA.

Selvaggio S L (1967), Carlson C C. Restraint in Fire Tests of Concrete Floors and Roofs. Fire Test Methods- Restraint and Smoke (1966), ASTM STP 422, pp. 21-39, Research Dept. Bulletin 220, PCA.

Smith C I (1982) Fire Regulations - Is There Something Better ? Public Works Congress 1982.

Stirland C (1980) Steel Properties at Elevated Temperatures for use in Fire Engineering Calculations. British Steel Corporation, Teeside Laboratory, Paper for ISO KC92/WG15 Committee.

Sullivan P J E (1983), Dougill J W. Developments in Design of Structural Concrete under Fire Conditions. Three Decades of Structural Fire Safety (BRE).

Taylor H P J (1974) — The Behaviour of Insitu Concrete Beam-Column Joints. Cement and Concrete Association. Technical Report. pp.32.

Thomas F C (1953)
Webster C T — Fire Resistance of Reinforced Concrete Columns. National Building Studies Research, Paper no. 18, pp. 80.

Weigler H (1967)
Fischer R — Beton bei Temperaturen von 100 bis 750°C. Mehmel-Festschrift, Beton-Verlag GmbH, Dusseldorf.

Wickström U (1979) — TASEF-2. A computer program for the Temperature Analysis of Structures Exposed to Fire. Department of Structural Mechanics, Lund Institute of Technology. Report no. 79-2.

Zoldners N G (1960) — Effect of High Temperatures on Concrete Incorporating Different Aggregates. Proc. ASTM Vol. 60, pp. 1087-1108.